CO_2 Storage and Enhanced Oil Recovery: Sugar Creek Oil Field Test Site, Hopkins County, Kentucky

Scott M. Frailey, Thomas M. Parris, James R. Damico, Roland T. Okwen, and Ray W. McKaskle

Technical Editors
Charles C. Monson and Jonathan H. Goodwin

Contributing Authors
E. Glynn Beck, Peter M. Berger, Robert Butsch, Damon A. Garner, John P. Grube, Keith C. Hackley, Jessica S. Hinton, Abbas Iranmanesh, Christopher P. Korose, Edward Mehnert, Charles C. Monson, William R. Roy, Steven L. Sargent, and Bracken Wimmer

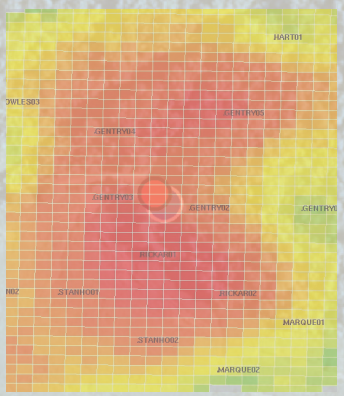

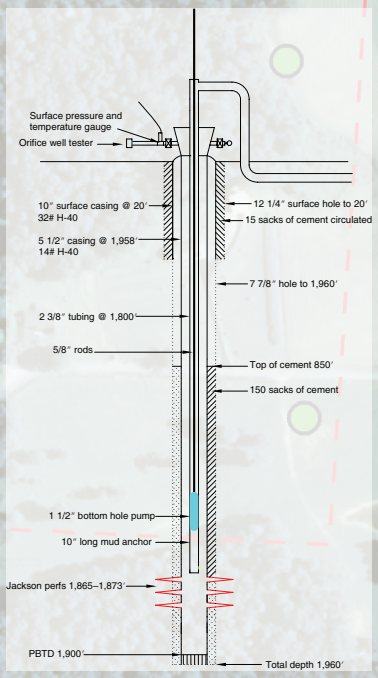

Open File Series 2012-4 2012

ILLINOIS STATE GEOLOGICAL SURVEY
PRAIRIE RESEARCH INSTITUTE

ILLINOIS STATE GEOLOGICAL SURVEY
Prairie Research Institute
University of Illinois at Urbana-Champaign

DISCLAIMER

Midwest Geological Sequestration Consortium

Final Report

October 1, 2007–March 30, 2012

Principal Investigator: Robert Finley
Illinois State Geological Survey
Prairie Research Institute
University of Illinois
(217) 244-8389
finley@isgs.illinois.edu

Report Issued: March 30, 2012

U.S. DOE Contract: DE-FC26-05NT42588

The Board of Trustees of the University of Illinois
Sandy Moulton, Director
c/o Grants & Contracts Office
1901 S. First Street, Suite A
Champaign, IL 61820
Illinois State Geological Survey
with Team Members:
Gallagher Drilling, Inc.
Kentucky Geological Survey
Trimeric Corporation

Frailey, S.M., T.M. Parris, J.R. Damico, R.T. Okwen, R.W. McKaskle. 2012. CO_2 Storage and Enhanced Oil Recovery: Sugar Creek Oil Field Test Site, Hopkins County, Kentucky. C.C. Monson and J. H. Goodwin (eds.): Illinois State Geological Survey, Open File Series 2012-4, 234 pp.

CO_2 Storage and Enhanced Oil Recovery: Sugar Creek Oil Field Test Site, Hopkins County, Kentucky

Scott M. Frailey, Thomas M. Parris, James R. Damico, Roland T. Okwen, and Ray W. McKaskle

Technical Editors
Charles C. Monson and Jonathan H. Goodwin

Contributing Authors
E. Glynn Beck, Peter M. Berger, Robert Butsch, Damon A. Garner, John P. Grube, Keith C. Hackley, Jessica S. Hinton, Abbas Iranmanesh, Christopher P. Korose, Edward Mehnert, Charles C. Monson, William R. Roy, Steven L. Sargent, and Bracken Wimmer

ILLINOIS STATE
GEOLOGICAL SURVEY
PRAIRIE RESEARCH INSTITUTE

ILLINOIS

ILLINOIS STATE GEOLOGICAL SURVEY
Prairie Research Institute
University of Illinois at Urbana-Champaign
615 E. Peabody Drive
Champaign, Illinois 61820-6964
http://www.isgs.illinois.edu

CONTRIBUTORS

Robert J. Finley and Scott M. Frailey, Illinois State Geological Survey (ISGS), Prairie Research Institute, conducted the technical review of this document. Charles C. Monson and Jonathan H. Goodwin (ISGS) worked with contributors and reviewers to assemble the report. Goodwin, Monson, and Frailey prepared the Abstract and Executive Summary.

Scott Frailey led the effort to find a suitable injection site as well as pilot planning, scheduling, and logistics of implementing the plan through post-carbon dioxide (CO_2) injection testing, including coordination with the field operator. Frailey monitored pressures and injection rates and performed real time analyses of the data for the CO_2 and water injection periods. He was the primary author for the introduction and sections on site selection, pilot site design and well arrangement, field observations during active CO_2 injection, conclusions, and recommendations. Text for these sections was also contributed by James R. Damico and John P. Grube (ISGS), Charles Monson, and Thomas M. Parris (Kentucky Geological Survey [KGS]).

Charles Monson and Roland Okwen (ISGS) wrote the field history section, based largely on data provided by Mike Gallagher and Gallagher Drilling, Inc. (GDI), the operators of the field. James Damico organized and processed much of the data provided by GDI and drafted some of the figures.

James Damico and John P. Grube (ISGS) and E. Glynn Beck and Thomas M. Parris (KGS) wrote the text for the geologic characterization section. Damico and Grube were responsible for conceptual and geocellular modeling, including core and log analyses. Beck and Parris were responsible for characterization of surface geology, bedrock, and general site hydrology and hydrogeology as well as x-ray diffraction analysis.

Thomas M. Parris (KGS) coordinated the monitoring, verification, and accounting (MVA) program at the Sugar Creek site. Parris wrote and edited the majority of the MVA strategies and methods and MVA observations and interpretations sections. Edward Mehnert (ISGS) was responsible for the groundwater modeling. Keith C. Hackley (ISGS) wrote the section dealing with isotopic characterization and oversaw lab work associated with this effort. Other contributors to these sections included Glynn Beck and Kathryn G. Takacs (KGS). ISGS contributors to both field and lab efforts and data analysis and interpretation included Peter M. Berger (geochemical modeling), Joseph Chou and Shari E. Fanta (gas chromatographic and isotopic characterization), William R. Roy (geochemical modeling, health and human safety), and Bracken Wimmer (soil gas work in response to line leak section). Randy Locke (ISGS) assisted in planning of the MVA effort and helped oversee ISGS MVA efforts. Bob Butsch (Schlumberger Carbon Services) completed the cased hole log analyses and contributed the text and figures for the appendix on the reservoir saturation tool interpretation. Kenneth Copenhaver (University of Illinois at Chicago) arranged for the acquisition and processing of the hyperspectral imagery of the July 2009 CO_2 leak.

Ray McKaskle, Kevin Fisher, Joe Lundeen, and Andrew Sexton (Trimeric) were responsible for injection equipment design, procurement, and testing; they also provided operational support. McKaskle was the primary author for the field operations section of this report. Additional contributors to this section were Scott Frailey, Damon A. Garner, Jessica Hinton, Charles Monson, and Steven L. Sargent (ISGS).

Mike Gallagher, Shawn Gallagher, Dan Gallagher, and Victor J. Gallagher of Gallagher Drilling, Inc. (GDI) provided site and field logistic support and engineering and geologic design. Mike Gallagher was the primary contact with ISGS throughout the project and provided information and feedback during the report writing stage. GDI also provided several of the figures used in this report.

Damon Garner provided extensive data management, archiving, and analysis tool development. Garner was responsible for calculating gas production at Sugar Creek wells throughout the project and was primary author for the appendix describing gas production calculation considerations (Daniel Klen and Charles Monson provided technical editing of this text). Steve Sargent supported the data acquisition program from inception through completion, including installation, calibration, and maintenance of monitoring equipment. Charles Monson also contributed to the data gathering effort in the field.

Roland Okwen (ISGS) was responsible for post-injection reservoir modeling and was the primary author for the CO_2 sequestration and EOR interpretation, analysis, and reservoir modeling section. Scott Frailey worked with Okwen on the modeling effort and write-up.

Charles Monson (ISGS) and E. Glynn Beck (KGS) were the authors of the pilot closure and site reclamation section.

Other ISGS personnel assisted with this report: Jessica Hinton was responsible for the early stages of report organization. Victoria Bobell, Megan Seger, Daniel Klen, Charles Monson, and Shannon Wilson provided editing, figure drafting, unit conversions, and data compilation. Daniel L. Byers (ISGS) contributed photographs of the equipment and site and technical drawings. Michael Knapp provided figure formatting and layout of final report. Christopher P. Korose contributed Geographic Information Systems and volumetrics figures and images. Don Luman contributed image processing. Cheryl K. Nimz provided technical editing and review.

ACKNOWLEDGMENTS

The Midwest Geological Sequestration Consortium is funded by the U.S. Department of Energy through the National Energy Technology Laboratory (NETL) via the Regional Carbon Sequestration Partnership Program (contract number DE-FC26-05NT42588), the Illinois Department of Commerce and Economic Opportunity, Office of Coal Development through the Illinois Clean Coal Institute (cost share agreement), and the Commonwealth of Kentucky, through the Kentucky Consortium for Carbon Storage (KYCCS) at the University of Kentucky, Lexington.

Through a university grant program, Landmark Software was used for the reservoir and geologic modeling.

ABSTRACT

The Midwest Geological Sequestration Consortium (MGSC) carried out a small-scale carbon dioxide (CO_2) injection test in the Jackson sandstone (Mississippian System Big Clifty Sandstone Member) in order to gauge the large-scale CO_2 storage that might be realized from enhanced oil recovery (EOR) of mature Illinois Basin oil fields via immiscible liquid CO_2 flooding.

As part of the MGSC's Validation Phase (Phase II) studies, the small injection pilot test was conducted at the Sugar Creek Field in Hopkins County, western Kentucky, which was chosen for the project on the basis of site infrastructure as well as reservoir conditions. Geologic data on the target formation were limited, but core analysis reports permitted the estimation of porosity and permeability, and geophysical logs were used to define the structure and architecture of the target formation. A geocellular model of the reservoir was constructed to improve understanding of CO_2 behavior in the subsurface.

At the time of site selection, the field was under secondary recovery through water injection. A water injection well surrounded by four nearby producing wells was converted to CO_2 injection, and several additional production and observation wells were instrumented to collect temperature and pressure response information. The CO_2 injection period lasted from May 13, 2009, through May 26, 2010, and was punctuated by multiple interruptions, which ranged from a few days to several weeks in length. These lapses were caused by line leaks and supply interruptions due to winter weather. A total of 6,560 tonnes (7,230 tons) of CO_2 were injected into the reservoir at rates that generally ranged from 18.2 to 27.3 tonnes (20 to 30 tons) per day. Injection pressure decreased slowly with time. The CO_2 injection was followed by more than a year of water injection and continued monitoring.

Pressure changes and elevated CO_2 levels in response to injection (breakthrough) occurred at five production wells during the one-year injection period, all within the first five months. The first breakthrough occurred one week after commencement of CO_2 injection, which was sooner than expected based on modeling; this difference was attributed to a previously undetected fracture network.

A monitoring, verification, and accounting (MVA) program was set up to document the fate of injected CO_2. Extensive sampling of brine, groundwater, and wellhead gas was carried out, beginning before CO_2 injection and continuing through the waterflooding period. Samples were gathered at Sugar Creek Field production and observation wells, newly constructed groundwater monitoring wells, and nearby domestic and agricultural wells. Samples underwent geochemical and isotopic analysis to reveal any CO_2-related changes. Groundwater and kinetic modeling and mineralogical analysis were also employed to better understand long-term dynamics of CO_2 in the reservoir. No CO_2 leakage into groundwater was detected, and analysis of brine and gas chemistry made it possible to track the path of plume migration and infer geochemical reactions and trapping of CO_2. Cased-hole logging at several wells did not detect any CO_2 in the near-wellbore region. An estimated 1,028 tonnes (1,133 tons) of CO_2 were produced at the surface from wells and the gas separator from May 13, 2009, through the end of September 2011, representing about 16% of the injected CO_2. Consequently, 84% of the injected CO_2 was stored at the Sugar Creek field after one year of post-CO_2 injection monitoring.

Project improved oil recovery (IOR) was estimated at 1,574 m^3 (9,900 bbls) and CO_2 enhanced oil recovery (EOR) at 429–509 m^3 (2,700–3,200 bbl), although estimation of an EOR baseline was difficult because recovery was also increased by pre-project well work. These figures would have been higher if not for variations in oil production rate due to operational problems. Oil production rates did not return to pre-shut-in level after the lengthy winter injection hiatuses, but they remained elevated relative to production rates immediately before the pilot.

The pilot was designed to measure and record data which could be used to calibrate a reservoir simulation model of the Jackson sandstone to project EOR potential of a larger-scale project at the field. A model calibrated to field data (including geologic data and oil and water production) was used to assess the full-field EOR potential at the Sugar Creek Field. Projections based on these models indicated that full-field CO_2 injection for 20 years could have 5.5% incremental oil recovery or 27,700 scm (174,000 stb), with a CO_2 net utilization of 160 scm/scm (880 scf/bbl). The potential CO_2 storage is estimated to be 5,200 to 9,500 tonnes (5,800 to 10,500 tons). At lower reservoir pressure, less CO_2 can be stored.

EXECUTIVE SUMMARY

Based on the results of the Characterization Phase (Phase I) studies carried out by the Midwest Geological Sequestration Consortium (MGSC), enhanced oil recovery (EOR) offers the most important economic offset to the costs associated with carbon storage in the Illinois Basin. As part of its Validation Phase (Phase II) studies, the MGSC carried out a small-scale carbon dioxide (CO_2) injection test in the Jackson sandstone (Mississippian System Big Clifty Sandstone Member), in order to gauge the potential for EOR and concomitant large-scale CO_2 storage via immiscible CO_2 flooding in mature Illinois Basin oil fields.

The Sugar Creek Field in Hopkins County, western Kentucky, was selected as the site for the MGSC's EOR III pilot study. The decision was based on screening of five factors: (1) conditions in the reservoir conducive to an immiscible CO_2 flood; (2) operation and development history of the field; (3) surface conditions to allow delivery of CO_2 via tanker trucks; (4) well-bore conditions for producing and injection wells, and (5) results of preliminary geologic and reservoir modeling.

Data for use in developing the geocellular and reservoir models of the oil reservoir were limited. Neither cores nor drilling samples were available for visual inspection within the pilot area, but some core analysis reports provided information about porosity and permeability. A limited suite of resistivity and spontaneous potential (SP) geophysical logs from 37 wells drilled in the mid-1960s were used to define the structure and architecture of the formation. A geocellular model of the reservoir was built for reservoir modeling to estimate CO_2 EOR and storage capacity and to quantify the distribution of CO_2 in the subsurface. The average porosity and permeability were 16% and 192×10^{-12} cm^2 (19.5 mD) from the normalized SP values and core analyses.

At the time of site selection, the field was under secondary recovery through water injection. A water injection well surrounded by four nearby producing wells was converted to CO_2 injection, and several additional production and observation wells were instrumented to collect temperature and pressure response information. The CO_2 injection period lasted from May 13, 2009, through May 26, 2010, during which time 6,560 tonnes (7,230 tons) of CO_2 were injected into the Jackson oil reservoir. One year of monitoring followed the CO_2 injection period; during this time the CO_2 injection well was returned to water injection. The CO_2 injection rates generally ranged from 18.2 to 27.3 tonnes (20 to 30 tons) per day. Bottomhole injection pressures remained close to 13 MPag (1,900 psig), but gradually decreased throughout injection. Injection of CO_2 was interrupted three times during the period from May 13 through August 20, 2009, because of leaks in the line that supplied CO_2 to the injection well. Winter road conditions that made CO_2 delivery impossible brought a halt to injection from December 27, 2009 to January 25, 2010. Injection was also interrupted from February 3 through February 21, 2010, when another leak developed in the line between the main CO_2 pump and the injection well. The first CO_2 injection line leak was used as an opportunity to test the performance of several near-surface MVA monitoring techniques. Notably, hyperspectral imagery was found to be ineffective in this case due to short leak duration and the inability to directly detect CO_2.

Pressure changes and elevated CO_2 levels in response to injection (breakthrough) occurred at five production wells during the one-year CO_2 injection period, all within the first five months. The first breakthrough occurred one week after commencement of CO_2 injection, which was sooner than expected based on modeling; this difference was attributed to a previously undetected high permeability geologic feature such as a fracture network. Breakthrough did not occur at several wells to the east and south of the injection well, suggesting that a portion of the field was not in communication with the injector.

Monitoring, verification, and accounting (MVA) strategies for the pilot study included (1) developing and implementing a health and safety plan; (2) monitoring air quality at strategic locations to ensure human safety during CO_2 transfer and injection operations; (3) monitoring volumes and rates of CO_2 injection; (4) monitoring the quality of shallow groundwater before, during, and after CO_2 injection and modeling of potential CO_2-rock-water interactions; (5) monitoring volumes and chemical properties of produced oil, gas, and water before, during, and after CO_2 injection; and (6) monitoring surface and subsurface CO_2 injection pressures and temperatures.

The collection and analysis of aqueous and gas chemistry data allowed the inference of reservoir characteristics and, to some degree, the fate of CO_2 in the reservoir. Dissolution of CO_2 into the reservoir brine in the Jackson sandstone caused pH to decrease by one pH unit from approximately 6.8 to 5.8. For some wells, the pH decrease occurred before the arrival of free-phase CO_2, indicating rapid dissolution of CO_2

into brine. The CO_2 dissolution and associated dissociation reactions increased alkalinity and dissolved inorganic carbon, indicating some solubility trapping of CO_2. Increased concentrations of Ca^{2+}, Mg^{2+}, and Fe^{2+} in the reservoir brines during and after CO_2 injection indicated that dissolution of calcite, ankerite, and siderite buffered the pH of the brine. Both $\delta^{13}C$ and ^{14}C were found to be viable tracers of injected CO_2, although ^{14}C was judged to be more effective. The chemical composition of groundwater samples from deep and shallow Pennsylvanian aquifers in and outside of the field did not change over the course of the project and showed that there was no leakage of injected CO_2 into the groundwater system.

A simplified model of the surficial groundwater aquifer was used to find the groundwater flow direction and to determine whether, in the event of a leak, CO_2 released into the shallow groundwater would escape from the site in 100 years. The model showed that in the absence of heavy groundwater pumpage, any CO_2 released into the groundwater would not escape the boundaries of the test site. However, particle tracking showed that a well located 518 m (1,700 ft) west of the injection well, which is currently pumped at a rate of 91,000 L (24,000 gallons) per day, would capture all the CO_2 leaked if pumping continued at that rate.

The mixing of injection freshwater from waterflooding with reservoir brines buffered geochemical changes and complicated (but did not preclude) efforts to identify isotopic responses to CO_2 injection. Interpretation and analyses of the MVA-related data concluded that there were no indications that the injected CO_2 was present in a geologic formation above the Jackson sandstone reservoir.

An estimated 1,028 tonnes (1,133 tons) of CO_2 were produced at the surface from wells and the gas separator between the start of CO_2 injection and the end of September 2011. This amount represented about 16% of the injected CO_2. Exact measurement of CO_2 production proved problematic due to technical concerns. Consequently, 84% of the injected CO_2 was stored at the Sugar Creek field after one year of post-CO_2 injection monitoring.

Project improved oil recovery (IOR) was estimated at 1,574 m^3 (9,900 bbls) and CO_2 EOR as 429–509 m^3 (2,700–3,200 bbl), although estimation of an EOR baseline was difficult because recovery was also increased by pre-project well work. These figures would have been higher if not for variations in oil production rate due to operational problems. Oil production rates did not return to the pre-shut-in level after the lengthy winter injection hiatuses, but they remained elevated relative to production rates immediately before the pilot.

The pilot was designed to measure and record data which could be used to calibrate a reservoir simulation model of the Jackson sandstone to project CO_2 storage and EOR potential of a larger-scale project at the field. A model calibrated to field data (including geologic data and oil and water production) was used to assess the full-field CO_2 storage and EOR potential at the Sugar Creek Field. Projections based on these models indicated that full field CO_2 injection for 20 years could have 5.5% incremental oil recovery or 27,700 scm (174,000 stb), with a CO_2 net utilization of 160 scm/scm (880 scf/bbl). The potential CO_2 storage is estimated to be 5,200 to 9,500 tonnes (5,800 to 10,500 tons). At lower reservoir pressure, less CO_2 can be stored.

CONTENTS

CONTRIBUTORS IV
ACKNOWLEDGMENTS V
ABSTRACT VI
EXECUTIVE SUMMARY VII
INTRODUCTION 1
Midwest Geological Sequestration Consortium Background 1
MGSC Phase I Illinois Basin Oil Reservoir Assessment Summary 1
Phase II Enhanced Oil Recovery Pilot Objectives 2
Site Screening: General Pilot Requirements 2
CO_2 Flood Classification 2
Operation and Development History 2
Surface Conditions 2
Wellbore Conditions 4
Geological and Reservoir Modeling 4
SITE SELECTION 4
Oil Characteristics and Geology 4
Geographic Description of Site Location 5
Site Logistics 5
FIELD HISTORY 8
Original Oil in Place and Wells 8
Field Development 11
Available Geologic and Production Data 18
Well Completion Data 18
Cumulative Production and Injection Maps 21
Tank Battery and Flow Lines 23
Brine Injection Equipment and Injection Lines 24
PILOT SITE DESIGN AND WELL ARRANGEMENT 25
Returning Wells to Production 25
Observation Wells 25
Well Preparation 26
Tank Battery Adaptations 26
Chemical Corrosion Treatment Plan 28
Pre-injection Reservoir Modeling 28
CO_2 UIC II Injection Permit 32
GEOLOGICAL CHARACTERIZATION 32
Area Geology 32
Surface Geology 32
Bedrock 32
General Site Hydrology and Hydrogeology 32
Hydrology 32
Hydrogeology 32
Reservoir Geology 37
Core Analyses 37
Log Analyses 37
Conceptual Geologic Model 37
Geocellular Model 44

MVA STRATEGIES AND METHODS 46
Objectives 46
Sampling Priorities 46
Health and Human Safety 46
Sampling Strategies 51
Design of a Groundwater Monitoring System for the Injection Site 51
Well Locations 51
Frequency of Brine Sampling 51
Sample Types 52
Groundwater 52
Brine 53
Gas 55
Sample Analysis Procedures 56
Brine Chemistry 57
Isotopes 59
X-ray Diffraction and Jackson Mineralogy 60
Baseline Data 60
Geologic Data 60
Pre-injection Chemistry and Characterization of Jackson Brine and Associated Gas 61
Bulk and Isotopic Chemistry 61
Gas Chemistry 61
Pre-injection Chemistry of Pennsylvanian Groundwater 62
Hydrogeologic Data from the Drilling and Monitoring Well Installation 65
Kinetic Modeling 70
Cased Hole Logging 77
FIELD OPERATIONS DURING CO_2 INJECTION 77
CO_2 Pumping Equipment 77
Overview 77
Portable Storage Tanks 78
Booster Pump 78
Main CO_2 Pump 80
Automated Injection-Pressure Control System 80
Flow Meters 83
Liquid Turbine 83
Vortex Meter 83
In-Line Heater 83
Data Acquisition 83
Pressure and Temperature Sensors 83
Data Transmission 85
Wellhead Design 85
Injection Well 85
Production Wells 85
Monitoring Wells PZ-1, PB-3, and JR-1 90
General Operations 90
Operational Challenges 90
Scheduling CO_2 Delivery 90
Line Heater Detonation 90
Metering CO_2 92

Liquid Turbine Meter 92
Vortex Meter 92
Flow Line Breaches 92
Corrosion Treatment and Well Workover Frequency 92
FIELD OBSERVATIONS DURING ACTIVE CO_2 INJECTION 95
Overview 95
Injection Schedule at Well RG-5 96
CO_2 Injection 96
Post-CO_2 Water Injection 98
Pilot Area's Oil, Gas, and Water Production and Pressure Response 99
Oil Production Field Data 100
Flat oil rate baseline 100
Decline oil rate baseline 102
Water Production Field Data 102
Oil Producing Wells' Rate (Oil, Gas, and Water) and Pressure Responses 102
Ross Gentry #1 104
Surface casing gas pressure 104
Casing gas composition 104
Casing gas production rate 104
Allocated oil and water production 105
Ross Gentry #2 105
Surface casing gas and downhole pressure 105
Casing gas composition 106
Casing gas production rate 106
Allocated oil and water production 106
Ross Gentry #3 107
Surface casing gas pressure 107
Casing gas composition 108
Casing gas production rate 108
Allocated oil and water production 108
Ross Gentry #4 109
Surface casing gas pressure 109
Casing gas composition 110
Casing gas production rate 110
Allocated oil and water production 110
Pressley-Hart #1 110
Surface casing gas and downhole pressure 110
Casing gas composition 110
Casing gas production rate 111
Allocated oil and water production 111
Wilbur-Todd #4, #8, and #9 112
Surface casing gas pressure 112
Casing gas composition 112
Casing gas production rate 112
Allocated oil and water production 112

Observation Well Responses 114
Pressley-Zogg #1 114
Peter Bowles #3 114
J Rickard #1 115
Ross Gentry #2 115
Water Injection Outside of CO_2 Injection Pilot Area 115
MVA OBSERVATIONS AND INTERPRETATIONS 116
Jackson Sandstone Geochemistry and Sampling Results 116
Jackson Brine and Associated Gas—Response to CO_2 Injection 116
pH 117
Alkalinity and Dissolved Inorganic Carbon 119
Brine Composition (Dissolved Constituents) 120
Ca^{2+} 120
Mg^{2+} and Fe^{2+} 122
Silica (Si) 124
K^+ 125
Isotopic Response of Jackson Brine and Associated Gas to CO_2 Injection 125
Gas Measurements ($\delta^{13}C$-CO_2 and ^{14}C-CO_2) 127
Aqueous Measurements ($\delta^{34}S$-SO_4, $\delta^{18}O$-SO_4, $\delta^{18}O$-H_2O, $\delta^{13}C$-DIC, ^{14}C-DIC) 130
Pennsylvanian Groundwater—Bulk and Isotopic Response to CO_2 Injection 138
Geochemistry and Sampling Results: Interpretation and Discussion 141
Salinity and CO_2 141
Pre-injection Data 141
Active CO_2 Injection Data 142
PH-1 142
WT-9 142
CO_2 Breakthrough Time and Relative Velocity 143
Mineral Dissolution 143
pH 146
Cations 146
Geochemistry Summary 146
Cased Hole Logging 147
Soil Gas Work in Response to Line Leak 147
CO_2 SEQUESTRATION AND ENHANCED OIL RECOVERY: INTERPRETATION, ANALYSIS AND RESERVOIR MODELING 150
Sugar Creek Pilot Area Reservoir Model Calibration 150
Description of the Geologic and Reservoir Models and Input Parameters 150
Description of the Calibrated Model 154
Primary Recovery 154
Waterflood Recovery 154
CO_2 Pilot 157
Explanation of Field Observations During CO_2 Injection 157
Early Gas Breakthrough at RG-2 157
No Gas Breakthrough at WT-4, 8, and 9 157

Pilot Projections Using Calibrated Model to Determine CO_2 Enhanced Oil Recovery, Storage, and Plume Size Distribution 157
Pilot Case 1: Continuous Production at RG-2 and PH-1 and Continuous Injection at Maximum Pressure at RG-5 161
Pilot Case 2: Continuous Injection of CO_2 for 5 Years with Pilot Case 1 Approach 161
Full-Field Projections Using Calibrated Model to Determine CO_2 Enhanced Recovery, Storage, and Plume Size Distribution 162
Field Case 1: Full-Field CO_2 Injection 162
Field Case 2: Modified Full-Field CO_2 Injection 162
Field Case 3: Infill Drilling and 5-spot Pattern Full-Field CO_2 Injection 162
Modeling Summary 163
PILOT CLOSURE 164
Plugging and Abandonment of Groundwater Monitoring Wells 164
Removal of Data Acquisition Equipment 164
Relocation of Injection Equipment 164
CONCLUSIONS 164
Enhanced Oil Recovery Estimate 164
CO_2 Storage Estimate 165
General Observations 165
Effectiveness of Operations 165
Effectiveness of Techniques for Monitoring, Verification, and Accounting 165
RECOMMENDATIONS 166
REFERENCES 166

APPENDICES
1 Injection permit 169
2 Drillers' logs. 179
3 Information on monitoring wells. 205
4 X-ray diffraction data. 206
5 Jackson brine properties. 207
6 Gas composition from production wells prior to breakthrough. 209
7 Pennsylvanian groundwater properties. 210
8 Jackson brine cation and anion concentrations. 211
9 Pennsylvanian groundwater cation and anion concentrations. 212
10 Interpretation of Reservoir Saturation Tool logging data. 213
11 Equipment specifications. 225
12 Gas production calculations. 226
13 Schematics of data acquisition equipment. 227
14 Timeline of events. 228
15 Water injection rates. 232
16 Casing gas production data. 233
17 Isotopic composition of gas phase hydrocarbons from production wells. 234

LIST OF TABLES
1 Reservoir test configuration wells for Sugar Creek Field, including well lease name, number, and abbreviation, well type, and date drilled. 10
2 Waterflood/CO_2 injection periods by well. Only RG-5 water injection rates were available through 2011; all other injection well data is through 2010. 12

3 Production history by well. At the time of this report, rate allocated well production data was available by well only through end of December 2010. 17
4 Summary of well completions data for Sugar Creek Field. 20
5 Oil and gas wells located within a 0.8-km (0.5-mi) radius of the injection well, RG-5. Permit numbers and other records are from the KGS oil and gas online database. 35
6 Hydrogeologic descriptions taken from drillers' logs listed in Table 5-1. The volume of a bailer is approximately 160 L (42 gallons). Permit numbers and other records are from the KGS oil and gas online database (http://kgs.uky.edu/kgsweb/DataSearching/OilGas/OGSearch.asp). 36
7 Summary of number of samples collected from monitoring wells and wells from which brine and groundwater samples were collected at different time periods. The list also includes the tank battery, TB-1. 52
8 Summary of the number of gas samples and IRGA measurements collected from each well. "Top of carboy" refers to gas measurements or samples collected during brine sampling from the headspace at the top of the carboy as well as fluids cycled through it. All other measurements and samples were collected at the surface from the casing-tubing annulus of the well. 55
9 Summary of field preservation and laboratory measurement techniques for brine and groundwater samples. Details of methods can be accessed at the websites for the Environmental Protection Agency (EPA, http://water.epa.gov/scitech/methods/) and the American Society for Testing and Materials (ASTM, http://www.astm.org/Standard/index.shtml). 56
10 Summary statistics for charge imbalances in samples of the Mississippian Jackson sandstone brines and Pennsylvanian groundwater. 57
11 Relative percent difference (RPD) between KGS and ISGS laboratories for select brine analytes. 58
12 Comparison of brine measurements among ISGS and KGS laboratories and an anonymous commercial lab to a brine standard developed by ERA. 59
13 Mean annual flow for streams in the study area. 67
14 Input parameters for GFLOW. 69
15 Comparison of predicted and observed values with and without active (pumping) groundwater wells. 70
16 Initial brine composition for the batch reaction model, based on the brine sample collected at RG-5. Elemental composition is in milligrams per liter. CO_2 was constrained by setting the initial solution to be in equilibrium with calcite. 74
17 Average mineralogical composition (%) adapted from XRD analysis of reservoir samples near RG-5. 74
18 Breakthrough dates as indicated by pressure response and significant increase in CO_2 concentration in gas samples. 95
19 Waterflood and CO_2 flood breakthrough time and associated rates. Rates are in barrels per day (calculated from monthly production) and concentration is in percent. 101
20 Average daily oil production in 2009 prior to CO_2 injection. 101
21 Isotopic composition of dissolved sulfate from production wells at Sugar Creek. 133
22 Estimated CO_2 migration velocities and the number of elapsed days between CO_2 breakthrough (as indicated by gas composition; see Table 8-1) and documented decreases in pH or cation increases. Negative and positive numbers refer to time before and after breakthrough, respectively. 144

23 Pre-CO_2 saturation indices (Q/K) for some minerals in Jackson sandstone brines having intermediate and high salinities calculated using Geochemist's Workbench (Schumacher, 2010). Inputs included brine chemistry measurements and CO_2 fugacities from CO_2 casing gas concentrations. The input reservoir temperature was 29°C (84°F), and the brine was assumed to be saturated with CH_4. 145
24 Soil temperatures (ºC) from the mornings of July 7 and July 8, 2009. Compass directions indicate locations where temperature was measured relative to hole. Temperatures inside the hole were on the order of −0.2°C (31.6°F), and ambient temperatures ranged from 26.2ºC (79.3ºF) to 31.5ºC (88.7ºF) during soil temperature measurements. 147
25 Mole fractions of the pseudo-components used in the five-component EOS to match crude oil properties at Sugar Creek. 152
26 Reservoir brine and rock parameters. 152
27 Saturation and relative permeability end points. 154
28 Enhanced oil recovery and CO_2 utilization for optimized pilot cases. 161
29 EOR and CO_2 utilization for optimized fieldwide cases. 163

LIST OF FIGURES

1 Potential enhanced oil recovery (EOR) resources in the Illinois Basin, mapped by oil field (from Midwest Geological Sequestration Consortium, 2005). 3
2 Location of Sugar Creek oil field relative to the nearest town and city (Earlington and Madisonville, KY) and other oil fields. 6
3 Aerial photograph of the northern portion of Sugar Creek oil field where the CO_2 pilot was conducted. Locations of wells and tank battery and general location of buried injection line are shown. Sugar Creek Road crosses the lower right corner of this map. 7
4 The tank battery at Sugar Creek, including tanks and pump house. Tanks are to the left, and the pump house is to the right. The oil-water separator and brine tanks are in the middle. 8
5 Isopach map used to estimate the bulk volume of sand in acre-feet for OOIP calculation (courtesy of Gallagher Drilling, Inc.). 9
6 Map of the well locations and the lease boundaries. The well names are in regular font while the lease names are in bold. The model area is encompassed by the red square. The tank battery is identified by a small, cross-hatched square at a bend in Sugar Creek Road. 10
7 Annual oil production from Sugar Creek Field for the entire history of the field (through December 4, 2011), including primary production, waterflooding, and CO_2 injection. Production data were not available for 1991 or 1992. 11
8 Monthly water injection averaged daily (bwpd) for each well (primary axis) and for Sugar Creek Field (secondary axis) during the waterflooding period, December 1992 to December 2010. (One outlying data point is not visible on the map: 238.71 bwpd at RW-2 in January 1998.) 13
9 Monthly oil production rates for Sugar Creek Field during the waterflooding period, December 1992–May 12, 2009, average barrels per day. 13
10a Monthly oil production averaged daily (bopd) at the Ross-Gentry wells (RG-1, RG-2, RG-3, RG-4) for the period from December 1992 through December 2010. 14
10b Monthly oil production averaged daily (bopd) at the Wilbur-Todd wells (WT-4, WT-6, WT-8, WT-9) for the period from December 1992 through December 2010. 15

10c Monthly oil production averaged daily (bopd) for Pressley-Hart #1 (PH-1), Pressley-Zogg #1(PZ-1), Peter Bowles #3 (PB-3), and J.C. Rickard #1 (JR-1) for the period from December 1992 through December 2010. 16
10d Monthly oil production averaged daily (bopd) for Mary Stanhope #1 and #3 (MS-1, MS-2), Bernice Marquess #1 (BM-1), E.O. Laffoon #1 (EL-1), and Albert Babb #2 (AB-2) (Sugar Creek Field wells outside the pilot area) for the period from December 1992 through February 2009. (There was no production at any of these wells from March 2009 through December 2010.) 16
11 Oil production for the field through the end of secondary production (waterflooding). Daily oil rates are based on annual oil production during primary production (1964–1992) and monthly oil production from 1992 to May 12, 2009 (the day preceding commencement of CO_2 injection). 18
12 Wellbore schematic of a typical Sugar Creek production well (courtesy of Gallagher Drilling, Inc.). 19
13 Sugar Creek lease map showing cumulative primary oil production (barrels) by lease. 21
14 Sugar Creek oil and water production and water injection bubble map for the waterflooding period, by well. Brown circles around individual wells (with black numbers above the well symbol) represent cumulative oil production at each well from December 1992–May 12, 2009. Dark blue circles around producing wells (with dark blue numbers to the right of the well symbol) represent the cumulative water production for the same time period. Light blue circles around injection wells (with numbers in blue type) indicate cumulative water injection from December 1992–May 12, 2009. Larger bubbles indicate higher total production or injection. Bubbles are overlapping circles, not concentric rings; each is measured from the center of the circle. Bubbles indicating injection volumes are at a different scale than production bubbles. All numbers are in thousands of barrels. 22
15 Top of the "gun barrel" oil-water separator at Sugar Creek Field tank battery. The separator is in the center of the photo. The top of an oil tank is in the foreground, and the two brine tanks are behind the separator. 23
16 Well and pump controls in the Sugar Creek pump house. The four gauges (bottom row, red boxes with circular displays) regulate pressure and water levels in the injection pump, water supply well, and water tank. The three red boxes in the top row contain electronic motor controllers. 24
17 Downhole assembly (courtesy of Gallagher Drilling, Inc.). 27
18 Partial view of surface wellhead at RG-4; gas meter is visible (short aluminum pipe at lower left). 27
19 Baker SPD inline choke valve used to regulate gas pressure and temporarily shut-in well during routine gas sampling. 27
20a Liquid-gas separator (left) with back-pressure regulator (center right) and Siemens pressure transducer (blue cap to right). 29
20b Electronic Siemens pressure gauge (blue cap) and Teledyne Merla orifice well tester (aluminum pipe to right) attached to the liquid-gas separator (out of picture, at left) at tank battery. 29
21 Wellhead at well RG-3; the batch chemical corrosion treatment pot is visible. Top photograph: Treatment pot is tall cylindrical object on far left of wellhead, to left of pumpjack, in front of pole. Bottom photograph: Close-up of treatment pot. 30
22 Texsteam chemical injection pump (green box) and chemical box (stainless steel) at RG-4 well. 31

23 Map of oil and gas wells located within a 0.8-km (0.5-mile) radius of the injection well RG-5 (red circle); water wells in the area; and wells that yielded rock samples for x-ray diffraction. Bedrock geology of the area is also shown. 33
24 Map showing the topography and hydrology of the Sugar Creek Field area, including all shallow groundwater wells, ponds, and creeks. 34
25 Structure map of the top of the Jackson sandstone. The blue dashed rectangle marks the boundaries of the geocellular model. The red lines and letters mark the traces of the cross sections in Figures 28 and 29. 38
26 Map of the gross Jackson sandstone. The white rectangle marks the boundaries of the geocellular model, and the pink rectangle contains the injection well and the five closest producing wells. 39
27 Isopach map of the Jackson sandstone showing the thickness of the 50% or greater clean sandstone. The white rectangle marks the boundaries of the geocellular model, and the pink rectangle contains the injection well and the five closest producing wells. 40
28 A north-to-south geophysical log cross section showing the unit of interest, the Jackson sandstone, and a reference unit, the Golconda Formation. The upper figure is a structural view, and the lower figure is a stratigraphic view with the Golconda serving as the origin. The top and base of the Jackson are marked by the red lines, and the base of the Golconda is marked by the green line. The boundary between the upper and lower units of the Jackson sandstone is marked by the thick black line. Abbreviation: KB, kelly bushing, a piece of equipment above ground elevation from which depth is measured. See Figure 5-3 for the location of the cross section. 41
29 A west-to-east geophysical log cross section showing the unit of interest, the Jackson Sandstone, and a reference unit, the Golconda Formation. The upper figure is a structural view, and the lower figure is a stratigraphic view with the Golconda serving as the origin. The top and base of the Jackson are marked by the red lines, and the base of the Golconda is marked by the green line. The boundary between the upper and lower units of the Jackson sandstone is marked by the thick black line. Abbreviation: KB, kelly bushing. See Figure 5-3 for the location of the cross section. 42
30 Isopach map of the lower portion of the Jackson sandstone showing the thickness of the 50% or greater clean sandstone. The white rectangle marks the boundaries of the geocellular model, and the pink rectangle contains the injection well and the five closest producing wells. 43
31 Variogram map (top) and variogram with the fitted models (bottom). The variogram map indicates a strong northeast-southwest anisotropy. However, there appears to be a secondary direction at 140° southeast-northwest, which could be the result of geometry of the sandstone shoals seen in the isopach map in Figure 5-8. In the top figure, the corresponding variograms calculated in the two directions are represented by the erratic, lighter lines, and the models are the smoother, darker lines. The number of pairs of data at each lag is represented by the histogram in the lower part of the top figure. The sill is the dashed horizontal line at 0.96. The range of the variogram model in the direction of maximum continuity (red line) was 1,372 m (4,500 ft). The range of the variogram model in the direction of minimum continuity (green line) was 1,067 m (3,500 ft). 45
32 Graphs illustrating the transforms created to convert normalized spontaneous potential (SP) data into permeability (top) and permeability into porosity (bottom). The data were derived from sidewall core analyses and geophysical log records. Data were first plotted on the graph, and then a curve was best fitted to the data regression techniques. 47

33 Images of the three-dimensional geocellular model. The top image shows the outline of the reservoir within the Jackson sandstone when a porosity cutoff is applied to the model. In the bottom image, the original isopach is overlain as a transparency to demonstrate the agreement between the original geologic model and the geocellular model. Except for a small discrepancy in the south due to poor data control, the two models match very well. Note that the geocellular model captures the northern part of the reservoir that is water-saturated. This area is not included in the original isopach. 47
34 North-to-south cross sections showing the distribution of permeability (top two images) and porosity (bottom two images). The cross sections are in structural space and stratigraphic space with the top of the Jackson sandstone serving as the origin. The injection well is marked in red. The trace of the cross section is shown as a green line on the map at the bottom of the figure. 48
35 West-to-east cross sections showing the distribution of permeability (top two images) and porosity (bottom two images). The cross sections are in structural space and stratigraphic space with the top of the Jackson sandstone serving as the origin. The trace of the cross section is shown as a green line on the map. 49
36 Planar slices through the geocellular model. The upper and lower two images are taken at depths of 1.8 and 3.4 m (6 and 11 ft), respectively, below the top of the Jackson sandstone. Images on the left show the distribution of permeability; images on the right show the distribution of porosity. The injection well, RG-5, is marked by a gold star. All images are taken from the geocellular model projected stratigraphically using the top of the Jackson sandstone as the origin. 50
37 Brine sampling apparatus. Critical components include the carboy and pre-filter (not visible) for separating oil from the brine; the flow-through cell that contains the probes for measuring pH, redox potential , temperature, dissolved oxygen, and conductivity; and the YSI data logger connected to the probe. The assembly is connected to the wellhead via ¼-inch Tygon tubing that connects to the top of the carboy. 54
38 Piper plot of Jackson brines prior to CO_2 injection shows that they are rich in NaCl. Water injected back into the Jackson reservoir (i.e., make-up water) consists of Jackson brine produced during oil production and dilute Pennsylvanian water from WT-3. The WT-3 water, in contrast, is rich in $NaHCO_3$. Variable mixing and communication in the Jackson reservoir has produced brine of intermediate salinity (“J”) that represent mixtures of saline Jackson (“I”) and dilute Pennsylvanian (“K”) waters. 62
39 Stiff plots for wells RG-4, RG-3, PH-1, and WT-3. The NaCl-rich samples from RG-4, RG-3, and PH-1 demonstrate the variation in Jackson brine salinity, expressed as milliequivalents per kilogram, before CO_2 injection. Intermediate salinities occur in RG-4 and RG-3, and high salinities occur in PH-1 (note scale difference). Pennsylvanian groundwater from WT-3 is rich in $NaHCO_3$ and even more dilute. 63
40 Sodium and chloride concentrations of Jackson brines from production wells and dilute Pennsylvanian groundwater from WT-3 before CO_2 injection. The distribution suggests that formation waters in the RG and WT-9 wells represent a composite formed by linear mixing between dilute WT-3 water and more saline water from PH-1 and WT-4. Moreover, lever-rule relationships suggest that dilute WT-3 water makes up 50% or more of the formation water in the RG and WT-9 wells. Comparison with regional brine data suggests that WT-4 and PH-1 waters are similar in composition to Mississippian-age formation waters that were not affected by waterflooding or other human influences. 63

41 Graphs showing how air contamination affected the concentration of hydrocarbons (C_1 to C_6) in the production wells. Air is represented by the sum of O_2+N_2 concentrations for samples prior to the day of CO_2 injection at the Sugar Creek site. 64
42 Concentration of CO_2 in the production wells leading up to and immediately preceding the day of CO_2 injection at the Sugar Creek site.Vertical dashed line indicates the day that CO_2 injection started (May 13, 2009). 65
43 Concentrations of CO_2 and (O_2 + N_2) for production wells RG-1, RG-2, and RG-3 during the initial weeks prior to CO_2 injection at the Sugar Creek site. Graphs show how contamination of air diluted the concentration of CO_2 observed in the gas sample bags. Duplicate samples were taken at RG-2 on April 8, 2009. 66
44 Stiff plots showing compositional diversity of shallow Pennsylvanian groundwater before CO_2 injection at wells DC-1 and KB-1, RG4-MW and RG5-MW, and PH-1MW. Solute concentration is expressed as milliequivalents per liter. 67
45 Map of study site and surrounding area. Streams are shown in brown and dark green. Roads appear as green linear features, while railroads are mustard color linear features. The olive-green colored polygons depict wetlands. A monitoring well is located at the study site. Test points for the model (streamflow) are depicted with turquoise markers along Clear Creek. The turquoise dashed lines are intermittent streams. 68
46 GFLOW output for the Clear Creek area. The estimated groundwater heads are contoured using dashed blue lines and have a 3-m (10-ft) contour interval. In the vicinity of the study site (green triangle) a northwest-southeast-trending groundwater divide is present. 71
47 GFLOW output for the Clear Creek area showing particle tracking for 100 years (no groundwater pumping). The 49 particles were included in the analysis, and are illustrated by the red points and attached lines near the study site. Contour interval is 3 m (10 ft). Black dashed lines are equipotential lines. 72
48 GFLOW output for the Clear Creek area showing particle tracking for 100 years with groundwater pumping from two local wells. The 49 particles were included in the analysis, and are illustrated by the red points and attached lines near the study site. Contour interval is 3 m (10 ft). Black dashed lines are equipotential lines. 73
49 Changes in mineralogical composition as the reservoir rock reacts with acidified brine. 75
50 Evolution of pH as the acidified brine reacts with the reservoir minerals. The initial value is buffered by calcite dissolution, followed by the precipitation and dissolution of clays. 75
51 Total amount of CO_2 sequestered in the brine and calcite. 76
52 Calcium carbonate equilibria of Ross Gentry #3 (RG-3) and Wilbur Todd #9 (WT-9) observation wells at Sugar Creek Field. Groundwater samples collected at RG-3 were supersaturated with respect to calcium carbonate before break-through at RG-2. Well WT-9 appeared to be unaffected. The chemical composition of the groundwater samples was input to the geochemical model PHREEQCi (version 2.15.0). Negative values indicate the number of days before CO_2 injection began. 76
53 The CO_2 injection pump skid and instrument diagram. 79

54 Booster pump (frosted over) and motor. Manual temperature gauge (circular object at center), Siemens pressure gauge (just above and to the left of manual gauge; blue cover), and temperature probe (largely obscured behind Siemens gauge; base visible to immediate right of stem of Siemens gauge). Lines are covered with neoprene pipe insulation. (Photograph courtesy of Trimeric Corp.) 80
55 Triplex pump in operation at the EOR II site (a photograph of the specific triplex pump used at Sugar Creek was not available) with input and output lines and valves (frosted over in foreground). The gray motor (center) is behind the blue pump crankcase. The storage tank is in the background. Aluminum housing covers the belt and pulleys between the motor and pump crankcase. (Photograph courtesy of Trimeric Corp.) 81
56 Globe Cast pressure control valve (BadgerMeter, Inc.) on the return line between the discharge of the main pump and storage tank. The electric actuator is shown top center (red base and equipment sitting on red base; the latter is usually covered in a red casing under operational conditions). The valve is below the actuator covered with black neoprene and gray duct tape. (Photograph courtesy of Trimeric Corp.) 82
57 Omega pressure controller panel cover and housing with pressure reading shown. (Photograph courtesy of Trimeric Corp.) 82
58 Cameron NuFlo liquid turbine meter (center left) and Sierra vortex flow meter (center, red) in series on frosted line. Front of inline heater is shown in upper left background. Pump discharge is shown frosted over in lower right. (Photograph courtesy of Trimeric Corp.) 84
59 Natco line heater (105,520 kJ/hr [100,000 Btu/hr]). Propane tank is shown in the background. Inline heater's CO_2 inlet is frosted over; the top of this line has the Siemens pressure gauge/transmitter that is connected to the Globe Cast pressure control valve. Also shown is the inline heater discharge (lower right) to the RG-5 injection line. (Photograph courtesy of Trimeric Corp.) 84
60 Data acquisition and transmission enclosure at a production well, showing the solar panel, datalogger box, and battery. 86
61 Surface wellhead and related piping of the injection well RG-5. Stainless steel lubricator at the top allowed the cable connected to the downhole pressure and temperature sensors to enter the tubing. 87
62 Photograph of a typical production wellhead, RG-4, at Sugar Creek Field. The schematic is stylized and not to scale. Orifice well tester at lower left in schematic is not visible in the wellhead photograph but can be seen in Figure 4-2. 88
63 Wellhead and data acquisition enclosure at well RG-4. The blue cable that emerges from a gland on the flowing wing of the wellhead and connects to the data acquisition enclosure is connected to the surface pressure gauge in the wellhead. 89
64 Wellhead of monitoring well JR-1 with solar panel, datalogger, and battery. Mechanical pressure gauge immediately above the riser pipe and Siemens gauge (blue face) to right. 91
65 Top graph: Comparison between CO_2 injection rates in tons per day as measured by Sierra vortex meter (SVM, blue line) and liquid turbine meter (LTM, red line). Bottom graph: Comparison between cumulative CO_2 delivered as measured by vendor (black line) and cumulative CO_2 injected (in tons), as metered by SVM (blue line) and LTM (red line). 93
66 Corrosion (top) and pit (bottom) rates at wells PH-1, RG-1, RG-2, RG-3, RG-4, and WT-4 over the life of the pilot project. General corrosion rate and pit rate are presented in mills per year. One outlier is not shown: on December 23, 2009, the corrosion rate measured for PH-1 was 12.6 mills per year. 94

67 The CO_2 injection rates (tons per day) measured by liquid turbine meter (LTM) and Sierra Vortex Meter (SVM) and injection well (RG-5) surface pressure (psig) during the first month of injection, from May 13, 2009, through June 10, 2009. 96
68 The CO_2 injection rates from June 8, 2009 through February 8, 2010 (top graph) and February 9, 2010 through May 26, 2010 (bottom graph). Continuous injection was resumed February 21, 2010 after interruptions due to weather-related delivery failure and line leaks. 97
69 Wells at Sugar Creek Field with CO_2 breakthrough dates shown. Breakthrough date based on pressure response is given first, followed by gas composition breakthrough date in parentheses. (For further discussion, see Table 8-1 and associated text.) Wells with no date shown did not undergo CO_2 breakthrough within the CO_2 injection period (May 13, 2009 through May 26, 2010), although monitoring well PZ-1 underwent a pressure increase attributable to CO_2 in August 2010. (Aerial photograph from Kentucky Geologic Map Information Service website at http://kgs.uky.edu/kgsmap/kgsgeoserver/viewer.asp.) 99
70 Cumulative field oil production by month (bopm) from 1993 to 2010 showing historical production increases and declines. 103
71 Cumulative field oil production by month (bopm) during the pilot project showing the most recent decline. 103
72 Surface pressure (psig), average gas and CO_2 rate (Mscfd), average CO_2 volume percent, and cumulative CO_2 produced (tons) for RG-1 from the beginning of the pilot project (May 2009) to late September 2011. 105
73 Surface and bottomhole pressures at RG-2 from approximately the start of pilot project (May 2009) to late September 2011. 106
74 Pressure at well RG-2 during the period from July–September 2009, showing pressure response to being shut-in on August 16, 2009. 107
75 Surface pressure (psig), average total gas and CO_2 rate (Mscfd), average CO_2 volume percent, and cumulative CO_2 produced (tons) for RG-3 from the beginning of the pilot project (May 2009) to early October 2011. 108
76 Surface pressure (psig), average total gas and CO_2 rates (Mscfd), average CO_2 volume percent, and cumulative CO_2 produced (tons) for RG-4 from the beginning of the pilot project (May 2009) to the end of September 2011. 109
77 Surface pressure (psig), average total gas and CO_2 rates (Mscfd), CO_2 volume percent, and cumulative CO_2 produced (tons) for PH-1 from the beginning of the pilot project (May 2009) through October 2009. Casing gas production data (gas rates, CO_2 volume %, and cumulative CO_2 produced) ends in September because the well was allowed to flow to the surface production flow line. 111
78 Surface pressure (psig), average total and CO_2 gas rates (Mscfd), and cumulative CO_2 produced (tons) for WT-4, WT-8, and WT-9, as well as CO_2 volume percent for WT-4 and WT-8. 113
79 Water injection rates (bwpd) for the pilot period (May 2009 through December 2010). May 2009 rates are average for entire month rather than for injection period (May 13–May 31, 2009) because daily injection rates were not available. 116
80 Infrared gas analyzer determined CO_2 concentrations before, during, and after CO_2 injection from casing gas and liberated gas from brine sampling (via carboy). Star symbols represent CO_2 breakthrough dates. Gray vertical lines designate start and end of CO_2 injection at RG-5. Vertical blue bars designate approximate periods of CO_2 injection shut-in. 117

81 Top: Evolution of pH for wells having large increases in CO_2 during breakthrough (RG-1, RG-2, RG-3, RG-4, and PH-1); bottom: evolution of pH for wells having subtle (WT-9) or no (WT-4) increases in CO_2 levels as determined by infrared gas analyzer. Star symbols represent CO_2 breakthrough dates. Gray vertical lines designate start and end of CO_2 injection at RG-5. Vertical blue bars designate approximate periods of CO_2 injection shut-in. 118

82 Top: Evolution of alkalinity for wells having large increases in CO_2 during breakthrough (RG-1, RG-2, RG-3, RG-4, and PH-1); (b) Evolution of alkalinity for wells having subtle (WT-9) or no (WT-4) increases in CO_2 levels as determined by infrared gas analyzer. Star symbols represent CO_2 breakthrough dates. Gray vertical lines designate start and end of CO_2 injection at RG-5. Vertical blue shaded areas designate approximate periods of CO_2 injection shut-in. 121

83 Evolution of Ca^{2+} before, during, and after CO_2 injection. Star symbols represent CO_2 breakthrough dates. Gray vertical lines designate start and end of CO_2 injection at RG-5. Vertical blue bars designate approximate periods of CO_2 injection shut-in. 122

84 Evolution of Mg^{2+} before, during, and after CO_2 injection. Star symbols represent CO_2 breakthrough dates. Gray vertical lines designate start and end of CO_2 injection at RG-5. Vertical blue bars designate approximate periods of CO_2 injection shut-in. 123

85 Evolution of Fe^{2+} before, during, and after CO_2 injection. Star symbols represent CO_2 breakthrough dates. Gray vertical lines designate start and end of CO_2 injection at RG-5. Vertical blue bars designate approximate periods of CO_2 injection shut-in. 124

86 Evolution of silicon before, during, and after CO_2 injection. Star symbols represent CO_2 breakthrough dates. Gray vertical lines designate start and end of CO_2 injection at RG-5. Vertical blue bars designate approximate periods of CO_2 injection shut-in. 125

87 Evolution of K^+ before, during, and after CO_2 injection. Star symbols represent CO_2 breakthrough dates. Gray vertical lines designate start and end of CO_2 injection at RG-5. Vertical blue bars designate approximate periods of CO_2 injection shut-in. 126

88 2009 CO_2 concentrations over time from gas chromatographic analyses of gas bag samples from various production wells at the Sugar Creek site. The vertical blue-dashed line indicates the startup of CO_2 injection. 127

89 Project CO_2 concentrations over time from gas chromatographic analyses of gas bag samples from various production wells at the Sugar Creek Site. The vertical blue-dashed line indicates the startup of CO_2 injection. 128

90 Carbon isotope ($\delta^{13}C$) composition of CO_2 of gas samples from production wells at Sugar Creek for 2009. The vertical blue-dashed line indicates the startup of CO_2 injection. 128

91 Carbon-14 concentration of CO_2 from various production wells at Sugar Creek Field. Top: concentration in first part of the pilot, from pre-CO_2 injection to November 2009; bottom, concentration over entire pilot, including post-CO_2 water injection period. Note the strong shift in ^{14}C activity of RG-2 and RG-3, which showed the earliest CO_2 breakthrough. Also, the accidental contamination of RG-4 with injection CO_2 is easily observed on the July 8, 2009 sampling event. The vertical blue-dashed line is the startup of CO_2 injection. 129

92 Complete carbon isotope composition ($\delta^{13}C$) of CO_2 of gas samples from production wells at Sugar Creek Field up to December 9, 2011. The vertical blue dashed line is the startup of CO_2 injection, and orange vertical lines indicate beginning and end of major interruptions in CO_2 injection in June and July 2009 and December 2009 through early 2010. 131
93 Carbon isotopic composition ($\delta^{13}C$) of methane from production wells at Sugar Creek Field. Note the steady isotopic composition after the initial degassing effects for most of the wells. 131
94 Isotopic composition ($\delta^{13}C$ and δD) of methane samples from production wells at Sugar Creek Field. 132
95 Carbon isotopic composition of hydrocarbons from Sugar Creek production wells. 132
96 Sulfur and oxygen isotopic composition of dissolved sulfate from brine samples collected at Sugar Creek Field. 133
97 Isotopic composition of water and brine samples from the Sugar Creek site. 134
98 Top: $\delta^{18}O$ of brine samples vs. time from the Sugar Creek site; bottom: δD of brine samples vs. time. 135
99 Top: $\delta^{13}C_{DIC}$ of brine samples that showed impact from injected CO_2. Middle: $\delta^{13}C_{DIC}$ and $\delta^{14}C_{DIC}$ activity of brine samples that showed impact from injected CO_2. Bottom: $\delta^{13}C_{DIC}$ of brine samples for full period of pilot study at Sugar Creek. 137
100 Variation in alkalinity, total CO_2 (TCO_2), dissolved inorganic carbon (DIC), and pH at WT-3. 139
101 Variation in alkalinity, total CO_2 (TCO_2), alkalinity, and dissolved inorganic carbon (DIC) at RG-5MW. 139
102 Top: Oxygen isotopic composition of shallow monitoring well water samples at Sugar Creek vs. time; bottom:$\delta^{13}C_{DIC}$ of shallow monitoring wells, as well as a domestic and livestock well, over time. Orange lines show major interruptions (greater than twenty consecutive days) in CO_2 injection. 140
103 Precipitation and groundwater elevation data from RG-4MW, RG-5MW, and PH-1MW. Precipitation data were recorded at the Hopkins County Mesonet weather station located approximately 8.8 km (5.5 miles) east of injection well RG-5 and downloaded from the Kentucky Mesonet website (http://www.kymesonet.org). 141
104 Evolution of alkalinity (solid lines) and Ca^{2+} concentration (dashed lines) before, during, and after CO_2 injection. Note that the concentration scales for alkalinity (left axis) differ from the Ca^{2+} concentration (right axis). Star symbols represent CO_2 breakthrough dates. Vertical bar designates approximate periods of CO_2 injection shut-in. 144
105 Soil surface expression of CO_2 injection line leak. The hole is surrounded by flux rings. 148
106 Monitoring grid and representative soil CO_2 fluxes during initial conditions on the morning of July 7, 2009 (left; with no injection) and on the afternoon of July 7, 2009 (right; after injection resumed). The central point filled with a plus sign represents the leak location. Abbreviation: IR, infrared. 148
107 Thermal imagery taken at the leak site, showing an ISGS staffer standing near the leak (upper left) and CO_2 escaping from the ground (upper right). Darker areas indicate colder temperatures; the dark area on the right photo (looking directly into the hole) shows the cold CO_2 leaking out. Images at lower left and right are photographs showing comparable views. 149

108 Monitoring grid and representative atmospheric CO_2 concentrations at 2.5 cm above ground level during initial conditions on July 6, 2009 (left; with no injection) and on July 7, 2009 (right; after injection resumed). The central point filled with a plus sign represents the leak location. 151
109 Hyperspectral imagery collected on July 8, 2009, during a monitoring, validation, and accounting (MVA) effort to study and ameliorate a CO_2 leak. The technique proved ineffective at detecting a CO_2 leak of such small size and short duration. The RG-5 site is within the red square. The gray-blue line is the lease road. The top of the figure is south. RG-2 is at the top of the picture at the inflection point in the lease road. 151
110 Porosity of model layer 4 showing grid size and shape of the Sugar Creek reservoir model. 153
111 Initial water-oil and gas-oil relative permeability curves. 153
112 Comparison of simulated values and field data, by lease, for oil production at the end of primary recovery. 155
113 Comparison of simulated values and field data, by well, for oil production at the end of waterflooding. 155
114 Comparison of simulated values and field data, by well, for water production at the end of waterflooding. 156
115 Comparison of simulated cumulative water injected and field data, by well, at the end of waterflooding. 156
116 Simulated and field oil production rate (QOP) and cumulative oil production rate (COP). 158
117 Simulated and field CO_2 injection rates for RG-5. 158
118a The CO_2 distribution in layer 3, displaying largest extent of CO_2 at the end of CO_2 injection. 159
118b The CO_2 distribution in layer 3, displaying largest extent of CO_2 at the end of one year of water injection following one year of CO_2 injection. 159
119a The CO_2 distribution in orthogonal cross-section through RG-5, displaying largest extent of CO_2 at the end of CO_2 injection. 160
119b The CO_2 distribution in orthogonal cross-section through RG-5, displaying largest extent of CO_2 at end of one year of water injection following one year of CO_2 injection. 160
120 Decline curve projections for CO_2 EOR cases. 163

INTRODUCTION

Midwest Geological Sequestration Consortium Background

The Midwest Geological Sequestration Consortium (MGSC) has been assessing the options for geological carbon dioxide (CO_2) storage, also called sequestration, in the 155,400 sq km (60,000 sq mi) Illinois Basin. Within the Basin, which underlies most of Illinois, western Indiana, and western Kentucky, there are deep, uneconomic coal resources, numerous mature oil fields, and deep saline reservoirs potentially capable of storing CO_2. The objective of the assessment is to determine the technical and economic feasibility of using these geological sinks for long-term storage to avoid atmospheric release of CO_2 from fossil fuel combustion at electrical generation facilities and industrial sources.

The MGSC is a consortium of the geological surveys of Illinois (ISGS), Indiana (IGS), and Kentucky (KGS), joined by subcontractors and consultants, to assess carbon capture, transportation, and storage processes and their costs and viability within the three-state Illinois Basin region. The ISGS serves as the lead technical contractor for the MGSC. The Illinois Basin region has annual CO_2 emissions of about 265 million metric tonnes (292 million tons), primarily from 122 coal-fired electric generation facilities, some of which burn almost 4.5 million tonnes/yr (5 million tons/yr) of coal (U.S. Department of Energy, 2010).

Initial MGSC work during 2003–2005, termed the Characterization Phase (Phase I), involved an assessment of carbon capture and transportation options in the region. All available data were compiled on potential CO_2 sinks and on applicable carbon capture approaches. Transportation options focused on small-scale options for field tests and the pipeline requirements for long-term sequestration. Research primarily focused on storage reservoirs in order to assess each of the three geological sinks: coals, oil reservoirs, and saline reservoirs. Results were linked with integrated options for capture, transportation, and geological storage and the environmental and regulatory framework to define sequestration scenarios and potential outcomes for the region. A final task was to generate an action plan for possible technology validation field tests involving CO_2 injection, thus setting the stage for the Validation Phase (Phase II) of the project, which involved small-scale field tests during 2005–2011. A 477-page final report (MGSC, 2005), plus two topical reports on Phase I results are available at www.sequestration.org, the MGSC website.

A key conclusion of the Phase I studies was that the geology of the Illinois Basin is favorable for CO_2 sequestration. In some localities, two or more potential CO_2 sinks are vertically stacked. The primary focus of the Phase II study, however, was the properties of the rock units that control injectability of CO_2, the total storage resources, the safety of injection and storage processes, and the security of the overlying rock units that act as seals for the reservoirs. For Phase II (2005–2011), a series of four small-scale field tests were conducted. They included testing of the ability of a deep, unminable coal seam to adsorb gaseous CO_2 (Frailey et al., 2012b) and the ability to store CO_2 and enhance oil production in mature oil fields (Frailey et al., 2012a). Each of these field tests had an extensive monitoring program for sampling of air, shallow groundwater, and fluids from the injection zone, as well as geophysical and cased hole logging and monitoring of pressure changes to understand the fate of injected CO_2 at our test sites. The integrity of the entire process is being scrutinized in detail to understand the contribution Illinois Basin geological sinks can make to national and international carbon sequestration goals and to determine what technology developed here can be extrapolated to other regions.

MGSC Phase I Illinois Basin Oil Reservoir Assessment Summary

Enhanced oil recovery (EOR) offers the most important economic offset to the costs associated with carbon sequestration in the Illinois Basin. To assess this potential, a Basin-wide EOR assessment was made based on a new understanding of the original-oil-in-place (OOIP) in the Basin, the CO_2 stored volume, the assessed EOR resource, the geographic distribution of EOR potential, and the type of recovery mechanism (miscible vs. immiscible).

With cumulative production for the Basin of about 0.67 billion stock tank cubic meters (scm) or 4.2 billion stock tank barrels (stb), a nearly 1.6 billion scm (10 billion stb) resource remains, primarily as unrecovered resources in known fields. To assess the recovery potential of a part of this resource, and the concurrent stored CO_2 volumes, reservoir modeling and computational simulations were carried out.

The resource target of CO_2 EOR is 140 to 210 million scm (860 to 1,300 million stb) of recoverable oil with resulting sequestered volume of 140 to 440 million tonnes of CO_2 (150 to 490 million tons). The distribution of the unrecovered EOR resource was mapped by field (Figure 1) with larger fields holding multiple reservoirs constituting a larger CO_2 EOR target.

Phase II Enhanced Oil Recovery Pilot Objectives

The purpose of this project was to determine the CO_2 injection and storage capability and the EOR recovery potential of Illinois Basin oil reservoirs. The results of the EOR pilot tests will be compared with the CO_2 storage and EOR estimates made in the Phase I assessment. The prolific oil-producing reservoirs in the Basin, particularly the Mississippian-age Aux Vases and Cypress Sandstones and the Ste. Genevieve Limestone, were the primary interest.

In the DOE Regional Carbon Sequestration Partnership Phase I, about half of the OOIP in the Basin was found to be at depths that would sustain immiscible CO_2 floods. Compared with models of miscible CO_2 floods, reservoir simulations showed oil recovery to be about 50% lower for immiscible floods, but CO_2 net utilization was only 20–35% of the miscible net utilization. In other words, immiscible CO_2 EOR may recover 50% less oil but require 65–80% less CO_2.

For an immiscible flood for reservoirs with temperatures below the critical temperature of CO_2, the reservoir pressure must be below the vapor pressure of pure CO_2. For a pilot project with a limited CO_2 budget, the reservoir pressure cannot be entirely depleted, or there will be inadequate CO_2 to pressurize the reservoir enough to have any significant mixing between CO_2 and the in situ crude oil. Therefore, a current average reservoir pressure of at least 1.7 MPa (250 psi) and preferably 2.1–5.0 MPa (350–700 psi) was desired.

For this pilot, MGSC EOR III, an immiscible flood was planned.

Site Screening: General Pilot Requirements

MGSC solicited oil field operators within the Illinois Basin to nominate geologic formations within oil fields for consideration of a CO_2 EOR pilot. Finding a reputable oil field operator and owner was recognized as a necessity for the EOR pilot projects.

For budgetary reasons and to meet the project timeline, the plan was to convert an existing water injection well to a CO_2 injection well. Consequently, the site screening process was based on an existing water injection well and surrounding wells. A five-tier screening process was used: CO_2 flood classification, operation/development history, surface conditions, wellbore conditions, and geologic/reservoir modeling.

CO_2 Flood Classification

The first tier screening was primarily designed to classify the projected CO_2-crude oil interaction as immiscible-gas, miscible-liquid, or miscible-critical fluid. (A fourth CO_2 flood classification for the pilot tests was for those reservoirs considered too close to the boundary between these three classifications; for pilot purposes only, reservoirs with less certain miscibility classification were avoided.) The screening was primarily based on current reservoir pressure and temperature, API gravity, and geologic formation.

Operation and Development History

The second tier was the number of geologic zones open to the injector, a centrally located injection well preferably surrounded by four existing producing wells. Surface injection pressure, water injection rate (barrels of water per day [bwpd]), and oil/water/gas production at the surrounding wells were considered in this tier.

Surface Conditions

The third tier was surface conditions that could accommodate the injection and data acquisition equipment and CO_2 tank truck delivery. Other surface features considered included proximity to lakes/ponds, floodplains, homes, and major roads, and cooperation of the county and township road commissioners. Early in the application of third-tier screening criteria, it became obvious that the only oil field roads that could withstand semi-trailer tanker truckloads of CO_2 were those roads that led to the oil tank battery (separators

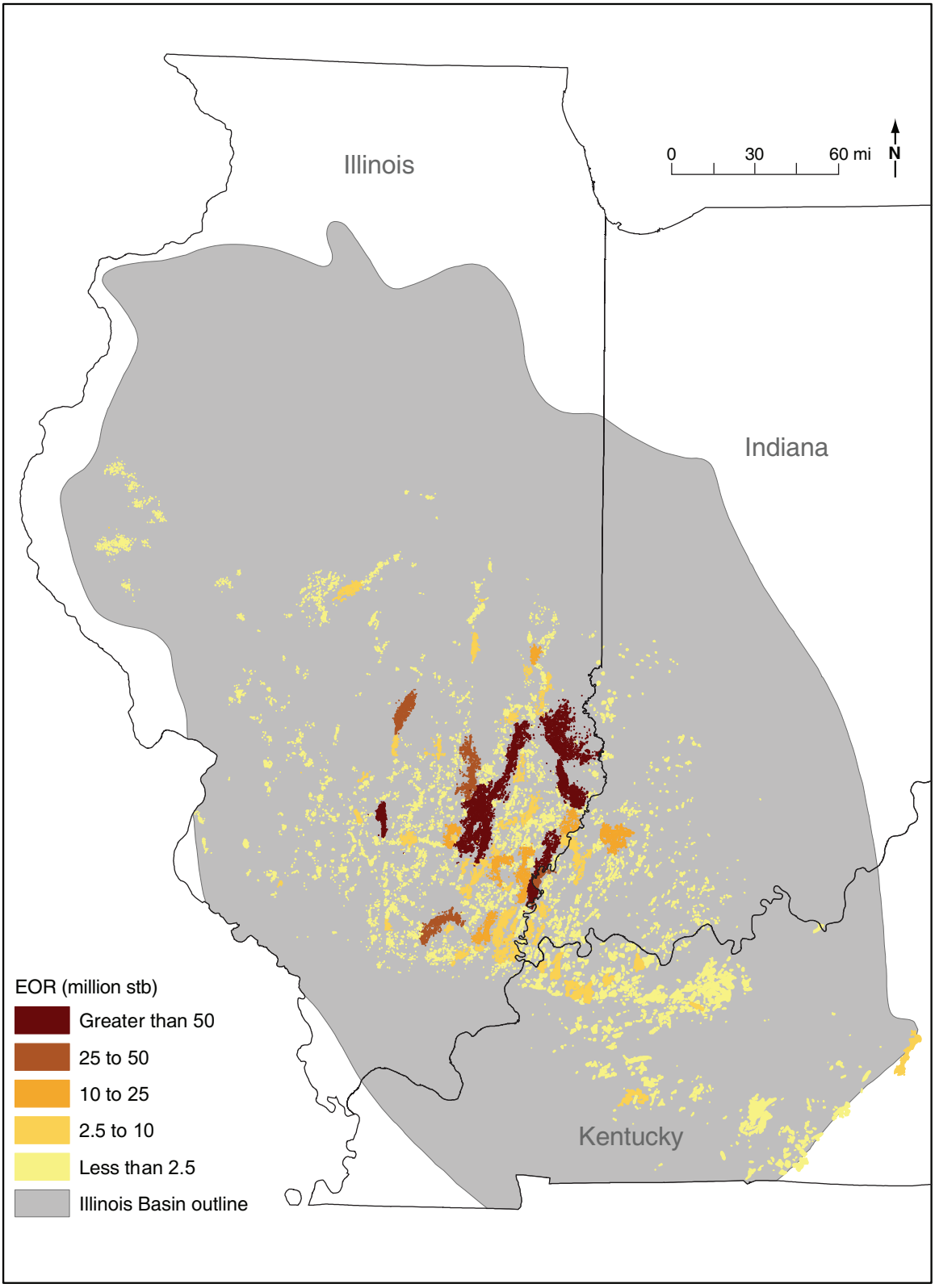

Figure 1 Potential enhanced oil recovery (EOR) resources in the Illinois Basin, mapped by oil field (from Midwest Geological Sequestration Consortium, 2005).

and stock tanks) and had regular pickup of bulk crude oil via semi-trailer tanker trucks. Consequently, areas surrounding the tank battery were considered ideal for locating the surface injection equipment (e.g., CO_2 storage tanks, injection, pumps, and inline heater), and injection wells located near the tank battery were considered better choices for an EOR pilot test.

Wellbore Conditions

The depths of multiple zones currently completed in the injector, and the ability to isolate zones, were considered in the fourth tier. Therefore, the type of completion (e.g., cased and perforated or openhole) was important. Injection pressure history over the most recent few months was reviewed. Workover type and frequency were important in the screening process. The sizes of casing and any casing liners were also important considerations for placement of an injection tubing packer.

Geologic and Reservoir Modeling

The fifth tier was the geologic and reservoir modeling results. More consideration was given to injection patterns and models that would give oil production and pressure results that were measurable and quantifiable within the CO_2 and time budget of the project. It was recognized that direct field data indicating increases in oil recovery were important, but a pilot to estimate EOR directly would likely require at least 2–3 years of injection and multiple injection patterns. Consequently, the CO_2 EOR estimate would be based on a reservoir model calibrated to the measured field results.

SITE SELECTION

This EOR III pilot site was screened to have current reservoir pressure and temperature sufficient to sustain an immiscible flood, but not at depleted pressure. After applying the rigorous EOR site screening criteria, the Sugar Creek oil field in Hopkins County, Kentucky, was chosen. The Sugar Creek Field is owned and operated by Gallagher Drilling, Inc. (GDI), based in Evansville, Indiana.

Using bottomhole pressure of the water injection well and the producing wells, the average pressure in the field was initially estimated at 3.5 MPa (500 psi). The reservoir temperature was found to be 27°C (78°F). The area of the field considered for this pilot produces from a single geologic formation with 28 wells drilled and completed, of which there were four active water injection wells and eight active oil production wells. The chosen CO_2 pilot area was central to the active oil-producing wells in the northern part of the field.

Although several wells in the field were temporarily or permanently abandoned, the oil field had some relatively new wells and no reports of major casing leaks or other production well problems. The site's tank battery had excellent year-round road access, and continuous CO_2 delivery was expected to be possible.

Analyses and interpretations of projections from a simplistic but representative geologic model of the Sugar Creek oil field suggested that the CO_2 injection rates and cumulative injection volume for the pilot design could be achieved in the timeframe and budget allotted.

Oil Characteristics and Geology

The geologic criteria required a formation that represented the types of producing units found in fields that would be prime candidates for CO_2 EOR activities in the Illinois Basin. The geologic zone selected for the pilot needed to represent one of the three formations accounting for a relatively large proportion of the Illinois Basin's oil production— the Cypress, Aux Vases, and Ste. Genevieve—or depositionally similar formations. Completion of the wells in a single geologic zone was desired. Surveillance of productivity and injectivity from wells completed in a single zone is much more certain than commingled production and injection in wells completed in multiple zones. Additionally, the amount of CO_2 injected would need to be significantly larger for a multi-zone oil field with wells completed in all zones.

The Jackson sandstone at the Sugar Creek Field, which lies stratigraphically above the Cypress Sandstone but closely resembles it in lithology and depositional environment, was the only formation producing at Sugar Creek. This target formation is referred to herein by its informal name, the Jackson sandstone. The Jackson sandstone or "Jackson sand" is a drillers' term for the Big Clifty Sandstone Member, which is part

of the Golconda Formation in Kentucky (Goudarzi and Smith, 1968; Gildersleeve and Johnson, 1978) or the Fraileys Shale of Illinois (Willman et al., 1975). Another requirement for the formation was that the API gravity of the crude oil in the reservoir needed to be representative of Illinois Basin oil. An API gravity value of 37 API is very common in the Illinois Basin, so only oils in the range of 35 to 40 API were considered acceptable. The gravity of the oil in the Sugar Creek Field is 37 API.

Geographic Description and Site Location

The Sugar Creek Field is located in Hopkins County, Kentucky, approximately 5.6 km (3.5 miles) southwest of the small town of Earlington (Figure 2). The town is located along US Highway 41 about 6 km (3.75 miles) south of Madisonville, the county seat of Hopkins County. From Earlington, Sugar Creek Field is reached by traveling 4.8 km (3 miles) west on Kentucky Highway 1337, turning left onto Sugar Creek Road, and traveling another 1.2 km (0.75 miles) along this road. Sugar Creek Field tank battery and pump house are on the west side. Most of the oil production and monitoring wells and the injection well in this study are within 0.8 km (0.5 mile) west and southwest of the tank battery (Figure 3).

Physiographically, the Sugar Creek Field is located in the Green River-Southern Wabash Lowlands. The area is characterized by variably forested bottomlands and uplands. Streams have low gradients and the area tends to be poorly drained. Row-crop farming is prominent, and corn and soybeans are the most common crops. Agriculture and surface mining for coal have removed large forested areas and altered drainage patterns. Both of these activities have increased siltation of streams and degraded their water quality.

There is a small tilled field (12–16 ha [30–40 acres]) in the middle of the Sugar Creek oil field. The northern and western portions of the oil field are wooded, and the southern and eastern portions of the field are in pasture. A rock chip and oil road (Sugar Creek Road) runs along the northeastern edge of the oil field, then turns to the west in the middle of the field and continues south, dividing the southern part of the oil field into east and west portions.

Site Logistics

Unlike the other active water injection wells in the field, the Ross-Gentry #5 (RG-5) water injection well was surrounded by several active and temporarily abandoned oil-producing wells. There were no wellbore- or injection-related problems associated with RG-5, so it was chosen as the CO_2 injection well primarily based on its proximity to the oil-producing wells. However, the injection well was 640 m (2,100 ft) from the tank battery. The water injection pumps and accessories (e.g., filters) were located immediately adjacent to the oil tank battery (Figure 4), and the water injection line leading to RG-5 started from this location.

The lease road leading to RG-5 was not capable of supporting semi-trailer truck and tanker traffic; therefore, the CO_2 injection equipment was placed near the tank battery to allow for regular CO_2 delivery. This location required either laying a new CO_2 injection line between the injection equipment and RG-5 or using the existing water injection flow line to carry the CO_2. The 13.8 MPag (2,000 psig) pressure rating of the injection line was well above the anticipated injection pressure 9.825 MPag (1,425 psig) and the composition of the injection line was fiberglass, so that compatibility with CO_2 was not a concern. However, the line was not laid in a direct line to the well because there was a modest hill between the tank battery and RG-5. The injection line was buried around the hill to the south, which took it relatively close to a residence. Figure 3 shows the general position of the line that carried the CO_2 from the tank battery to the injection well.

The actively producing wells surrounding RG-5 were the Ross-Gentry #1 (RG-1), Ross-Gentry #2 (RG-2), Ross-Gentry #3 (RG-3), Ross-Gentry #4 (RG-4), Wilbur-Todd #4 (WT-4), Wilbur-Todd #8 (WT-8), and Wilbur-Todd #9 (WT-9) (Figure 3). Because of the hill's location, WT-4, WT-8, and WT-9 were drilled slightly farther away from RG-5 than typical offset wells within this field. Another well, the Pressley-Hart #1 (PH-1), was temporarily abandoned, but was returned to production for this pilot. There were no producing wells to the northwest of RG-5. Except for WT-9, all of the wells were accessible by the same oil field lease road, which made a large circle around the edge of the tillable acreage and the edge of the wooded areas near the pastures. Well WT-9 was accessible via Sugar Creek Road.

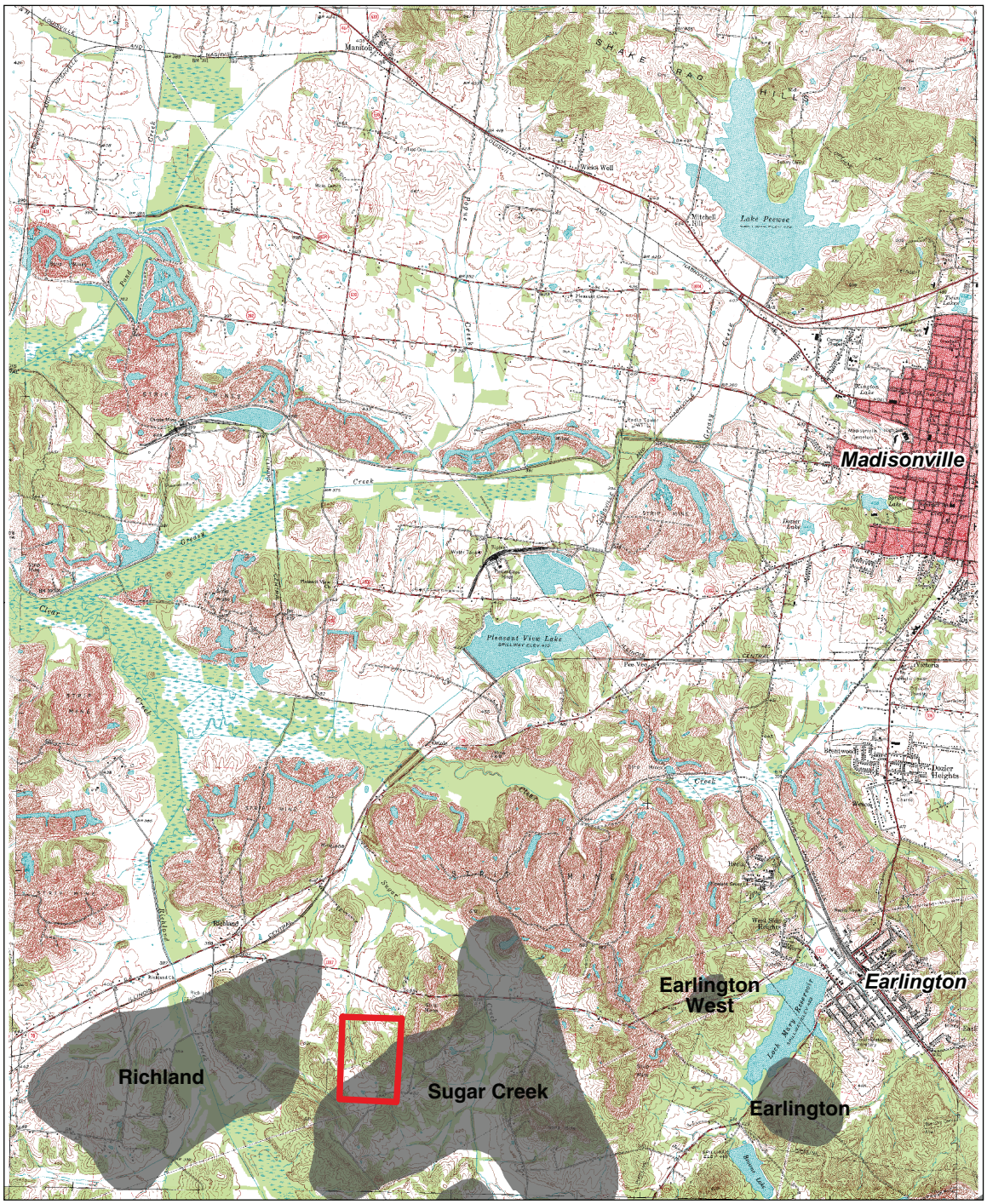

Figure 2 Location of Sugar Creek oil field relative to the nearest town and city (Earlington and Madisonville, KY) and other oil fields.

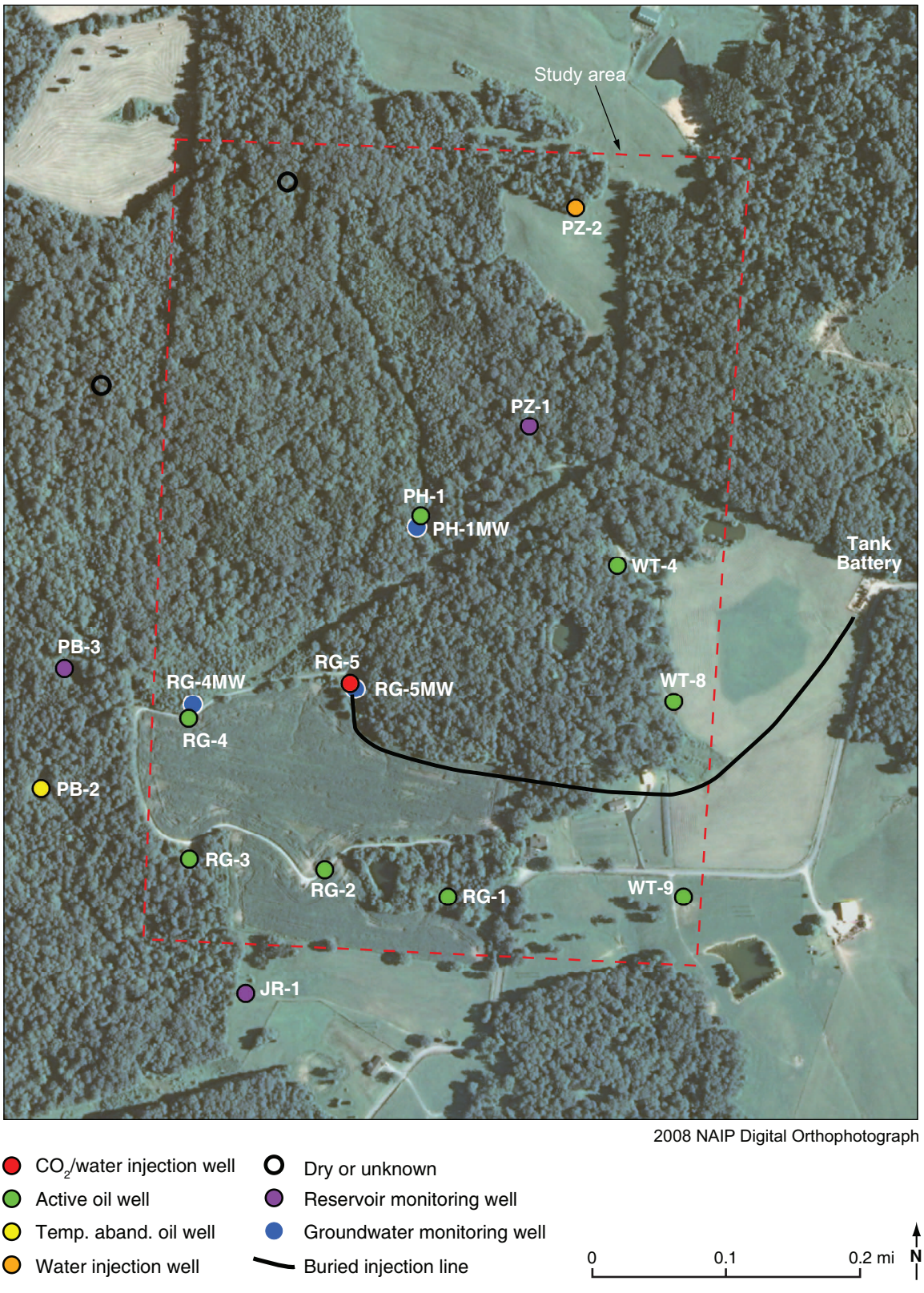

Figure 3 Aerial photograph of the northern portion of Sugar Creek oil field where the CO_2 pilot was conducted. Locations of wells and tank battery and general location of buried injection line are shown. Sugar Creek Road crosses the lower right corner of this map.

Figure 4 The tank battery at Sugar Creek, including tanks and pump house. Tanks are to the left, and the pump house is to the right. The oil-water separator and brine tanks are in the middle.

FIELD HISTORY

Original Oil in Place and Wells

The Sugar Creek Field was discovered in 1963. Individual leases were operated by several independent oil companies until 1991 when GDI acquired a large portion of the field. Production throughout the history of the field has been exclusively from the Mississippian Jackson sandstone.

The original-oil-in-place (OOIP) estimate for Sugar Creek Field is 383,190 scm (2,410,000 bbl), according to an estimate provided by the field operator. The volumetric formula for calculating OOIP (bbl) is

$$OOIP = 7758\ V_b\ \phi\ (1–S_w)/B_o \quad (1)$$

where V_b is the bulk volume of sandstone reservoir in acre-ft, ϕ is porosity fraction, S_w is water saturation fraction, B_o is the oil formation volume factor, and 7,758 is a conversion factor (7,758 bbl/acre-ft equals one acre-ft per barrel). To estimate V_b, a planimeter was used to measure the area encompassed by each contour of the isopach map (Figure 5). Constant porosity of 16.7% and an assumed water saturation of 30% were used.

Figure 6 is a map of well locations for Sugar Creek Field. There are a total of 49 wells on eleven leases in the field, 44 of which were used in the geologic and reservoir modeling for this pilot project. The pilot included 12 wells on six leases, including 8 production wells, 3 reservoir monitoring wells, and 1 water/CO_2 injection well (Figure 3, Table 1).

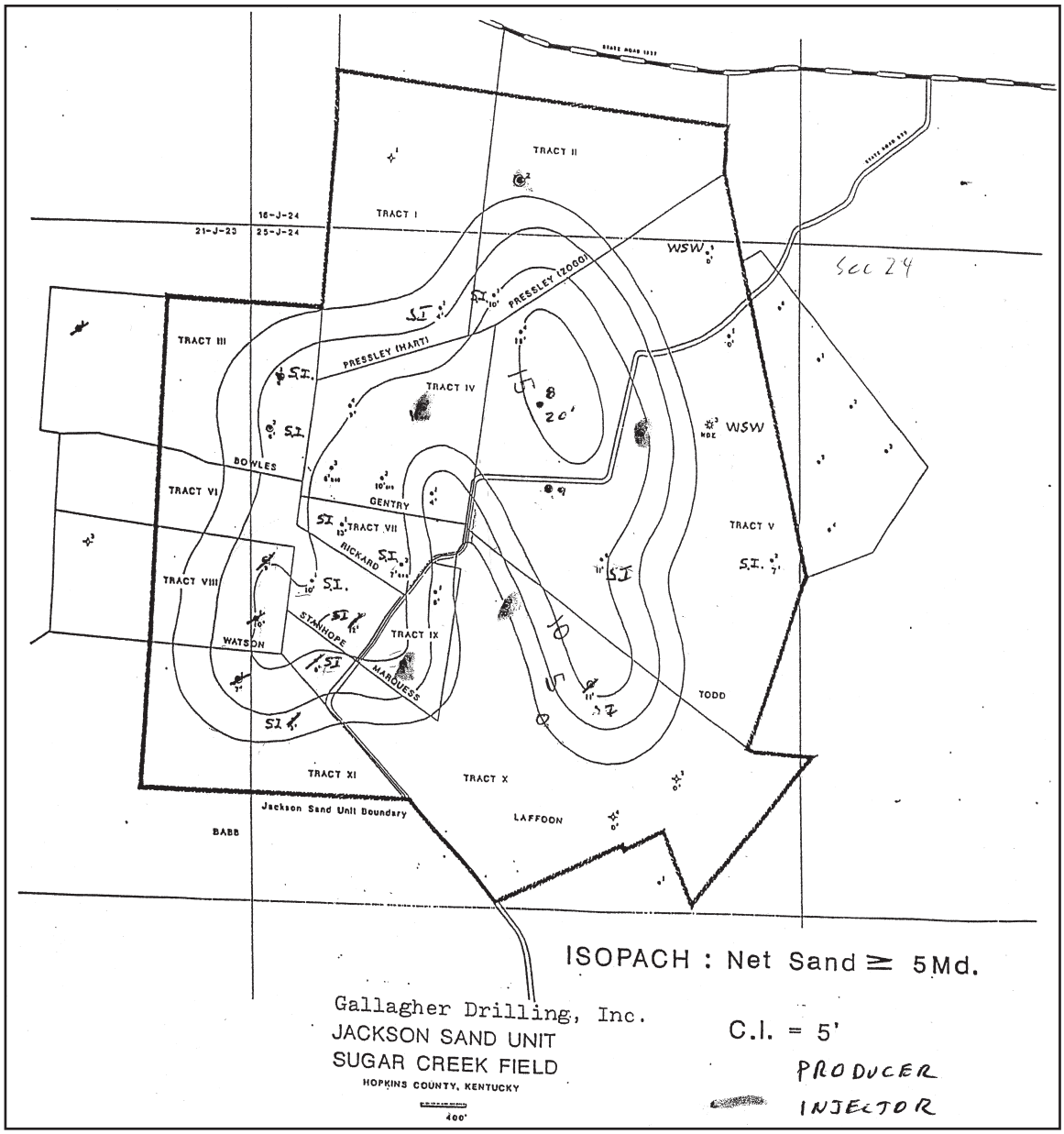

Figure 5 Isopach map used to estimate the bulk volume of sand in acre-feet for OOIP calculation (courtesy of Gallagher Drilling, Inc.). Contour interval = 5 feet.

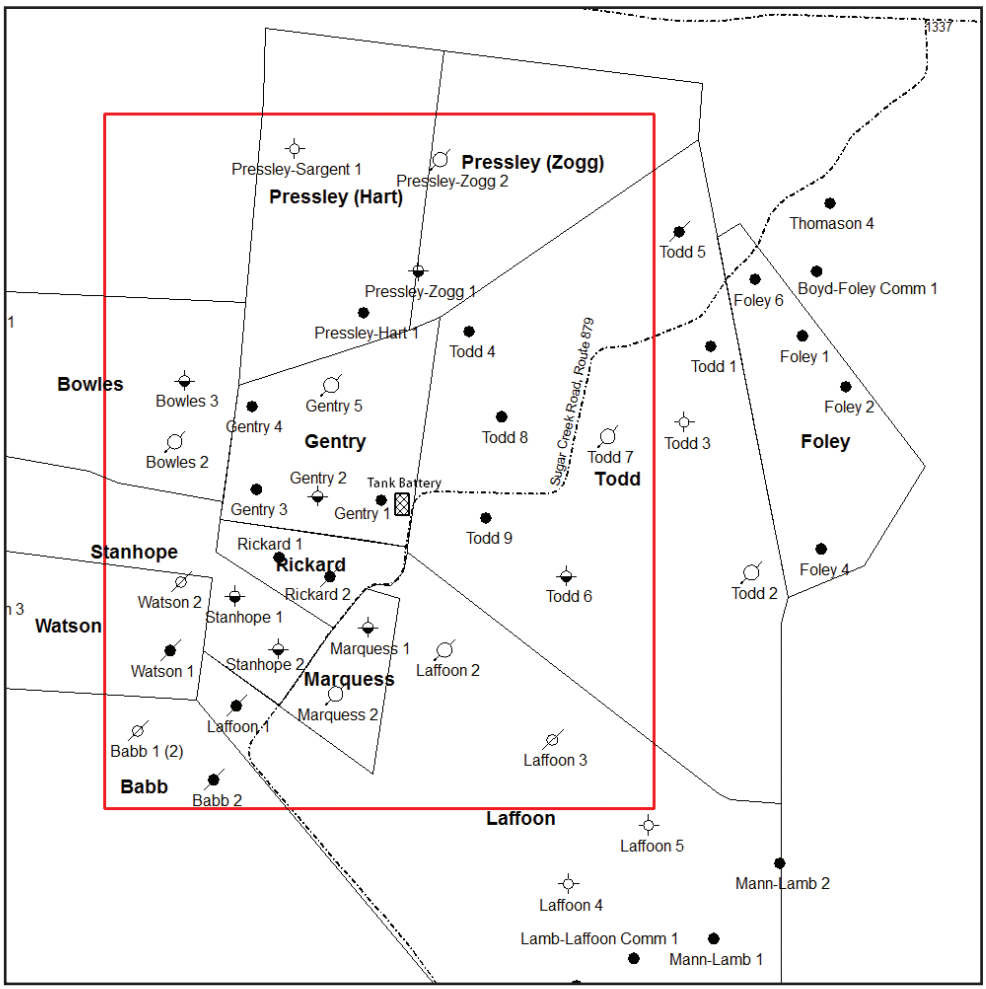

Figure 6 Map of the well locations and the lease boundaries. The well names are in regular font while the lease names are in bold. The model area is encompassed by the red square. The tank battery is identified by a small, cross-hatched square at a bend in Sugar Creek Road.

Table 1 Reservoir test configuration wells for Sugar Creek Field, including well lease name, number, and abbreviation, well type, and date drilled.

Well name	Well type	Date drilled
Ross-Gentry #1 (RG-1)	Production	July 2, 1964
Ross-Gentry #2 (RG-2)	Production	September 30, 1964
Ross-Gentry #3 (RG-3)	Production	October 17, 1964
Ross-Gentry #4 (RG-4)	Production	May 18, 1965
Ross-Gentry #5 (RG-5)	Water/CO_2 injection	June 25, 1965
Wilbur-Todd #4 (WT-4)	Production	August 10, 1965
Wilbur-Todd #8 (WT-8)	Production	December 5, 2003
Wilbur-Todd #9 (WT-9)	Production	January 5, 2007
Pressley-Hart #1 (PH-1)	Production	August 20, 1965
Pressley-Zogg #1 (PZ-1)	Monitoring	July 12, 1965
Peter Bowles #3 (PB-3)	Monitoring	August 23, 1965
J.C. Rickard #1 (JR-1)	Monitoring	August 24, 1964

Field Development

Most of the wells in the pilot area were drilled between July 1964 and August 1965. WT-8 and WT-9 (oil production wells) were drilled in December 2003 and January 2007, respectively.

Primary production lasted until November 1992 when water injection began. The sole well (PH-1) on the Pressley-Hart lease ceased production in 1972, but wells on the 10 other leases continued to produce through at least 1990, two years prior to the start of the waterflood. (Records provided to ISGS are incomplete for 1991 and 1992, when ownership and management of the field transitioned to GDI; however, there was probably production at some of the wells during this period.) Peak annual oil production for the field was 14,775 m^3 (92,931 bbls) in 1965 (Figure 7). Annual production dropped below 3,180 m^3 (20,000 bbls) in 1971 and below 1,590 m^3 (10,000 bbls) in 1984. Total primary oil production was 86,455 m^3 (543,783 bbl) through the end of 1990. Although water production volumes during primary production were not available, the oil-producing wells in the northern part of the field (PH-1, PZ-1, and WT-4) likely produced water directly from the oil reservoir's aquifer, and the remainder of the wells produced very little water.

Water injection commenced in December 1992 and was continuous at some injection wells but intermittent at others (Table 2; Figure 8). PH-1 returned to production. Two wells (Albert Babb #1 [AB-1] and Peter Bowles #2 [PB-2]) underwent sustained water injection for a few years before being shut-in during the mid-1990s. Ruby Watson #2 (RW-2) underwent nearly ten years of continuous water injection (December 1992–October 2002), and E.O. Laffoon #2 (EL-2), Bernice Marquess #2 (BM-2), and Pressley-Zogg #2 (PZ-2) all had continuous injection from December 1992 to present. RG-5, E.O. Laffoon #3 (EL-3), and Wilbur-Todd #7 (WT-7) underwent intermittent water injection during this time. Water injection at EL-3 terminated in October 1998 after three injection periods totaling 58 months; total downtime was 9 months. (Note that production and injection periods for 1992 through 2010 were reported by month; the actual days per month of active injection were not available.) WT-7 underwent 64 months of water injection through May 2001 with three interruptions totaling 10 months. After May 2001, injection at WT-7 ceased until January 2009 (except for two isolated months of injection, October 2001 and April 2005), before continuous water injection resumed in January 2009.

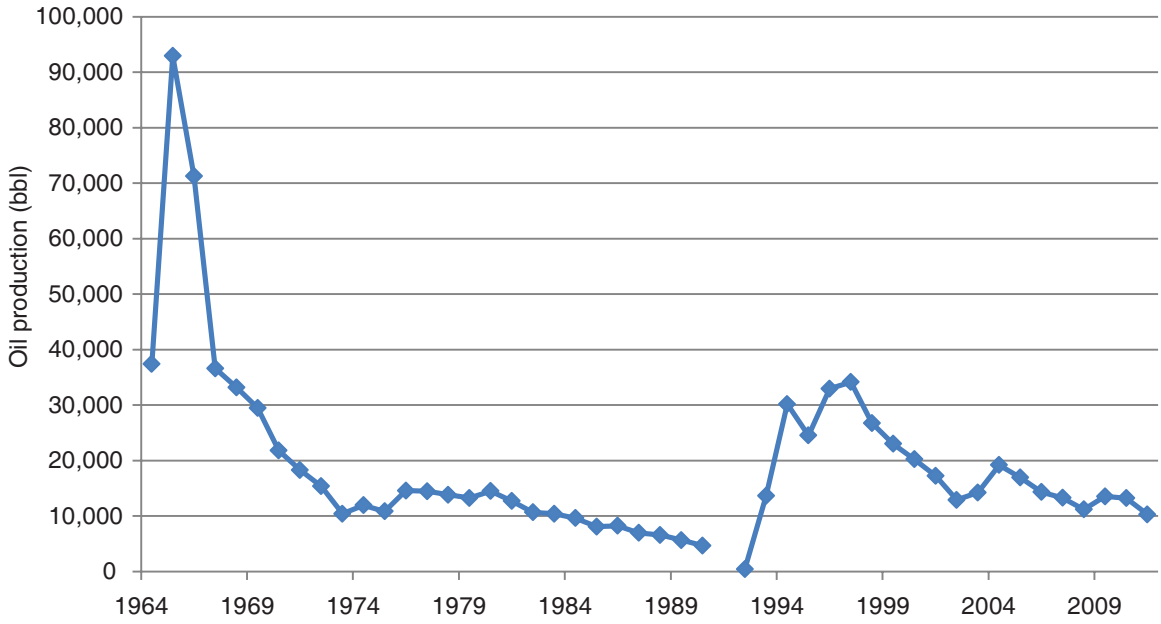

Figure 7 Annual oil production from Sugar Creek Field for the entire history of the field (through December 4, 2011), including primary production, waterflooding, and CO_2 injection. Production data were not available for 1991 or 1992.

The average RG-5 water injection rate for the 12 months preceding CO_2 injection was about 9.1 m^3/d (57 bwpd); however, the rate for April 2009 was 19 m^3/d (120 bwpd) following a field shut-down during February when reservoir pressure was much lower due to no injection.

Total field water injection was reported to be 383,000 m^3 (2,400,000 bbls).

Table 2 Waterflood/CO_2 injection periods by well. Only RG-5 water injection rates were available through 2011; all other injection well data is through 2010.

Well name	Injection periods
Albert Babb #1 (AB-1)	December 1992–March 1998
Peter Bowles #2 (PB-2)	December 1992–December 1995
Ross-Gentry #5 (RG-5)	December 1992–October 2002 December 2002–May 15, 2009 May 16, 2009–May 2010[1] June 2010–December 2011
E.O. Laffoon #2 (EL-2)	December 1992–December 2010
E.O. Laffoon #3 (EL-3)	December 1992–September 1997 February 1998–April 1998 October 1998[2]
Bernice Marquess #2 (BM-2)	December 1992–December 2010
Wilbur-Todd #7 (WT-7)	December 1992–February 1993 June 1993–December 1995 February 1996–January 2000 December 2000–May 2001 October 2001[2] April 2005[2] January 2009–December 2010
Ruby Watson #2 (RW-2)	December 1992–October 2002
Pressley-Zogg #2 (PZ-2)	December 1992–December 2010

[1] CO_2 injection.
[2] Single month water injection.

Monthly oil production for the field for the waterflooding period of December 1992–May 12, 2009 (Figure 9) peaked at 515.5 m^3 (3,242 bbl) in July 1996. Production dropped below 318 m^3 (2,000 bbl) for the first time in December 1998 and declined relatively consistently until February 2003, when it hit a low of 95.1 m^3 (598 bbl) but then began an upward climb to a peak of 357.6 m^3 (2,249 bbl) in December 2003 as a result of drilling and completing WT-8 and WT-9. Production dropped quickly to 292.4 m^3 (1,839 bbl) in January 2004 and then went into a slow overall decline (with some minor month-by-month increases and decreases in production) over the next several years, dropping below 159 m^3 (1,000 bbl) for the first time in November 2006 and declining to a low of 44.7 m^3 (281 bbl) in February 2009 before rebounding to 202.6 m^3 (1,274 bbl) in April 2009, shortly before the start of CO_2 injection for this pilot. Total waterflood oil production was 52,400 m^3 (329,000 bbls) through May 12, 2009. Total water production was 114,000 m^3 (719,000 bbl).

Prior to CO_2 injection, the field's daily oil production and injection rates were 5–6 m^3/d (30–40 bopd) and 48–56 m^3 (300–350 bwpd), respectively. The daily injection rate at RG-5 was 10–13 m^3 (60–80 bwpd).

None of the oil production wells underwent sustained oil production for the entire water injection period, although some were interrupted only briefly (Table 3). The Ross-Gentry (RG) wells (Figure 10a) were all in production for the majority of the period spanning December 1992 through December 2010, but with multiple interruptions ranging in duration from a month to several months; the exception was RG-3, which sustained only a single month of production interruption between December 1992 and December 2010. Two of the Wilbur-Todd wells (Figure 10b), WT-4 and WT-6, were also in production beginning in December 1992 and continuing for the majority of the waterflooding period, but with frequent production gaps of

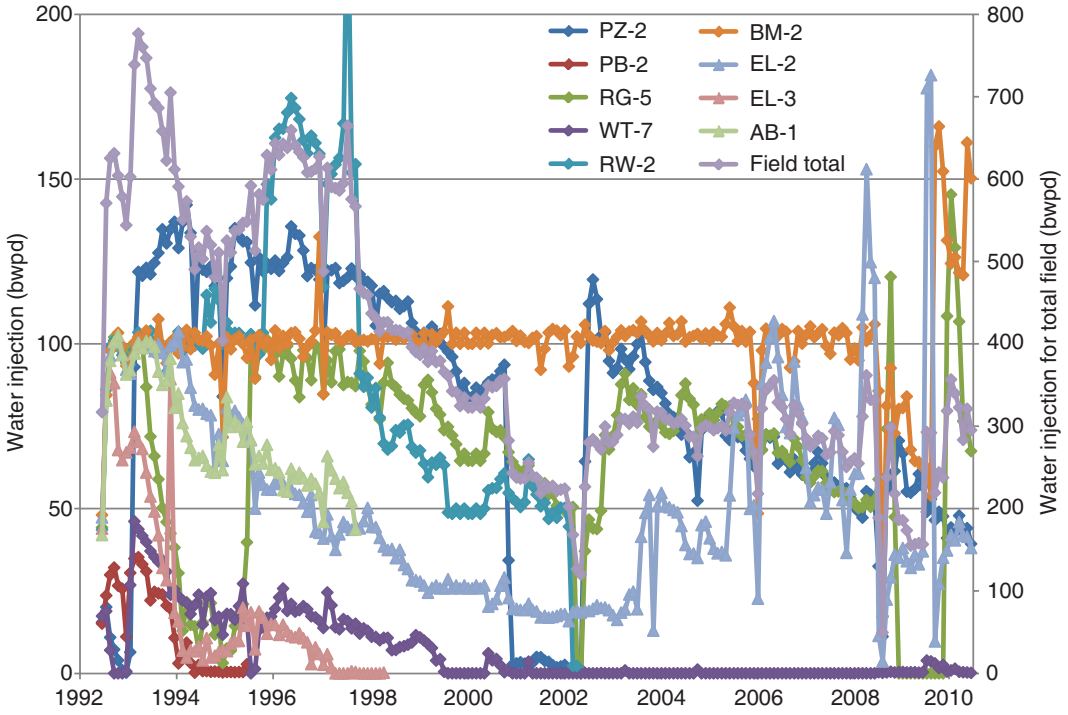

Figure 8 Monthly water injection averaged daily (bwpd) for each well (primary axis) and for Sugar Creek Field (secondary axis) during the waterflooding period, December 1992 to December 2010. (One outlying data point is not visible on the map: 238.71 bwpd at RW-2 in January 1998.)

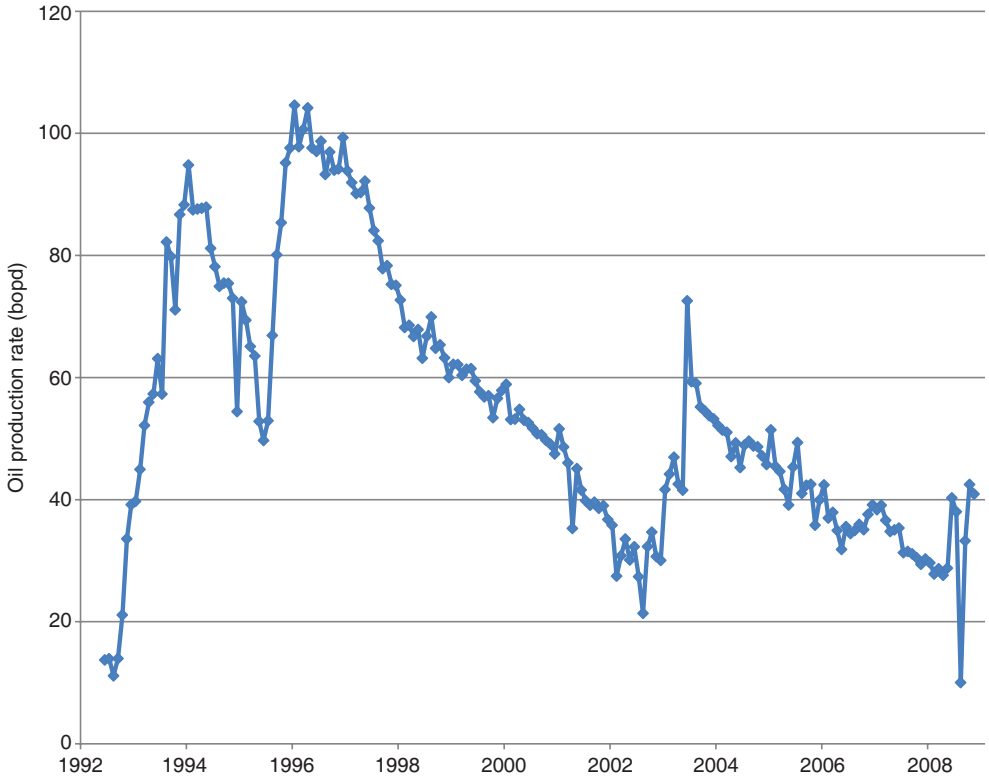

Figure 9 Monthly oil production rates for Sugar Creek Field during the waterflooding period, December 1992–May 12, 2009, average barrels per day.

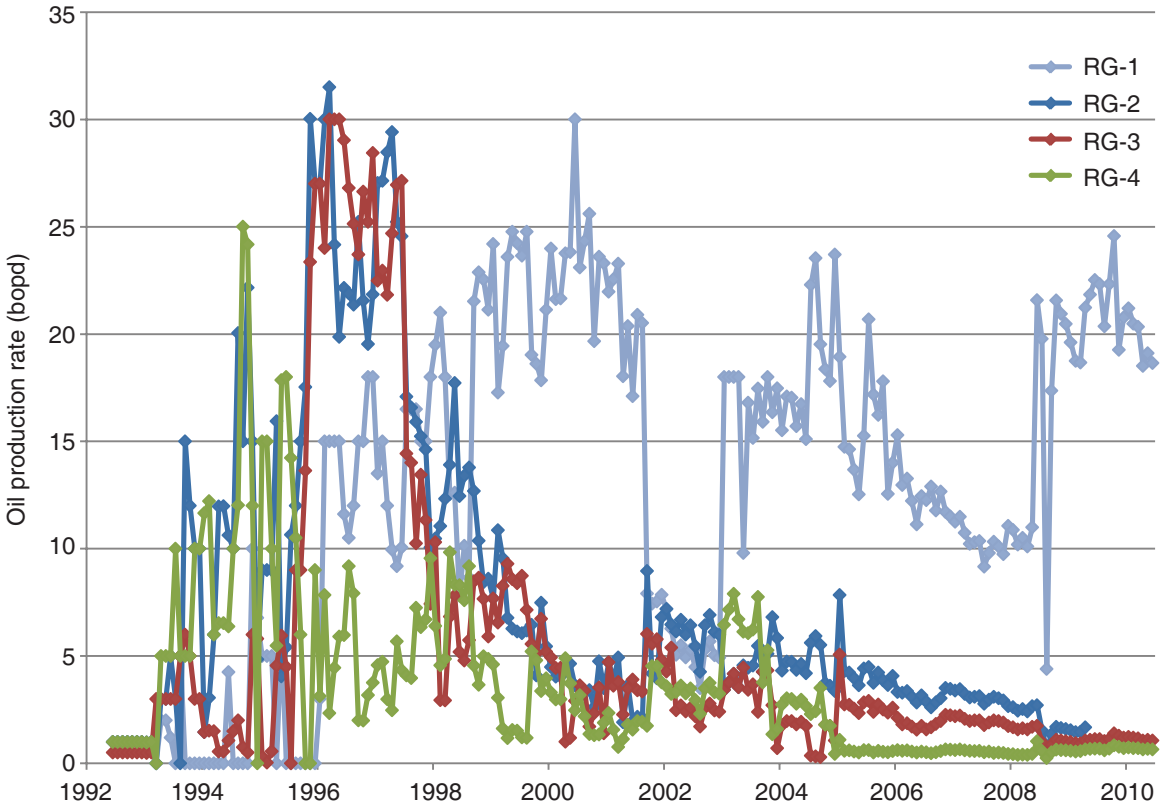

Figure 10a Monthly oil production averaged daily (bopd) at the Ross-Gentry wells (RG-1, RG-2, RG-3, RG-4) for the period from December 1992 through December 2010.

anywhere from a month to a few years. The longer gaps were sometimes punctuated with single months of production. Wells WT-8 and WT-9 were not drilled until 2003 and 2007, respectively, and continued production until December 2010.

Oil production by month for wells on adjacent leases is shown in Figures 10c and 10d and Table 3. Babb #2 (AB-2), PB-3, Laffoon #1 (EL-1), Stanhope #1 (MS-1), and PZ-1 underwent relatively sustained production (only one or two interruptions of a few months each) for a few years before ceasing production in the mid-1990s. Production at JR-1 ceased in October 2000 after about eight years of continuous production, and Stanhope #2 (MS-2) ceased production a year later having undergone only about two months of interrupted operation during that period. Well PH-1 was in production for the majority of the period spanning December 1992 through December 2004, but with multiple interruptions ranging in duration from 1 to 2 months. Marquess #1 (BM-1) ceased production in February 2009 after relatively continuous production that was interrupted by several periods of downtime lasting up to several months.

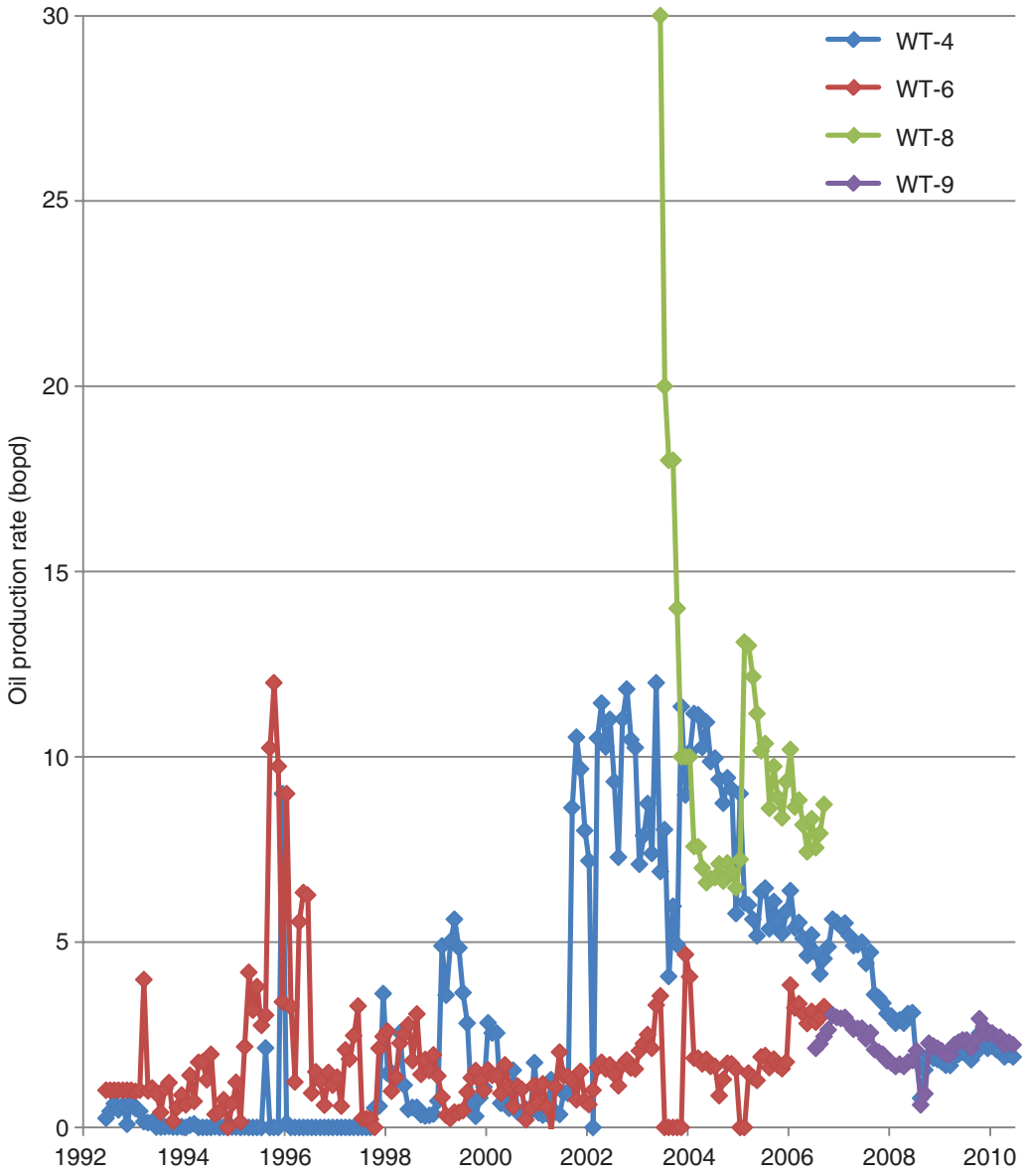

Figure 10b Monthly oil production averaged daily (bopd) at the Wilbur-Todd wells (WT-4, WT-6, WT-8, WT-9) for the period from December 1992 through December 2010.

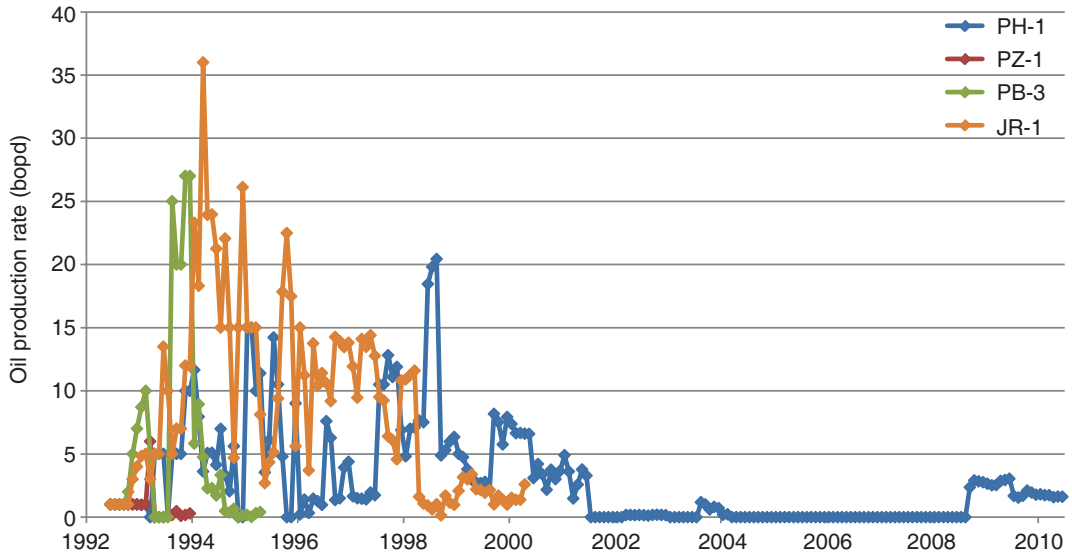

Figure 10c Monthly oil production averaged daily (bopd) for Pressley-Hart #1 (PH-1), Pressley-Zogg #1 (PZ-1), Peter Bowles #3 (PB-3), and J.C. Rickard #1 (JR-1) for the period from December 1992 through December 2010.

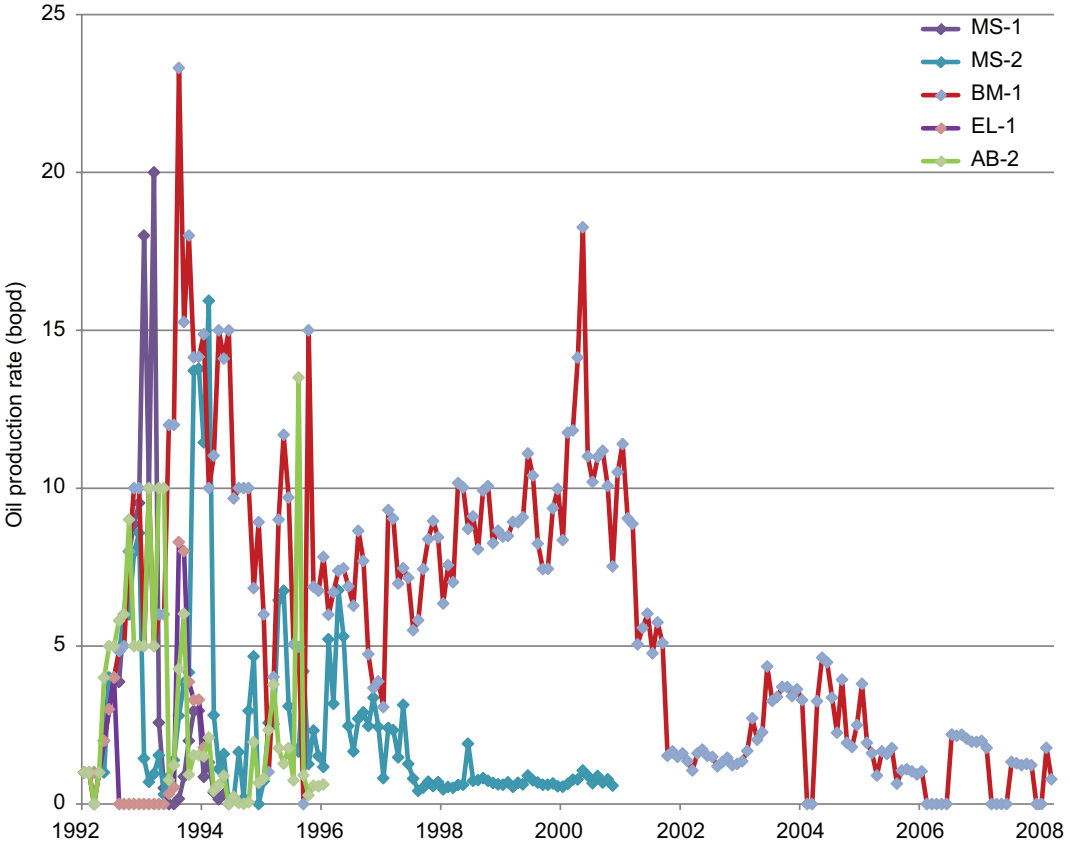

Figure 10d Monthly oil production averaged daily (bopd) for Mary Stanhope #1 and #2 (MS-1, MS-2), Bernice Marquess #1 (BM-1), E.O. Laffoon #1 (EL-1), and Albert Babb #2 (AB-2) (Sugar Creek Field wells outside the pilot area) for the period from December 1992 through February 2009. (There was no production at any of these wells from March 2009 through December 2010.)

Table 3 Production history by well. At the time of this report, rate allocated well production data was available by well only through end of December 2010.

Well name	Production period		
Albert Babb #2 (AB-2)	1964–1990 Dec 1992–Jan 1993 Mar 1993–Dec 1996		
Peter Bowles #3 (PB-3)	1964–1990 Dec 1992–Sep 1993 Feb 1994–Oct 1995		
Ross-Gentry #1 (RG-1)	1964–1990 Dec 1992–Aug 1993 Oct 1993–Jan 1994	Mar 1994–Oct 2009	
Ross-Gentry #2 (RG-2)	1964–1990 Dec 1992–Aug 1993 Oct 1993–Jan 1994	Mar 1994–Oct 2009	
Ross-Gentry #3 (RG-3)	1964–1990 Dec 1992–Dec 1995 Feb 1996–Dec 2010		
Ross-Gentry #4 (RG-4)	1964–1990 Dec 1992–Aug 1993 Oct 1993–May 1995	Jul 1995–Mar 1996 Jun 1996–Dec 2010	
Pressley Hart #1 (PH-1)	1965–1969 1972–1972 Dec 1992–Aug 1993	Oct 1993–Apr 1995 Jul 1995–Mar 1996 Jun 1996–Dec 2001	Sep 2002–Jan 2003 Feb 2004–Aug 2004 Mar 2009–Dec 2010
E.O. Laffoon #1 (EL-1)	1964–1972 1974–1990 Dec 1992–Jun 1993	May 1994–Dec 1994	
Bernice Marquess #1 (BM-1)	1964–1990 Dec 1992–Jan 1993 Mar 1993–Jul 1996	Sep 1996–Dec 2004 Mar 2005–Dec 2006 Jun 2007–Jan 2008	Jun 2008–Oct 2008 Jan 2009–Feb 2009
J.C. Rickard (JR-1)	1964–1990 Dec 1992–Oct 2000		
Mary Stanhope #1 (MS-1)	1964–1990 Dec 1992–Jan 1993 Mar 1993–Apr 1994	Jul 1994–Apr 1995	
Mary Stanhope #2 (MS-2)	1964–1990 Dec 1992–Apr 1995 Jun 1995–Oct 1995	Dec 1995–Oct 2001	
Wilbur-Todd #4 (WT-4)	1965–1990 Dec 1992–Jun 1994 Aug 1994–Sep 1994 Feb 1995[1]	Apr 1995[1] Jun 1995–Sep 1995 Feb 1996[1] Jun 1996–Jul 1996	Apr 1998–Jul 2002 Sep 2002–Dec 2010
Wilbur-Todd #6 (WT-6)	1965–1990 Dec 1992–Apr 1995 Jun 1995–Mar 1998	May 1998–Dec 2003 Jun 2004–Jun 2005 Sep 2005[1]	Mar 2007[1]
Wilbur-Todd #8 (WT-8)	Dec 2003–Dec 2010		
Wilbur-Todd #9 (WT-9)	Jan 2007–Dec 2010		
Pressley-Zogg (PZ-1)	1965–1972 1974–1990 Dec 1992–Sep 1993	Jan 1994–Jun 1994	

[1] Single month production.

The field had 26 years of primary production and over 18 years of waterflooding. Figure 11 is the oil production for the field (by year before 1992 and monthly for 1992 and after). Total production was 142,387 m^3 (895,575 bbl), which represents 33% oil recovery as a percent of the field operator's original OOIP estimate. Similar to most Illinois Basin oil fields, gas production was very low and vented at the casing heads of individual wells and at the production tank battery.

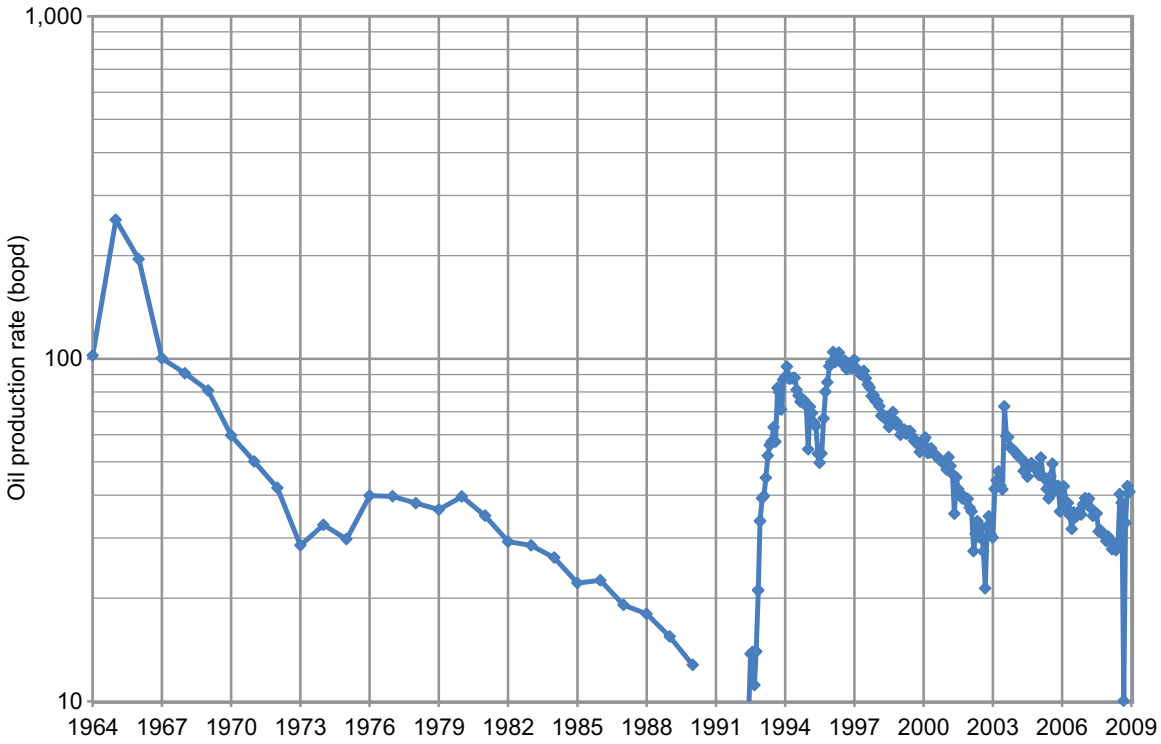

Figure 11 Oil production for the field through the end of secondary production (waterflooding). Daily oil rates are based on annual oil production during primary production (1964–1992) and monthly oil production from 1992 to May 12, 2009 (the day preceding commencement of CO_2 injection).

The Wilbur Todd #3 (WT-3) well, located a good distance outside the boundary of the test site, was the make-up water supply well for water injection.

Available Geologic and Production Data

Geologic data available at Sugar Creek Field were limited. Neither cores nor drilling samples were available; however, core analysis reports were available for a limited number of wells and provided a sample of reservoir porosity and permeability. The geophysical logs available predated the porosity logs and included predominantly spontaneous potential (SP) and resistivity. Schlumberger's reservoir saturation tool (RST) and cement bond logs (CBL) were run in many of the wells as part of the CO_2 pilot project's monitoring, verification, and accounting (MVA) program to determine the presence of CO_2 behind pipe in the near-wellbore region. These data provided the opportunity for a modern, in-situ estimate of porosity; unfortunately, the cased hole logging tool was unable to reach the Jackson sandstone due to the original total depth (TD) of the well or other obstructions and the length of the logging tool.

Gallagher Drilling, Inc. provided production data back to 1964 based on a combination of records from the original well operators and GDI's own post-1990 records. Production data for primary recovery were generally available only by lease rather than by well and were less comprehensive than the waterflood data because they were compiled mostly as monthly production totals. GDI also provided structure and isopach maps.

Well Completion Data

The surface wellbore for a typical Sugar Creek production well (Figure 12) was drilled with a 31.12-cm (12¼-inch) bit and cased with 25-cm (10-inch) surface casing to a depth of 6.1 m (20 ft). The production wellbore was drilled with a 20-cm (7⅞-inch) bit and cased with 14-cm (5½-inch) production casing. Casing

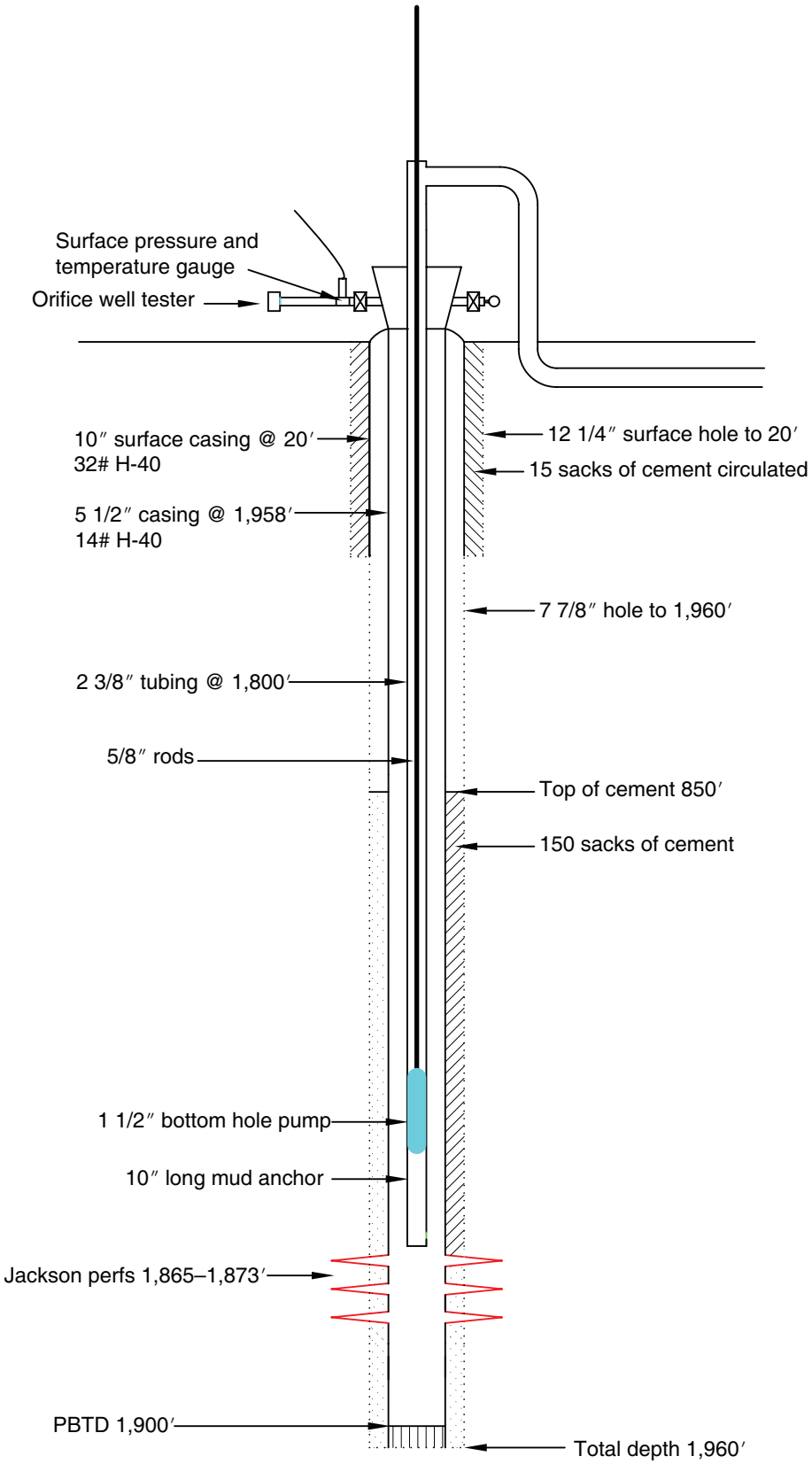

Figure 12 Wellbore schematic of a typical Sugar Creek production well (courtesy of Gallagher Drilling, Inc.).

grade for both production and surface casing was H-40; surface casing weighed 48 kg/m (32 lb/ft) and production casing weighed 21 kg/m (14 lb/ft).

Typically, the surface casing was cemented with 15 sacks of cement. Below that was a 20-cm (7⅞-inch) hole to about 597 m (1,960 ft) with 596.8 m (1,958 ft) of 14-cm (5½-inch) casing. The 20-cm (7⅞-inch) hole was cemented from TD to a depth of 259 m (850 ft) using 150 sacks of cement.

Tubing that was 6 cm (2⅜ inch) in diameter extended from the surface to 548 m (1,800 ft), enclosing 1.6-cm (⅝-inch)-diameter sucker rods which connected downhole to a 3.8-cm (1.5-inch) bottomhole pump with a 6-cm (2⅜ inch) diameter, 3-m (10-ft) long mud anchor. Well TD was about 609 m (2,000 ft), and the well was plugged back to the bottom of the Jackson sandstone, typically about 580 m (1,900 ft).

This wellbore description characterizes a typical wellbore, but there were variations in well design. Exact lengths of casing and tubing, total depths of wells, and other parameters differed slightly from well to well. Production casing was 11.4 cm (4½ inch) rather than 14 cm (5½ inch) for some wells. Figure 12 shows a well with perforations in the Jackson sandstone beginning at a depth of around 568 m (1,865 ft). However, the majority of wells at Sugar Creek are open-hole. Wells RG-2, RG-3, RG-4, RG-5, WT-4, JR-1, PZ-1, and PB-3 are all open-hole, with typical open-hole intervals of 3 to 6 m (10 to 20 ft) at depths between 564 and 584 m (1,850 and 1,915 ft). Wells RG-1, WT-8, WT-9, and PH-1 were cased to TD and perforated. Table 4 summarizes basic information for the wells of Sugar Creek Field, including completion types, depths, and elevations, length of transducer cable and elevation of transducer, and bottomhole depth and elevation.

Table 4 Summary of well completions data for Sugar Creek Field.[1]

Well	Ground level elev. (ft)	Trans. cable length (ft)	Trans. elev. (ft)	Completion depths (ft)	Completions top and bottom elev. (ft)	Bottom-hole depth (ft)	Bottom-hole elev. (ft)
RG-1	493	-	-	Perf; 1865–1873	–1,372, –1,380	1,907	–1,414
RG-2	508	1,870	–1,362	Open; 1877–1888	–1,369, –1,380	1,888	–1,380
RG-3	493	-	-	Open; 1852–1867	–1,359, –1,374	1,867	–1,374
RG-4	506	-	-	Open; 1878–1892	–1,372, –1,386	1,892	–1,386
RG-5	493	1,868	–1,375	Open; 1867–1879	–1,374, –1,386	1,883	–1,390
PB-3	477	365	112	Open; 1871–1876	-1,394, –1,399	1,871	–1,394
PZ-1	481	950	–469	Open; 1874–1894	–1,393, –1,413	1,894	–1,413
JR-1	496	-	-	Open; 1845–1859	–1,349, –1,363	1,859	–1,363
PH-1	488	-	-	Perf; 1877–1897	–1,389, 1,409	1,897	–1,409
WT-4	502	-	-	Open; 1893–1913	–1,391, –1,411	1,913	–1,411
WT-8	498	-	-	Perf; 1887–1907	–1,389, –1,409	1,912	–1,414
WT-9	494	-	-	Perf; 1860–1879	–1,366, –1,385	1,879	–1,385

[1] Abbreviations: elev., elevation with respect to sea level; trans., transducer; Perf., perforated interval; Open, open-hole below casing.

Figure 13 Sugar Creek lease map showing cumulative primary oil production (barrels) by lease.

Cumulative Production and Injection Maps

Production maps for Sugar Creek during the primary production period (by lease) and waterflooding period (by well) are shown in Figures 13 and 14, respectively. Figure 13 shows cumulative oil production by lease for the primary production period (individual well data were not available). The Gentry lease was the most productive with 16,770 m^3 (105,480 bbls), followed by Laffoon with 15,896 m^3 (99,979 bbl). Figure 14 is a bubble diagram showing cumulative oil and water production by well for the waterflooding period (December 1992–May 12, 2009). The most productive wells during waterflooding were on the Gentry lease; RG-1 produced the most oil at 11,715 m^3 (73,686 bbls). Injection wells with cumulative injection totals are also shown in Figure 14.

Well RG-5, the water injection well in the most prolific part of the oil field, was chosen as the CO_2 injection well.

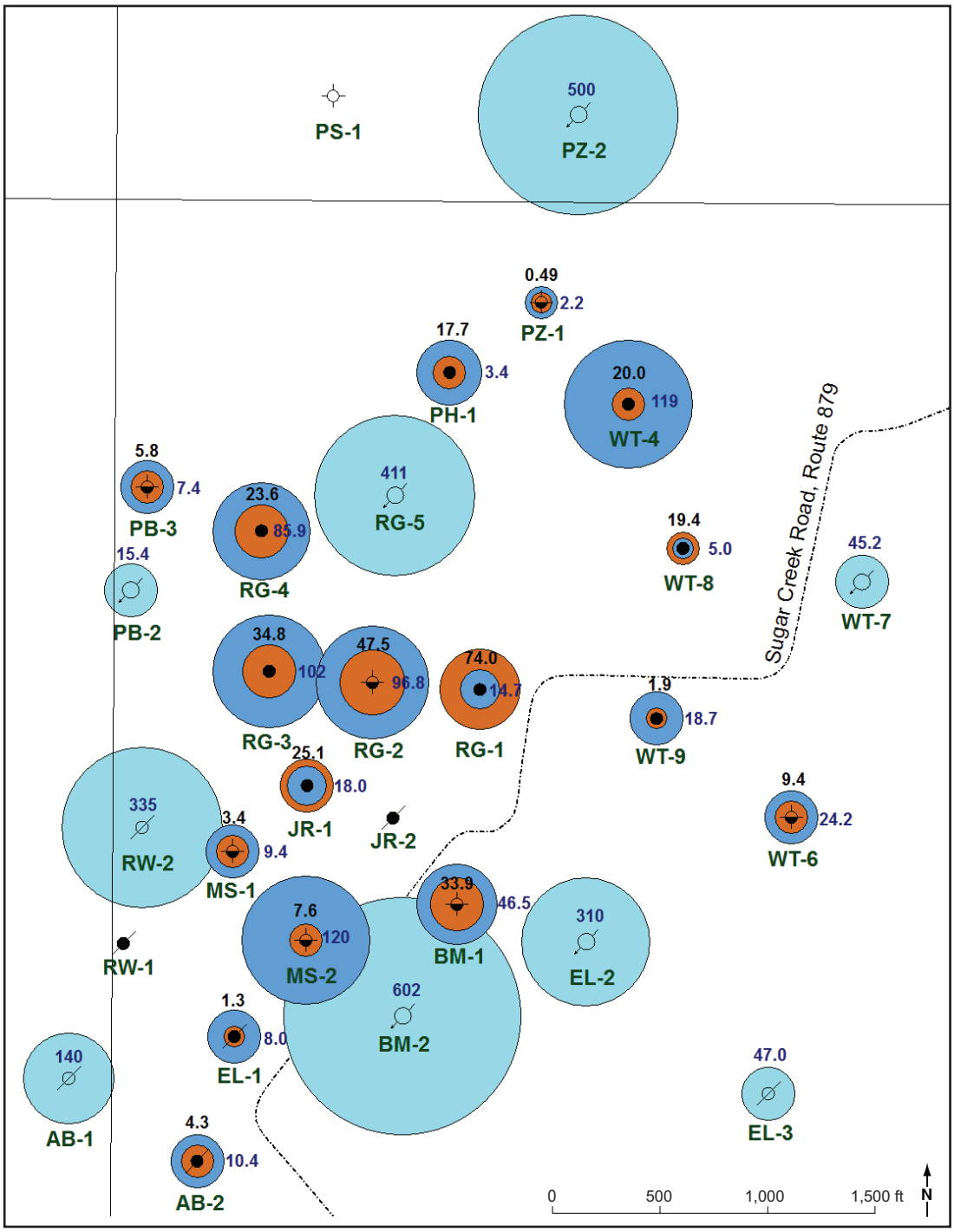

Figure 14 Sugar Creek oil and water production and water injection bubble map for the waterflooding period, by well. Brown circles around individual wells (with black numbers above the well symbol) represent cumulative oil production at each well from December 1992–May 12, 2009. Dark blue circles around producing wells (with dark blue numbers to the right of the well symbol) represent the cumulative water production for the same time period. Light blue circles around injection wells (with numbers in blue type) indicate cumulative water injection from December 1992–May 12, 2009. Larger bubbles indicate higher total production or injection. Bubbles are overlapping circles, not concentric rings; each is measured from the center of the circle. Bubbles indicating injection volumes are at a different scale than production bubbles. All numbers are in thousands of barrels.

Figure 15 Top of the "gun barrel" oil-water separator at Sugar Creek Field tank battery. The separator is in the center of the photo. The top of an oil tank is in the foreground, and the two brine tanks are behind the separator.

Tank Battery and Flow Lines

Squibb Tank Company, Inc. manufactured the tank battery, which consisted of three oil tanks, two brine tanks, and a "gun barrel" oil-water separator. The steel oil tanks were 3 m (10 ft) in diameter and 4.6 m (15 ft) in height. The two brine tanks were of similar dimensions to the oil tanks but were made of fiberglass. The nominal capacity of each oil and brine tank was 33.4 m^3 (210 bbl). The fiberglass oil-water separator was 1.8 m (6 ft) in diameter and 6 m (20 ft) tall and had a nominal capacity of 15.9 m^3 (100 bbl). A dike surrounded the tank battery. According to regulations, the dike volume must be 1.5 times the volume of the largest tank within the battery. The dike was approximately 30 m (100 ft) × 11 m (35 ft); the longer sides of the rectangle run parallel to the row of oil tanks. The height of the dike ranged from a minimum of approximately 51 cm (20 in) to a maximum of approximately 86 cm (34 in) above the adjacent level ground surface, and its average width was approximately 2 m (6 ft).

Buried production flow lines (2 inch nominal; 6.03 cm [2⅜ inch] OD) made from schedule 40 PVC running from the individual production wells in the field merged into a single line (2 inch nominal; 6.03 cm [2⅜ inch] OD), also made from schedule 40 PVC which was connected to a gas-liquid separator.

Liquid flowed from the oil-gas separator into the "gun barrel" oil-water separator, a tall narrow tank (Figure 15). Oil segregated to the top of the gun barrel and was flowed to one of three oil tanks (foreground, Figure 15), while the denser brine at the bottom of the separator flowed to one of two brine tanks (background, Figure 15).

Brine Injection Equipment and Injection Lines

A pump house containing the water injection equipment was located immediately adjacent to the brine tanks at the north end of the tank battery near the driveway entering the tank battery area from Sugar Creek Road. Produced brine from the tanks was piped to the pump house for re-injection. The brine is supplemented with water from water supply well WT-3 when the amount available from the brine tanks was inadequate.

Figure 16 shows the control panels in the pump house. The four instruments on the bottom row are OPLC series Swichgage® pressure gauges and switches manufactured by FW Murphy. The boxes above the dials are TR-1760 electronic motor controllers. The gauges were used to monitor pressures and tank water levels. If the measured parameter exceeded an upper limit or dropped below a lower limit set by the operator, the controller was engaged and shut down the motor. The first and second gauges from the left both connected to the same TR-1760 assembly, which controlled the injection pump motor. The first gauge on the left shut down the injection pump if the pressure exceeded or dropped below a specified range, and the second gauge from the left shut down the pump if the level of water in the water tank got too low. The third gauge from the left started and stopped the water supply well based on the height of fluid in the water tank. The gauge farthest to the right shut down the field by cutting power to all pumping units if the water tank got too full.

The water injection line was a 3.8 cm (1.5 inch) i.d. fiberglass pipe rated to 13.8 MPa (2,000 psi). The connections were threaded with double O-rings as part of the threaded end of each 9-m (30-ft) length of pipe. Between the pump house and RG-5, approximately 760 m (2,500 ft) of water injection line is in place.

Figure 16 Well and pump controls in the Sugar Creek pump house. The four gauges (bottom row, red boxes with circular displays) regulate pressure and water levels in the injection pump, water supply well, and water tank. The three red boxes in the top row contain electronic motor controllers.

The water injection pump was a triplex pump type B-323, size 6.4 × 7.6 cm (2.5 inches × 3 inches), manufactured by Wilson-Snyder Works. (The maximum plunger size and fixed stroke are 2.5 inches and 3 inches, respectively; at Sugar Creek, the plungers were 4.45 cm [1.75 inches], less than the maximum). Water entered the injection pump and exited through one of three filter lines. One line went to RG-5 and another to PZ-2. These lines passed through medium-flow Nowata Filtration liquid filter housings (Model 2AH-S12C), each containing 12 cartridges. Maximum working pressure on these housings was 9.93 MPa (1,440 psi). The pressure of the water immediately upstream of the inlet was measured by a mechanical pressure gauge, and pressure of the fluid downstream of the outlet was measured by an electronic MC-II flow analyzer from Halliburton Services and measured again by a mechanical gauge before entering the ground. The third filter line passed through a larger Nowata housing on its way to the injection wells in the south part of the field (WT-7, EL-2, and BM-2). This filter housing also had a maximum operating pressure of 9.93 MPa (1,440 psi). There was a mechanical pressure gauge attached to the filter housing, a Halliburton MC-II flow analyzer downstream of the filter system, and a Lenz mechanical pressure gauge further downstream toward the injection wells.

PILOT SITE DESIGN AND WELL ARRANGEMENT

The RG-5 waterflood "pattern" is not a regular pattern (e.g., a 5-spot pattern) but an area flood with eight oil-producing wells immediately surrounding the water injection well. Although there were questions regarding the connectivity of the Wilbur-Todd wells to the east, all wells immediately adjacent to RG-5 were considered as part of the floodable part of the pilot. Three of the four wells surrounding the immediate pilot area were instrumented with pressure monitoring equipment.

In preparation for liquid CO_2 in transit to the site and on location, emergency medical service providers in the area were contacted to discuss the project scope and operations. This provided information to local officials that could provide answers to questions from the community and increase their preparedness in the case of an emergency. Maps of the oil field and a summary of project operations were given to local first responders (e.g., fire and emergency medical services).

Returning Wells to Production

With the exception of PH-1, all of the oil-producing wells surrounding RG-5 were active at the time the oil field was chosen for the pilot. Well PH-1 had been temporarily abandoned in September 2004 due to its low fluid production and high water cut. Because of low reservoir pressure, the rods, tubing, and pump were left in the wellbore without a downhole packer.

It was desirable to have as much information about pre-CO_2 injection production rates for well PH-1 as possible. To return PH-1 to production, the rods and pump were pulled from this well. The pump was reconditioned, and routine maintenance was performed on the rocking beam pumping unit. Well PH-1 was returned to production on March 1, 2009.

Observation Wells

In order to detect out-of-pattern migration of CO_2, observation wells immediately outside of the pilot area were desired. At the RG-5 site test site, there were four wells immediately offset to the oil producing wells: PB-2 and PB-3 to the west, PZ-1 to the northeast, and JR-1 to the southwest (Figure 3). All of these wells were temporarily abandoned and were available for monitoring the CO_2 pilot test. Due to budgetary constraints and its proximity to the CO_2 injection well, well PB-2 was not instrumented as an observation well. However, as part of routine oil field procedure, its surface tubing pressure was periodically measured and logged.

The observation wells all had tubing and packers inside the casing. JR-1 had fluid to the surface, while PB-3 and PZ-1 had fluid levels several hundred ft below surface. (Fluid levels of each well were determined during the pre-CO_2 injection cased hole well log runs.)

Well Preparation

In spring 2009 during preparation for the pre-CO_2-injection cased-hole logging runs, the rods, pumps, and tubing of pilot area wells were pulled. (RG-5 was logged through the tubing.) After the logging runs were completed, a downhole assembly designed for CO_2 and relatively higher gas rates was installed. Excessive gas entering the pump may lead to valves not opening and closing properly and pumping action failure of the pump. This failure, commonly called gas-locking, can require intervention at the surface or a well workover that entails pulling the rods and pump from the well.

The downhole assembly consisted of a 2.54-cm (1-inch) gas anchor at the bottom of the tubing and a 7.3-cm (2⅞-inch) mud anchor placed at the bottom of the pump (Figure 17). These anchors are designed to separate gas from liquid at the bottom of the wellbore prior to fluids entering the ball and seat arrangement of the insert pump. (In anticipation of higher gas rates, the 6.03-cm [2⅜-inch] mud and gas anchors were replaced with 7.3-cm [2⅞-inch] diameter anchors.)

Each well's Harbison-Fischer insert pump was a two-stage, hollow rod pump with 4-cm (1.5-inch) i.d., a 2.4-m (8-ft) barrel, and a 0.9-m (3-ft) plunger. Special stuffing boxes adapted for higher gas rates were considered for this project. For budgetary reasons, it was decided to wait until there were field indications that they were required. No problems occurred with the existing stuffing boxes, and stuffing boxes specifically designed for CO_2 service were not required.

Except for well RG-5, the existing rods and tubing were run in each well. New tubing was acquired for CO_2 injection at RG-5. Plastic-lined tubing was used for water injection, and unlined steel tubing was selected for use during CO_2 injection. The chosen packer was the same AD-1 type packer used for water injection; however, the 60-durometer elastomer used during water injection was replaced with a harder rubber element, 80-durometer.

Wells RG-1, RG-4, PH-1, and WT-8 were acidized prior to injection. A 1,900-L (500-gallon) treatment of 10% xylene and 15% HCl was used. No other wellbore cleanouts or stimulations were performed prior to CO_2 injection.

To measure casing gas production at individual wells, gas meters were placed at the end of a short length of pipe (visible in Figure 18). On this run was a Baker SPD aluminum bronze inline choke valve with a 1.3 cm (½ inch) choke (Figure 19) that could be used to regulate gas pressure or to shut-in the casing gas temporarily. Maximum pressure of the choke was 25.53 MPa (3,705 psi), and maximum orifice diameter was 1.7939 cm (0.70625 inch).

The gas meter used was a Teledyne Merla orifice well tester. Gas rate is calculated from calibrations from the manufacturer. The calibrations are a function of the orifice plate size and the pressure upstream of the well tester; each wellhead was instrumented with an electronic pressure gauge to calculate flow rate. These pressure gauges also were used to monitor pressure changes caused by the breakthrough of CO_2 at individual wells during active CO_2 injection. The orifice plate size chosen for each well was based on the pressure caused by the reduction in flow rate of the plate. In order to protect the casing, pressure less than 688 kPa (100 psi) was desirable. (Additional information on pressure gauges and metering is in the data acquisition equipment and wellhead design subsections of the Injection Operations section.)

Tank Battery Adaptations

In the Illinois Basin, crude oil production has very little associated gas production, and most gas is vented to the atmosphere at the wellhead or the stock tanks. An important aspect of CO_2 sequestration and EOR is accurate accounting of the CO_2 produced from an oil field. Because the casing annulus of the producing wells is open to the atmosphere, CO_2 at the individual wells may be separated from the reservoir fluids (oil and water) near the bottom of the wellbore and produced at the surface from the casing-tubing annulus. The CO_2 that remained dissolved in the oil and water at the bottomhole pressure and temperature was produced through the tubing and pumped through the production flow lines to the tank battery.

To measure the CO_2 at the tank battery, a Waterford Tank and Fabrication gas-liquid separator was placed in series upstream of the gun-barrel style oil/water separator. The separator had a maximum allowable work-

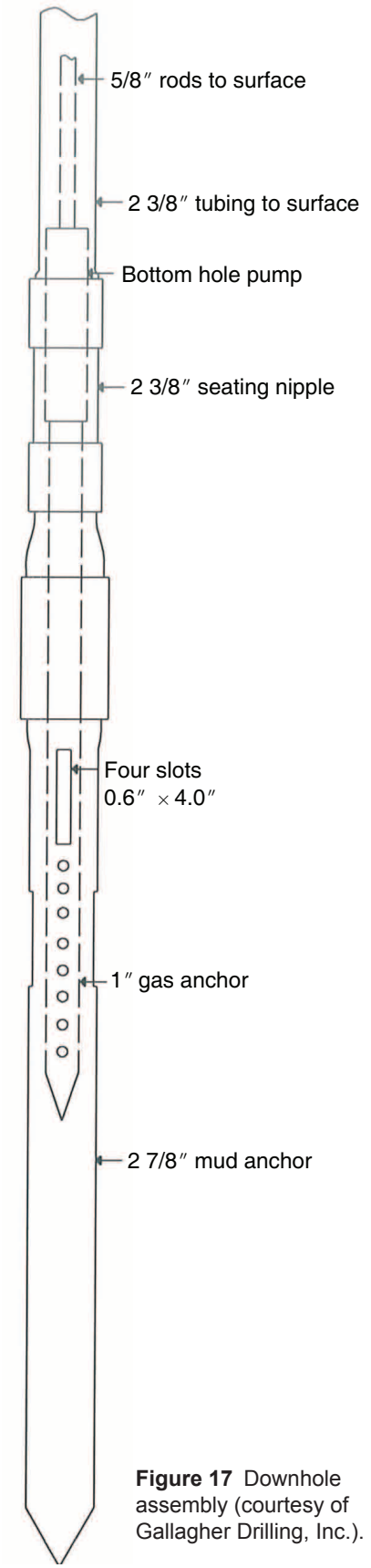

Figure 17 Downhole assembly (courtesy of Gallagher Drilling, Inc.).

Figure 18 Partial view of surface wellhead at RG-4; gas meter is visible (short aluminum pipe at lower left).

Figure 19 Baker SPD inline choke valve used to regulate gas pressure and temporarily shut-in well during routine gas sampling.

ing pressure of 1.72 MPa (250 psi) at 93°C (200°F) and a minimum design metal temperature of −29°C (−20°F) at 1.72 MPa (250 psi). A U-bend of pipe was connected to the top of the separator. This pipe connected to a horizontal gas pipe that allowed collection of gas samples, monitoring of gas pressure, and metering and venting of gas. A Kimray cast-iron back-pressure gas regulator, located at the proximal end of the gas pipe (red apparatus on pipe in Figure 20a), sets pressure at 138 kPa (20 psi), as measured by a mechanical gauge. If pressure exceeds this value, the gas regulator opens to vent gas through the well tester (aluminum colored device at the distal end of the pipe, Figure 20b, right side of photo). An electronic pressure gauge (left side of Figure 20b, adjacent to gas regulator) is also used to measure pressure at the distal end of the gas regulator. The 0.64-cm (¼-inch) ball valve on the well tester was included for gas sampling and field measurements of gas composition. (The Siemens pressure transducer shown in Figures 20a and 20b was used to calculate the gas flow rate through the well tester at the gas-liquid separator.)

No gas metering or detection equipment was placed on the oil or water stock tanks.

Chemical Corrosion Treatment Plan

As part of the routine field operations at Sugar Creek, batch chemical corrosion treatment pots were permanently installed on each well for regular chemical treatments for brine-related corrosion and scale (Figure 21; chemical treatment pot). Chemicals are added to the pot while it is isolated from the rest of the tubing and production equipment. The assembly is plumbed so that produced fluids from the tubing are diverted through the chemical pot by opening and closing three ball valves. The produced fluids flush the specific chemicals from the pot and into the tubing-casing annulus where they fall to the bottom of the wellbore and are pumped to surface to coat the pump, rods, and inside of the tubing. The rod pump operates during this treatment, and the chemicals are circulated continuously with oil and brine for about six hours every two weeks.

In addition to the existing chemical treatments to inhibit CO_2-related corrosion, Baker Hughes CRO195 was chosen for its ability to provide excellent corrosion protection from CO_2 and H_2S on downhole production equipment. After completion of the batch treatment, any residual chemical that makes it back to surface will further protect steel flow lines and the tank battery.

Prior to this CO_2 pilot, the produced fluids were treated with de-emulsifying chemicals to prevent oil-water emulsions at two different locations within the field. The de-emulsifying chemical Tretolite DMO5060 was administered continuously at 2 L (0.5 gallons) per week. Small Texsteam chemical injection pumps are actuated by the pumping units at two different well sites. A galvanized lever arm attaches to the box assembly and pump, and this arm connects to the well pumping unit so that each stroke of the well pumping unit also strokes the chemical pump. The chemical flow line starts submerged in a chemical drum and leads to the chemical pump (Figure 22; the smaller box contains the pump, and the larger box contains the chemical). The chemical enters the production flow line and commingles with the other wells' production in the flow line network. Positioning the treatment at two different wells provided de-emulsifier chemicals at optimal locations to treat most of the oil prior to its entering the tank battery. The de-emulsifying chemical treatment continued during the CO_2 injection pilot.

Pre-injection Reservoir Modeling

As part of the site selection process, a simple geologic model was used for reservoir modeling to provide general design specifications such as CO_2 injection rate; CO_2, oil, and water production rates; injection pressure; CO_2 distribution; and time to CO_2 breakthrough. The model covered 1.6 million square meters (16.9 million ft^2) or 388 acres. The top of the model was assigned a constant elevation of –419.1 m (–1,375 ft) (i.e., 419.1 m [1,375 ft] below msl) and was based on average elevation of the top of the Jackson taken from the geophysical well logs. The grid had 40 cells in the x-direction, 66 cells in the y-direction, and 2 cells in the z-direction. Each cell was 11 m × 11 m × 1.5 m (80 ft × 80 ft × 5 ft). Permeability and porosity values were based on core data and field performance and assigned values of 2.5×10^{-10} cm^2 (25 mD) and 18%. Based on general Mississippian reservoir trends, the vertical to horizontal permeability ratio (k_v/k_h) was set at 0.84.

Figure 20a Liquid-gas separator (left) with back-pressure regulator (center right) and Siemens pressure transducer (blue cap to right).

Figure 20b Electronic Siemens pressure gauge (blue cap) and Teledyne Merla orifice well tester (aluminum pipe to right) attached to the liquid-gas separator (out of picture, at left) at tank battery.

Figure 21 Wellhead at well RG-3; the batch chemical corrosion treatment pot is visible. Top photograph: Treatment pot is tall cylindrical object on far left of wellhead, to left of pumpjack, in front of pole. Bottom photograph: Close-up of treatment pot.

Figure 22 Texsteam chemical injection pump (green box) and chemical box (stainless steel) at RG-4 well.

The general MGSC Illinois Basin oil field reservoir model was used with the simple geologic model. CO_2 injection rates of 7 to 12 tonnes (8 to 13 tons) per day or 4 to 5.7 million scm (140 to 200 million scf/d) and 5 to 7 months until CO_2 breakthrough were projected. The reservoir model suggested that 5,000 to 7,000 tonnes (6,000 to 8,000 tons) of CO_2 followed by water injection would be required to cause a measureable oil production response in some of the offset wells. Consequently, contingent plans were made to have up to three wells converted to CO_2 injection. Injection of CO_2 followed by water was not likely to influence oil production at wells WT-4, WT-8, or WT-9 because of the relatively greater distance between these wells and RG-5. At peak oil production, an increase in oil production of 0.8 to 1.6 scm/d (5 to 10 stb/d) was projected based on model results.

CO_2 UIC II Injection Permit

Well RG-5 was previously permitted as a water injection well (UIC Class II) with the U.S. Environmental Protection Agency (USEPA) Region 4. It was permitted at 31.8 m^3 (200 bbl) of water per day at 9.31 MPag (1,350 psig) surface injection pressure. Because CO_2 density is less than brine density, for this project an application was made to USEPA Region 4 to increase the surface pressure that would correspond to the same bottomhole pressure. The existing bottomhole injection pressure for water was 14.88 MPag (2,158 psig). For injecting the less dense CO_2, an increase in the surface injection pressure to 9.818 MPag (1,424 psig) was requested and approved. A copy of the permit is in Appendix 1.

GEOLOGIC CHARACTERIZATION

Area Geology

Surface Geology

As shown in the Madisonville West and Saint Charles Geologic Quadrangles (Kehn, 1964; Palmer, 1967), bedrock exposed at the surface in the Sugar Creek area consists of sandstone, shale, and coal of the Pennsylvanian Carbondale Formation (Figure 23). The Pennsylvanian strata dip gently to the north-northeast at less than one degree. The upper part of the Carbondale Formation includes the No. 9 and No. 11 coals, which were extensively mined in the area, as evidenced by the large surface-mined areas north of the Sugar Creek site. The only notable structural features in the area include a series of southwest to northeast trending dip-slip faults that have offsets on the order of tens of feet.

Bedrock

Sugar Creek Field is located in the southeastern part of the Illinois Basin, an intracratonic basin that contains up to 4,900 m (16,000 ft) of Paleozoic strata. With the exception of some major fault zones (e.g., Rough Creek, Wabash Valley), the strata dip gently toward the Basin center. The Paleozoic strata consist primarily of dolostone and smaller, but still significant, amounts of sandstone, limestone, shale, and coal (Buschbach and Kolata, 1990).

General Site Hydrology and Hydrogeology

Hydrology As mapped on the Madisonville West and Saint Charles Geologic Quadrangles (Kehn, 1964; Palmer, 1967), two perennial streams, Richland Creek and Sugar Creek, are present within a 1.6 km (1 mile) radius of the injection well, RG-5. Richland Creek is approximately 1.6 km (1 mile) southwest of the injection well, and Sugar Creek is approximately 1.4 km (0.87 mile) east of the injection well. There are numerous intermittent tributaries of Richland and Sugar Creeks mapped within a 1.6 km (1 mile) radius of the injection well. In addition, numerous farm ponds were mapped within a 1.6-km (1-mile) radius of the injection well, and two ponds were within 0.4 km (0.25 mile) (Figure 24).

Hydrogeology Because no water wells are located within the Sugar Creek EOR site, records from 26 oil and gas wells located within a 0.8 km (0.5 mile) radius of the injection well were used to assess the local hydrogeology (Figure 24). Each well and the type of available log (drillers' log or wireline log) are listed in Table 5. Copies of drillers' logs for wells listed in Table 5 are presented in Appendix 2.

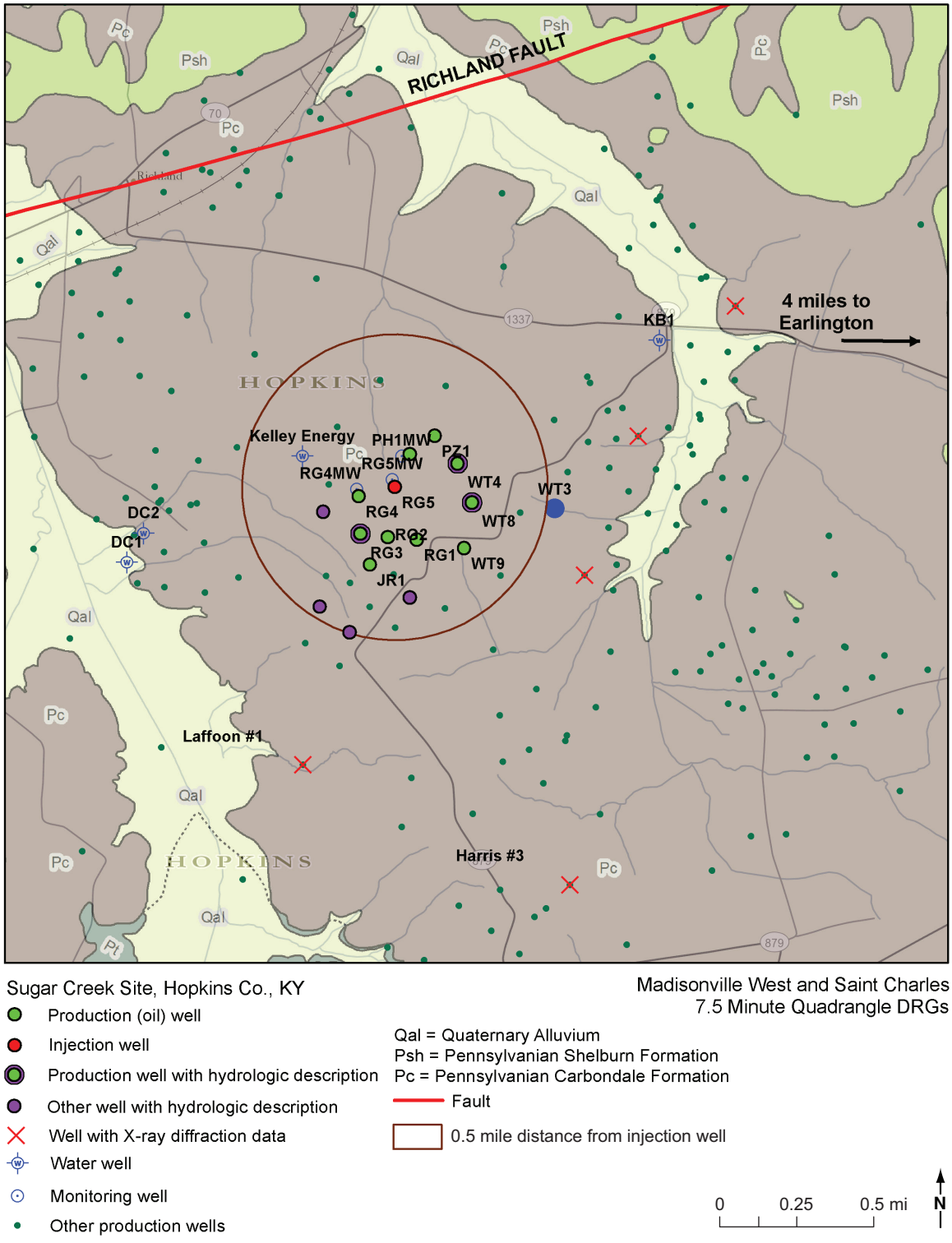

Figure 23 Map of oil and gas wells located within a 0.8-km (0.5-mile) radius of the injection well RG-5 (red circle); water wells in the area; and wells that yielded rock samples for x-ray diffraction. Bedrock geology of the area is also shown.

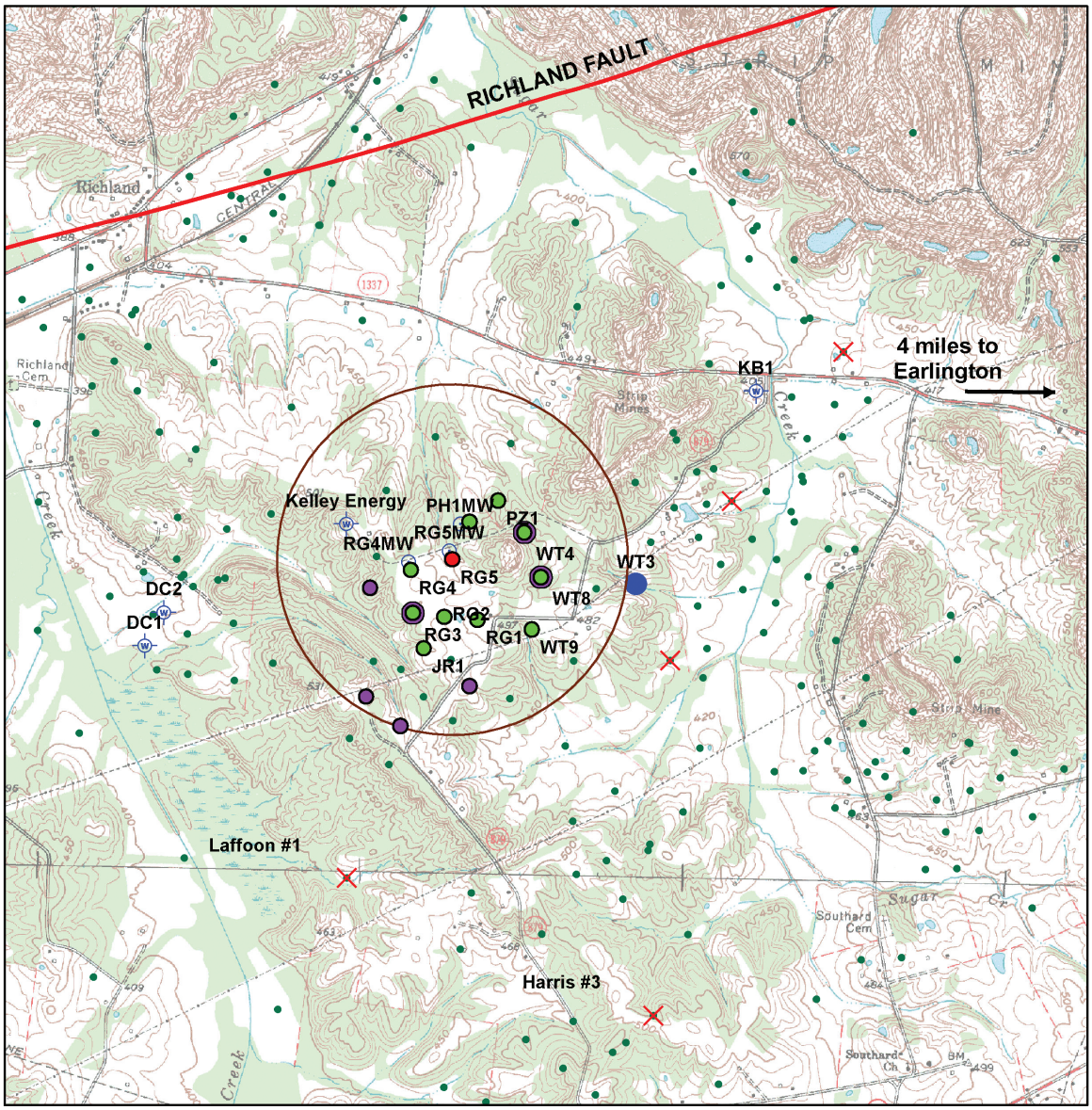

Figure 24 Map showing the topography and hydrology of the Sugar Creek Field area, including all shallow groundwater wells, ponds, and creeks.

Table 5 Oil and gas wells located within a 0.8-km (0.5-mi) radius of the injection well, RG-5. Permit numbers and other records are from the KGS oil and gas online database (http://kgs.uky.edu/kgsweb/DataSearching/OilGas/OGSearch.asp).

Permit no.	Well no.	Farm name	Original operator names	Total depth (ft)	Driller's log	Wireline log
10853	1	Pressley	Sargent	2,338	yes	yes
11673	1	Watson	Zogg	1,864	yes	yes
11986	1	Gentry	Mullenax	2,275	yes	yes
12241	1	Laffoon	Zogg	1,869	yes	no
12298	1	Stanhope	Mitchell	1,880	yes	no
12397	1	Rickard	Tuttle	1,859	yes	yes
12409	2	Watson	Zogg	1,974	yes	yes
12468	1	Marquess	Tuttle	1,878	yes	yes
12620	2	Gentry	Mullenax	1,891	yes	yes
12697	2	Stanhope	Mitchell	1,850	yes	no
12783	3	Gentry	Mullenax	1,868	yes	yes
12985	2	Bowles	Tuttle	1,850	yes	no
12986	2	Marquess	Tuttle	1,838	yes	no
12987	2	Rickard	Tuttle	1,866	yes	no
13693	2	Laffoon	Zogg	2,265	yes	yes
13864	4	Gentry	Mullenax	1,892	yes	yes
14041	5	Gentry	Mullenax	1,880	yes	yes
14342	1	Pressley	Zogg	1,894	yes	yes
14513	3	Bowles	Tuttle	1,879	yes	no
14514	4	Todd	Zogg	1,912	yes	yes
14578	1	Pressley	Hart	1,886	yes	no
20186	6	Todd	Zogg	2,170	yes	yes
20270	7	Todd	Zogg	2,209	yes	yes
57326	2	Pressley	Zogg	2,360	yes	yes
95402	8	Todd	Gallagher	1,942	yes	yes
99990	9	Todd	Gallagher	1,894	yes	yes

Most of the 26 listed drillers' logs indicate that there are sandstone units (potential aquifers) of various thicknesses distributed between 0 and 110 m (0 and 370 ft) below land surface. These references generally are recorded as "sand and shale." Seven drillers' logs specifically reference the presence of groundwater (Table 6). Four of these seven wells are oil production wells associated with this project. Data from these seven logs indicate that groundwater may be present at several intervals between 30 and 110 m (90 and 370 ft) below land surface. There are no data available on groundwater quality for the waters associated with these intervals. Some groundwater production data are available, but they are estimates and are considered less reliable (Table 6).

Table 6 Hydrogeologic descriptions taken from drillers' logs listed in Table 5. The volume of a bailer is approximately 160 L (42 gallons). Permit numbers and other records are from the KGS oil and gas online database (http://kgs.uky.edu/kgsweb/DataSearching/OilGas/OGSearch.asp).

Permit no.	Well associated with project	Distance from injection well (ft)	Direction from injection well	Interval (ft)	Hydrogeologic description
11673	WNA[1]	2423	SW	6–20 120–138 155–160 232–250 250–275	Sand Sand (1/2 bailer/hour) Sand Sand (5 bailers/hour) Sand (HFW)
12241	WNA	2,604	SW	7–35 115–143 155–165 210–307	Sand Sand Sand (WD) Sand (HFW)
12468	WNA	1,922	S	115–150 320–344	Sand Sand
12783	RG-3	948	SW	150–340 340–375	Sand and shale Sand (water)
12985	PB-2	1,285	WSW	90–128 218–300	Sand (making some water) Sand (HFW)
14514	WT-4	1,132	ENE	15–75	Hard sand
95402	WT-8	1,338	ESE	280–370	Sand (water)

[1] Well not associated with project.
[2] HFW, hole full of water; WD, well makes enough water to drill with.

A water-supply well, WT-3, used to supplement the oil field brine water injection is located approximately 823 m (2,700 ft) east of the injection well (Figure 23). According to the Kentucky Division of Oil and Gas Completion Report, well WT-3 was initially drilled as an oil well to a TD of 474 m (1,555 ft), back-plugged to 281 m (922 ft), and then converted to a water-supply well. Well WT-3 was perforated at the following intervals: 83.5–86.6 m (274–284 ft); 171–174 m (562–572 ft); 187–190 m (614–624 ft); 202–205 m (662–672 ft); and 241–250 m (790–820 ft), which are assumed to correlate with various unnamed Pennsylvanian sandstones. Groundwater quality samples collected from well WT-3 as part of this project's deep aquifer monitoring program have a low total dissolved solids (TDS) concentration (940 mg/L). Previously collected groundwater quality data are not available, and production rates are unknown.

Using the KGS Water Well and Spring online database (http://www.uky.edu/KGS/water/research/gwreposit.htm), one water well, well 004, was identified within a 1.6 km (1 mile) radius of the injection well (Figure 24). Well 004 was completed in a 9-m (30-ft) thick sandstone aquifer, which ranges in depth between 41.1 and 50.9 m (135 and 167 ft) below land surface. The well was reported by the driller to produce 190 L (50 gallons) per minute. Groundwater quality data are not available for the Kelly Energy well, well 004. An attempt to inspect and gain access to well 004 was made, but the well owner was not cooperative. No springs were found within a 1.6-km (1-mile) radius of the injection well. The KGS online database does indicate that there are recently-constructed (post-1990) water wells outside of the 1.6 km (1 mile) radius. According to digital orthoimagery, these wells are associated with poultry farms. Data from these wells were not included because they were considered to be too far from the injection site.

In an attempt to identify and locate additional water wells within the 1.6-km (1-mile) radius of the injection well, house-to-house well reconnaissance was conducted on February 13, 2009. Interviews with landowners revealed the location of two abandoned hand-dug wells within 0.8 km (0.5 mile) of the injection well, one abandoned domestic well, and two livestock wells within 1.6 km (1 mile) of the injection well (Figure 24). Both hand-dug wells were not in use and were not accessible. Specific information pertaining to the

two hand-dug wells is not known. The abandoned domestic well, KB-1, has a total depth of 39.9 m (131 ft) and produces 8–11 L (2–3 gallons) per minute (personal communication with well owner). Both livestock wells, DC-1 and DC-2, are approximately 57 m (187 ft) deep and produce approximately 76 L (20 gallons) per minute (personal communication with well owner). Wells KB-1, DC-1, and DC-2 were sampled during this project as part of the shallow-aquifer monitoring program. Groundwater quality results indicated that groundwater associated with these wells was low in TDS (300 to 800 mg/L). Prior to this sampling, groundwater quality data were not available for wells KB-1, DC-1, and DC-2.

Preliminary oil and water well data indicate that there are underground sources of drinking water (USDWs) within a 1.6 km (1-mile) radius of the CO_2 injection well. The depth of these USDWs ranges from possibly 27–250 m (90 to 820 ft) below land surface, which is over 300 m (1,000 ft) from the Jackson sandstone. Prior to groundwater sampling conducted as part of this project, there was no groundwater quality data reported for water wells located within a 1.6-km (1-mile) radius of the injection well.

Reservoir Geology

Core Analyses

No physical cores or samples were available for study at the beginning of the pilot. However, the field operator provided 13 core analyses from 13 different wells in the Sugar Creek oil reservoir. Geophysical logs were available on four of the 13 wells with core analyses. The overall mean porosity and permeability from the core analyses for the Mississippian Jackson sandstone was 15.3% and 1.57×10^{-10} cm^2 (15.9 mD) respectively. When samples taken from non-reservoir intervals (i.e., permeability $< 1 \times 10^{-12}$ cm^2 [0.1 mD]) were removed, the mean porosity and permeability increased to 16.0% and 1.85×10^{-10} cm^2 (18.7 mD).

Drill cuttings were not available for the central portion of the field specific to the pilot area, but for some wells on the outskirts of the field, cuttings were available and were used for x-ray diffraction (XRD) (see further explanation in MVA Methods section).

Log Analyses

Geophysical logs from 37 wells were available to study; 21 wells penetrated the target reservoir for the pilot; the rest either penetrated unconnected reservoirs surrounding the pilot area or contained impermeable sandstone or shale. The majority of the wells were drilled in 1964 and 1965 and, with the exception of two recently drilled wells, the log suites consisted of the SP, the 16-inch short normal, the 64-inch long normal, and the 18 ft, 8 inch lateral logs. The two recent wells had an induction package only. There were no porosity logs available. The average TD of all the wells in the field was 621.8 m (2,040 ft). Many of the wells did not log the entire reservoir interval, which complicated the geologic modeling.

Conceptual Geologic Model

In addition to the data just described, the conceptual geologic model was based on mapping and cross sections digitally constructed using Landmark Corporation's Geographix® software. Formation tops for the Jackson sandstone were picked, and a structure contour map (Figure 25) was generated. Reservoir thickness data was collected, and isopach maps for the Jackson sandstone (Figures 26 and 27) were constructed. Cross sections were constructed using the geophysical logs, and formation tops above and below the Jackson sandstone were correlated (Figures 28 and 29). The base of the Golconda limestone, a regionally continuous limestone that lies above the Jackson, was used as a correlative stratigraphic reference in the cross sections. The structure map (Figure 25) demonstrates a monoclinal structure with a 1-degree dip into the basin toward the north. The isopach map in Figure 26 shows the gross thickness of the Jackson sandstone (average thickness 3.4 m [11 ft]). Figure 27 is a net isopach map showing the thickness of the 50% or greater clean sandstone (average thickness 1.5 m [5 ft]) within the field area. Thickness data for the 50% or greater clean sandstone were acquired from normalized SP logs. The shale baseline, or 0% clean sandstone, for normalizing the SP logs was established by using the consistently flat line of the shale between the Jackson sandstone and the Golconda Limestone. The 100% clean sandstone SP response was calibrated using sandstones with the greatest amount of SP deflection 30 to 46 m (100 to 150 ft) above or below the Jackson sandstone. When the 0% and 100% endpoints are used to calibrate the SP curve, the 50% clean sandstone can be established as that part of the SP curve that deflects to the left of the shale baseline one-half or more

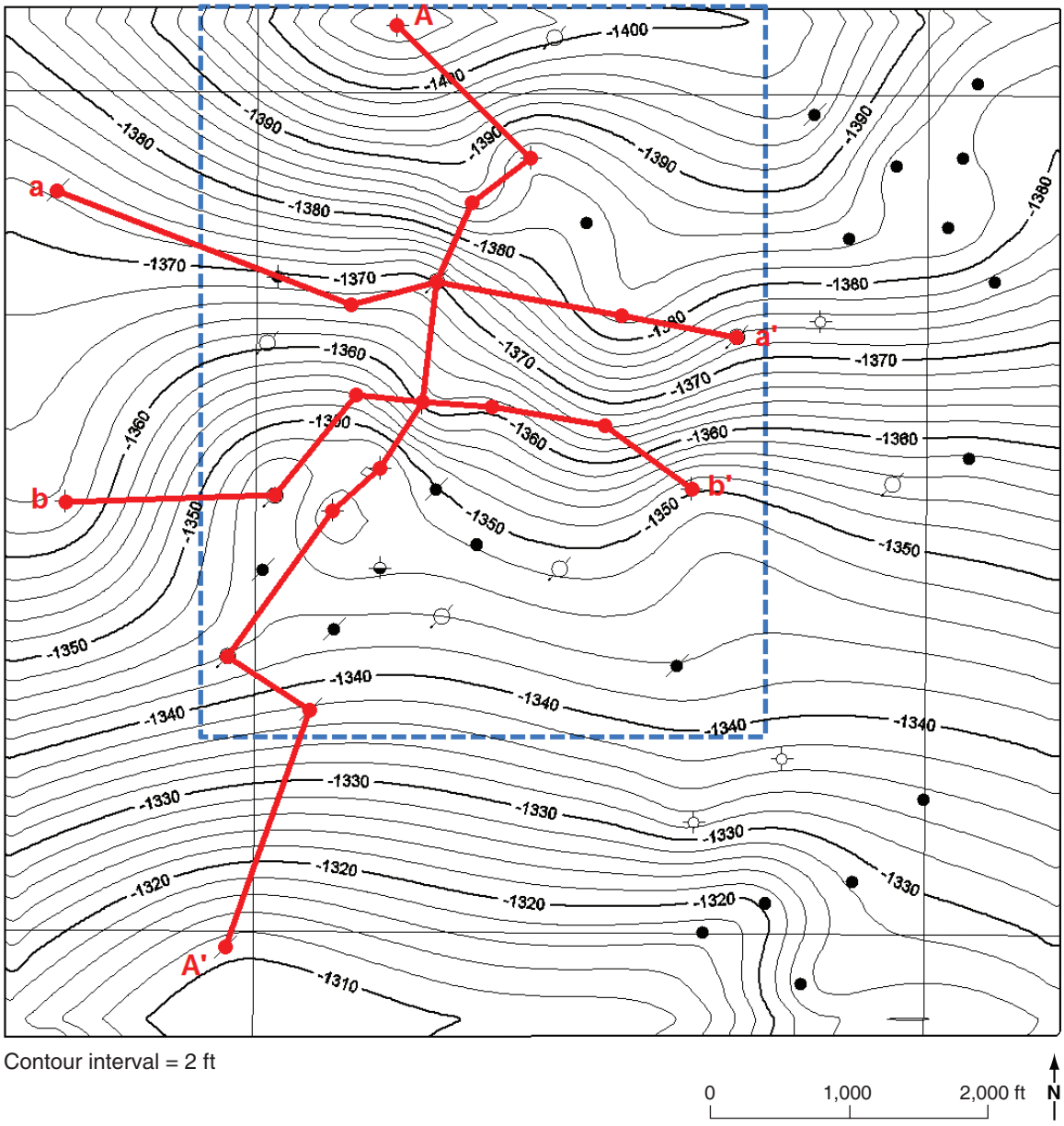

Figure 25 Structure map of the top of the Jackson sandstone. The blue dashed rectangle marks the boundaries of the geocellular model. The red lines and letters mark the traces of the cross sections in Figures 28 and 29.

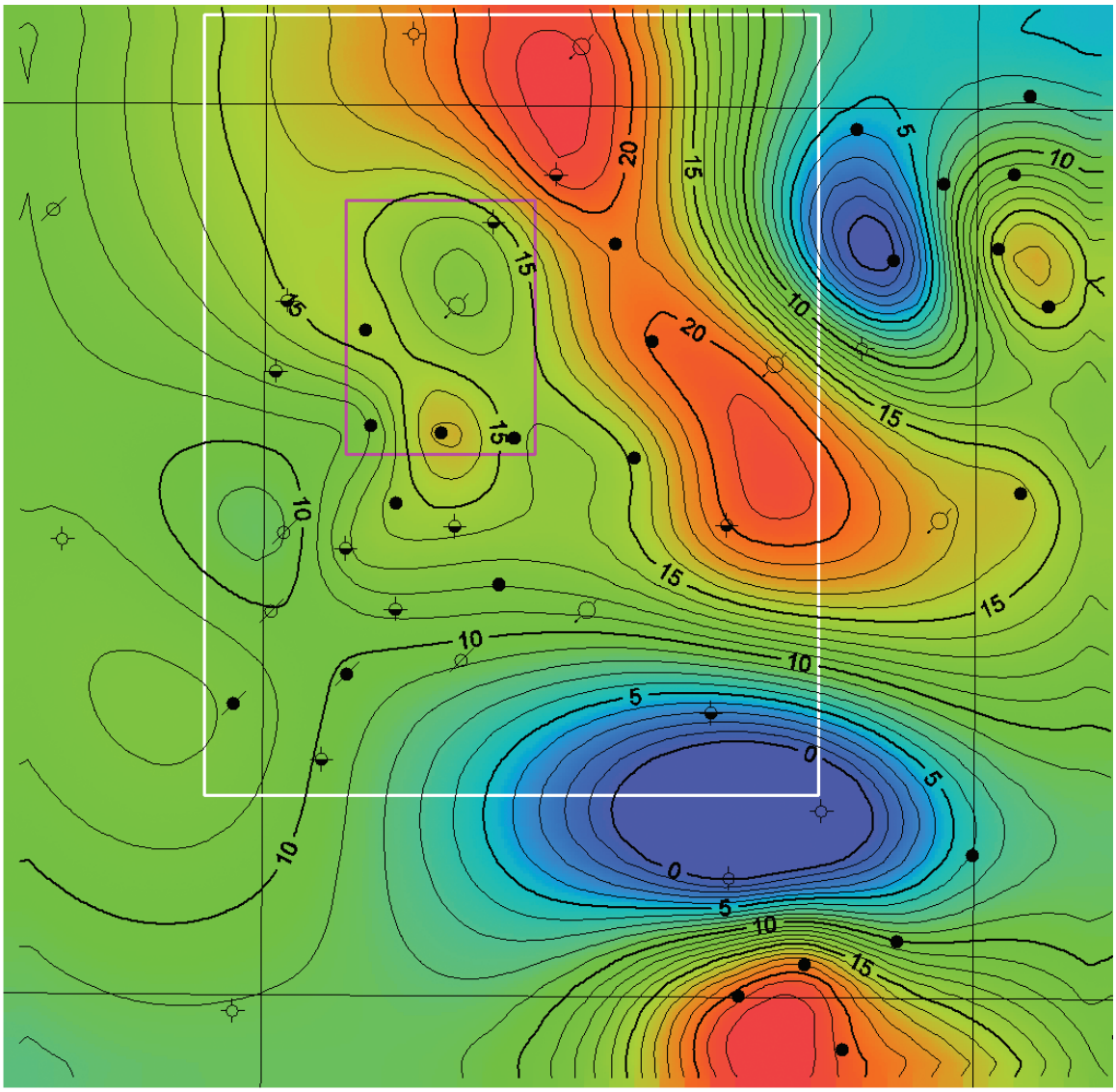

Figure 26 Map of the gross Jackson sandstone. The white rectangle marks the boundaries of the geocellular model, and the pink rectangle contains the injection well and the five closest producing wells.

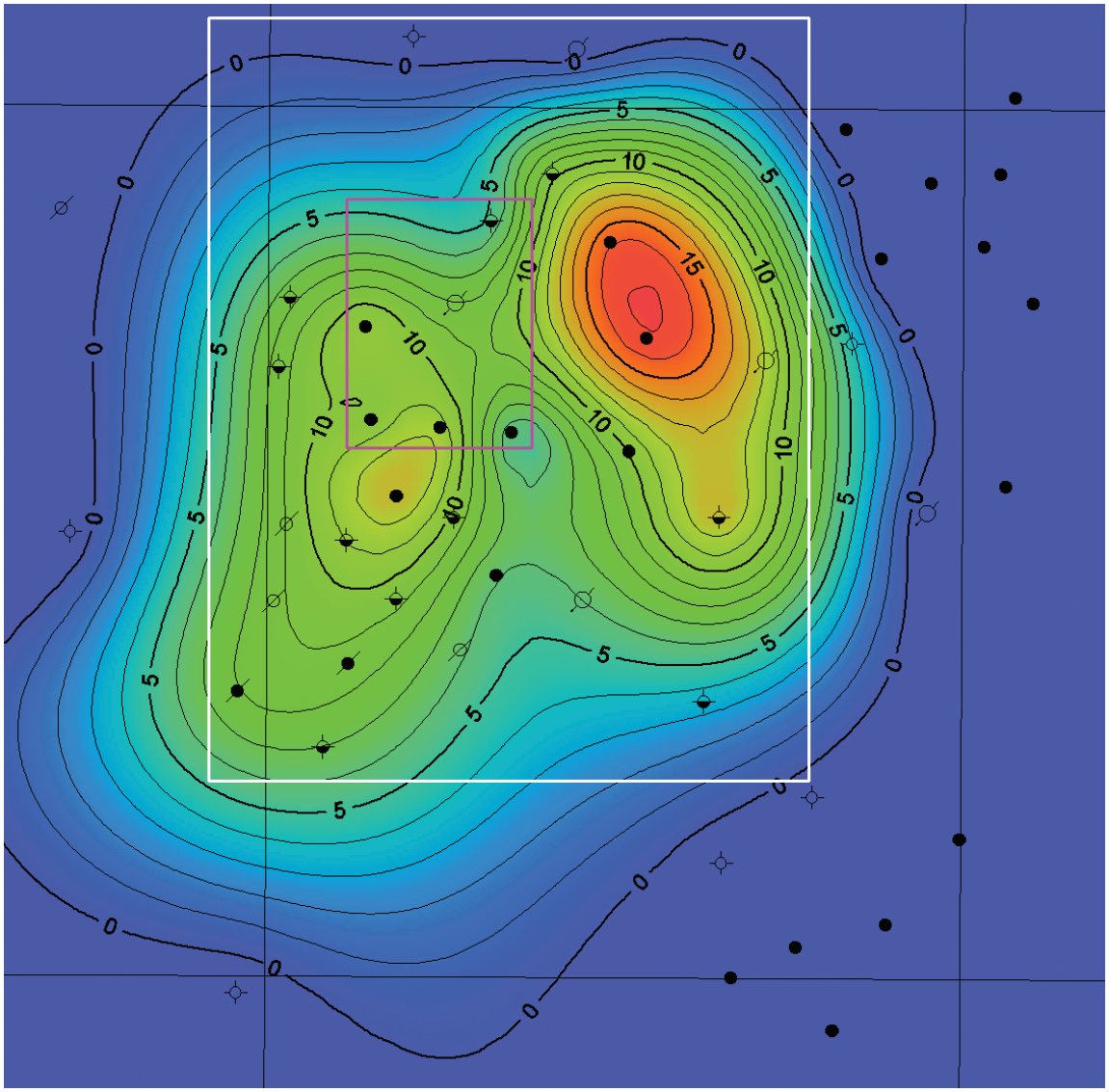

Figure 27 Isopach map of the Jackson sandstone showing the thickness of the 50% or greater clean sandstone. The white rectangle marks the boundaries of the geocellular model, and the pink rectangle contains the injection well and the five closest producing wells.

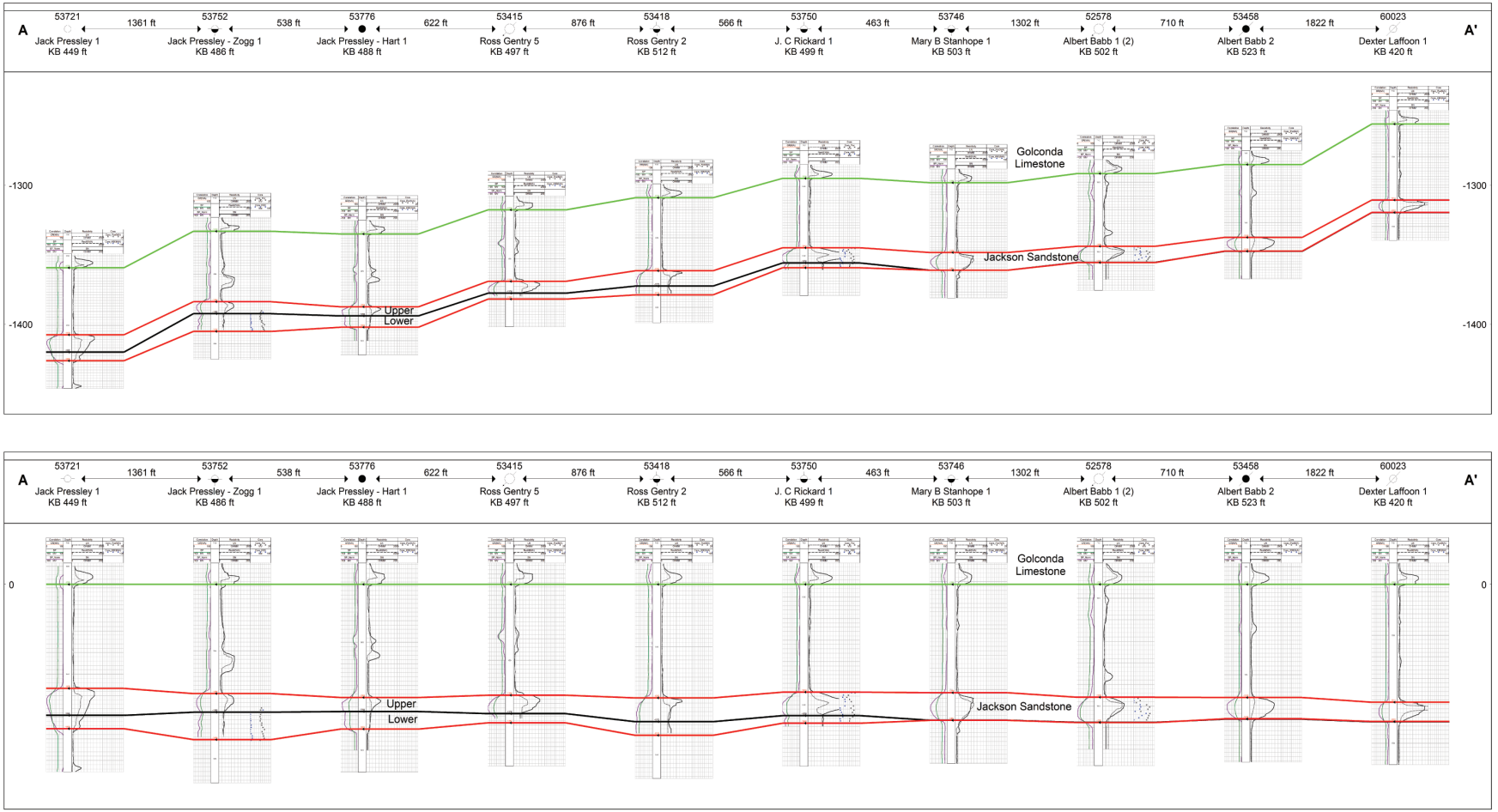

Figure 28 A north-to-south geophysical log cross section showing the unit of interest, the Jackson sandstone, and a reference unit, the Golconda Formation. The upper figure is a structural view, and the lower figure is a stratigraphic view with the Golconda serving as the origin. The top and base of the Jackson are marked by the red lines, and the base of the Golconda is marked by the green line. The boundary between the upper and lower units of the Jackson sandstone is marked by the thick black line. Abbreviation: KB, kelly bushing, a piece of equipment above ground elevation from which depth is measured. See Figure 25 for the location of the cross section.

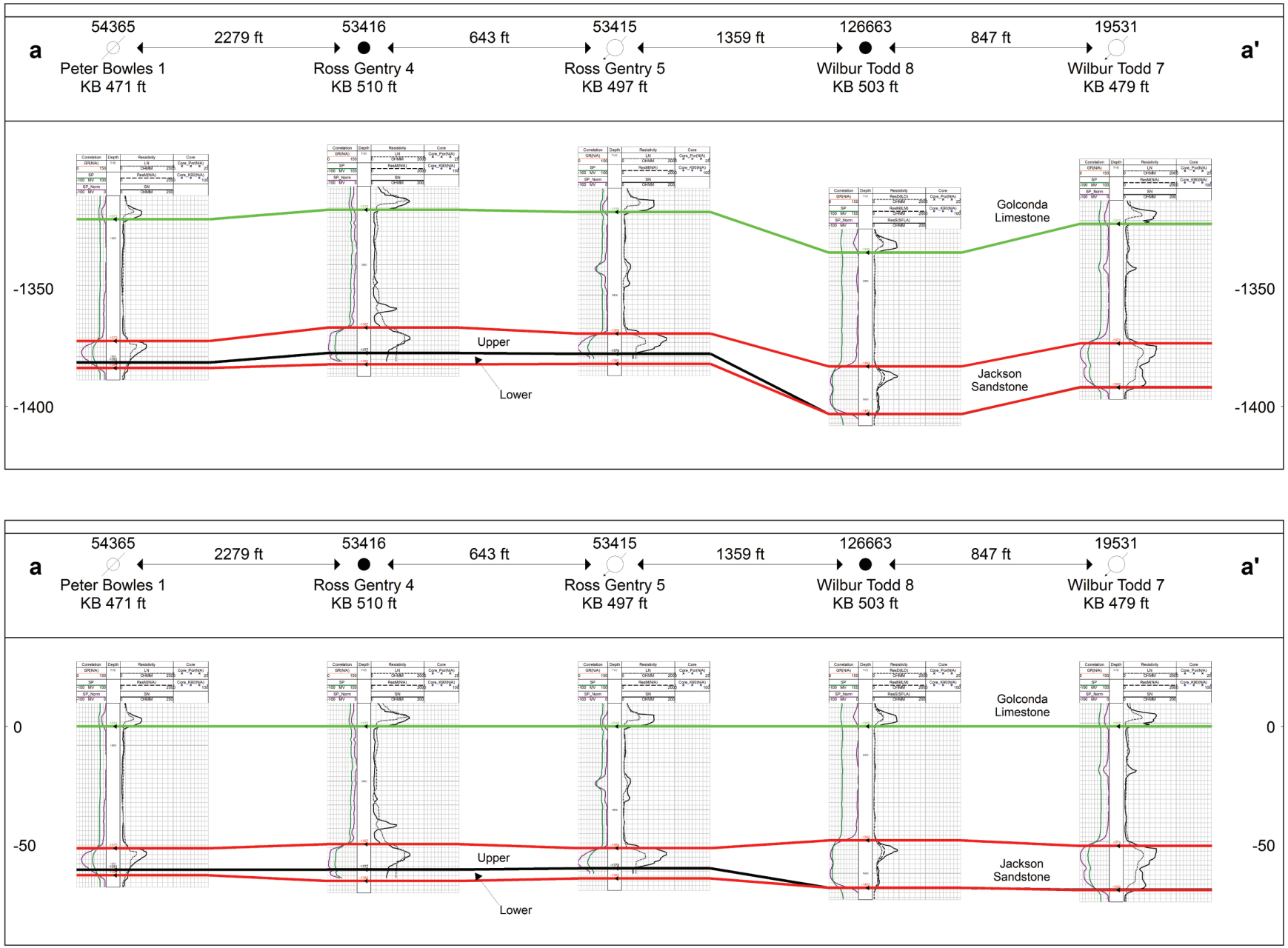

Figure 29 A west-to-east geophysical log cross section showing the unit of interest, the Jackson Sandstone, and a reference unit, the Golconda Formation. The upper figure is a structural view, and the lower figure is a stratigraphic view with the Golconda serving as the origin. The top and base of the Jackson are marked by the red lines, and the base of the Golconda is marked by the green line. The boundary between the upper and lower units of the Jackson sandstone is marked by the thick black line. Abbreviation: KB, kelly bushing. See Figure 25 for the location of the cross section.

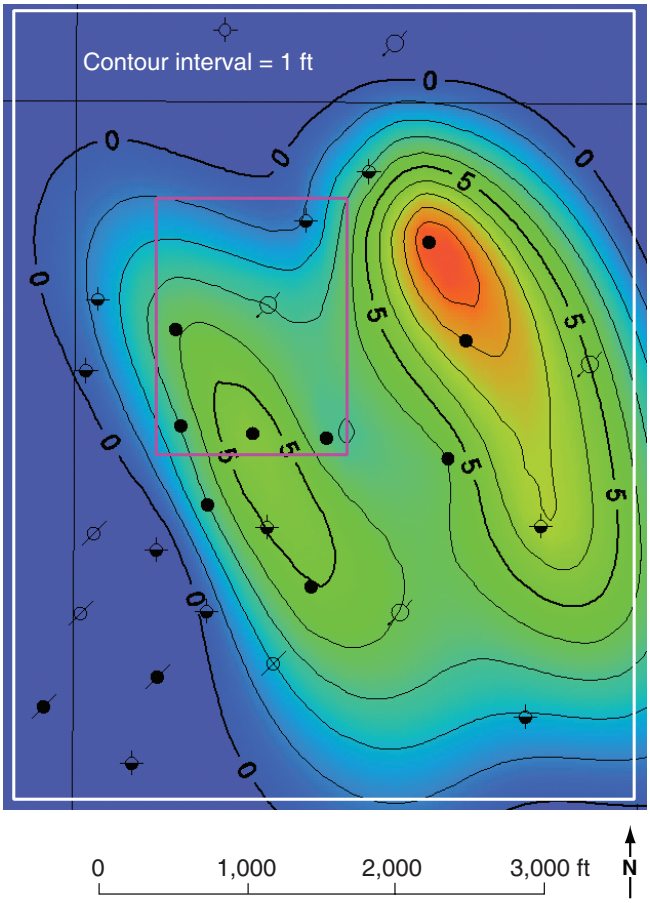

Figure 30 Isopach map of the lower portion of the Jackson sandstone showing the thickness of the 50% or greater clean sandstone. The white rectangle marks the boundaries of the geocellular model, and the pink rectangle contains the injection well and the five closest producing wells.

of the distance between the 0% and 100% endpoints. Basin experience indicates that reservoir quality sandstones must have normalized SP values greater than 50%. As shown in Figure 26, the Jackson sandstone continues to the north, where it becomes an aquifer, and to the west and south, where apparently the permeability decreases to the point that the sandstone is no longer reservoir quality.

From studying the geophysical logs' cross sections, it was noted that the Jackson sandstone is composed of upper and lower sandstones separated by a thin layer of shaly sandstone. Figure 30 is an isopach map of the 50% clean sand of the lower Jackson sandstone. These sandstones on the eastern side of the field tend to coalesce into a single layer. In addition, a layer of calcareous sandstone (~0.3 m [1 ft] thick) was also noted in both the core descriptions and the logs. This cemented sandstone tends to occur in the upper part of the Jackson sandstone and is commonly capped by a 0.3- to 0.6-m-[1- to 2-ft-] thick, porous, and permeable sandstone bed.

Whole core samples were not available for the interpretation of depositional environments for the reservoir in this field. However, the widespread distribution of the Jackson sandstone encapsulated in thick marine shales, the reservoir architecture, and the presence of sporadic, thin beds of carbonate-cemented sandstone indicate that the sandstone was deposited in a nearshore marine environment. The geometry and orientation of the sandstone bodies shown in the isopach map (Figure 30) are similar to tidal shoal deposits found in other Mississippian sandstone reservoirs in the Illinois Basin.

Although the oil in the field appears to be stratigraphically trapped, the trapping mechanism remains in question. Visual inspection of the log signatures of many wells outside the field shows that those signatures are identical to the sandstone signatures of wells inside the field. Although the logs indicated that the sandstone continues to the east, west, and south, none of these wells produced significant amounts of oil. In addition, the core analyses of non-productive wells on the edge of the field demonstrated a poor correlation between porosity and permeability; for example, analyses of samples from these wells can have non-reservoir quality permeability measurements of less than 5.0×10^{-11} cm^2 (5 mD), whereas measured porosities can be greater than 15%. Mississippian marine sandstones in the Illinois Basin commonly exhibit quartz overgrowths (Grube and Frankie, 1999), which reduce permeability, particularly within the pore throats, while maintaining porosity. These sandstones, therefore, have pore space, but blocked pore throats restrict the flow of oil.

A cursory inspection of the structure map (Figure 25) shows a general alignment of the contours east to west with regularly spaced intervals. The map also shows that production in Sugar Creek is associated with areas where the contours deviate from the trend and reflect subsurface deformation. This is also true of other nearby fields to the southeast and northeast. The association of oil production with these areas of deformation indicates that it is possible that permeability was enhanced by fracturing and faulting in these areas.

Geocellular Model

The approach to building the geocellular model followed a workflow that uses geostatistical methods to describe the heterogeneity of the reservoir. The workflow was developed during the course of preparing models for other EOR fields within the Illinois Basin and employs the geostatistical geologic modeling software Isatis® by Geovariance Corporation. The Sugar Creek model was developed using log suites that did not include modern neutron density or gamma-ray packages. Instead, the log suites consisted of normal/lateral resistivity logs and an SP log. Geostatistical modeling requires greater data distribution than that offered by the available core analysis data. Modern logs were not available, so the SP log was chosen as an indicator of reservoir quality because of its availability in the older log suites. The SP log correlates with porosity and permeability core data via a porosity-permeability-based transform. First, the SP logs were normalized using the process described in the previous section in order to produce a curve or value that was an approximate indicator of the percentage of sandstone relative to shale. The normalization process reduces well-to-well SP variation that results from fluid chemistry (electrical activity) and other borehole conditions. Geocellular models were built based on the normalized SP data, then the normalized SP values were converted into the desired petrophysical properties utilizing a transform equation relating permeability and porosity values to the normalized SP values.

The normalized SP values were used on a quantitative basis for the geostatistical analysis. After transforming the normalized SP data into a Gaussian distribution, the data set was used to create semivariogram maps and directional semivariograms, as shown in Figure 31. The semivariogram maps indicated a northeast-southwest trend of NE 15º. However, there is a secondary direction in the southeast-northwest direction that could be a reflection of the geometry of the shoal deposits. The models fitted to the semivariograms (Figure 31) had a range of 1,371.6 m (4,500 ft) in the northeast-southwest direction and a range of 1,066.8 m (3,500 ft) in the northwest-southeast direction. The semivariogram models used an exponential structure with a sill of 0.96. For the geostatistical model, a grid was built with a total volume of 1.70×10^7 m^3 (6.02×10^8 ft^3) and covering a surface area of 2.33×10^6 m^2 (2.51×10^7 ft^2) or 233.10 ha (576 acres). The grid initially consisted of cells with x and y dimensions of 12.19 m (40 ft) in the horizontal direction and 0.3048 m (1 ft) in the vertical direction. Later, the cell dimensions were increased to 24 m (80 ft) in the horizontal direction and 0.61 m (2 ft) vertically, with 56 cells in the x direction, 70 in the y direction, and 16 in the z direction. The semivariogram models were used in turning band method simulations, first proposed by Matheron (1973) and Journel (1974). The simulations produced 100 unique, equiprobable realizations. The median (P50) and the mean of the realizations were used as the most representative models of the reservoir.

After the geostatistical model had been selected, the model was populated with permeability and porosity core-derived values using a transform to convert the synthetic, normalized SP values. The transform was derived from regression analysis techniques on the permeability and normalized SP log data. A large amount of scatter in the data made it difficult to fit a curve that had a high level of correlation; therefore, the

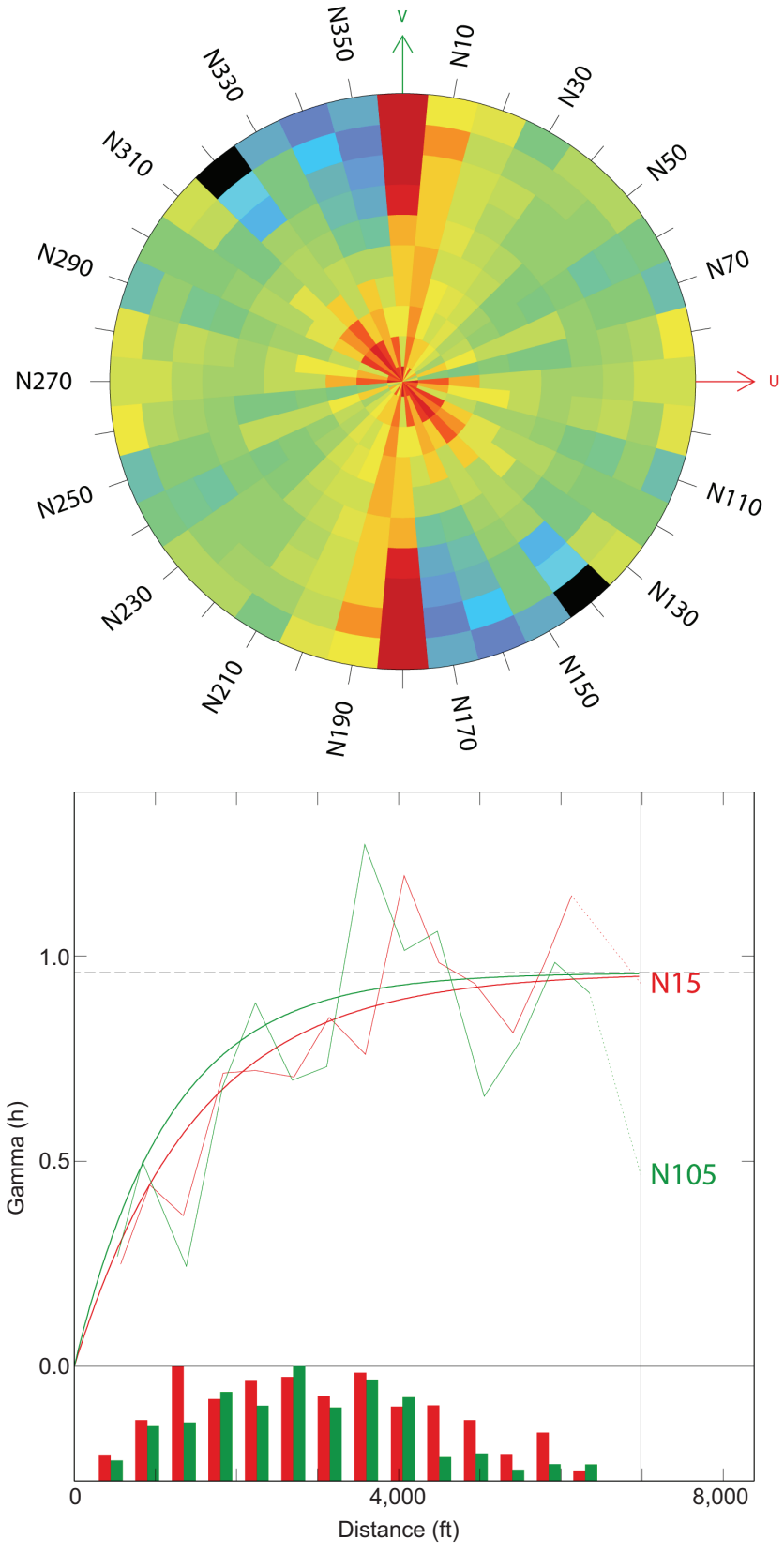

Figure 31 Variogram map (top) and variogram with the fitted models (bottom). The variogram map indicates a strong northeast-southwest anisotropy. However, there appears to be a secondary direction at 140° southeast-northwest, which could be the result of geometry of the sandstone shoals seen in the isopach map in Figure 30. In the top figure, the corresponding variograms calculated in the two directions are represented by the erratic, lighter lines, and the models are the smoother, darker lines. The number of pairs of data at each lag is represented by the histogram in the lower part of the top figure. The sill is the dashed horizontal line at 0.96. The range of the variogram model in the direction of maximum continuity (red line) was 1,372 m (4,500 ft). The range of the variogram model in the direction of minimum continuity (green line) was 1,067 m (3,500 ft).

curve chosen was based on experience and expectations regarding the reservoir characteristics commonly found in other Illinois Basin reservoirs. The final transform curves and corresponding equations are shown in Figure 32.

Figures 33, 34, 35, and 36 show a selection of images from the final geocellular model. The average porosity of the model was 16% and the average permeability was 1.92×10^{-10} cm^2 (19.5 mD), which compares favorably with the 16% and 1.85×10^{-10} cm^2 (18.7 mD) averages determined for the reservoir from the core analyses. The geocellular model was able to reasonably approximate the boundaries of the field, when compared with the isopach map shown in Figure 33. Also, the model was successful in capturing the dual-layer nature of the Jackson sandstone (Figures 34 and 35).

The geocellular model was then utilized for reservoir simulation. As new data were acquired or revelations made over the course of the pilot study, the geocellular model was modified in an iterative process. For example, a fault/fracture network that was undetectable before the actual CO_2 injection began was noted based on the timing of individual wells' response to CO_2 injection at RG-5. The model was subsequently updated to reflect this new information.

MVA STRATEGIES AND METHODS

Objectives

The success of a CO_2 EOR and sequestration project depends, in part, on accurately documenting the fate of CO_2 in the subsurface and demonstrating that the project is an effective greenhouse gas control technology (NETL, 2009). Moreover, it is important that the project be conducted in an environmentally safe manner. Attainment of these broad goals is achieved through a portfolio of protocols and measurements generally called monitoring, verification, and accounting (MVA).

Sampling Priorities

The MVA strategies and measurements specific to Sugar Creek included (1) monitoring air quality at strategic locations to ensure health and human safety; (2) monitoring volumes and rates of injected CO_2; (3) monitoring shallow groundwater quality; (4) measuring volumes of produced oil, gas, and water and changes in their chemical properties; (5) monitoring surface and subsurface injection pressure and temperature; and (6) developing and implementing a health and safety plan.

To cover the project life cycle, MVA measurements were conducted in three stages corresponding to time periods before, during, and after CO_2 injection. Pre-injection MVA work focused on characterizing ambient aqueous fluid and gas chemistry and developing a baseline data set against which changes due to CO_2 interactions could be documented. The MVA work during injection provided the basis for documenting types of CO_2-water-rock interactions, the magnitudes of the reactions, and their spatial distribution in the field. Post-injection MVA work focused on documenting the extent to which fluid chemistry in the oil reservoir returned to pre-injection values and ensuring that CO_2 did not migrate into the shallower groundwater.

Health and Human Safety

The MGSC had a health and safety plan (HASP) addressing the activities related to the Sugar Creek pilot. The purpose of the HASP was to assign staff responsibilities, establish safety standards and procedures, and address contingencies that might arise during operation. Each HASP contained the emergency telephone numbers for the local first responders (fire, law enforcement, and ambulance services). A map was provided for the nearest clinic and the nearest major hospital. The HASP also included information on occupational hazards (e.g., CO_2 exposure, high pressures) and field hazards (e.g., heat and cold exposure, Lyme disease, snakebites, tornadoes, lightning, and poison ivy).

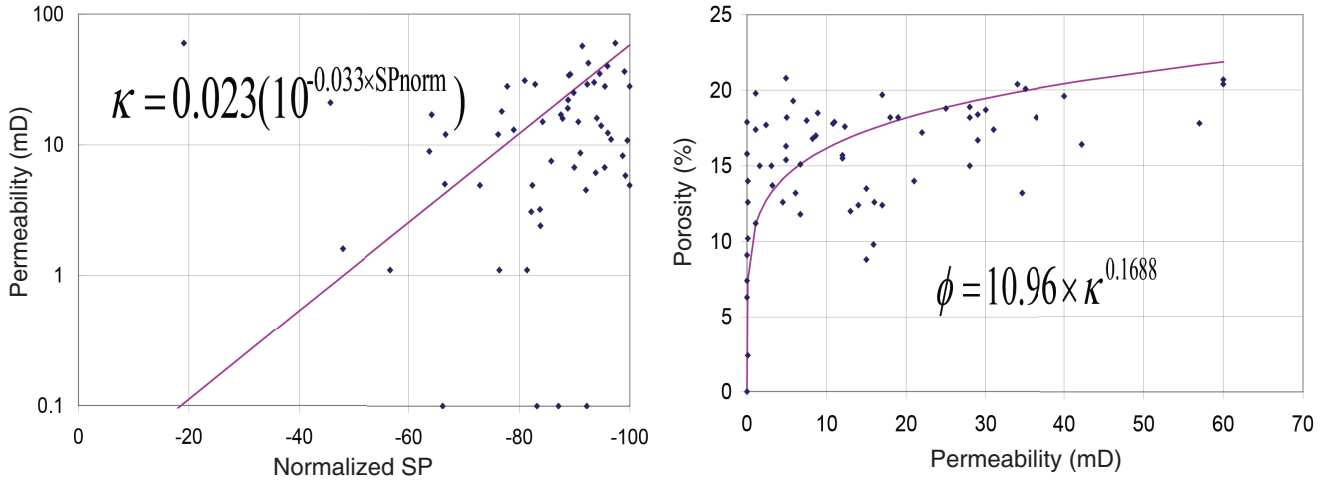

Figure 32 Graphs illustrating the transforms created to convert normalized spontaneous potential (SP) data into permeability (left) and permeability into porosity (right). The data were derived from core analyses and geophysical logs. Data were first plotted on the graph, and then a curve was best fitted to the data regression techniques.

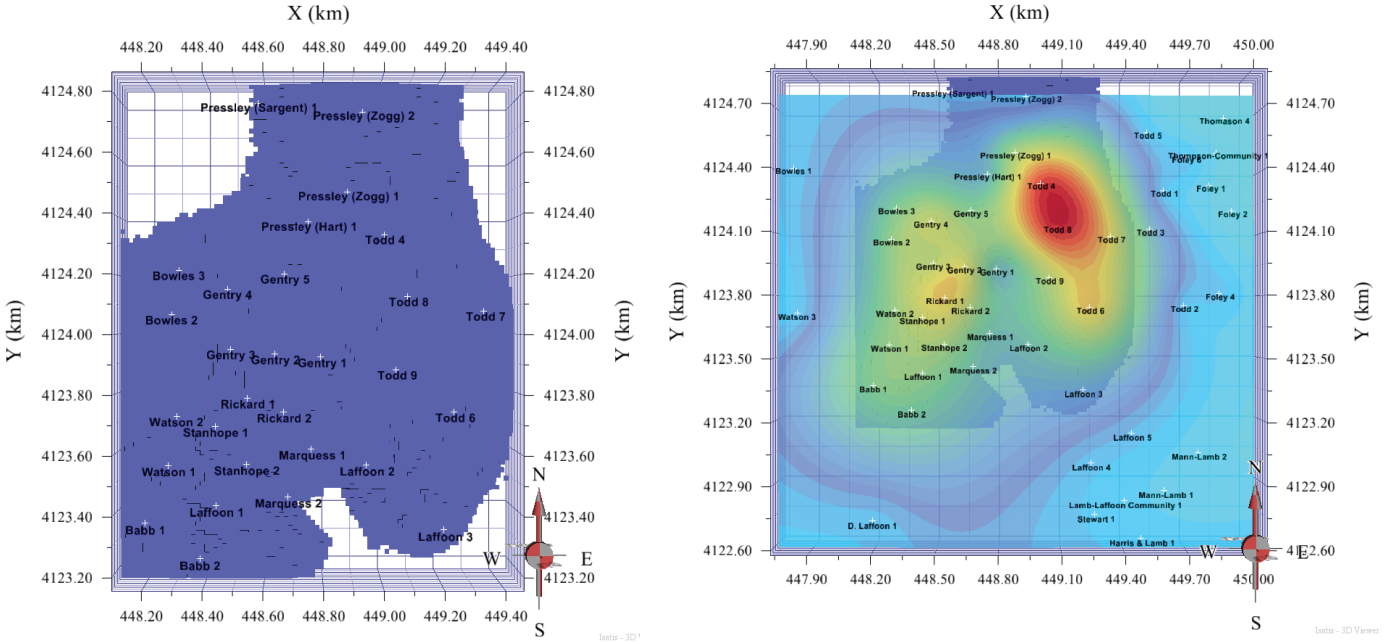

Figure 33 Images of the three-dimensional geocellular model. The left image shows the outline of the reservoir within the Jackson sandstone when a porosity cutoff is applied to the model. In the right image, the original isopach is overlain as a transparency to demonstrate the agreement between the original geologic model and the geocellular model. Except for a small discrepancy in the south due to poor data control, the two models match very well. Note that the geocellular model captures the northern part of the reservoir that is water-saturated. This area is not included in the original isopach.

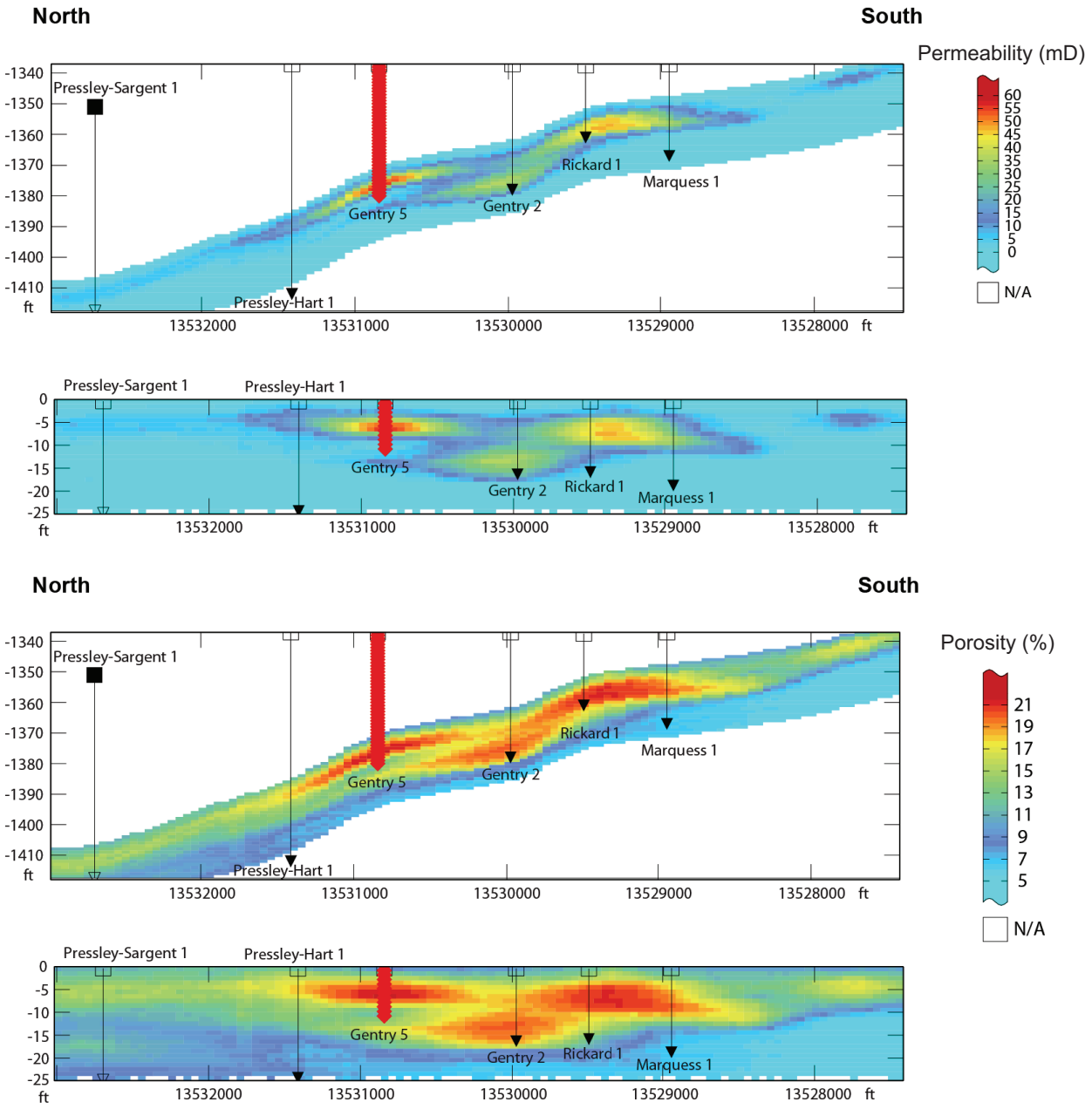

Figure 34 North-to-south cross sections showing the distribution of permeability (top two images) and porosity (bottom two images). The cross sections are in structural space and stratigraphic space with the top of the Jackson sandstone serving as the origin. The injection well is marked in red. The trace of the cross section is shown as a green line on the map at the bottom of the figure.

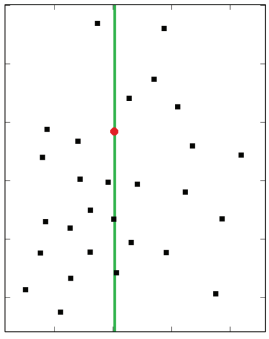

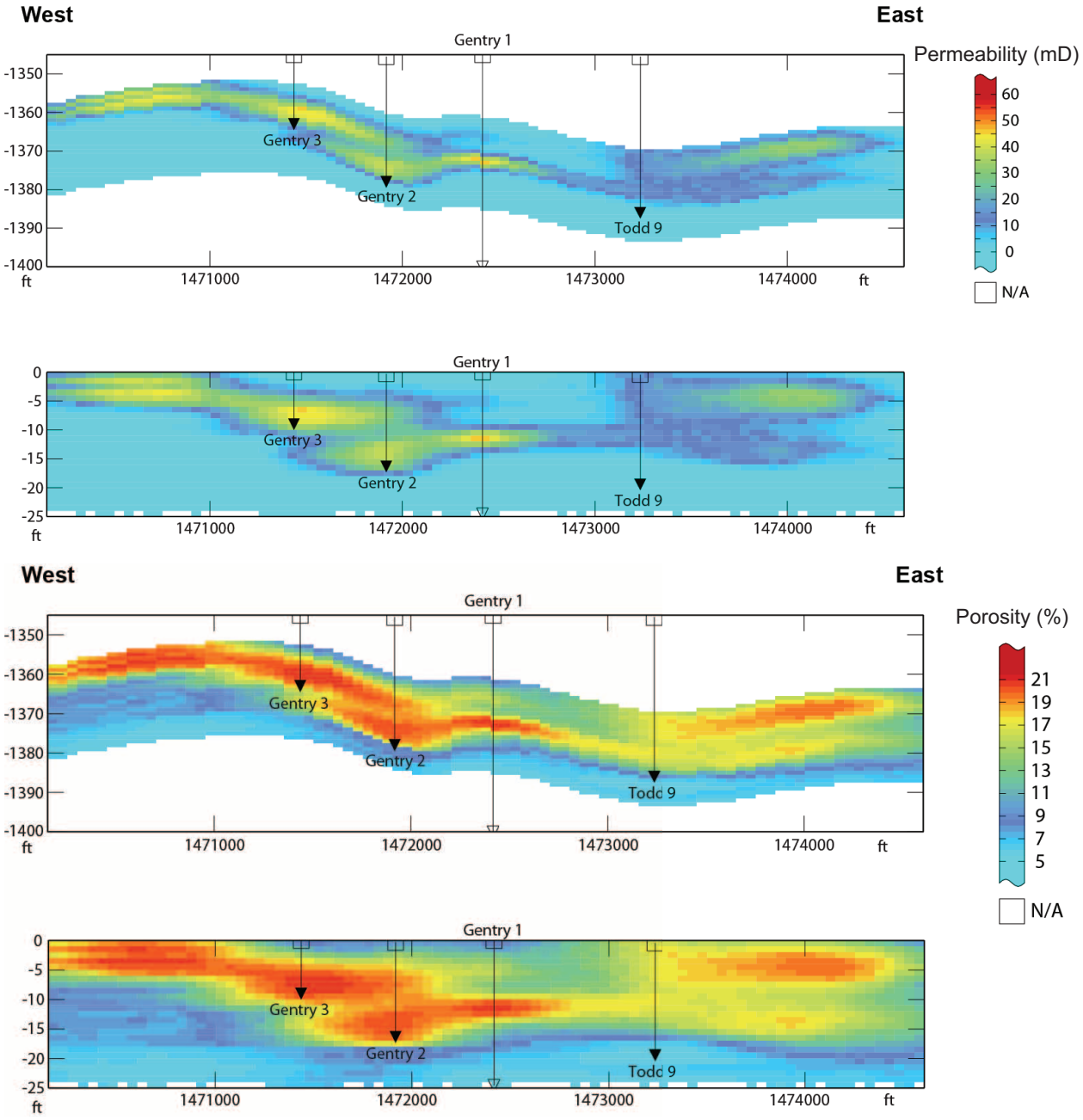

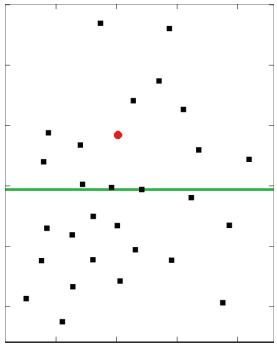

Figure 35 West-to-east cross sections showing the distribution of permeability (top two images) and porosity (bottom two images). The cross sections are in structural space and stratigraphic space with the top of the Jackson sandstone serving as the origin. The trace of the cross section is shown as a green line on the map.

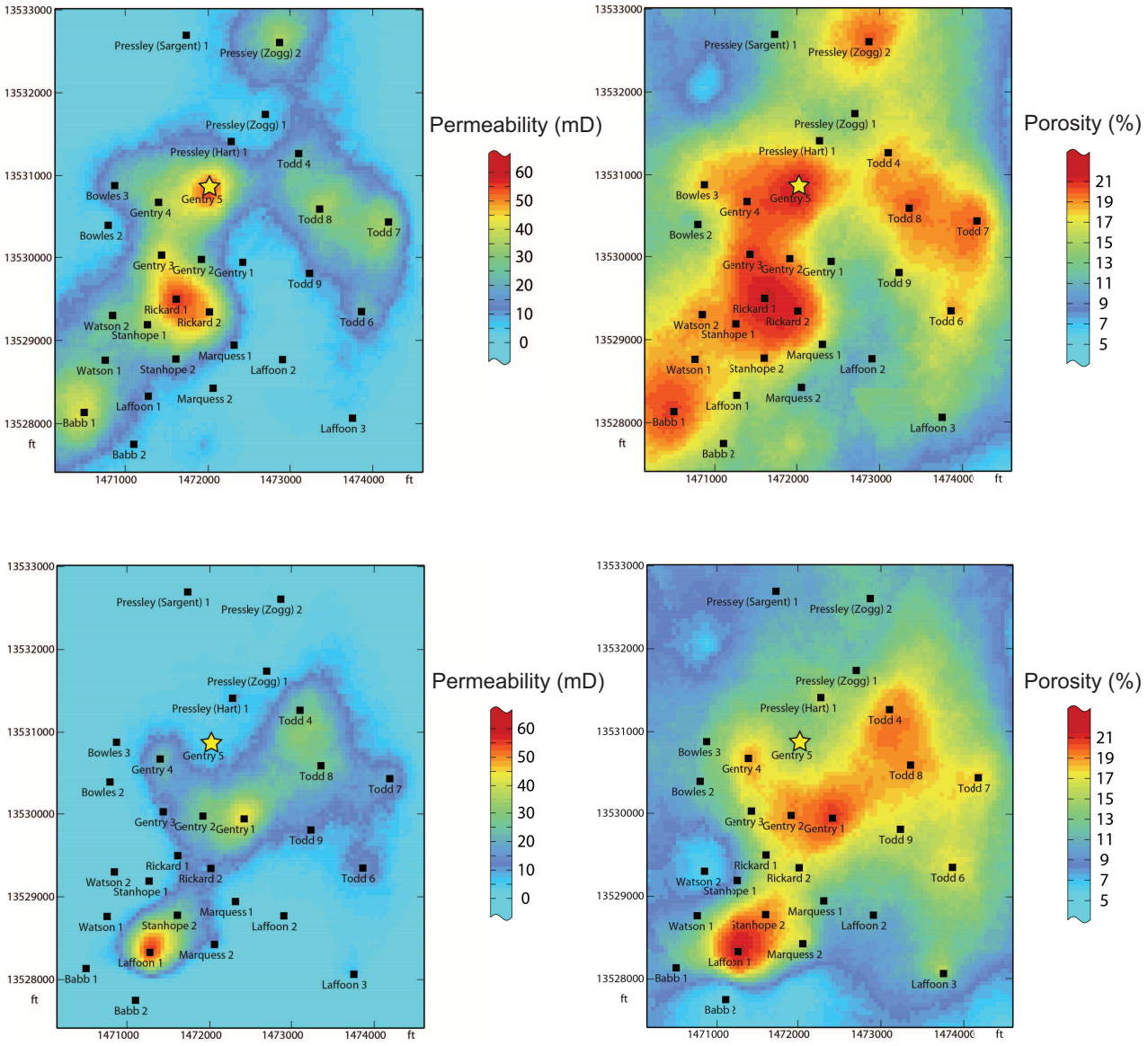

Figure 36 Planar slices through the geocellular model. The upper and lower two images are taken at depths of 1.8 and 3.4 m (6 and 11 ft), respectively, below the top of the Jackson sandstone. Images on the left show the distribution of permeability; images on the right show the distribution of porosity. The injection well, RG-5, is marked by a gold star. All images are taken from the geocellular model projected stratigraphically using the top of the Jackson sandstone as the origin.

All employees from the MGSC who visited or worked at the EOR site were required to attend a HASP training session. A printed copy of the HASP was kept on-site during injection activities. Level D personal protective equipment (PPE)—which includes safety glasses, hard hats, gloves, steel-toed boots, and hearing protection where appropriate—was required for all workers. In the immediate area of the injection equipment, air sampling was conducted to monitor CO_2 levels in the air in real time.

Sampling Strategies

Design of a Groundwater Monitoring System for the Injection Site

Spatially, measurements were conducted at locations and stratigraphic depth intervals that provided the best opportunity to document water-rock interactions in response to CO_2 injection, and that ensured that the CO_2 remained in the Jackson sandstone oil reservoir. The targeted stratigraphic-depth intervals included the Mississippian Jackson sandstone oil reservoir at a depth of approximately 564 m (1,850 ft), the overlying deep Pennsylvanian aquifers, at depths of 60 to 275 m (200 to 900 ft), and the shallow Pennsylvanian aquifer at depths less than 60 m (less than 200 ft) (reference to ground surface).

Well Locations

The Jackson sandstone reservoir brine was sampled from the seven oil production wells (RG-1, RG-2, RG-3, RG-4, PH-1, WT-4, and WT-9), one monitoring well (JR-1), and the injection well, RG-5 (Figure 3). (RG-5 was only sampled prior to CO_2 injection). The production and monitoring wells almost completely circumscribe the injection well and thus provided good coverage to detect CO_2 migration in the Jackson oil reservoir. The brine also was sampled from a sample port attached to the brine tank at the tank battery, TB-1. (TB-1 refers to any sample taken from a tank at the tank battery.)

The deep Pennsylvanian groundwater was sampled from multiple Pennsylvanian sandstones over the broad interval of 83–250 m (274–820 ft) at WT-3. Water from WT-3 (located outside the EOR III site boundaries), along with Jackson brines, made up the water used for waterflooding in the field (Figure 23).

In order to monitor potential geochemical changes in the shallow Pennsylvanian aquifer within the EOR test site, three shallow groundwater-monitoring wells were installed. Monitoring well RG-4MW was installed approximately 15 m (50 ft) northeast of production well RG-4; well RG-5MW was located approximately 15 m (50 ft) south of the injection well RG-5; and well PH-1MW was located approximately 15 m (50 ft) southwest of production well PH-1 (Figure 3). Outside of the field, the previously described KB-1, located about 1.6 km (1 mile) northeast of the injection well, and DC-1 and DC-2, located approximately 1.6 km (1 mile) west of the injection well (Figure 23), also were sampled to monitor the composition of the groundwater from the shallow Pennsylvanian aquifer.

Frequency of Brine Sampling

Samples of the Jackson reservoir brine were collected from most of the oil production wells multiple times before CO_2 injection. Injection well RG-5 was sampled once before CO_2 injection and was not sampled thereafter. Monitoring well JR-1 was sampled three times before injection and once afterwards. During injection and for approximately a year afterward, an effort was made to sample the production wells monthly (Table 7). Production well WT-8, also located in the immediate field area, was not brine sampled because of a low water cut. The tank battery, TB-1, was also sampled at the same frequency as the production wells. Overall, the monthly sampling protocol provided a balance between manpower availability, the need to obtain a robust data set, and the need to spatially and temporally resolve CO_2 movements in the Jackson reservoir.

Table 7 Summary of number of samples collected from monitoring wells and wells from which brine and groundwater samples were collected at different time periods. The list also includes the tank battery, TB-1.

Sampling site	Pre-injection (3/16/09–4/27/09)	Injection (6/2/09–5/18/10)	Post-injection (6/7/10–6/6/11)	Total sampling events
Brines				
RG-1	3	5	13	21
RG-2	3	1	3	7
RG-3	3	12	12	27
RG-4	3	11	8	22
RG-5	1	0	0	1
PH-1	3	4	3	10
WT-4	3	11	12	26
WT-8	0	0	0	0
WT-9	3	13	11	27
JR-1	3	0	0	3
TB-1	2	12	13	27
Groundwater				
WT-3	2	4	4	10
RG-4MW	2	4	4	10
RG-5MW	2	4	4	10
PH-1MW	2	4	4	10
DC-1	2	4	3	9
DC-2	2	0	0	2
KB-1	3	4	4	11

The deep Pennsylvanian aquifer was sampled from WT-3 twice before injection began and quarterly during and after CO_2 injection.

The shallow Pennsylvanian aquifer was sampled as follows: KB-1 was sampled three times before CO_2 injection began and quarterly thereafter; DC-1 and DC-2 were sampled twice during the pre-injection stage; and thereafter DC-1 was sampled four times during injection and three times after injection. The three monitoring wells drilled in the EOR site were sampled twice pre-injection and quarterly thereafter.

Sample Types

Groundwater

Water samples collected from the Pennsylvanian sandstone aquifers were more dilute (~300–850 mg/L, TDS) than Jackson reservoir waters, and the water samples from the Pennsylvanian are henceforth referred to as groundwater. To better understand potential water-rock interactions with CO_2 in the Jackson reservoir, it was necessary to characterize the deeper Pennsylvanian groundwater used by the field operator as injection water for pressure maintenance. Sampling and characterization of the shallow Pennsylvanian aquifer was necessary to ensure that CO_2 did not leak into the shallow groundwater zone. Data acquired from both aquifers also provided inputs for geochemical modeling (e.g., Schumacher et al., 2010).

Samples of the groundwater from the deep Pennsylvanian aquifer were collected only from WT-3, which was perforated over multiple intervals from 83.5 to 250 m (274 to 820 ft) in undifferentiated Pennsylvanian

sandstones. Therefore, the WT-3 samples likely represent contributions from multiple sandstone aquifers within the perforated intervals. The WT-3 well, like the oil wells, is configured with a pumping unit, but the well does not produce oil. Also like the oil production wells, the WT-3 well was pumped on an intermittent schedule, and was pumped several hours before sampling to allow sufficient time for water from the reservoir to fill the wellbore and reach the surface. Well WT-3 was monitored and sampled in a manner similar to the oil production wells, but oil separation was not necessary and probe fouling was not an issue. Sampling of this well and the other shallow (<60 m [<200 ft]) groundwater wells was done with a clean set of Tygon tubing to avoid contamination from oil.

Samples of the shallow Pennsylvanian groundwater collected from the three wells outside the EOR site provided a broader characterization of the shallow aquifer away from the area of active oil field operations. Domestic well KB-1, located approximately 1.6 km (1 mile) northeast of the injection well (Figure 23), had a total depth of 40 m (131 ft) and was constructed as an open borehole well with 12 m (40 ft) of 15 cm (6 inch) diameter PVC surface casing. Well KB-1 was no longer in use by the owner, and the existing pump was not operational. Therefore, the well was purged and sampled using a 5 cm (2 inch) diameter Redi-Flo Grundfos submersible pump. Typically, 144 L (38 gallons) were purged from the well before steady-state water properties were recorded with the YSI multi-probe (see brine sampling methods) and samples were collected.

Wells DC-1 and DC-2, located at poultry farms approximately 1.6 km (1 mile) west of the injection well, were sampled using their existing submersible pumps. Both wells were constructed with a sand-packed screen and 10 cm (4 inch) diameter PVC casing to a depth of 57 m (187 ft). Because livestock well DC-2 was less than 150 m (500 ft) from well DC-1, well DC-2 was sampled only twice, both times during the pre-injection stage; DC-1 was sampled during the injection and post-injection stages as well. Like well KB-1, these wells also were tested with the YSI multi-probe until steady state was observed, and only then were samples collected for analysis.

The three shallow groundwater monitoring wells (RG-4MW, RG-5MW, and PH-1MW) were installed to a depth of approximately 52 m (170 ft) in the vicinity of the injection well. (Details of groundwater monitoring well construction are given in Appendix 3.) These wells provided data regarding shallow groundwater chemistry in the area of active oil field operations, and they were the closest monitoring wells to the CO_2 injection well. Each monitoring well was constructed with 5-cm (2-inch) diameter PVC casing with a 6-m (20-ft) screened interval at the bottom of the borehole. Each monitoring well was equipped with a dedicated bladder pump, which was used to purge the wells and collect groundwater samples. As with well KB-1, the monitoring wells were purged until steady state water properties were recorded with the YSI and then samples were collected. Purge volumes typically were on the order of 25 to 80 L (6.6 to 21.1 gallons).

Gamma-ray logs were taken for the domestic water well KB-1 and the three shallow groundwater monitoring wells (RG-4MW, RG-5MW, and PH-1MW) using the 2PGA-1000 Poly-Gamma logger manufactured by Mount Sopris Instruments.

Brine

Water samples collected from the Jackson oil reservoir were saline (~17,000–63,000 mg/L, TDS) and are hence referred to as brines. The collection of deep, brine-bearing reservoirs often presents challenges in getting samples from a discrete stratigraphic interval in which the water sample is representative of reservoir water at the time of sampling. This problem was avoided at Sugar Creek because the oil production wells contained casing down to the top of the Jackson and were perforated through casing or open-hole in the interval corresponding to the Jackson. Moreover, because the wells were pumped more or less continuously, the sampled brines generally were not stagnant in the wellbore and not re-equilibrating for extended periods of time.

The tank battery is the central collection point for produced fluids in the field. At TB-1, brine was sampled from the brine tank downstream of the gun barrel oil-water separator. Brine samples collected from TB-1 during the pre-and post-injection stages represent a composite sample of brine from all production wells and groundwater from the water supply well, WT-3. Because CO_2 replaced the brine injection volume at

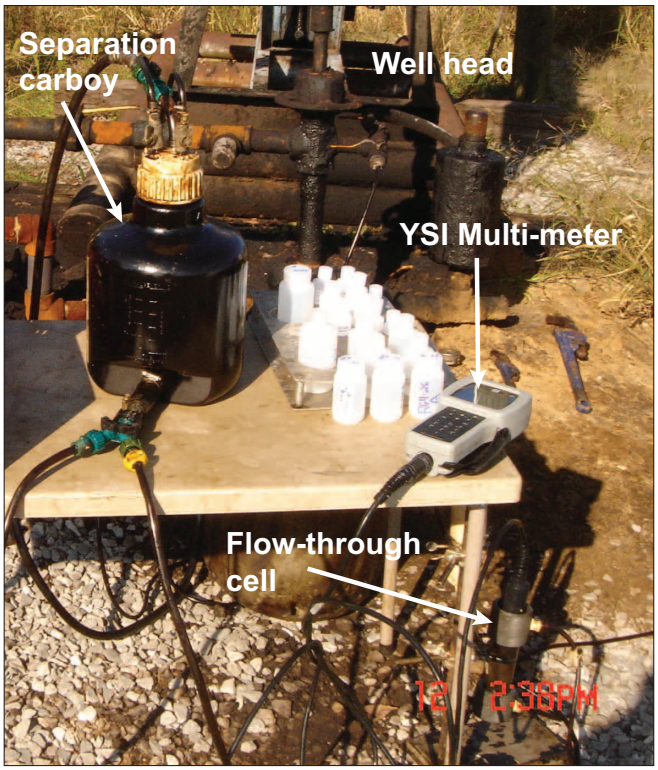

Figure 37 Brine sampling apparatus. Critical components include the carboy and pre-filter (not visible) for separating oil from the brine; the flow-through cell that contains the probes for measuring pH, redox potential, temperature, dissolved oxygen, and conductivity; and the YSI data logger connected to the probes. The assembly is connected to the wellhead via ¼-inch Tygon tubing that connects to the top of the carboy.

RG-5, no WT-3 water was required to supplement the field's brine injection volume; consequently, brine collected during the CO_2 injection period is produced brine only.

To ensure that representative samples of the reservoir brine were collected, field measurements were taken while formation fluids were being pumped to the surface with minimal contact with the atmosphere. To achieve this, formation fluids were pumped from the production well through Tygon tubing into a carboy fabricated to function as a very small-scale oil-water separator. The continuous flow rate through the carboy was low, allowing oil and water to separate. The brine was drained through the bottom spigot of the carboy to a pre-filter chamber filled with glass wool. The pre-filter chamber removed most of the remaining oil, after which the brine passed through a flow-through cell containing a YSI 556 MPS multi-probe. The YSI multi-probe recorded the pH, temperature, conductivity, redox potential (Eh), and dissolved oxygen content of the fluid (Figure 37). Field measurements with the multi-probe were monitored until they stabilized as fluids were passing through the flow-through cell, at which time the values were recorded, flow was shut off, and samples were collected. Attainment of stable field measurements provided confidence that the sampled brine water was representative of that in the reservoir.

The multi-probe was calibrated according to the manufacturer's specifications at the beginning and end of each sample day. Conductivity standards that closely matched the conductivity of the reservoir brine were developed in the laboratory. Based on the two calibrations on a given sampling day, instrument drift appeared to be minor. A bigger issue, however, was fouling of the probes by oil when sampling the oil pro-

duction wells. Any fouling required cleaning and recalibration of the probes. The pH and dissolved oxygen probes were the most sensitive to contact with oil.

Brine samples were collected directly from the oil-separation carboy in pre-rinsed Nalgene bottles for measurements of dissolved CO_2, alkalinity, dissolved inorganic carbon (DIC), anions, cations-metals, NH_4-NH_3, and TDS (Table 9). All sample bottles were filled to remove headspace, and the cations-metals samples were acidified in the field with nitric acid to pH equal to or less than 2. If required, samples were filtered in the field using a 0.45 µm (1.8×10^{-5} inches) high-flow inline filter. After collection, all samples were chilled for transport. With the exception of the NH_4-NH_3 measurements done at the ISGS laboratories, the bulk chemistry measurements were performed at both the KGS and ISGS labs, which required collection of duplicate samples in the field. After May 2010, however, bulk chemistry measurements were conducted at KGS only. Samples for analysis of total organic carbon (TOC) and dissolved organic carbon (DOC) were collected from selected wells during the post-injection phase. These samples were preserved in the field with sulfuric or phosphoric acid and stored in amber bottles. Finally, samples were collected for measurement of stable isotopes (δ^{13}C-DIC, δD-H_2O, and δ^{18}O-H_2O) at the ISGS laboratories.

Gas

Changes in gas chemistry in a reservoir can be a sensitive indicator of CO_2 migration and geochemical interactions in the subsurface (Kharaka et al., 2006a, 2006b); therefore, gas monitoring and sampling was a critical part of the MVA program and general surveillance of the EOR process. Field gas readings and samples were taken from eight production wells (RG-1, RG-2, RG-3, RG-4, PH-1, WT-4, WT-8, and WT-9), two observation wells (JR-1 and PZ-1), and the Sugar Creek Field's tank battery (TB-1) and gas separator (GS-1) (Figure 3; GS-1 is unmarked, but is immediately adjacent to the tank battery). Gases in the Jackson sandstone reservoir represented gases associated with the in situ oil and injected CO_2. Gas compositions were determined in the field using a Geotechnical Instruments GA 2000 infrared gas analyzer (IRGA). The IRGA was calibrated using N_2, 50% CH_4(+), and 35% CO_2 standards. The CH_4(+) standard included higher molecular weight gases (e.g., ethane, propane). The IRGA measurements were conducted weekly from the start of the project until August 18, 2010, after which they were conducted once every two weeks (Table 8).

Table 8 Summary of the number of gas samples and IRGA measurements collected from each well. "Top of carboy" refers to gas measurements or samples collected during brine sampling from the headspace at the top of the carboy as well as fluids cycled through it. All other measurements and samples were collected at the surface from the casing-tubing annulus of the well.

Well	IRGA (annulus)	IRGA (top of carboy)	Gas samples (annulus)	Gas samples (top of carboy)
RG-1	87	0	29	0
RG-2	12	3	7	3
RG-3	86	0	30	0
RG-4	88	0	31	0
RG-5	0	0	0	0
PH-1	29	3	11	3
WT-4	86	0	29	0
WT-8	85	0	25	0
WT-9	8	7	3	3
JR-1	2	2	1	1
GS-1	59	0	14	0
TB-1	23	0	5	0
PZ-1	1	0	1	0

Gas samples were collected in Cali-5 Bond gas sample bags, which were analyzed at the ISGS laboratories for both bulk and isotopic composition. The gas samples were collected monthly coincident with sampling of the Jackson brines. Production well gas readings and samples were typically taken from the well annulus. Casing or annulus gas sampling was carried out by removing the bull plug atop the chemical pot, attaching the gas sampling bushing to the pot, and fully opening the casing kill wing valve for gas to flow from the annulus.

For shut-in wells, gas readings and samples were taken from the top of the separation carboy during brine sampling. Observation well gas readings and samples were taken from the well tubing or the top of the separation carboy during brine sampling. Gas readings and samples from the tank battery (TB-1) were taken from the oil tank exhaust pipe and from the atmospheric end of the well tester on the gas-liquid separator (GS-1).

Sample Analysis Procedures

Laboratory methods used to characterize water chemistry are summarized in Table 9.

Table 9 Summary of field preservation and laboratory measurement techniques for brine and groundwater samples. Details of methods can be accessed at the websites for the Environmental Protection Agency (EPA, http://water.epa.gov/scitech/methods/) and the American Society for Testing and Materials (ASTM, http://www.astm.org/Standard/index.shtml).

Analyte and field preservation	Details	Method (reference)	Laboratory (personnel)
Cations: filtered, HNO_3 to pH 2, cool to 4°C (39°F)	Al, Sb, As, Ba, Be, B, Cd, Cr, Co, Cu, Au, Fe, Pb, Li, Mg, Mn, N, P, K, Se, Si, Ag, Na, Sr, Tl, Sn, V, Zn	ICP (EPA SW 846.6010B, 1996)	KGS (Backus), ISGS (Webb)
Anions: filtered, cool to 4°C (39°F)	Cl, NO_3, SO_4, Br, F, I	IC (EPA 300.0; ASTM D4327, 1996)	KGS (Mock), ISGS(Chou)
Alkalinity: filtered, cool to 4°C (39°F)	mg/L $CaCO_3$	Field: Titration with H_2SO_4 to pH 4 Lab: Electrometric titration (EPA 310.1, 1978; ASTM D1067, 1996)	Field: ISGS (Wimmer, Iranmanesh), KGS lab (Conner)
DIC: filtered, cool to 4°C (39°F)		CO_2 Coulometer (ASTM D513B)	KGS (Conner)
Total dissolved CO_2: cool to 4°C (39°F)		Gas-sensing electrode (ASTM D513A, 1988)	KGS (Conner), ISGS (Wimmer, Iranmanesh)
TOC: amber bottle, H_3PO_4 to pH 2, cool to 4°C (39°F)		High temperature combustion (EPA 415.2, 1982)	KGS (Conner), ISGS (Berger)
DOC: amber bottle, filtered, H_3PO_4 to pH 2, cool to 4°C (39°F)		High temperature combustion (EPA 415.2, 1982)	KGS (Conner), ISGS (Berger)
NH_3-NH_4: amber bottle, filtered, H_2SO_4 to pH 2, cool to 4°C (39°F)		Method 4500-NH_3 (Std. methods of water and wastewater, 1998)	ISGS (Wimmer, Iranmanesh)
TDS: filter, cool to 4°C (39°F)		Gravimetric (EPA 160.1)	KGS (Conner), ISGS (Henderson)

Isotopes: filter, cool to 4°C (39°F)	δ^2H of H_2O $\delta^{13}C$ of DIC $\delta^{14}C$ of DIC $\delta^{18}O$ of H_2O ^3H (enrichment)	$\delta^{18}O$ and δ^2H of H_2O: wavelength-scanned cavity ring-down spectroscopy DIC extraction for $\delta^{13}C$ and $\delta^{14}C$: gas evolution $\delta^{14}C$ of extracted CO_2: AMS ^3H: enrichment (Vaughn et al., 2008; Hackley et al., 2007; Linick et al., 1989; Ostlund and Dorsey, 1977)	ISGS (Hackley, Fanta)

Brine Chemistry

Along with separating water from the oil, perhaps the most significant challenge in conducting analyses on the Jackson reservoir brines was their high salinity and the large range of concentrations of the various ions. For example, chloride values were typically on the order of 10^4 mg/L, major cations (e.g., Ca, Mg, Na) 10^2–10^3 mg/L, and trace metals 10^{-1}–10^{-2} mg/L. This large range of concentrations required numerous dilutions in order to conduct ion chromatography (IC) and inductively coupled plasma (ICP) measurements within the optimal working ranges of the instruments for the species being measured. For example, dilutions for IC analysis ranged from 5 for sulfate to 5,000 for chloride. Dilutions for ICP measurements ranged from 41 for sodium to none for the trace metals.

The dilution process inherently introduces error into the concentration measurements and consequently accuracy was a concern, especially in the early project stages.

Accuracy and precision were addressed by charge balance analysis (Table 10), comparison of measurements between the KGS and ISGS labs, and comparison with synthetic brine samples developed for the project. This analysis covers the period April 2009 through May 2010 when samples were collected and measured at both labs.

Table 10 Summary statistics for charge imbalances in samples of the Mississippian Jackson sandstone brines and Pennsylvanian groundwater.

Sample	Measurements (no.)	Average	Standard deviation	Median	Samples with charge imbalance ≤10%	Samples with charge imbalance ≤5%
Brine	163	2.9	2.6	2.2	98%	85%
Groundwater	56	6.4	8.0	4.7	87%	54%

Charge balance among measured cation and anion concentrations provided an important criterion for determining the quality of water chemistry measurements (Freeze and Cherry, 1979). Assuming that the analyzed waters are overall electrically neutral, the electrical charges contributed by cations and anions—reported as milliequivalents per liter—should be close to zero. Large departures indicate that a major anion or cation was not included in the analysis and/or that there were problems with sampling, sample preservation and handling, or laboratory errors. Charge balance was determined using Equation (2):

$$\% \text{ Imbalance} = 100 \times (\sum\text{cations} - \sum\text{anions})/(|\sum\text{cations}| + |\sum\text{anions}|) \quad (2)$$

The analysis showed that charge imbalance errors for the brines were relatively small (Table 10). Depending on whether a 5% or 10% imbalance error is used, then 85% or 98% of samples had errors less than the

respective thresholds. Groundwater samples, in contrast, had higher average imbalance error and 54% and 87% of samples had errors less than the 5% and 10% thresholds, respectively (Table 10). From an analytical perspective, measurements in the more dilute groundwater samples should be more straightforward as they do not require the extensive dilutions associated with the brine samples. The dilute character of the groundwater samples, however, also made laboratory measurement errors more pronounced. Measurement errors in the brine samples, unless truly large, were less pronounced because of the overall higher salinity.

To further investigate reproducibility between labs, the relative percent difference (RPD) for specific cation and anion measurements was determined according to the equation

$$RPD = 100 \times \left| (ISGS\ meas - KGS\ meas)/[(ISGS\ meas + KGS\ meas)/2)] \right| \quad (3)$$

where "ISGS meas" and "KGS meas" represent measured concentrations of a cation or anion from samples collected at the same time and under the same field conditions. The criterion RPD < 15% was used for acceptance. The results (Table 11) suggest that, except for sulfate and potassium, measurements were consistent between the laboratories, suggesting a fairly high degree of precision on most of the major cation and anion measurements. Differences between the labs for sulfate and potassium measurements seemed to persist over the course of the project and their cause is not clear.

Table 11 Relative percent difference (RPD) between KGS and ISGS laboratories for select brine analytes.

Analyte	Average RPD	Standard deviation	Median RPD	Measurements meeting criteria (%)[1]
Anions				
Cl (n = 85)	7	10	5	92
Br (n = 84)	7	7	5	93
SO_4 (n = 79)	27	28	17	41
Cations				
Na (n = 81)	6	5	5	96
Ca (n = 80)	4	3	4	100
Sr (n = 78)	4	2	3	100
Mg (n = 81)	5	4	4	99
K (n = 81)	32	21	27	25
Ba (n = 81)	7	7	5	90

[1] Refers to percentage of measurements meeting the criteria: RPD <15%

To better assess the accuracy of the brine measurements, a synthetic brine was developed by Environmental Resource Associates (ERA) to mimic the Sugar Creek brine. The composition of the brine was decided jointly by ISGS and KGS personnel. The ERA synthetic brine was taken into the field coincident with the monthly sampling program. While in the field, the synthetic brine was collected and preserved in bottles in the same manner that natural brine samples were collected. The synthetic brine was not, however, cycled through the carboy. Bottles containing the synthetic brine samples were also labeled in the same manner as bottles containing natural brines so that laboratory personnel could not distinguish them from natural brines. Splits from the synthetic brine were distributed to ISGS and KGS labs and an independent commercial lab for analysis. The ISGS laboratory had one analyte, chloride, that differed from the standard by more than 10%. The KGS laboratory had two analytes, potassium and lithium, that differed by more than 10% (Table 12). The error for potassium accords with the problem previously noted for this analyte in the RPD analysis (Table 11). The commercial laboratory had two analytes, alkalinity, and TDS, that departed from the standard by more than 10%.

Table 12 Comparison of brine measurements among ISGS and KGS laboratories and an anonymous commercial lab to a brine standard developed by ERA.[1]

ERA standard (actual)	ISGS measured	% Error	KGS measured	% Error	Commercial laboratory measured	% Error
Anions						
Cl = 36,300	40,301	–11	35,100	3.3	36,700	–1.1
Br = 180	170	5.6	190	–5.6	163	9.4
Cations						
Na = 20,000	19,555	2.2	19,220	3.9	19,000	5
Ca = 2,000	1,890	5.5	1,920	4	1,910	4.5
Sr = 648	634	2.2	655	–1.1	663	–2.3
Mg = 650	614	5.5	635	2.3	682	–4.9
K = 125	136	–8.8	156	–24.8	154	–23.2
Li = 2.04	2.2	–7.8	2.64	–29.4	1.57	23
B = 303	304	–0.3	303	0	282	6.9
Other						
Alkalinity = 702	710	–1.1	720	–2.6	800	–14
TDS = 60,100	62,208	–3.5	62,440	–3.9	46,900	22

[1] Percent error = 100 × (actual–measured)/actual.

The interlab comparisons and comparison with a known standard underscore the challenges in conducting accurate water chemistry measurements on brines. The high salinities allow some measurement error within the context of keeping charge balances at an acceptable level. Cations and anions of specific interest should, however, be checked against known standards to ensure accurate measurements of the brine chemistry.

Isotopes

The gas samples were analyzed on a Varian 3800 gas chromatograph equipped with a thermal conductivity detector (TCD) for fixed gases (CO_2, N_2, O_2, and CH_4) and a flame ionization detector (FID) for hydrocarbons from methane (CH_4) through hexane (C_6H_{14}). Gas samples with sufficient CO_2 were analyzed for stable carbon isotopes ($\delta^{13}C$). Selected samples containing sufficient CH_4 were analyzed for $\delta^{13}C$ and hydrogen isotopes (δD). The aqueous samples were analyzed for stable carbon ($\delta^{13}C$), oxygen ($\delta^{18}O$), and hydrogen (δD) isotopes.

The gas samples were extracted from the sample bags through a septum fitted onto the Luer valve using a syringe. For those gas samples containing very low to no hydrocarbons heavier than methane, the extracted gas sample was then injected into a vacuum line, and the CO_2 was cryogenically purified and sealed in a 6 ml (0.4 inch^3) Pyrex tube for isotopic measurement. For gas samples that contained heavy hydrocarbons, the sample had to be sent to an outside laboratory equipped with a gas chromatograph separation method connected to a vacuum line for $\delta^{13}C$ analysis of the CO_2. The $\delta^{13}C$ of DIC was determined using a gas evolution technique described by Hackley et al. (2007). Approximately 10 ml (0.6 in^3) of water was injected into an evacuated vial containing crystalline phosphoric acid and a stir bar. The CO_2 evolved from the water sample was cryogenically purified on a vacuum system using liquid nitrogen followed by a dry-ice and isopropyl alcohol trap and sealed into a Pyrex break tube for isotopic analysis. The CO_2 evolved from DIC for those samples that contained hydrocarbons such as propane was prepared using liquid nitrogen followed by a pentane and liquid nitrogen trap. For the stable isotopes of the brine samples, the brine was first vacuum distilled, and the purified water was collected in a vial using liquid nitrogen. The distilled water from the brines and the freshwater samples was then sent to an outside lab for $\delta^{18}O$ and δD analysis.

The isotopic compositions ($\delta^{13}C$ and δD) of the gas samples separated on a vacuum line were determined on a dual inlet isotope ratio mass spectrometer (IRMS); those samples with hydrocarbons heavier than CH_4 were analyzed on a flow-through GC-IRMS. Each sample was compared to an internal standard calibrated versus an international reference standard. The $\delta^{18}O$ and δD isotopic analyses for aqueous samples were determined by Wavelength-Scanned Cavity Ring-Down Spectroscopy (WS-CRDS) (Vaughn et al, 2008). The final results are reported versus the international reference standards. The $\delta^{13}C$ results are reported versus the Vienna PeeDee Belemnite (V-PDB) reference standard. The $\delta^{18}O$ and δD results are reported versus the

international Vienna-Standard Mean Ocean Water (V-SMOW) standard. Analytical reproducibility is equal to or less than ±0.15‰ for $\delta^{13}C$, ±0.1‰ for $\delta^{18}O$, and ±1.0‰ for δD.

The ^{3}H analyses were done by the electrolytic enrichment process (Ostlund and Dorsey, 1977) and the liquid scintillation counting method. The electrolytic enrichment process consists of distillation, electrolysis, and purification of the ^{3}H enriched samples. The precision for the tritium analyses reported in this study is ±0.25 tritium units (TU).

The ^{14}C activity of the DIC was analyzed using acceleration mass spectrometry (AMS). The DIC was extracted from the water samples by acidification; the released CO_2 was quantitatively collected and purified on a vacuum line and sent to an AMS laboratory along with background, modern, and intermediate standards for ^{14}C analysis. The ^{14}C concentrations are reported as percent modern carbon (pMC). The primary ^{14}C standard is the National Institute of Standards and Technology (NIST) Oxalic Acid #1, of which 95% of the activity is equal to 100 pMC which by convention is equivalent to the year 1950 AD (Stuiver and Polach, 1977).

X-ray Diffraction and Jackson Mineralogy

The XRD measurements for mineralogic composition of the Jackson sandstone were conducted on 14 drill cutting samples collected from wells located within 2.4 km (1.5 miles) of RG-5 (Appendix 4). The depths from which the cuttings were collected were based on driller's log descriptions and correlations with geophysical logs. Collection of cuttings from the selected depths was based on macroscopic examination with hand lens and stereo-microscope. The XRD data are critical as they provide a semi-quantitative mineralogic characterization of the Jackson sandstone and overlying seal rocks needed to interpret potential interactions among rock-forming minerals, reservoir fluids, and injected CO_2.

The XRD measurements were conducted on the whole-rock and clay fraction (<5 μm [0.0002 inch]) by K/T GeoServices. After the samples were cleaned of contaminants, XRD measurements were performed using a Rigaku automated diffractometer equipped with a copper x-ray source and a scintillation x-ray detector. Determination of mineral amounts was done by using integrated peak areas and empirical reference intensity ratio factors. The weight percentage data from this method are semi-quantitative and can quantify crystalline material only. The percentages reported for each mineral depend on the percentages of the other materials. One limitation of this method is that if one mineral is underestimated, then the others will be overestimated. Additionally, detection limits differ for each mineral species and are on the order of 1 to 5 wt% (K/T GeoServices, 2008).

Baseline Data

Geologic Data

The predominant mineral in the Jackson sandstone is quartz (70.6–89.5 wt%, Appendix 4). Numerous studies show the Jackson and other Mississippian Chesterian sandstones to be mature quartz-rich sandstones in which the main framework grain is quartz (Sable and Dever, 1990). Although no petrographic studies were done for this project, some of the quartz is likely cement in the form of syntaxial overgrowths. K-feldspar and plagioclase are likely present as framework grains, but they make up a relatively small percentage with the latter ranging up to approximately 4%. The amounts of calcite and ankerite are variable, but can be significant with respective values ranging up to 14.6 and 17.6 wt%. Clays occur in modest amounts with kaolinite ranging up to 6.5 wt% in EL-1 (530–532 m [1,740–1,745 ft]) and chlorite up to approximately 5% in Harris-3 (547–550 m [1,795–1,805 ft]) (Figure 23). It is not known whether the chlorite in these samples is Fe- or Mg-rich or some combination. Pyrite occurs in small amounts (≤0.3 wt%) in a few samples.

Studies show that rocks in the Golconda Formation, which constitute the overlying seal or confining layer, consist primarily of shales, mudstones, and limestones (Sable and Dever, 1990). The total clay content is up to 60% by weight in the Golconda samples (Appendix 4). Mixed-layer illite/smectite (19.8–35.2 wt%) is the main mineral, followed by quartz (25.7–28.6 wt%) and illite-mica (16.2–18.8 wt%). Calcite content is

up to 19.4 wt%, dolomite is absent, and ankerite (1.7–1.9 wt%) is lower than in the Jackson. Pyrite occurs in small amounts (0.4–0.6 wt%) and gypsum was detected in one sample (WT-2, 543–544 m [1,780–1,785 ft]).

Pre-injection Chemistry and Characterization of Jackson Brine and Associated Gas

Bulk and Isotopic Chemistry Chemical characterization of the Jackson brine samples before CO_2 injection shows that they are NaCl-rich, but with a wide range of salinities (Figure 38, Appendix 5). The highest salinities occurred in PH-1 and WT-4 (50,420–59,000 mg/L). Excluding a likely erroneous measurement in RG-1 (111,124 mg/L TDS), variable but lower salinities were measured in RG-1, RG-2, RG-3, and WT-9 (23,536–31,472 mg/L); and RG-5 and RG-4 (18,438–22,316 mg/L) (Figure 39).

The large variation in salinity is best explained by considering that a portion of the injection water for the waterflood operation was taken from Pennsylvanian sandstone in WT-3. The salinity of the Pennsylvanian water is approximately 850 mg/L, and it is $NaHCO_3$-rich (Figures 38 and 39). Thus the lower and intermediate salinities in the Jackson reservoir brine samples likely represent a mixture of Jackson brine with Pennsylvanian groundwater.

The extent of mixing and groundwater migration can be assessed by plotting concentrations of sodium and chloride, the latter of which is largely geochemically conservative (Figure 40). This plot shows a linear distribution of concentration in which the endpoints are defined by samples from WT-4 and PH-1 at higher concentration and WT-3 at lower concentration. The distribution supports the linear character of the mixing process, and use of the lever-rule indicates that, excepting samples from PH-1 and WT-4, the Jackson brines were diluted by more than 50% by Pennsylvanian groundwater from WT-3.

The contrast in salinity among wells also suggests that the Jackson sandstone may be a compartmentalized reservoir within Sugar Creek Field. Wells with lower and intermediate salinities were diluted with Pennsylvanian groundwater and are therefore in hydraulic communication with RG-5, the injector well. In contrast, the higher salinities at PH-1 and WT-4 show no evidence of dilution and thus appear to be hydraulically isolated from RG-5 and other wells. If the higher salinities are representative of values from the Jackson sandstone aquifer to the north of the oil reservoir, then it is likely that brines at WT-4 and PH-1 represent pristine Jackson formation waters.

Gas Chemistry There were three to four samples of gas from seven of the production wells leading up to and immediately preceding the day of CO_2 injection (March 17, 2009 to May 12, 2009). Hydrocarbons made up the majority of the gas composition for the production wells during this initial sampling period. Gas composition of the production wells appeared to vary significantly from one well to another as well as from one sampling event to another during this period. However, much of the variation could be attributed to air contamination of the samples. With such elevated concentrations of methane and other hydrocarbons, the oxygen concentration should be negligible. The sum of the hydrocarbons, including methane (CH_4), ethane (C_2H_6), propane (C_3H_8), isobutane (iC_4H_{10}), n-butane (nC_4H_{10}), isopentane (iC_5H_{12}), n-pentane (nC_5H_{12}), and hexane+ (C_6H_{14}) ranged from approximately 20% to greater than 99% by volume. Those samples with significant oxygen (O_2) concentrations (i.e., >0.5%) also showed increased nitrogen (N_2) concentrations and corresponding lower hydrocarbon concentrations. Figure 41 shows a comparison of the sum of hydrocarbon concentrations and the sum of $O_2 + N_2$ concentrations of all the production wells sampled prior to injection. Those wells with greater air contamination (higher $O_2 + N_2$ values) showed corresponding decreases in overall hydrocarbon concentrations. Thus, the concentration of hydrocarbons in these wells without air contamination would generally range from approximately 88% to greater than 99% by volume.

Prior to CO_2 injection at RG-5, the CO_2 concentration was fairly significant in some of the production wells. The CO_2 concentration ranged from 0.04 to 7.8% (Figure 42). The greatest concentrations were observed in production wells RG-2 and RG-3. The smallest concentrations were observed in production wells WT-8, PH-1, and WT-4. Some of the production wells showed significant variation in CO_2 concentration prior to injection; again, however, most of the variation could be explained by air contamination of the samples. As observed with the hydrocarbon results, the increases in oxygen and nitrogen concentrations

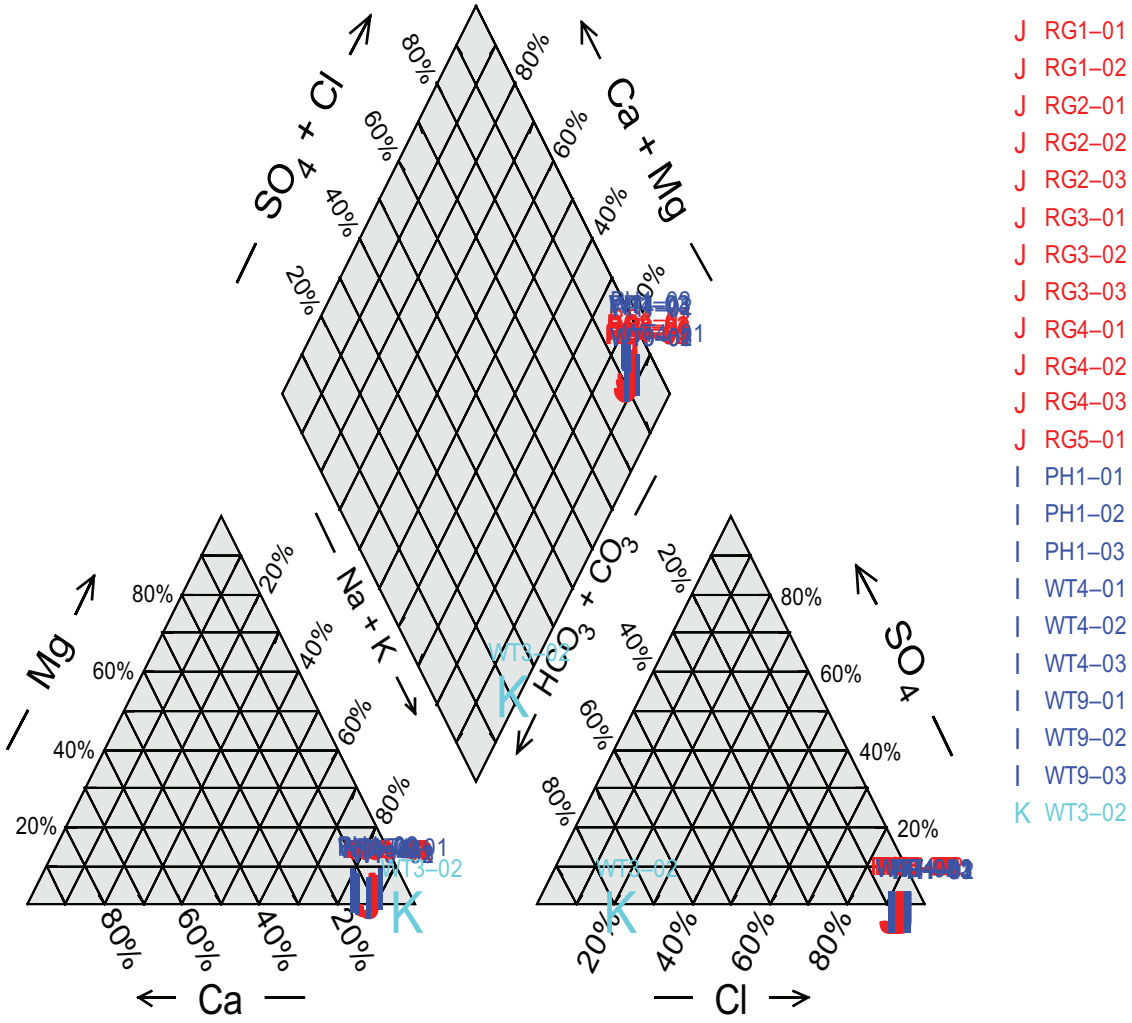

Figure 38 Piper plot of Jackson brines prior to CO_2 injection shows that they are rich in NaCl. Water injected back into the Jackson reservoir (i.e., make-up water) consists of Jackson brine produced during oil production and dilute Pennsylvanian water from WT-3. The WT-3 water, in contrast, is rich in $NaHCO_3$. Variable mixing and communication in the Jackson reservoir has produced brine of intermediate salinity ("J") that represent mixtures of saline Jackson ("I") and dilute Pennsylvanian ("K") waters.

frequently diluted the concentration of CO_2. This effect can be observed in Figure 6-7 where concentrations of CO_2 are often inversely correlated to (O_2 + N_2) concentrations for RG-1, RG-2, and RG-3. The gas samples with the least amount of O_2 contamination should give the best indications of the natural CO_2 and hydrocarbon concentrations for the production wells. Appendix 6 shows the gas chromatograph results for production well gas samples prior to breakthrough of injected CO_2 that also had low O_2 concentrations.

Pre-injection Chemistry of Pennsylvanian Groundwater

Prior to CO_2 injection, two samples were collected from WT-3 to determine baseline geochemical conditions within the deep Pennsylvanian groundwater aquifer. The samples are $NaHCO_3$-rich waters and have TDS ranging from 842 mg/L to 1,077 mg/L (Figures 38, 39; Appendix 7). Groundwater-quality data from deep Pennsylvanian sandstone aquifers compiled by Davis et al. (1974) indicate that $NaHCO_3$-rich waters are the dominant water type associated with these deep aquifers. Groundwater salinities for WT-3 are similar to those presented by Davis et al. (1974). Alkalinity, pH, DIC, and dissolved CO_2 ranged from 633–652 mg/L, 8.54–8.84 pH units, 129–158 mg/L, and 480–526 mg/L, respectively (Appendix 7). Pre-injection pH values are very similar to those listed in Davis et al. (1974). Pre-injection concentration ranges for cations and anions are listed in Appendix 8.

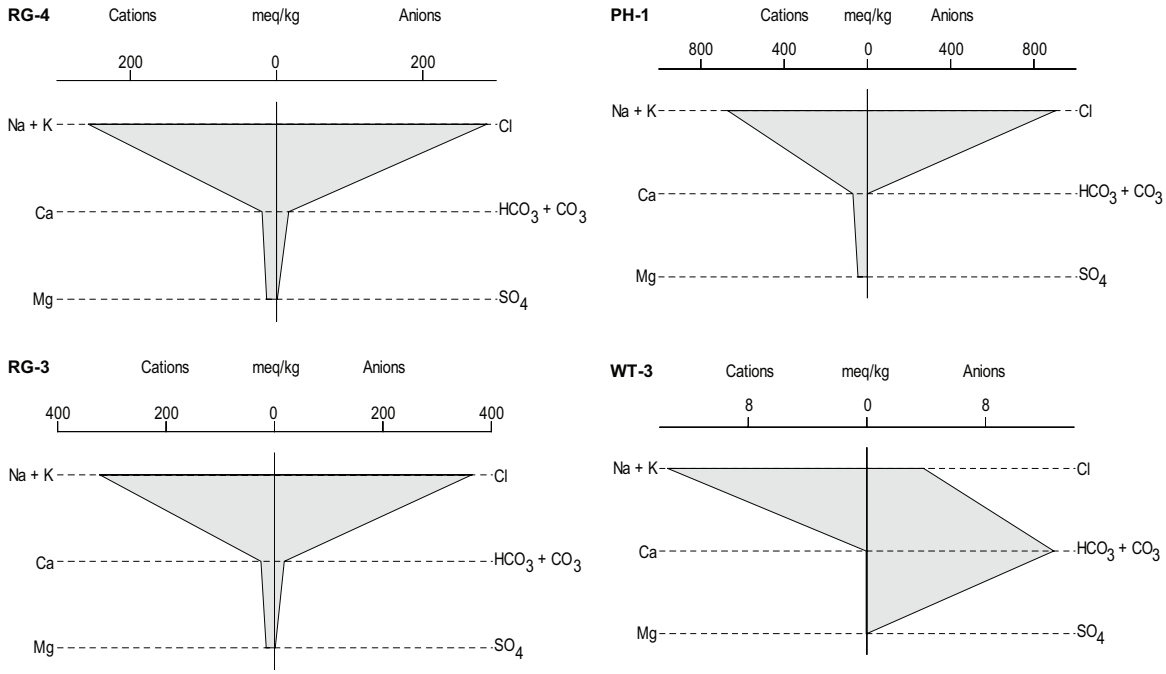

Figure 39 Stiff plots for wells RG-4, RG-3, PH-1, and WT-3. The NaCl-rich samples from RG-4, RG-3, and PH-1 demonstrate the variation in Jackson brine salinity, expressed as milliequivalents per kilogram, before CO_2 injection. Intermediate salinities occur in RG-4 and RG-3, and high salinities occur in PH-1 (note scale difference). Pennsylvanian groundwater from WT-3 is rich in $NaHCO_3$ and even more dilute.

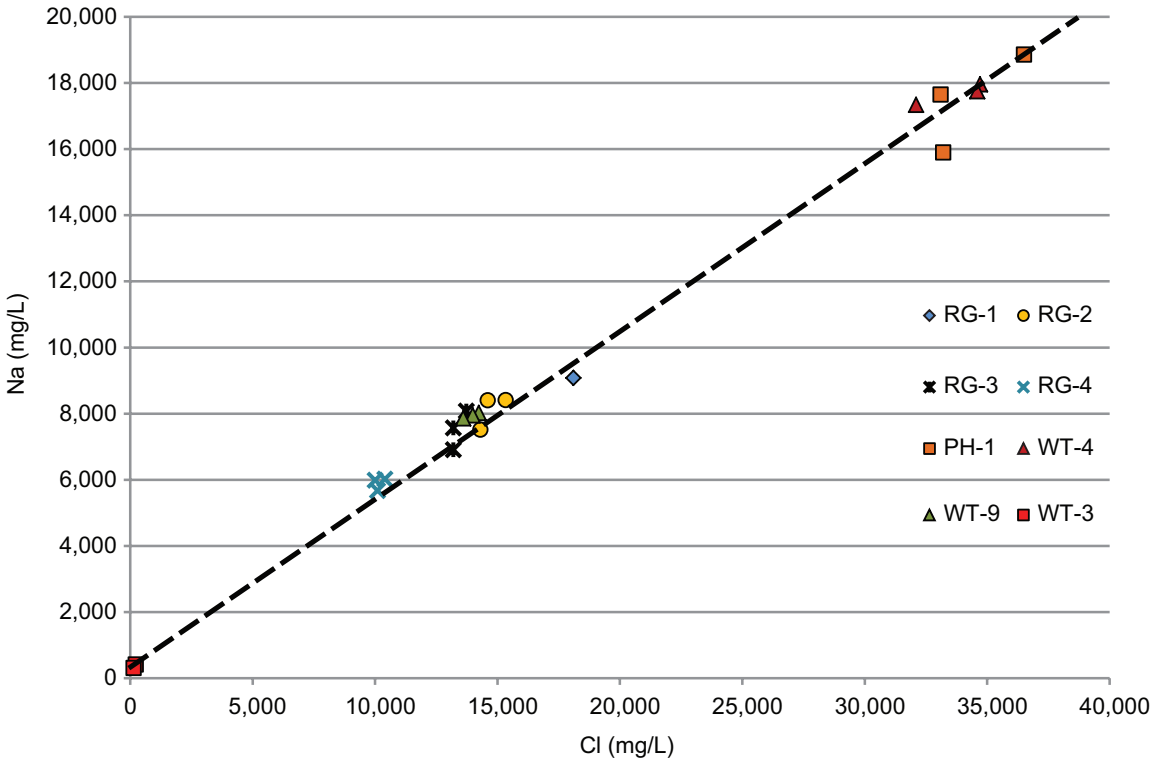

Figure 40 Sodium and chloride concentrations of Jackson brines from production wells and dilute Pennsylvanian groundwater from WT-3 before CO_2 injection. The distribution suggests that formation waters in the RG and WT-9 wells represent a composite formed by linear mixing between dilute WT-3 water and more saline water from PH-1 and WT-4. Moreover, lever-rule relationships suggest that dilute WT-3 water makes up 50% or more of the formation water in the RG and WT-9 wells. Comparison with regional brine data suggests that WT-4 and PH-1 waters are similar in composition to Mississippian-age formation waters that were not affected by waterflooding or other human influences.

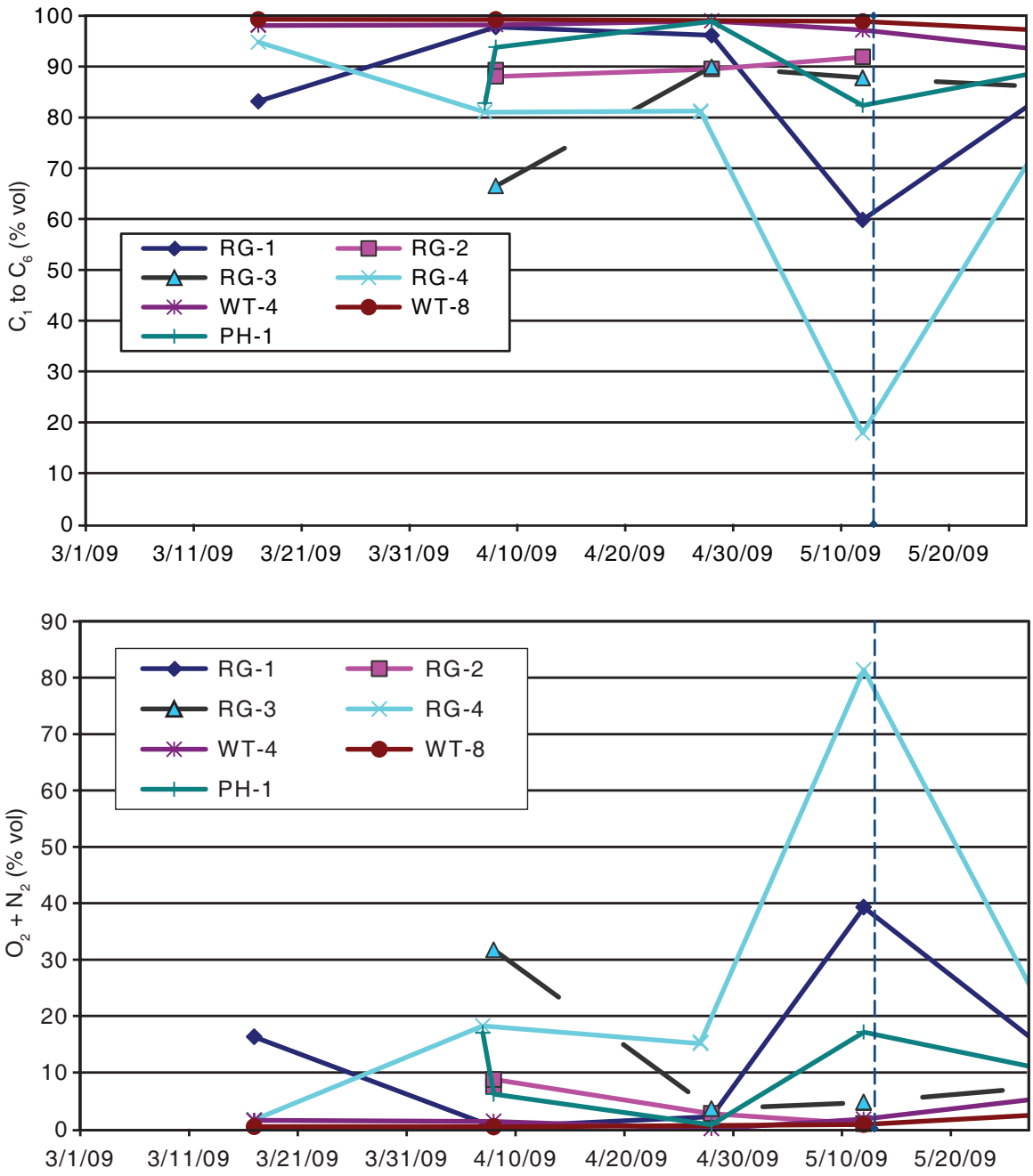

Figure 41 Graphs showing how air contamination affected the concentration of hydrocarbons ($C_1$to C_6) in the production wells. Air is represented by the sum of O_2+N_2 concentrations for samples prior to the start of CO_2 injection at the Sugar Creek site. Vertical dashed line indicates the day that CO_2 injection started (May 13, 2009).

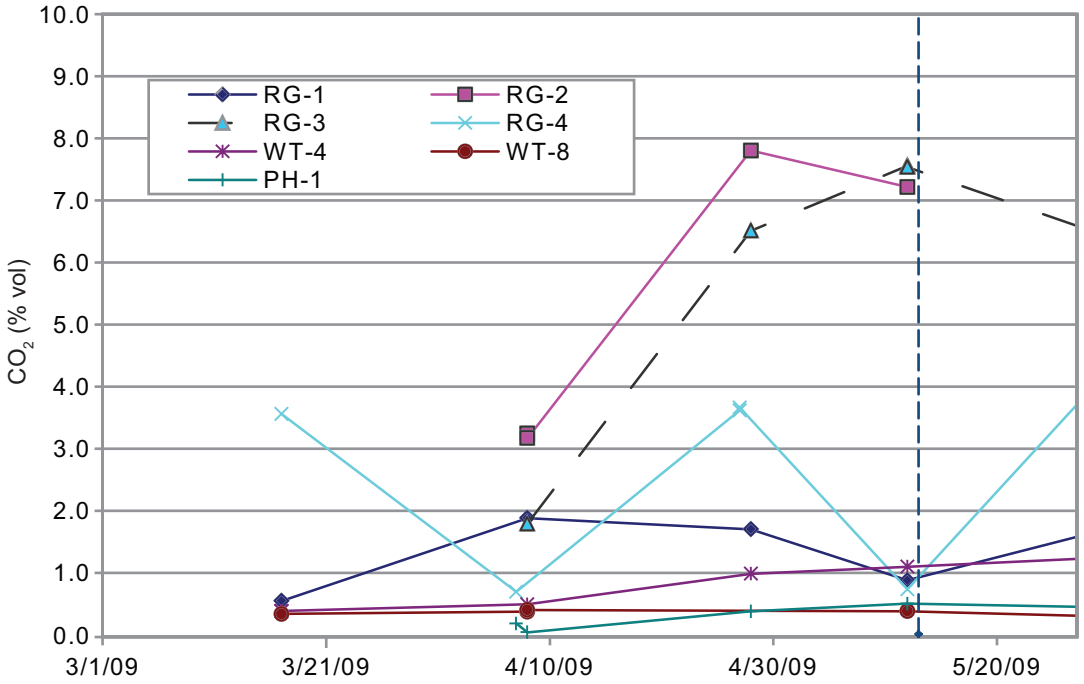

Figure 42 Concentration of CO_2 in the production wells leading up to and immediately preceding the start of CO_2 injection at the Sugar Creek site. Vertical dashed line indicates the day that CO_2 injection started (May 13, 2009).

Pre-injection shallow Pennsylvanian groundwater samples were collected from DC-1 (two samples) and KB-1 (three samples) outside of the field. Within the field boundaries, three samples each were collected from RG-4MW, RG-5MW, and PH-1MW (Figure 3). These samples provided data used to determine local baseline geochemical conditions within the shallow Pennsylvanian aquifers. As discussed in the MVA Strategies section, these data were important because no groundwater quality data were available for shallow Pennsylvanian aquifers within a one-mile radius of the injection well.

Groundwater samples collected from DC-1 and KB-1 are similar to those from WT-3 in that they are $NaHCO_3$-rich (Figure 44). However, TDS values for DC-1 (304–528 mg/L) are lower than those for KB-1 (688–828 mg/L), which are closer to TDS values of WT-3. Bicarbonate, sulfate, sodium, and chloride concentrations are much higher in KB-1 than in DC-1 (Appendix 9), which accounts for the difference in TDS. Pre-injection alkalinity, pH, DIC, dissolved CO_2, and other solute concentration ranges for DC-1 and KB-1 are listed in Appendices 7 and 9.

Groundwater from RG-4MW, RG-5MW, and PH-1MW are Na-Ca-HCO_3-SO_4-type waters (Figure 44). Salinity ranges from 712–996 mg/L. Alkalinity, pH, DIC, dissolved CO_2, and other solute concentration ranges are listed in Appendices 7 and 9.

Hydrogeologic Data from the Drilling and Monitoring Well Installation

A shallow groundwater monitoring system was designed based on hydrogeologic modeling of a hypothetical CO_2 release to the shallow groundwater in the vicinity of the test site. The objectives of the groundwater modeling were (1) to design a groundwater monitoring system that would detect any CO_2 leaked to shallow groundwater, and (2) to determine the rate of flow and transport direction of any CO_2 that leaked into the shallow groundwater from the injection point. The model was initially based on available information prior to drilling new wells. The model was revised based on geologic and hydrologic data collected at the new wells drilled at the site. The results of this model were used to predict the fate and transport of any CO_2 that might leak from the injection zone.

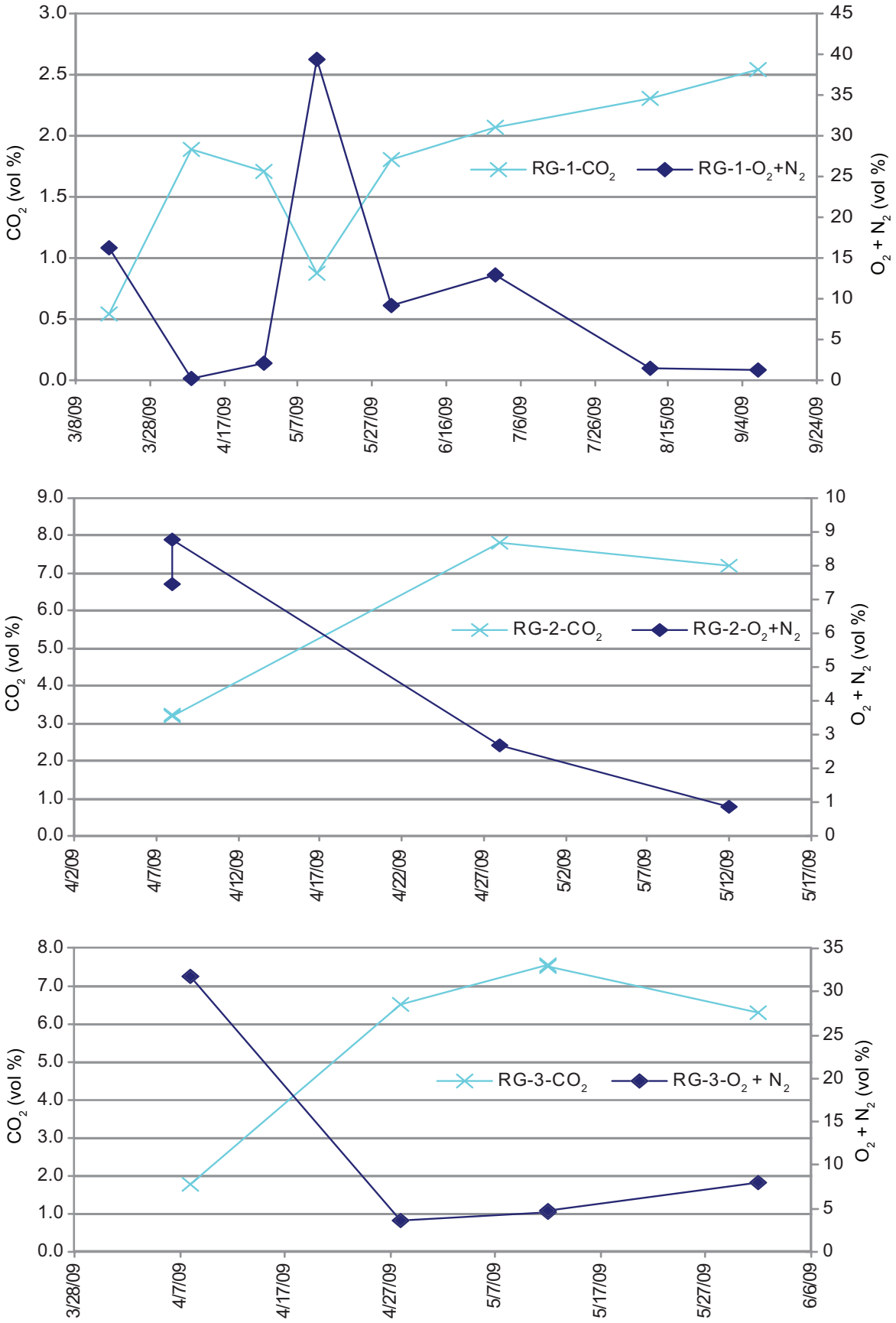

Figure 43 Concentrations of CO_2 and (O_2 + N_2) for production wells RG-1, RG-2, and RG-3 during the initial weeks prior to CO_2 injection at the Sugar Creek site. Graphs show how contamination by air diluted the concentration of CO_2 observed in the gas sample bags. Duplicate samples were taken at RG-2 on April 8, 2009.

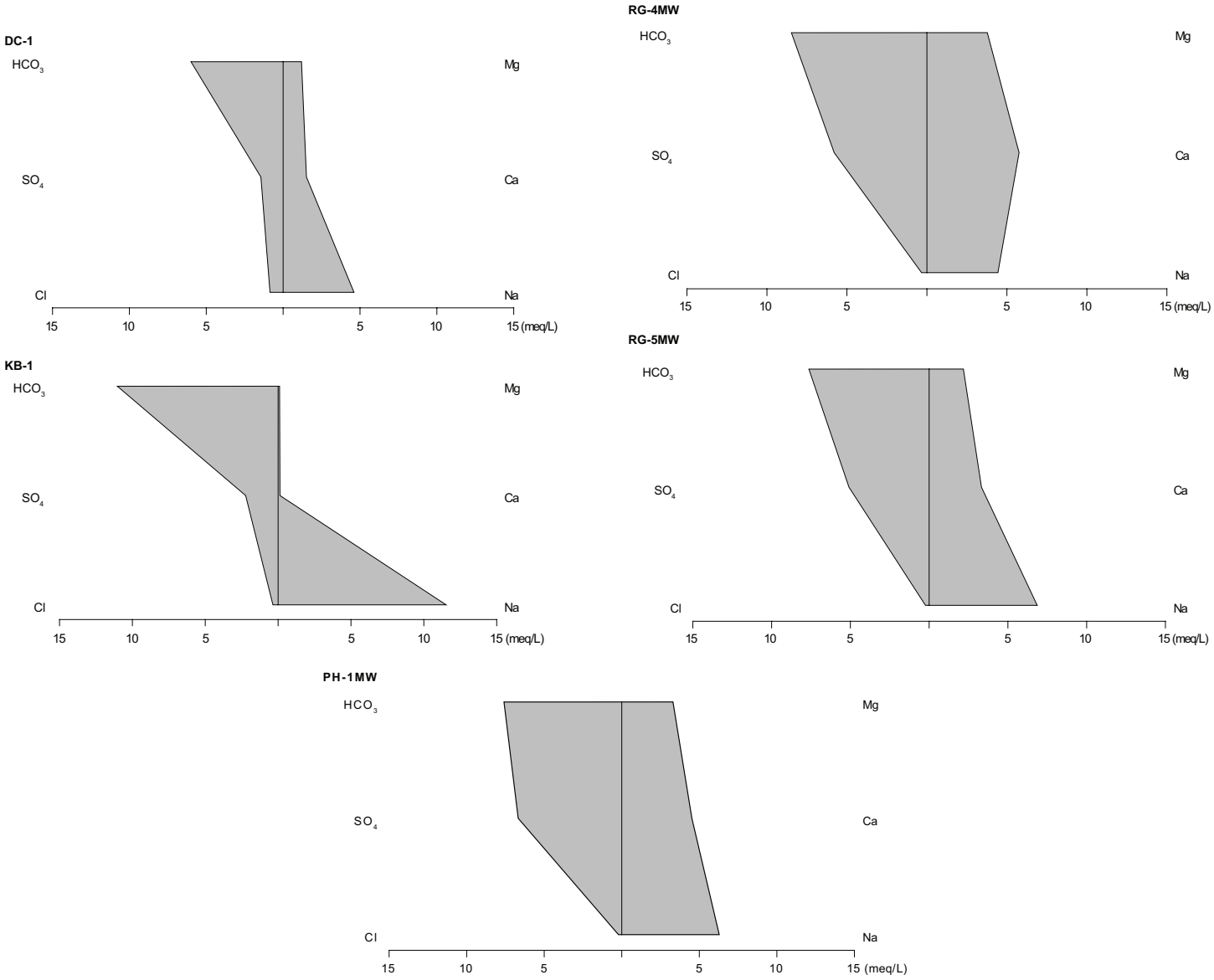

Figure 44 Stiff plots showing compositional diversity of shallow Pennsylvanian groundwater before CO_2 injection at wells DC-1 and KB-1, RG4-MW and RG5-MW, and PH-1MW. Solute concentration is expressed as milliequivalents per liter.

Data on mean annual flow for three streams near the EOR III test site (Sugar Creek, Clear Creek, and Richland Creek; Figure 45), available at the Hydrology of Kentucky website (http://kygeonet.ky.gov/kyhydro/main.htm), were used as the major input to the groundwater model. Table 13 shows the mean annual flow for these three streams.

Table 13 Mean annual flow for streams in the study area.

Stream	Location	Mean annual flow (cfs)
Richland Creek	Just upstream of confluence with Clear Creek	20.4
Sugar Creek	Just upstream of confluence with Clear Creek	8.1
Clear Creek	Just upstream of Route 70	20.9

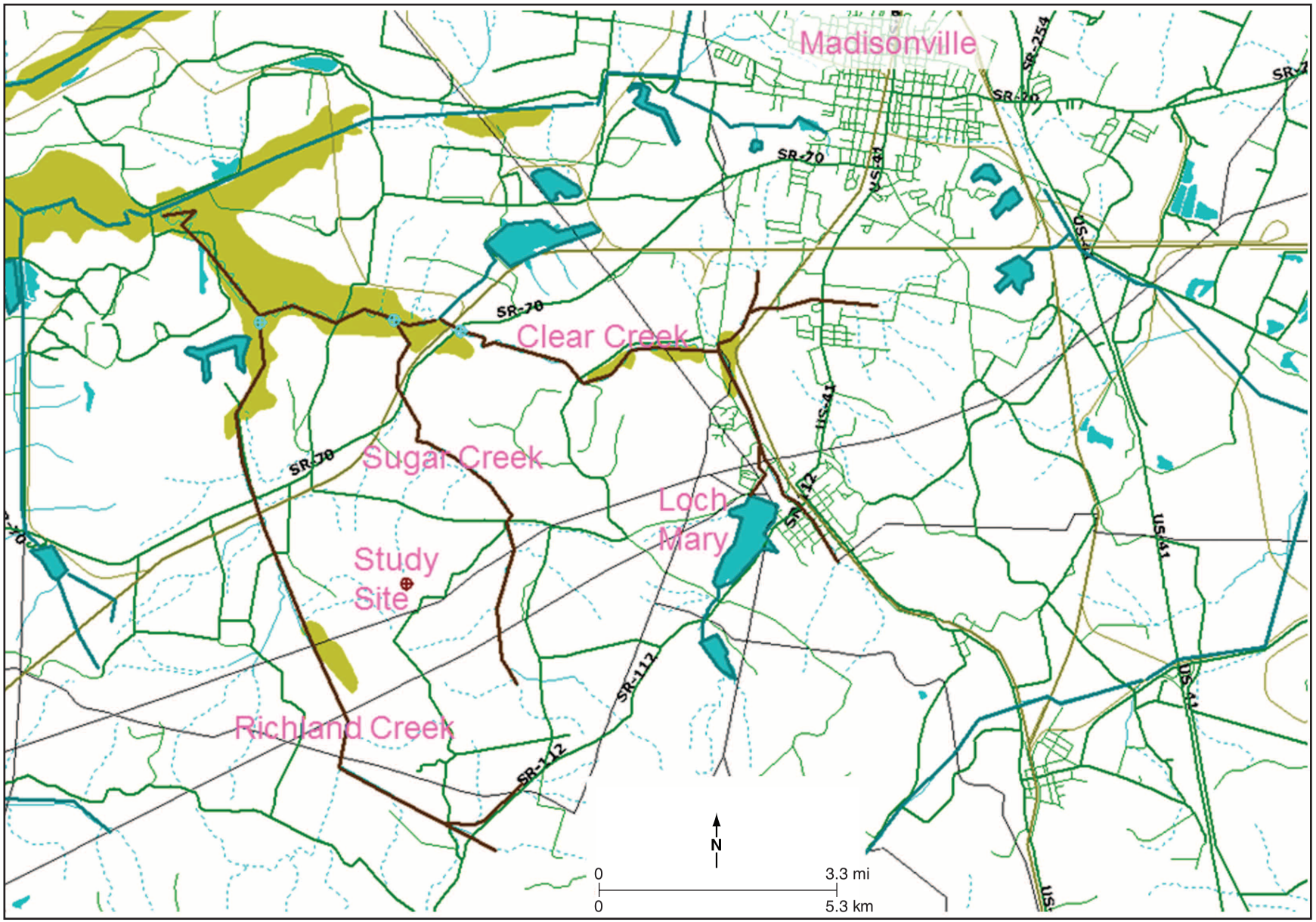

Figure 45 Map of study site and surrounding area. Streams are shown in brown and dark green. Roads appear as green linear features, while railroads are mustard color linear features. The olive-green colored polygons depict wetlands. A monitoring well is located at the study site. Test points for the model (streamflow) are depicted with turquoise markers along Clear Creek. The turquoise dashed lines are intermittent streams.

At the Hydrology of Kentucky website, *Low-flow and mean annual flow* is a vector data set representing streams in Kentucky. Each line segment is attributed with the 7-day 2-year low-flow frequency values (lf7Q2), 7-day 10-year low-flow frequency values (lf7Q10), and the mean annual streamflow values (MEAN_ANNUAL_FLOW) for the downstream end of that stream segment (all in cubic feet per second [cfs]). For example, the "7-day 2-year low-flow" is the flow rate, averaged over seven days, that has a 50% chance (i.e., one of every two years) of being exceeded in any year; the 10-year value has a 10% chance of being exceeded in any year (i.e., one of every ten years). Low-flow values were calculated using the equations in Ruhl and Martin (1991). Mean annual streamflow values were calculated using the equation in Martin (2002).

Analytic element modeling (AEM) was used because shallow groundwater and surface water flow can be modeled simultaneously using a relatively simple data set. The AEM method is suitable for modeling steady state flow, but transient flow and three-dimensional flow can only be partially represented in the model, and aquifer properties that change gradually from one place to another are difficult to represent. However, these issues were not considered for this simplified groundwater model based on limited data.

Analytic elements were chosen to best represent certain hydrologic features. For instance, stream sections and lake boundaries were represented by line sinks, and small lakes or wetlands were represented by areal sink distributions. Areal recharge was modeled by an areal sink with a negative strength. Streams and lakes that were not fully connected to the aquifer were modeled by line sinks or area sinks with a bottom resistance. Discontinuities in aquifer thickness or hydraulic conductivity were modeled by use of line doublets (double layers). Specialized analytic elements were used for special features such as drains or slurry walls. Locally, three-dimensional solutions such as a partially penetrating well (Haitjema, 1985) may be added where necessary.

A simple conceptual model was adopted for the local hydrogeology. A single surficial aquifer was assumed to extend from ground surface to a base elevation of 98 m (320 ft) below ground level, which was considered the base of the shallow Pennsylvanian sandstone that is used locally for domestic and commercial water supplies. This aquifer was assumed to have uniform properties (hydraulic conductivity, porosity, etc.).

The software used for analytic element modeling was GFLOW v2.1.2 (www.haitjema.com). Input parameters were either estimated from available information or calibrated in the modeling process (Table 14). The model was calibrated using three values of streamflow and a single value for groundwater head at the study site. Because groundwater discharge is more significant to total streamflow at low flows, 5% of the mean annual streamflow was adopted as the calibration target for streamflow from the model. The model was calibrated using streamflow data from the three streams listed in Table 13. After the flow model was calibrated, particle tracking was used to determine the flow paths and travel time for CO_2 from a hypothetical leak at the injection well. The model was used to assess impacts to the streams and the surficial aquifer from any CO_2 leakage.

Table 14 Input parameters for GFLOW.

Aquifer parameters	Value			Source
Base elevation (ft)			320	Field data
Thickness (ft)			145	Estimate
Porosity			0.2	Estimate
Hydraulic conductivity (ft/day)			2	Model calibration
Recharge (inches/year)			0.75	Model calibration
Stream parameters	Richland Creek	Sugar Creek	Clear Creek	Source
5% of mean annual streamflow (cfs)	1.02	0.41	1.05	Hydrology of Kentucky website
Width (ft)	10	10	10	Field data
Depth (ft)	2	2	2	Field data
Resistance (ft)	0	0	0	Estimate

Model results indicated that a groundwater divide was present at the site; groundwater flowed towards Richland Creek to the northwest and Sugar Creek to the northeast (Figure 46). For the calibrated model, recharge was set at 1.9 cm/yr (0.75 in/yr) and hydraulic conductivity at 2 ft/d or 7.1×10^{-4} cm/s. The modeled and target streamflow for the three streams differed by less than 15% for the calibrated model, while the groundwater head at the study site was 3 m (9 ft) higher than the observed value (Table 15, case without pumping). The values of recharge and hydraulic conductivity (K) used in the calibrated model are about an order of magnitude lower than values used in AE models for Illinois watersheds (Mehnert et al., 2005).

Table 15 Comparison of predicted and observed values with and without active (pumping) groundwater wells.

		Case without pumping		Case with pumping	
Test points	Observed value	Predicted value	Difference (%)	Predicted value	Difference (%)
Head in monitoring well (ft)	405	414	+2.2	410	+1.2
Streamflow in Richland Creek (ft^3/day)	88,000	94,000	+6.8	90,000	+2.3
Streamflow in Sugar Creek (ft^3/day)	35,000	30,000	–14.3	28,000	–20
Streamflow in Clear Creek (ft^3/day)	90,000	90,000	+0	91,000	+1.1

Particle tracking was used to determine the direction and travel time for CO_2, assuming that there was leakage at the injection point into the surficial aquifer and that the CO_2 was dissolved but did not react during transport. The leak was modeled as being continuous and of sufficient size (e.g., 929 m^2 or 10,000 ft^2) to be monitored; the software did not have the capability of modeling a leak with a specified magnitude or duration. Using these initial input data, the model results indicated that the CO_2 plume did not migrate very far from the site. No particles reached Richland Creek or Sugar Creek after 100 years of transport (Figure 47).

In this area of Hopkins County, groundwater is pumped from the bedrock for domestic and commercial uses. Two local wells were included in the model to evaluate the effects of these wells on the transport of any CO_2 leaked. Both wells were located on the southwest side of the groundwater divide. The westernmost of the two wells had a pumping rate of 91 m^3/d (3,200 ft^3/d or 24,000 gal/d). The east well was originally assigned a pumping rate of 310 m^3/d (11,000 ft^3/d or 82,000 gal/d), but this rate dewatered the aquifer. The east well was then also assigned a pumping rate of 91 m^3/d (3,200 ft^3/d or 24,000 gal/d). The presence of the pumping wells altered the groundwater heads and particle tracking results (Figure 48). The east well captured approximately two-thirds of the particles over the 100 year modeled period. The other particles remained flowing in the aquifer, but would eventually be captured by the east well.

The sensitivities of two key model outputs (streamflow and groundwater heads) were determined with respect to changes in recharge. A 100% increase in recharge resulted in an average increase of 79% for the three streamflow values predicted by the model, but caused only a 2.4% increase in groundwater head at the observation well.

The results from the groundwater modeling showed that, under natural flow conditions in the shallow Pennsylvanian aquifer, transport of any CO_2 leaked to the groundwater would be very slow. However, transport rates in the shallow groundwater increased significantly when groundwater pumpage in two different wells was included in the model. As shown in Figure 48, over the 100-year period of the model, the easternmost of the two wells, located approximately 518 m (1,700 ft) west of the injection well, appeared to be susceptible to any leaked CO_2 when it was pumped at the rate of 91 m^3/d (3,200 ft^3/d or 24,000 gallons) per day.

Kinetic Modeling

A batch reaction model of the injection process was first constructed using React software (Bethke and Yeakel, 2007). The model input was the brine composition of a sample collected on-site (Table 16) at the injection well, RG-5. In the model, this brine equilibrated with CO_2 at reservoir fugacity of 33.7.

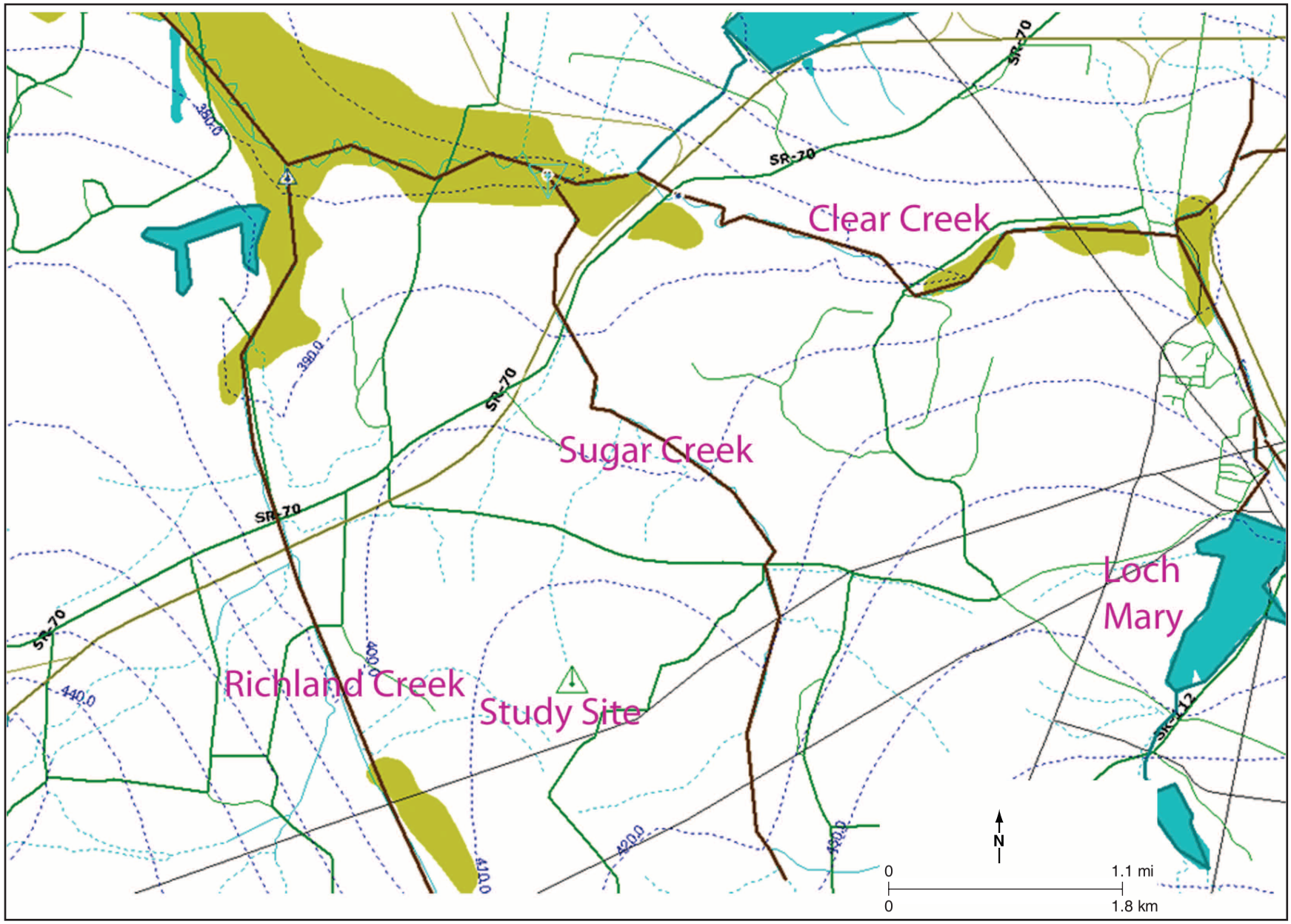

Figure 46 GFLOW output for the Clear Creek area. The estimated groundwater heads are contoured using dashed blue lines and have a 3-m (10-ft) contour interval. In the vicinity of the study site (green triangle) a northwest-southeast-trending groundwater divide is present.

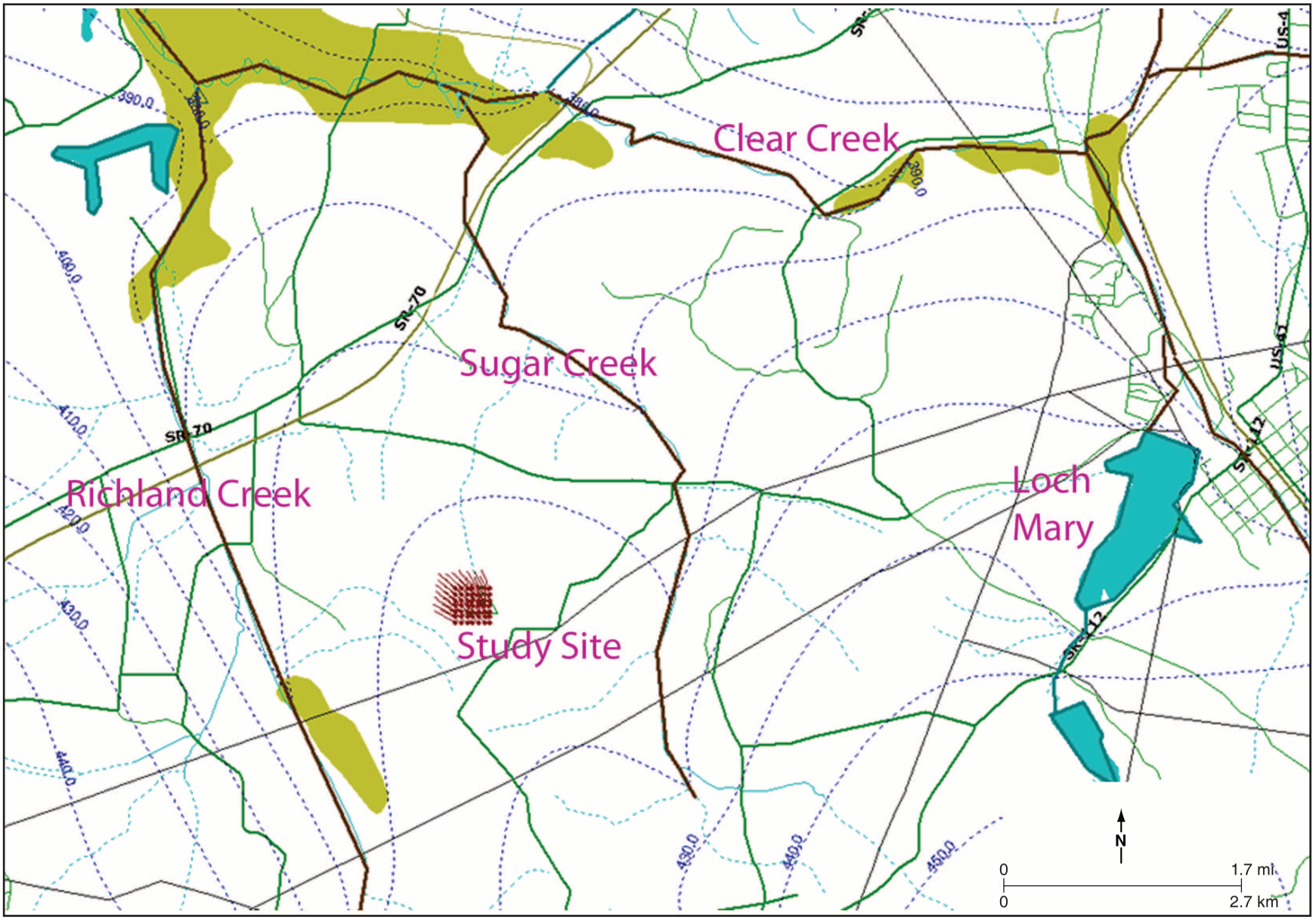

Figure 47 GFLOW output for the Clear Creek area showing particle tracking for 100 years (no groundwater pumping). The 49 particles included in the analysis are illustrated by the red points and attached lines near the study site. Contour interval is 3 m (10 ft). Blue dashed lines are equipotential lines.

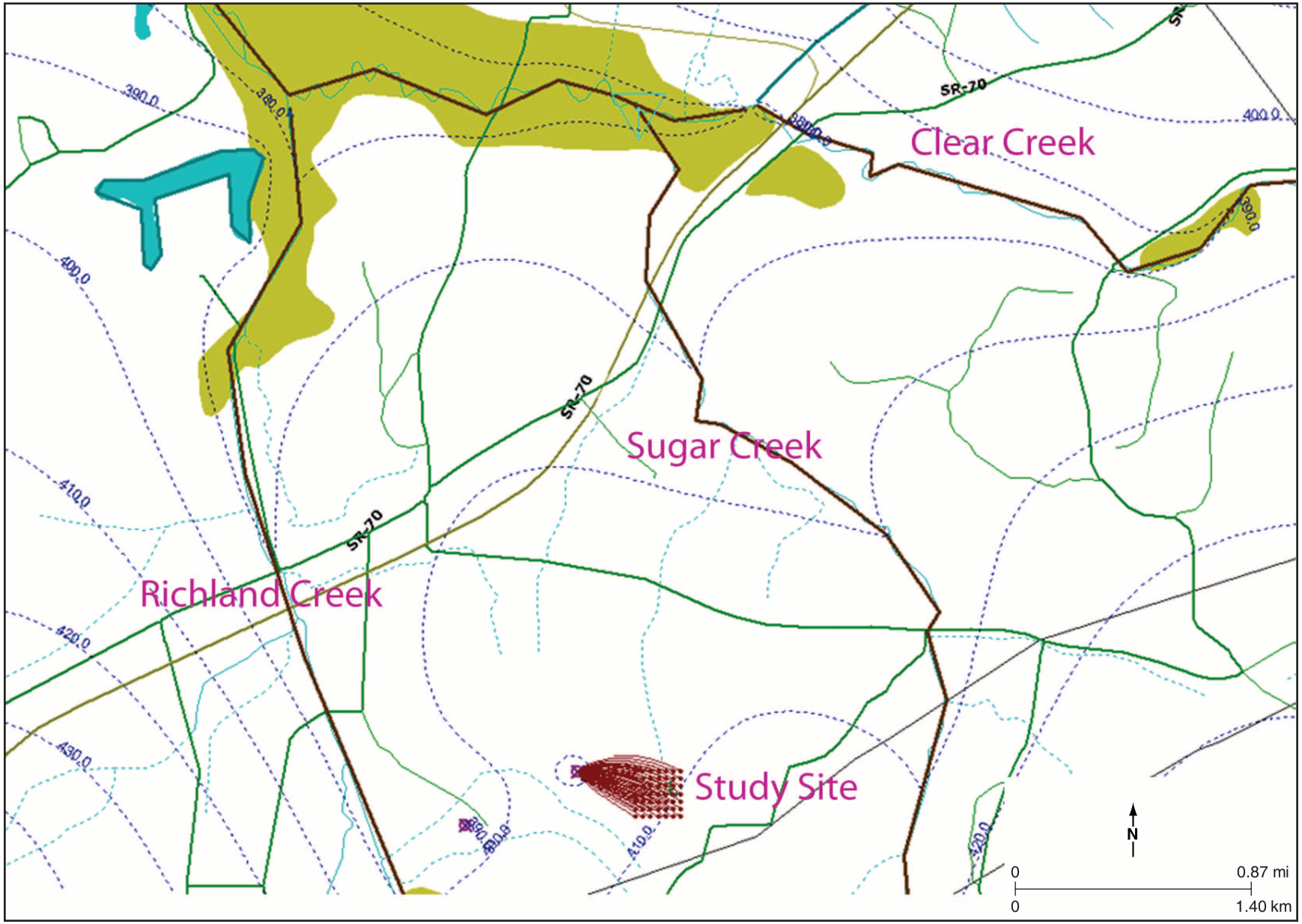

Figure 48 GFLOW output for the Clear Creek area showing particle tracking for 100 years with groundwater pumping from two local wells. The 49 particles included in the analysis are illustrated by the red points and attached lines near the study site. Blue dashed lines are equipotential lines showing groundwater head. Contour interval is 3 m (10 ft).

Table 16 Initial brine composition for the batch reaction model, based on the brine sample collected at RG-5. Elemental composition is in milligrams per liter. CO_2 was constrained by setting the initial solution to be in equilibrium with calcite.

pH 7.10	Temperature (°C) 16.3	Eh (mV) −161	Cl 11,164	Br 46.7	SO_4 32.4	PO_4 7.38	NH_4 2.62	Al 0.061
B 1.26	Ba 2.84	Ca 451	Fe 0.05	K 27.4	Li 1.41	Mg 181	Mn 0.13	Na 6,434
Ni 0.09	Pb 0.05	Se 0.26	Si 6.67	Sr 295				

The next stage in the model was the reaction of the acidified brine with reservoir rocks. The mineralogical composition of those rocks was determined from XRD analysis (Table 17, Appendix 4). The kinetic rates for the brine-rock interactions for the second stage from the compilation of Palandri and Kharaka (2004) were used. A reaction interval of 1,000 years was studied.

Table 17 Average mineralogical composition (%) adapted from XRD analysis of reservoir samples near RG-5.

Quartz 80.4	K-Feldspar 0.3	Na-Plagioclase 2.8	Calcite 2.6	Ankerite 6.2
Dolomite 0.4	Pyrite 0.1	Illite and mica 2.6	Kaolinite 2.4	Chlorite 2.2

Calcite dissolution controlled the system in the initial equilibrium model by consuming some of the added CO_2 and buffering the pH.

$$CaCO_3 + CO_2 + H_2O \leftrightarrow Ca^{2+} + 2\ HCO_3^- \quad (4)$$

This reaction was the only solid phase reaction allowed to take place during the initial modeling because reactions with silicate minerals are expected to take too long to treat as equilibrium processes. Without the buffering action of the calcite, the pH would decrease to about 3.5.

After this initial reaction, the conversion of illite to smectite became the dominant cause of change in pH (Figures 49 and 50). This reaction buffered the pH to less acidic values (Figure 50). However, the reactions took longer because of the slower kinetics of silicate dissolution and precipitation (Palandri and Kharaka, 2004). The overall porosity changes caused by these reactions were negligible because the reactions were simply the alteration of one clay to another with little new material precipitating.

The increase in pH allowed more CO_2 to enter the brine and form calcite, increasing the amount of both mineral and solubility sequestration (Figure 51). Overall, the amount of CO_2 sequestered in this model is a best case scenario because of the assumption that CO_2 pressure will maintain its maximum value. A more realistic case would be a decrease and equilibration of CO_2 pressure resulting from the dissolution into the brine and spreading of the plume. This spreading would lead to less sequestration per unit volume of the reservoir, but allow more of the reservoir to act as a CO_2 sink.

The CO_2 breakthrough event impacted the phase equilibria of groundwater at WT-9 and RG-3. The chemical composition of groundwater samples collected at the monitoring wells was input to the geochemical model PHREEQCi (Parkhurst and Appelo, 1999; Charlton and Parkhurst, 2002). Before the injection of CO_2, the groundwater at both wells appeared to be slightly supersaturated with respect to calcium carbonate, favoring the precipitation of some type of calcium carbonate phase (Figure 52). The Day 48 sample collected at RG-3 was, however, undersaturated with respect to calcium carbonate. It was speculated that

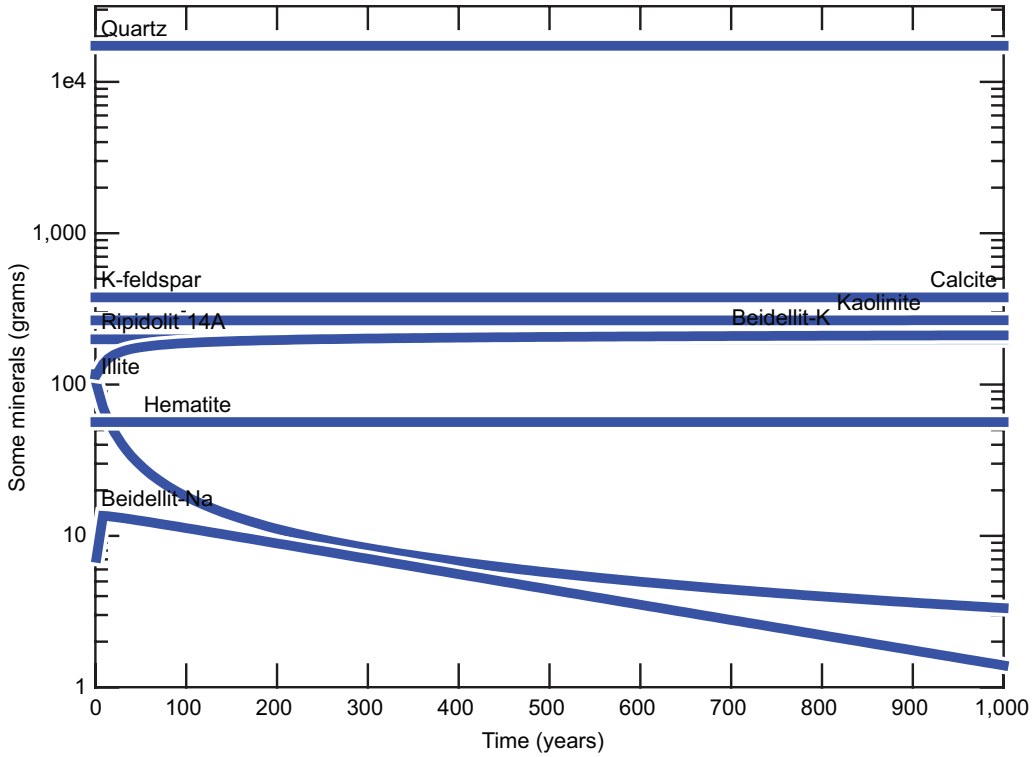

Figure 49 Changes in mineralogical composition as the reservoir rock reacts with acidified brine.

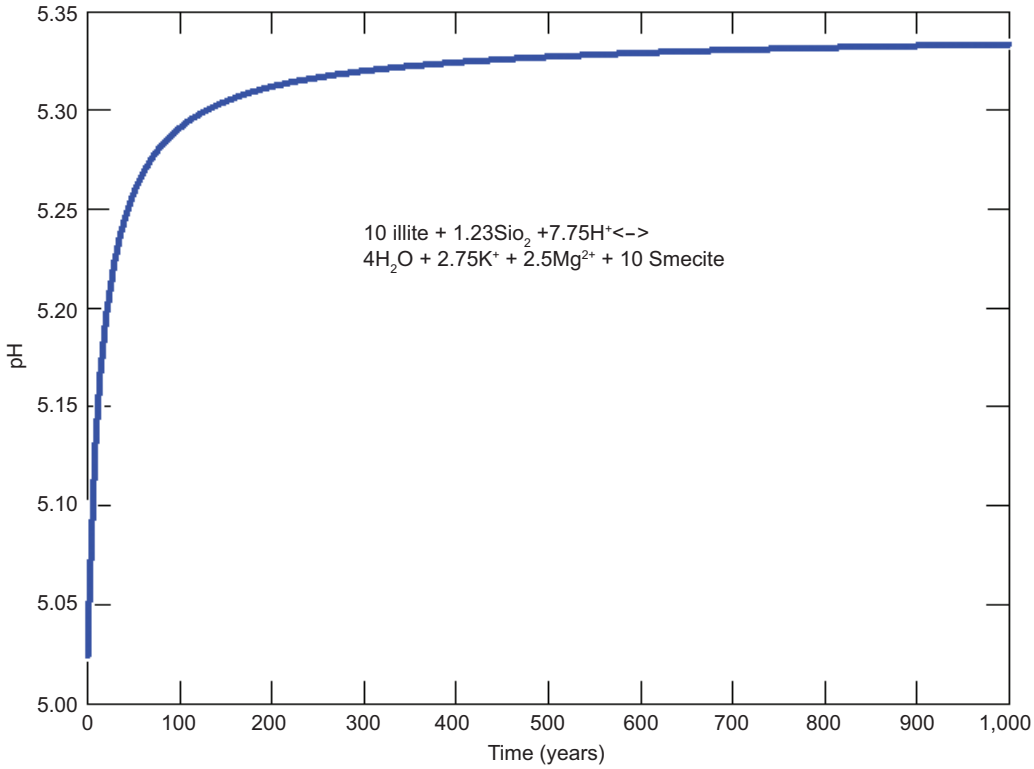

Figure 50 Evolution of pH as the acidified brine reacts with the reservoir minerals. The initial value is buffered by calcite dissolution, followed by the precipitation and dissolution of clays.

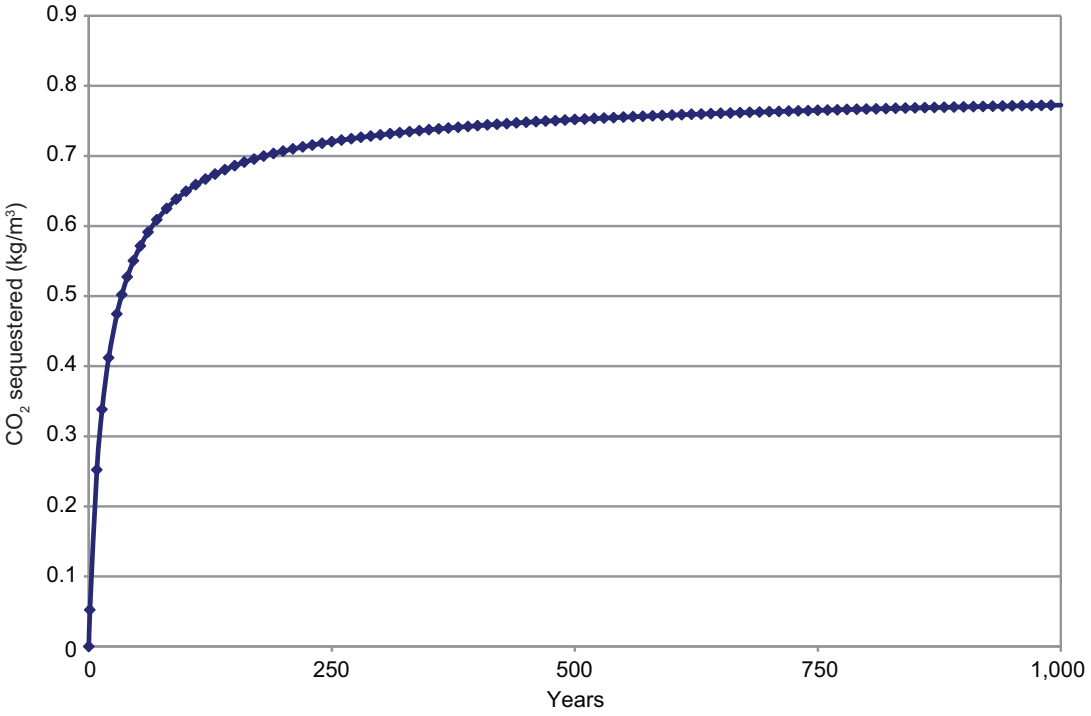

Figure 51 Total amount of CO_2 sequestered in the brine and calcite.

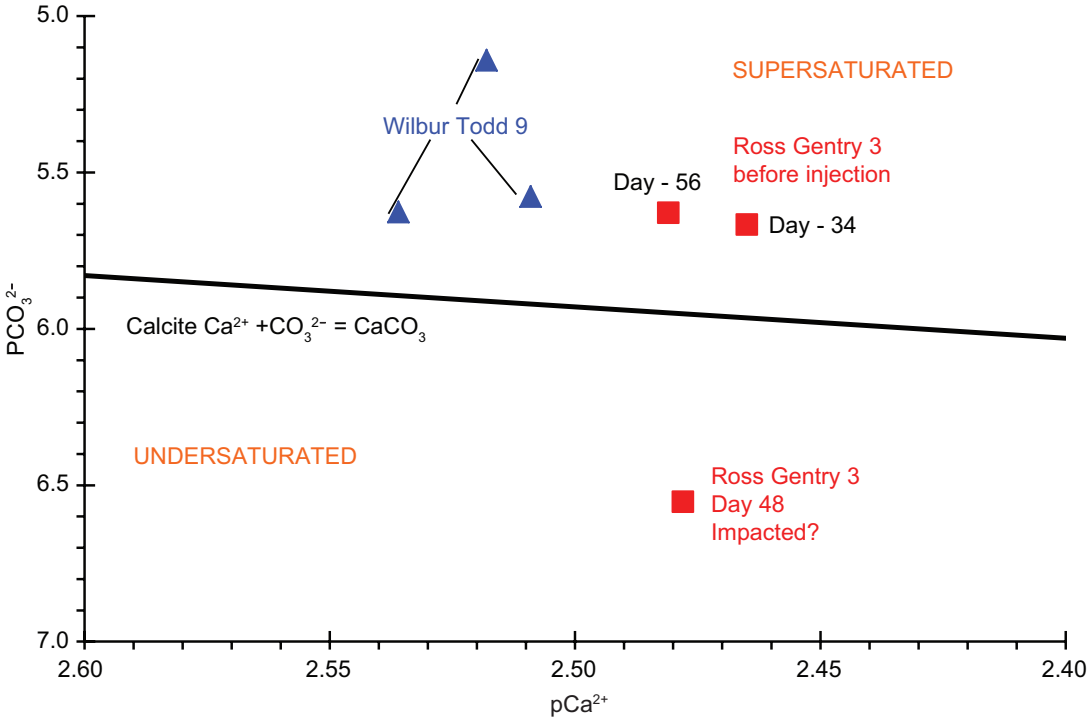

Figure 52 Calcium carbonate equilibria of Ross Gentry #3 (RG-3) and Wilbur Todd #9 (WT-9) observation wells at Sugar Creek Field. Groundwater samples collected at RG-3 were supersaturated with respect to calcium carbonate before breakthrough at RG-2. Well WT-9 appeared to be unaffected. The chemical composition of the groundwater samples was input to the geochemical model PHREEQCi (version 2.15.0). Negative values indicate the number of days before CO_2 injection began.

the uncontrolled release of CO_2 resulted in acidification of the groundwater, yielding a decrease in the concentration of bicarbonate ions, which would promote calcium carbonate dissolution.

Cased Hole Logging

Schlumberger Carbon Services provided the reservoir saturation tool (RST) log runs for monitoring of wellbore integrity and near-wellbore changes to saturation in any zones above the injection zone. To monitor the possible movement of CO_2 into the zones above the injection zone, the RST was used; the RST is a wireline pulsed neutron logging tool. The primary measurements are the macroscopic capture cross section and the neutron porosity of the formation. Appendix 10 relates primarily to the analysis of the RST data collected on RG-5 and eight of the oil producing and monitoring wells. The RST is considered most accurate within a few feet from the wellbore and diminishes in relevance radially from the wellbore.

The cased hole logging program consisted of running two passes of the RST to evaluate the containment of the CO_2. The first logging runs (base pass) of the RST were made in late March 2009, prior to CO_2 injection. In early October 2011, after injection of CO_2 and about 16 months of water injection, the post-CO_2 injection run of the RST log was made in each well.

On the baseline runs, no abnormalities were identified.

FIELD OPERATIONS DURING CO_2 INJECTION

CO_2 Pumping Equipment

Overview

The pump skid used at the Sugar Creek EOR III site was designed to inject CO_2 at surface pressures up to 14 MPag (2,000 psig). A rotary vane booster pump was used to reduce or prevent vapor locking in the main triplex plunger pump by increasing the pressure of the feed to the plunger pump to approximately 140 kPa (20 psi) above the inlet pressure from the storage tanks. A triplex plunger pump specifically designed for liquid CO_2 was installed downstream of the booster pump. There was a CO_2 return line to the storage tanks on the discharge lines of both the booster pump and the main triplex pump. The two CO_2 storage tanks were connected with vapor and liquid pressure equalization lines between them.

The pump skid was equipped with a liquid turbine flow meter used to measure the injection flow rate and a transmitter to send a 4–20 mA signal, proportional to the flow rate, to a data recorder. Temperature and pressure indicators were available for manual recording of the triplex pump suction and discharge temperatures and pressures. Temperature and pressure data used to estimate CO_2 density and calculate mass flow from the volumetric flow rate data were measured by a Sierra vortex meter.

There was an automated pressure control valve (PCV) on the recycle line of the triplex pump discharge. The automated pressure control valve at the EOR III site was connected to a pressure transmitter located immediately upstream of the line heater. If the discharge/injection set pressure was not exceeded, all of the CO_2 flowed out into the discharge line and to the injection well. If the discharge set pressure was exceeded, a portion of the CO_2 was diverted back to the storage tank through the PCV in order to meet the surface injection pressure set point on the main discharge line. The set point was typically around 9,100 kPa (1,320 psi) but was periodically adjusted up or down by a few psi in order to inject approximately one truckload of CO_2 per day and to keep the storage tanks approximately half full. (Later in the injection period, about 1½ truckloads per day were injected.)

A propane-fired line heater downstream of the liquid turbine flow meter heated the liquid CO_2 prior to delivery to the injection well. Temperature and pressure gauges were installed between the line heater and the wellhead (close to the line heater) so that the temperature and pressure of the CO_2 injected into the wellhead could be manually recorded.

In addition to measuring and recording CO_2 injection rate, the surface facilities at the Sugar Creek site provided for automatic measurement and recording of the following parameters:

- Booster pump inlet temperature and pressure
- Booster pump outlet temperature and pressure
- Main pump outlet temperature and pressure
- Line heater outlet temperature
- Wellhead (surface tubing) temperature and pressure

Equipment specifications for some of the equipment used to measure these above parameters are given in Appendix 11.

Typical operations at the Sugar Creek pilot test site, as indicated by field temperature, pressure, and flow meter readings, were as follows:

- CO_2 injection rates ranged from 18 to 27 tonnes/day (20 to 30 tons/day) (17.4–26.7 m^3/day [3.2–4.9 gpm], 111–167 bbl/day).
- Typical CO_2 supply conditions to the booster pump inlet were –20 to –17°C (–4 to 2°F) and 1.9 to 2.1 MPag (270 psig to 300 psig).
- The booster pump raised the pressure by about 170 kPag (25 psig).
- Typical CO_2 discharge conditions from the main (triplex) pump were –14 to –11°C (6 to 12°F) and 8.8 to 9.03 MPag (1,270 to 1,310 psig).
- CO_2 leaving the line heater was heated to about 16°C (60°F).

These values are representative of typical operations and are presented here to provide an understanding of the operational requirements of the CO_2 storage, pumping, and heating equipment during CO_2 injection at this site.

Figure 53 shows the piping and instrument diagram for the EOR III test site.

Portable Storage Tanks

At the Sugar Creek site, the CO_2 was stored on site in two unrefrigerated, insulated 45-tonne (50-ton) capacity storage tanks leased from Praxair. One tank served as the primary feed tank, and the second storage tank held a reserve supply in case of CO_2 delivery problems. Each tank had two 10-cm (4-inch) liquid CO_2 connections and three 5-cm (2-inch) vapor CO_2 connections. The tanks were each approximately 14 m (45 ft) long, 2.4 m (8 ft) wide, and 4.0 m (13 ft) high and weighed approximately 20,000 kg (45,000 lbs) at 0 kPa (0 psi) (i.e., when empty).

Booster Pump

A booster pump was used to improve the reliability of the main triplex plunger pump by increasing the pressure of the feed to the main pump to approximately 138 kPa (20 psi) above the pressure of the liquid CO_2 in the storage tanks. (Because CO_2 vapor is in equilibrium with CO_2 liquid in the storage tank, the pressure at the vapor-liquid interface is the vapor pressure of CO_2.) This reduced the possibility of vapor locking of the plunger pump. The booster pump, which is shown frosted-over in Figure 54, is a model CRL1.25 rotary vane pump manufactured by Blackmer. The booster pump was driven by a 0.75 kW (1 hp) motor equipped with a 0.75 kW variable frequency drive (VFD) made by Toshiba (left foreground). The VFD speed settings were manually adjusted to maintain the approximate 138 kPa (20 psi) differential between the suction and discharge pressures on the booster pumps.

The booster pump was rated for 71 m^3/day (13 gpm) at a differential pressure of 138 kPa (20 psi), requiring 1.1 kW (1.5 hp) of power at an impeller speed of 1,150 rpm. The maximum capacity of the booster pump was approximately 82 m^3/day (15 gpm) at 34 kPa (5 psi) of differential pressure. Because the motor used on the booster pump was rated for only 0.75 kW (1 hp), the maximum capacity and/or the discharge pressure of the pump was less than the values listed in the specification sheets for the pump.

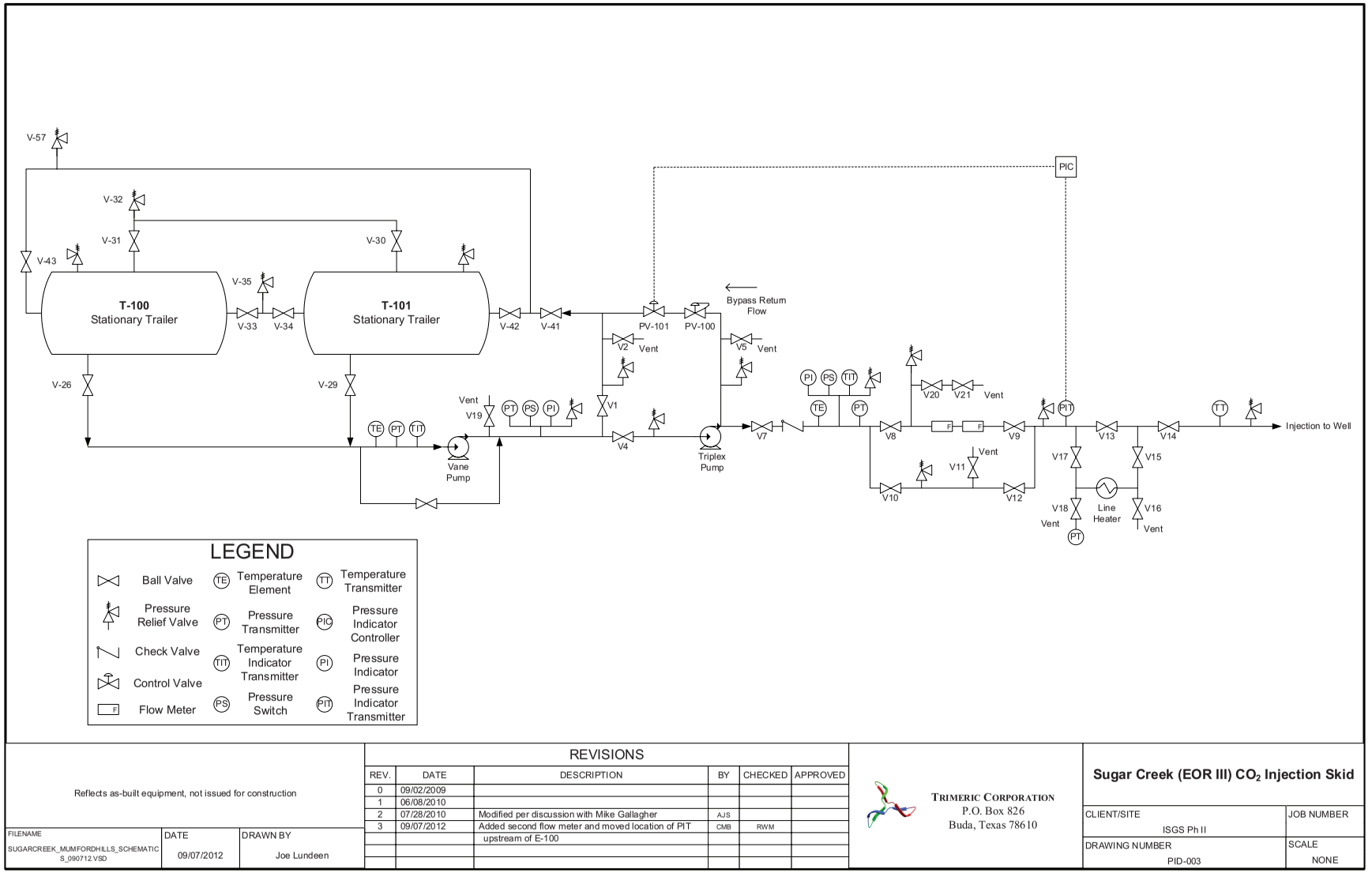

Reflects as-built equipment, not issued for construction

FILENAME	DATE	DRAWN BY
SUGARCREEK_MUMFORDHILLS_SCHEMATICS_090712.VSD	09/07/2012	Joe Lundeen

REVISIONS

REV.	DATE	DESCRIPTION	BY	CHECKED	APPROVED
0	09/02/2009				
1	06/08/2010				
2	07/28/2010	Modified per discussion with Mike Gallagher	AJS		
3	09/07/2012	Added second flow meter and moved location of PIT upstream of E-100	CMB	RWM	

TRIMERIC CORPORATION
P.O. Box 826
Buda, Texas 78610

Sugar Creek (EOR III) CO_2 Injection Skid

CLIENT/SITE	JOB NUMBER
ISGS Ph II	
DRAWING NUMBER	SCALE
PID-003	NONE

Figure 53 The CO_2 injection pump skid and instrument diagram.

Figure 54 Booster pump (frosted over) and motor. Manual temperature gauge (circular object at center), Siemens pressure gauge (just above and to the left of manual gauge; blue cover), and temperature probe (largely obscured behind Siemens gauge; base visible to immediate right of stem of Siemens gauge). Lines are covered with neoprene pipe insulation. (Photograph courtesy of Trimeric Corp.)

Main CO_2 Pump

The main CO_2 pump at the site was a model 3521 triplex plunger pump manufactured and supplied by CAT Pumps® and driven by an 11.2 kW (15 hp) motor equipped with an 11-kW variable frequency drive made by Toshiba. The drive speed settings were manually adjusted to achieve the desired CO_2 injection rate. The triplex plunger pump itself was capable of delivering liquid CO_2 at 125 m^3/day (23 gpm) and discharge pressures up to 13.8 MPa (2,000 psi) with a power requirement of 23.6 kW (31.6 hp). However, because the motor used on the pump at the Sugar Creek site was rated for only 11.2 kW (15 hp), the maximum capacity and/or discharge pressure of the pump was significantly less than the maximum values listed in the specification sheets. Figure 55 shows an identical triplex pump in operation at the Mumford Hills site.

Automated Injection-Pressure Control System

The automatic injection-pressure control system was designed to return a portion of the CO_2 discharged from the main pump back to the storage tanks in order to maintain constant discharge pressure on the line going to the injection well. A pressure transmitter measured the pressure of the CO_2 in the line going to the injection well and sent a signal to a controller that adjusted the pressure control valve, which regulated the amount of CO_2 returned to the storage tank as needed to maintain the pressure set point in the injection line. At the Sugar Creek site, the pressure transmitter was installed between the main CO_2 pump and the inlet to the line heater. Placing the transmitter near the line heater separated it from the main pump's vibrations.

The pressure control valve (Figure 56) was a 2.5-cm (1-in) Type 1711 Globe Cast Control Valve manufactured by BadgerMeter, Inc. The valve had an EVA-200 electric actuator, a 4–20 mA input signal, and linear

Figure 55 Triplex pump in operation at the EOR II site (a photograph of the specific triplex pump used at Sugar Creek was not available) with input and output lines and valves (frosted over in foreground). The gray motor (top) is behind the blue pump crankcase. Aluminum housing covers the belt and pulleys between the motor and pump crankcase. (Photograph courtesy of Trimeric Corp.)

size “G” trim with a Cv (flow coefficient) of 0.2. In case of a loss of signal, the control valve failed in the open position, which ensured that CO_2 was diverted back to the storage tank if it could not continue to the injection line. For example, if the wellhead inlet valve was closed due to a mistake or failure, then the automated pressure control valve would divert the CO_2 back to the storage tank instead of forcing mechanical pressure relief valves to open. If the site lost power, the valve remained in its position prior to the loss of electricity. The pressure transmitter was a Siemens Model Sitrans P 7MF4033-1EA10-1AC1-Z with flush-mounted process connections.

The Model # CNi3253-C24 Omega Controller (Figure 57) compared the actual pressure relayed from the pressure transmitter to the pressure set point and provided an output to the pressure control valve.

Figure 56 Globe Cast pressure control valve (BadgerMeter, Inc.) on the return line between the discharge of the main pump and storage tank. The electric actuator is shown top center (red base and equipment sitting on red base; the latter is usually covered in a red casing under operational conditions). The valve is below the actuator covered with black neoprene and gray duct tape. (Photograph courtesy of Trimeric Corp.)

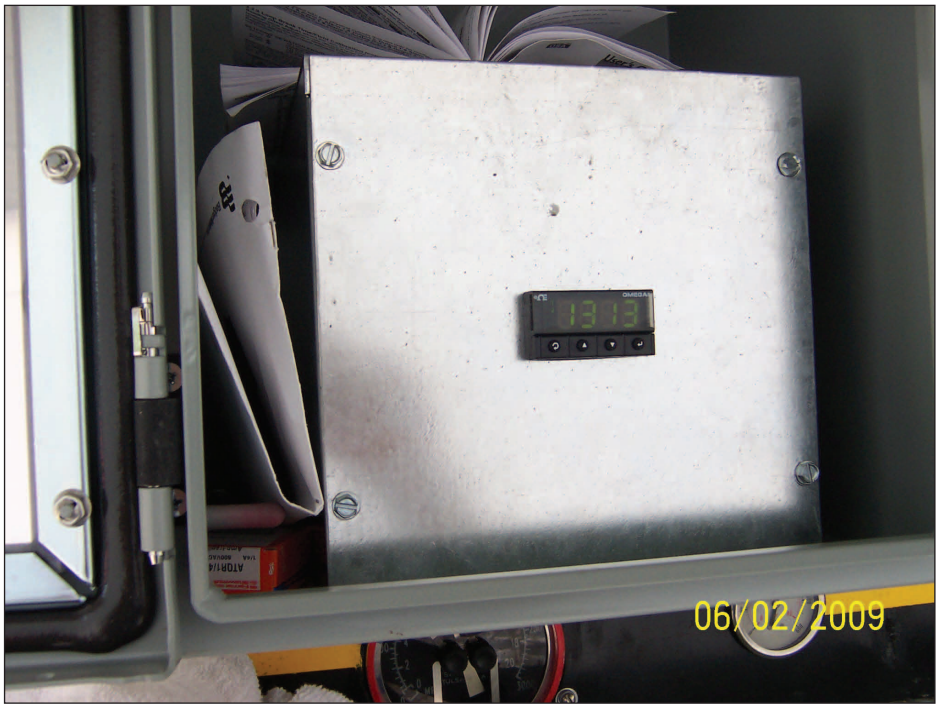

Figure 57 Omega pressure controller panel cover and housing with pressure reading shown. (Photograph courtesy of Trimeric Corp.)

Flow Meters

Liquid Turbine A Cameron NuFlo™ 1.3-cm (0.5 in) liquid turbine flow meter was installed to measure the CO_2 injection rate (Figure 58). This flow meter can accurately measure flows between 4 and 41 m^3/d (0.75 to 7.5 gpm or 25 to 250 barrels per day) of liquid CO_2. This particular type of flow meter is a volumetric measuring turbine type; the flowing CO_2 fluid engages the vaned rotor, causing it to rotate at an angular velocity that is proportional to the fluid flow rate. The angular velocity of the rotor results in the generation of an electrical signal (AC sine wave type) in the pickup. The summation of the pulsing electrical signal is directly related to the total flow. The frequency of the signal relates directly to the flow rate. Pressure and temperature measurements are required to estimate the mass flow rate from this meter.

Vortex Meter A Sierra Instruments Vortex Multivariable Mass Vortex Flow Meter model 240-VTP-H2-E2-DD-PV1-V6M-ST-MP5 was installed to provide an additional flow measurement option (Figure 58). This flow meter measured the liquid CO_2 velocity, temperature, and pressure, and calculated a mass flow rate, volumetric flow rate, and density in a single integrated meter with a digital display. The 1.3-cm (0.5-in) flow meter used had a 12–36 VDC input power source and three 4–20 mA analog outputs. It was capable of measuring CO_2 flow rates of 4.9 to 120 m^3/d (0.9 to 22 gpm, 31 to 754 barrels per day) at temperatures between –40 and 260°C (–40 and 500°F) and at pressures up to 10.3 MPa (1,500 psi).

In-line Heater

The line heater (Figure 59), supplied by Natco, had a design capacity of 105,520 kJ/hr (100,000 Btu/hr). The line heater was 0.6 m (24 in) in diameter and 3 m (10 ft) long and was equipped with four internal horizontal passes of 5-cm (2 in) diameter tubing, each approximately 2.7 m (9 ft) long, joined by 180-degree elbows connecting each pass.

The shell side of the line heater was partially filled with a 50/50 (by volume) mixture of propylene glycol and water. Propane fuel gas was burned in a burner that discharged hot flue gas into a horizontal U-shaped fire tube immersed in the lower portion of the solution. Heat released by the burning fuel gas was transmitted through the fire tube wall to the solution of propylene glycol and water. The desired propylene glycol/water bath temperature was maintained within upper and lower dead band limits by turning on and off the fuel gas flow to the burner based on thermostatic control of the solution temperature. The CO_2 on its way to the injection well passed through the flow coil of the heater immersed in the upper portion of the solution. Heat was transmitted from the propylene glycol/water solution through the tube wall to the CO_2 inside the flow coil.

Data Acquisition

Pressure and Temperature Sensors

Geokon 4500-series vibrating wire pressure transducers were used to measure surface and downhole pressures and temperatures of the pilot wells. Based on the manufacturer's specifications, the resolution and accuracy of the pressure transducers were at least 0.025% full scale (F.S.) and ± 0.1% F.S., respectively, with a maximum drift of 0.05% F.S. per year. (F.S. indicates the measurement range of the transducer.) Each of the pressure transducers also contained a thermistor with a temperature range of −20 to 80°C (−4 to 176°F) and thermal zero shift of <0.05% F.S./°C. Pressure ranges and installed locations for each sensor are given in Appendix 11.

The transducers performed to manufacturer specifications. However, over the course of the project, it became apparent that the surface wellbore environment posed special data collection challenges, and the gauges were not designed to deliver the desired levels of precision and accuracy under these conditions. Thermal disequilibrium between the diaphragm and thermistor affected the readings. Efforts to correct for this disequilibrium were complicated by hysteresis related to diurnal and seasonal temperature variation. Pressure and temperature data gathered from the transducers were still usable, but these complications imposed a larger-than-desired margin of error on calculations of gas production. The use of pressure gauges set to measure wide pressure ranges also introduced unnecessary error and uncertainty. As noted, resolution and accuracy of the gauge is a certain percentage of F.S., meaning that gauges with larger ranges also have larger errors and less ability to resolve low pressures. Lower pressures usually prevailed at the surface, so in most cases gauges with smaller F.S. (and therefore smaller errors and greater resolution) could have been used instead. Further information on gas production calculations is given in Appendix 12.

Figure 58 Cameron NuFlo liquid turbine meter (center left) and Sierra vortex flow meter (center, red) in series on frosted line. Front of inline heater is shown in upper left background. Pump discharge is shown frosted over in lower right. (Photograph courtesy of Trimeric Corp.)

Figure 59 Natco line heater (105,520 kJ/hr [100,000 Btu/hr]). Propane tank is shown in the background. Inline heater's CO_2 inlet is frosted over; the top of this line has the Siemens pressure gauge/transmitter that is connected to the Globe Cast pressure control valve. Also shown is the inline heater discharge (lower right) to the RG-5 injection line. (Photograph courtesy of Trimeric Corp.)

Atmospheric pressure was measured at the WT-8 wellhead using a Geokon 4580-1 (barometer) vibrating wire pressure transducer, which was programmed for a range of 0 to 17 kPa (0 to 2.5 psi). Based on the manufacturer's specifications, the resolution and accuracy of the barometer was at least 0.025% F.S. and ±0.1% F.S., respectively, with a maximum drift of 0.05% F.S. per year.

Data Transmission

Each Geokon vibrating wire pressure transducer was connected to a vibrating wire spectrum analyzer, housed within the data acquisition enclosure at the wellhead. The analyzer measured the wire resonant frequency and resistivity, which were then transmitted to a datalogger and converted to digital pound-force per square inch and Fahrenheit degrees. Figure 60 shows a typical data acquisition enclosure. Additionally, surface pressure of the JR-1 monitoring well and the RG-3 production well were measured using a Siemens Sitrans P Pressure Transmitter. Schematics of the data acquisition equipment can be found in Appendix 13.

The pressure and temperature of the CO_2 were measured upstream of the injection pumps using a Siemens Sitrans P Pressure Transmitter and a Siemens Sitrans TK-H Temperature Transmitter. Pump discharge flow rate, pressure, and temperature were measured using a Sierra Innova-Mass 240 Vortex Meter. Additionally, a Cameron NuFlo Liquid Turbine Flowmeter was installed downstream from the pumps to verify the vortex meter flow rate. Line heater discharge temperature was measured using a Siemens Sitrans TK-H Temperature Transmitter. All pressure, temperature, and flow rate measurements at the pump skid and line heater were sent by 4–20 mA signal to the pump skid datalogger.

Radio transmitters connected to each datalogger sent pressure and temperature data to a common receiver, housed within the WT-9 enclosure. The data (5-minute intervals) were sent by cellular transmission every hour to the ISGS. Removable flash cards within each datalogger served as a backup in case of interrupted transmission. (The flash cards had data collected at 1-minute intervals.) Each datalogger had an independent power supply (battery) that was continually recharged by solar panel.

Wellhead Design

Injection Well

The wellhead of the injection well, RG-5, is shown in Figure 61. At left is the top part of the uppermost joint of injection tubing (vertical pipe), which extends upward through the casing head. This joint is topped with a valve, a pipe cross, and a stainless steel lubricator that seals off the wellhead while still accommodating the transmission cable connected to the electronic downhole temperature and pressure gauges. The lubricator is a Type C lubricator manufactured by Double E and is rated to 34 MPa (5,000 psi). The pipe cross is beneath the lubricator and is connected to a short horizontal pipe (at left in Figure 61) and a longer horizontal pipe (at right). The longer arm contains instrumentation and connects to the CO_2 injection line from the pump skid at the tank battery. In the upper horizontal length of this arm, proximal to the injection tubing above the wellhead, is the electronic surface pressure and temperature gauge. The cable for this gauge emerges from a cable gland at the distal end of the top length of the right arm. Beneath the cable gland, in the lower horizontal length of the right pipe arm, is an isolation valve which can be used to block the CO_2 inlet to the wellhead (which is immediately downstream of this valve). Upstream of the isolation valve is a pipe elbow. A mechanical pressure gauge is attached to the vertical pipe segment upstream of (below) the elbow. The CO_2 line (dark-colored pipe running into the background in the picture) connects with this vertical length of pipe near ground level.

Production Wells

A typical wellhead for the production wells used in this pilot test, the RG-4 wellhead (Figure 62), is described here. However, it should be noted that there was some variation in the wellhead designs of Sugar Creek production wells.

Two pipe arms were connected to the casing head on opposite sides of the wellhead near ground level (Figure 62). The kill wing (shorter arm to right) connects the bottom of the chemical treatment pot to the casing head. A shut-off ball valve in the middle of this arm was opened during chemical circulation. The longer pipe arm (the flowing wing) was composed of two lengths of horizontal pipe connected by a short length of vertical pipe. A Geokon 4500 pressure transducer, for measuring surface pressure and temperature, was

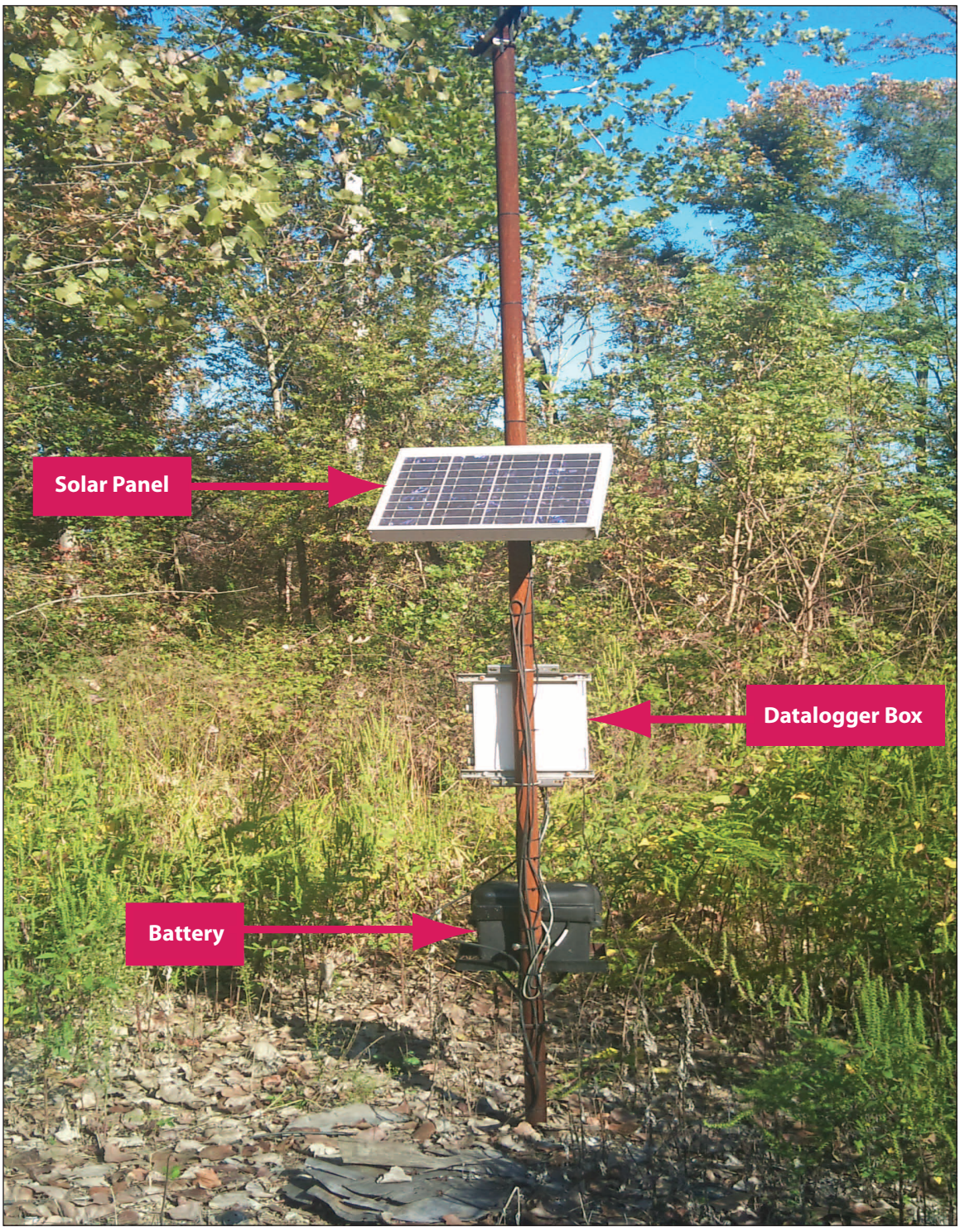

Figure 60 Data acquisition and transmission enclosure at a production well, showing the solar panel, datalogger box, and battery.

Figure 61 Surface wellhead and related piping of the injection well RG-5. Stainless steel lubricator at the top allowed the cable connected to the downhole pressure and temperature sensors to enter the tubing.

installed in the upper length of vertical pipe. (Because these wells were actively producing via rod pumps, there were no downhole pressure or temperature sensors installed.) The cable for the pressure transducer emerged from a cable gland on the upper length of vertical pipe and connected to the nearby data acquisition enclosure (Figure 63). At the end of the pipe (Figure 18, lower left) was a Teledyne Merla orifice well tester, a device into which different sized orifice plates could be inserted. (Orifice plates are thin circular metal plates which have a small hole in the center. Gas production from the wellhead can be regulated by changing the orifice plate; a larger hole allows more gas to escape and results in a lower gas pressure at the surface gauge. A 'blank' plate with no center hole can also be inserted to shut off external gas venting entirely.) There was an adjustable choke valve between the orifice well tester and the pipe elbow. Maximum pressure of the choke was 25.53 MPa (3,705 psi), with a maximum orifice diameter of 1.8 cm (0.70625 inch) (Figure 19). Upstream of the orifice plate, but attached to the well tester, was a ball valve that served as a coupling port for annulus gas sampling.

The top of the uppermost joint of tubing passed through the casing head. Atop the tubing was a pipe cross fitting. Above the cross-fitting was a stuffing box, and the polished pump rod entered the well through the stuffing box. The short arm of the cross was on the same side of the casing head as the kill wing and chemical pot. This arm connected to a perpendicular pipe length; one end was tipped with a ball valve and a mechanical backup surface pressure gauge. The other arm of the cross was a pipe connected to the buried production flow line that directed oil to the tank battery. This line included ball valves, a check valve, and a tee that provided entry of de-emulsifying chemical injected continuously into the production flow line.

Figure 62 Photograph of a typical production wellhead, RG-4, at Sugar Creek Field. The schematic is stylized and not to scale. Orifice well tester at lower left in schematic is not visible in the wellhead photograph but can be seen in Figure 18.

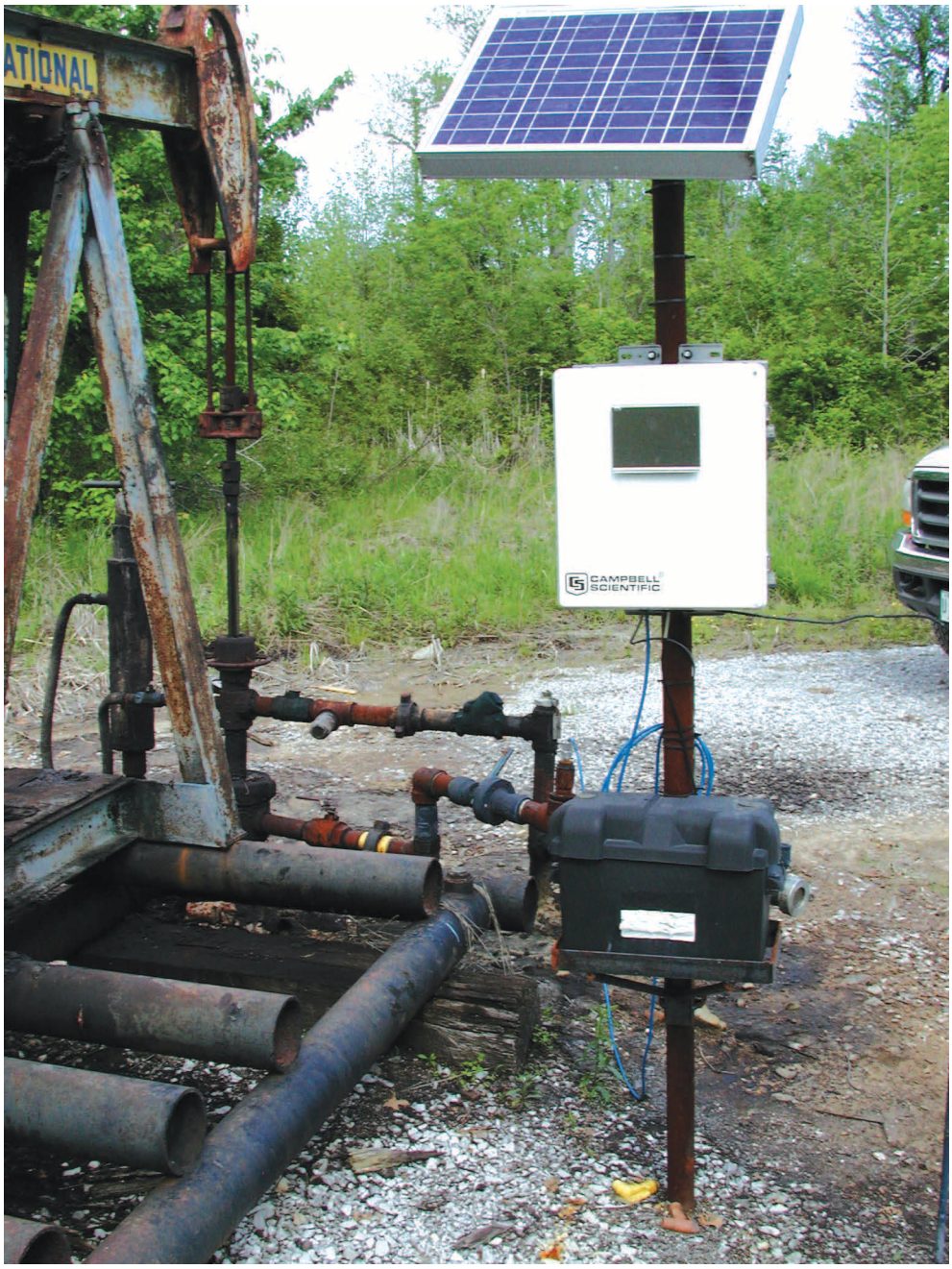

Figure 63 Wellhead and data acquisition enclosure at well RG-4. The blue cable that emerges from a gland on the flowing wing of the wellhead and connects to the data acquisition enclosure is connected to the surface pressure gauge in the wellhead.

Monitoring Wells PZ-1, PB-3, and JR-1

There was significant variation in the design of the monitoring wells, but JR-1 is given as a representative example (Figure 64). The main body of the primary wellhead was a riser pipe (uppermost joint of tubing) passing through a production well casing head. The nature of the horizontal pipes attached to the casing head varied among the different wells, but they were typically simpler than production and injection well heads, although in some cases a ball valve was present. Instrumentation on the wellheads varied among wells and is described in some detail in the section on field observations.

JR-1 was liquid filled and was gauged at the surface only; a mechanical pressure gauge and an electronic pressure gauge were both installed. The monitoring wells that did not contain fluid to surface (PZ-1 and PB-3) were equipped with downhole pressure and temperature sensors, the cable for which emerged from a gland at the top of the wellhead and connected with the datalogger enclosure. A special lubricator adaptation was installed at the top of the riser pipe in each well to accommodate the cable connected to the downhole pressure and temperature gauges.

General Operations

Liquid CO_2 was delivered in road transport tank trucks that had capacities of about 18 tonnes (20 tons). On site, the CO_2 was transferred to the storage tanks and pumped through an inline heater to ensure that the liquid CO_2 temperature was at least 10°C (50°F) but stayed in the liquid phase from the pump storage tank to the bottom of the injection well, RG-5. There were concerns about contraction of flow line connections if CO_2 started through the flow line at −14 to −11°C (6 to 12°F).

The CO_2 injection system was designed to minimize the need for a regular on-site operator of the equipment. The system was designed to shut down safely when operator-specified pressures and temperature thresholds were exceeded under various conditions. The GDI and ISGS staff monitored the data remotely several times a day. The data acquisition system allowed an instantaneous download of data or monitoring of updated data every hour. A pumper made visual inspection of all pumping equipment, the tank battery, and the production and injection wellhead areas once per day. Monitoring the CO_2 tank levels was the most critical task, because continuous injection was only possible when adequate CO_2 volume was maintained in the tanks. If the tank levels were too low, operators communicated directly with the CO_2 supply company, Air Liquide, to obtain additional supply or make plans for a temporary, controlled shut down.

Operational Challenges

Scheduling CO_2 Delivery

Winter weather caused interruption in CO_2 delivery to the EOR III site because trucks were unable to reach the site. An ice storm at the EOR III site interrupted delivery for approximately 10 days.

The initial plan called for one storage tank, but Air Liquide would not deliver to the site at night because of night-time safety concerns, including the narrow road and the need to turn into the site on a poorly illuminated road. To maintain operations without night delivery, a second storage tank was added at the site. Delivery of one truckload per day was the target.

Operating the storage tanks at lower pressure, either by reducing the pressure relief valve set point or by the addition of refrigeration systems to the CO_2 storage tanks, would have simplified storage tank reloading operations. Delivery personnel frequently had to vent some CO_2 from the storage tanks before filling them in order to lower the pressure in the CO_2 storage tanks to allow loading.

Line Heater Detonation

Upon introduction of fuel gas at initial startup, soot and smoke emerged from the back end of the Natco line heater. The soot and smoke were preceded by a loud boom, which was the result of an improper air to fuel ratio in the pilot burner. The issue was resolved by adjusting the air valve (open three to four turns) and the gas valve (open 1 to 1.5 turns) to achieve the proper air to fuel ratio. After this correction, the inline heater operated relatively uninterrupted.

Figure 64 Wellhead of monitoring well JR-1 with solar panel, datalogger, and battery. Mechanical pressure gauge immediately above the riser pipe and Siemens gauge (blue face) to right.

Metering CO_2

Liquid Turbine Meter Based on a comparison of each meter's cumulative mass of CO_2 injected and the delivered CO_2 during the first month of injection, the turbine meter was determined to be more accurate than the vortex meter. From May 13 through June 11, 2009 the total mass delivered as measured by the vendor was 535 tonnes (590 tons); total injected mass measured by the liquid turbine meter was 487 tonnes (537 tons), and total injected mass measured by the vortex meter was 446 tonnes (492 tons). The only concern with operation of the liquid turbine meter was that pumping CO_2 at excessively high rates through the meter at startup could break the turbine shaft, which was small (0.16 cm [1/16 inch]) and relatively fragile. In order to avoid this problem, a bypass was used during startup until the pressure stabilized (stabilization of the pressure was taken to also indicate stabilization of the rate). Pressure stabilization took only a few minutes, and once it was achieved, the bypass was shut and CO_2 was sent through the liquid turbine meter.

Vortex Meter The vortex meter sometimes gave unreliable readings. The exact reason for this is unknown, but the pump skid was located under an electrical transformer, so the operator concluded that the unstable readings were likely caused by electrical interference. The operator activated a filter function on the vortex meter, which seemed to improve performance, but in general the liquid turbine meter still appeared to give more reliable readings, so its readings were used for tracking system performance and operations. Both meters were nevertheless kept in use for the duration of the project. Figure 65 shows the difference in performance between the two meters over the injection period.

Flow Line Breaches CO_2 injection was shut down for about 1 month (combined) due to three leaks in the injection flow line. The first two leaks took place in June and July 2009 and together prevented operations for about 11 days (addressed in more detail later in the "Field observations during active CO_2 injection" section). Following these leaks, MVA techniques were employed to evaluate the leaks and the MVA techniques themselves prior to resuming injection. The third leak occurred in February 2010 and prevented operations for about 21 days. During restart of injection after this leak was repaired, plugging in the injection line was reported. The plugging was thought to be caused by the formation of H_2O-CO_2 hydrates at temperatures of about 3°C (38°F) in the injection line. Water may have gotten into the injection line while it was down for repair. Additional purging and heating of the line using dry, heated CO_2 was required to clear the obstruction.

Corrosion Treatment and Well Workover Frequency

No well workovers for pump failure, parted rods, or tubing leaks were required during the entire 2.25 years of this project. Historically at the Sugar Creek Field at least one well workover per year had been required, most often for a parted rod.

Corrosion rates were monitored by Baker-Hughes with the use of a MultiCorr meter and Pair probes installed on the tubing flow line near each producing well. Throughout the project there were no indications of CO_2-related corrosion (Figure 66). A relatively large increase in the pit rate, with a pit rate 3–5 mils per year (mpy) greater than the general corrosion rate, is considered indicative of corrosion by CO_2. The very early high values are associated with oxygen (via air) being present due to a small leak in the stuffing box.

At the time of the post-CO_2 cased hole logging, when the wellbore tubulars were removed from each well, the rods and tubing were visually inspected and found to be clean with only very minor corrosion exhibited on just a few rods.

The chemical treatment plan was effective in controlling CO_2-related corrosion and may also be responsible for the reduction in well workovers required compared to previous years.

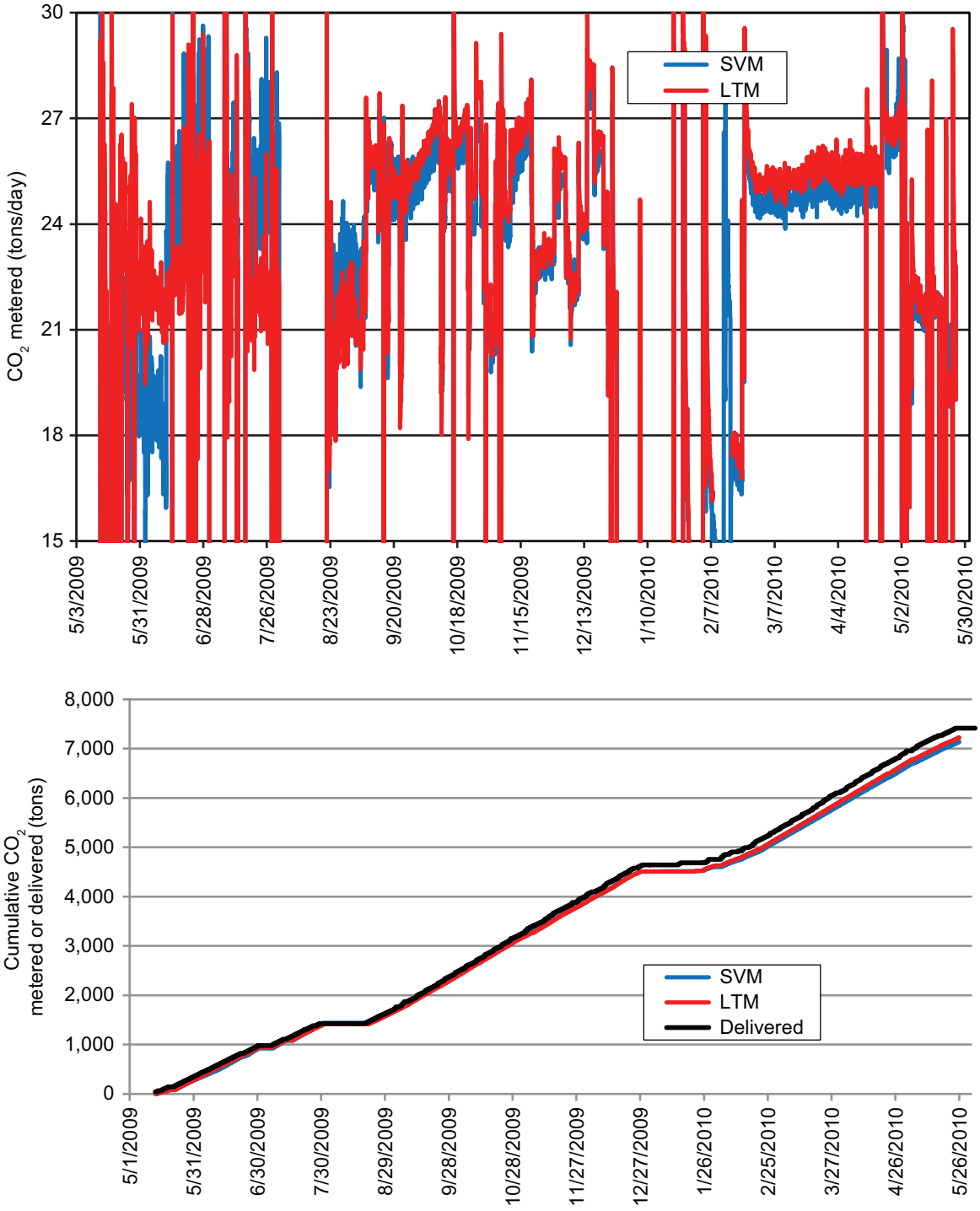

Figure 65 Top graph: Comparison between CO_2 injection rates in tons per day as measured by Sierra vortex meter (SVM, blue line) and liquid turbine meter (LTM, red line). Bottom graph: Comparison between cumulative CO_2 delivered as measured by vendor (black line) and cumulative CO_2 injected (in tons), as metered by SVM (blue line) and LTM (red line).

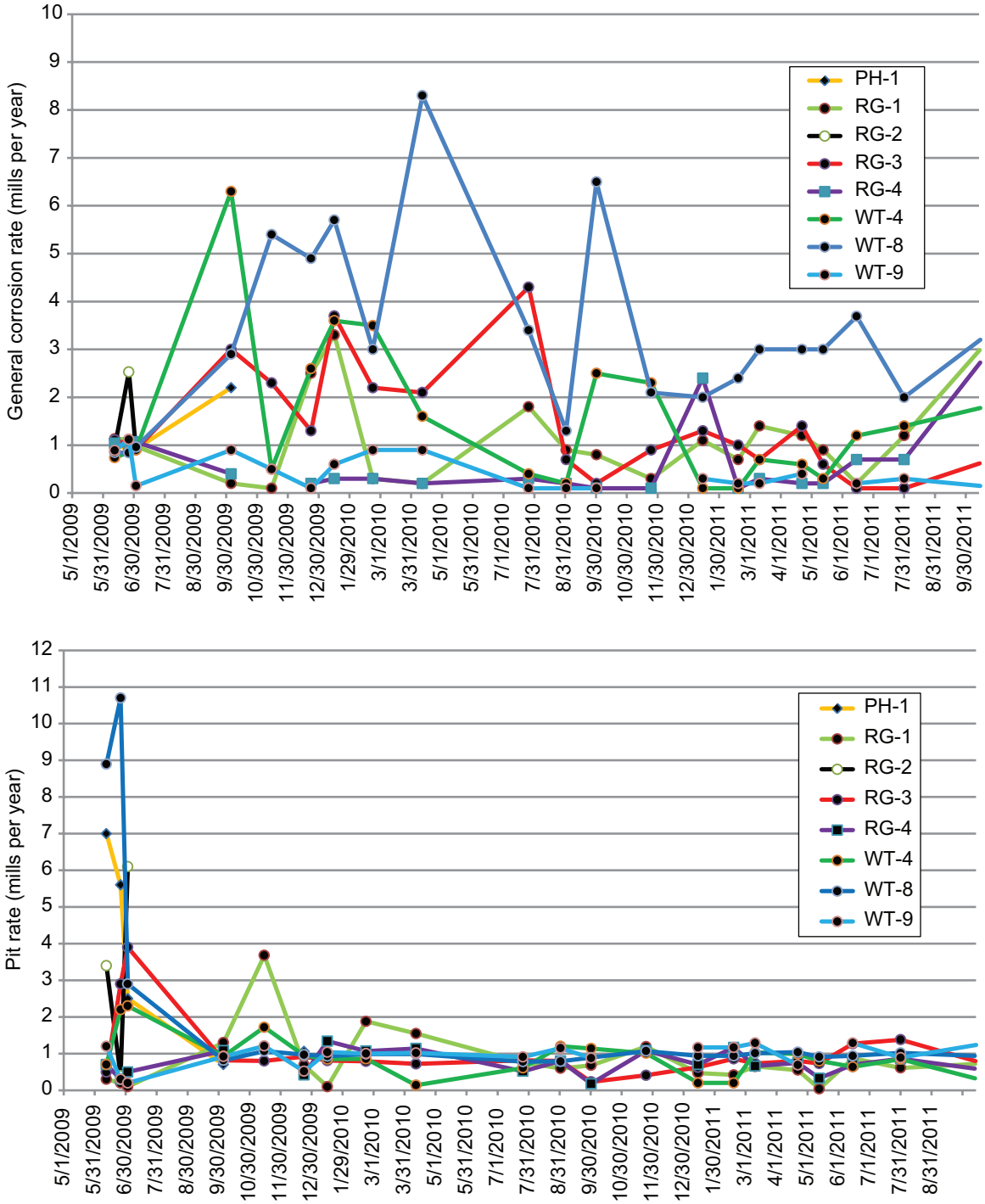

Figure 66 Corrosion (top) and pit (bottom) rates at wells PH-1, RG-1, RG-2, RG-3, RG-4, WT-4, WT-8, and WT-9 over the life of the pilot project. General corrosion rate and pit rate are presented in mills per year. One outlier is not shown: on December 23, 2009, the corrosion rate measured for PH-1 was 12.6 mills per year.

FIELD OBSERVATIONS DURING ACTIVE CO_2 INJECTION

Overview

Appendix 14 contains a timeline of events at the injection and monitoring wells.

On May 13, 2009, CO_2 injection started at well RG-5. Injection rates were constrained by CO_2 availability rather than pressure. Injection rates were relatively constant, but injection pressure decreased slowly with time.

After about one week of CO_2 injection, CO_2 was detected at one of the eight producing wells, RG-2, which was eventually converted to a pressure-monitoring well after the CO_2 production became excessive. Eventually CO_2 was detected at all the wells to the north, west, and south of the injection well, but not in the wells to the east in the Wilbur Todd lease (WT-4, WT-8, and WT-9). (Breakthrough dates are listed in Table 18.)

Table 18 Breakthrough dates as indicated by pressure response and significant increase in CO_2 concentration in gas samples.

Well	Pressure breakthrough	CO_2 concentration breakthrough
RG-1	September 11, 2009	September 15, 2009
RG-2	May 19, 2009	May 20, 2009
RG-3	June 22, 2009	June 10, 2009
RG-4	September 25, 2009	September 15, 2009
PH-1	October 6, 2009	October 7, 2009

Oil production increased by nearly 1.6 m^3 (10 bbl) per day after 3 months of CO_2 injection. The increased production was sustained for the next 3 months until CO_2 injection was temporarily suspended due to a leak in the injection line from the pump skid to the injection well, and winter road conditions that were unsafe for the CO_2 delivery truck. The rate of oil production slowed for about 2 months, but increased modestly again until near the end of CO_2 injection.

By the time injection ceased at the end of May, 2010, 6,560 tonnes (7,230 tons) of CO_2 had been injected. After a pressure falloff test of well RG-5, water injection was restarted in early June 2010 and continued through the end of the MGSC monitoring period in September, 2011. Contrary to most observations of post-CO_2 water injection in West Texas fields (e.g., Henry and Metcalfe, 1983; Chopra et al., 1990), water injection rates in well RG-5 were not adversely affected and pre- CO_2 water injection rates were achieved immediately.

The CO_2 produced from the casing-tubing annulus of individual wells and at the tank battery was 1,090 tonnes (1,200 tons) or 16.6% of the injected CO_2.

Monitoring of the observation wells continued until September 2011, when the data acquisition equipment was removed in preparation for the post-CO_2 cased-hole logging runs.

Through September 30, 2011,[1] increased oil production due to pre-CO_2 injection well work was estimated as 1,065–1,145 m^3 (6,700–7,200 bbl) and increased oil production due to CO_2 as 429–509 m^3 (2,700–3,200 bbl). Project improved oil recovery (IOR) was estimated at 1,574 m^3 (9,900 bbl). Increased oil production includes variations in oil production due to operational problems (e.g., flowline breach) and does not necessarily reflect the CO_2 EOR completely. The pilot project data were used to calibrate a numerical model that was used to improve the CO_2 EOR estimate. Modeling is able to investigate scenarios with longer periods of uninterrupted CO_2 injection and multiple CO_2 injectors in the field.

[1] Oil rates through December 31, 2010 are corrected for sales volumes. At the time of this report only the daily pumper measured rates via gauged oil tank levels were available from January 1 through September 31, 2011. Additionally, no oil and water rates allocated to individual wells were available for this period.

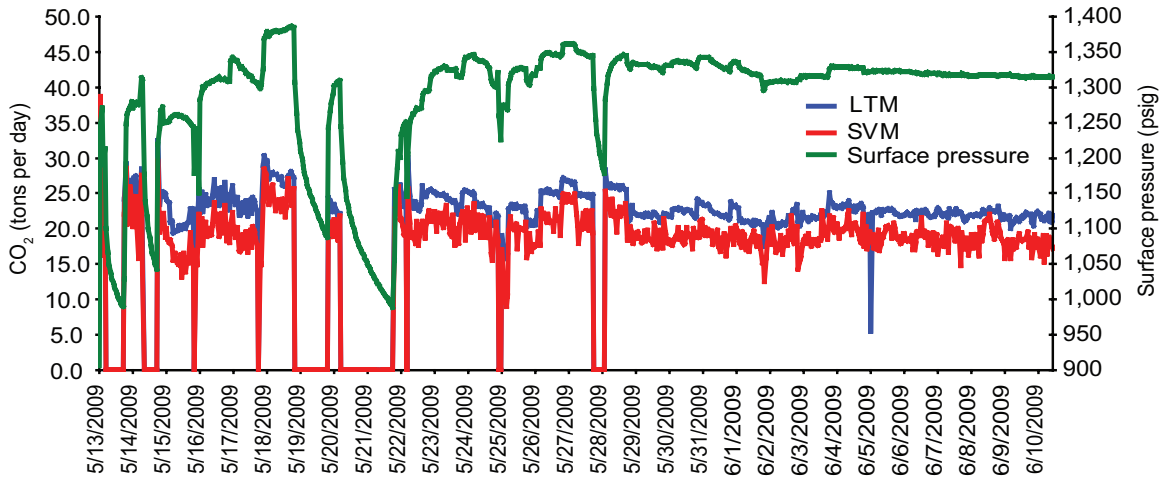

Figure 67 The CO_2 injection rates (tons per day) measured by liquid turbine meter (LTM) and Sierra Vortex Meter (SVM), and injection well (RG-5) surface pressure (psig) during the first month of injection, from May 13, 2009, through June 10, 2009.

Injection Schedule at Well RG-5

CO_2 Injection

Because of permit regulations, pumping operations were constrained by the maximum surface injection pressure of 9.82 MPag (1,425 psig) and maximum bottomhole pressure of 14.88 MPag (2,158 psig). The downhole pressure gauge was placed at 569.4 m (1,868 ft) measured depth from ground level.

CO_2 injection began on May 13, 2009, and continued through May 26, 2010, with a few interruptions that lasted from a few days to 1 month. Active injection occurred for 311 of the 377 days of operation at the test site, or 82.5% on-time injection. During this time, bottomhole injection pressure ranged from 11.7 to 14.5 MPag (1,700 to 2,100 psig) during active injection and bottomhole shut-in pressure fell to 8.82 MPag (1,280 psig) during the first long shut-in period, which ended on August 21, 2009. Injection was not constrained by regulated pressure or equipment ability, but by CO_2 delivery (which initially was limited to no more than one truckload per day) and the operator's need to gain familiarity with the pumping equipment and general operations.

For the first month (through June 10), injection rates were generally between 13.6 and 22.7 tonnes (15 and 25 tons) per day and averaged 17.5 tonnes (19.2 tons) per day, with a few hours of downtime every few days (Figure 67). Bottomhole injection pressure was at its highest during the first few weeks of injection, but decreased nearly linearly with time at about 7 to 14 kPag (1 to 2 psig) per day even though injection rates increased or were relatively constant.

After a month of gaining experience with the equipment and availability of additional CO_2, on June 11, 2009, injection rates were increased and generally ranged from 18.2 to 27.3 tonnes (20 to 30 tons) per day (Figure 68). (The delivery schedule was one truckload per day plus a second truckload every other day.) Bottomhole injection pressure continued to decrease somewhat linearly to 13.42 MPag (1,947 psig). From May 13 through August 20, 2009, there were three major shutdown periods (lasting 4, 7, and 21 days) due to injection flow line leaks. Bottomhole shut-in pressures decreased to 10.64, 10.52, and 8.81 MPag (1,544, 1,526, and 1,278 psig), respectively, at the end of each shut-in period.

The first two shut-ins started on June 30 (7 days) and July 13, 2009 (4 days). Both of these shut-downs were due to a single CO_2 injection line leak near the RG-5 injection well. This leak was detected as a result of modest soil heaving about 18 m (60 ft) south of the injection well during routine sampling of the ground water monitoring well near RG-5. The short injection period between these two shut-in periods allowed the MVA team to observe a real leak and test their equipment and procedures for detecting CO_2 (Wimmer et al., 2011). This injection line repair required excavation to the depth of the injection line (about 0.9 m [3 ft])

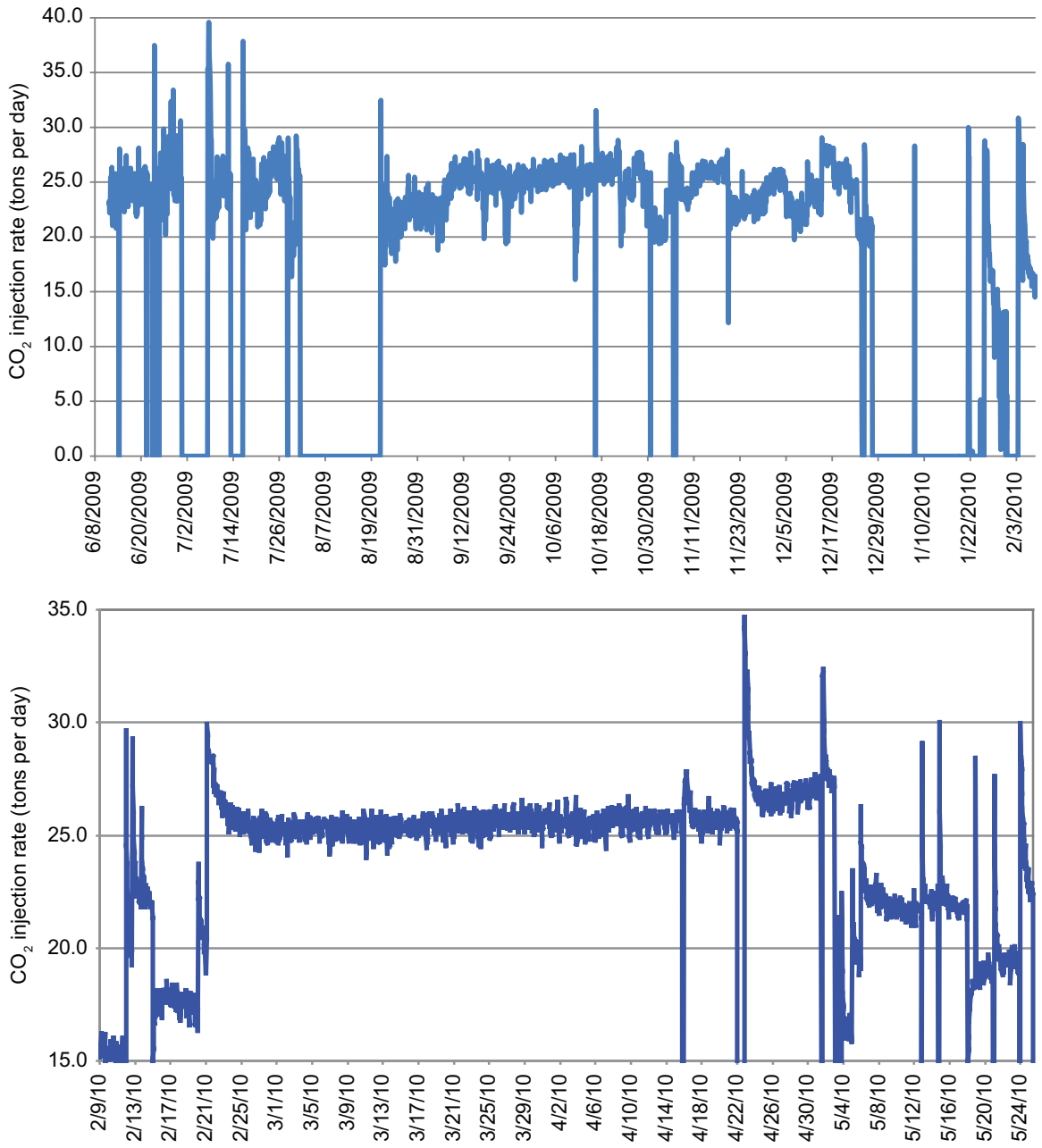

Figure 68 The CO_2 injection rates from June 8, 2009 through February 8, 2010 (top graph) and February 9, 2010 through May 26, 2010 (bottom graph). Continuous injection was resumed February 21, 2010 after interruptions due to weather-related delivery failure and line leaks.

and replacement of two joints of the 3.8 cm (1½ in) PVC injection line. It was determined that a glued-on thread coupling failed. After joint of pipe replacement, the hole was backfilled with dirt.

The third shut-in period began on July 31, 2009 (21 days) and was due to a second injection line leak in nearly the same place as the first repair. Because the repair was in the same area, steel pipe was used to replace the two joints of previously replaced PVC pipe. No other leaks occurred at this location near the injection well.

From August 20, 2009, through May 26, 2010, there was only one additional major shutdown. For about 1 month from December 27, 2009, through January 25, 2010, CO_2 delivery was not possible due to icy road conditions. Prior to this shut-in, injection rates were between 18.2 and 27.3 tonnes (20 and 30 tons) per day with an average of 22.0 tonnes (24.1 tons) per day. Bottomhole injection pressure gradually decreased from 13.46 to 12.96 MPag (1,954 to 1,881 psig). By the end of this shut-in period, the bottomhole shut-in pressure had fallen to 9.83 MPag (1,426 psig).

Following the shut-in due to icy road conditions, the injection flow line between the pump skid and well RG-5 developed another leak (third injection line leak). It was not immediately obvious that a leak was present. Immediately prior to finding the leak, injection rates were highly variable from 4.5 to 27.3 tonnes (5 to 30 tons) per day (beginning about January 25). Additionally, bottomhole pressure was variable but had a general trend increasing from 9.83 to 13.11 MPag (1,426 psig to 1,902 psig). In other words, rates were relatively high and pressure was relatively low at the pump skid. The general area along the underground injection line was walked. A bulge was found in the ground and a field IR identified elevated CO_2 concentrations. The location of this leak was different from the first two leaks. It was about 300 m (1,000 ft) west of the tank battery/injection equipment, in a farm pasture/hay field. The leak was the result of a crack in a single joint of pipe. Injection was interrupted on February 3, 2010. The repair included excavation with a backhoe to the depth of the line (about 0.9 m [3 ft]), joint of pipe replacement, and back-filling with sand and dirt.

Continuous injection resumed on February 21, 2010, at a relatively constant rate of a little over 22.7 tonnes (25 tons) per day through April 22, 2010 (Figure 68). From April 22, 2010, there were three relatively continuous injection periods with only a few hours of down-time. Rates were between 13.6 and 31.8 tonnes (15 and 35 tons) per day with nearly constant but decreasing rates of 23.6, 20.0, and 18.2 tonnes (26, 22, and 20 tons) per day. Bottomhole injection pressure continued its gradual and linear decrease from 13.11 to 13.04 MPag (1,902 to 1,892 psig).

The injection of CO_2 was completed on May 26, 2010. Cumulative CO_2 injection was 6,560 tonnes (7,230 tons) into RG-5. Of the 378 days between startup and shutdown of CO_2 injection, active injection occurred over 311 days at an average rate of 21.3 tonnes (23.4 tons) per day. The average rate over 378 days was 17.5 tonnes (19.2 tons) per day.

Post-CO_2 Water Injection

Water injection resumed at well RG-5 on June 7, 2010, after a 12-day pressure falloff test immediately following termination of CO_2 injection. The water injection rate was up to 19.9 m^3/day (125 bwpd) for the first 2 days, reaching 25.4 m^3/day (160 bwpd) in 5 days. Bottomhole injection pressure was maintained between 13.8 and 14.5 MPag (2,000 and 2,100 psig) during active water injection. During the next 1.5 months (through July 20, 2010) the sustained rates were between 23.9 and 28.6 m^3/day (150 and 180 bwpd). The pre-CO_2 water injection rate at RG-5 was about 9.5 m^3/day (60 bwpd).

No decrease in water injectivity was observed in the field immediately upon return to water injection following CO_2 injection. However, due to improved CO_2 injectivity with time and fixed tank-delivered CO_2 schedule, average reservoir pressure and CO_2 injection pressure decreased about 1 MPag (150 psig) with time (from about 14.1 MPag to 13.1 MPag [2,050 psig to 1,900 psig]) over the entire injection period. A portion of the high water injection may therefore be due to lower average reservoir pressure.

Through the remainder of 2010, the bottomhole injection pressure was kept relatively constant between 13.8 and 14.1 MPag (2,000 and 2,050 psig). Despite the constant bottomhole pressure, the injection rate decreased somewhat linearly through the beginning of December and started to stabilize at 9.5 to 11.1 m^3/day (60 to 70 bwpd).

The lower water injection rates continued through the end of February 2011. At that time, an acid treatment was administered on well RG-5 by pumping 1,900 L (500 gallons) of 15% HCl plus 10% xylene through the injection tubing. The HCl was intended to dissolve hydrogen sulfide scale suspected of precipitating at the bottom of the well; the xylene is a solvent to oil designed to reduce the presence of oil and improve acid contact with the scale. Following the acid treatment, water injection rate increased to 17.5 to 20.7 m^3/day (110 to 130 bwpd) without any change in the injection pressure. On March 12, the bottomhole injec-

tion pressure was increased to 14.1 to 14.5 MPag (2,050 psig to 2,100 psig), and the water injection rate increased to 32 m^3/day (200 bwpd). Bottomhole injection pressure was maintained between 14.5 and 14.8 MPa (2,100 and 2,150 psig) through the end of September, and water injection rates decreased exponentially to 14.3 to 15.9 m^3/day (90 to 100 bwpd).

The cumulative water injected during this time was 8,124.25 m^3 (51,100 barrels). The average RG-5 water injection rate was 15.9 m^3 (100 bbl/day) compared with 9.54 m^3 (60 bbl/day) prior to CO_2 injection.

Pilot Area's Oil, Gas, and Water Production and Pressure Response

RG-2 gas breakthrough occurred relatively quickly in one week (Table 18; Figure 69). Over the next few months CO_2 broke through at relatively low rates at four more wells to the south, west, and north. The next well to have CO_2 present was RG-3 toward the end of June 2009. About 2½ months later, CO_2 broke through at RG-1 and RG-4. PH-1 had CO_2 present in early October 2009. Table 18 has CO_2 breakthrough times; Table 19 summarizes waterflood breakthrough times.

Monitoring well PZ-1 had a relatively sharp increase in pressure in early August 2010 that was suspected to be attributable to CO_2, which was confirmed by gas composition analysis in early summer 2011.

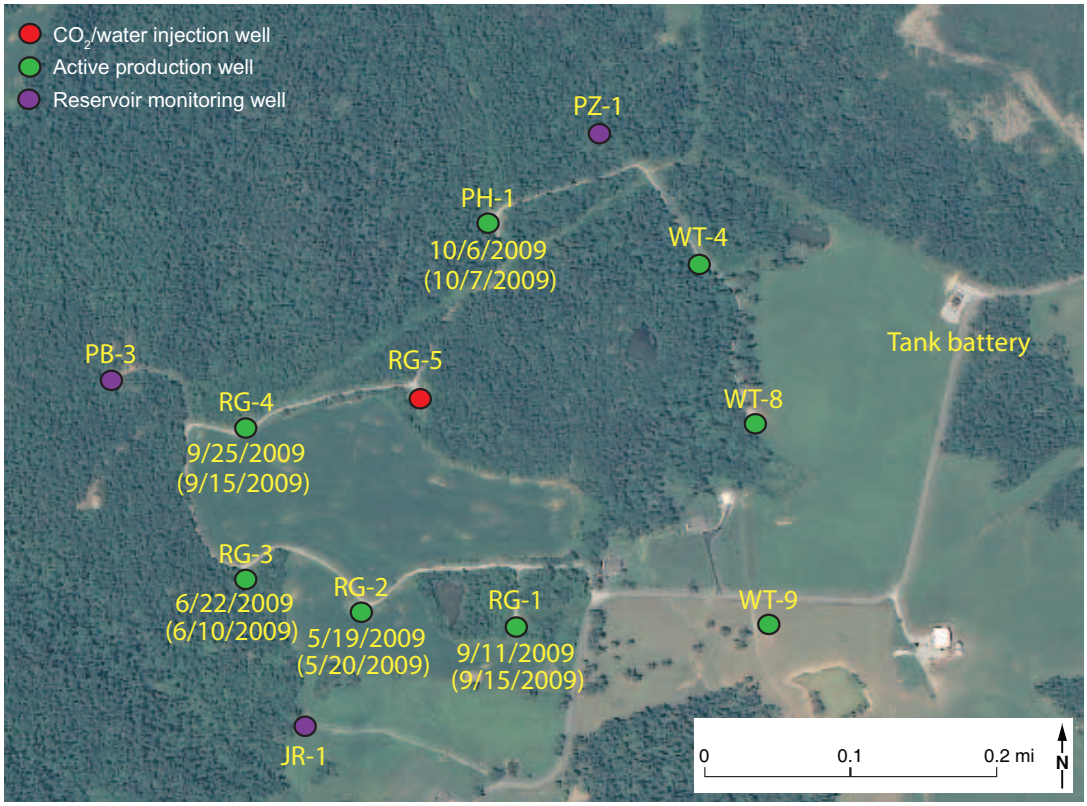

Figure 69 Wells at Sugar Creek Field with CO_2 breakthrough dates shown. Breakthrough date based on pressure response is given first, followed by gas composition breakthrough date in parentheses. (For further discussion, see Table 18 and associated text.) Wells with no date shown did not undergo CO_2 breakthrough within the CO_2 injection period (May 13, 2009 through May 26, 2010), although monitoring well PZ-1 underwent a pressure increase attributable to CO_2 in August 2010. (Aerial photograph from Kentucky Geologic Map Information Service website at http://kgs.uky.edu/kgsmap/kgsgeoserver/viewer.asp.)

About 3½ months after the start of injection, field oil rates declined from pre-injection rates of 6.4–7.2 m^3/day (40–45 bopd) to about 5.6 m^3/day (35 bopd) by September 1, 2009. This decline is attributed to loss of oil production at RG-2, relatively low reservoir pressure due to CO_2 delivery schedule shortage, and lower CO_2 injection rates at RG-5. During September 2009, the oil production rate stabilized and started to climb to more than 8.0 m^3/day (50 bopd) in early November. Daily oil rate was between 6.4 and 8.0 m^3/day (40 and 50 bopd) until the end of December, when icy road conditions precluding CO_2 delivery and an injection flow line leak both caused CO_2 injection operations to be shut down for nearly 2 months.

During this shut-down period, the field oil rate decreased to 5.6 to 6.4 m^3/day (35 to 40 bopd). In early March 2010, oil rates started to climb to 6.4 to 7.2 m^3/day (40 to 45 bopd) until CO_2 injection was stopped in May 2010. Oil rate declined linearly to 4.8 to 5.1 m^3/day (30 to 32 bopd) by February 2011. In early March, oil rate increased to 5.6 to 5.7 m^3/day (35 to 36 bopd) and declined linearly through September 2011 to 4.1 to 4.5 m^3/day (26 to 28 bopd).

Breakthrough of CO_2 can be indicated by a pressure increase or a CO_2 concentration increase in gas samples and/or field IR readings at a producing well. Surface pressure at the production wells was measured every 5 minutes for the life of the project, whereas gas samples and field IR readings were taken on an approximately weekly basis (usually at the same time, but in some cases only field IR samples were taken). As a result, breakthrough dates based on CO_2 concentration increases were usually different from those based on pressure responses. Table 18 compares CO_2 breakthrough time based on pressure response and CO_2 concentration increases in gas samples. In cases where pressure breakthrough date significantly preceded the CO_2 response date, it is possible that the gap between the two breakthrough times would have been smaller if gas had been sampled more frequently. In some cases, CO_2 concentration increased before the pressure response; this increase is likely explained by low volume breakthrough of CO_2 that was not adequate to increase the pressure of wells on the pumping units that are venting gas to the atmosphere via the casing tubing annulus.

The peak oil production for individual wells is given in Table 19.

Oil Production Field Data

In preparation for the CO_2 pilot study, well work was started near the end of 2008, which led to an increase in oil production. The well work included acid treatments at RG-1, RG-4, PH-1, and WT-8. A severe ice storm that hit the region in February 2009 disabled electricity delivery to Sugar Creek. As such, very little oil production occurred in February. The pre-CO_2 cased-hole logging required the wells to be shut-in for about one week in March 2009, during which time wells produced significantly less oil.

Because of the variations in oil production prior to CO_2 injection, estimating the pre-CO_2 oil production baseline was not straightforward. There are two reasonable means of estimating the baseline: a flat average oil rate or a decline curve based oil rate.

Because additional oil production occurred as a result of well treatments and workovers in preparation for CO_2 injection, estimates of project improved oil recovery (IOR) and the incremental CO_2 EOR must include these changes to the pre-CO_2 injection oil production baseline. Three projections are necessary: pre-project projection, IOR projection, and CO_2 EOR projection.

Flat oil rate baseline The use of a constant oil rate baseline is convenient for discussion and quick interpretation of field data. However, an increase in oil production due to workovers typically is defined by a sharp increase in oil rate followed by a decline. The opposite can occur following a temporary shut-in (e.g., due to electricity availability); the oil rate decreases instantly (maybe to zero) and increases quickly after the problem is resolved. Depending on the occurrence and duration of this event, it can lead to an estimate of a flat oil rate baseline that is not useful. Arguably, the baseline should include these types of operational increases and decreases because these types of random events are likely to occur during CO_2 injection. These operational aspects need to be considered when selecting a constant rate baseline.

The 2008 average daily oil production was 4.9 m^3/day (30.6 bopd), but the December 2008 average was the highest for 2008 (6.4 m^3/day [40.30 bopd]). The average oil rate in 2009 prior to CO_2 injection was 5.3 m^3/day (33.4 bopd). The average daily oil production for each month before injection began in 2009 is shown in Table 20.

Table 19 Waterflood and CO_2 flood breakthrough time and associated rates. Rates are in barrels per day (calculated from monthly production) and concentration is in percent.

Waterflood								
Well	RG-1	RG-2	RG-3	RG-4	PH-1	WT-4	WT-8	WT-9
Date and oil rate increase (bopd)	Jul 1996 15–20	Sep 93 5	Jan 1996 8	Dec 1993 10 Feb 1995 25	Dec 1997 11 September 1993 5	Mar 02[1] 11	No or nil response	No response
Date and peak oil rate (bopd)	Nov 2000 31	Aug 1996 32	Aug 1996 30	Feb 1995 25	Jan 1999 20 June 1995 15	Mar 02 11	Dec 03 30	-
Date and water rate increase (bwpd)	Sep 2008 4	Oct 1995 14 Oct 1996 9	Dec 1996 5	Jul 1996 10	Jan 1995 10	Mar 98 26	- Nil	-
Date and water rate peak (bwpd)	Nov 1999 14	Apr 2001 34	Aug 1998 36	May 98 35	Mar 2000 25 Feb 1995 23	Jun 2003[1] 65 Sep 1998 51	Oct 05 9	-
CO_2 Flood								
Well	RG-1	RG-2	RG-3	RG-4	PH-1	WT-4	WT-8	WT-9
Date and oil rate increase (bopd)	Dec 2009 2.5	Oct 2009 0.2	Apr 2010 0.3	Apr 2010 0.2	Dec 2009 0.2	No response	No response	No response
Date and increase (%)	Dec 2009 12	Oct 2009 14	Apr 2010 27	Apr 2010 33	Dec 2009 7			
Date of pressure breakthrough	9/11/09	5/19/09	9/8/09[2]	9/25/09	10/6/09	-	-	-
Date and CO_2 sample	9/15/09 70	5/20/09 82	6/22/09[3] 58	9/15/09 81	10/7/09 31	-	-	-

[1] WT-4 has two relative peaks and subsequent water declines. The first major water increase had no significant oil increase before or after the first peak. One year prior to the second water peak, oil rate increased from 0.16 to 1.59 m^3 per day (1 to 10 bopd).
[2] On June 22, 2009, RG-3 exhibited a small, transitory pressure increase which may have been related to injection. Pronounced, consistent increase in pressure did not occur untill 9/8/09.
[3] Based on lab data. 6/10 breakthrough based on Field IR data.

Table 20 Average daily oil production in 2009 prior to CO_2 injection.

2009	January	February	March	April	May
Average daily oil production (bopd)	38.0	10.1	33.2	42.5	41.2

The average daily oil production rate for the 3 and 6 months preceding injection was 4.6 m^3/day (29.1 bopd) and 5.2 m^3/day (32.5 bopd). Flat oil rate baselines that include operational downtime and natural decline are between 5.1 and 6 m^3/day (32 and 38 bopd). The choice in a flat baseline is significant in a relatively small pilot test. Each 0.16 m^3/day (1 bopd) increase above the baseline results in nearly 63.6 m^3/day (400 bbls) increase in the CO_2 EOR estimate for the one year period of injection. The 0.95 m^3/day (6 bopd) difference between the minimum and maximum production rates results in a difference in the CO_2 EOR estimate of as much as 348 m^3 (2,190 bbls) of oil.

Decline oil rate baseline Historical oil production from January 1993 to before CO_2 injection had four major production increases and subsequent declines (Figure 70). Two of these decline periods cover nearly 60% of this time period: July 1996 to February 2003 and January 2004 to November 2008. Using monthly oil production the nominal decline rate for these two periods was 0.0321/month and 0.0276/month. The latter decline rate was continued through December 2011 to project the oil production that would have occurred with no CO_2 injection project. This estimate was 2,496 m^3 (15,700 stb) oil production (Figure 71). The actual production during this time was 4,070 m^3 (25,600 stb). The difference between these two numbers is the field measured oil production attributable to the pre-CO_2 injection well work and CO_2 related oil recovery, 1,574 m^3 (9,900 stb). Because this oil production estimate includes actual production, the effects of typical field operations (e.g., shut-in wells due to logging, pipeline leaks, delivery of CO_2, and reduced sales during periods of poor weather) are included in the estimates. If fewer detrimental operation-related problems had occurred, the project IOR would be higher.

The field-measured oil production attributable to CO_2 is the difference between the actual production and the projected oil production from the pre-CO_2 injection workovers. Because of the uncertainty in the decline rate following the workovers, the two decline period decline rates were appended to the December 2008 monthly production to estimate the project oil production (as if CO_2 injection had not occurred). Through the end of September 2011, these two decline rates project 3,545 and 3,625 m^3 (22,300 and 22,800 stb) oil production. The oil production attributable to CO_2 is the difference between these estimates and the pre-project forecast: 445 and 525 m^3 (2,800 and 3,300 Mstb).

Project IOR and CO_2 EOR are estimated from numerical modeling calibrated to the field measurements. The modeling details and results are documented in a subsequent section of this report.

Water Production Field Data

Prior to CO_2 injection, the Sugar Creek Field water injection rate was 40–56 m^3/day (250–350 bwpd). (Field water injection rates are in Appendix 15.) During active CO_2 injection the non-pilot injection well water rates were 24–48 m^3/day (150–300 bwpd) with the lowest rates during the first 6 months of injection. After CO_2 injection with RG-5 returning to water injection, the field water injection rate was 44–56 m^3/day (275 to 350 bwpd).

Oil Producing Wells' Rate (Oil, Gas, and Water) and Pressure Responses[2]

The oil production from all wells was measured once a day by gauging the daily volume of oil accumulated in the oil tanks at the tank battery. However, these measurements could be inaccurate due to routine operations such as draining water from tanks. The actual oil production was calculated using tank volumes at the beginning and ending of each month and sales during the month and cross-checked with the period oil sales volume reported by the crude oil transport truck service. Water production was metered using a ¾ inch Cameron NuFlo turbine meter with a range of 10.8–81.9 m^3/day (68–515 bwpd). This meter had frequent problems with plugging and use of the meter was discontinued after January 11, 2010. (The produced water had more solid material entrained than expected and even addition of a filter was insufficient to keep the

[2] Note that, throughout the following section, pressure readings described in the text for each well may differ slightly from pressures shown on the accompanying figures. These differences are artifacts of the time-averaging process used to simplify the data for graphing and/or the result of slightly different baseline pressures used in plotting the data. Differences in magnitude are small, and pressure changes and trends (which, generally speaking, are the focus of the following section) are accurately reflected in the figures as well as the text. Some of the pressure spikes shown in the figures may not be discussed (or may be given a lower magnitude) because they were brief and were related to equipment maintenance or similar technical concerns rather than reflecting injection-related trends in reservoir pressure.

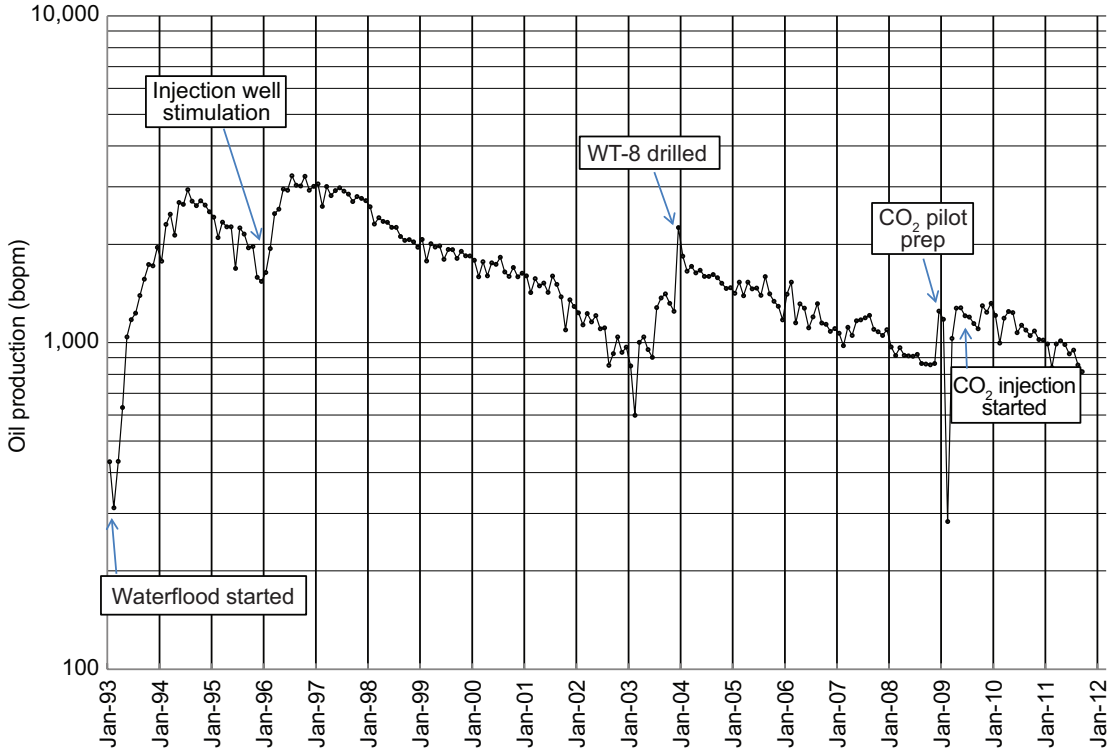

Figure 70 Cumulative field oil production by month (bopm) from 1993 to 2010 showing historical production increases and declines.

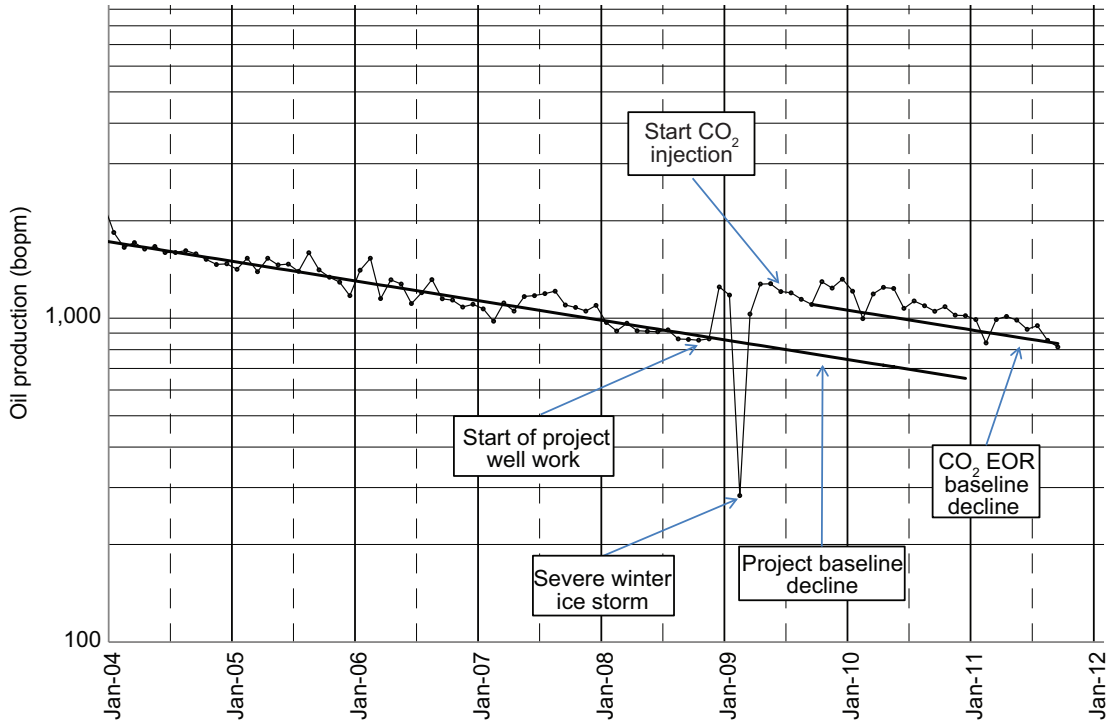

Figure 71 Cumulative field oil production by month (bopm) during the pilot project showing the most recent decline.

meter operable.) After this time water production was estimated using well tests. Separator gas production was metered using a Teledyne Merla orifice well tester and Siemens electronic pressure gauge on the gas-liquid separator.

Oil and water production rates of individual wells were allocated based on results of "barrel" tests which determined the fraction of the field's production that was assigned to each individual well. The barrel tests were conducted at various times throughout the project life. Allocated oil and water rates for individual wells, corrected for sales, were available through end of 2010. For 2011, only field rates based on the pumper's daily tank levels was available. The monthly allocated oil and water rates for individual wells were available from 1992 to the present. Prior to 1992, only the monthly oil production by lease was available.

Gas production of individual wells was measured by using a Teledyne Merla orifice plate well tester and a pressure gauge upstream of the orifice plate at each well's casing-tubing annulus vent. (The downstream side of the orifice plate is open to the atmosphere.) This pressure gauge allowed for calculation of the gas rate and the detection of pressure buildup in the annulus. Rates of CO_2 and methane production were determined by using the overall gas rate and the gas composition data. Because the original design was for all producing wells to be pumped with a rod pump, it was not practical to have a subsurface gauge in these wells. Gas rates are calculated from casing pressure, so any operational causes of pressure fluctuations will have the same effect on gas rates. The biweekly corrosion chemical treatment required the casing pressure to be temporarily lowered. Larger orifice plates would also be used to reduce pressure in order to prevent excessive casing pressure. In some instances this resulted in excessively low pressure, and reliable gas rates could not be measured during these periods. Appendix 16 summarizes gas production at five of the production wells and the gas separator.

Ross Gentry #1

Figure 72 shows surface pressure, average total gas and CO_2 rate, CO_2 volume percent, and cumulative CO_2 in tons for RG-1 from the beginning of the pilot project (May 2009) to October 2011.

Surface casing gas pressure By September 13, 2009, about 4 months after the start of injection, casing pressure increased slightly (by about 14–28 kPag [2-4 psig]). The average pressure declined by about 7 kPag (1 psig) over the next few days before jumping to 55 kPag (8 psig) on September 16. Pressure then increased relatively linearly to about 140 kPag (20 psig) by early November, then decreased to about 70 kPag (10 psig) on November 8. Casing pressure rose again to about 210 kPag (30 psig) on December 6 and dropped back to a low of about 103 kPag (15 psig) on December 11. The pressure then climbed to 140–170 kPag (20–25 psig) by December 16 and stayed in that range for several days before beginning to decrease by the end of December 2009 as a result of a decrease in CO_2 injection mid-month. Because of the cooler winter temperatures, ice developed within the orifice of the orifice plate and plugged the meter. On January 4, 2010, the orifice plate was removed and was not reinserted until February 26. At that time, the pressure returned to 70–140 kPag (10–20 psig) until the end of May, when a larger plate was used to reduce the casing pressure to zero. After 1 month at the end of June 2010, the smaller size was used, but pressure was relatively low and did not indicate large gas production.

Casing gas composition Pre-CO_2 injection casing gas composition at well RG-1 was hydrocarbon gases, predominantly methane. These samples contained 0.5 to 2% CO_2. During the first few months of injection, CO_2 concentration increased very slightly from 1.8 to 2.6% until mid-September, when the CO_2 concentration increased to 70%. The CO_2 concentration varied from 65 to 92% until August 30, 2010, when the concentration fell to about 60%. The concentration remained between 54 and 60% through June 2011. No samples were collected in July–September 2011. The final samples were taken on October 19 and November 1, 2011, when the concentrations were 53.9% and 52.5%, respectively.

Casing gas production rate After CO_2 breakthrough on September 12, 2009, gas production rates increased steadily until an interruption in CO_2 injection in December 2009 and January 2010 caused a decline. Once CO_2 injection resumed, production rates increased until they peaked between 200 and 280 scm/day (7,000 and 10,000 scf/day) between February 2010 and May 2010. After CO_2 injection ended on May 26, 2010, gas rates rapidly declined. The cumulative total gas production and CO_2 gas production for RG-1

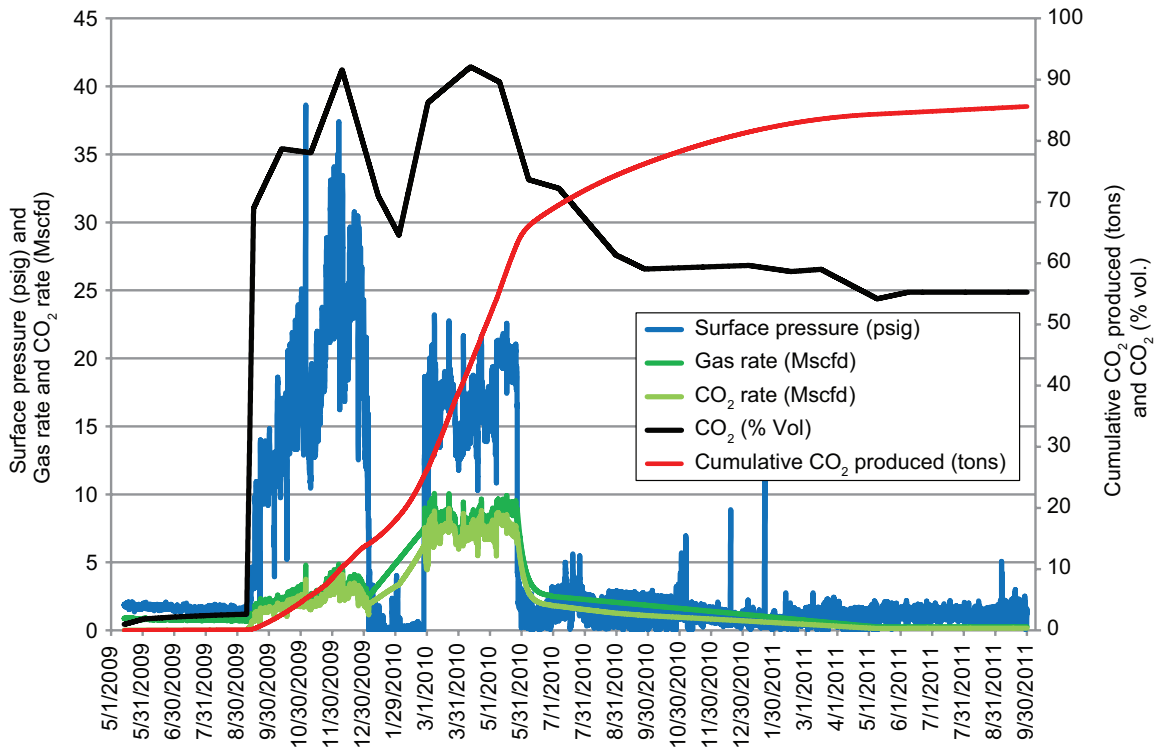

Figure 72 Surface pressure (psig), average gas and CO_2 rate (Mscfd), average CO_2 volume percent, and cumulative CO_2 produced (tons) for RG-1 from the beginning of the pilot project (May 2009) to late September 2011.

estimated from May 2009 through September 2011 is 56,300 scm (1,988,000 scf) and 77.7 tonnes (85.6 tons), respectively.

Allocated oil and water production The daily oil rates were relatively low (0 to 0.8 m^3/day [0 to 5 bopd]) for RG-1 until July 1996 when the oil rate increased to about 2.4 m^3/day (15 bopd). Oil rates stayed at this level until February 1999, when they increased to 3.2 to 4.0 m^3/day (20 to 25 bopd). During this period, water rates increased from nearly zero to 0.8 to 1.6 m^3/day (5 to 10 bwpd). In January 2002, oil and water rate both were substantially reduced (0.8 m^3/day [5 bopd] and 0 m^3/day [0 bwpd]) through April and August 2003, respectively, after which oil and water increased noticeably. (This rate change is thought to be attributable to the rate allocation method used by the operator.) From September 2004 through the end of September 2008 oil rate decreased somewhat exponentially from 3.2 to 1.6 m^3/day (20 to 10 bopd), and water varied from near zero up to 0.6 to 0.8 m^3/day (4 to 5 bwpd).

During fall 2008, in preparation for CO_2 pilot activities, RG-1 was treated with acid, and the oil rate increased to 3.5 m^3/day (22 bopd) and then decreased to 3.0 m^3/day (19 bopd). CO_2 injection increased the oil rate to 3.5 m^3/day (22 bopd), with a peak of 4.0 m^3/day (25 bopd) in February 2010. The peak CO_2 EOR oil rate was very similar to the peak waterflood oil rate.

Since the time of waterflood startup, RG-1 produced 14,000 m^3 (87,000 stb) oil and 2,700 m^3 (17,000 stb) water.

Ross Gentry #2

Surface casing gas and downhole pressure After about one week of CO_2 injection, CO_2 was detected at RG-2. The CO_2 production rate was initially relatively low, but increased quickly. Pressure in the tubing-casing annulus was considered too high (Figure 73), so the well was worked over, and a packer was placed in the well so that the casing pressure could be lowered and the reservoir fluids produced through the production tubing only. Gas rates continued to increase with little additional oil production; consequently, on

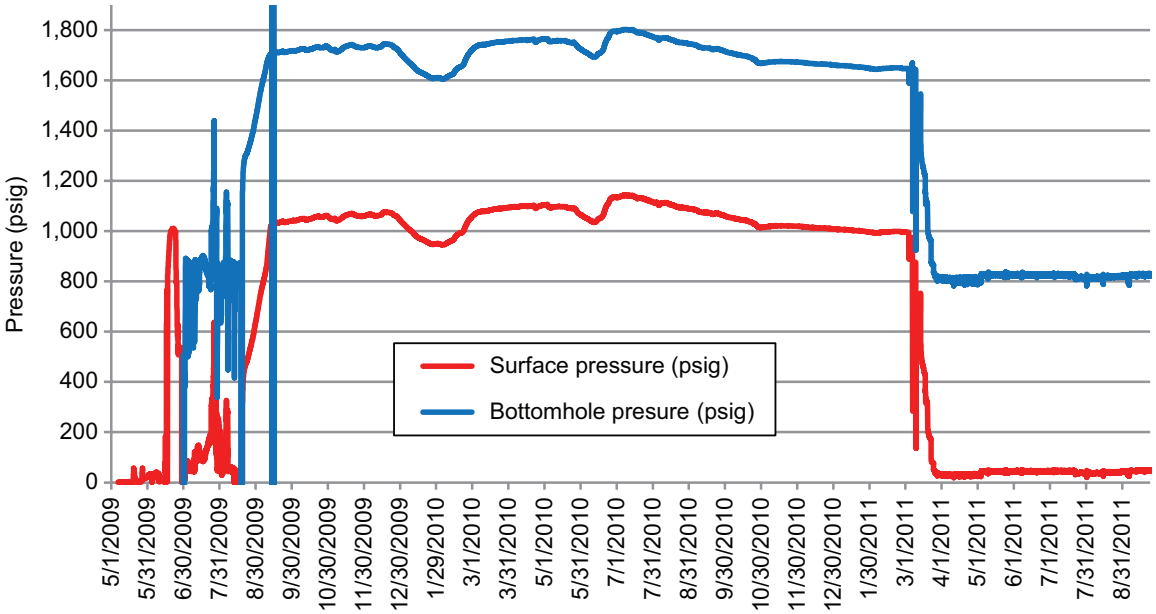

Figure 73 Surface and bottomhole pressures at RG-2 from approximately the start of pilot project (May 2009) to late September 2011.

June 14, 2009, RG-2 was shut-in. A downhole pressure gauge was lowered into the tubing and placed at 570 m (1,870 ft) MD (GL). The well was flowed to surface through tubing July 2 through August 16, 2009; bottomhole flowing pressure ranged from 3.4 to 6.2 MPag (500 to 900 psig) with a few shut-in pressure spikes up to 9.9 MPag (1,440 psig). On August 16, it was decided that too little fluid was being produced from RG-2 in relation to the CO_2 production, and the well was shut-in for the remainder of the CO_2 injection period and used as a pressure monitoring well. Pressure increased relatively quickly and stabilized at 11.8 MPag (1,710 psig) over the next month (Figure 74). At the time of breakthrough RG-2 had a modest increase in oil production of 0.8–1.3 m^3 (5–8 bbl) per day over its base oil rate. After the well was shut-in, total field production was below the baseline (pre- CO_2 injection) rate. Figure 73 shows surface and bottomhole pressures at RG-2 from approximately the start of pilot project to mid-September 2011.

Casing gas composition Pre-CO_2 injection casing gas composition at RG-2 was hydrocarbon gases, predominantly methane. There was 3 to 8% CO_2 in these samples. In about a week from the start of CO_2 injection, on May 20, 2009, CO_2 concentration increased to 82% and continued to increase to 98% by June 1, 2009. After the downhole packer was placed in the well, surface gas sampling of the casing-tubing annulus was no longer possible. In March 2011, when attempts were made to return RG-2 to production, gas samples were taken, and the CO_2 concentration was between 72 and 85% through June 8, 2011. No samples were taken in July through October 2011. A final sampling event on November 1, 2011, showed 92% CO_2.

Casing gas production rate CO_2 breakthrough initially occurred on May 19, 2009 when gas production rapidly peaked then declined to pre-CO_2 injection rates by May 21. On May 27 gas production rates rapidly increased to 600 scm/day (20,000 scf/day) then increased steadily from 600 scm/day to 1,400 scm/day (20,000 to 50,000 scf/day) through June 14, the end of casing gas production at RG-2. The cumulative total gas production and CO_2 gas production for RG-2 estimated from May 2009 through June 14, 2009 is 20.2 × 10^3 scm (714,000 scf) and 36.4 tonnes (40.1 tons), respectively.

Allocated oil and water production The daily oil rates for RG-2 were low (0.16 m^3/day [1 bopd]) until October 1993. Thereafter, the oil rate increased to about 0.75–3.18 m^3/day (5–20 bopd) through May 1996. At that time, the oil rate increased (likely due to waterflood response) to a maximum rate of 5.1 m^3/day (32 bopd), but had decreased to 0.3 m^3/day (2 bopd) by January 2002. This oil decrease was accompanied by an increase in the water production rate (up to 4.8 m^3/day [30 bwpd]). Water rates were relatively constant at 4

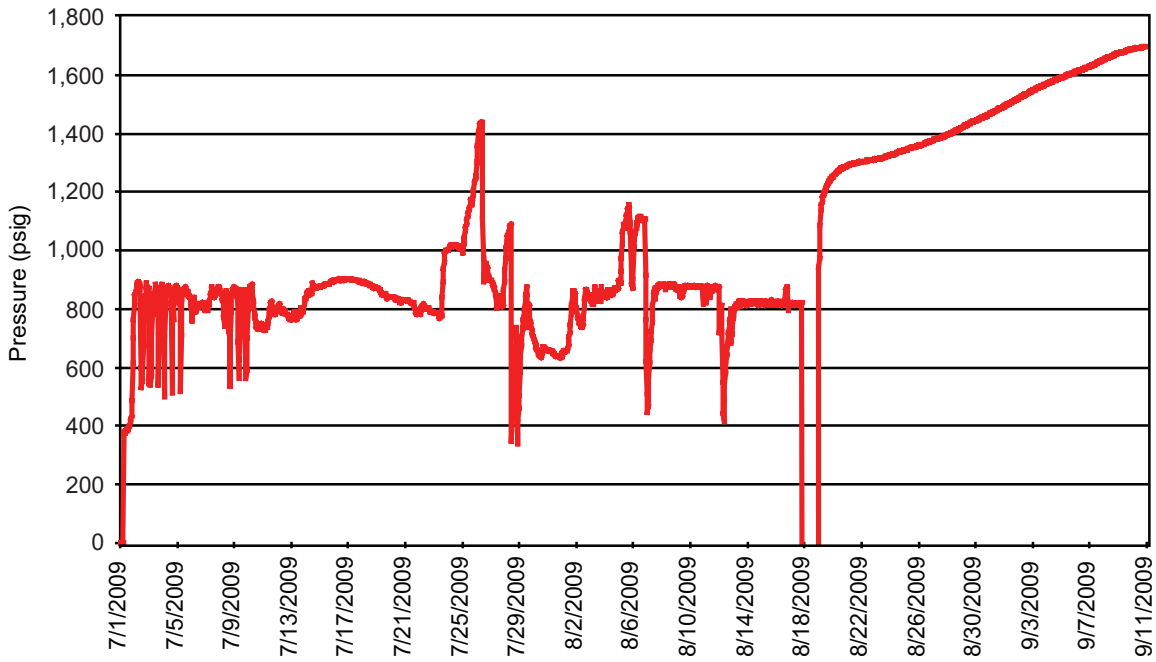

Figure 74 Pressure at well RG-2 during the period from July–September 2009, showing pressure response to being shut-in on August 16, 2009.

to 4.8 m^3/day (25 to 30 bopd) through January 2002. At this time the water rate decreased to about 3.2 m^3/day (20 bwpd), and the oil rate increased slightly to 0.8 to 1.4 m^3/day (5–9 bopd). In May 2003 the water rate increased and remained relatively constant at 3.6 to 4.6 m^3/day (23 to 29 bwpd) through December 2005; the oil rate also remained relatively constant at 0.5 to 1.3 m^3/day (3 to 8 bopd). After December 2005, the oil rate slowly decreased to about 0.3 m^3/day (2 bopd) while the water rate remained relatively constant at 2.4 to 3.2 m^3/day (15 to 20 bwpd). (These rate changes are thought to be attributable to the rate allocation method used by the operator.)

In fall 2008, during preparation for CO_2 pilot study activities, the oil rate remained unchanged at about 0.3 m^3/day (2 bopd) while the water rate was relatively flat at 2.4 to 2.5 m^3/day (15 to 16 bwpd). There was a modest increase in oil production before the well was shut-in.

Since waterflood start-up, well RG-2 has produced 7,600 m^3 (48,000 stb) of oil and 15,700 m^3 (99,000 stb) of water.

Ross Gentry #3

Figure 75 shows surface pressure, average total gas and CO_2 rate, CO_2 volume percent, and cumulative CO_2 in tons for RG-3 from the beginning of the pilot project (May 2009) to October 2011.

Surface casing gas pressure By September 8, 2009, almost 4 months from the start of injection (September 8, 2009) casing pressure (70 kPag–140 kPag [10–20 psig]) increased sharply in well RG-3. This was the start of several swings of increasing and decreasing pressure that ranged between about 170 kPag and 14 kPag (about 25 to 2 psig). Over the next month (until October 10, 2009) the pressure stayed between 103 and 140 kPag (15 and 20 psig); thereafter the casing pressure increased again, reaching 240 to 280 kPag (35 to 40 psig) in early January. From January 4 through February 26, 2010, the orifice plate was removed from the annulus vent because of observed ice buildup in the orifice. Once the orifice plate was re-installed at the end of February, the pressure increased to 35 to 70 kPag (5 to 10 psig), but the casing pressure climbed steadily through early April 2010 to in excess of 410 kPag (60 psig). To reduce the casing pressure, the next largest orifice plate size was installed (early April 2010), and the pressure decreased to about 70 kPag (10 psig) and slowly decreased to nearly 0 kPag (0 psig) through the rest of September 2011.

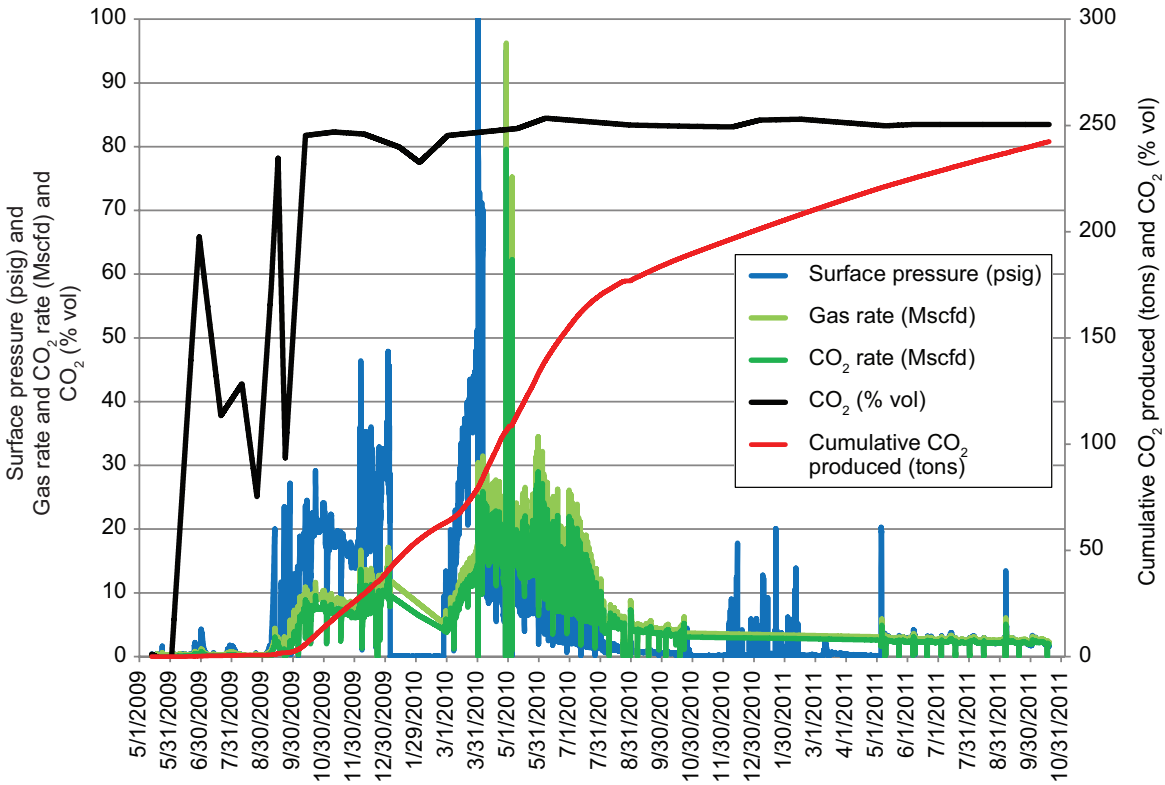

Figure 75 Surface pressure (psig), average total gas and CO_2 rate (Mscfd), average CO_2 volume percent, and cumulative CO_2 produced (tons) for RG-3 from the beginning of the pilot project (May 2009) to early October 2011

Casing gas composition Pre-CO_2 injection casing gas composition at RG-3 was hydrocarbon gases, predominantly methane. There was 1.7 to 8% CO_2 in these samples. During the first months of injection, CO_2 remained relatively constant until June 22, 2009, when the CO_2 concentration increased to 58%. The CO_2 concentration varied from 27 to 77% until October 12, 2009, when the concentration increased again to 81%. The CO_2 concentration remained relatively constant and high, between 79 and 84%, through June 2011. After a sampling gap from July to September 2011, a final sample was taken on October 19, 2011, when CO_2 concentration was 93%.

Casing gas production rate After CO_2 breakthrough, gas production rates increased rapidly in September 2009, slowly increased until an interruption in CO_2 injection in December 2009, and then declined. Once CO_2 injection resumed in late January 2010, production rates increased until they peaked between 425 and 708 scm/day (15,000 and 25,000 scf/day) between April 2010 and the end of injection on May 26, 2010. After CO_2 injection, gas rates rapidly declined. The cumulative total gas production and CO_2 gas production for RG-3 estimated from May 2009 through September 2011 was 142,200 scm (5,025,000 scf) and 218 tonnes (240 tons), respectively.

Allocated oil and water production The daily oil rates were relatively low (0.16 to 0.79 m^3/day [1 to 5 bopd]) for RG-3 until January 1996 when the oil rate started increasing and peaked at 4.8 m^3/day (30 bopd) in August 1996. By December 1997, the oil rate was between 3.66 and 4.77 m^3/day (23 and 30 bopd). Water rates started to increase in December 1996 and peaked at 5.72 m^3/day (36 bwpd) in July 1998. Oil rates decreased sharply as water rates increased. At peak water production, the oil rate was down to 0.48 m^3/day (3 bopd). From September 1998 through November 2005, the water rate was relatively constant at 3.2 to 4.8 m^3/day (20 to 30 bwpd). The oil rate was also relatively constant at 0.08 to 1.4 m^3/day (0.5 to 9 bopd) through most of this period. From June 2006 through December 2010, water production was down to 2.5 to 2.7 m^3/day (16 to 17 bwpd); the oil rate remained at 0.16 to 0.48 m^3/day (1 to 3 bopd). (These rate changes are thought to be attributable to the rate allocation method used by the operator.)

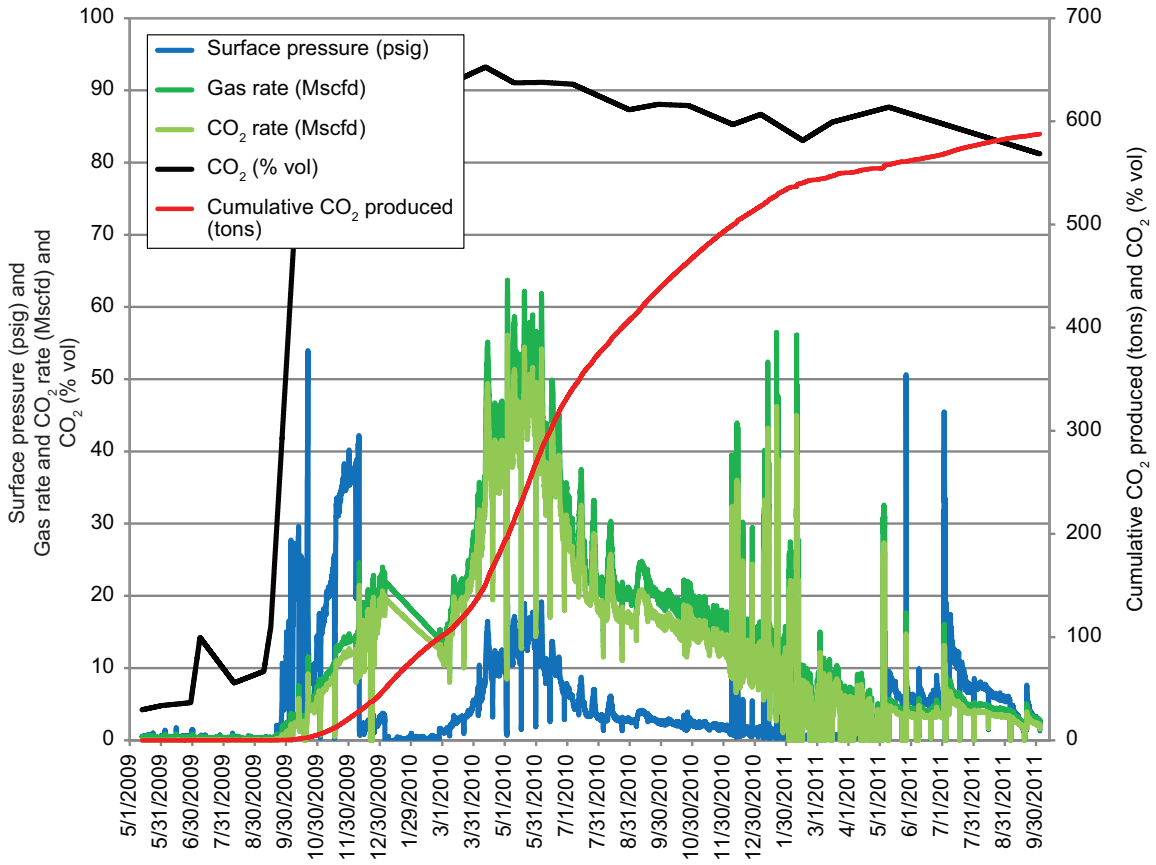

Figure 76 Surface pressure (psig), average total gas and CO_2 rates (Mscfd), average CO_2 volume percent, and cumulative CO_2 produced (tons) for RG-4 from the beginning of the pilot project (May 2009) to the end of September 2011.

In fall 2008, during preparation for CO_2 pilot activities, the oil rate remained unchanged at about 0.16 m^3/day (1 bopd), and the water rate was relatively flat at 2.38 to 2.54 m^3/day (15 to 16 bwpd).

Since waterflood start-up, well RG-3 has produced 5,565 m^3 (35,000 stb) of oil and 17,488 m^3 (110,000 stb) of water.

Ross Gentry #4

Figure 76 shows surface pressure, average total gas and CO_2 rates, CO_2 volume percent, and cumulative CO_2 in tons for RG-4 from the beginning of the pilot project (May 2009) to October 2011.

Surface casing gas pressure The casing pressure at RG-4 remained near zero until September 25, 2009, when the pressure rose to about 69 kPag (10 psig). The pressure climbed to 140 kPag (20 psig) and then stayed fairly constant during the first half of October. After the pressure spiked to more than 340 kPag (50 psig) on October 21, the orifice plate was changed to the next larger size and the pressure decreased to 40 to 62 kPag (6–9 psig). The pressure had climbed to about 280 kPag (40 psig) on December 10, 2009, when the orifice plates were again changed, and the pressure again fell to nearly zero. On January 4, 2010, the plate was removed because of ice buildup in the orifice. The pressures remained nearly zero until near the end of February when the orifice plate was returned, and pressure slowly increased, reaching 70–104 kPag (10–15 psig) by early May. The pressure was relatively constant until early June, when pressure started to slowly decrease, reaching zero by September 2010 and staying at that level until May 2011. At this time, a smaller orifice plate was used and a very slight increase in pressure started and continued through the end of September 2011 when pressure monitoring ended.

Casing gas composition At RG-4, pre-CO_2-injection casing gases were hydrocarbon gases, predominantly methane. These samples contained 1.2 to 3.7% CO_2. During the first months of injection, CO_2 increased slightly to 9 to 14% until October 12, 2009, when the CO_2 concentration increased to 81%. The CO_2 concentration continued to climb slowly, reaching 93% on April 12, 2010, generally decreasing after that time; CO_2 concentration reached 88% on May 10, 2011, varying between 83 to 91% over this period. A gas sample taken at RG-4 on June 8, 2011 had a CO_2 concentration of 61%, but this sample also had a high nitrogen content, suggesting air contamination. A sampling gap of several months followed, and then a final sample was taken in October 19, 2011, when the CO_2 concentration was 88%.

Casing gas production rate After CO_2 breakthrough on September 25, 2009, gas production rates increased steadily to roughly 622 scm/day (22,000 scf/day) in late December when an interruption in CO_2 injection caused rates to decline. Once CO_2 injection resumed in late January 2010, production rates increased until they peaked between 1,274 and 1,699 scm/day (45,000 and 60,000 scf/day) in May 2010. After CO_2 injection ended, gas rates rapidly declined. The cumulative total gas production and CO_2 gas production for RG-4 estimated from May 2009 through September 2011 are 333,000 scm (11,760,000 scf) and 533 tonnes (587 tons), respectively.

Allocated oil and water production The daily oil production rates for well RG-4 were low (0.16 m^3/day [1 bopd]) until October 1993. Thereafter, the oil rate increased to about 0.8–1.6 m^3/day (5–10 bopd) through January 1995. At that time, the oil rate increased (likely in response to the waterflood) to a maximum rate of nearly 4 m^3/day (25 bopd), but decreased back to 0.8–1.6 m^3/day (5–10 bopd) by February 1996. This oil rate decrease was accompanied by a relatively low water production rate of 0.3–1.6 m^3/day (2–10 bwpd). By mid-1996, the water rate reached a maximum of 5.6 m^3/day (35 bwpd) and remained between 2.4 and 4.8 m^3/day (15 and 30 bwpd) through September 2008. During this period of higher water production rates, the oil production rate was relatively constant between 0.3 and 1.3 m^3/day (2 and 8 bopd) until May 2005, when the oil rate decreased to between 0.08 and 0.11 m^3/day (0.5 and 0.7 bopd) through the start of CO_2 injection.

In fall 2008, during the preparation for CO_2 pilot activities, RG-4 was treated with acid. The oil rate remained between 0.08 and 0.11 m^3/day (0.5 and 0.7 bopd), but the water rate increased sharply to nearly 7.9 m^3/day (50 bwpd). There was no noticeable change in oil and water production due to CO_2 injection.

Since waterflood startup, well RG-4 has produced 3,816 m^3 (24,000 stb) of oil and 17,488 m^3 (110,000 stb) of water.

Pressley-Hart #1

Figure 77 shows surface pressure, average total gas and CO_2 rates, CO_2 volume percent, and cumulative CO_2 for PH-1 from the beginning of the pilot project (May 2009) through October 2009.

Surface casing gas and downhole pressure After nearly 5 months of CO_2 injection, on October 6, 2009, pressure began to increase at PH-1 and rose to about 210–240 kPag (30–35 psig) by October 24. Production problems associated with its downhole, insert pump were suspected and the well was shut-in at various times while attempts were made to return the well to production. Efforts included reducing the casing pressure to atmospheric pressure until November 6. At that time, the rods and insert pump were pulled and the well was allowed to flow directly into the surface production flow line. The pump did not appear to be impaired by paraffin or any mechanical failure, and a flow line obstruction (paraffin) was suspected.

The flow line was treated on November 11 by pumping 420 L (110 gallons) of xylene into the flow line to remove any paraffin build-up. The pressure started to increase again. By November 15, 2009, flow line pressure was in excess of 1.1 MPag (160 psig). Consequently plans were made to pull the tubing and add a packer to protect the casing. (The packer chosen was the same as that for RG-2 and the injection well RG-5, an AD-1 type with an 80-durometer rubber element.) At this time the casing surface pressure gauge was connected to the flow line, and no additional pressures were recorded directly for PH-1.

Casing gas composition Pre-CO_2 injection casing gas composition at PH-1 was hydrocarbon gases, predominantly methane. These samples contained 0.2 to 0.5% CO_2. Over the next four months, the CO_2 concentration increased very slightly to 1.3%. On October 7, 2009, the CO_2 concentration increased to 31%

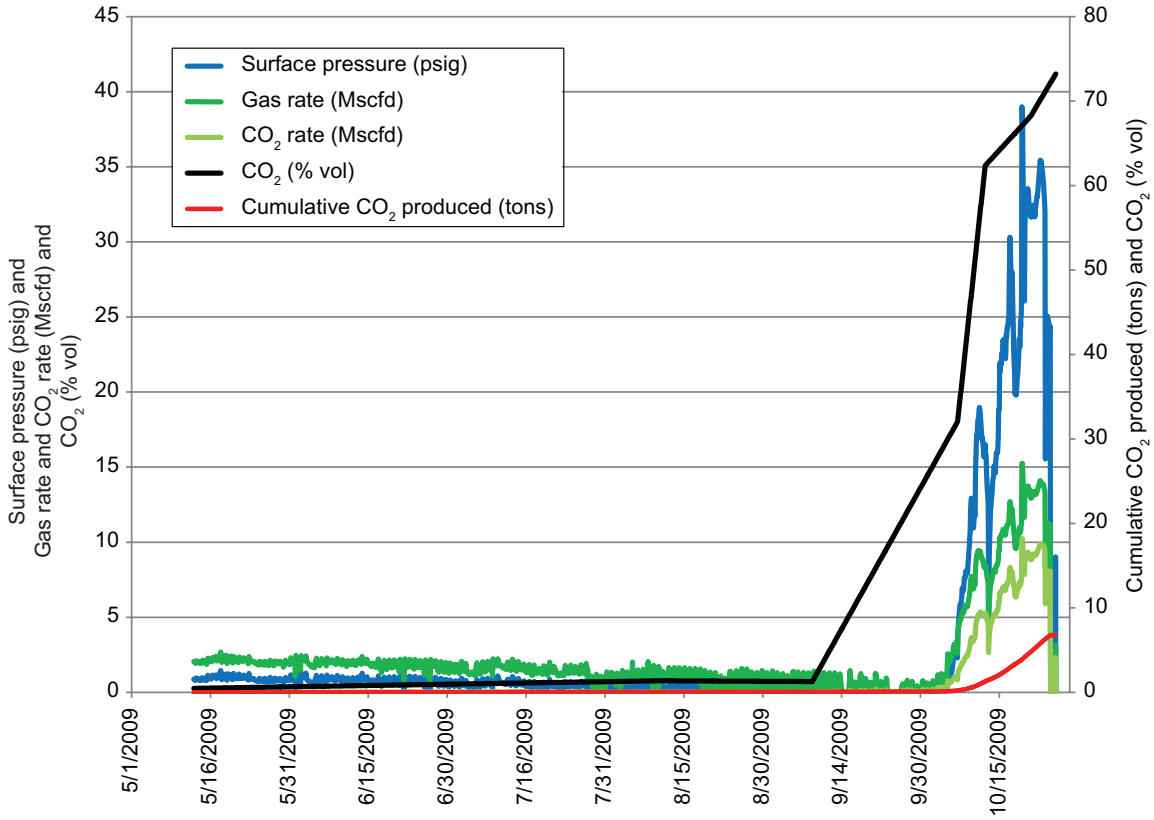

Figure 77 Surface pressure (psig), average total gas and CO_2 rates (Mscfd), CO_2 volume percent, and cumulative CO_2 produced (tons) for PH-1 from the beginning of the pilot project (May 2009) through October 2009. Casing gas production data (gas rates, CO_2 volume %, and cumulative CO_2 produced) ends in October because the well was allowed to flow to the surface production flow line.

and had risen to 63% by October 12, 2009. After CO_2 broke through at this well, production problems associated with pumping the well eliminated the possibility of sampling the casing gas directly from the wellhead. After the downhole packer was placed in the well, surface gas sampling directly from the wellhead was also no longer possible. After a field IR reading of 82.7% on November 4, 2009, no gas samples were collected nor field IR readings taken from PH-1 until April 2011. At that time, gas collected from the top of the carboy during brine sampling was used for field IR readings and laboratory samples. Field IR readings taken in April, May, and June 2011 showed 86–91% CO_2 concentration. Laboratory results showed slightly higher (91–92%) concentrations. The final sampling event took place on November 2, 2011, and yielded a field IR result of 85.4% CO_2 and a laboratory result of 91.9% CO_2.

Casing gas production rate After CO_2 breakthrough on October 6, 2009, gas production rates increased steadily from less than 28 to roughly 400 scm/day (1,000 to roughly 14,000 scf/day) on October 25, 2009, the end of casing gas production. The cumulative total gas production and CO_2 gas production for PH-1 estimated from May 2009 through September 2011 are 10,300 scm (362,000 scf) and 6.2 tonnes (6.8 tons), respectively.

Allocated oil and water production Based on the oil and water production data, there were two water and oil responses for well PH-1. Daily oil rates were low (0.16 m^3/day [1 bopd]) until September 1993. The oil rate increased at that time and ranged from 0.8 to 2.4 m^3/day (5 to 15 bopd) through May 1996. Water rates were as high as 3.7 m^3/day (23 bwpd) and declined with the oil rate. Water and oil rates remained relatively low from June 1996 through December 1997. The oil rate increased to a peak of 3.2 m^3/day (20 bopd) in January 1999; water production also increased during this time but was delayed by about 5 months relative to the oil production.

The rates decreased thereafter to 0.3 to 0.8 m^3/day of oil (2 to 5 bopd) and 0.8 to 1.6 m^3/day of water (5 to 10 bwpd) until the well was shut-in in December 2001. Two additional attempts to produce from PH-1 were made prior to returning the well to production as part of the CO_2 injection pilot, but these attempts resulted in relatively high water rates and low oil reports and were discontinued after 5 to 8 months.

In January 2009, during the preparation for CO_2 pilot activities, PH-1 produced at about 0.5 m^3/day of oil (3 bopd) and 2.4 m^3/day of water (15 bwpd). When excessive CO_2 caused the rod pump to fail and the well was allowed to flow, the water rate decreased to 1.3 m^3/day (8 bwpd) and oil production was about 0.2 m^3/day (1.5 bopd).

Since waterflood startup, well PH-1 produced 3,020 m^3 (19,000 stb) of oil and 6,360 m^3 (40,000 stb) of water.

Wilbur-Todd #4, #8, and #9

There was no reportable change in fluid production, composition, or pressure at WT-4, WT-8, and WT-9, likely because of the greater distance of these wells from RG-5 than the other wells or lower hydraulic conductivity between the Gentry and Wilbur-Todd leases.

Figure 78 shows surface pressure, average total gas and CO_2 rates, CO_2 volume percent, and cumulative CO_2 in tons for WT-4, WT-8, and WT-9.

Surface casing gas pressure In general, the casing pressures at WT-8 were relatively low, flat, and constant, staying below 35 kPag (5 psig) for the entire project with a slight (7–14 kPag [1–2 psig]) increase over the course of injection and a drop of about 7 kPag (1 psig) at the end of injection. Pressures at WT-4 averaged around 14–21 kPag (2–3 psig), but with frequent brief spikes as high as 110 kPag (16 psig) during injection and one spike up to 124 kPag (18 psig) in November 2010. WT-9 was flat at nearly 0 kPag (0 psig) and based on regular field observations, the casing pressure was considered to be on a vacuum. No change in casing gas production occurred during CO_2 injection or the post-CO_2 water injection period.

Casing gas composition No large increases in CO_2 concentration were detected at any of the WT wells in the pilot area from pre-CO_2 injection through May 2011. At well WT-4, the CO_2 concentration was between 0.4 and 2.2%, but with a relatively consistent average concentration of about 1.5%; at well WT-8 it was between 0.1 and 2% with an average value of 0.5%. To simplify calculation of gas rates, the average values were used and are shown in Figure 78. No positive casing pressure existed at WT-9, and no gas samples were taken. Although there were no large increases, the concentration of CO_2 in the casing gas at well WT-4 did have a generally increasing trend from 0.4 up to 2.2% CO_2 from March 2009 to May 2011. Final readings taken at WT-4 on October 19, 2011, and November 2, 2011, show concentrations of 1.3% both days. Field readings were also taken at WT-8 on those dates, yielding a CO_2 concentration of 3.4% on October 19 but a lower reading of 0.7% on November 2. A field IR reading taken at WT-9 on November 2, 2011, showed a CO_2 concentration of 2.3%. Laboratory (GC) results showed a CO_2 concentration of 2.4% at WT-4 on November 2, 2011, and 4.0% at WT-8 on October 19, 2011.

Casing gas production rate Gas production rates at WT-4 were relatively constant and less than 34 scm/day (1,200 scf/day) from May 13, 2009, to October 1, 2011. Similarly, gas production rates at WT-8 were relatively constant and less than 40 scm/day (1,400 scf/day) from May 13, 2009, to October 1, 2011. (Pressures were not accurate enough to calculate good estimates; however, since the $^1/_{16}$-inch orifice plate was installed, rates were not very sensitive to pressure and setting a maximum pressure did not generate large error.) Gas production rates at WT-9 were constant with an average of roughly 10.7 scm/day (377 scf/day) from May 13, 2009, to April 1, 2011. (The pressure transducer was damaged on April 1, 2011 and measurement ended.) There was no evidence of pressure breakthrough, and CO_2 concentrations were roughly 2% with no trend.

Allocated oil and water production Well WT-4 oil and water production was relatively low (0.16–0.318 m^3/d [1–2 bpd]) until March 1998 when water rate increased to above 3 m^3/d (20 bwpd) and peaked in excess of 8 m^3/d (50 bwpd) in September 1998. Water rate stabilized at about 5 m^3/d (30 bwpd) through November 2001. Oil rate had very little change to a few barrels of oil per day to 0.8 m^3/d (5 bopd) until November 2001. Oil rates were about 2 m^3/d (10 bopd) from November 2001 to June 2005 and then decreased to a few barrels of oil per day through the end of 2010.

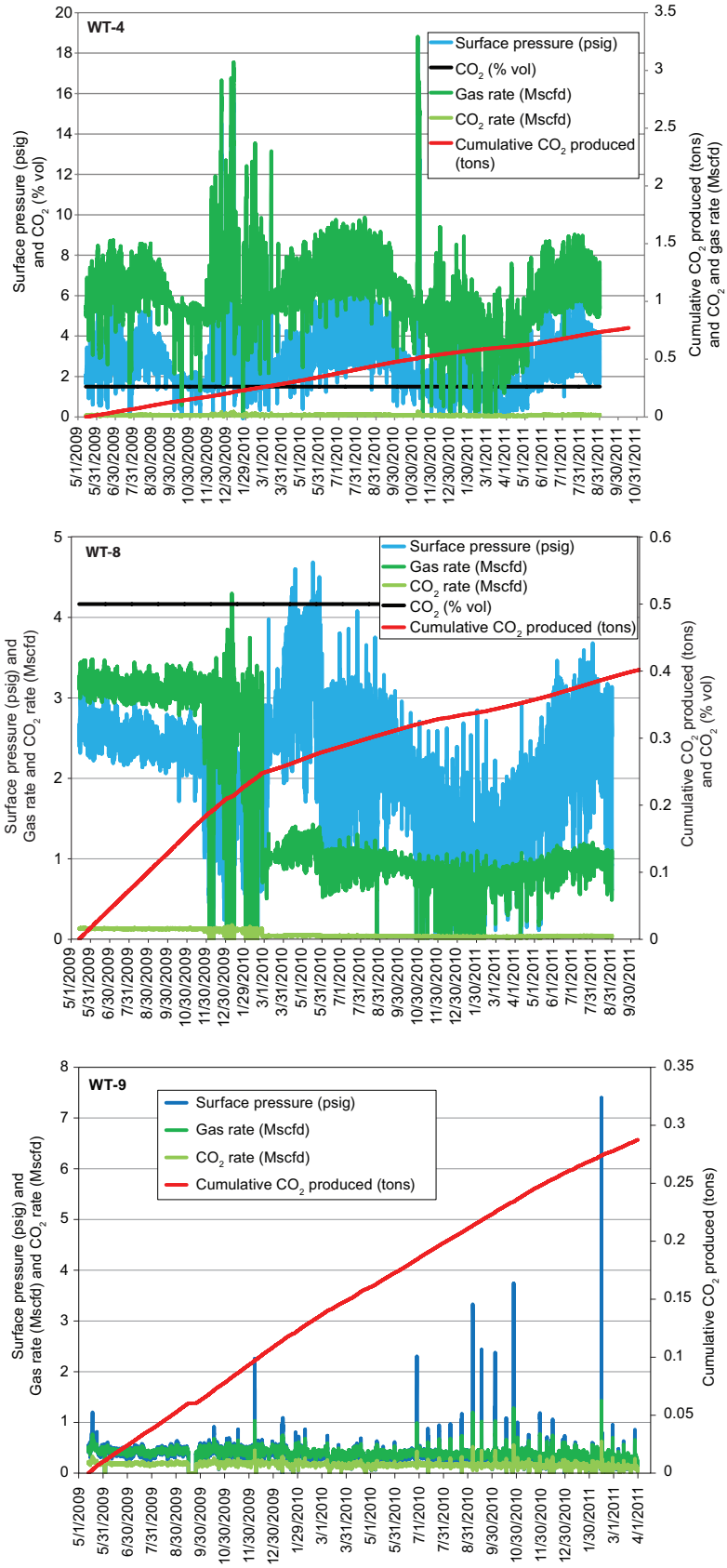

Figure 78 Surface pressure (psig), average total and CO_2 gas rates (Mscfd), and cumulative CO_2 produced (tons) for WT-4, WT-8, and WT-9, as well as CO_2 volume percent for WT-4 and WT-8.

Well WT-8 started at about 3 m^3/d (20 bopd) at the end of 2003. Oil production was relatively constant between 1 and 1.7 m^3/d (7 and 11 bopd) through the end of 2011. Water rate was relatively flat from 0.2 to 0.8 m^3/d (1 to 5 bwpd). The oil rate at WT-9 was consistently between 0.24 to 0.5 m^3/d (1.5 to 3 bopd) from April 2007 through the end of 2011. Water rate decreased over this period from 4.0 to 3.0 m^3/d (25 to 19 bwpd). Neither well had a change in oil or water rate during the CO_2 injection period or the subsequent water injection period.

Since waterflood start-up, well WT-4 produced 3,300 m^3 (21,000 stb) of oil and 2,100 m^3 (13,000 stb) water, well WT-8 produced 3,800 m^3 (24,000 stb) of oil and 950 m^3 (6,000 stb) water, and WT-9 produced 530 m^3 (3,300 stb) of oil and 4,600 m^3 (29,000 stb) water.

Observation Well Responses

In the original plan for this pilot, three wells were designated and instrumented to measure pressure immediately outside of the "ring" of producers surrounding RG-5: PZ-1 located 356 m (1,170 ft) to the northeast, PB-3 located 352 m (1,115 ft) to the west, and JR-1 located 407 m (1,335 ft) to the south from RG-5. After RG-2 was shut-in due to excessive CO_2 production, it, too, became a pressure observation well.

In the first few weeks of operation, an attempt was made to collect a brine sample at JR-1. Only oil was recovered, and the resulting pressure decrease rendered JR-1 relatively useless as a pressure monitoring well. Because it was not possible to both sample brine and monitor pressure, fluid sampling at JR-1 was discontinued in early June 2009. Wells PZ-1 and PB-3 were not sampled for brine because they had gas heads.

Pressley-Zogg #1

Well PZ-1 was not liquid-filled so a subsurface gauge was deployed at a depth of 290 m (950 ft) MD (GL). This was datum-corrected to −420 m (−1,380 ft) below sea level using a fluid density gradient of 9.80 kPa/m (0.433 psi/ft). The datum-corrected pressure was 4.27 MPag (620 psig) on May 15, 2009. The pressure underwent a general decrease until mid-September, reaching 4.05 MPag (589 psig) on September 11, 2009. At that time it started to increase and reached nearly 4.69 MPa (680 psig) on May 9, 2010, then fell to 4.58 MPa (665 psig), and thereafter remained relatively constant at that pressure until the end of the CO_2 injection period. The cause of this rise and fall in pressure is not known.

After CO_2 injection stopped, the pressure at well PZ-1 started to increase linearly to 4.84 MPa (702 psig) through July 8, 2010, at which time a relatively large pressure increase occurred, reaching a maximum of 5.46 MPag (793 psig) on August 8, 2010. Pressure ranged between 5.20 and 5.48 MPag (755 and 795 psig) through March 22, 2011, at which time another relatively large pressure increase occurred, increasing to a maximum of 6.26 MPag (909 psig) on May 27, 2011. To check whether the pressure increase was due to CO_2, the tubing pressure was relieved slowly through a 0.64 cm (¼-inch) valve for about 2 hours until a light mist of oil sprayed from the valve; at this time the valve was shut. This gas relief event caused a rapid decrease in pressure to 4.27 MPag (620 psig), followed immediately by a rebound to about 5.1 MPag (740 psig). The pressure increased to about 6.06 MPag (880 psig) through September 9, 2011. The pressure was released from the well as before, and pressure fell to 5.58 MPag (810 psig) by September 18, 2011. The final measured pressure was about 4.96 MPag (720 psig).

Peter Bowles #3

Well PB-3 was not liquid-filled, so a subsurface gauge was deployed to a depth of 111 m (365 ft), which was datum-corrected to −420.6 m (−1,380 ft) ss using a fluid density gradient of 9.80 kPa/m (0.433 psi/ft). The datum-corrected pressure was 5.44 MPag (789 psig) on May 15, 2009. Pressure slowly increased to 5.79 MPag (840 psig) through November 20, 2009. Over the next 3 months the pressure increased and decreased very rapidly during four different events. The four pressure peaks were 5.99, 6.48, 7.20 and 7.03 MPag (870, 940, 1,045, and 1,020 psig). After this period, the pressure was relatively constant between 5.44 and 5.65 MPag (790 and 820 psig) through the end of CO_2 injection. The cause of these pressure peaks is not known. Interference from offsite wells is possible; the nearest oil field is about 0.8 to 1.6 km (½ to 1 mile) from this well site.

During the following water injection period, pressure at well PB-3 was relatively constant at 5.48 MPag (795 psig) through July 8, 2010, at which time the pressure began to increase rapidly, reaching 5.72 MPag (830 psig) by July 14, 2010. Pressure then remained relatively stable through September 13, 2010. Over the next 6 to 7 months the pressure increased and decreased very rapidly during multiple different events, hitting a maximum of 7.37 MPag (1070 psig) on December 30, 2010. From April 2011 through September 26, 2011, pressure fluctuated between 5.48 and 6.17 MPag (795 and 895 psig) with one spike. Toward the end of the monitoring period, the pressure in the well was trending upward; pressure reached 6.51 MPag (945 psig) on September 29, 2011, before dropping to about 5.41 MPag (785 psig) and then remaining steady for the next few days until monitoring ended.

J Rickard #1

Because the well was filled with liquid, a surface gauge could be used on well JR-1 to calculate the bottomhole pressure (BHP). For about a month, from June 16 to July 23, 2009, the automated BHP gauges frequently failed to log their data. Most of these failures occurred because the transmission line was lying on the ground and cattle frequently tripped over it and disconnected or broke the wire. Radio transmission was installed to overcome this problem. The datum-corrected initial pressure of well JR-1 was 12.95 to 13.06 MPag (1,880 to 1,895 psig), and the pressure decreased to 12.85 MPag (1,865 psig) on August 19, 2009. Afterward the pressure increased to between 13.02 and 13.16 MPag (1,890 and 1,910 psig) through February 2, 2010. From this time onward, the pressure gradually increased and was up to 13.37 MPag (1,940 psig) at the end of CO_2 injection (May 26, 2010).

During the subsequent water injection period, the pressure at JR-1 reached a maximum of 13.40 MPag (1,945 psig) on June 7, 2010. The pressure then decreased somewhat linearly to 12.75 MPag (1,850 psig) through October 29, 2010. From then through Sept. 26, 2011, the pressure varied between 12.75 and 13.02 MPag (1,850 and 1,890 psig). The final measured pressure was closer to 12.64 MPag (1,835 psig).

Ross Gentry #2

On June 14, 2009, gas production and pressure from the annulus of RG-2 was too great and the well was shut-in. Casing pressure was up to 276 kPag (40 psig) on June 8. (In general the operator maintained casing annulus pressure below 689 kPag [100 psig.]) Until the pulling unit could arrive on location, the annulus was left open to protect the casing by preventing higher pressure on the casing. When the workover rig arrived, the pump, rods, and tubing were pulled and tubing with packer was run back in the well; this isolated the casing from the excessive pressure associated with the high volume and pressure of CO_2 at this well. The packer chosen was the same as that for the injection well RG-5, an AD-1 type with an 80-durometer rubber element.

By September 2009, during active CO_2 injection, the pressure at RG-2 was relatively constant and between 11.9 and 12.1 MPag (1,720 and 1,750 psig). When CO_2 injection at RG-5 ceased due to failure of delivery of CO_2 during icy road conditions, the pressure decreased to 11.10 MPag (1,610 psig). When CO_2 injection resumed, pressure increased to 12.13 to 12.23 MPag (1,760–1,775 psig). A small decrease in pressure to 11.71 MPag (1,700 psig) started a few days before CO_2 injection ceased and continued through June 13, 2010, when the pressure began to increase, reaching 12.41 MPag (1,800 psig) on June 26 and then staying between about 12.41–12.47 MPag (1,800–1,810 psig) until July 14. At that point the pressure decreased slowly to about 11.54 MPag (1,675 psig) in late October, followed by a slight, slow increase to 11.58–11.61 MPag (1,680–1,685 psig) through most of November, followed by a steady drop to about 9.85 MPag (1,430 psig) on March 14, 2011. At this time attempts were made to return RG-2 to production. At the end of March, 2011, RG-2 was producing regularly and the bottomhole pressure decreased to and remained relatively constant between 5.52 and 5.72 MPag (800 and 830 psig).

Water Injection Outside of CO_2 Injection Pilot Area

Historically there were nine water injection wells including RG-5 in the Sugar Creek oil field. Since 2003, however, only five injectors have been active: RG-5, PZ-2, EL-2, WT-7, and BM-2. Water injection rates are measured with turbine meters and reported daily.

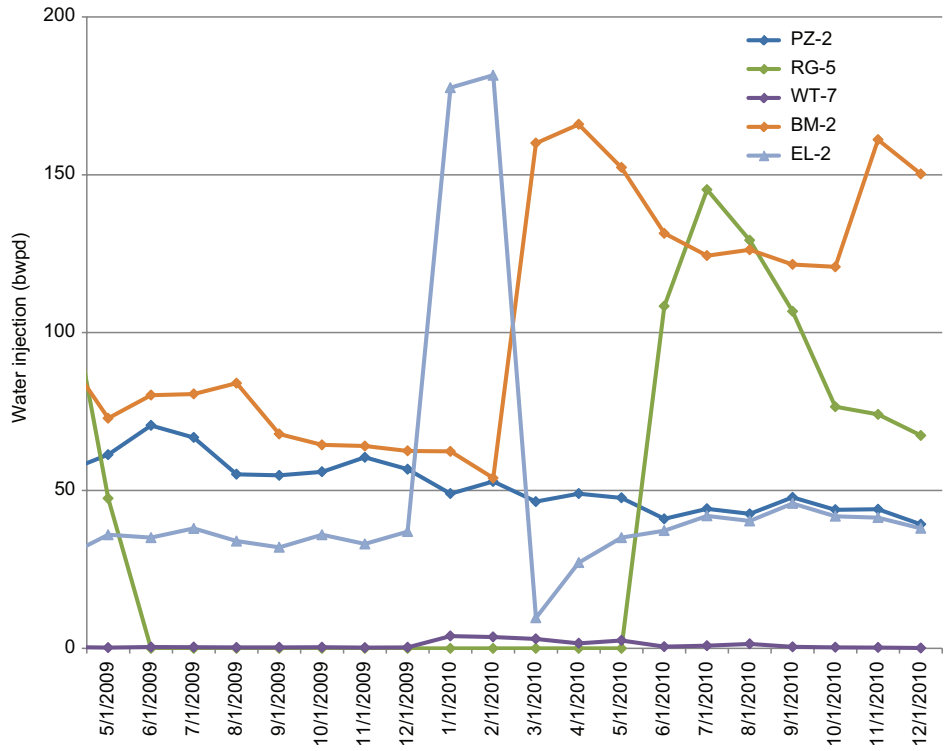

Figure 79 Water injection rates (bwpd) for the pilot period (May 2009 through December 2010). May 2009 rates are average for entire month rather than for injection period (May 13–May 31, 2009) because daily injection rates were not available.

Injection well rates ranged from 4.77 to 12.72 m^3/d (30 to 80 bwpd) for BM-2, EL-2, and PZ-2 through the beginning of 2010. During the period from the start of CO_2 injection through the end of 2010, BM-2 usually had the highest injection rates, although it was briefly exceeded by EL-2 in January and February 2010 (Figure 79). Rates for EL-2 and BM-2 climbed above 23.85 m^3/d (150 bwpd) from January through February 2010 and March through May 2010, respectively; EL-2 dropped precipitously after its high of 28.9 m^3/d (182 bwpd) in February 2010 to less than 8 m^3/d (50 bwpd) for the remainder of 2010. BM-2 had rates of 19.2–20.8 m^3/d (121–131 bwpd) for June–October 2010 and then climbed above 23.85 m^3/d (150 bwpd) for November and December.

Rates at PZ-2 peaked at 13 m^3/d (71 bwpd) in June 2010 and then entered an almost uniform decline, dropping to 6.2 m^3/d (39 bwpd) by December 2010. RG-5 started water injection after CO_2 injection termination and reached a high of 23.1 m^3/d (145 bwpd) in July 2010 but dropped to 10.7 m^3/d (67 bwpd) by December 2010. WT-7 had water injection rates of less than 0.8 m^3/d (5 bwpd) throughout the period.

During active CO_2 injection, cumulative water injection for the non-pilot injection wells was 12,300 m^3 (77,200 bbl). For the year following CO_2 injection, cumulative water injection for these wells was 6,710 m^3 (42,200 bbl).

MVA OBSERVATIONS AND INTERPRETATIONS

Jackson Sandstone Geochemistry and Sampling Results

Jackson Brine and Associated Gas—Response to CO_2 Injection

The geochemical response of coproduced Jackson sandstone brine, gas, and oil to CO_2 injection was variable in timing and character. This variability was exemplified by the IRGA measurements used to detect the occurrence of free-phase CO_2 in the annulus space of the production wells (i.e., CO_2 breakthrough; Figure 80). The first well to show breakthrough was RG-2 where CO_2 concentrations increased to 75 to 80% on

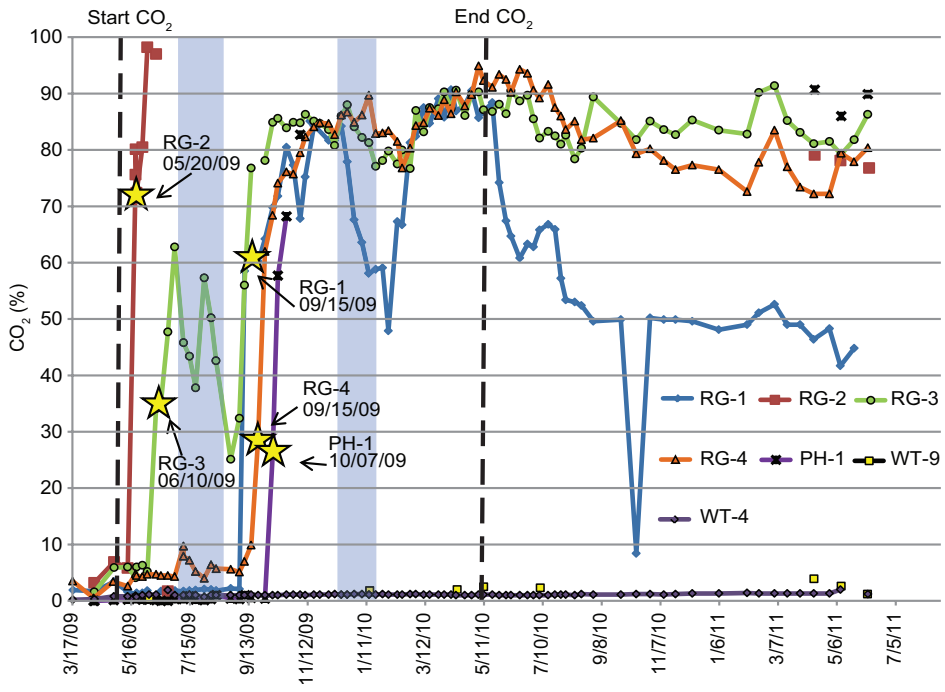

Figure 80 Infrared gas analyzer determined CO_2 concentrations before, during, and after CO_2 injection from casing gas and liberated gas from brine sampling (via carboy). Star symbols represent CO_2 breakthrough dates. Black vertical dashed lines designate start and end of CO_2 injection at RG-5. Vertical blue bars designate approximate periods of CO_2 injection shut-in.

May 20, 2009 up from pre-CO_2 injection values of 3 to 7%. This pronounced increase occurred within one week of the start of injection. In order of increasing time from the onset of injection, order of magnitude increases in CO_2 also characterized breakthrough at RG-3, RG-4, and PH-1.

In contrast, WT-9 showed a more subtle increase in CO_2; a June 2009 measurement showed 0.3% CO_2, and the next measurement in January 2010 showed 1.8% CO_2. The 6-month gap in measurements reflected the difficulty in making IRGA measurements at WT-9 where little or no positive pressure existed in the annulus. Consequently, IRGA measurements and gas samples were mostly collected from gases evolved as headspace in the top of the carboy. (Only seven IRGA measurements were conducted after CO_2 injection for WT-9.)

WT-4 showed no evidence of increased CO_2.

pH The dissolution of CO_2 into water and attendant dissociation reactions are well documented (e.g., Cotton and Wilkinson, 1976):

$$CO_2(g) = CO_2(aq) \quad (5)$$

$$H_2O + CO_2(aq) = H_2CO_3 \quad (6)$$

$$H_2CO_3 = H^+ + HCO_3^- \quad (7)$$

$$HCO_3^- = H^+ + CO_3^{2-} \quad (8)$$

The dissolution of CO_2 into water and subsequent dissociation steps proceed at relatively rapid rates. The sequence of reactions acts to lower solution pH and drive other reactions, such as carbonate dissolution. Therefore, documenting the pH and alkalinity response to CO_2 injection was important (Figures 81 and 82; Appendix 5). Values for pH were typically on the order of 6.8 to 7.2 before CO_2 injection and decreased to 5.7 to 6.2 (as measured at the surface) within several weeks of CO_2 breakthrough for RG-2, RG-4, and

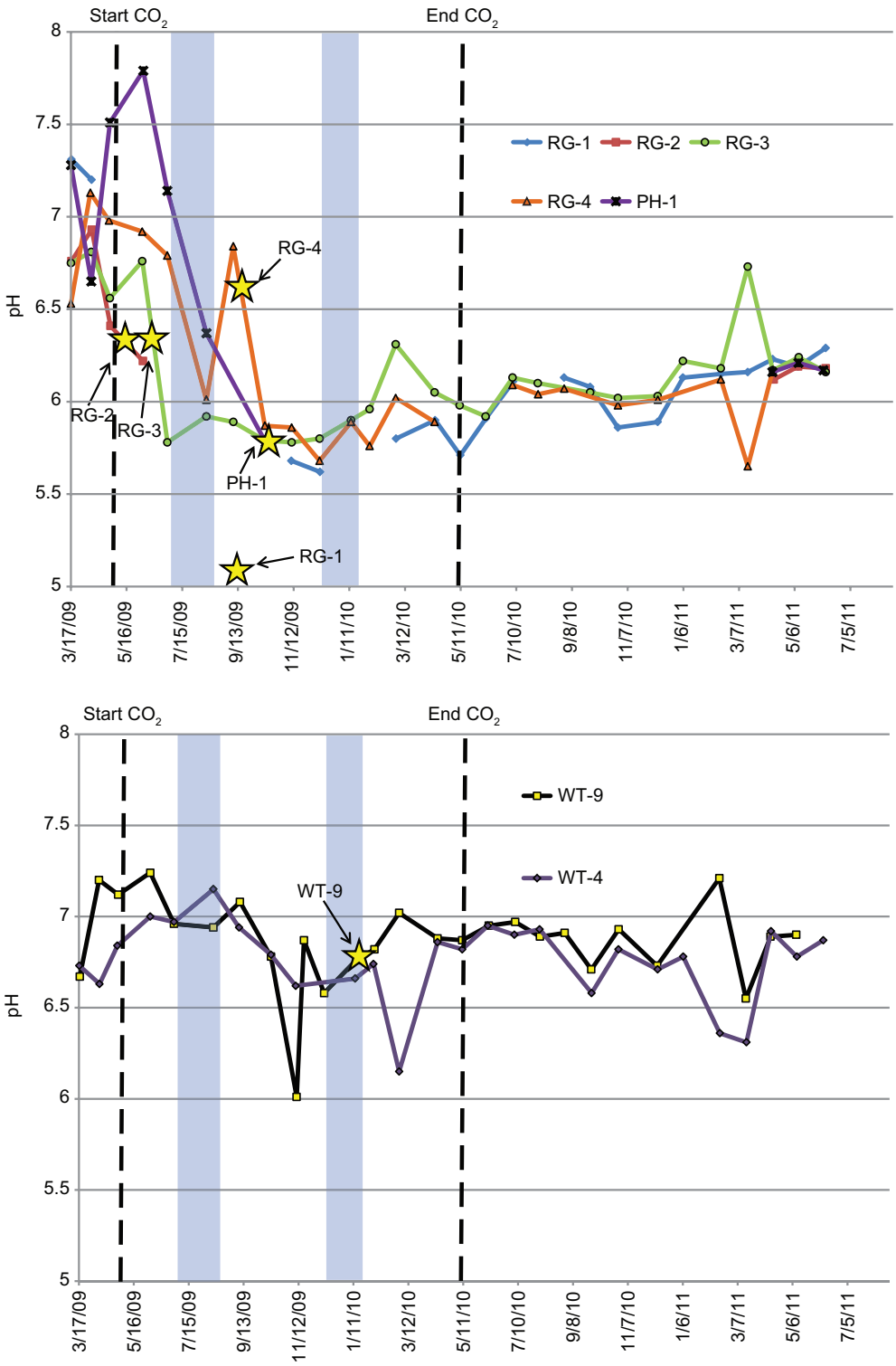

Figure 81 Top: Evolution of pH for wells having large increases in CO_2 during breakthrough (RG-1, RG-2, RG-3, RG-4, and PH-1); bottom: evolution of pH for wells having subtle (WT-9) or no (WT-4) increases in CO_2 levels as determined by infrared gas analyzer. Star symbols represent CO_2 breakthrough dates. Black vertical dashed lines designate start and end of CO_2 injection at RG-5. Vertical blue bars designate approximate periods of CO_2 injection shut-in.

PH-1. Moreover, in RG-4 and PH-1, and possibly RG-2, pH appears to have decreased ahead of CO_2 breakthrough (Figure 81).

A strong pH decrease was documented at RG-1 approximately 2 months after CO_2 breakthrough. The apparent time lag between CO_2 breakthrough and pH response in RG-1, however, is likely a sampling artifact because no brine samples were collected in September, when CO_2 breakthrough was documented, or subsequently in October. Specifically, high oil cut in the produced fluids precluded the collection of brines. A similar problem occurred at RG-2 and later at PH-1, albeit due to high CO_2 content, which eventually caused the wells to be temporarily shut-in. Data gaps in the time series plots for given wells are the result of periods when it was not possible to collect brine (e.g., Figures 81 and 82).[3] This characteristic applies not only to pH and alkalinity, but also other chemical parameters for which temporal evolution is analyzed in this section.

Except for the 6.0 measurement on November 10, 2009, the pH response at WT-9 showed a possible subtle decrease from about 7.2 to 6.6, although the month-to-month variations made recognition of a trend ambiguous. The WT-4 showed no discernible trend and, with a few exceptions, pH generally varied between 6.6 and 6.9.

Following the end of CO_2 injection on May 10, 2010, the field was continuously sampled on a monthly basis from June 2010 through June 2011 and one additional time, November 2011. The 18-month, post-CO_2 sampling period was important for assessing the longer-term geochemical behavior in the reservoir, especially with respect to pH buffering and aqueous fluid reactivity. Moreover, the post-CO_2 monitoring provided further confirmation that the project was implemented safely and without adverse effect on the shallow groundwater resources.

The IRGA showed that the concentrations of CO_2 in the post-injection period remained elevated at 72 to 91% for the RG and PH-1 wells (Figure 80). However, RG-4 and RG-1 showed declines when compared with the measured CO_2 concentrations of about 90% near the end of the injection period. Concentrations post-CO_2 injection at RG-4 declined to 72%, and those at RG-1 declined further to 49%. The November 2011 measurements for RG-1 continued to decline to 42%, whereas CO_2 concentrations in the other wells remained similar to the June 2011 measurements. The CO_2 concentration at WT-9 was low (2.3%) but still elevated with respect to pre-injection CO_2 values while those at WT-4 remained unchanged.

Minimum pH values of 5.6 to 5.8 developed in the RG wells and PH-1 6 to 7 months after the start of CO_2 injection (Figure 81). Remarkably, regardless of when CO_2 breakthrough occurred, the RG wells and PH-1 reached pH minima at nearly the same time from about September 2009 through January 2010. Subsequently, their pH values rose gradually and steadily, and pH values in June 2011 equaled 6.2 to 6.3. The pH values measured November 2011 equaled 6.1 to 6.2. WT-9 and WT-4 had a few unexplained excursions to higher and lower pH values in the post-CO_2 period, but otherwise maintained pH values in the mid- to upper-6 range (Figure 81).

Alkalinity and Dissolved Inorganic Carbon The CO_2 aqueous speciation reactions further predict that the concentration of HCO_3^- and CO_3^{2-} should increase and consequently lead to increases in alkalinity and DIC. Wells that had large increases in annulus CO_2 and attendant decreases in pH during CO_2 injection showed strong increases in alkalinity and DIC (Figure 82, Appendix 5). For example, the RG wells had pre-CO_2 alkalinity values on the order of 700 to 800 mg/L, and these values increased to 1,000 to 2,400 mg/L during CO_2 injection. Pre-CO_2 DIC values on the order of 100 to 200 mg/L sometimes increased by a factor of 4 during CO_2 injection, such as in RG-3 (Appendix 5). Increases in alkalinity and DIC were often quick relative to the time of CO_2 breakthrough; for example, at PH-1 alkalinity and DIC increased within a week of CO_2 breakthrough. Alkalinity and DIC measurements at WT-9 showed unambiguous increases during injection, providing strong evidence for the influence of CO_2 and clarifying the subtle pH response (Figure 82, Appendix 5).

[3] Some of the later data (e.g., November 2011) were not included on the figures to avoid a large gap in the data after the preceding measurement.

Pre-CO_2 alkalinity and DIC values at PH-1 and WT-4 were lower than those at the RG wells and WT-9, which likely reflects the lack of mixing with dilute HCO_3-rich Pennsylvanian groundwater from WT-3 injected during waterflood operations (Figure 82, Appendix 5). (PH-1 was shut-in for several years prior to the start of this project and likely had less RG-5 injected water around it at the start of the CO_2 injection pilot.) PH-1 was eventually influenced by CO_2 as shown by breakthrough (January 14, 2010) and the aforementioned decrease in pH and increase in alkalinity and DIC. WT-4, however, showed no increase in CO_2 or changes in alkalinity or DIC.

Alkalinity and DIC values in the post-CO_2 period remained elevated for the RG wells, PH-1, and WT-9 (Figure 82, Appendix 5). The range of values and trends in the post-CO_2 period is variable, even for wells that experienced significant increases in CO_2 associated with breakthrough. For example, alkalinity and DIC values at RG-1 peaked at 3 to 5 months (1,754 mg/L and 654 mg/L, respectively) following injection and decreased thereafter. Alkalinity at RG-3 and RG-4, in contrast, peaked (~2,700 mg/L) at 9 and 11 months following CO_2 injection, respectively. Moreover, RG-4 continued to show an upward trend through the November 2011 measurements. The persistence of high alkalinity and DIC at PH-1 would appear to be the result of CO_2 breakthrough; however, as the cation response shows other factors are likely influencing the aqueous geochemistry. Although WT-9 did not have the large IRGA CO_2 response, it shows a trend of increasing alkalinity and DIC, albeit at lower values. Post-CO_2 alkalinity and DIC at WT-4 remain unchanged.

Brine Composition (Dissolved Constituents) Changes in pH, alkalinity, and DIC arise not only from the aqueous CO_2 speciation reactions, but also because of interactions with rock-forming minerals in the reservoir and confining strata. More specifically, buffering of pH by dissolution of carbonate and silicate minerals yields changes in solution chemistry. Some representative reactions show the dissolution of calcite ($CaCO_3$), albite ($NaAlSi_3O_8$), and muscovite [$2KAl_2(AlSi_3O_{10})(OH)_2$]:

$$CaCO_3 + H^+ = Ca^{2+} + HCO_3^- \quad (9)$$

$$NaAlSi_3O_8 + 2H^+ + 6H_2O = Na^+ + Al(OH)^{2+} + 6H_2O + 3SiO_2 \quad (10)$$

$$2KAl_2(AlSi_3O_{10})(OH)_2 + 2H^+ + 3H_2O = 3Al_2Si_2O_5(OH)_4 + 2K^+ \quad (11)$$

Along with these minerals, strata in the Jackson sandstone and overlying Golconda intervals contain variable amounts of potentially reactive ankerite, dolomite, K-feldspar, illite, kaolinite, and chlorite (Appendix 4).

Ca^{2+} A variety of experimental and field studies have demonstrated that reactions with carbonate minerals are typically faster than those with silicate minerals (Palandri and Kharaka, 2004). Divalent calcium is found in these carbonate minerals, and increases in Ca^{2+} solution concentration would thus provide strong evidence that pH was buffered through dissolution of carbonate. Even before CO_2 injection, however, concentrations of Ca^{2+} were much higher in PH-1 and WT-4 versus the RG wells and WT-9 (Figure 83, Appendix 8). As with alkalinity and DIC, the difference can be attributed to injected WT-3 waters mixing with and diluting the in situ Jackson sand water at the RG wells and WT-9 but not PH-1 and WT-4.

Wells RG-1, RG-2, RG-3, and PH-1 showed rapid responses with increased Ca^{2+} concentrations within 30 days of CO_2 breakthrough (Figure 83). The quickest response was at PH-1 where Ca^{2+} concentration increased by about 200 mg/L within six days of breakthrough. Unfortunately, high levels of CO_2 production in PH-1 required a packer to be placed downhole to protect the casing, and the well flowed through tubing without a pump; consequently, collection of additional samples was not possible until the last several months of the project. For RG-1, an unambiguous increase in Ca^{2+} was documented approximately 11 months after breakthrough. This comparatively late Ca^{2+} increase is likely an artifact, however, as variable pre-CO_2 measurements precluded establishment of an accurate reference baseline for Ca^{2+}, and the inability to brine sample RG-1 for 8 months during injection rendered a poor time resolution. At WT-9 a subtle increase in Ca^{2+} from approximately 460 to 480 mg/L was documented on December 10, 2009, ahead of the documented breakthrough on January 14, 2010. Again, however, this is likely an artifact of the aforementioned difficulties in getting IRGA measurements at WT-9. Concentrations of Ca^{2+} at WT-4 showed no significant changes in accordance with observations that this well was not influenced by CO_2 injection.

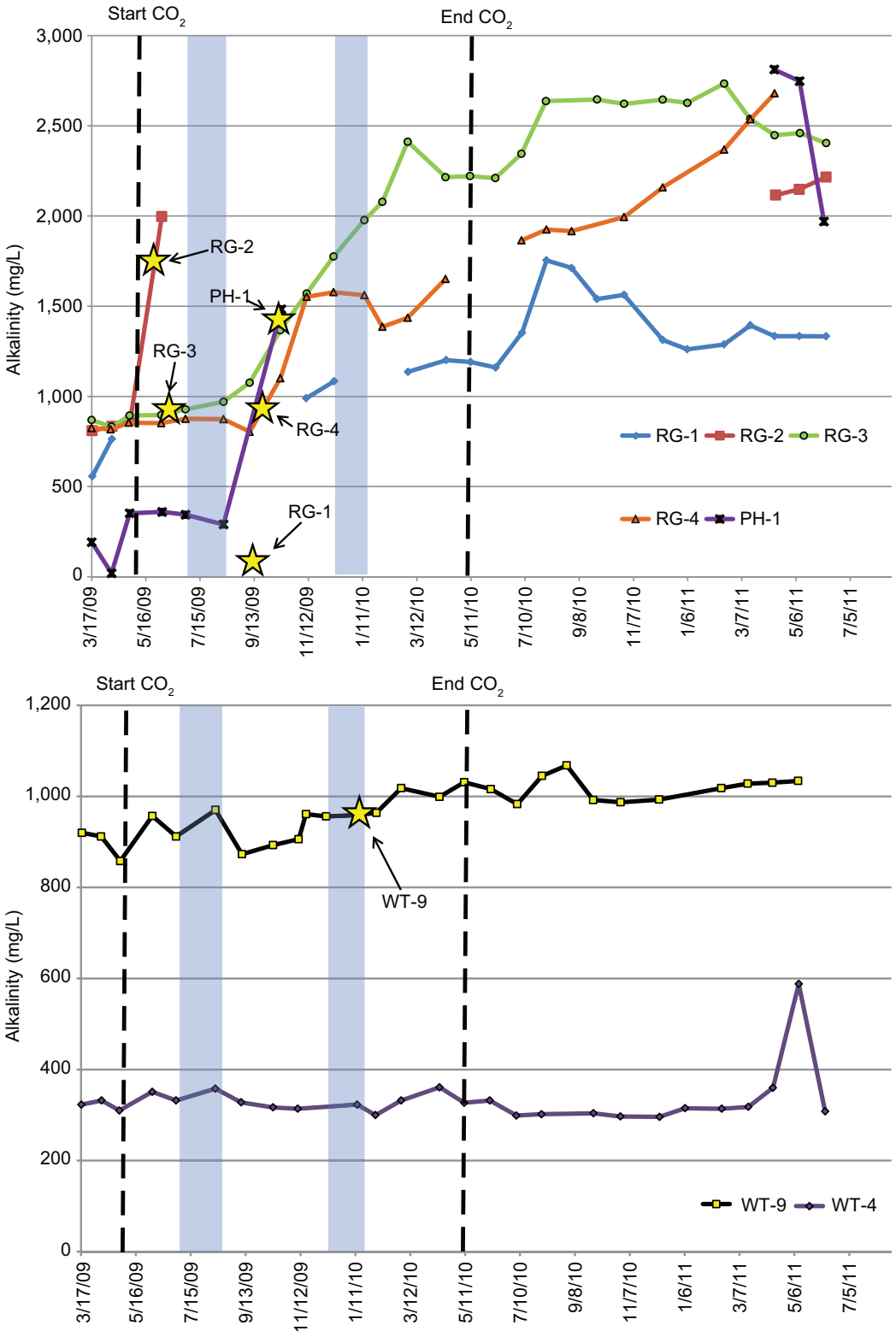

Figure 82 Top: Evolution of alkalinity for wells having large increases in CO_2 during breakthrough (RG-1, RG-2, RG-3, RG-4, and PH-1); (b) Evolution of alkalinity for wells having subtle (WT-9) or no (WT-4) increases in CO_2 levels as determined by infrared gas analyzer. Star symbols represent CO_2 breakthrough dates. Black vertical dashed lines designate start and end of CO_2 injection at RG-5. Vertical blue shaded areas designate approximate periods of CO_2 injection shut-in.

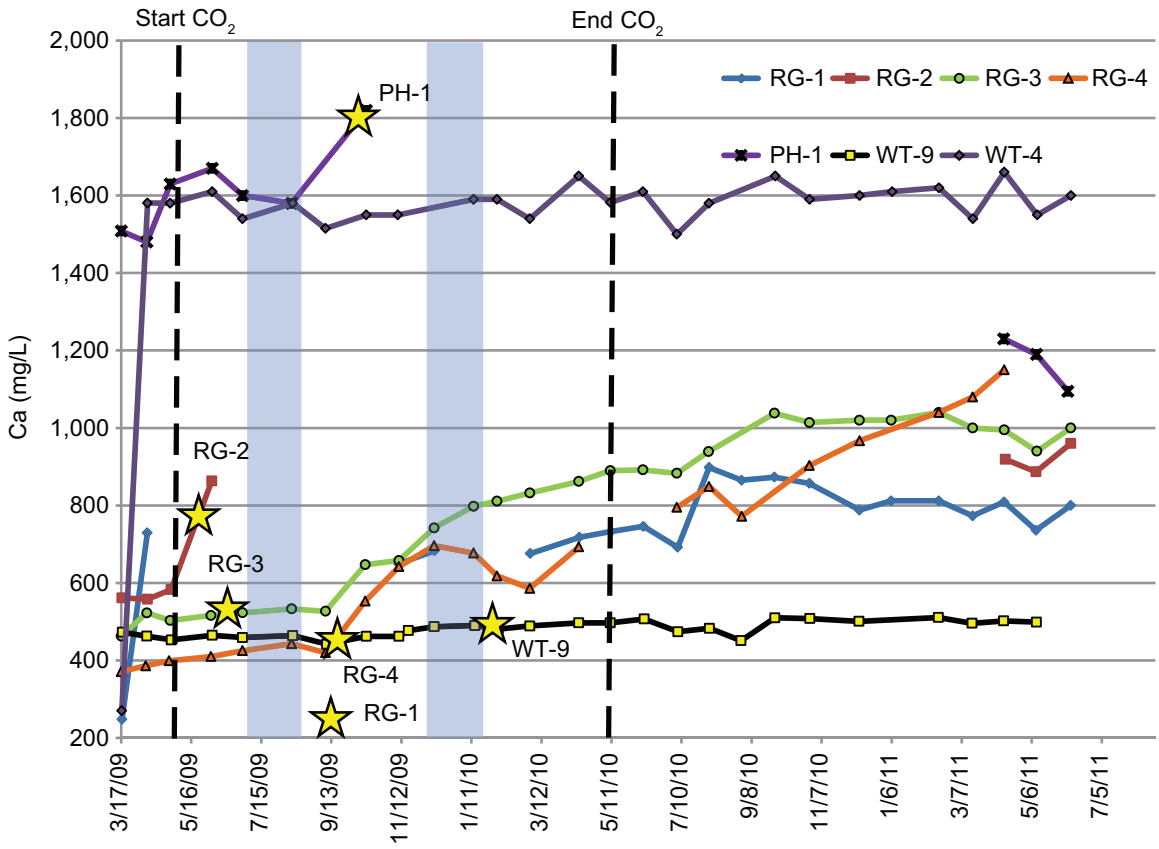

Figure 83 Evolution of Ca^{2+} before, during, and after CO_2 injection. Star symbols represent CO_2 breakthrough dates. Black vertical dashed lines designate start and end of CO_2 injection at RG-5. Vertical blue bars designate approximate periods of CO_2 injection shut-in.

The post-CO_2 concentrations of Ca^{2+} remain elevated for wells influenced by CO_2; however, their evolution during this period is variable (Figure 83). Many wells influenced by CO_2 continued to show increasing Ca^{2+} for 3 to 5 months after CO_2 injection. After reaching maxima, Ca^{2+} concentrations in RG-1, RG-3, and WT-9 plateaued or showed modest declines. Although RG-2 contains a significant data gap that spans most of the injection period, measurements during the last several months of the post-CO_2 monitoring period and in November 2011 suggest that Ca^{2+} concentrations remain elevated. Remarkably, Ca^{2+} concentrations at RG-4 showed an overall increase and the November 2011 measurements (1,112 mg/L) confirm that the increase continues.

PH-1 showed dramatic increases in alkalinity in the post-CO_2 period as compared to values both pre-CO_2 and immediately after breakthrough (Figure 82). Although some of the alkalinity increase was attributed to the influence of CO_2, it was not clear that it was the sole cause. In contrast, when Ca^{2+} concentration is examined over the same period for PH-1, it shows a dramatic decrease from 1,820 mg/L immediately after breakthrough to 1,100 to 1,200 mg/L in the post-CO_2 period (Figure 83). This decrease does not indicate a CO_2 influence, but rather suggests that dilute water with lower Ca^{2+} concentration started to influence PH-1 at some point after breakthrough and before collection of the final four samples in the post-CO_2 period. This is likely due to the production of injected water at PH-1 when RG-5 returned to water injection following the CO_2 injection period. The change in water composition greatly complicates the ability to interpret the influence of CO_2 on reservoir geochemistry at PH-1.

Mg^{2+} and Fe^{2+} Changes in solution concentration of Mg^{2+} and Fe^{2+} were also examined as they could indicate dissolution of dolomite, ankerite, and/or chlorite. Again, because of variable mixing with dilute waters from WT-3, pre-CO_2 concentrations of Mg^{2+} were higher in PH-1 and WT-4 than in the RG wells and WT-9

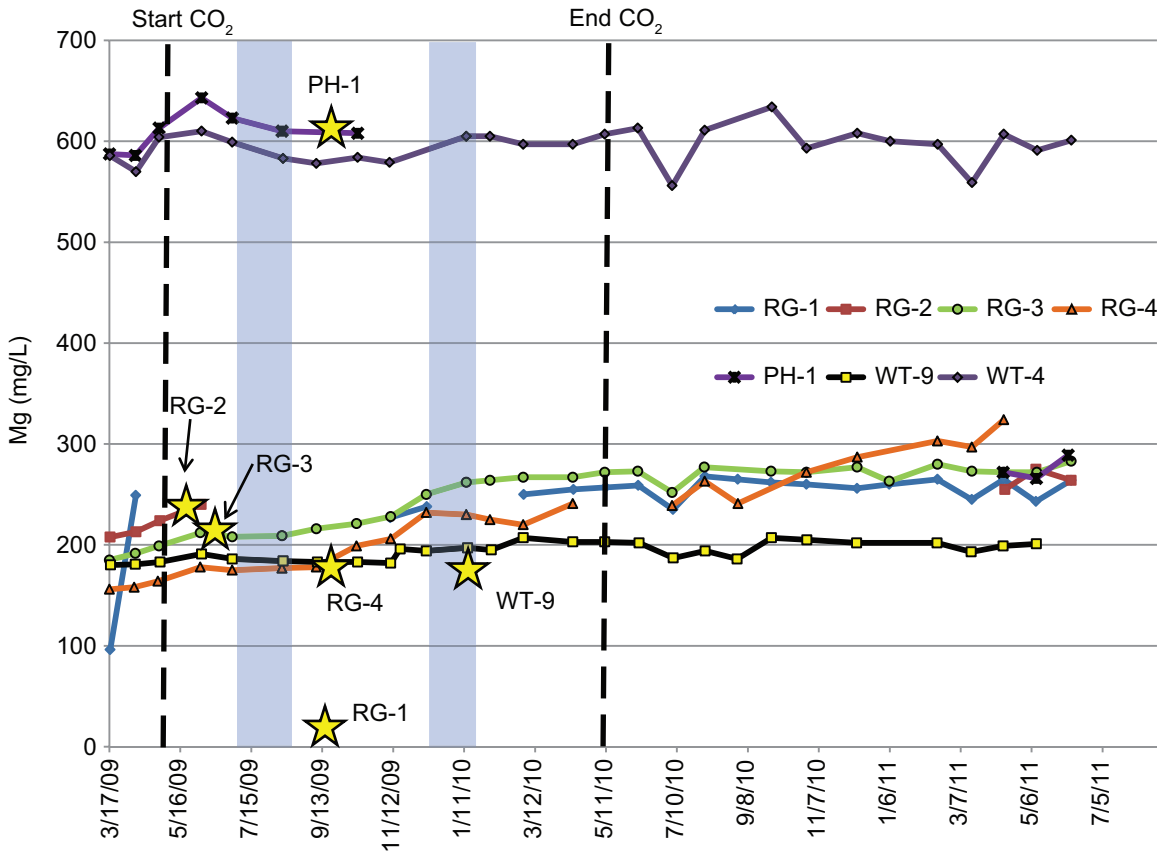

Figure 84 Evolution of Mg^{2+} before, during, and after CO_2 injection. Star symbols represent CO_2 breakthrough dates. Black vertical dashed lines designate start and end of CO_2 injection at RG-5. Vertical blue bars designate approximate periods of CO_2 injection shut-in.

(Figure 84). Increases in Mg^{2+} concentration on the order of 20 to 100 mg/L were observed after breakthrough at RG-2, RG-3, and RG-4 (Appendix 8). Increased Mg^{2+} at RG-3 occurred approximately 3 months after CO_2 breakthrough and was later than that observed for increased Ca^{2+} at RG-3. The increase in Mg^{2+} at RG-4, in contrast, occurred approximately 1 month after breakthrough similar to that for Ca^{2+}. A possible increase also occurred at RG-1, although the highly variable pre-CO_2 measurements precluded defining an accurate reference baseline. Increases at WT-9 were subtle and on the order of 10 to 25 mg/L. The elevated Mg^{2+} concentrations at these wells were maintained in the post-CO_2 period. The dramatic drop in Mg^{2+} concentration at PH-1 is attributed to mixing of dilute water as previously described for Ca^{2+}. No change in Mg^{2+} concentration was observed at WT-4.

Unlike differences in Ca^{2+} and Mg^{2+}, differences in pre-CO_2 values for Fe^{2+} were not observed for PH-1 and WT-4 versus the RG wells and WT-9 (Figure 85). With the exception of PH-1, pre- CO_2 Fe^{2+} concentrations were on the order of 0.4 to less than 0.002 mg/L, the latter representing a method detection limit (<MDL, Appendix 8). The low values and lack of a difference in Fe^{2+} concentration among the wells prior to CO_2 injection likely reflects the typically low solubility of Fe^{2+} in most natural solutions (Hem, 1992). The notable exception to the concentration pattern was in PH-1 where Fe^{2+} values were considerably higher and more variable before, during, and after CO_2 injection. The reason for the significant difference is unknown, but may be related to the shut-in period of the well prior to the start of pilot activities. All of the RG wells showed increased Fe^{2+} after CO_2 breakthrough, but the timing relative to breakthrough was variable. For example, at RG-3, which has a complete record of brine measurements during and after injection, Fe^{2+} increased approximately 4 months after CO_2 breakthrough. RG-2, in contrast, showed increased Fe^{2+} 12 days from CO_2 breakthrough. Neither WT-9 nor WT-4 showed changes in Fe^{2+} concentration. Concentrations

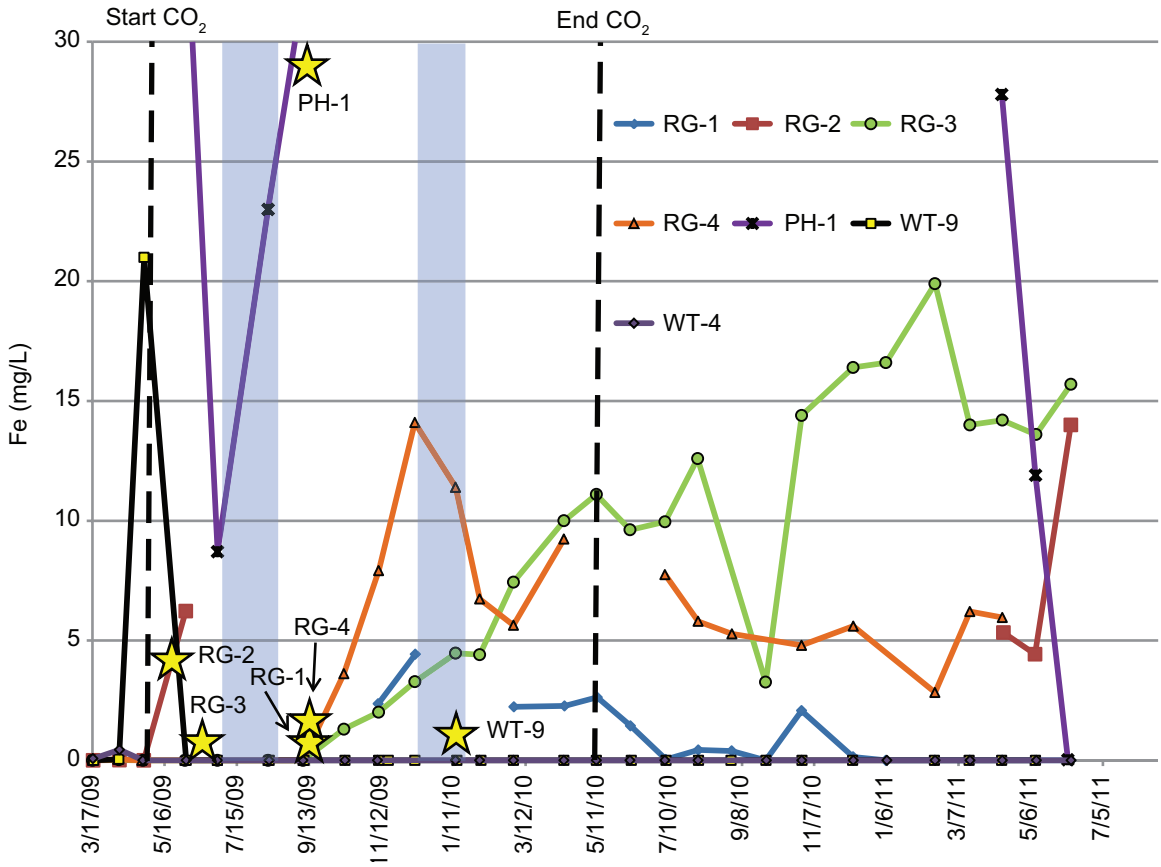

Figure 85 Evolution of Fe^{2+} before, during, and after CO_2 injection. Star symbols represent CO_2 breakthrough dates. Black vertical dashed lines designate start and end of CO_2 injection at RG-5. Vertical blue bars designate approximate periods of CO_2 injection shut-in.

for Fe^{2+} in the RG wells remained elevated in the post-CO_2 period, but RG-1 and RG-3 showed a trend of increasing values, whereas RG-2 and RG-4 showed a decreasing trend.

Silica (Si) Temporal changes in silica (shown as Si, but actually the sum of ionized and un-ionized silica species) and K^+ concentrations were examined to assess possible pH buffering by aluminosilicate minerals. Pre-CO_2 Si values among the wells were similar and ranged from 4.2 to 8.0 mg/L (Figure 86, Appendix 8). Again, however, PH-1 values were much more variable (2.4–11.2 mg/L) due to the production of RG-5 injection water and the Jackson sand native brine. RG-3 and RG-4 showed similar decreasing Si values during the early stages of CO_2 injection, but from September to October 2009 the values started trending upward and those overall upward trends were maintained through the end of CO_2 injection and into the post-CO_2 period (Figure 86). The shift to increased Si values for RG-3 and RG-4 developed approximately 4 and 2 months after CO_2 breakthrough, respectively. For RG-1, Si values that are unambiguously above background levels did not develop until the post-CO_2 period approximately 10 months after breakthrough. This result must be viewed within the context of the data gaps for RG-1. Data gaps for RG-2 preclude any meaningful analysis of Si increase relative to CO_2 breakthrough, but Si values clearly are elevated for the last measurements in the post-CO_2 period. Similarly, PH-1 did not show increased Si with the single measurement immediately following CO_2 breakthrough, but the post-CO_2 values were elevated. No discernible changes in Si concentration were detected at WT-9 or WT-4. As noted, RG-1, RG-3, and RG-4 showed trends of increasing Si values into the post-CO_2 period and, along with RG-2 and PH-1, Si values in these wells remain elevated. Relative to the June 2011 measurements, samples collected November 2011 show slightly increased Si values at RG-1, RG-2, RG-4, and PH-1.

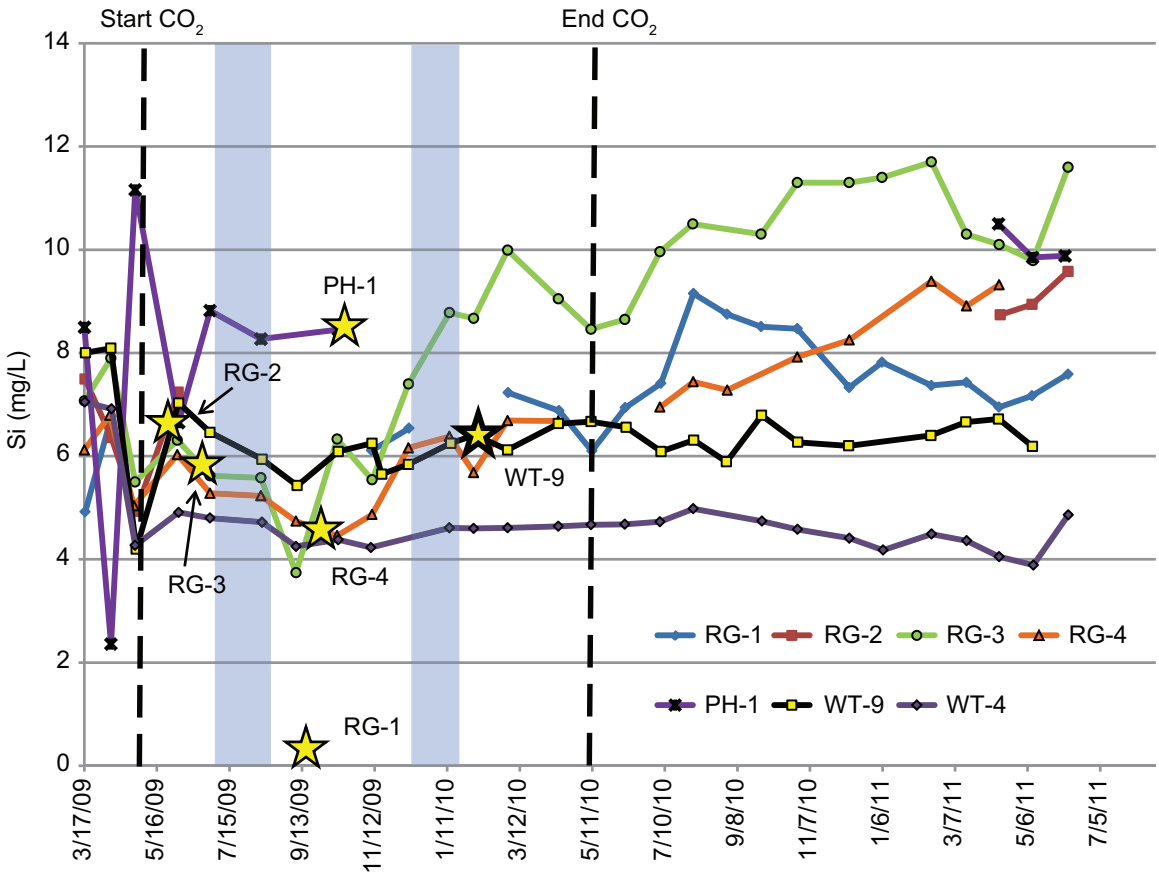

Figure 86 Evolution of silicon before, during, and after CO_2 injection. Star symbols represent CO_2 breakthrough dates. Black vertical dashed lines designate start and end of CO_2 injection at RG-5. Vertical blue bars designate approximate periods of CO_2 injection shut-in.

***K*⁺** Concentrations of K^+ before injection were variable but became more consistent during the early stages of injection (Figure 87). It appears that dilute injected WT-3 water influenced concentrations in the wells before CO_2 injection as K^+ values in PH-1 and WT-4 were greater than those for the RG wells and WT-9 (Appendix 8). Most of the wells maintained consistent K^+ concentrations throughout most of the injection period. It was not until the last 4 to 5 months of injection that increases occurred at RG-1, RG-3, and WT-9. For RG-1 and RG-3 the increases occurred approximately 7 to 8 months after CO_2 breakthrough. The increase in K^+ at RG-4 occurred in the post-CO_2 period at about 13 months after CO_2 breakthrough. At RG-2 the variable pre-CO_2 K^+ concentrations along with the large data gap during and after injection precluded a meaningful interpretation of K^+ changes. In the post-CO_2 period, K^+ values at RG-1, RG-3, and WT-9 decreased back to near baseline values within a month of the end of injection. Only RG-4 showed persistent elevated K^+ values in the post-CO_2 period. Concentrations of K^+ for PH-1 dropped dramatically in the post-CO_2 period, which was attributed to the influence of RG-5 injection water. At WT-4, the K^+ concentrations were variable over the course of the project, but showed no persistent trends. Part of the variation might be attributed to the analytical error (see section 6) associated with K^+ measurement. The analytical error might have been exacerbated by the bimodal distribution of K^+ concentrations wherein the GC column was optimized for measurement of lower K^+ concentrations thereby producing more error in samples with higher K^+ concentration. Data in Figure 87, where the lower K^+ concentration measurements show less variation, support this idea.

Isotopic Response of Jackson Brine and Associated Gas to CO_2 Injection

The source of the injected CO_2 at the Sugar Creek site varied with time. For the first three months about 92 % of the injected CO_2 was from an ethanol processing plant in Washington, IN. This CO_2 had a $\delta^{13}C$ value of

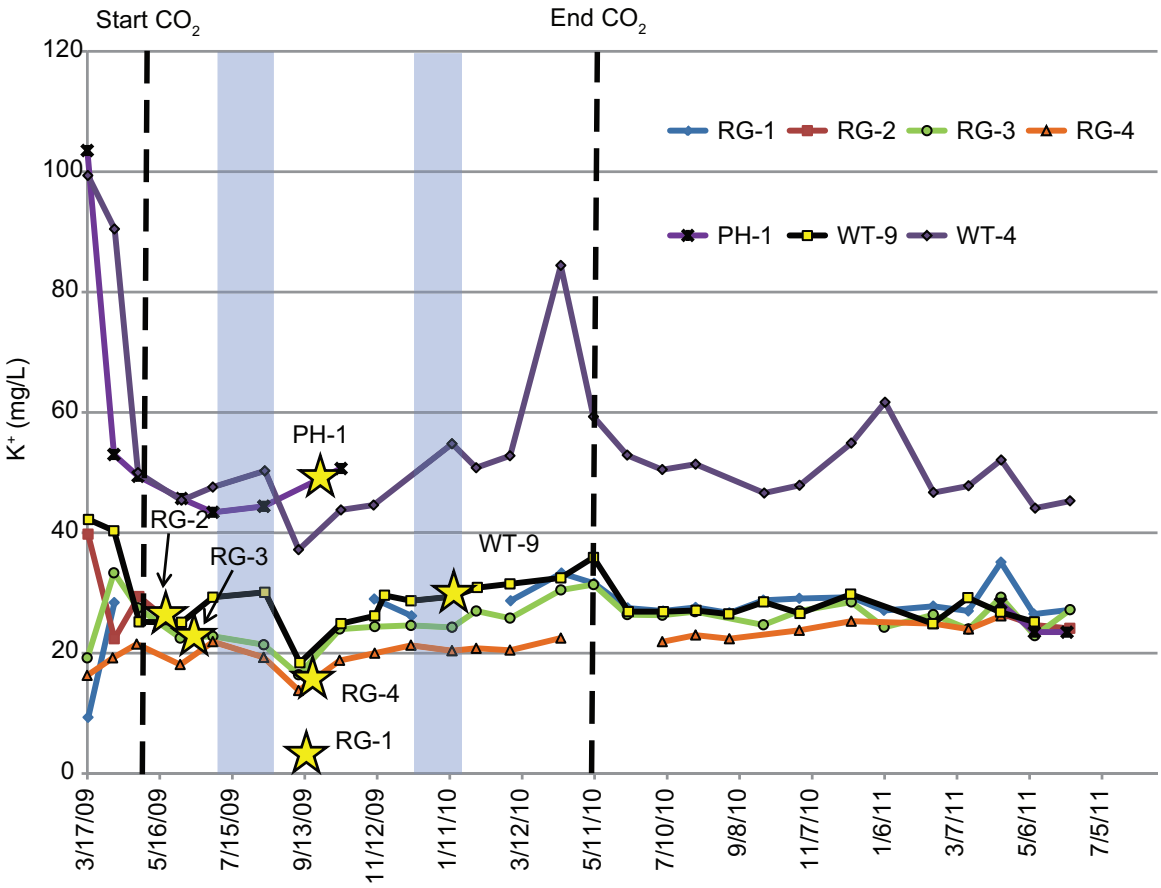

Figure 87 Evolution of K^+ before, during, and after CO_2 injection. Star symbols represent CO_2 breakthrough dates. Black vertical dashed lines designate start and end of CO_2 injection at RG-5. Vertical blue bars designate approximate periods of CO_2 injection shut-in.

–10.8‰ and a modern carbon-14 (^{14}C) activity of about 104 pMC (percent modern carbon), as measured in the summer of 2008. Because the ethanol plant could not provide a continuous supply of CO_2 to the Sugar Creek and Mumford Hills EOR sites, CO_2 was trucked in from another source. The other 8% of the injected CO_2 during the first three months originated from a refinery in Wood Dale, IL. The refinery CO_2 had a more negative $\delta^{13}C$ value equal to –34.4‰ and a ^{14}C activity of 1 pMC, as measured from a sample collected from a delivery truck at Mumford Hills, IN. As the pilot study progressed at Sugar Creek, a greater percentage of the injected CO_2 came from the refinery so that by the end of the project it constituted nearly 40% of the injected CO_2. The mixing of CO_2 sources turned out to have a significant impact on the isotopic composition measured on the gas and aqueous samples from the production wells.

Prior to CO_2 breakthrough, the concentration of CO_2 in the samples collected from production wells RG-1, RG-2, RG-3, and RG-4 contained relatively significant amounts of CO_2, ranging from approximately 1.8 to 7.5% by volume (Figure 88, Appendix 6). However, the concentrations of CO_2 in the other three production wells sampled (WT-4, WT-8, and PH-1) were relatively low, ranging from approximately 0.38 to 0.78% by volume (Appendix 6). These pre-CO_2 GC concentrations, measured on samples collected in the Cali-5 bond gas bags, tracked closely with CO_2 concentrations measured in the field with the IRGA (Figure 80).

Like the IRGA measurements, the GC measurements on the gas bag samples showed CO_2 breakthrough at different times soon after the start of injection on May 13, 2009. The first CO_2 breakthrough occurred within about one week at RG-2 where the concentration of CO_2 jumped from about 7.2% to 84%, followed by 91% and 98% over the next several days. Breakthrough was later detected at RG-3 (6/10/09) and eventually

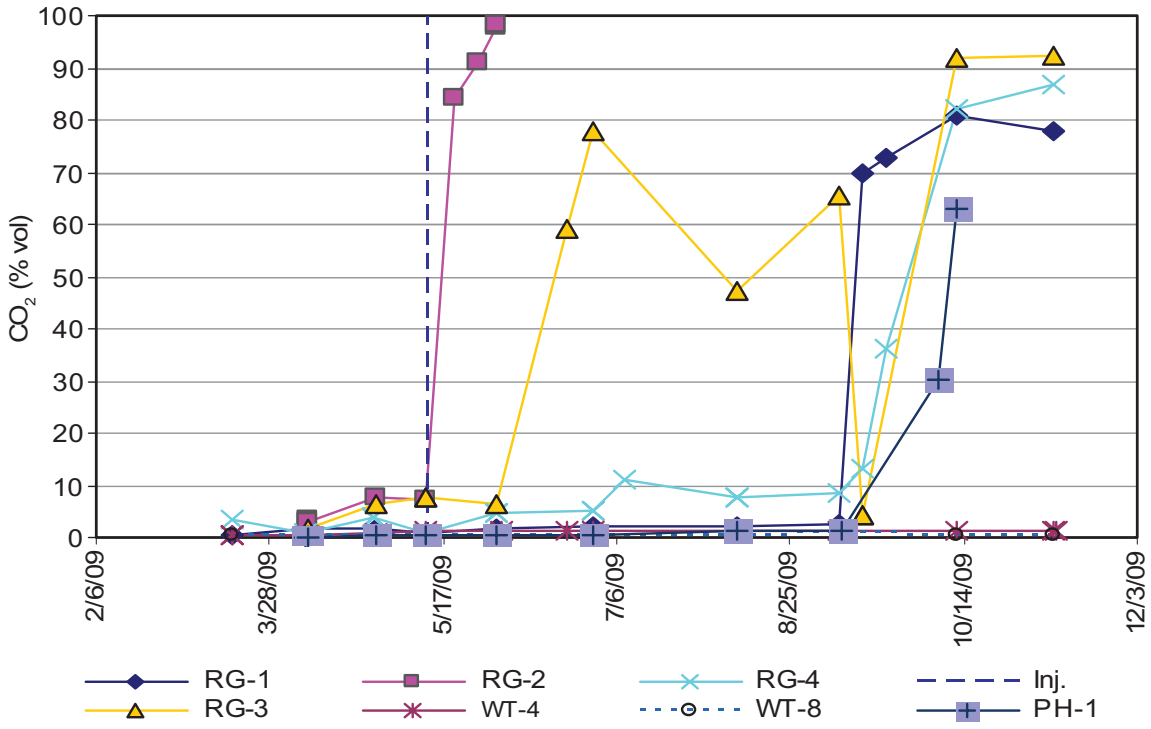

Figure 88 2009 CO_2 concentrations over time from gas chromatographic analyses of gas bag samples from various production wells at the Sugar Creek site. The vertical blue-dashed line indicates the startup of CO_2 injection.

at RG-4 (9/15/09), RG-1 (9/15/09), and PH-1 (10/7/09) (Figure 88; Table 18). The GC results did not show evidence of CO_2 breakthrough at WT-4 (Figure 89). However, WT-8 did begin to show small increases in CO_2 concentration (from a few tenths to 1.5 and 4%) approximately one year after CO_2 injection was completed.

Gas Measurements ($\delta^{13}C$-CO_2 and ^{14}C-CO_2) The $\delta^{13}C$ values of CO_2 sampled from the production wells before the start of CO_2 injection ranged from –29.3 to –10.8‰ with one isotopically heavy value of +1.3‰ (Figure 90). The $\delta^{13}C$-CO_2 of WT-4 for the pre-CO_2 period had the isotopically heaviest (most positive) values, ranging from –10.8 to –11.3‰ (with one anomalous value of +1.3‰). The $\delta^{13}C$-CO_2 for WT-8 ranged from –18.5 to –21.4‰. The RG and PH-1 wells had similar $\delta^{13}C$-CO_2 values, ranging from –22.2 to –29.3‰ prior to injection and showed a similar pattern of gradually becoming more negative from the initial sampling event in mid-March to the start of CO_2 injection. This shift to more negative isotopic values is probably because, during the preparation procedures for this pilot study, acid pretreatment was carried out at RG-1, RG-4, PH-1, and WT-8, as well as cased-hole geophysical logging at each borehole. During geophysical logging, the tubing was pulled from the production wells and make-up water was put into the wells from WT-3. The $\delta^{13}C$ of the CO_2 from WT-3 is –11.2‰. As WT-3 water filled the borehole, degassing probably occurred and CO_2 originating from the WT-3 water penetrated the annulus, resulting in a $\delta^{13}C$ composition which was isotopically more enriched in ^{13}C (more positive values). After the tubing was reinserted into the boreholes and the WT-3 water was pumped out, the annulus gas composition gradually re-equilibrated with the formation water, which was substantially more negative isotopically. Thus, both acid pre-treatment and geophysical well logging could have affected the $\delta^{13}C$ of the CO_2 in the annulus of the boreholes. This would explain the gradual decrease in $\delta^{13}C$ of the CO_2 observed at nearly all the production wells during the initial few sampling events. These results point out the importance of obtaining background data for each well prior to injection.

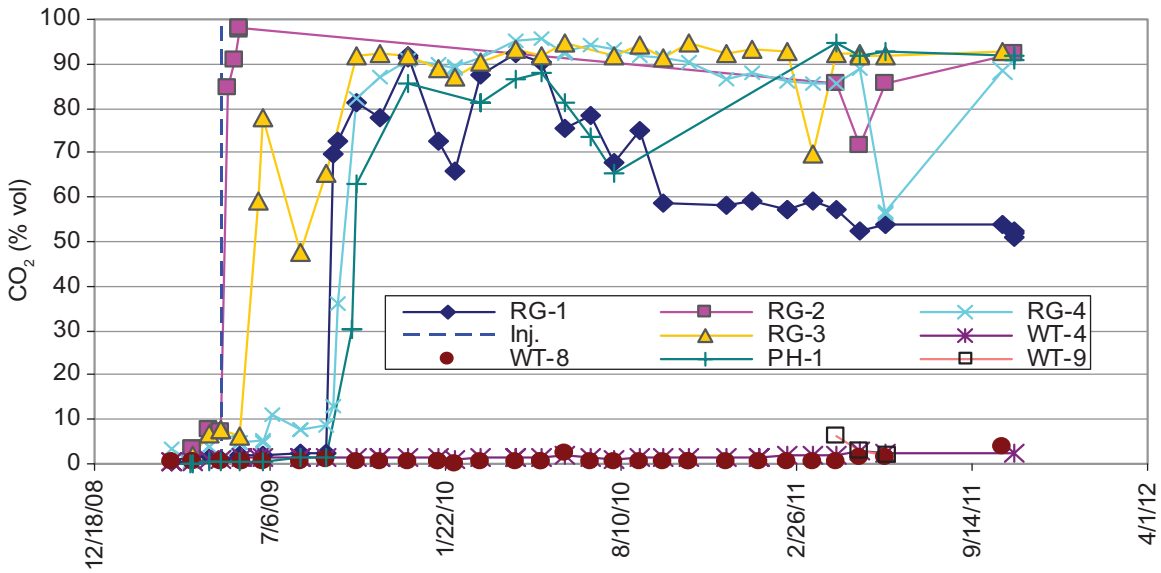

Figure 89 Project CO_2 concentrations over time from gas chromatographic analyses of gas bag samples from various production wells at the Sugar Creek Site. The vertical blue-dashed line indicates the startup of CO_2 injection.

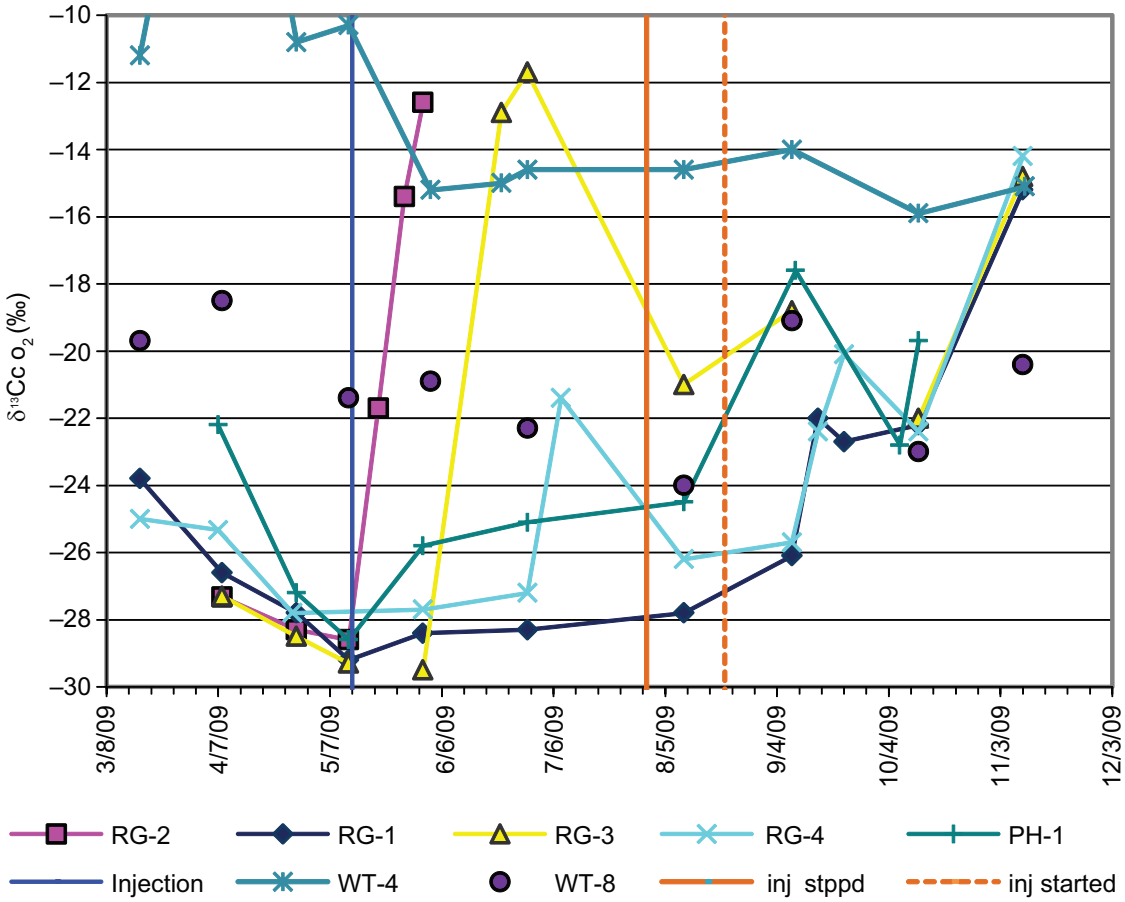

Figure 90 Carbon isotope ($\delta^{13}C$) composition of CO_2 of gas samples from production wells at Sugar Creek for 2009. The vertical blue line indicates the startup of CO_2 injection.

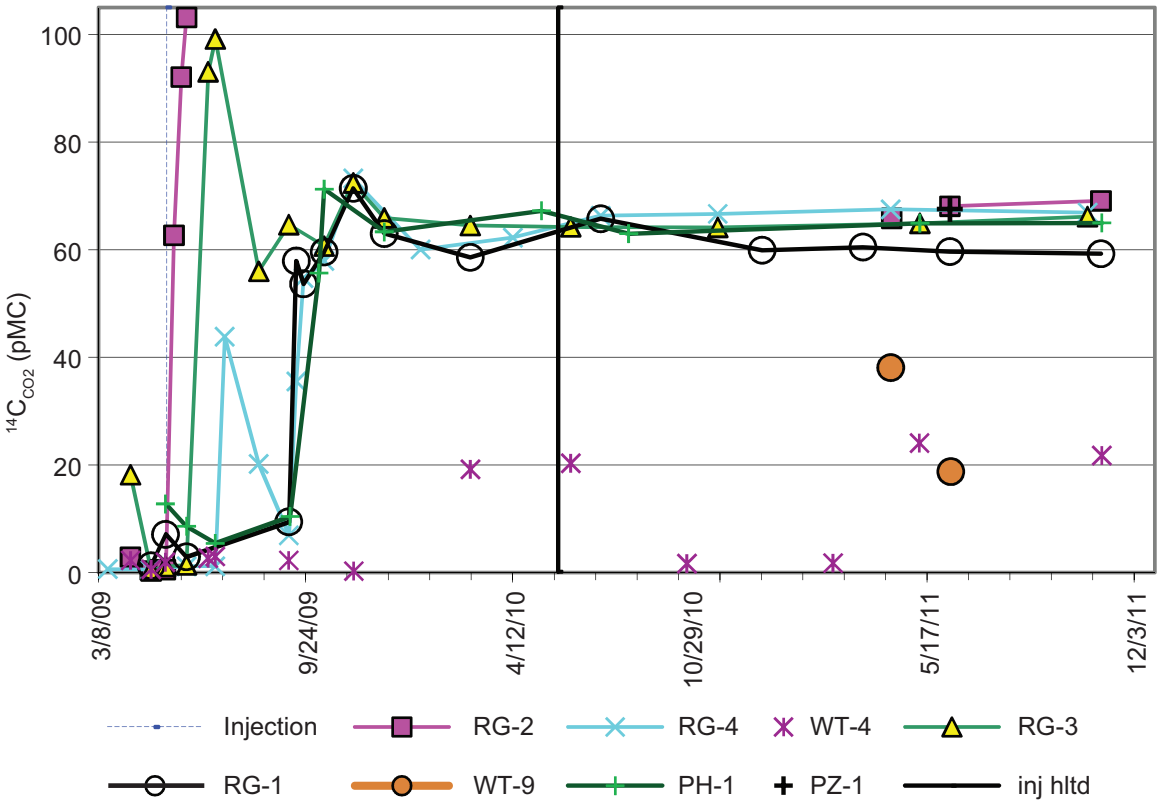

Figure 91 Carbon-14 concentration of CO_2 from various production wells at Sugar Creek Field. Top: concentration in first part of the pilot, from pre-CO_2 injection to November 2009; bottom, concentration over entire pilot, including post-CO_2 water injection period. Note the strong shift in ^{14}C activity of RG-2 and RG-3, which showed the earliest CO_2 breakthrough. Also, the accidental contamination of RG-4 with injection CO_2 is easily observed on the July 8, 2009 sampling event. The vertical blue-dashed line is the startup of CO_2 injection.

The $\delta^{13}C$-CO_2 values in each of the RG wells and PH-1 increased significantly as the concentration of CO_2 increased associated with breakthrough. The $\delta^{13}C$ increase was especially pronounced for the first two wells impacted, RG-2 and RG-3 (Figure 90).

Similarly, the ^{14}C activity increased dramatically as CO_2 concentrations increased in the production wells (Figure 91). Even when a small amount of injected CO_2 was accidently introduced into RG-4, the few percent change in CO_2 concentration produced a marked change in $\delta^{13}C$ and ^{14}C (7/8/09, Figures 9-11 and 91). The ^{14}C was probably the most definitive tracer for the injected CO_2 since the difference between the injected CO_2 and the background CO_2 was greater for ^{14}C compared to $\delta^{13}C$. The ^{14}C results even suggest the possibility of minor influence of injected CO_2 at WT-4, although very intermittent. Alternatively, this could be due to air contamination in the gas sample. These results indicate that both $\delta^{13}C$ and ^{14}C are good tracers and useful for confirming the provenance and movement of injected CO_2 in the subsurface so long as the isotopic composition of the injected CO_2 is distinct from inherent CO_2 in the reservoir.

After the initial increase in $\delta^{13}C$-CO_2 composition associated with CO_2 breakthrough, the $\delta^{13}C$-CO_2 values began to decrease and eventually settled to a consistent composition of approximately –19 to –20‰ (Figure 92). This shift to more negative $\delta^{13}C$ compositions with time can be explained by the blending of the injected CO_2 from the ethanol plant with additional CO_2 from the refinery. Based on the CO_2 delivery records, approximately 37% of the injected CO_2 came from a refinery plant while 63% of the CO_2 came from an ethanol plant. Using the measured isotopic compositions of each source of CO_2 (–10.8‰ and 104 pMC for ethanol and –34.4‰ and 1 pMC for the refinery), the resultant mixed CO_2 would have a $\delta^{13}C$ composition of approximately –19.5‰ and a ^{14}C activity of about 65.9 pMC. This is almost exactly what is observed

at the end of the injection cycle (Figures 91 and 92). Other possible sources of isotopically negative CO_2 produced from within the formation include oxidation of methane and other volatile hydrocarbons or microbial oxidation of dissolved organic carbon (DOC) through sulfate reduction. These other sources will be discussed elsewhere in this section.

The aforementioned increase in ^{14}C activity of CO_2, which coincided with increased CO_2 concentrations and the shift to more enriched $\delta^{13}C$-CO_2 values (Figures 89 and 90), was transient as ^{14}C activity was lower in the August and September 2009 samples (Figure 91). Much of this decrease was most likely the result of a line leak that halted CO_2 injection during much of July and August, 2009. Once injection resumed, ^{14}C activity increased to values on the order of 70 pMC and then leveled off to approximately 60 to 65 pMC that persisted into the post-CO_2 period (Figure 91). The persistent lower ^{14}C activity compared to the initial injected CO_2 agrees with the continuous addition of the CO_2 from the refinery plant. As mentioned above, it is possible that some of the old carbon could come from sources within the formation itself such as organic compounds (e.g., hydrocarbons or DOC) or inorganic sources such as carbonates. Increasing concentrations of Ca^{2+} suggest that some carbonate dissolution occurred. Carbonate dissolution should, however, enrich the $\delta^{13}C$ values of CO_2 toward more positive values rather than make them more negative. Despite evidence for continued carbonate dissolution in the form of increasing Ca^{2+} concentrations for many of the wells during and following CO_2 injection (Figure 83), the shift back to more negative $\delta^{13}C$ values indicates that carbonate dissolution exerted little influence on the $\delta^{13}C$ composition of CO_2 in the reservoir. On the contrary, the shift back to more negative $\delta^{13}C$-CO_2 values suggests that injected CO_2 from the refinery was the stronger influence. Both the refinery and carbonate dissolution likely contributed to the reduced ^{14}C activity.

If methane oxidation was the source of some of the negative CO_2, then we would expect a shift in the $\delta^{13}C$ of methane toward more positive values with time. While some variation was observed, by and large the $\delta^{13}C$-CH_4 values remained constant during and after CO_2 injection (Figure 93). Thus, it does not appear that the oxidation of methane contributed to the isotopically negative shift in CO_2. There were a few gas samples that showed more positive $\delta^{13}C$-CH_4 values but these were determined to be a result of diffusion of methane from the gas bags after collection because the δD did not show a corresponding shift to more positive values for those samples that had a more positive $\delta^{13}C$ composition compared to the majority (Figure 94). Acetate fermentation (conversion of acetate or fatty acids to methane) by methanogens also provides another potential mechanism for the production of CO_2 and CH_4; however, this mechanism is unlikely as none of the methane showed isotopic evidence of a microbial signature—that is, further depleted $\delta^{13}C$ and δD values (Figure 94).

In addition to methane, compound-specific isotopic analyses of ethane, propane, butane, and pentane (C_2–C_5) did not show any difference between the production wells that had significant impact from the injected CO_2 and those that did not (Figure 95). The lack of difference indicates that oxidation of volatile hydrocarbons besides methane does not appear to have contributed to the negative carbon input and low ^{14}C activity observed with time in the CO_2 reservoir (Figure 95).

Aqueous Measurements ($\delta^{34}S$-SO_4, $\delta^{18}O$-SO_4, $\delta^{18}O$-H_2O, $\delta^{13}C$-DIC, ^{14}C-DIC) Sulfur and oxygen isotopes were measured on sulfate dissolved in the Jackson brine ($\delta^{34}S$-SO_4, $\delta^{18}O$-SO_4) to help evaluate whether sulfate reduction could have contributed to the negative $\delta^{13}C$ shift and decrease in ^{14}C of the DIC pool. The sulfate reduction reaction can be shown as follows (Lovley and Phillips, 1988):

$$CH_3COO^- + SO_4^{2-} + H^+ \rightarrow HS^- + HCO_3^- + CO_2 + H_2O \quad (12)$$

The isotopic results show similar $\delta^{34}S$ values between wells that had pronounced CO_2 breakthrough (RG-1–RG-4, PH-1) and WT-4, which did not show CO_2 gas phase breakthrough (Figure 96, Table 21). Even though the $\delta^{34}S$ measurements were conducted over a short time interval (April 12–13, 2011) and therefore represent a geochemical 'snapshot', the similarity among the wells regardless of CO_2 influence suggests that sulfate reduction was not an important influence on the $\delta^{13}C$ or ^{14}C composition of CO_2.

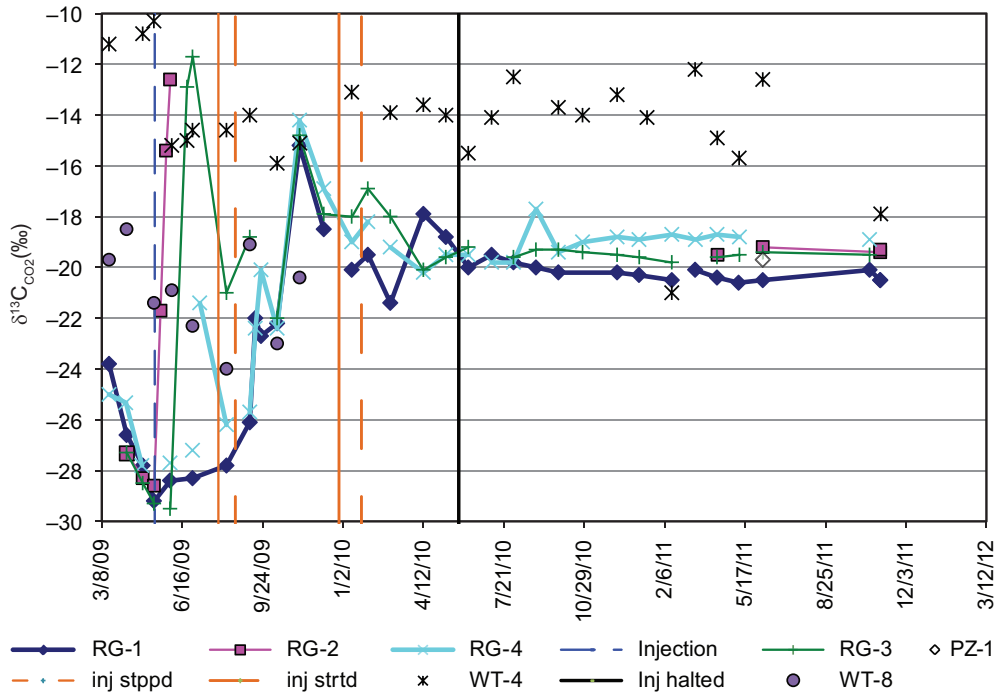

Figure 92 Complete carbon isotope composition ($\delta^{13}C$) of CO_2 of gas samples from production wells at Sugar Creek Field up to December 9, 2011. The vertical blue dashed line is the startup of CO_2 injection, and orange vertical lines indicate beginning and end of major interruptions in CO_2 injection in June and July 2009 and December 2009 through early 2010.

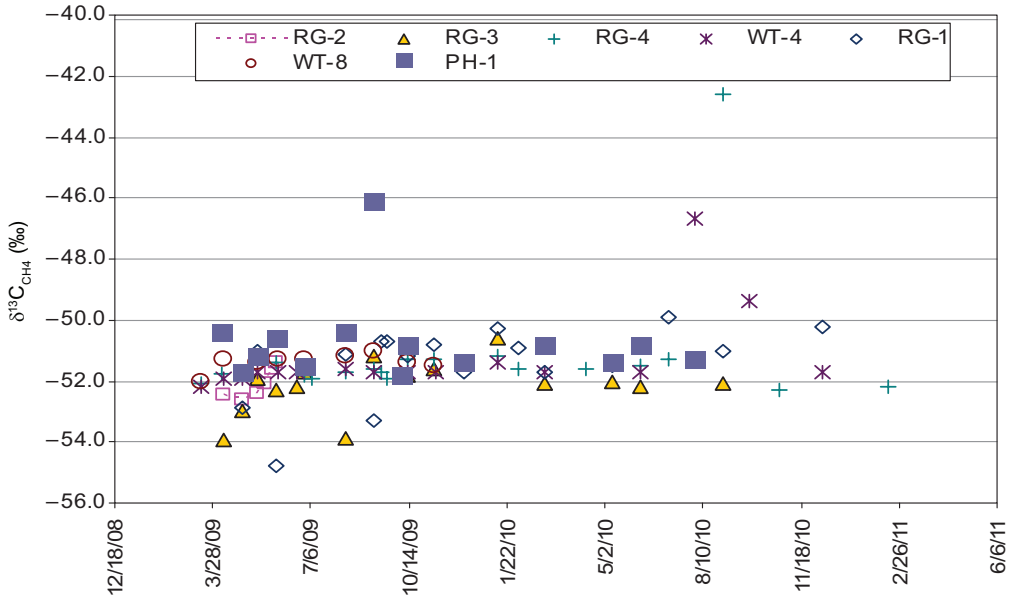

Figure 93 Carbon isotopic composition ($\delta^{13}C$) of methane from production wells at Sugar Creek Field. Note the steady isotopic composition after the initial degassing effects for most of the wells.

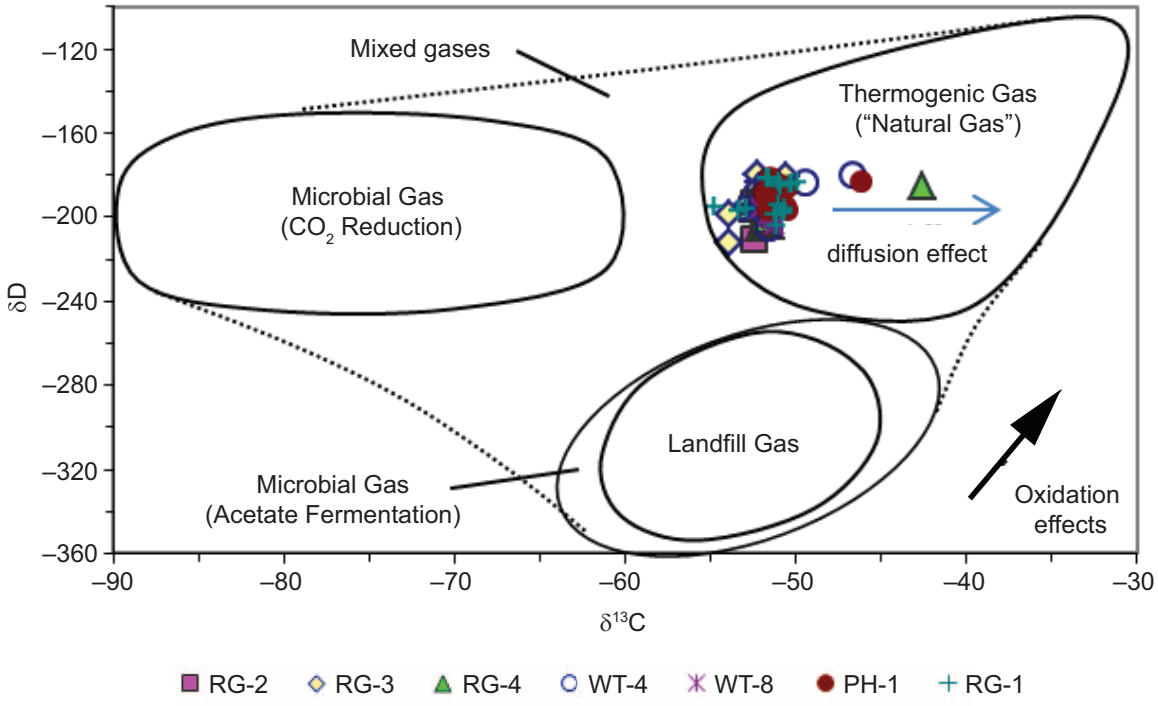

Figure 94 Isotopic composition ($\delta^{13}C$ and δD) of methane samples from production wells at Sugar Creek Field.

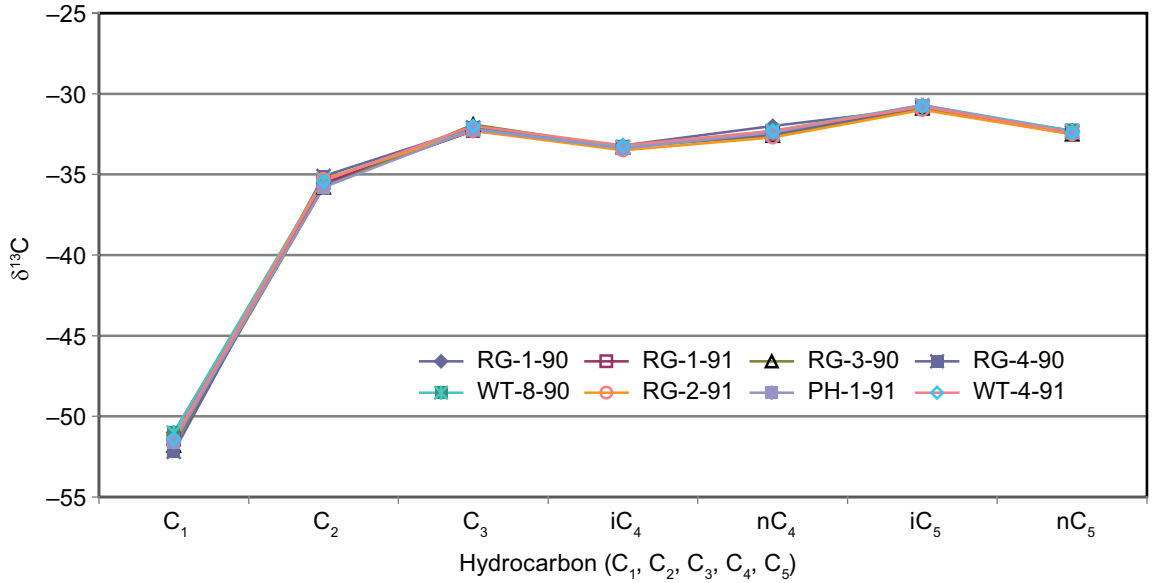

Figure 95 Carbon isotopic composition of hydrocarbons from Sugar Creek production wells.

Table 21 Isotopic composition of dissolved sulfate and sulfide from production wells at Sugar Creek.

Sample ID	$\delta^{34}S_{sulfide}$	$\delta^{34}S_{SO4}$	$\delta^{18}O_{SO4}$
SC-RG1-85 4/12/11		30.4	10.8
SC-RG2-85 4/13/11		30.0	16.7
SC-RG3-85 4/12/11		28.2	11.3
SC-RG4-85 4/12/11		27.6	12.3
SC-PH1-85 4/13/11		28.0	18.6
SC-TB1-85 4/13/11		28.2	10.2
SC-WT4-85 4/12/11		29.7	15.8
SC-WT9-85 4/12/11	16.3	22.4	7.5

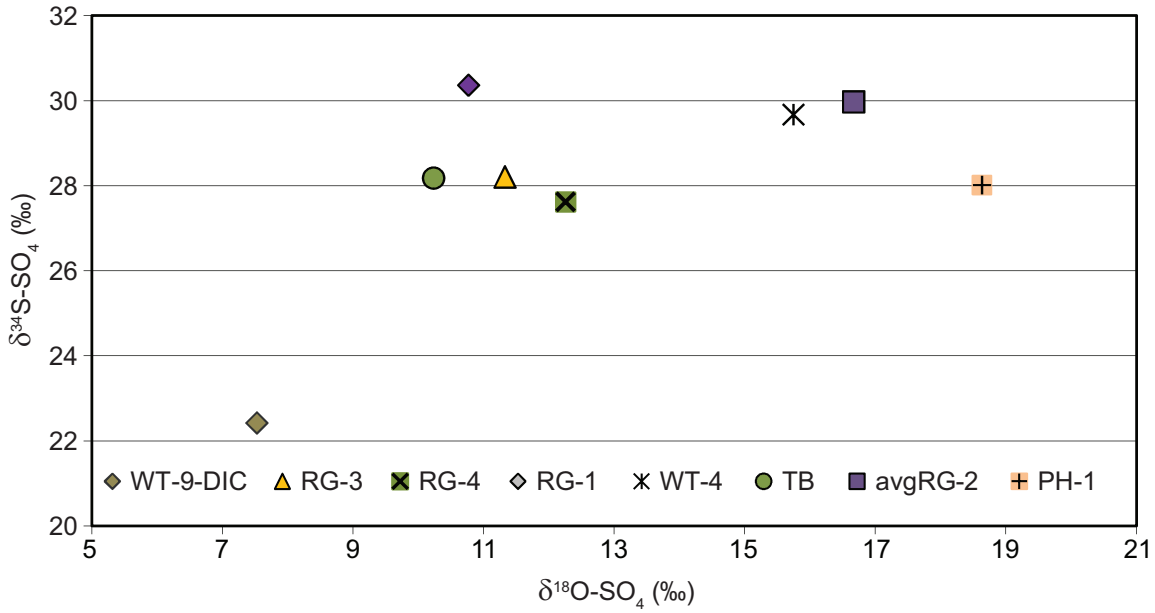

Figure 96 Sulfur and oxygen isotopic composition of dissolved sulfate from brine samples collected at Sugar Creek Field.

The isotopic composition ($\delta^{18}O$-H_2O and δD-H_2O) of the water samples varied, not surprisingly, between the shallow Pennsylvanian groundwater and Jackson brine, but also within the Jackson brines even before CO_2 injection. The pre-CO_2 water data for $\delta^{18}O$ and δD fall into three groups (Figure 97) with the division of wells mimicking the division documented with salinity (Figure 40). The most negative isotopic group was made up of the residential wells, monitoring wells, and water supply well, WT-3. The $\delta^{18}O$ for this group ranged from –6.7 to –5.8‰; WT-3 had the most negative values, –6.4 to –6.7‰. The next group was made up of most of the production wells including the RG wells, JR-1, WT-9, and the post-CO_2 samples from PH-1 samples, all of which had $\delta^{18}O$ values ranging from about –5.5 to –4‰. The third group of samples, from WT-4 and early samples from PH-1, showed the most isotopically heavy values, ranging from –3.2 to –2.4‰. The RG, JR-1, WT-9, WT-4, and PH-1 wells are all screened in the same Jackson sandstone formation, most within 500 m (1640 ft) of one another, and would be expected to have a similar $\delta^{18}O$ and δD composition. Similar to the postulated mixing mechanism proposed for the salinity distribution, the more negative isotopic composition exhibited by the middle group (RG wells, JR-1, and WT-9) relative to the third group (WT-4 and several PH-1 samples) is probably due to mixing between the most negative water injected into this formation from well WT-3 with the more positive isotopic brines of the Jackson Sandstone formation water represented by WT-4 and the initial samples from the PH-1 well.

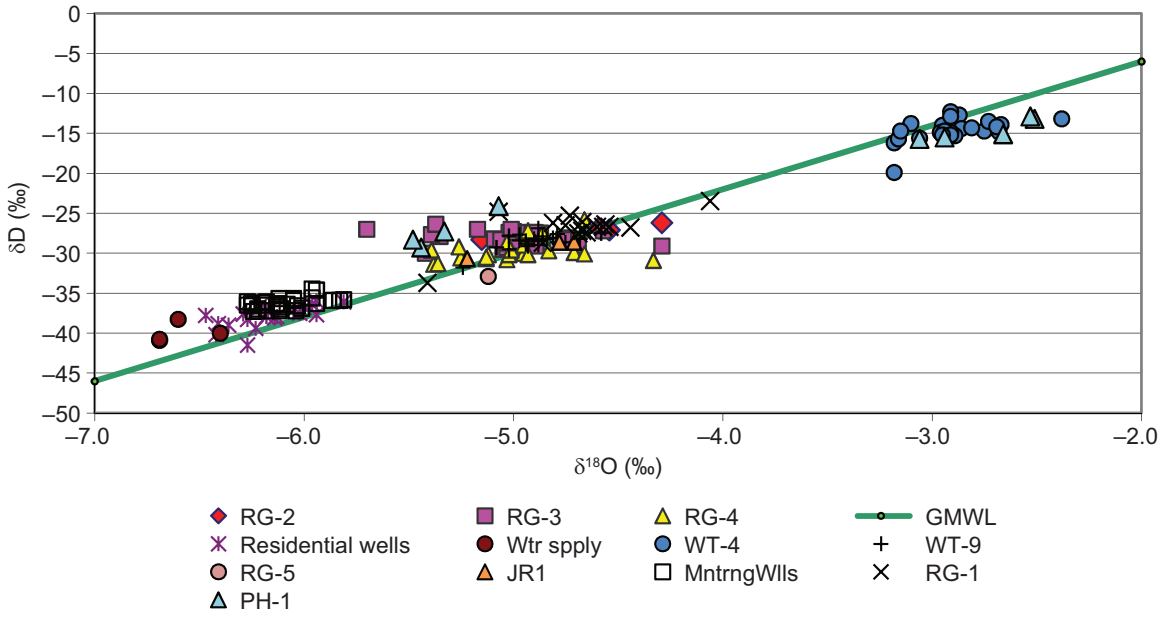

Figure 97 Isotopic composition of water and brine samples from the Sugar Creek site.

When examined in a time series, the $\delta^{18}O$-H_2O measurements define three groups of wells for the reasons discussed above and the grouping largely persisted during and after CO_2 injection. The production wells all showed approximately a 0.5‰ shift in $\delta^{18}O$ to more negative values on June 2, 2009, immediately after the start of CO_2 injection on May 13, 2009 (Figure 98). The reason for the shift is not known but it was consistent among all the production wells, including WT-4, which never showed CO_2 breakthrough or other geochemical evidence of injected CO_2 impact. The 0.5‰ shift may have been due to the injected CO_2 pushing make-up water, which included water from WT-3 having more negative $\delta^{18}O$ values, to the surrounding production wells.

After the decrease in $\delta^{18}O$-H_2O right after the start of CO_2 injection, most of the production wells did not show additional decreases in $\delta^{18}O$ during or after CO_2 injection (Figure 98). The exceptions to this pattern included PH-1 and RG-3. PH-1 showed a dramatic decrease in the $\delta^{18}O$-H_2O values in the post-CO_2 period, most of which is the result of dilute injection waters from RG-5 migrating into the Jackson reservoir surrounding PH-1 (Figure 98). This change agrees with similar changes in bulk chemistry documented, for example, with chloride which dropped from approximately 33,500 mg/L to 13,570 mg/L. Unfortunately, for PH-1 we do not have a continuous sequence of samples, so we cannot evaluate the full impact on the $\delta^{18}O$ at this well during and after CO_2 injection. During the post-CO_2 water injection period, an excursion to more depleted $\delta^{18}O$-H_2O values was observed at RG-3 from approximately October 2010 through April 2011, followed by an increase. Possible explanations for this excursion could be a greater degree of mixing with injection water, which had a more negative $\delta^{18}O$ value, or perhaps impacts from carbonate dissolution or, more likely, isotopic exchange between the injected CO_2 and the water sampled at RG-3. An examination of other parameters that should reflect an increase in make-up water, such as a decrease in chloride and hydrogen isotopes, was not observed and so did not support greater amounts of injection water at RG-3.

As far as carbonate dissolution impact goes, we can estimate the degree of carbonate dissolution from the total increase in calcium concentration in the system during the pilot study and thus evaluate the amount of oxygen available from the carbonates that could impact the brine $\delta^{18}O$ value. Using data from RG-3, Figure 83 shows that the calcium increased approximately 500 mg/L. This equates to the dissolution of approximately 0.0125 moles/L calcite, which would result in about 0.0375 moles/L oxygen, or 0.6 g/L of oxygen. If all of the CO_2 released from the carbonate dissolution were saturated in the water, 0.6 g would only represent 0.067% of the oxygen of the water and thus would not cause any significant changes in the $\delta^{18}O$ of the brine reservoir. Thus, the drop in $\delta^{18}O$ observed for RG-3 is most likely due to isotopic exchange between the injected CO_2 and brine water at RG-3.

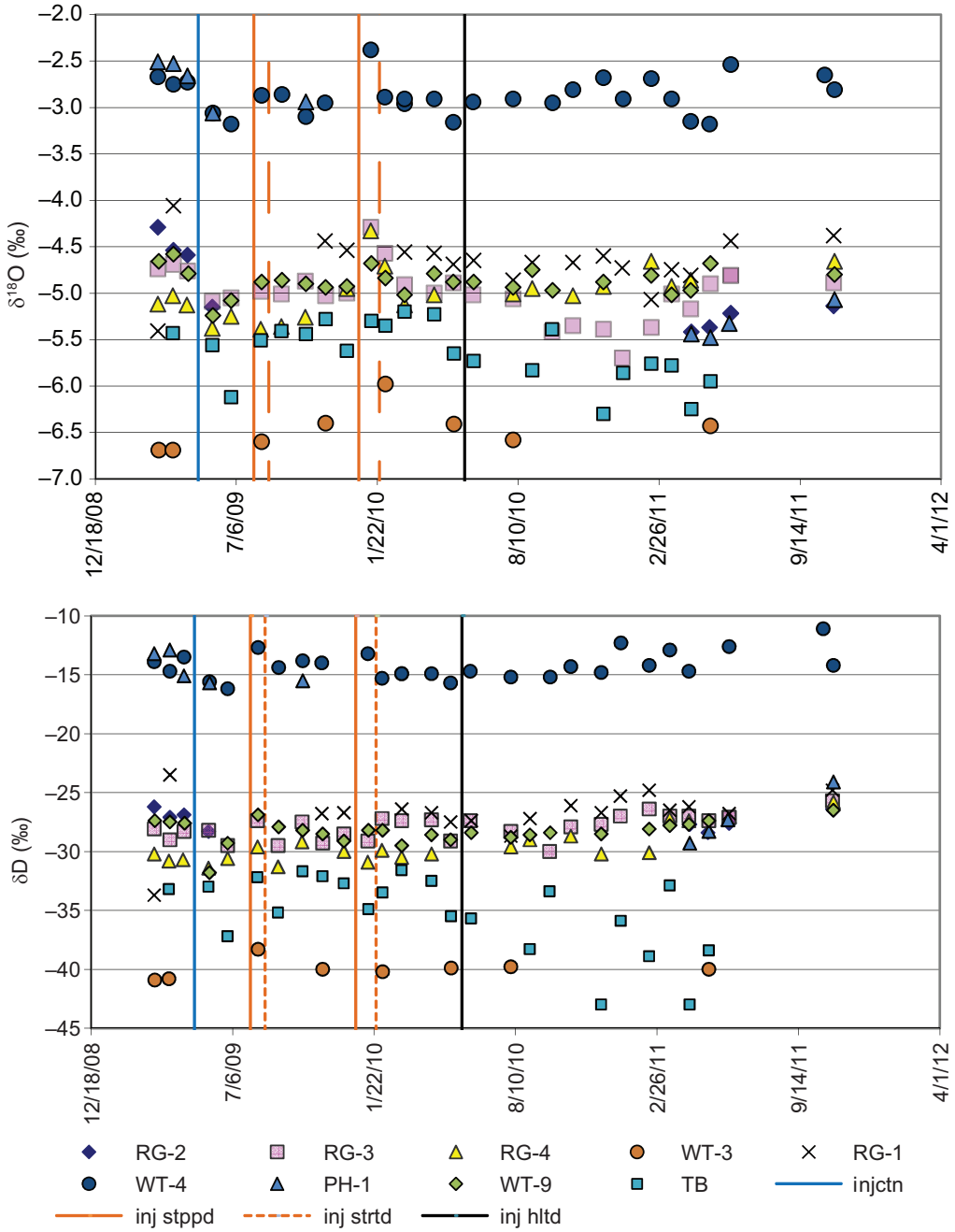

Figure 98 Top: $\delta^{18}O$ of brine samples vs. time from the Sugar Creek site; bottom: δD of brine samples vs. time.

Equilibrium oxygen isotopic fractionation between CO_2 and H_2O causes the latter to become more enriched in ^{16}O resulting in a much more negative $\delta^{18}O$ value by approximately 41‰ for H_2O (Freidman and O'Neil, 1977). Thus the more negative shift in $\delta^{18}O$ values observed for RG-3 was probably due to some equilibrium exchange between the brine and the injected CO_2, which ISGS researchers previously measured as 23.6‰ for the CO_2 from the ethanol plant and 0.9‰ for the CO_2 from the refinery plant. However, besides the initial 0.5‰ drop in $\delta^{18}O$ at the beginning of the injection experiment, the other production wells that showed significant CO_2 breakthrough, RG-1 and RG-4, did not show an additional negative shift in $\delta^{18}O$ values. Interestingly, of the production wells that showed CO_2 gas phase breakthrough, the greatest impact from the injected CO_2 on chemical parameters such as alkalinity, calcium, and silica (Figures 82, 83, and 86) was observed at RG-3 which showed the most impact from isotopic exchange between CO_2 and H_2O.

It was also observed that the brine samples from the tank battery (TB) gradually became more negative during the second half of the pilot study which could be evidence that there was oxygen isotopic exchange between the CO_2 and the formation brine water (Figure 98). However, this effect was most likely caused by an increase in volume of make-up water from WT-3 added to TB, because the hydrogen isotopic composition also showed a negative shift for the TB samples (Figure 98). Thus any negative oxygen isotopic shift in the TB samples due to equilibrium exchange reactions would have been overshadowed by the addition of make-up water from WT-3.

The RG wells along with PH-1 and WT-9 all showed increases in δ^{13}C-DIC at different times during CO_2 injection and these elevated values persisted into the post-CO_2 period (Figure 99). The increases were especially prominent for wells that had strong CO_2 breakthrough (e.g., RG-2–RG-4). The shift most certainly reflected the impact of the isotopically heavier injected CO_2 as it dissolved into the Jackson brine and then underwent the previously discussed dissociation reactions. The δ^{13}C-DIC isotopic shift observed for RG-2 was large and approximately 13‰ compared to pre-CO_2 values. The isotopic increase at RG-2 occurred within 13 days of CO_2 breakthrough.

The initial positive shift in δ^{13}C-DIC at RG-3 and RG-4 (~3 to 4‰) was observed June 2, 2009, prior to when the gas phase actually showed up at the well screen (Figure 99, top graph). The ^{14}C-DIC data suggests that the initial increase in the δ^{13}C-DIC values at these two wells is probably not associated with the injected CO_2 because the ^{14}C activity did not shift significantly for either RG-3 or RG-4 during the June 2, 2009 sampling event (Figure 99, middle graph). Thus, this initial positive shift in δ^{13}C-DIC values for RG-3 and RG-4 may be due to contributions of DIC from the make-up water, WT-3, which had a more positive δ^{13}C-DIC value (Figure 99, bottom graph). As mentioned earlier, RG-5 was a water injection well prior to the CO_2 injection pilot study, and so the make-up water from WT-3 would have been used at RG-5. This is exemplified by the more positive δ^{13}C-DIC value measured for RG-5 prior to CO_2 injection (Figure 99, bottom graph). The water from RG-5 could have been pushed through the system subsequent to CO_2 injection causing an impact on the geochemistry, such as increased δ^{13}C-DIC values, at the production wells prior to CO_2 breakthrough. There was a very large positive shift in the δ^{13}C-DIC value (~10‰) for RG-3 on June 29, 2009 which correlated with a large jump in the ^{14}C activity of the DIC as well for RG-3 during this same sampling event. These jumps in isotopic composition on June 29 also agreed with the CO_2 breakthrough at this well.

There was also a significant ^{14}C activity shift for RG-4 during the June 29, 2009 sampling, which reflected the accidental contamination of RG-4 with the use of tank CO_2 instead of N_2 gas when measuring water depths for this well as described earlier (Figure 99, middle graph). A jump in ^{14}C activity was also observed for RG-4 during the pre-injection period (April 7, 2009, second sampling event of the pilot study) which can be explained by atmospheric contamination of the gas sample. This April 7 gas sample only showed 0.7% CO_2 compared to the other pre-injection gas samples for RG-4, which contained 3.6% CO_2.

Other production wells also showed significant variations in δ^{13}C-DIC values over the course of the project (Figure 99, bottom graph). PH-1 showed extreme fluctuations in δ^{13}C-DIC values, especially during the pre-CO_2 period. The first two samples yielded very positive δ^{13}C-DIC values, –1.4 and 4.0‰. Such positive values suggest input of very isotopically positive carbon into the system. PH-1 was treated with acid just prior to the start of the pilot study which would have dissolved carbonates (typically 0 ±4‰; Craig, 1953) in the vicinity of the well releasing isotopically positive carbon into the dissolved inorganic carbon reservoir. Besides the impact of acid treatment at PH-1, mixing of injection water with PH-1 brine may also have contributed to some of the variation of the δ^{13}C-DIC observed at PH-1.

The δ^{13}C-DIC also showed variations at WT-9, where pronounced CO_2 breakthrough did not occur. At WT-9 the δ^{13}C-DIC was observed to jump to more positive values by approximately 4 to nearly 7‰ on June 29, 2009, after which values decreased but still remained above pre-CO_2 values. The elevated δ^{13}C-DIC values persisted through the remainder of the injection and post-CO_2 injection periods. The increase in δ^{13}C-DIC correlates with the increase in alkalinity and DIC (Figure 82). Given the absence of a pronounced CO_2 breakthrough at WT-9, it is possible that the change in δ^{13}C-DIC was related to the influence of re-injected water from wells surrounding the pilot study area. As compared to the other sampled production wells, WT-9 is the farthest from RG-5, the injection well. Thus an alternative explanation is that WT-9 was

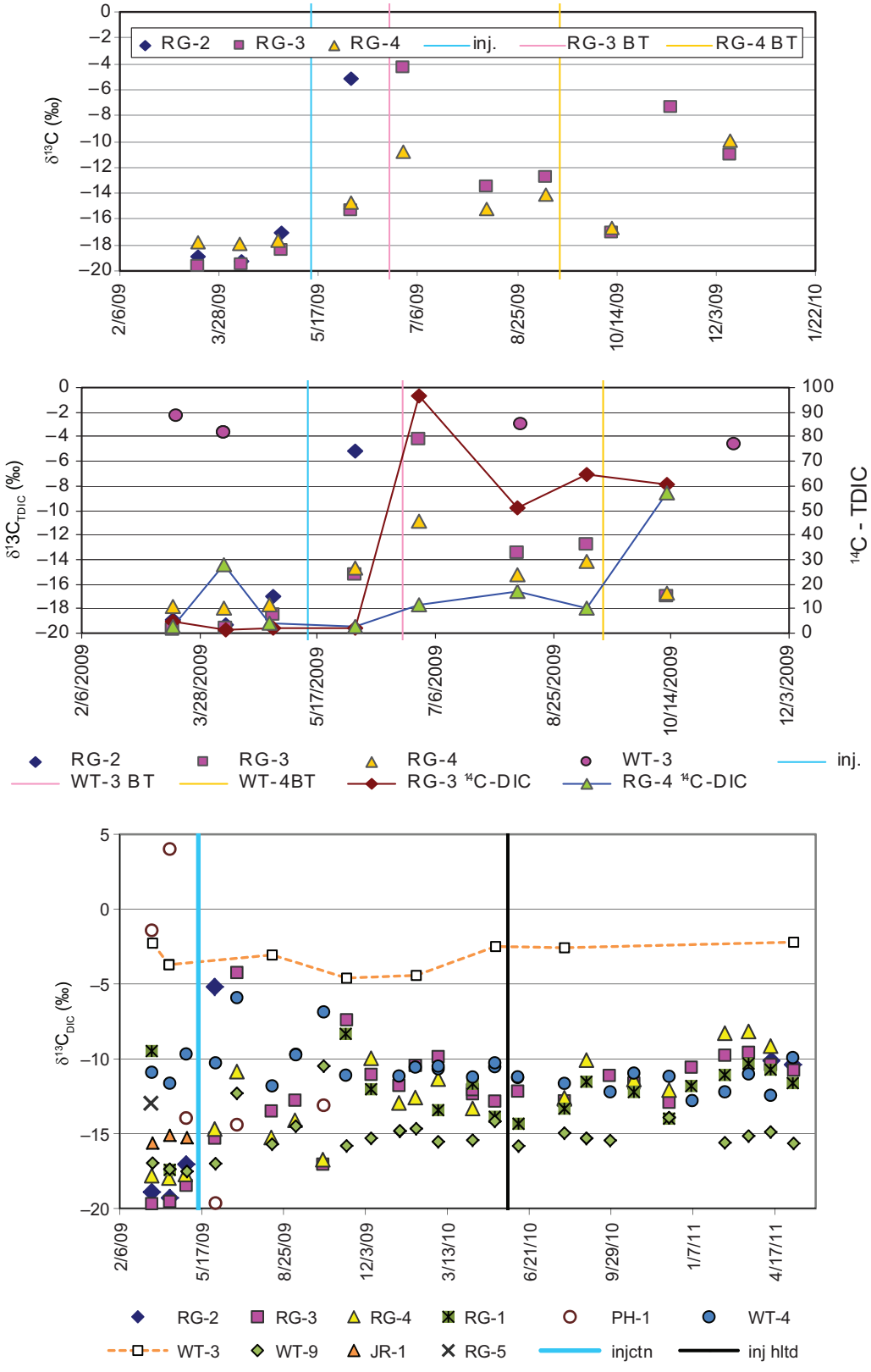

Figure 99 Top: $\delta^{13}C_{DIC}$ of brine samples that showed impact from injected CO_2. Middle: $\delta^{13}C_{DIC}$ and $^{14}C_{DIC}$ activity of brine samples that showed impact from injected CO_2. Bottom: $\delta^{13}C_{DIC}$ of brine samples for full period of pilot study at Sugar Creek. BT=breakthrough.

too far from RG-5 to have free-phase CO_2, but rapid dissolution of CO_2 into the Jackson brines caused changes in water composition, albeit more subtle changes compared to those at the other production wells.

As with the bulk chemistry data, the δ^{13}C-DIC data for WT-4 are mostly consistent and vary little during and after CO_2 injection. A couple of positive shifts on the order of 4 to 5‰ occurred in samples collected on June 29, 2009 and October 13, 2009 (Figure 9-20, bottom graph). The causal mechanism for the shifts is unknown, but after each increase the δ^{13}C-DIC values returned to baseline. Although the bulk chemistry data suggest that WT-4 was not affected by CO_2, it is possible that the δ^{13}C-DIC increases represent transient effects of injected CO_2. Alternatively, the increased δ^{13}C-DIC values could represent the influence of well treatments at the nearby PH-1 or WT-8. This latter alternative would accord with the transient character of the isotope increases.

Pennsylvanian Groundwater—Bulk and Isotopic Response to CO_2 Injection

Injection water supply well WT-3 was sampled three times during the CO_2 injection phase and five times post-CO_2 injection (Appendix 7). Changes in alkalinity, pH, DIC, and dissolved CO_2 are very good indicators of subtle geochemical changes associated with the presence of CO_2 within an aqueous system (e.g., Kharaka et al., 2006a, 2006b). During the life of this project there were no significant changes associated with these geochemical indicators at WT-3, which indicates that no injected CO_2 migrated into the deeper Pennsylvanian aquifers from which WT-3 produced water (Figure 9-21). (As described in the MVA Strategies and Methods section, the deeper Pennsylvanian aquifers are those sampled by WT-3 at depths of >60 to 275 m [>200 to 900 ft], in contrast to the shallow Pennsylvanian aquifer sampled by the groundwater monitoring wells, which lies at depths of <60 meters [<200 ft].)

Each of the five shallow Pennsylvanian groundwater wells was sampled three times during the injection phase and five times during the post-injection phase (Appendix 7). The shallow groundwater monitoring well RG-5MW was located approximately 16 m (50 ft) south of RG-5 to serve as a shallow Pennsylvanian aquifer monitoring well in order to examine water chemistry characteristics that may be indicative of CO_2 leakage. As depicted in Figure 9-22, alkalinity, pH, DIC, and dissolved CO_2 were fairly consistent throughout the life of the project, which indicates that injected CO_2 did not mix with shallow groundwater. Groundwater quality data at RG-4MW and PH-1MW yielded similar results, further supporting the conclusion that injected CO_2 remained in the Jackson sandstone.

Like the bulk chemistry measurements above, the δ^{13}C-DIC and δ^{18}O-H_2O measurements in the Pennsylvanian groundwater samples were fairly constant during and after CO_2 injection (Figure 9-23). The δ^{13}C-DIC measurements in DC-1 and the RG monitoring wells appear to be cyclic and this might be related to input of meteoric runoff having variable amounts of DIC.

In addition to groundwater quality data, groundwater pressure data for each of the shallow groundwater-monitoring wells does not show a perturbation during the CO_2 injection or post-CO_2 periods (Figure 9-24). Such perturbations could be associated with CO_2 leakage across confining layers or along the wellbore casing. Instead the groundwater elevation data closely correlated with precipitation patterns determined from the Hopkins County Kentucky Mesonet[4] weather station located approximately 8.9 km (5.5 miles) east of the injection well. The close correlation between precipitation and elevation head further suggests that the shallow Pennsylvanian aquifer at all the monitoring well locations is quickly recharged by meteoric water. Moreover, the similar elevation head patterns among the wells suggest that the Pennsylvanian aquifers are potentially in hydraulic communication.

The collective groundwater quality and elevation head data from WT-3 and shallow monitoring wells therefore strongly suggest that there was no CO_2 leakage across confining layers above the Jackson sandstone reservoir or along casing in the production wells.

[4] The following disclaimer is from the Kentucky Mesonet website (http://www.kymesonet.org/): "While many aspects of the Kentucky Mesonet are functional, the development of systems, procedures, and controls necessary to produce and deliver operational data continues. While Mesonet data is adequate for many purposes, any data displayed from the network should be considered experimental until the time that the State Climatologist declares them to be of operational quality. Data should not be published in any manner without including this notice."

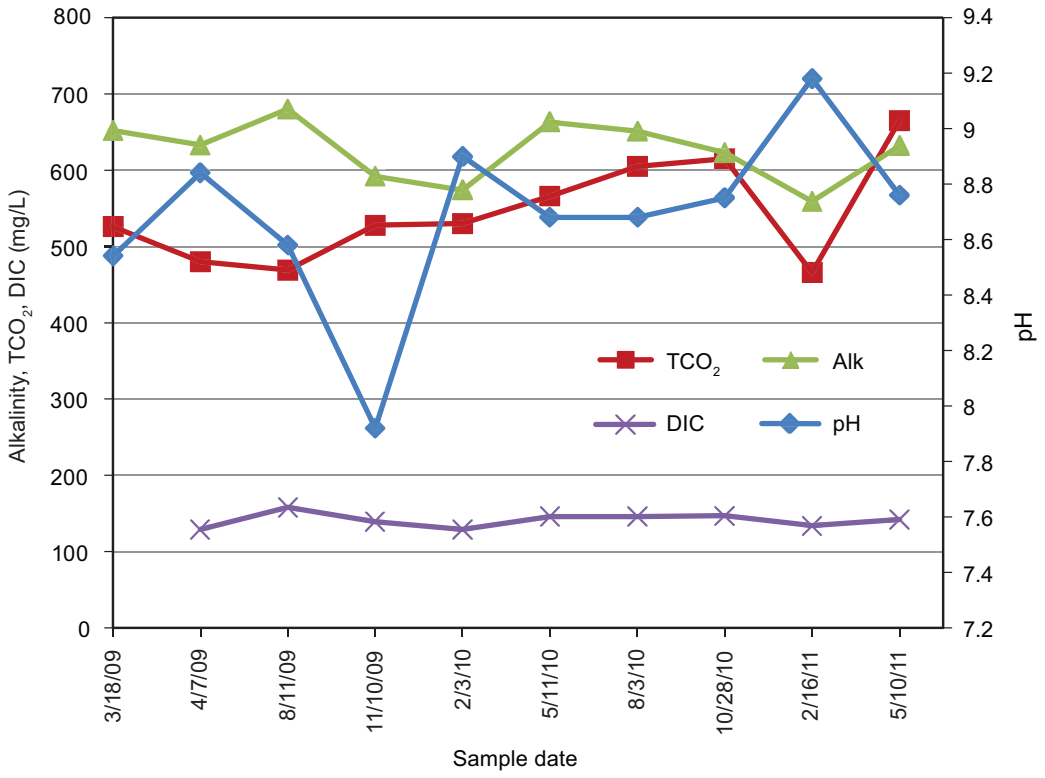

Figure 100 Variation in alkalinity, total CO_2 (TCO_2), dissolved inorganic carbon (DIC), and pH at WT-3.

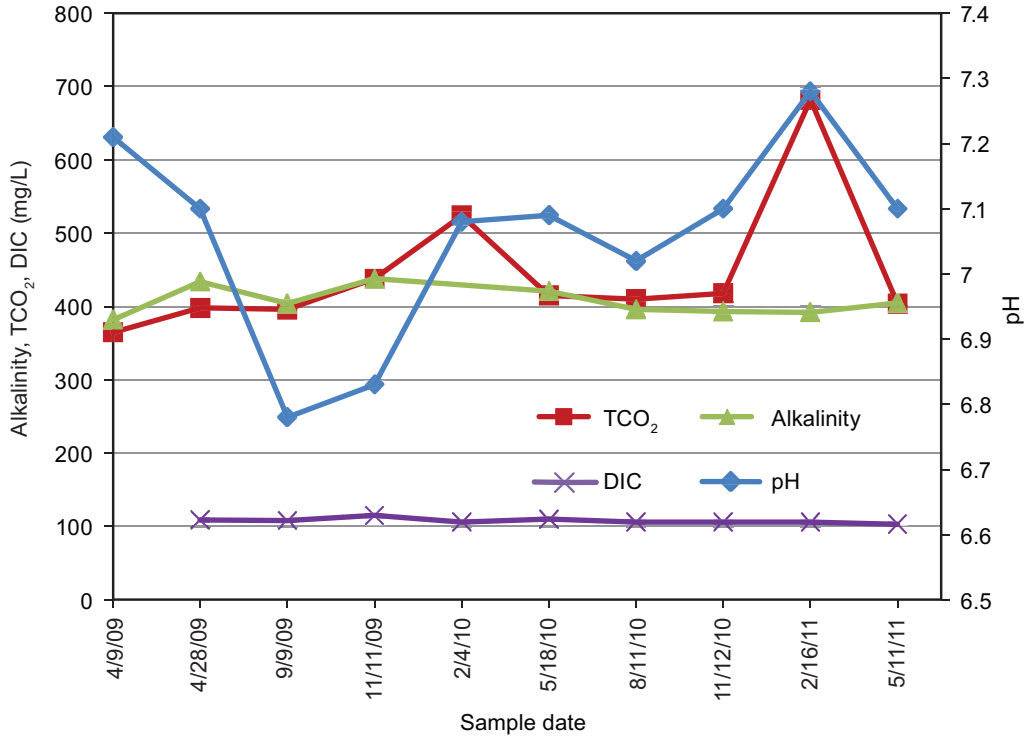

Figure 101 Variation in alkalinity, total CO_2 (TCO_2), alkalinity, and dissolved inorganic carbon (DIC) at RG5-MW.

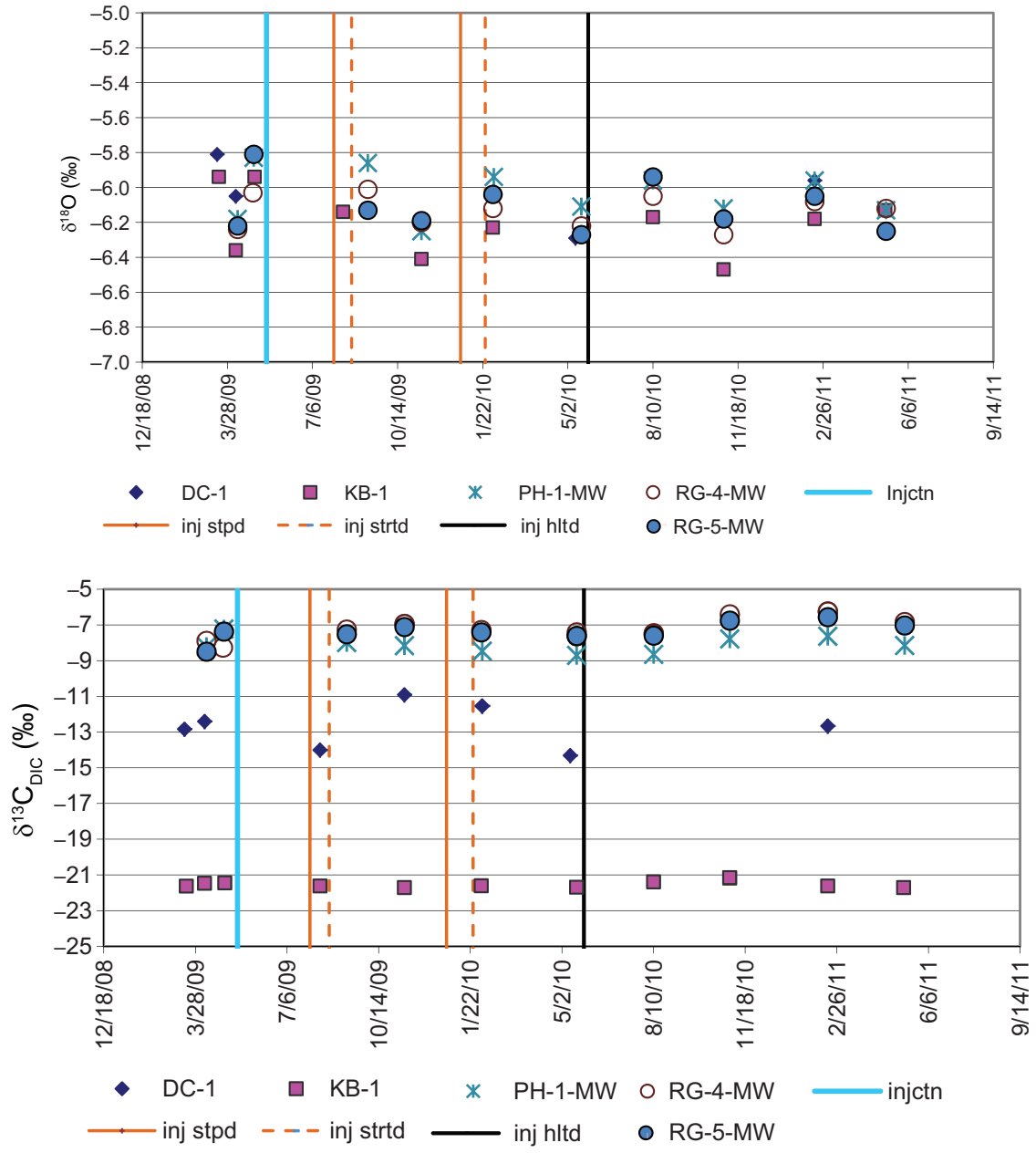

Figure 102 Top: Oxygen isotopic composition of shallow monitoring well water samples at Sugar Creek vs. time; bottom:$\delta^{13}C_{DIC}$ of shallow monitoring wells, as well as a domestic and livestock well, over time. Orange lines show major interruptions (greater than twenty consecutive days) in CO_2 injection.

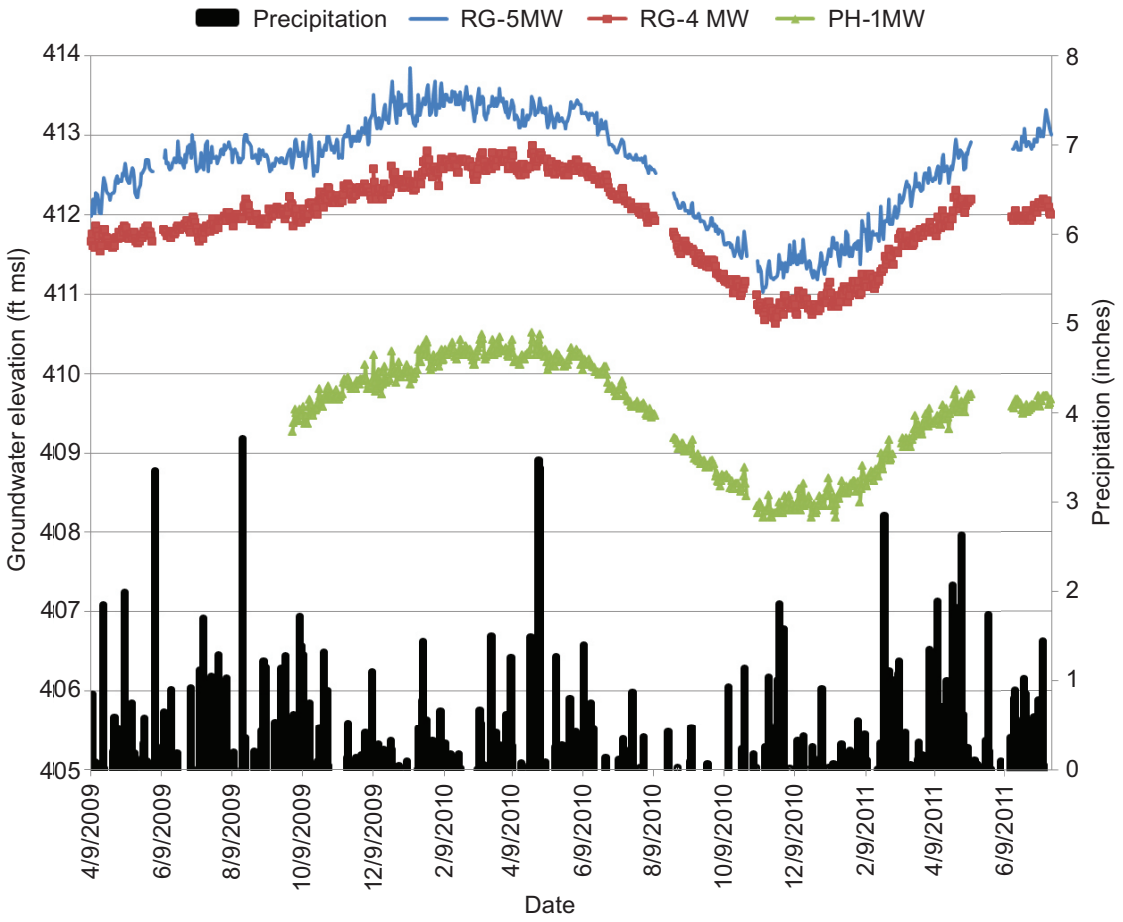

Figure 103 Precipitation and groundwater elevation data from RG4-MW, RG5-MW, and PH1-MW. Precipitation data were recorded at the Hopkins County Mesonet weather station located approximately 8.9 km (5.5 miles) east of injection well RG-5 and downloaded from the Kentucky Mesonet website (http://www.kymesonet.org).

Geochemistry and Sampling Results: Interpretation and Discussion

Monitoring groundwater chemistry in the Pennsylvanian aquifers and brine and gas chemistry in the Jackson oil reservoir was an important part of the MVA effort at Sugar Creek. More specifically, the collection and analysis of aqueous and gas chemistry data allowed the inference of the migration paths and, to some degree, the fate of CO_2 in the Jackson reservoir as well as qualitative data useful in developing the geologic and reservoir models. Moreover, the data provided confirmation that the injected CO_2 did not affect the shallow groundwater system.

Salinity and CO_2

Pre-injection Data The utility of the aqueous and gas chemistry analysis was demonstrated even before CO_2 was injected. The pre-CO_2 distribution of salinity by well, represented by the Na versus Cl plot in Figure 40 (also visible in the Stiff plots in Figure 39), showed that the production wells had near-bimodal distribution. The RG wells and WT-9 had intermediate salinity (~18,000–31,000 mg/L), and WT-4 and PH-1 had higher salinity (57,000–59,000 mg/L). WT-3, the Pennsylvanian groundwater well used to supplement the Jackson sandstone injection wells, had low salinity (~850 mg/L). The higher salinities are interpreted to represent native Jackson brines, and the intermediate salinities are interpreted to represent an in situ mixture of Jackson brines with the WT-3 produced water.

Spatially, the higher salinities occur north and east of the injection well, RG-5, whereas the intermediate salinities occur in wells south and west of RG-5. While drilled and completed in the oil-saturated portion of the Jackson sandstone, the proximity of PH-1 and WT-4 to the original oil-water contact explains the higher-salinity water present in these wells. During RG-5's post-CO_2 water injection, PH-1 salinities were intermediate, which suggested that it was producing RG-5 injected water. The high-salinity water at PH-1 prior to CO_2 injection is likely a result of the relatively long period during which it was shut in prior to this project such that the aquifer encroached in the area of this well due to the PZ-2 injection directly into the aquifer in the northern part of the oil field. WT-4 water chemistry never changed but continued to reflect the signature of the native Jackson brine, which may indicate that WT-4 is hydraulically isolated from the other parts of the oil reservoir.

The pre- CO_2 IRGA measurements are in agreement with the salinity measurements on the brine. The wells with higher pre- CO_2 injection brine salinity had lower background CO_2 concentrations (0–0.8%) than did the intermediate salinity wells (0.5–6.9%) (Appendix 5). Although brine production at WT-8 was too low to sample, it had low casing gas CO_2 concentrations (0–0.2%), suggesting that WT-8 may be less connected to the injector, RG-5. However, WT-8 and WT-4 are considerably farther from RG-5 than the other wells in the pilot. It is possible that distance alone is responsible for the lack of CO_2 response at these wells.

Active CO_2 Injection Data Indicative of a distinct front of CO_2 moving through the reservoir, concentrations of CO_2 measured with the IRGA in the annulus of the well or headspace of the carboy increased by an order of magnitude—often greater than 90%—for the RG wells and PH-1 (Figure 80, Appendix 5). These increases, or CO_2 breakthrough, occurred within 5 months of the onset of CO_2 injection. Elsewhere, the geologic model based on the pre-CO_2 chemistry correctly predicted the absence of CO_2 at WT-4 and WT-8.

PH-1 The change in salinity at PH-1 is best explained by considering its production history. Prior to CO_2 injection, PH-1 was shut-in and therefore would not have acted as a pressure sink to draw in intermediate salinity water (produced water diluted with WT-3 water) from RG-5. At the time PH-1 was shut-in, large amounts of make-up water were injected into PZ-2, located north of PH-1 (Figure 23). Despite being in a downdip direction relative to PH-1, water injection at PZ-2 displaced higher salinity native Jackson water updip into the reservoir surrounding PH-1. This would account for the higher salinities measured at PH-1 before CO_2 injection (Figure 40, Appendix 5). After CO_2 injection commenced and PH-1 was put back into production, PH-1 would have acted as a pressure sink to draw in CO_2; hence, the breakthrough on October 7, 2009. The large increase in CO_2 resulted in PH-1 flowing through tubing only until the last several months of sampling in the post-CO_2 period of RG-5 water injection. At that time the brine salinities had decreased by more than 50%, suggesting that PH-1 was in communication with RG-5 (Appendix 5). Based on CO_2 breakthrough and the changes in brine chemistry at PH-1, it is in good hydraulic communication with RG-5, but possibly not as good as RG-2.

WT-9 The CO_2 increase at WT-9 was more subtle and occurred later (Figure 80, Appendix 5). It was not clear from the IRGA CO_2 and pH data that WT-9 was influenced by CO_2. Only alkalinity and DIC data provided an unambiguous CO_2 influence (Figure 82). The different chemical response, compared with those at the RG and PH-1 wells, may be attributed to the greater distance between WT-9 and RG-5 and the rate of CO_2 dissolution into the brine (see discussion). Alternatively, very small amounts of CO_2 likely remained dissolved in the produced water and were re-injected into the field via the water injection wells. Consequently, a secondary source of injected CO_2 was likely. A very large injection well, EL-2, is immediately south of WT-9 and this well's injected water with a small amount of CO_2 may have reached WT-9 much later than was observed for the injected CO_2 at RG-5.

CO_2 Breakthrough Time and Relative Velocity

The different CO_2 breakthrough times suggest that porosity and permeability are not isotropic in the Jackson reservoir. This potential heterogeneity is exemplified in RG-2, where CO_2 breakthrough occurred 11 days after the start of injection. In contrast, RG-4 and PH-1, which are closer to the injection well, both had later breakthrough dates. To normalize for distance and to estimate CO_2 migration velocities, the straight line distances between the production wells and the injection well were divided by the elapsed time between CO_2 injection start and breakthrough for each well (Table 22). The results show that CO_2 migration velocities at RG-2 and RG-3 (9.6–24.3 m/day) were considerably greater than the other wells (1.3–2.5 m/day). The high migration velocity in RG-2 and RG-3 would suggest that CO_2 migration occurred at least partly through a fracture network. The smaller range of values for wells having apparent slower velocities suggests that migration, on average, occurred primarily through porous media.

The large increases in CO_2 in the RG wells and PH-1 produced predictable aqueous geochemical responses with decreases in pH, increases in alkalinity and DIC, and enrichment of δ^{13}C-DIC (Figures 81, 82, and 99; Appendix 5). The geochemical behavior provides strong evidence for solubility trapping of CO_2 through the aqueous speciation reactions.

Relative to the time of CO_2 breakthrough, the response of pH, alkalinity, DIC, and δ^{13}C-DIC was often rapid with changes occurring in weeks. The most notable of these was the apparent decrease in pH at RG-2, RG-4, and PH-1 before CO_2 breakthrough. The rapidity of the geochemical responses strongly suggests that the dissolution of CO_2 into water and the subsequent dissociation of H_2CO_3 to produce H^+ ions were relatively fast. The linkage among these reactions and their sensitivity to CO_2 injection pressure, which controls the partial pressure and hence fugacity of CO_2, can be demonstrated by examining the pH response of certain wells to the injection shut-in periods (e.g., injection line leaks) that occurred during CO_2 injection (Figure 81). The longer CO_2 shut-in periods resulted in reduced reservoir pressure and CO_2 partial pressure. The reduced CO_2 partial pressure would shift the CO_2 speciation reactions to the left and cause an increase in pH. Such a response is observed with RG-3 and RG-4 during the first two shut-in periods (late June 2009 to early July) and possibly the third (July 31 to August 21, 2009; Figure 81). There are more data gaps for RG-1, but it too might show an increase after the third major shut-in (late December 2009 to early February). A similar response between pH and CO_2 injection pressure was observed at the Frio project in Texas (Kharaka et al., 2006a, 2006b).

Mineral Dissolution

As previously noted, wells with large increases in CO_2 developed pH minima at about the same time from October 2009 to January 2010, after which overall pH values increased slowly but steadily (Figure 81). Although some of the pH increase is attributable to decreased CO_2 partial pressure associated with the second line leak, the longer term pH increase is likely due to buffering through mineral dissolution. The role of mineral dissolution is apparent when changes in alkalinity are compared with changes in Ca^{2+} concentration, which is used as a proxy for carbonate dissolution (Figure 104). RG-1, RG-3, and RG-4 are used as examples because they have fairly complete data sets. Data from these wells show that Ca^{2+} concentrations closely track changes in alkalinity, and that increases in Ca^{2+} often occurred soon after CO_2 breakthrough (Figure 83, Table 22). The Ca^{2+} increase therefore strongly suggests that carbonate dissolution buffered pH even during active CO_2 injection and that dissolution started anywhere from a week up to approximately 4 months after CO_2 breakthrough. Similar responses were documented with Mg^{2+} and Fe^{2+} as proxies for dolomite, ankerite, and/or chlorite dissolution (Table 22).

Table 22 Estimated CO_2 migration velocities and the number of elapsed days between CO_2 breakthrough (as indicated by gas composition; see Table 18) and documented decreases in pH or cation increases. Negative and positive numbers refer to time before and after breakthrough, respectively.[1]

Well	CO_2 breakthrough date	Velocity (m/s)	Elapsed time for pH or cation changes after CO_2 breakthrough (days)					
			pH	Ca^{2+}	Mg^{2+}	Fe^{2+}	Si	K^+
RG-1	9/15/2009	2.5	55	55	55	55	294	211
RG-2	5/20/2009	24.3	12	12	12	12	ambig.	ambig.
RG-3	6/10/2009	9.6	19	124	124	124	183	~307
RG-4	9/15/2009	1.5	−36	27	27	27	~86	~210
PH-1	10/7/2009	1.3	−58	6	ambig.	6	ambig.	ambig.

[1] Abbreviations: ambig., ambiguous well response because of data gaps (e.g., RG-2), changes in water chemistry due to operational changes in the well (e.g., PH-1), inconsistent pre-CO_2 measurements that precluded an accurate reference baseline (e.g., K+), or indistinct trends (e.g., pH in WT-9); tilde (~), approximate date of change because the change was subtle.

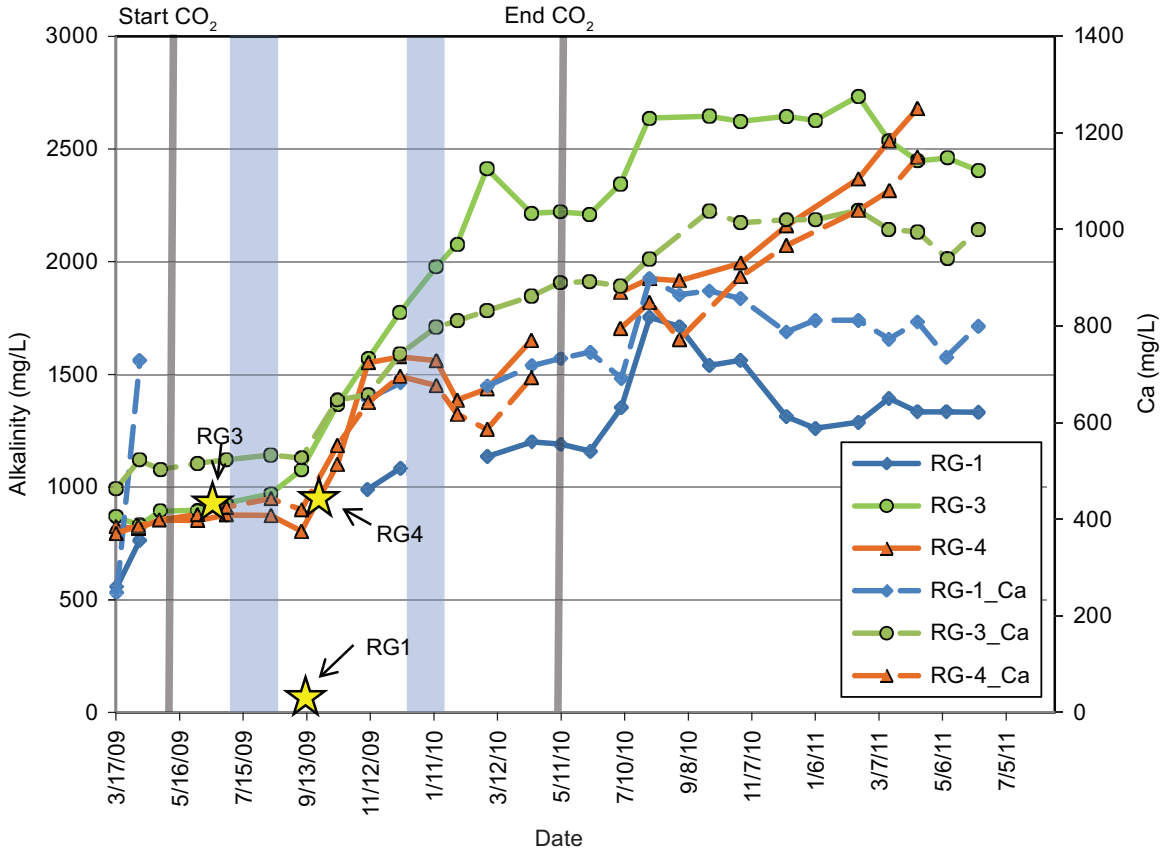

Figure 104 Evolution of alkalinity (solid lines) and Ca^{2+} concentration (dashed lines) before, during, and after CO_2 injection. Note that the concentration scales for alkalinity (left axis) differs from the Ca^{2+} concentration (right axis). Star symbols represent CO_2 breakthrough dates. Vertical bar designates approximate periods of CO_2 injection shut-in.

Increases in Si and K^+ concentrations were also documented, albeit at longer time scales on the order of 90 to 300 days following CO_2 breakthrough. The increases in Si and K^+ were often difficult to resolve because changes in Si concentration were frequently subtle (Figure 86), and pre-CO_2 concentrations of K+ showed significant variation (Figure 87). Relative to CO_2 breakthrough, the longer time periods for increases in Si and K^+ concentrations agrees with the generally lower solubility of Si and, compared with carbonates, the typically slower reaction kinetics of aluminosilicate minerals (Palandri and Kharaka, 2004). Notwithstanding the analytical obstacles, it is clear that, along with carbonates, dissolution of aluminosilicate minerals contributed to buffering of pH.

The rapidity with which apparent mineral dissolution occurred after CO_2 breakthrough was somewhat surprising. For example, at RG-1, RG-2, and RG-4, increases in Ca^{2+} along with Mg^{2+} and Fe^{2+} suggest that not only is calcite dissolving, but also dolomite and/or ankerite. Dissolution of aluminosilicate minerals, although later, appears to have occurred within the one year of post-CO_2 monitoring. One possible explanation for the quick response is the influence of the dilute Pennsylvanian groundwater from WT-3 on the mineral saturation states in the make-up water.

Using Geochemist's Workbench, Schumacher et al. (2010) analyzed the mineral saturation states of the intermediate-salinity waters—that is, waters representing a mixture of native Jackson brines and dilute WT-3 water—and high-salinity waters representing the undiluted native Jackson brine before the injection of CO_2. In this analysis, the mineral saturation state in solution is given by the parameter Q/K in which Q represents the actual solution concentration of species comprising a mineral (e.g., Ca^{2+} and CO_3^{2-} in calcite) and K represents the theoretical equilibrium concentration of the same for a given temperature and pressure. Thus Q/K values of 1 signify that the solution is in equilibrium with the mineral of interest; values greater or less than 1 signify supersaturated and undersaturated solutions, respectively. With the exception of quartz, which is close to equilibrium in the intermediate and high salinity brines, the results show that mineral saturation in the intermediate salinity brines is clearly lower than in brines with higher salinity (Table 23). Lower mineral saturation levels would have made minerals in the part of the reservoir containing the intermediate salinity brines potentially more predisposed to dissolution during CO_2 injection.

Table 23 Pre-CO_2 saturation indices (Q/K) for some minerals in Jackson sandstone brines having intermediate and high salinities calculated using Geochemist's Workbench (Schumacher et al., 2010). Inputs included brine chemistry measurements and CO_2 fugacities from CO_2 casing gas concentrations. The input reservoir temperature was 29°C (84°F), and the brine was assumed to be saturated with CH_4.

Mineral	High salinity	Intermediate salinity
Quartz	1.05	0.98
K-feldspar	16.6	2.3
Albite	12.6	1.48
Calcite	1.01	0.53
Siderite	4.27	0.36
Dolomite	13.18	2.39
Illite/mica	4,677	549
Kaolinite	17,378	13,803
Chlorite	19.49	0.002

pH

Although pH values increased in the post-CO_2 period, most values (6.2–6.3) remained a half pH unit or more below the pre-CO_2 injection values (Appendix 5, Figure 81). Similarly, alkalinity and DIC concentrations remain elevated in the post-CO_2 period, although some wells showed declines (RG-1, RG-3, and PH-1) whereas others showed increases (RG-4, WT-9) (Appendix 5). Measurements and samples collected during November 2011, although values are not shown in the figures, show that these parameters have not changed significantly.

Cations

Similarly, cation concentrations in the post-CO_2 period remained higher than pre-CO_2 concentrations, but trends toward increasing or decreasing concentrations varied from well to well. RG-4 and PH-1 continued to show increasing concentrations of Ca^{2+}, Mg^{2+}, Fe^{2+}, and Si, although neither well displayed all of the trends (Appendix 8). The continued increase in cation concentrations at RG-4 and PH-1 suggests that, despite their close proximity to the injection well, the Jackson brines in and around these wells remained very reactive and were not being buffered by injection water in the post-CO_2 waterflood period. Indeed, this lack of response is not surprising given that during CO_2 injection, breakthrough at PH-1 and RG-4 developed after breakthrough at the other RG wells. By comparison, some of the cation concentrations and other water quality parameters in RG-2 and RG-3 have stabilized in the post-CO_2 period (Appendices 5, 8). RG-1, which is farther from the injection well than the other RG wells, has showed decreasing values for all of the discussed cations in this section.

Cation concentrations at WT-9 were still slightly elevated but have remained steady in the post-CO_2 period. Compared with the other wells with CO_2 breakthrough, WT-9 was not as greatly impacted by CO_2. Similarly, the brine chemistry, and hence chemical equilibrium, at WT-9 was changed less, as indicated by the subtle increases in cation concentrations. Consequently, chemical equilibrium theory predicts that the return to pre-CO_2 values will be slower as those values are approached.

Geochemistry Summary

Bulk and isotopic chemistry measurements before CO_2 injection showed significant variability in the Jackson sandstone reservoir. The geochemical heterogeneity reflected geologic influences, such as possible compartmentalization, but also operational influences in the field. The geochemical variability underscores the importance of baseline geochemical measurements prior to CO_2 injection, so that geochemical responses to CO_2 injection can be better understood.

Collectively, the water parameters such as pH, alkalinity, and DIC, and the cation responses in the post-CO_2 period point to a reservoir that is still moderately acidic and reactive. The narrow range of pH values suggests relatively uniform buffering across the field. In parts of the field where Ca^{2+} and even Si concentrations are elevated and even increasing, such as at RG-4 and PH-1, the respective dissolution of carbonates and silicates is still likely playing an important role in buffering. Elsewhere, where cation concentrations are declining or holding steady, the influx of post-CO_2 injection water, supplemented with dilute Pennsylvanian groundwater, is also likely a significant buffering mechanism.

Increases in alkalinity and DIC and the shift to more positive δ^{13}C-DIC values collectively reflect the dissolution of CO_2 into water and storage of CO_2 through solubility trapping. The CO_2 aqueous speciation reactions developed early in the injection stage and continued for many wells into the post-CO_2 period.

The isotopic measurements provided further accuracy in documenting the movement of the injected CO_2 and additional information about reservoir geochemical reactions. The δ^{13}C and ^{14}C measurements showed strong responses in both gas and aqueous phases and therefore were good indicators of subsurface CO_2 movement and CO_2-water-rock interactions. The strong contrast between the injected CO_2 and inherent CO_2 in the Jackson reservoir made measurements of ^{14}C activity particularly effective at tracking CO_2 movement.

Cased Hole Logging

A comprehensive report comparing and interpreting the pre- and post-CO_2 cased hole logs is in Appendix 10. The interpretations show no indication of CO_2 in the near-wellbore region of the wells logged. The RST reading Sigma was considered identical and was interpreted as the presence of liquid only. The RST was able to detect a change in produced water salinity in PH-1. Because this well had been shut-in prior to CO_2 injection, the brine present was significantly different from the brine injected at RG-5. Based on regional information, this brine was thought to be native aquifer water from the northern part of the Jackson sand. Post-CO_2 injection of brine at RG-5 and subsequent brine sampling at PH-1 showed a change in brine composition at PH-1 that was much more similar to the RG-5 injected brine than it was pre-CO_2 injection. Other anomalies detected with the RST tool were the presence of tubing and difference in casing-tubing annular fluids.

Soil Gas Work in Response to Line Leak

On June 30, 2009, a leak in the injection line between the CO_2 injection equipment and RG-5 was discovered. The leak was detected when site personnel observed dust circulating into the air and layers of vapor hovering near the ground surface in the vicinity of the leak. The leak was shallow enough and at a sufficiently high rate that it was discovered via direct observation by personnel. The injection line was buried approximately 1 m (3 ft) underground, and the soil surface expression caused by the leak consisted of a hole (Figure 105) approximately 1.9 m long × 1.7 m wide × 0.7 m deep (6.2 ft × 5.6 ft × 2.3 ft). Injection of CO_2 was immediately halted upon discovery of the leak.

This incident was a unique opportunity to test the performance of monitoring equipment in the presence of a known leak of a pipeline. The leak detection methods employed included thermal infrared imagery, aerial hyperspectral imagery, determination of near-surface gas concentrations, soil CO_2 fluxes, and vadose zone gas composition. The plan was to set up these methods in the immediate area of the leak and restart CO_2 injection so that direct measurements and observations could be made.

Twenty-six soil flux measurement rings with a diameter of 20 cm (8 in) were installed. These rings were oriented radially around the leak (Figure 106). Rings were generally located at distances of 1, 1.5, 3.5, and 5.5 m (3, 5, 11, and 18 ft) away from the leak. The rings were hammered into the soil to a depth of about 8 cm (3 in). Atmospheric CO_2 concentrations were also measured at the ring locations at 2.5, 25, 50, 75, and 165 cm (1, 10, 20, 30, and 65 in) above the ground surface. Soil CO_2 fluxes were determined by a LI-COR 8100® single chamber survey system, and atmospheric CO_2 concentrations were measured using a portable non-dispersive infrared gas analyzer (NDIR). The rapid release of CO_2 froze the soil, making conditions ideal for thermal imagery (Figure 107), which was periodically collected at the leak site using an IR Snapshot model 525™ by Infrared Solutions, Inc. Reference points were set up on the boundaries of the leak to maintain orientation. To complement thermal imagery, soil temperatures were taken in the top 10 cm (4 in) of the soil surface by an Omega 865 Thermometer (Table 24). Hyperspectral imagery was collected nine times from altitudes of 0.6 km, 1.1 km, and 2.1 km (0.4, 0.7, and 1.3 mi) on July 8, eight days after the leak was detected.

Table 24 Soil temperatures (ºC) from the mornings of July 7 and July 8, 2009. Compass directions indicate locations where temperature was measured relative to hole. Temperatures inside the hole were on the order of −0.2°C (31.6°F), and ambient temperatures ranged from 26.2ºC (79.3ºF) to 31.5ºC (88.7ºF) during soil temperature measurements.

	Distance	July 7, 2009					July 9, 2009		
Ring	from leak (m)	N	NE	S	SW	W	E	SE	NW
1	1.0	14.2	NM[1]	13.3	16.6	10.8	15.2	13.8	13.3
2	1.5	16.9	NM	15.9	18.6	16.9	18.9	17.3	17.8
3	3.5	21.0	--	20.5	22.3	21.4	20.7	--	22.8
4	5.5	21.3	--	21.1	26.5	21.7	--	--	23.8

[1] Not measured.

Figure 105 Soil surface expression of CO_2 injection line leak. The hole is surrounded by flux rings.

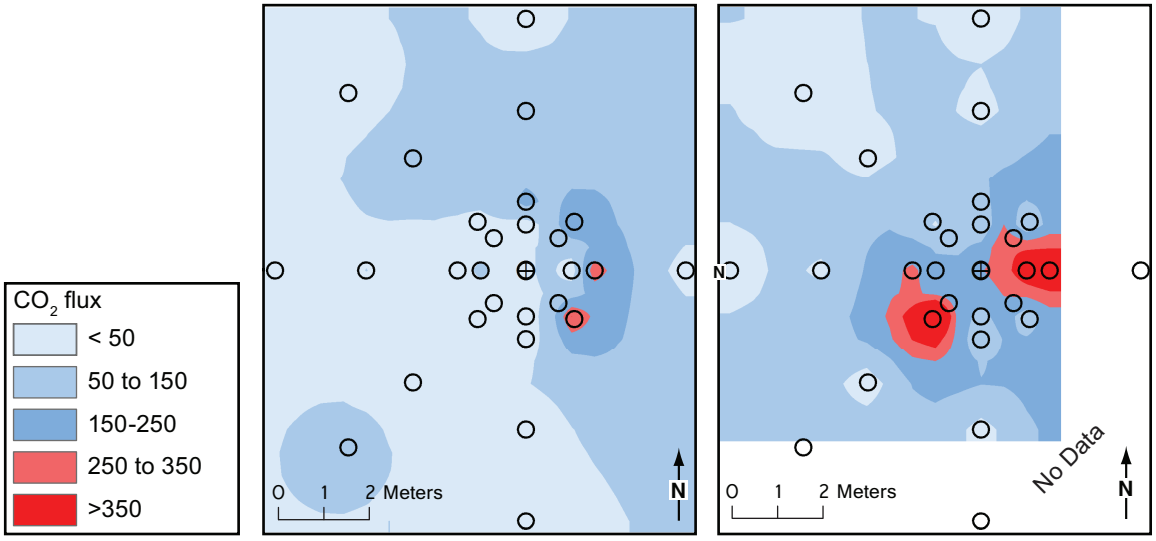

Figure 106 Monitoring grid and representative soil CO_2 fluxes during initial conditions on the morning of July 7, 2009 (left; with no injection) and on the afternoon of July 7, 2009 (right; after injection resumed). The central point filled with a plus sign represents the leak location. Abbreviation: IR, infrared.

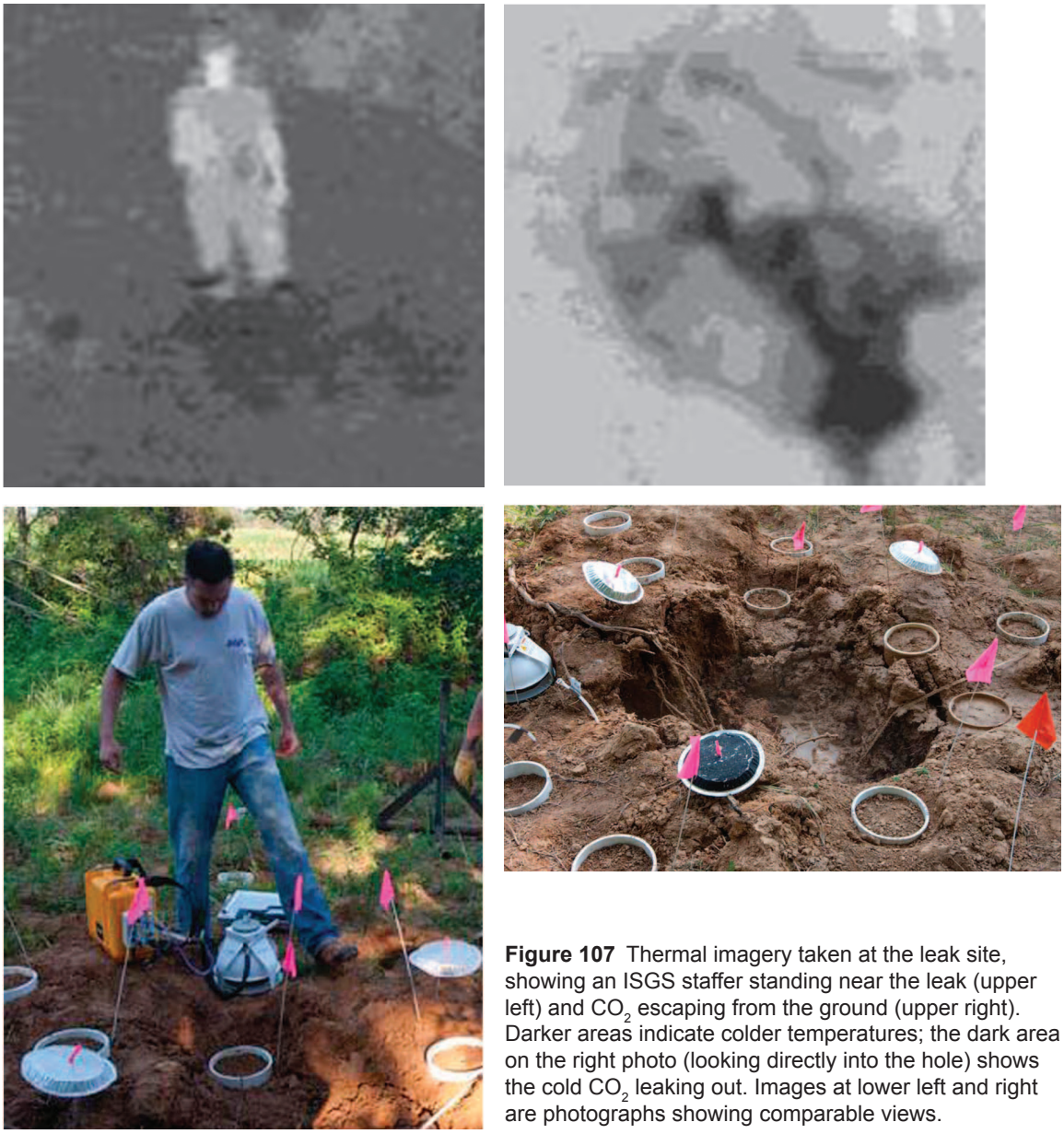

Figure 107 Thermal imagery taken at the leak site, showing an ISGS staffer standing near the leak (upper left) and CO_2 escaping from the ground (upper right). Darker areas indicate colder temperatures; the dark area on the right photo (looking directly into the hole) shows the cold CO_2 leaking out. Images at lower left and right are photographs showing comparable views.

Initial condition data were collected on July 6, 2009. Although CO_2 injection had been terminated, CO_2 was still escaping from the soil surface, likely due to CO_2 saturation of the soil, CO_2 remaining in the pipeline, and possibly a very small amount of CO_2 from the injection well. (A check valve may have allowed a very small amount of continued CO_2 release.) Atmospheric CO_2 measurements indicated for the initial condition that CO_2 concentrations were less than 20% CO_2 at 2.5 cm (1 inch) above the ground surface except directly above the leak. At the hole, where the leak was visible, CO_2 concentrations ranged from 86.6% at 2.5 cm (1 inch) above the leak to 0.2% at 75 cm (30 inches) above the leak. Soil CO_2 fluxes on the same day ranged from 0.47 to 713.6 µmol/m^2/s.

The injection of CO_2 resumed July 7, 2009, and monitoring continued for an additional 2 days. On July 7 and 8, atmospheric CO_2 concentrations ranged from <0.1% to 97.7% at 2.5 cm (1 inch) above the ground surface, while concentrations measured at greater heights were less than 0.1%. CO_2 concentrations at the leak ranged from 99.9% at 2.5 cm (1 in) above the leak to 0.1% at 75 cm (30 inches) above the leak. Soil CO_2 fluxes ranged from 0.51 µmol/m^2/s to greater than the upper measurement range of the instrument.

Figures 106 and 108 are maps of the atmospheric and soil flux measurements. Contour intervals represent averaged concentrations or soil CO_2 flux values. On July 7, 2009, 42 of 67 fluxes collected were above the upper measurement range of the single chamber survey system, while on July 8, 15 of 51 fluxes were above this range. Fewer flux measurements were out of range on July 8 because of the disruption to the soil surface during the CO_2 leak such that some of the rings were displaced or contained thicker layers of soil within the rings. Fluxes were not collected directly above the leak.

The leak provided an opportunity to evaluate the advantages and disadvantages of several potential near-surface MVA monitoring techniques. This unique monitoring opportunity led us to these conclusions:

- Hyperspectral imagery (Figure 109) was not effective in detecting this relatively small short-term CO_2 leak because the sensor used on the aircraft did not have wavelengths in the shortwave infrared spectrum to detect CO_2 directly. Also, the short-term nature of the leak did not provide sufficient time to alter surrounding vegetation.
- Rapid deployment and maintenance of surface and shallow subsurface monitoring equipment was possible with minimal manpower. However, the active nature of the leak proved to be destructive of the soil surface and interfered with data collection.
- Soil CO_2 flux data were successful in showing high rates of release of CO_2 into the atmosphere from the leak. However, concentrations encountered outside of the equipment's operational range caused difficulty in quantifying flux values.
- Atmospheric CO_2 measurements collected near the soil surface using a portable NDIR analyzer were able to track soil CO_2 emissions. Elevated CO_2 concentrations were not detected at heights greater than 2.5 cm (1 inch) above the ground surface except directly above the leak.
- Ground thermal imagery (Figure 107) successfully differentiated between frozen soil and soil that had not been affected by the release of CO_2.

A faulty connection between joints of pipe in the injection line was determined to be the cause of the leak.

CO_2 SEQUESTRATION AND ENHANCED OIL RECOVERY: INTERPRETATION, ANALYSIS AND RESERVOIR MODELING

Sugar Creek Pilot Area Reservoir Model Calibration

The design of the pilot was to measure and record data that could be used to calibrate a reservoir simulation model of the Jackson sandstone of the Sugar Creek oil field to estimate the CO_2 EOR and storage capacity. The field pilot data collected directly does not adequately quantify the CO_2 EOR or storage capacity. For example, with field data it is not possible to directly eliminate the effect of the loss of CO_2 EOR as a result of periods when CO_2 was not delivered to the site. A model calibrated to the measured field data can provide more representative CO_2 EOR and storage estimates. Through the use of a calibrated model, continuous CO_2 injection can be simulated and the resulting EOR estimated. Other examples of model scenarios to improve the EOR estimate are injection rates at higher pressures (the regulated injection pressure), adding additional CO_2 injection wells, placing back pressure on the producing wells to estimate a miscible flood, and infill drilling to achieve smaller CO_2 injection patterns.

The Sugar Creek model calibration included 28 years of primary production and 16 years of waterflooding, followed by 1 year of CO_2 injection and a subsequent year of water injection at RG-5. The calibration included changes to the geologic model, injection and production pressures, relative permeability, aquifer properties, and each well's skin factor.

Description of the Geologic and Reservoir Models and Input Parameters

The reservoir model used to conduct reservoir simulations used a geostatistically generated geologic model (as described in the Geologic Characterization: Reservoir Geology section). The geological model was generated using the Isatis ® software package and then input to the VIP Reservoir Simulation Suite for reservoir modeling. Permeability, porosity, reservoir thickness, well locations, and depth from the upscaled geostatistical model were used as inputs in the reservoir model. The reservoir model consisted of 56 × 70 ×

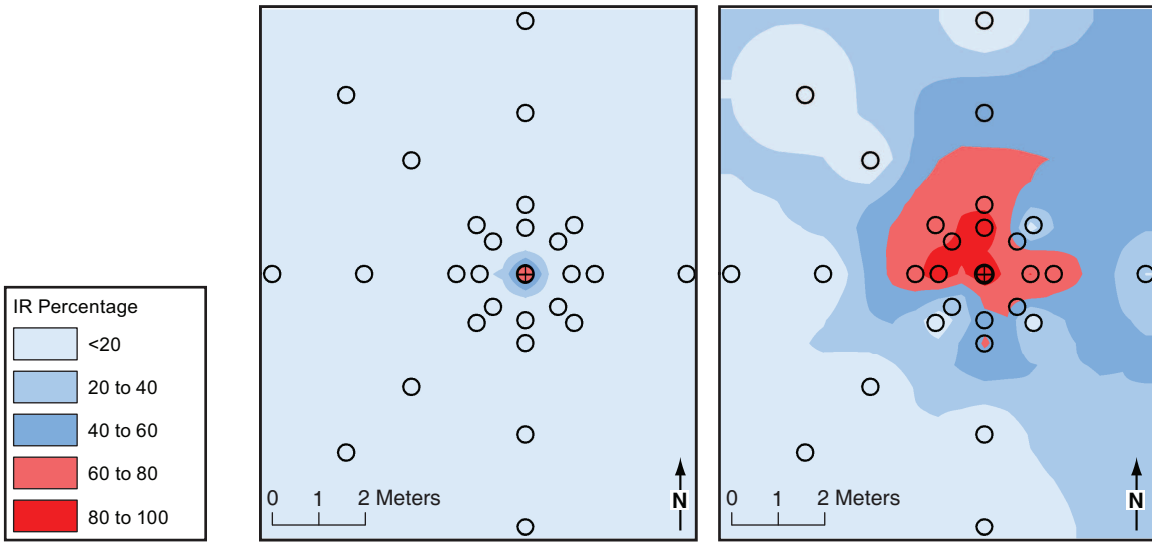

Figure 108 Monitoring grid and representative atmospheric CO_2 concentrations at 2.5 cm above ground level during initial conditions on July 6, 2009 (left; with no injection) and on July 7, 2009 (right; after injection resumed). The central point filled with a plus sign represents the leak location.

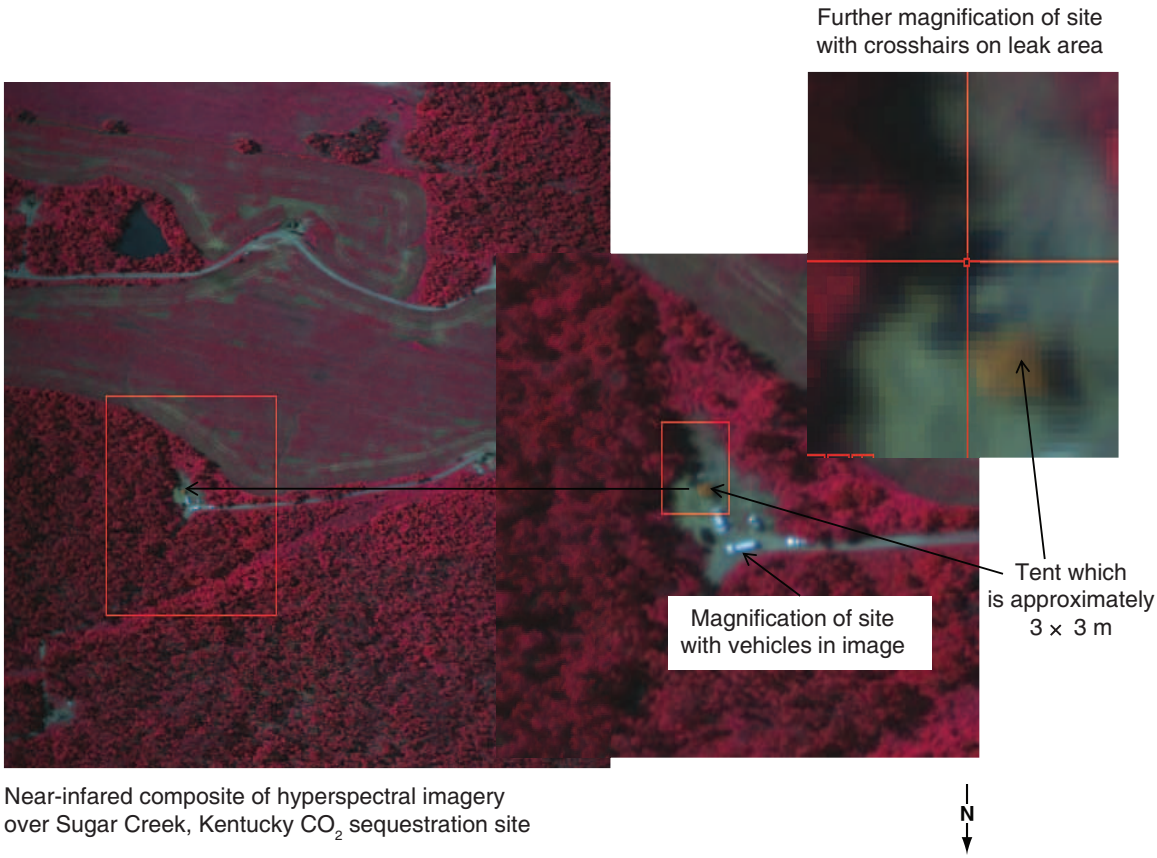

Figure 109 Hyperspectral imagery collected on July 8, 2009, during a monitoring, validation, and accounting (MVA) effort to study and ameliorate a CO_2 leak. The technique proved ineffective at detecting a CO_2 leak of such small size and short duration. The RG-5 site is within the red square. The gray-blue line is the lease road. The top of the figure is south. RG-2 is at the top of the picture at the inflection point in the lease road.

12 gridblocks in the x-, y-, and z-directions, respectively, i.e., 47,040 gridblocks (Figure 10-1). Each gridblock has dimensions of 24.4 m × 24.4 m × 0.610 m (80 ft × 80 ft × 2 ft).

To eliminate portions of the model considered non-reservoir, a porosity cutoff was imposed. A porosity cutoff of 14.4%, which is equivalent to a permeability cutoff of approximately 5.0×10^{-11} cm^2 (5 mD), was applied to the model. The number of active gridblocks was 20,064.

The reservoir datum is located about 561.4 m (1842 ft) below ground level, and the water-oil contact is 568.5 m [1,865 ft] below ground level. Completion intervals of the wells were estimated from a combination of well log data, core data, and communication with GDI. A five-component Peng–Robinson equation of state (EOS) was used to generate pressure-volume-temperature (PVT) properties of the crude oil. The five pseudo-components used to characterize the crude oil were CO_2, C_1, C_2, C_6, and C_{25}. The mole fractions of the pseudo-components (Table 25) were adjusted until the EOS-derived fluid properties matched the observed density and viscosity of the Sugar Creek fluids, which were 0.83 g/cm^3 and 4.78 cP, respectively, at initial reservoir pressure (~893 psia) and temperature (~78°F). Pederson's correlation was used to calculate the viscosity of the crude oil. Generalized water-oil and gas-oil relative permeability correlations were used in the simulations. Figure 111 shows the initial water-oil relative permeability curves. The irreducible water saturation employed was 0.35. Capillary pressure was assumed negligible and as a result, relative permeability hysteresis effect was assumed to be negligible.

Table 26 shows the brine properties and rock compressibility.

Table 25 Mole fractions of the pseudo-components used in the five-component EOS to match crude oil properties at Sugar Creek.

Component	Mole fraction
CO_2	0.01
C_1	0.08
C_2	0.12
C_6	0.13
C_{25}	0.66

Table 26 Reservoir brine and rock parameters.

Parameter[1]	Value
ρ_{wb}	1.1 g/cm^3 (69 lb/ft^3)
B_{wi}	1.01 rb/stb
μ_w	0.8 cP
c_w	3.0×10^{-6} psi^{-1}
c_r	5.0×10^{-6} psi^{-1}

[1] Abbreviations: ρ_{wb}, stock tank water density; B_{wi}, water formation volume factor; μ_w, water viscosity; c_w, water compressibility; and c_r, rock compressibility.

Based on generalities of Illinois Basin geology and oil field operations, the following assumptions were made in the simulations:

- All wells were considered pumped-off during production. As a result, bottomhole pressure (BHP) of 34.5 kPa (5 psi) during primary and 170 kPa (25 psi) during water and CO_2 flooding were applied at all production wells during primary recovery and waterflooding, respectively.
- No-flow boundaries were imposed on the western, southern, and eastern edges of the geologic model. Aquifer support to the reservoir was from the northern edge of the model.
- Capillary pressures between oil and water and between gas and water were considered negligible. As such, the numerical model assumed that the thickness of the transition zone between oil and water was zero, i.e., there was a sharp interface between oil and water.
- Pressure within the reservoir was hydrostatic, i.e., the reservoir was considered to be neither over-pressured nor under-pressured.
- The crude oil in the reservoir was assumed to contain very small amounts or proportions of dissolved hydrocarbon gas.

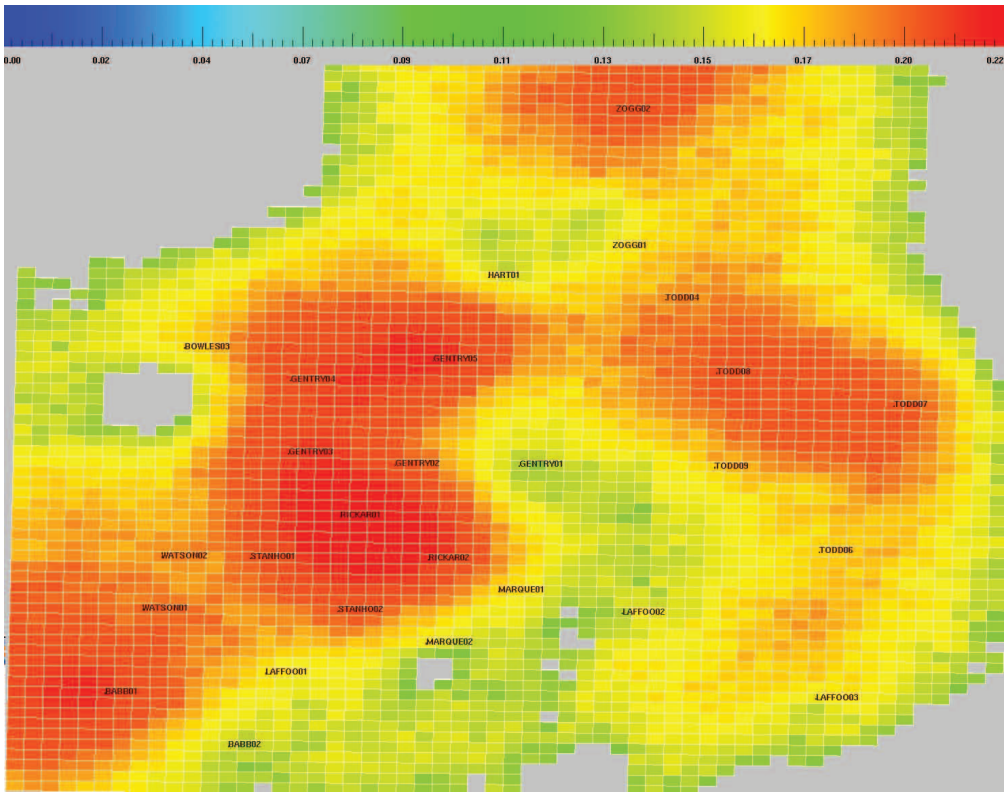

Figure 110 Porosity of model layer 4 showing grid size and shape of the Sugar Creek reservoir model.

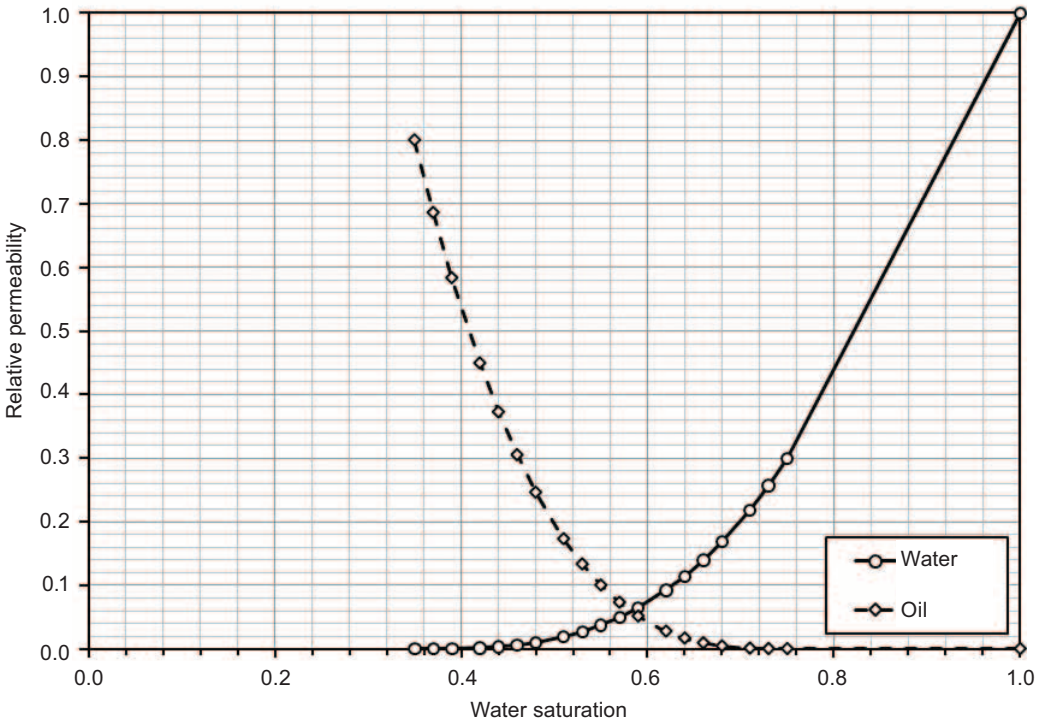

Figure 111 Initial water-oil relative permeability curves.

No relative permeability data were available for the Jackson sandstone reservoir. The values in Table 27 were the initial values for the history match based on sandstones in general, and the final or calibrated relative permeability end-points to the Sugar Creek history match.

Table 27 Saturation and relative permeability end points.

Parameter[1]	Initial value	Calibrated value
S_{wr}	0.35	0.35
$k_{rw@Sor}$	0.5	0.5
$S_{g,max}$	0.65	0.65
$k_{rg,max}$	0.90	0.9
$k_{row,max}$	0.80	0.8
$k_{rog,max}$	0.80	0.8

[1] Abbreviations: S_{wr}, irreducible water saturation; k_{rw}, relative permeability of water at residual oil saturation; $S_{g,max}$, maximum gas saturation; $k_{rg,max}$, maximum relative permeability of gas; $k_{row,max}$, oil relative permeability at irreducible water saturation; and $k_{rog,}$ oil relative permeability at residual gas saturation in the reservoir.

Description of the Calibrated Model

The reservoir model was calibrated by specifying the total liquid production and matching historical oil and water production data and water injection history data for all 11 leases at the Sugar Creek Field. Primary oil production was available only by lease; consequently, a history match of individual wells was not possible. Even though field data during waterflooding were available by well, fluid production values were allocated based on periodic barrel tests. Fluid relative permeability values used in the simulations were iteratively adjusted to achieve a good match with oil and water production and water injection. The exact dates when wells became active or were shut-in were implemented in the simulations. In cases where precise dates were unavailable the last day of the month was used.

Primary Recovery All of the wells except WT-8, WT-9, and PZ-2 were simulated as production wells during primary recovery: WT-8 and WT-9 were drilled after 1992, and PZ-2 was a water injection well. Figure 112 shows column charts of simulated and field cumulative oil production by lease at the end of primary recovery. The simulated values closely matched the field data. A similar chart for water production during primary recovery is not presented because field data on water production were not available.

To match primary production, a much larger OOIP (726,333.5 m^3 or 4,568,500 bbl) was required compared to that provided by the operator, which is an indication that more reservoir energy is required to match the historical oil production, not necessarily that the OOIP is this high.

Waterflood Recovery Producing wells AB-1, PB-2, RG-5, EL-2, EL-3, BM-2, WT-7, and RW-2 were converted to injection wells during waterflooding. From December 1992 until mid-May 2009, half of these injection wells (AB-1, PB-2, EL-3, and RW-2) were shut-in prior to the start of the CO_2 pilot. In addition, the RG-5, EL-3, and WT-7 wells were intermittently shut-in and brought online during waterflooding. Based on tubing head pressure (THP) data provided by GDI, the BHP for injection wells was set at 15.2 MPa (2,200 psi).

Adjustments to the oil-water relative permeability were made to match the waterflood history; the calibrated model's relative permeability curves are in Table 27. A comparison of simulated and field cumulative (oil and water) production by well (Figures 113 and 114) shows an acceptable match between the simulated

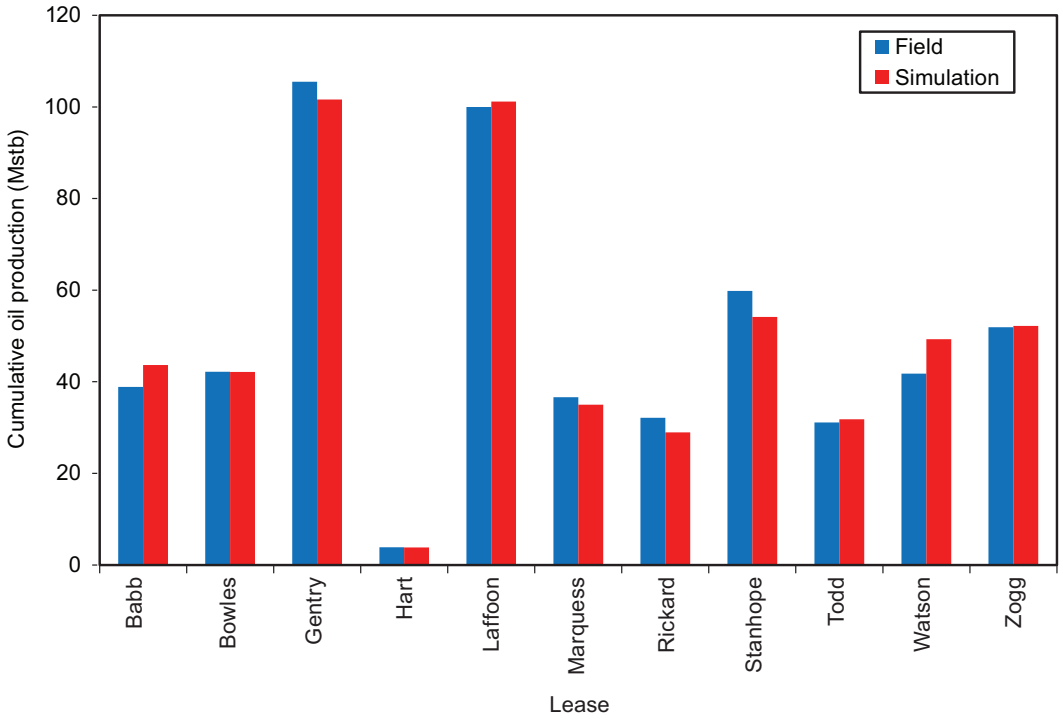

Figure 112 Comparison of simulated values and field data, by lease, for oil production at the end of primary recovery.

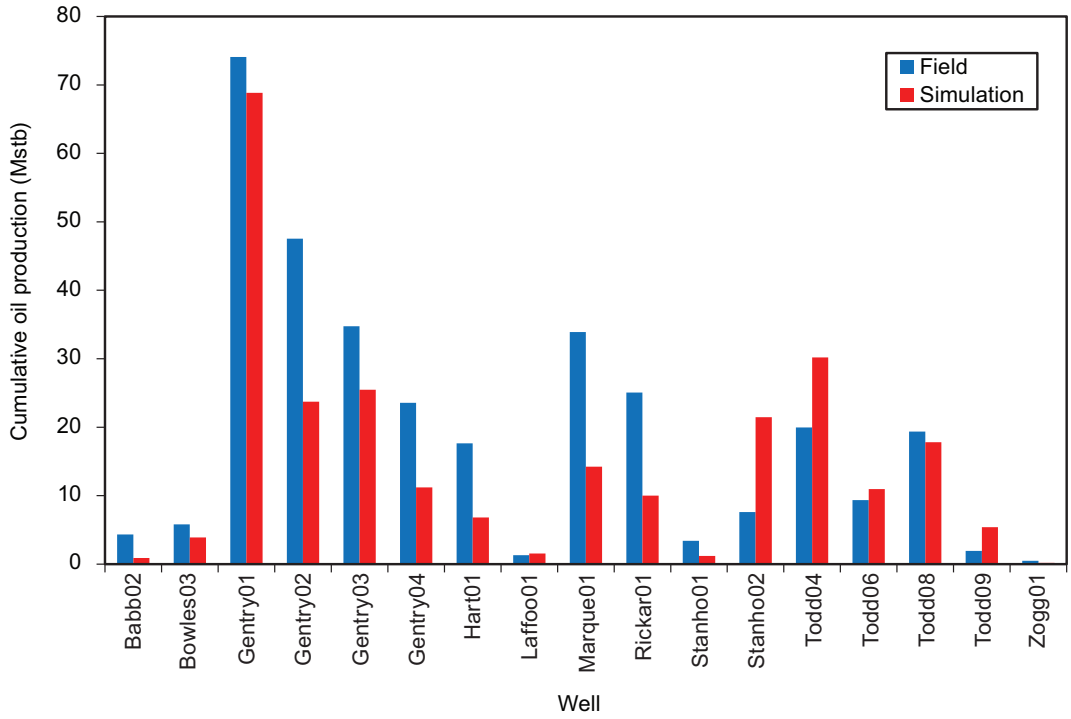

Figure 113 Comparison of simulated values and field data, by well, for oil production at the end of waterflooding.

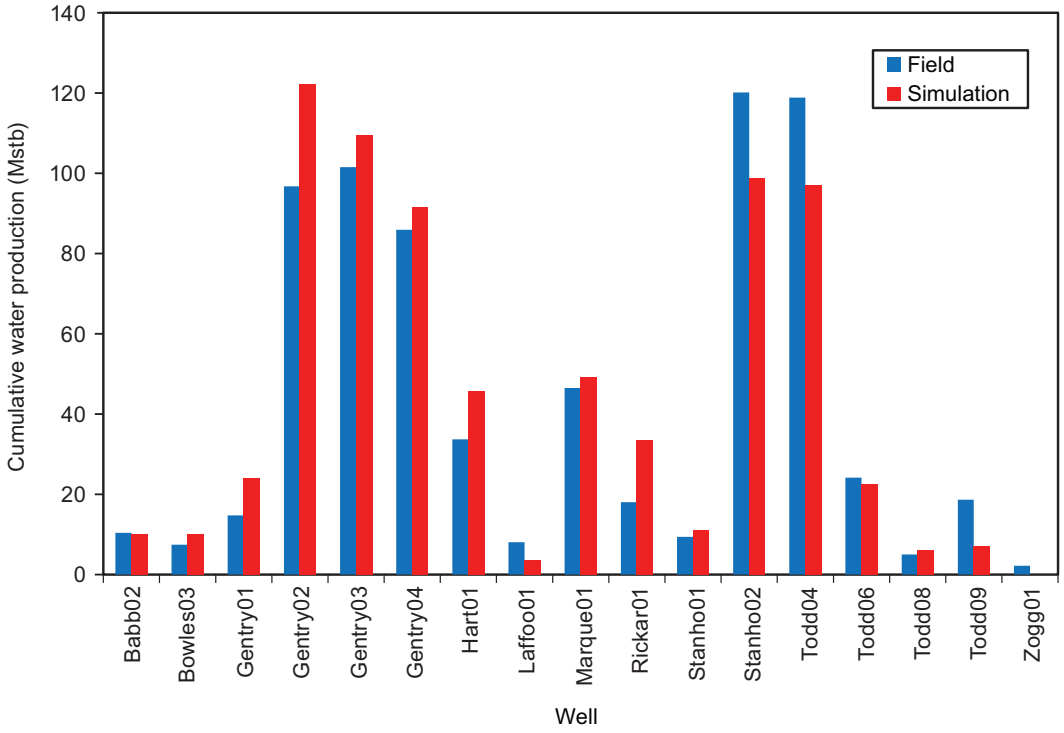

Figure 114 Comparison of simulated values and field data, by well, for water production at the end of waterflooding.

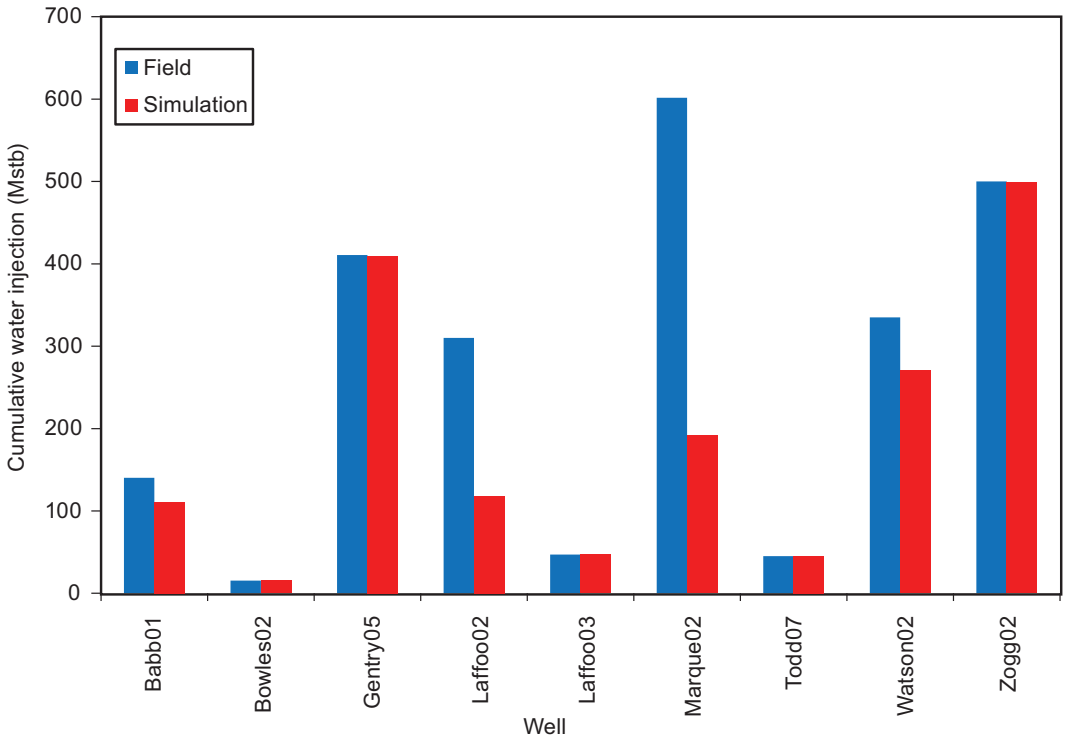

Figure 115 Comparison of simulated cumulative water injected and field data, by well, at the end of waterflooding.

and field cumulative oil production. However, a good match was achieved between the simulated and field cumulative water production (Figure 114). Figure 115 also shows irregularities between the simulated cumulative water injected during waterflooding and the field data (allocated water injection). By specifying total liquid production and matching oil and water production, it was not possible to match the early and late waterflood oil and water production simultaneously. More emphasis was placed on matching more recent data (1999 to 2010) to build a better model for matching data from the CO_2 injection pilot (Figure 116).

Additional modifications to the geologic model included the following:

Linear fault zones trending generally north and south were simulated by changing the transmissibility between cells. Length of zone, general direction, and magnitude of transmissibility were determined based on history match of affected wells and their respective production or injection. These modifications were added as a result of the relatively fast breakthrough of CO_2 during the pilot and geologists' interpretation of structure and isopach maps.

A low-permeability flow barrier between the upper and lower sand bodies was simulated by changing the transmissibility between model layers 5 and 6 across the model field. This was added as a result of geologists' concern with preliminary reservoir model that showed too much communication between wells that did not exhibit this historically in the field.

CO_2 Pilot CO_2 was injected into RG-5 for about one year, followed by water injection for 12 months. The simulated and field cumulative CO_2 injected were 6,572 tonnes (7,229 tons) and 6,560 tonnes (7,230 tons). The post-CO_2 injection simulated and field cumulative water injected was 2,650 m^3 (22,200 bbls) and 2,580 m^3 (21,600 barrels).

The modeled RG-5 CO_2 injection rates were matched (Figure 117); however, the breakthrough of CO_2 at various wells and CO_2 production rate were not matched. The simulated and field oil rates matched well (Figure 116).

Areal distribution (Figures 10-9a and b) and cross section (Figures 10-10a and b) of the injected CO_2 at the end of the CO_2 injection and after one year of water injection are shown at its greatest extent in layer 3 and by an orthogonal cross section through RG-5.

Explanation of Field Observations During CO_2 Injection

Early Gas Breakthrough at RG-2 The initial reservoir model did not predict the early breakthrough of CO_2 at RG-2 and the high CO_2 rate at PH-1. No geologic feature was identified on logs or core analyses that could cause the CO_2 production at these wells. Only the presence of a relatively small, relatively high permeability zone between these wells can explain this early CO_2 breakthrough. Therefore, a "fault or fracture zone" passing through RG-5 and passing near RG-2 and PH-1 was incorporated in the model. High transmissibility values were assigned to gridblocks intersected by the fault zone. To achieve CO_2 breakthrough earlier, a very high transmissibility layer within the fault zone connecting RG-2 and RG-5 was also included in the model; however, this was not adequate to have CO_2 breakthrough in one week. There are geologic features present in the Sugar Creek model that are not identified on logs or core analyses. Additionally, they may be smaller than the grid cells used in the model.

No Gas Breakthrough at WT-4, 8, and 9 A comparison of the reservoir characterization and the production history of the Gentry lease and the Todd lease indicated better reservoir quality at the Gentry lease. Also, the distance between RG-5 and the WT wells (>366 m; >1,200 ft) is much greater compared to the remaining RG wells (244–274 m [800–900 ft]). As a result, communication between the injection well in the Gentry lease and wells in the Todd lease may be limited by the differences in reservoir quality. Consequently, CO_2 breakthrough should be expected at wells in the Gentry lease prior to those in the Todd lease.

Pilot Projections Using Calibrated Model to Determine CO_2 Enhanced Oil Recovery, Storage, and Plume Size Distribution

In a pilot operation, oil rate increases and decreases occur for reasons other than the EOR process. In the Sugar Creek case, pre-injection oil rate increases occurred due to pilot well preparation, and oil rate

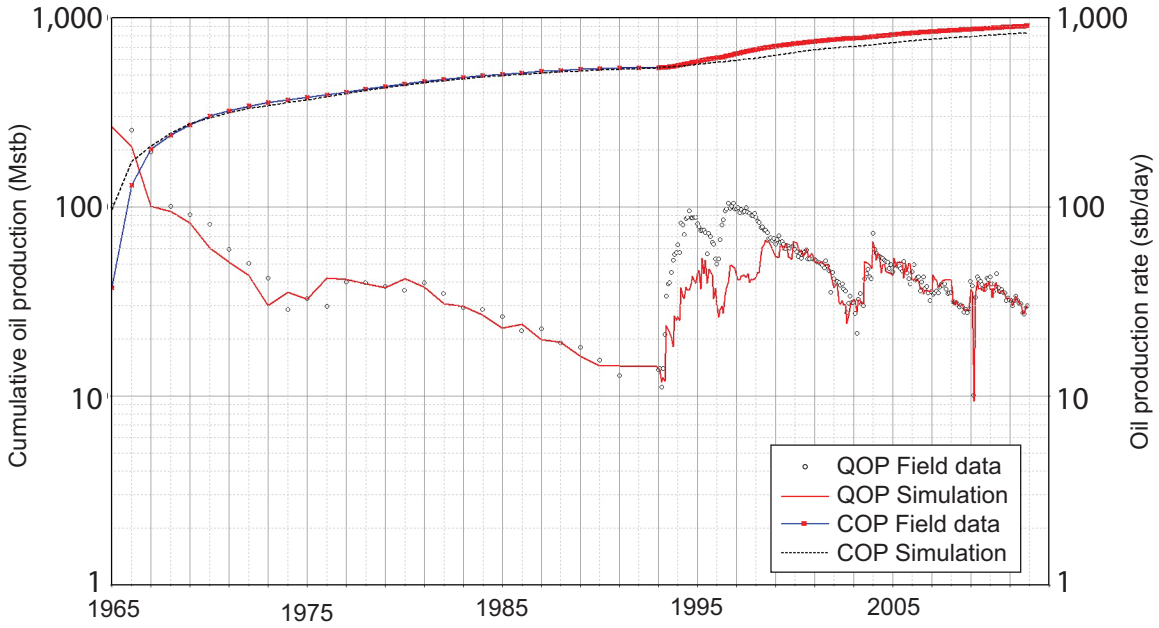

Figure 116 Simulated and field oil production rate (QOP) and cumulative oil production rate (COP).

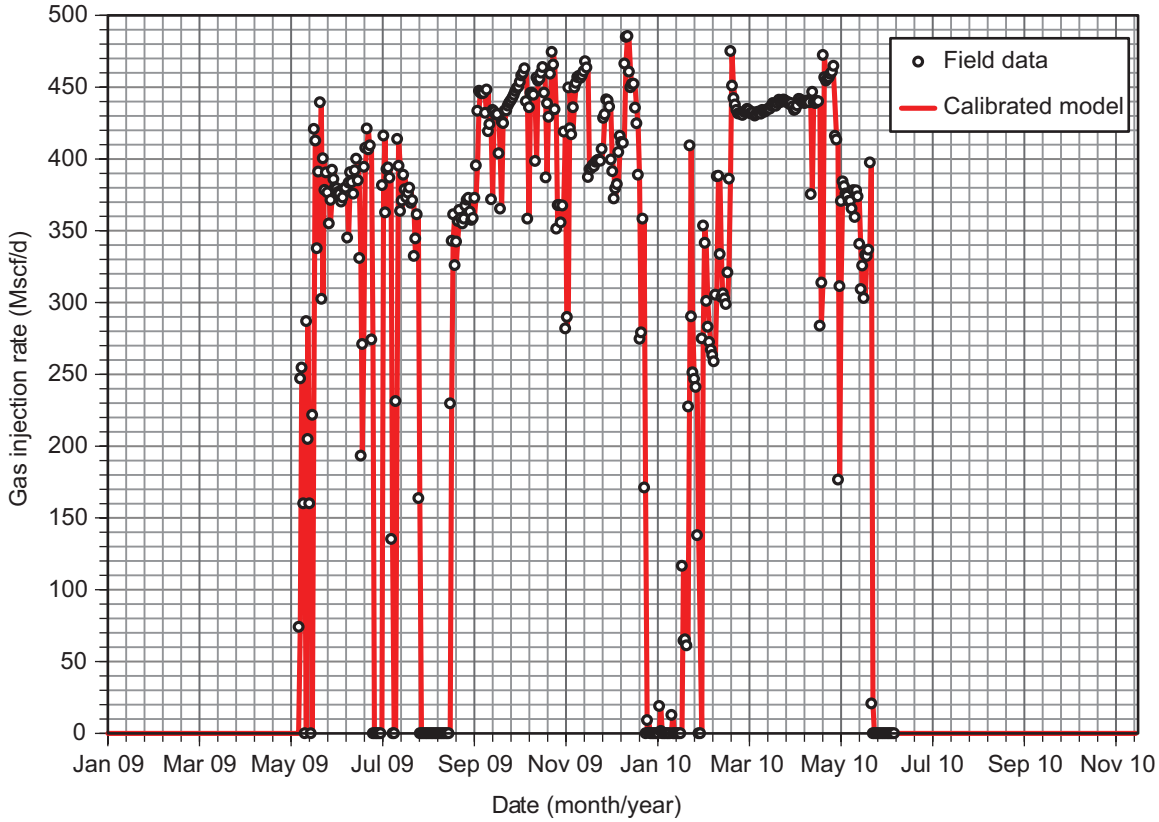

Figure 117 Simulated and field CO_2 injection rates for RG-5.

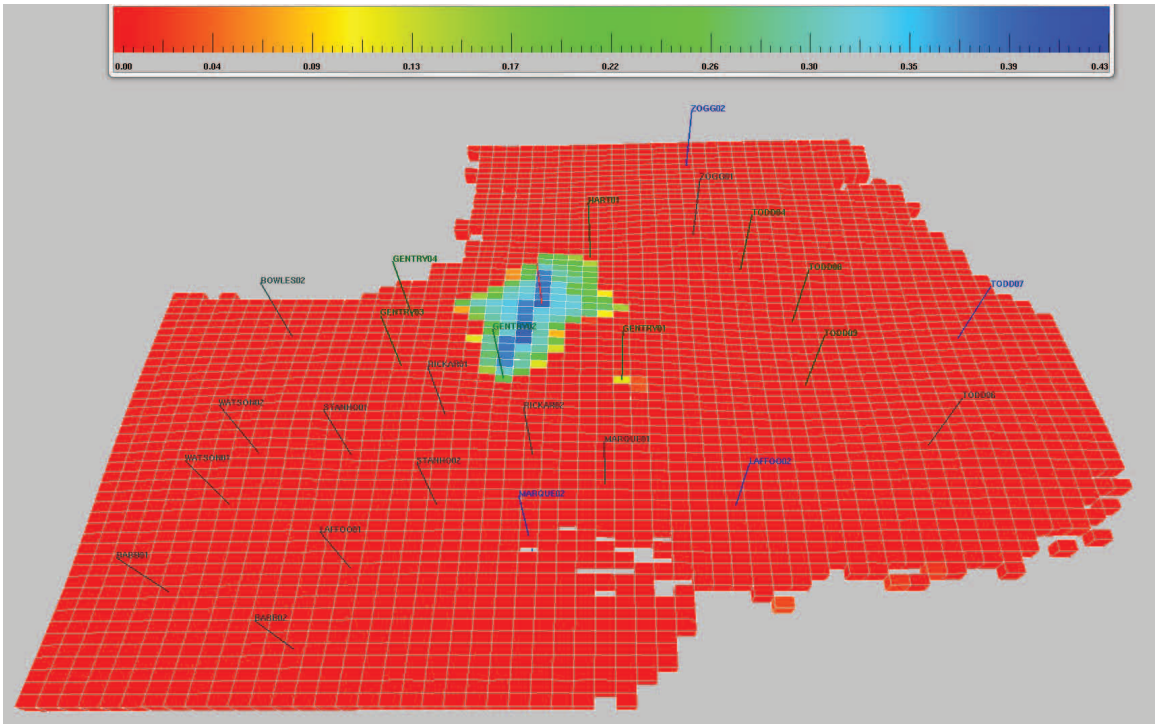

Figure 118a The CO_2 distribution in layer 3, displaying largest extent of CO_2 at the end of CO_2 injection.

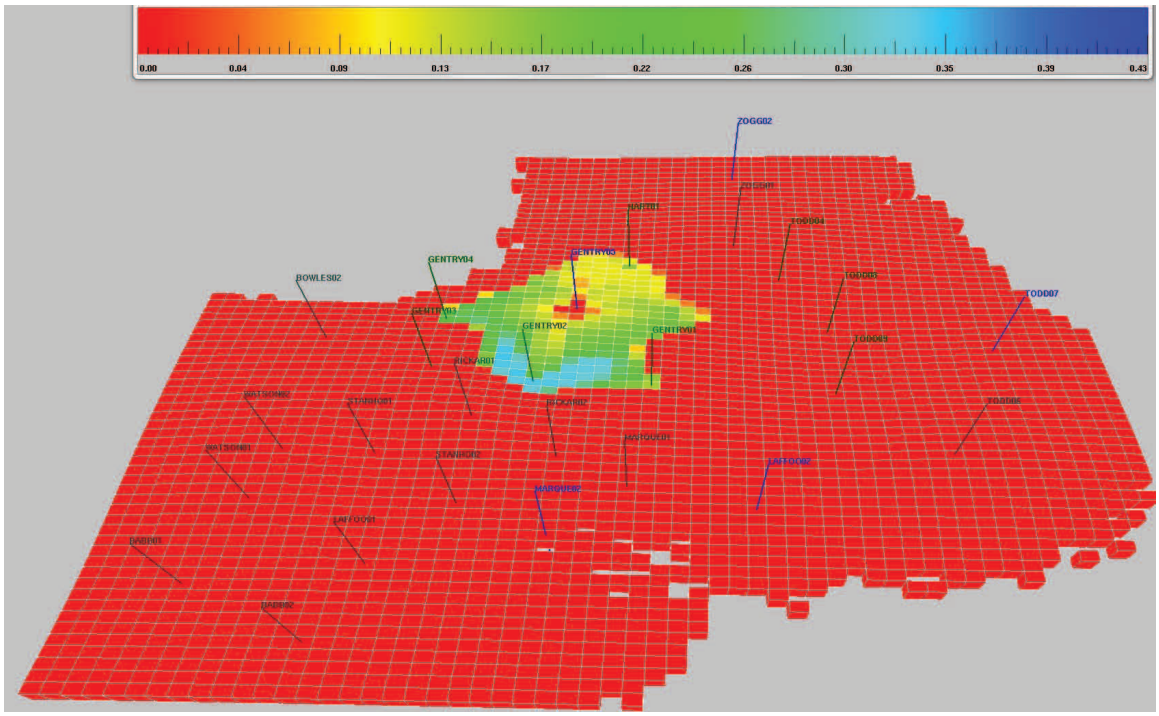

Figure 118b The CO_2 distribution in layer 3, displaying largest extent of CO_2 at the end of one year of water injection following one year of CO_2 injection.

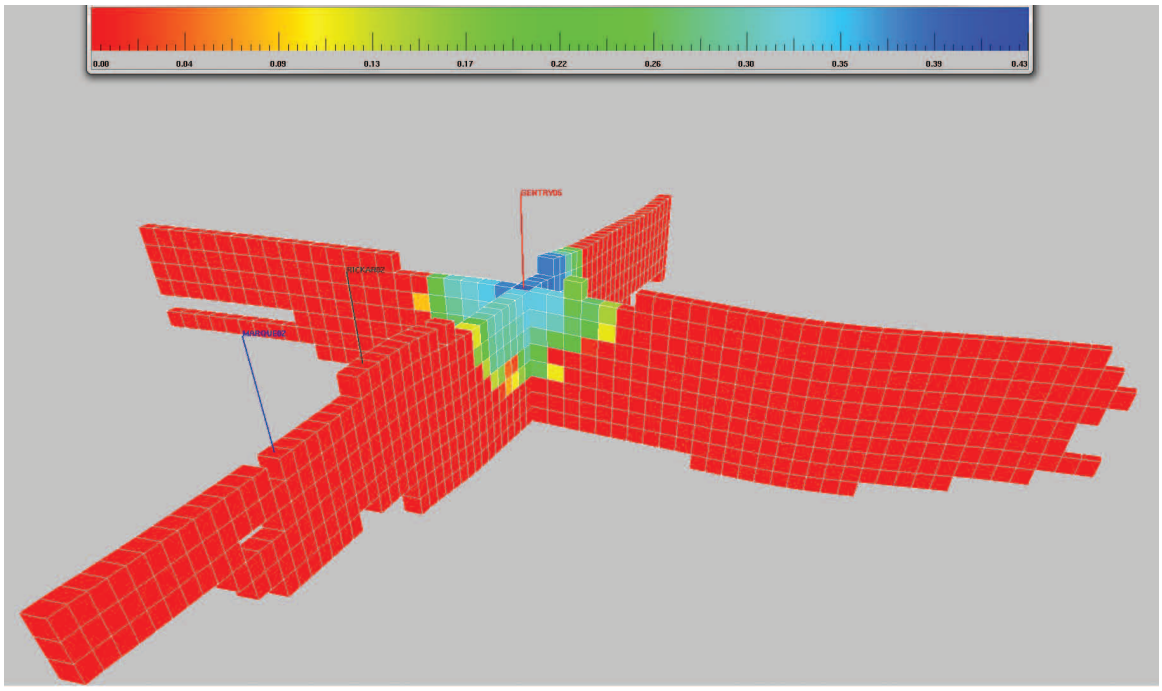

Figure 119a The CO_2 distribution in orthogonal cross-section through RG-5, displaying largest extent of CO_2 at the end of CO_2 injection.

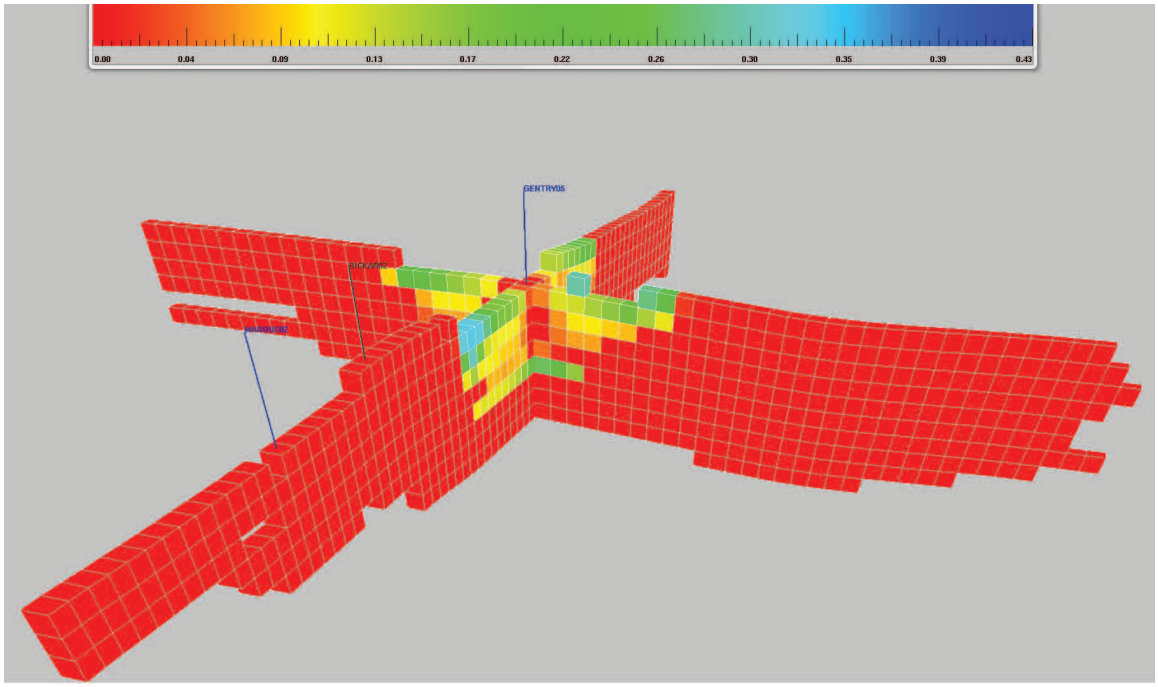

Figure 119b The CO_2 distribution in orthogonal cross-section through RG-5, displaying largest extent of CO_2 at end of one year of water injection following one year of CO_2 injection.

decreases occurred due to temporarily shutting-in wells and suspension of injection. The oil loss from these problems needs to be quantified and excluded from an estimate of CO_2 EOR.

The most significant operational problems that occurred were (1) loss of RG-2 production due to excessive flowline pressure due to CO_2 production rate, (2) loss of oil production when the injection line leaked and CO_2 injection was stopped, (3) loss of oil production when CO_2 delivery was halted due to icy road conditions, and (4) loss of oil production when the PH-1 downhole pump failed and was eventually removed so that the well could flow to the tank battery.

In addition to operational effects on oil production during this pilot, the daily delivery of CO_2 and budget constraints kept the field oil response to CO_2 from being maximized. RG-5 was injection rate constrained and not pressure constrained. Delivery of additional CO_2 each day would have allowed maximum injection rates. The logistics in planning truck delivery of CO_2 did not allow day-to-day changes in delivery, so a more regular plan was adopted (one truckload per day and a 2nd truckload every other day). Also, a larger CO_2 budget and injection period would have increased and sustained the field oil production rates.

To study the effect on oil recovery, CO_2 storage, and plume size and distribution on the pilot field results, the following scenarios were simulated in the two pilot cases:

- uninterrupted injection,
- longer period of continuous CO_2 injection,
- higher CO_2 injection rate, and
- increased injection pressure.

A waterflood baseline case was run to reflect similar scenarios. The CO_2 EOR cases were compared to their respective waterflood baselines to determine the incremental oil production, which was added to the decline curve projection of the actual field oil production rates.

Pilot Case 1: Continuous Production at RG-2 and PH-1 and Continuous Injection at Maximum Pressure at RG-5

In Pilot Case 1, production wells RG-2 and PH-1 are not shut-in. Injection of CO_2 at RG-5 is continuous, and bottomhole pressure constrained. The CO_2 injection is for 12 months only. This approach eliminates effects of CO_2 delivery schedule, injection interruptions due to bad weather, injection line leakages and repairs, and loss of RG-2 and PH-1 production due to flow line and maximum casing pressure constraints.

For this scenario, the calibrated model results presented in Table 28 show CO_2 EOR estimates of 1,300 to 6,300 scm (7,900 to 13,000 stb) oil production, which is an oil recovery of 1.7 to 2.7% of OOIP and a CO_2 net utilization of 410 to 520 scm/scm (2,300 to 2,900 scf/stb).

Pilot Case 2: Continuous Injection of CO_2 for 5 Years with Pilot Case 1 Approach

Using the Pilot Case 1 approach, CO_2 injection was continued for 5 years using bottom hole pressure constraints. Pilot Case 2 eliminates the effects of the duration and budget constraints of the first pilot case.

For this second scenario, the calibrated model results presented in Table 28 show CO_2 EOR estimates of 3,900 to 2,100 scm (24,530 to 39,390 stb) oil production, which is an oil recovery of 3.7 to 5.9% of OOIP and a CO_2 net utilization of 640 to 710 scm/scm (3,600 to 4,000 scf/stb).

Table 28 Enhanced oil recovery and CO_2 utilization for optimized pilot cases.

	Pilot Case 1		Pilot Case 2	
	Low	High	Low	High
EOR (stb)	7,920	12,690	24,530	39,390
EOR (%OOIP)	1.71	2.74	3.69	5.93
Net utilization (scf/stb)	2,330	2,900	3,620	4,010
Gross utilization (scf/stb)	23,690	29,560	38,170	47,530
CO_2 storage (tons)	1,078	2,147	5,180	9,218
CO_2 storage factor (Mscf/stb OOIP)	0.0399	0.0794	0.134	0.238

Full-Field Projections Using Calibrated Model to Determine CO_2 Enhanced Oil Recovery, Storage, and Plume Size Distribution

Based on the pilot-calibrated model, estimates of full-field implementation of CO_2 injection were of interest. Estimates were achieved by simulating three scenarios in which some water injectors are converted to CO_2 injectors, and temporarily abandoned wells are produced or injected with CO_2. Wells that are currently temporarily abandoned include AB-1, AB-2, PB-2, PB-3, EL-1, EL-3, BM-1, JR-1, JR-2, MS-1, MS-2, WT-6, RW-1, RW-2, and PZ-1. The Field Case 1 and 2 used all existing wells. Field Case 3 infill-drilled several new producing wells and converted many of the existing wells to CO_2 injection wells.

A waterflood baseline case was run to reflect similar scenarios. The CO_2 EOR cases were compared with its respective waterflood baselines to determine the incremental oil production, which was added to the decline curve projection of the actual field oil production rates (Figure 120).

The scenarios considered follow.

Field Case 1: Full-Field CO_2 Injection

In this case, RG-5 and all water injection wells, except PZ-2, were converted to CO_2 injection wells. PZ-2 was not considered for conversion because it is located far into the aquifer located at the north end of Sugar Creek. However, injecting CO_2 at PZ-2 might be beneficial for increasing CO_2 storage into the Jackson sandstone aquifer. CO_2 was injected continuously for 20 years at maximum pressure. All temporarily abandoned production wells were brought online.

Results presented in Table 29 suggest that expansion of simultaneous injection of CO_2 at all Sugar Creek water injection wells would increase oil recovery by 18,000 scm (113,000 stb) after 20 years of CO_2 injection. This is an oil recovery of 2.8% of OOIP and a CO_2 net utilization of 160 scm/scm (880 scf/stb). The potential CO_2 storage is estimated to be 5,200 tonnes (5,800 tons). Because of the relatively high perm or fault zones, sweep efficiency is lower in parts of the field. Also, a longer period of injection would increase oil production.

Field Case 2: Modified Full-Field CO_2 Injection

Field Case 2 is similar to Field Case 1 except that RG-4, RG-2, JR-2, MS-2, AB-2, WT-9, and PZ-1 production wells were also converted to CO_2 injectors.

Results presented in Table 29 suggest that expansion of simultaneous injection of CO_2 at all Sugar Creek water injection wells and some of the oil producing wells would increase oil recovery by 23,500 scm (148,000 stb) after 20 years of CO_2 injection. This is an oil recovery of 4.1% of OOIP and a CO_2 net utilization of 210 scm/scm (1,200 scf/stb). The potential CO_2 storage is estimated to be 9,500 tonnes (10,500 tons).

Field Case 3: Infill Drilling and 5-spot Pattern Full-Field CO_2 Injection

Field Case 3 is similar to Field Case 2 except that seven infill production wells are drilled across the field, almost all existing wells at Sugar Creek are converted to injection wells, and a few existing wells were relocated to improve well spacing within specific patterns.

By drilling new wells a better estimate of CO_2 EOR is possible, but at a substantial increase in well count. The effect was a total of 22 injection wells and 12 production wells on 11 regular 5-spot patterns.

Results presented in Table 29 suggest that expansion of simultaneous injection of CO_2 at almost all Sugar Creek wells and drilling new wells across the field would increase oil recovery by 27,700 scm (174,000 stb) after 20 years of CO_2 injection. This is an oil recovery of 5.5% of OOIP and a CO_2 net utilization of 160 scm/scm (880 scf/stb). The potential CO_2 storage is estimated to be 8,100 tonnes (8,900 tons).

Even though a lower recovery is obtained for Field Case 3 compared to Pilot Case 2, a larger volume of oil is produced in the former than in the latter. This is partly due to the longer duration of the field cases, but also because the field cases are full-field and therefore have different reservoir volume and OOIP estimates.

Table 29 EOR and CO_2 utilization for optimized fieldwide cases.

	Field Case 1	Field Case 2	Field Case 3
EOR (stb)	112,671	147,886	173,976
EOR, % OOIP	2.8	4.1	5.5
Net Utilization (scf/stb)	880	1,214	876
Gross Utilization (scf/stb)	23,993	19,452	24,892
CO_2 Storage (tons)	5,785	10,479	8,893
CO_2 Storage Factor, (Mscf/stb-OOIP)	0.0247	0.0502	0.0485
Storage Efficiency, % HCPV*	12.6	22.3	20.6
EOR as % of primary and waterflood production	12.9	16.9	19.9

* Hydrocarbon pore volume

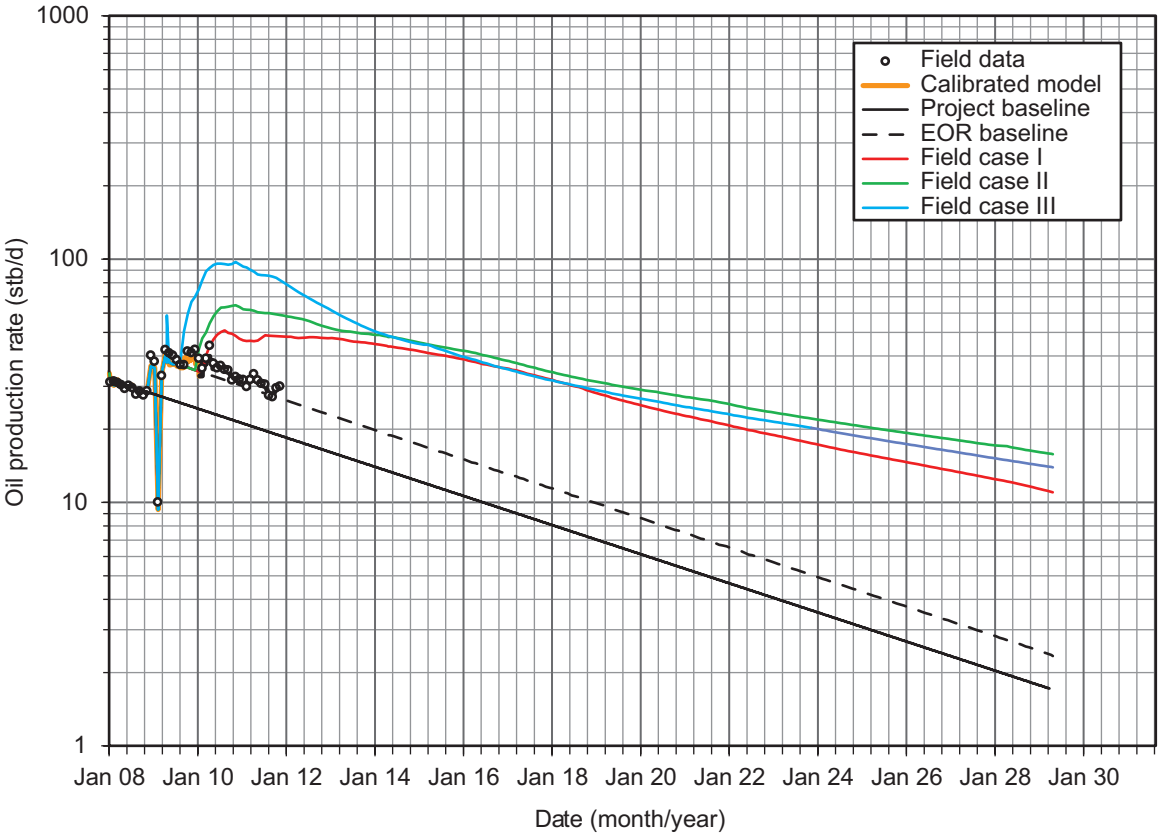

Figure 120 Decline curve projections for CO_2 EOR cases.

Modeling Summary

The pilot case in general has many more producers than injectors and results in a very low pressure for the area immediately surrounding RG-5. The pressure is relatively low at 2.76 MPa (400 psia); the CO_2 flood simulated is immiscible. The low CO_2 storage and oil recovery values in Table 10-4 show this. Similar to conclusions from the MGSC Phase I modeling, the net utilization of CO_2 was also significantly lower than for a miscible flood.

The field case results were similar to the pilot area. CO_2 EOR and storage were higher because of the area. The normalized values of recovery, utilization, and storage factor were similar. Average pressure for the field cases was slightly higher at 3.4 to 4.5 MPa (500 to 650 psia). Field Case 2 and 3 had nearly twice the CO_2 storage efficiency of Field Case 1, primarily due to the addition of more injection wells and injected CO_2 volume.

The oil recovery estimated from the Sugar Creek Field Case 3 compares well to the MGSC Phase I estimates of 4.5 to 7.1%. The CO_2 net utilization is low relative to MGSC Phase I results (250 to 960 scm/scm; 1,400 to 5,400 scf/bbl). A low net utilization means that it takes less CO_2 to recover oil compared to a higher net utilization; moreover, a high net utilization is indicative of storage of CO_2 per barrel of oil produced. A comparison of CO_2 EOR to the cumulative primary and waterflood oil production ranges from 13 to 20% (Table 29). For miscible CO_2 floods in West Texas, a rule-of-thumb is 25% of cumulative production. For immiscible modeling results, the Sugar Creek model compares favorably to this production based rule-of-thumb.

PILOT CLOSURE

Sugar Creek Field remained in operation under waterflooding conditions after completion of the CO_2 injection pilot, so relatively little in the way of site reclamation was required. Pilot closure consisted primarily of plugging and abandoning the groundwater monitoring wells, removing data acquisition equipment from the injection and production wells, and relocating injection equipment from the site.

Plugging and Abandonment of Groundwater Monitoring Wells

Groundwater monitoring wells were plugged and abandoned in October 2011. As required by Kentucky regulations, the plugging and abandonment of the monitoring wells was done by a Kentucky Certified Monitoring well driller. Each monitoring well was over-drilled so as to remove all PVC casing, grout seal, screen, and sand pack. Once all materials were removed, each borehole was filled with bentonite pellets from the bottom of the borehole to land surface.

Removal of Data Acquisition Equipment

Surface and downhole pressure and temperature gauges were removed from the wells in late September and early October 2011. The gauges' calibration was checked to confirm accurate pressure data were recorded.

Relocation of Injection Equipment

After completion of CO_2 injection, the injection pump skid and line heater were removed from the Sugar Creek tank battery area. A fence at the Sugar Creek tank battery was moved before CO_2 injection in order to accommodate the CO_2 storage tanks and other equipment. This fence was moved back to its original location after CO_2 injection was complete.

CONCLUSIONS

Enhanced Oil Recovery Estimate

Based on reservoir and geologic modeling, the implementation of fullfield CO_2 EOR at Sugar Creek Field would be 3 to 4% of OOIP or 17,500 to 24,000 scm (110,000 to 150,000 stb), with a CO_2 net utilization of 160 to 220 scm/scm (880 to 1200 scf/bbl).

This oil recovery is the low range of the 4 to 5% based on West Texas rules-of-thumb and the 4.5 to 7.1% from MGSC Phase I results. The net utilization is also low relative to the West Texas rules-of-thumb (900 to 1,800 scm/scm; 5,000 to 10,000 scf/bbl) and MGSC Phase I results (250 to 960 scm/scm; 1,400 to 5,400 scf/bbl).

CO_2 Storage Estimate

Assuming 100% recycling of produced CO_2, the CO_2 storage efficiency factor of the Jackson sandstone of the Sugar Creek oil field is 13 to 22% of HCPV. This is lower than MGSC RCSP Phase I results and is attributed to the geologic heterogeneity present in Sugar Creek Field. An estimated 1,028 tonnes (1,133 tons) of CO_2 were produced at the surface from wells and the gas separator between the start of CO_2 injection and the end of September 2011. This amount represented about 16% of the injected CO_2. Exact measurement of CO_2 production proved problematic due to technical concerns. Consequently, 84% of the injected CO_2 was stored at the Sugar Creek field after one year of post-CO_2 injection monitoring. The potential CO_2 storage is estimated to be 5,200 to 9,500 tonnes (5,800 to 10,500 tons).

General Observations

Oil production directly from the field was immediately affected by all shut-in periods of CO_2 injection. After the lengthier shut-in due to the flow line leak and poor road conditions, the oil rate did not reach the pre-shut in level. The reason for the reduction in oil rate is not certain but it is likely due to reduction in pressure which caused expansion of in situ CO_2 and decrease in solubility of CO_2 in the oil at reservoir pressure and temperature. It is likely that any oil bank that was created by the CO_2 was compromised and was not achieved again after CO_2 injection resumed.

Chemical treatment was effective in minimizing corrosion related to CO_2 and may have contributed to the low workover rate required during the 2 years of operations.

Establishing a CO_2 EOR oil production baseline is difficult when pre-CO_2 injection well work is required to prepare wells for the pilot. Optimally, well work would occur several months before start-up so that the baseline could be identified more clearly.

Geologic features are present in the reservoir sandstone that were not identified on logs or core analyses. These features are likely responsible for the early breakthrough of CO_2 at RG-2 and the relatively high volume of CO_2 at PH-1.

Effectiveness of Operations

Overall the operations were effective at meeting the project objectives with the given budget and project duration constraints. In general, pilots that have multiple injectors and patterns can give better representation of actual full-field deployment of CO_2 injection than a single injection well pilot.

An injection skid was designed and built that worked similarly to waterflood operations in the Illinois Basin. Consequently, an oil field operator familiar with waterflooding technology may find this design similar to currently used water injection equipment. The data acquisition system allowed for remote monitoring of operations such that a 24-hour operator was not required.

Real operational problems were encountered which was beneficial to improve the general understanding of CO_2 EOR. These problems were unavoidable but could have had lower impact on oil production if more wells and patterns had been involved in the pilot.

Effectiveness of Techniques for Monitoring, Verification, and Accounting

Measurements of groundwater chemistry before, during, and after CO_2 injection confirmed that shallow Pennsylvanian aquifers at the Sugar Creek pilot site were not affected by CO_2 injection. Measurements of brine and gas chemistry in the Jackson sandstone oil reservoir over the same period were successful in tracking the path of CO_2 migration. Moreover, the measurements provided sufficient data from which to infer the potential trapping of CO_2 through solubility trapping and to infer geochemical reactions among CO_2, brine, and rock-forming minerals.

Pre-injection brine characterization had an important role in reservoir characterization. pH measurements in the field are relatively simple and reliable for early indication of CO_2 breakthrough.

RECOMMENDATIONS

CO_2 EOR will always result in CO_2 production. In the CO_2 EOR process the volume of CO_2 stored will always be less than the volume injected even when produced CO_2 is recycled. It is unreasonable to expect that all injected CO_2 can be accounted for in an active oil field operation. Leaks around producing and injection wellheads and related plumbing, injection line leaks, well workovers, and cased hole logging procedures all have CO_2 leaving the CO_2 EOR system of reservoir, wells, and surface facilities. Some type of general and reasonable accounting guidelines for various types of CO_2 releases must be developed to account for the released CO_2 but not necessarily exactly quantify it for a specific event. For example, a producing well may be assigned a specific value of released CO_2 via a leaky wellhead based on its CO_2 production rate. Additionally, well workovers may be assigned a certain mass of CO_2 release instead of attempting to devise some means of measuring CO_2 that would be nearly impossible to meter and quantify during a well workover. Organizations and societies that deal with auditing (e.g., American Institute of Certified Public Accountants) have general guidelines for other industries that can likely be adapted to CO_2 sequestration in general and specifically to oil field EOR projects.

More single well production tests would improve the rate allocation at each well. The method for allocating the oil and water rates to each well was suspect and introduced an unquantifiable amount of uncertainty into the analysis of the pilot performance. A better constraint on the amount of oil and water produced at each well would greatly improve the reservoir model calibration as well as the assessment of the overall of the pilot performance.

More regular delivery of CO_2 would have maintained the injection at the regulated bottomhole pressure and kept average reservoir pressure higher which would have improved oil recovery. However, flow line breaches and poor road conditions were unavoidable and adversely affected direct measurements of CO_2 EOR. Additional injection wells with dedicated injection lines could eliminate operations-related problems.

Surface measurement of produced gas was made through well testers that required back pressure to use correlation to calculate gas rate. The pressure gauges used at this site were significantly affected by surface temperature and caused problems in the analyses of gas production. Also, in general the buildup of casing gas pressure in producing wells should be avoided to minimize excessive pressure on the casing, which could lead to a casing breach or force gas into the rod pump and cause gas-lock. Metering of produced water was deemed impossible due to foreign material in the brine and plugging and clogging of the meters.

To improve the geologic model and understanding of producing wells in hydraulic communication with specific injection wells, water injection tracers, and/or injection pulse tests would be very useful. Additional core samples would greatly improve the understanding of the geology at the site in addition to improving the characterization of the reservoir petrophysical properties. The absence of physical specimens for examination prevented any meaningful interpretation of geologic environment of deposition.

REFERENCES

Bethke, C.M., and S. Yeakel. 2007. The Geochemist's Workbench, Release 7.0: Reaction Modeling Guide: Urbana, University of Illinois Urbana-Champaign, 84 pp.

Buschbach, T.C., and D.R. Kolata. 1990. Regional setting of the Illinois basin, *in* M.W. Leighton, D.R. Kolata, D.F. Oltz, and J.J. Eidel, eds., Interior Cratonic Basins: AAPG Memoir 51, pp. 29–55.

Charlton, S.R., and D.L. Parkhurst. 2002. PhreeqcI—A graphical user interface to the geochemical model PHREEQC: Reston, VA, U.S. Geological Survey Fact Sheet FS-031-02, 2 pp.

Chopra, A.K., M.H. Stein, and C.T. Dismuke. 1990. Prediction of performance of miscible-gas pilots: Journal of Petroleum Technology, vol. 42, no. 12, pp. 1564-72.

Cotton, F.A., and G. Wilkinson. 1976. Basic Inorganic Chemistry: New York City, John Wiley and Sons, 579 pp.

Craig, H. 1953. The geochemistry of the stable carbon isotopes: Geochimica et Cosmochimica Acta, vol. 3, pp. 53–92.

Davis, R.W., R.O. Plebuch, and H.M. Whitman. 1974. Hydrology and geology of deep sandstone aquifers of Pennsylvanian age in part of the western coal field region, Kentucky: Lexington, KY, Kentucky Geological Survey, Series 10, Report of Investigation 15, 26 pp.

Frailey, S.M., I.G. Krapac, J.R. Damico, R.T. Okwen, and R.W. McKaskle. 2012a. CO_2 Storage and Enhanced Oil Recovery: Bald Unit Test Site, Mumford Hills Oil Field, Posey County, Indiana, J.H. Goodwin and C.C. Monson (eds.): Illinois State Geological Survey, Open File Series 2012-5, 172 pp.

Frailey, S.M., D.G. Morse, I.G. Krapac, and R.W. McKaskle. 2012b. Sequestration and Enhanced Coal Bed Methane: Tanquary Farms Test Site, Wabash County, Illinois, C.C. Monson (ed.), Illinois State Geological Survey, Open File Series 2012-2, 182 pp.

Freeze, J.A., and R.A. Cherry. 1979. Groundwater: Upper Saddle River, NJ, Prentice Hall, 604 pp.

Gildersleeve, B., and W.D. Johnson, Jr. 1978. Geologic map of the Spring Lick quadrangle, western Kentucky: Reston, VA, U.S. Geological Survey, scale 1:24,000.

Goudarzi, G.H., and A.E. Smith. 1968. Geological map of the Dundee quadrangle, Ohio County, Kentucky: Reston, VA, U.S. Geological Survey, scale 1:24,000.

Grube, J., and W.T. Frankie. 1999. Reservoir characterization and its application to improved oil recovery from the Cypress Formation (Mississippian) at Richview Field, Washington County, Illinois: Champaign, IL, Illinois State Geological Survey, Illinois Petroleum 155, 39 pp.

Hackley, K.C., S.V. Panno, H.H. Hwang, and W.R. Kelly. 2007. Groundwater quality of springs and wells of the sinkhole plain in southwestern Illinois: Determination of the dominant sources of nitrate: Champaign, IL, Illinois State Geological Survey, Circular 570, 39 pp.

Haitjema, H.M. 1985. Modeling three-dimensional flow in confined aquifers by superposition of both two- and three-dimensional analytic functions: Water Resources Research, vol. 21, no. 10, pp. 1557–1566.

Hem, J.D. 1992. Study and interpretation of the chemical characteristics of natural water: Reston, VA, U.S. Geological Survey Water Supply Paper 2254, 264 pp.

Henry, R.L. and R.S. Metcalfe. 1983. Multiple-phase generation during carbon dioxide flooding: Society of Petroleum Engineering Journal, vol. 23, no. 4, pp. 595–601.

Journel, A.G. 1974. Geostatistics for conditional simulation of ore bodies: Economic Geology, vol. 69, no. 5, pp. 673–687.

Kehn, T.M. 1964. Geology of the Madisonville West quadrangle, Kentucky: Reston, VA, U.S. Geological Survey Geologic Quadrangle Map GQ-346, scale 1:24,000.

Kharaka, Y.K., D.R. Cole, S.D. Hovorka, W.D. Gunter, K.G. Knauss, and B.M. Freifeld. 2006a. Gas-water-rock interactions in Frio Formation following CO_2 injection: Implications for the storage of greenhouse gases in sedimentary basins: Geology, vol. 34, pp. 577–580.

Kharaka, Y. K., D. R. Cole, J.J. Thordsen, E. Kakouros, and H.S. Nance. 2006b. Gas-water-rock interactions in sedimentary basins: CO_2 sequestration in the Frio Formation, Texas, USA: Journal of Geochemical Exploration, vol. 89, pp. 183–186.

Linick, T.W., P.I. Damon, D.J. Donahue, and A.J.T. Lull. 1989. Accelerator mass spectrometry: The new revolution in radiocarbon dating: Quaternary International, vol.1, pp. 1–6.

Lovley, D.R., and E.J.P. Phillips. 1988. Novel mode of microbial energy metabolism: Organic carbon oxidation coupled to dissimilatory reduction of iron or manganese: Journal of Applied and Environmental Microbiology, vol. 54, no. 6, pp. 1472–1480.

Martin, G.R. 2002. Estimating Mean Annual Streamflow of Rural Streams in Kentucky: Reston, VA, U.S.Geological Survey, Water-Resources Investigations Report 02-4206, 35 pp.

Matheron, G. 1973. The intrinsic random functions and their applications. Advances in Applied Probability, vol. 5, no. 3, pp. 439–468.

Mehnert, E., W.S. Dey, H.H. Hwang, D.A. Keefer, T.R. Holm, T.M. Johnson, W.C. Beaumont, M.C.F. Wander, R.A. Sanford, J.M. McDonald and S.M. Shiffer. 2005. Mass balance of nitrogen and phosphorus in an agricultural watershed: The shallow groundwater component. Champaign, IL, Illinois State Geological Survey, Open File Report 2005-3, 121 pp.

Midwest Geological Sequestration Consortium. 2005. An Assessment of Geological Carbon Sequestration Options in the Illinois Basin. DOE Report, DE-FC26-03NT41994, 581 pp. (Issued December 31, 2005.)

National Energy Technology Laboratories. 2009. Monitoring, verification, and accounting of CO_2 stored in deep geologic formations. DOE Report, 311/081508, 132 pp. (Issued January 2009.)

Ostlund, H.G., and H.G. Dorsey. 1977. Rapid electrolytic enrichment and hydrogen gas proportional counting of tritium, *in* Low-Radioactivity Measurements and Applications: Proceedings of the International Conference on Low-Radioactivity Measurements and applications, October 6–10, 1975, The High Tatras, Czechoslovakia, Slovenske Pedagogicke Nakladatel'stvo, Bratislava, pp. 55–60.

Palandri, J. L., and Y. K. Kharaka. 2004. A compilation of rate parameters of water-mineral interaction kinetics for application to geochemical modeling: Menlo Park, CA, U.S. Geological Survey, Open File Report 2004-1068.

Palmer, J.E. 1967. Geologic map of the Saint Charles Quadrangle, Hopkins and Christian Counties, Kentucky: Reston, VA, U.S. Geological Survey Geologic Quadrangle Map GQ-674, scale 1:24,000.

Parkhurst, D.L., and C.A.J. Appelo. 1999. User's guide to PHREEQC (Version 2) —A computer program for speciation, batch-reaction, one-dimensional transport, and inverse geochemical calculations: Reston, VA, U.S. Geological Survey, Water-Resources Investigations Report 99-4259, 312 pp.

Ruhl, K.J., and G.R. Martin. 1991. Low-Flow Characteristics of Kentucky Streams: Reston, VA, U.S. Geological Survey, Water-Resources Investigations Report 91-4097, 50 pp.

Sable, E.G., and G.R. Dever, Jr. 1990. Mississippian rocks in Kentucky: Reston, VA, U.S. Geological Survey Professional Paper 1503, 125 pp.

Schumacher, A.M., T.M. Parris, and A. Fryar. 2010. Modeling of CO_2-water-rock interactions in Mississippian sandstone and carbonate reservoirs of Kentucky. Geological Society of America, North-Central and South-Central Section 2010 Meetings, April 11–13, Branson, MO, Abstracts with Programs, vol. 42, no. 2, p. 52.

Stuiver, M., and H.A. Polach. 1977. Reporting of C-14 data—Discussion: Radiocarbon, vol. 19, no. 3, pp. 355–363.

Vaughn, B.H., E.R. Crosson, J.W.C. White, and C. Sweeney. 2008. Wavelength-scanned cavity ring down spectroscopy: Opening new doors for tracing water isotopes in the hydrosphere, biosphere, and atmosphere. American Geophysical Union, Fall Meeting 2008, December 15–19, San Francisco, CA, Abstract #A23C-0311.

William, H.R., E. Atherton, T.C. Buschbach, C. Collinson, J.C. Frye, M.E. Hopkins, J.A. Lineback, and J.A. Simon. 1975. Handbook of Illinois Stratigraphy: Champaign, IL, Illinois State Geological Survey, Bulletin 95, 261 pp.

Wimmer, B.T., I.G. Krapac, R. Locke, and A. Iranmanesh. 2011. Applying monitoring, verification, and accounting techniques to a real-world, enhanced oil recovery operational CO_2 leak: Energy Procedia, vol. 4, pp. 3330–3337.

Appendix 1 Injection permit.

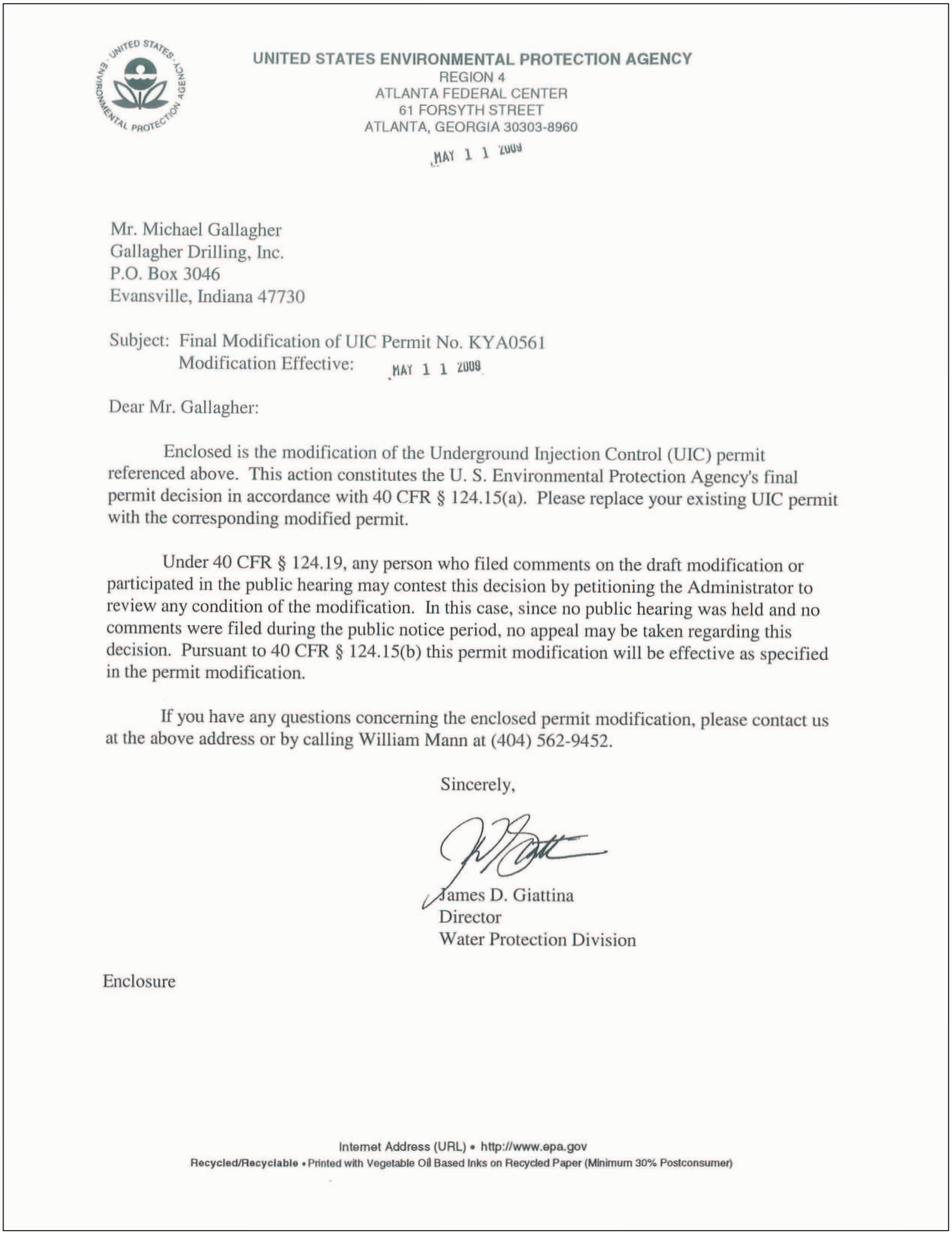

UNITED STATES ENVIRONMENTAL PROTECTION AGENCY
REGION 4
ATLANTA FEDERAL CENTER
61 FORSYTH STREET
ATLANTA, GEORGIA 30303-8960

MAY 11 2009

Mr. Michael Gallagher
Gallagher Drilling, Inc.
P.O. Box 3046
Evansville, Indiana 47730

Subject: Final Modification of UIC Permit No. KYA0561
Modification Effective: MAY 11 2009

Dear Mr. Gallagher:

Enclosed is the modification of the Underground Injection Control (UIC) permit referenced above. This action constitutes the U. S. Environmental Protection Agency's final permit decision in accordance with 40 CFR § 124.15(a). Please replace your existing UIC permit with the corresponding modified permit.

Under 40 CFR § 124.19, any person who filed comments on the draft modification or participated in the public hearing may contest this decision by petitioning the Administrator to review any condition of the modification. In this case, since no public hearing was held and no comments were filed during the public notice period, no appeal may be taken regarding this decision. Pursuant to 40 CFR § 124.15(b) this permit modification will be effective as specified in the permit modification.

If you have any questions concerning the enclosed permit modification, please contact us at the above address or by calling William Mann at (404) 562-9452.

Sincerely,

James D. Giattina
Director
Water Protection Division

Enclosure

Internet Address (URL) • http://www.epa.gov
Recycled/Recyclable • Printed with Vegetable Oil Based Inks on Recycled Paper (Minimum 30% Postconsumer)

Injection permit.

MODIFICATION OF

U. S. ENVIRONMENTAL PROTECTION AGENCY
UNDERGROUND INJECTION CONTROL PERMIT
AUTHORIZATION TO OPERATE CLASS II INJECTION WELLS
EPA UIC PERMIT NUMBER KYA0561

Pursuant to the Underground Injection Control regulations of the U. S. Environmental Protection Agency codified at Title 40 of the Code of Federal Regulations, Parts 124, 144, 146, and 147,

Gallagher Drilling, Inc.
P.O. Box 3046
Evansville, Indiana 47730

is hereby authorized to operate, and plug and abandon six existing Class II enhanced recovery injection wells in:

Sugar Creek Field
Hopkins County, Kentucky
Approximate center of project at
Carter Coordinate 25-J-24
1600' FNL x 1600' FWL

This authorization is in accordance with the limitations, monitoring requirements and other conditions as set forth in the original permit. This modification permit consists of this cover sheet; Part I, 8 pages; and Part II, 13 pages.

All references to Title 40 of the Code of Federal Regulations are to regulations that are in effect on the date that this permit modification becomes effective.

This modification permit shall become effective on MAY 1 1 2009.

This permit modification and the authorization to inject shall remain in full force and effect during the operating life of the well unless otherwise modified, revoked and reissued, terminated or a minor modification is made as provided at 40 CFR §§ 144.39, 144.40 and 144.1. This permit shall be reviewed at least once every five years from the effective date.

MAY 1 1 2009
Date

James D. Giattina, Director
Water Protection Division
U. S. Environmental Protection Agency
Region 4

PART I

WELL SPECIFIC CONDITIONS

SECTION A. AREA AND WELLS AUTHORIZED

1. Area Within Which Underground Injections are Authorized

The permittee is authorized to convert, operate and plug and abandon six enhanced recovery injection wells in Sugar Creek Field. This project area is described in the UIC Permit Application, with an approximate center at Carter Coordinate 25-J-24 leases.

2. Specific Wells Authorized for Conversion and Operation

The following wells are specifically authorized by this permit for conversion and operation within the permitted area:

Lease and Well No.	Carter Coordinate	Location
Bowles #2	25-J-24	1800' FNL x 0075' FWL
Gentry #5	25-J-24	1350' FNL x 1300' FWL
Lafoon #2	25-J-24	2650' FSL x 2220' FWL
Marquess #2	25-J-24	2300' FSL x 1350' FWL
Pressley (Zogg) #2	16-J-24	0420' FSL x 2140' FWL
Todd #7	25-J-24	1740' FNL x 1380' FEL

3. Construction of Additional Injection Wells

The permittee is authorized to construct, convert, operate or plug and abandon additional enhanced recovery wells within the permitted area provided:

(a) The permittee notifies the Director sixty (60) days, or less if approved by the Director, before construction or conversion is scheduled to begin; and

(b) The permittee submits, with his notification to construct or convert, all information required under 40 C.F.R. Part 146 to demonstrate how the additional well will meet the construction, operating, monitoring, reporting, and plugging and abandonment requirements of this permit; and

(c) The permittee, to the satisfaction of the Director, demonstrates that the cumulative impacts of drilling or operating the additional well will not result in the movement

of fluids into or between underground sources of drinking water; and

(d) The permittee obtains approval from the Director before beginning construction or conversion.

If the Director determines that any additional well constructed or converted pursuant to this section does not satisfy the requirements listed in (a) through (d) above, the Director may modify this permit under 40 CFR § 144.39, terminate it under 40 CFR § 144.40, or take enforcement action.

SECTION B. CONSTRUCTION REQUIREMENTS

1. Casing and Cementing

The permittee shall case and cement each well and maintain all casing and cement so as to prevent the movement of fluids into or between underground sources of drinking water. Conversion of each well shall be performed as described in Attachments L and M of the permit application.

2. Tubing and Packer

Injection may only take place through tubing with a packer set within the casing no higher than the depth given below for each specific well authorized by this permit under Part I, Section A, Item 2. The tubing and packer shall be maintained in a manner which is compatible with the injection operation specified in Part I, Section C, and to prevent the movement of fluids into or between underground sources of drinking water.

Lease and Well No.	Minimum Packer Depth, Feet Below Land Surface
Bowles #2	1790
Gentry #5	1817
Lafoon #2	1794
Marquess #2	1781
Pressley (Zogg) #2	1802
Todd #7	1802

3. Logs, Tests and Reports

The following logs, tests and reports shall be prepared and submitted to EPA for wells specifically authorized under Part I, Section A, Item 2. Logging and testing requirements or wells authorized under Part I, Section A, Item 3 will be prescribed by the Director

before drilling or conversion of such wells begins.

(a) A demonstration of the mechanical integrity of the well is required before injection can be authorized. The demonstration will consist of a pressure test on the tubing/casing annulus to at least 300 psig with less than three percent (3%) pressure loss in 30 minutes. The permittee shall contact EPA to arrange a date to conduct this test. A representative of EPA will be present to witness this test. If the well fails the test, the permittee shall not commence injection operations until the problem is corrected and mechanical integrity can be demonstrated.

(b) The permittee shall prepare a report, including procedures and results, of the logging and testing programs. Each log shall include a written interpretation prepared by a knowledgeable log analyst. The report must be submitted in accordance with Part I, Section B, Item 4 and shall be signed in accordance with Part II, Section E, Item 11 of this permit.

4. Commencing Injection

Any well authorized by this permit may not commence injection until:

(a) Conversion is completed, and the permittee has submitted to the Director, by Certified Mail with return receipt requested, a notice of completion using EPA Form 7520-10, and either:

(i) The Director has inspected or otherwise reviewed the injection well and finds it is in compliance with the conditions of the permit; or

(ii) The permittee has not received, within thirteen (13) days of the date of the Director's receipt of the notice required above, notice from the Director of his or her intent to inspect or otherwise review the new injection well, in which case prior inspection or review is waived and the permittee may commence injection.

(b) The permittee has demonstrated to EPA that the injection well has mechanical integrity, and has submitted the reports as specified in Part I, Section B, Item 3.

SECTION C. OPERATING REQUIREMENTS

1. Injection Operation

Beginning on the effective date lasting through the term of this permit, the permittee is

EPA
KENTUCKY

authorized to inject a mixture of freshwater and brine brought to the surface in connection with conventional oil and natural gas production from the operations in the Sugar Creek Field for enhanced recovery operations. The permittee is also authorized to inject CO2 into the Gentry #5. Upon approval by the Director, three additional water injection wells may be converted to CO2 injectors. The maximum amount of CO2 that can be injected into the Sugar Creek Field will be 8000 tons.

(a) Injection Zone

Injection shall be limited to the Jackson Sand of the Golconda Formation. For each specific well authorized by this permit under Part I, Section A, Item 2, injection shall be limited to the open hole/perforated interval between 1750 feet and 1900 feet below land surface. For all wells authorized by Part I, Section A, Item 3, the specific injection interval must be approved by the Director before construction or conversion begins.

(b) Injection Pressure Limitation

(i) The maximum allowable wellhead injection pressure for the fluids comprised of a mixture of freshwater and brine brought to the surface in connection with conventional oil and natural gas production will be 1350 psig. The maximum allowable wellhead injection pressure for the CO2 will be 1425 psig.

(ii) Injection at a pressure which initiates or propagates fractures in the confining zone or causes the movement of injection or formation fluids into an underground source of drinking water is prohibited.

(iii) Injection between the outermost casing protecting underground sources of drinking water and the well bore is prohibited.

2. Annulus Operation

The annulus between the tubing and the long-string casing shall be filled with fresh water, brine, or other fluid as approved by the Director. The annulus pressure shall be maintained at 0 psig.

The annulus shall be monitored with a gauge designed to indicate both a vacuum (below atmospheric) and positive pressure (above atmospheric). The permittee shall comply with Part I, Section C, Item 3 when a change in the annulus pressure of -10 psig or +20 psig occurs. The permittee shall provide an explanation to the Director for the change in

pressure, and measures that will be taken to restore annulus pressure to achieve compliance with this section. If the cause of annulus pressure change is not corrected within 48 hours, the permittee shall cease injection unless such order to cease operation is waived by the Director.

3. Loss of Mechanical Integrity During Operation

The permittee shall cease injection if a loss of mechanical integrity as defined at 40 CFR § 146.8 becomes evident during operation. Operation shall not be resumed until the permittee has complied with the provisions of Part II, Section G, of this permit regarding mechanical integrity demonstration and testing.

The permittee shall notify the Director of the loss of mechanical integrity in accordance with the reporting procedures in Part II, Section E, Item 12(d).

SECTION D. MONITORING REQUIREMENTS

1. Sampling and Analysis Methods

Samples and measurements taken for the purpose of monitoring shall be representative of the monitored activity. Grab samples shall be used for the laboratory analysis of the physical and chemical characteristics as specified in Part I, Section D, Item 3(a). Test methods and procedures shall be as specified at 40 CFR § 136.3 or 40 CFR Part 261, Appendix III. When the analytical method for a particular parameter is not specified at either 40 CFR § 136.3 or 40 CFR Part 261, Appendix III, the permittee must obtain the Director's approval of the methods used to generate all monitoring data. Reports to be generated from monitoring data are specified in Part I, Section E.

2. Injection Operation Monitoring

The permittee shall monitor the operation of each injection well as follows:

Parameter	Monitoring Frequency
Injection Pressure (psig) at Wellhead	Weekly
Annulus Pressure (psig) at Wellhead	Weekly

Flow Rate (barrels/day) of Injected Fluid (brine + freshwater)	Weekly
Flow Rate (tons/day) of Injected Fluid (CO2)	Weekly
Cumulative Volume (barrels) of Injected Fluid (brine + freshwater)	Monthly
Cumulative Volume (tons) of Injected Fluid (CO2)	Monthly

Observation and recording of injection pressure, annulus pressure, flow rate, and cumulative volume shall be made over equal time intervals beginning on the date on which each well commences operation. Recordings shall be of representative values.

3. Injection Fluid Analysis

The permittee shall conduct an injection fluid analysis at least once every twelve months and whenever changes are made to the injection fluid. Analyses shall be made beginning within twelve months from the effective date of this permit, or twelve months from the most recent analysis, whichever is later. An analysis must include:

(a) pH, total dissolved solids, CO2, and specific gravity; and

(b) a list of all chemicals and their composition used for any well stimulation and fracturing during that sampling year; and a list of any additives used and their chemical composition, including any inhibitors used to prevent scaling, corrosion, or bacterial growth. These lists should indicate the brand name of the product and the manufacturer.

On the written request of EPA, an injection fluid analysis shall include the following additional constituents: barium, calcium, total iron, magnesium, sodium, bicarbonate, carbonate, chloride, sulfate, carbon dioxide, dissolved oxygen, hydrogen sulfide, and purgeable aromatic hydrocarbons.

SECTION E. REPORTING REQUIREMENTS

1. Reports on Well Tests and Workovers

Within thirty (30) days after the completion of the activity, the permittee shall report to

the Director the results of the following:

(a) Mechanical integrity tests other than those specified in Part I, Section B, Item 3; and

(b) Any well workover, logging or other test data, other than those specified in Part I, Section B, Item 3, revealing downhole conditions.

2. Reporting of Monitoring Results

Monitoring results, as specified in Part I, Section D, shall be reported each year on EPA Form 7520-11 and must be postmarked by the 28th day of the month following the first full year after the effective date of this permit.

Copies of the monitoring results and reports required by Part I, Section D, and all other reports required by Part II, shall be submitted to the Director at the following address:

U. S. Environmental Protection Agency
Region 4, Water Protection Division
Safe Drinking Water Branch
GW & SDWA Enforcement Section
61 Forsyth Street, SW
Atlanta, Georgia 30303-8960

3. Reporting of New Wells Drilled Within the AOR

Within ten (10) days after spud date, the permittee shall report to the Director by certified mail, return receipt requested, the construction plans for any new well within the AOR of the permitted facility that will penetrate the confining zone or injection zone. The permittee shall provide information on proposed construction (including location and quantities of cement), location and depth. This requirement applies to any construction activity regardless of ownership of the well.

If the construction of the new well will not protect USDWs from contamination, the Director may terminate the permit under 40 CFR § 144.40(3) if he or she determines that continued injection may endanger human health or the environment.

SECTION F. PLUGGING AND ABANDONMENT PLAN

Plugging and abandonment (P&A) of the permitted injection wells shall be in accordance with Part II, Section F of this permit and 40 CFR § 146.10.

During the operating life of the wells, the injection facility may be screened for naturally occurring radioactive material (NORM) by EPA or another party. If the permittee becomes aware at any time that elevated levels of NORM have been detected at this injection facility, the permittee must notify EPA in writing of that fact no later than 45 days prior to the permittee's intent to P&A the well. EPA may require the permittee to revise the P&A plan to insure the safe disposal and proper management of elevated levels of NORM waste.

The plugging of these injection wells shall be performed in the manner described in Attachment Q of this permit application.

Appendix 2 Drillers' logs.

Copies of drillers' logs for wells listed in Table 5-1.

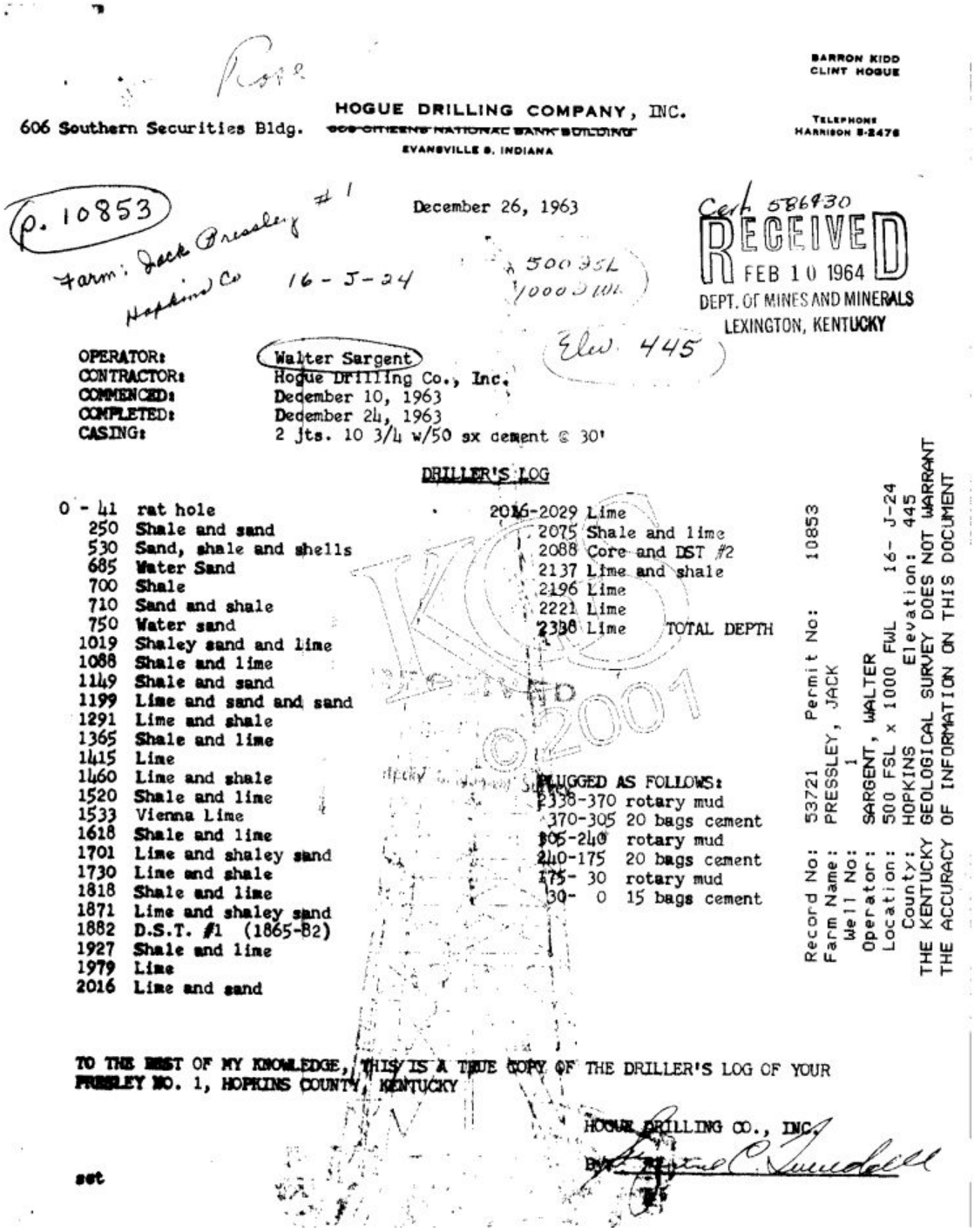

BARRON KIDD
CLINT HOGUE

HOGUE DRILLING COMPANY, INC.
606 Southern Securities Bldg. ~~600 CITIZENS NATIONAL BANK BUILDING~~
EVANSVILLE 8, INDIANA

TELEPHONE
HARRISON 8-2476

P. 10853
Farm: Jack Bressley #1
Hopkins Co 16 - J - 24

December 26, 1963

Cert. 586930
RECEIVED
FEB 10 1964
DEPT. OF MINES AND MINERALS
LEXINGTON, KENTUCKY

500 FSL
1000 FWL
Elev. 445

OPERATOR: Walter Sargent
CONTRACTOR: Hogue Drilling Co., Inc.
COMMENCED: December 10, 1963
COMPLETED: December 24, 1963
CASING: 2 jts. 10 3/4 w/50 sx cement @ 30'

DRILLER'S LOG

0 - 41	rat hole	2016-2029	Lime
250	Shale and sand	2075	Shale and lime
530	Sand, shale and shells	2088	Core and DST #2
685	Water Sand	2137	Lime and shale
700	Shale	2196	Lime
710	Sand and shale	2221	Lime
750	Water sand	2338	Lime TOTAL DEPTH
1019	Shaley sand and lime		
1088	Shale and lime		
1149	Shale and sand		
1199	Lime and sand and sand		
1291	Lime and shale		
1365	Shale and lime		
1415	Lime		
1460	Lime and shale	PLUGGED AS FOLLOWS:	
1520	Shale and lime	2338-370	rotary mud
1533	Vienna Lime	370-305	20 bags cement
1618	Shale and lime	305-240	rotary mud
1701	Lime and shaley sand	240-175	20 bags cement
1730	Lime and shale	175- 30	rotary mud
1818	Shale and lime	30- 0	15 bags cement
1871	Lime and shaley sand		
1882	D.S.T. #1 (1865-82)		
1927	Shale and lime		
1979	Lime		
2016	Lime and sand		

Record No: 53721 Permit No: 10853
Farm Name: PRESSLEY, JACK
Well No: 1
Operator: SARGENT, WALTER
Location: 500 FSL x 1000 FWL 16- J-24
County: HOPKINS Elevation: 445
THE KENTUCKY GEOLOGICAL SURVEY DOES NOT WARRANT
THE ACCURACY OF INFORMATION ON THIS DOCUMENT

TO THE BEST OF MY KNOWLEDGE, THIS IS A TRUE COPY OF THE DRILLER'S LOG OF YOUR PRESSLEY NO. 1, HOPKINS COUNTY, KENTUCKY

HOGUE DRILLING CO., INC.
BY [signature]

set

2630 5 3/4
50 7EL

R0019529P0027DC

DRILLERS

MAP NO. _____

WELL LOG

SERIAL NO. _____

ELEVATION 507
Derrick Floor - Ground

PERMIT NO. 11673

COMPANY: Zegg Oil Company
ADDRESS: 1520 Sweeney St., O'boro, Ky.
COMMENCED DRILLING: May 6, 1964
COMPLETED DRILLING: July 22, 1964
CONTRACTOR: Warren Drilling Company
ADDRESS: 1520 Sweeney Street, Owensboro, Ky.
TOOLS: CABLE from 0 to 1864
ROTARY from to

FARM: Ruby Watson
WELL NO. 1
ACRES:
FIELD NAME:
QUADRANGLE OR TOWNSHIP:
Sec. 21 TWP 9 Rge 23

COUNTY: Hopkins
STATE: Kentucky
SHOT from to
QUART

Cert. 209112

RECEIVED
AUG 17 1964
DEPT. OF MINES AND MINERALS
LEXINGTON, KENTUCKY

FROM DEPTH	TO	FORMATION
0	6	Soil and Clay
6	20	Sand
20	25	Sandy Shale
25	80	Shale
80	120	Sandy Shale
120	138	Sand ½Bailer per hr.
138	155	Shale
155	160	Sand
160	232	Shale
232	250	Sand 5-Bailers per hr.
250	275	Sand HFW
275	300	Sand (Broken)
300	310	Sand (Hard
310	325	Sand (Broken)
325	390	Sandy Shale
390	400	[illegible]
400	410	Sandy Shale
410	415	Shale
415	437	Sandy Shale
437	459	Sand (Broken)
459	465	Shale
465	490	Sandy Shale
490	528	Shale
528	560	Sandy Shaley
560	620	Sand
620	675	Sand y Shale
675	735	Sand
735	800	Sandy Shale'
800	860	Sand
860	945	Sandy Shale
945	963	Shale
963	980	Sand
980	987	Shale
987	990	Lime
990	994	Shale
994	1028	Lime
1028	1031	Shale
1031	1035	Lime
1035	1040	Shale
1040	1045	Lime
1045	1060	Lime (Broken)
1060	1094	Shale and Lime Shells
1094	1105	Lime
1105	1125	Shale and Lime Shells
1125	1167	Lime
1167	1208	Shale and Lime Shells
1208	1215	Lime
1215	1248	Shale and Lime Shells
1248	1270	Lime
1270	1307	Shale and Lime Shells
1307	1315	Lime
1315	1350	Lime Shells and Shale
1350	1365	Lime
1365	1375	Shale and Lime
1375	1378	Shale

RECEIVED
AUG 19 1964

CASING LANDED		
1378	1420	Shale
1420	1426	Lime
1426	1428	Shale
1428	1440	Lime
1440	1450	Shale
1450	1492	Lime (Broken)
1492	1500	Lime
1500	1520	Shale
1520	1525	Sandy Shale
1525	1530	Sand (Broken)
1530	1547	Shale
1547	1551	Sandy Shale
1551	1554	Sand)Hard)
1554	1560	Sandy Shale
1560	1572	Sand
1572	1580	Lime
1580	1601	Sand (Broken)
1601	1607	Sandy Shale
1607	1611	Shale
1611	1649	Lime
1649	1655	Shale
1655	1675	Sand (Broken)
1675	1685	Sand (Water)
1685	1700	Sand HFW
1700	1738	Lime
1738	1745	Shale
1745	1748	Lime
1748	1750	Lime and Shale
1750	1765	Lime
1765	1783	Lime (Broken)
1783	1800	Lime
1800	1802	Shale SLM
1802	1848	Sand
1848	1850	Sand S.O.
1850	1852	Sand-Oil
1852	1856	Sand Oil
1856	1862	Shale
1862	1864	TD.
1864		

CASING RECORD

Size	Run	Pulled
12½	16'	16'
10"	1285'	1285'
8"	1491'	1491'
7"	1703'	1783'
5½"	1852'	0
8"	16'	0

Cemented with 5 sacks of cement.
I hereby certify the within Well Log is a true and correct copy, as taken from the Daily Drillers Reports.

BY: George W. Warren Jr.
by Juanita Bennett

P. 11986

NAME OF WELL: Ross Gentry #1, Hopkins County, Kentucky
OPERATOR: Grant Mullenax,401 St. Claire Dr.,Owensboro, Ky.
CONTRACTOR: Weal Drilling Co.,Inc.,P.O.Box 140, Carmi, Illinois
DATE COMMENCED: 6/23/64
DATE COMPLETED: 7/7/64

Formation record of Ross Gentry #1, Hopkins County, Kentucky

From	To	Formation
0	60	Surface shale
60	548	Shale & sand
548	760	Sand
760	830	Sand & shale
830	930	Sand
930	975	Shaley sand
975	1028	Shale & sand
1028	1045	Lime & shale
1045	1212	Shale & sand
1212	1552	Shaley lime
1552	1595	Shale & lime
1595	1667	Sand & shale
1667	1680	Lime
1680	1726	Sand
1726	1743	Sandy shale
1743	1791	Lime
1791	1853	Lime & shale
1853	1878	Sand
1878	1917	Shaley sand
1917	2017	Shale & lime
2017	2029	Sand
2029	2275TD	Lime

RECEIVED
JAN 15 1965
DEPT. OF MINES AND MINERALS
LEXINGTON, KENTUCKY

Record No: 53419 Permit No: 11986
Farm Name: GENTRY, ROSS C
Well No: 1
Operator: MULLENAX, GRANT
Location: 2250 FNL x 1700 FWL 25- J-24
County: HOPKINS Elevation: 493
THE KENTUCKY GEOLOGICAL SURVEY DOES NOT WARRANT
THE ACCURACY OF INFORMATION ON THIS DOCUMENT

I, the undersigned, do hereby certify that the above is a true and complete copy of the Driller's Log of the Ross Gentry #1, Hopkins County, Kentucky, as taken from the Daily Drilling Reports.

WEAL DRILLING COMPANY, INC.

John T Wallace

RECEIVED
JAN 15 1965
Kentucky Geological Survey

Record No: 53455 Permit No: 12241
Farm Name: LAFFOON, E O
Well No: 1
Operator: ZOGG OIL CO, INC
Location: 2200 FSL x 570 FWL 25- J-24
County: HOPKINS Elevation: 507

2200' 3SL
570' 3WL

SERIAL NO.

PERMIT NO. 12241 12241

THE KENTUCKY GEOLOGICAL SURVEY DOES NOT WARRANT
THE ACCURACY OF INFORMATION ON THIS DOCUMENT

ADDRESS: 1520 Sweeney St. O'boro, Ky.

COMMENCED DRILLING: July 23, 1964

COMPLETED DRILLING: October 27, 1964

CONTRACTOR: Warren Drilling Co.

ADDRESS: 1520 Sweeney St. O'boro, Ky.

TOOLS CABLE from 0 to 1362
ROTARY from to

FARM: E.O. Laffoon

WELL NO. 1

ACRES:

FIELD NAME:

QUADRANGLE OR TOWNSHIP:

Sec. 25 Rge 24 Twp J

25 - J - 24

COUNTY: Hopkins

STATE: Kentucky

SHOT from to

QUART

FROM DEPTH	TO	FORMATION
0	7	Soil and Clay
7	35	Sand
35	115	Shale
115	143	Sand
143	155	Shale
155	165	Sand-Making enough water to drill with
165	195	Shale and Sandy Shale
195	210	Shale
210	307	Sand HFW
307	310	Shale
310	335	Sand and Shale
335	360	Shale
360	432	Sandy Shale
432	460	Sand-Good Show of Oil
460	470	Sandy Shale
470	510	Shale
510	565	Sandy Shale
565	625	Sand-12 Bailers per hr. Water
625	725	Sand HFW
725	740	Sand and Shale
740	845	Shale and Sandy Shale
845	860	Sand
860	875	Shale (Sandy)
875	950	Sandy Shale
950	975	Sand
975	995	Shale
995	997	Lime
997	1025	Shale
1025	1035	Shale and Lime Shells
1035	1043	Lime
1043	1052	Shale
1052	1065	Sandy Shale
1065	1080	Shale and Lime Shells
1080	1092	Sand
1092	1105	Shale
1105	1120	Shale and Lime Shells
1120	1125	Lime
1125	1163	Shale and Lime Shells
1163	1247	Lime
1247	1270	Shale and Shells
1270	1305	Lime
1305	1314	Shale and Shells
1314	1326	Lime
1326	1340	Shale and Lime
1340	1350	Lime
1350	1360	Shale and Shells
1360	1376	Lime
1376	1416	Shale
1416	1420	Lime
1420	1424	Shale
1424	1435	Lime
1435	1444	Shale
1444	1491	Lime (Broken) SLI
1491	1493	Lime
1493	1515	Sandy Shale
1515	1532	Sand (Broken)
1532	1547	Sand Shale
1547	1555	Sand
1555	1562	Sandy Shale
1562	1578	Sand (Broken)
1578	1592	Lime (Broken)
1592	1598	Sand (Broken)
1598	1607	Shale
1607	1650	Lime
1650	1654	Shale (Sandy)
1654	1690	Sand HFW
1690	1748	Lime and Shale
1748	1755	Lime
1755	1795	Shale
1795	1846	Sand
1846	1852	Shale
1852	1853	Sand
1853	1867	Shale-Shot of Oil
1867	1890	Sand Shale
1890		TOTAL DEPTH

CASING RECORD

Size	Run	Pulled
13-3/8"	15'	15'
10"	337'	337'
8"	1127'	1127'
7"	1496'	1496'
5"	1955	0 Cement with 65 sacks cement

Ran Surface Joint 10" 21' cemented.

I hereby certify the within drill log is a true and correct copy, as taken from the daily Drillers reports.

By George E. Warren, Jr.

Cert. 298115

RECEIVED
NOV 3 1964
DEPT. OF MINES AND MINERALS
LEXINGTON, KENTUCKY

P. 12298 Mary Belle MARRYBELLE STANHOPE #1 Elev 503.2

3060' FSL
555' FWL

RECEIVED
OCT 5 1964
DEPT. OF MINES AND MINERALS
LEXINGTON, KENTUCKY

Well Record

LOCATION: Marrybelle Stanhope, Section 25-J-24, Hopkins County, Kentucky
OPERATOR: R. L. Mitchell Oil Co
CONTRACTOR: Kendall-Davis Drilling Company, Inc.
CASING: Set 60' of 8 5/8" @ 65' w/80 sks. ; 1884' set @ 1882' w/125 sks.
STARTED: July 27, 1964
COMPLETED: August 1, 1964

Record No: 53746 Permit No: 12298
Farm Name: STANHOPE, MARY BELLE
Well No: 1
Operator: MITCHELL, R L
Location: 3060 FSL x 555 FWL 25- J-24
County: HOPKINS Elevation: 503
THE KENTUCKY GEOLOGICAL SURVEY DOES NOT WARRANT
THE ACCURACY OF INFORMATION ON THIS DOCUMENT

FROM	TO	FORMATIONS
0	69	surface
69	130	shale
130	425	sand, shale & lime
425	575	shly sand & lime
575	640	sand
640	775	sand
775	845	shale & lime
845	1011	sand & shly sand
1011	1025	lime (U. Kincaid)
1025	1095	shale & lime
1095	1132	lime
1132	1212	lime & shale
1212	1314	shale, lime & sand
1314	1329	shale
1329	1389	shale & lime
1389	1417	lime
1417	1456	shale & sand
1456	1497	shale
1497	1516	lime (Vienna)
1516	1541	lime
1541	1581	shly sand
1581	1593	lime
1593	1633	SHALE
1633	1646	shale
1646	1653	lime (Olen Dean)
1653	1708	shale sand
1708	1781	sand & shale
1781	1790	sand & shale
1790	1797	lime
1797	1847	shale & lime
1847	1850	shale & sand
1850	1865	sand
1865	1880	shale
1880		T. D.

I, the undersigned do hereby certify thet the foregoing well record of the Marybelle Stanhope #1, Section 25-J-24, Hopkins County, Kentucky, is a true and correct well log of the formations encountered, as reflected by the Daily Drilling Report.

BY: Beverly A. Elder
BEVERLY A. ELDER

Form G

Rose #804

WELL RECORD

COMMONWEALTH OF KENTUCKY
DEPARTMENT OF MINES AND MINERALS
OIL AND GAS DIVISION
P. O. Box 660
Lexington, Ky.

RECEIVED
DEC 18 1964
DEPT. OF MINES AND MINERALS
LEXINGTON, KENTUCKY

Permit No. 12397 Oil or Gas Well Oil (Kind)

Company John Tuttle
Address Owensboro, Ky.
Farm D.C.Rickard Acres
Location (waters) 2,700'FNLx900'FWL
Well No. 1 Elev. 496'
District County Hopkins
Drilling Commenced August 11, 1964
Drilling Completed August 24, 1964
Name of Contractor Miro Drilling Co., Inc.
Address of Contractor Owensboro, Ky.
Date Shot From To
With
Open flow /10ths Water in Inch
/10ths Merc. in Inch

Casing and Used in Left in Tubing Drilling Well

Size
16
13
10
8¼
6⅝
5 5/16
3
2
Liners Used

Kind of Packer
Size of
Depth Set
Perf. top
Perf. bottom
Perf. top
Perf. bottom

Casing Cemented 8-5/8" Size No. Ft. 181 Date
w/8 sks cement

Formation	Color	Hard or Soft	Top	Bottom	Oil, Gas & Coal or Water	Depth Found	Remarks
surface			0	18			
sandy shale			18	35			
sand & shale			35	320			
sand & shale			320	510			
sand & sdy shale			510	680			
lime, sand & shale			680	889			
			889	1021			
lime & shale			1021	1058			
			1058	1139			
lime & shale			1139	1186			
lime & shale			1186	1232			
			1232	1290			
shale & lime			1290	1342			
lime & shale			1342	1363			
lime & shale			1363	1410			
lime & shale			1410	1450			
lime			1450	1452			
shale			1452	1494			
lime			1494	1515			
lime			1515	1522			
shale			1522	1534			
lime			1534	1538			
shale			1538	1558			
sand, shale & lime			1558	1585			
lime			1585	1608			
shale			1608	1625			
			1625	1665			
sand & shale			1665	1723			
sand			1723	1735			
lime			1735	1742			
sandy shale			1742	1783			
lime & shale			1783	1835			
shale			1835	1843			
sand			1843	1844			
Coring			1844	1859			
TD			1859				

Section 25-J-24

Record No: 53750 Permit No: 12397
Farm Name: RICKARD, J C
Well No: 1
Operator: TUTTLE, JOHN W
Location: 2700 FNL x 900 FWL 25- J-24
County: HOPKINS Elevation: 496
THE KENTUCKY GEOLOGICAL SURVEY DOES NOT WARRANT
THE ACCURACY OF INFORMATION ON THIS DOCUMENT

Form G

WELL RECORD

RECEIVED
SEP 29 1964
DEPT. OF MINES AND MINERALS
LEXINGTON, KENTUCKY

2900' FNL
135' FWL

COMMONWEALTH OF KENTUCKY
DEPARTMENT OF MINES AND MINERALS
OIL AND GAS DIVISION
P. O. Box 606
Lexington, Ky.

Permit No. 12409 — Oil or Gas Well Oil (Kind)

Company Zogg Oil Company
Address Owensboro, Ky.
Farm Watson Acres
Location (waters)
Well No. 2 Elev. 458
District 25-J-24 County Hopkins
Drilling Commenced Aug 12, 1964
Drilling Completed Aug 22, 1964
Name of Contractor Miro Drlg. Co.
Address of Contractor Owensboro, Ky.
Date Shot From To
With
Open flow /10ths Water in Inch
/10ths Merc. in Inch

Ruby Watson

Casing and Used in Left In Tubing / Drilling Well

Size
16
13
10
8¼
6¾
5 3/16
3
2
Liners Used

Kind of Packer
Size of
Depth Set
Perf. top
Perf. bottom
Perf. top
Perf. bottom

Casing Cemented Size No. Ft. Date

Formation	Color	Hard or Soft	Top	Bottom	Oil, Gas & Coal or Water	Depth Found	Remarks
surface			0	69			
sd & sh			69	210	Coal		
sd & sh			210	800			
sd & sh			800	944	Water		
lime			944	958			
L & sh			958	1407			
shale			1407	1445			
L & sh			1445	1455			
L & sh			1455	1487			
sd & sh			1487	1523			
sd & sh			1523	1543			
L & sh			1543	1562			
shale			1562	1603			
Lime			1603	1609			
Sd Sh			1609	1634			
sand			1634	1670			
sd & sh			1670	1722			
sd & sh			1722	1797			
L & sh			1797	1804			
Core #1			1804	1819			
sd & sh			1819	1836			
L & sh							
Barlow			1836	1839			
sd & sh							
Cyp.			1839	1871			
Shale			1871	1874			
Lime upc			1874	1901			
L & sh			1901	1940			
sd & sh			1940	1953			
sd & sh			1953	1974			

Record No: 54152 Permit No: 12409
Farm Name: WATSON, RUBY
Well No: 2
Operator: ZOGG OIL CO, INC
Location: 2900 FNL x 135 FWL 25- J-24
County: HOPKINS Elevation: 458
THE KENTUCKY GEOLOGICAL SURVEY DOES NOT WARRANT
THE ACCURACY OF INFORMATION ON THIS DOCUMENT

Form G

25-8-24

2820'FSL
1600'FWL

WELL RECORD

RECEIVED
OCT 7 1964
DEPT. OF MINES AND MINERALS
LEXINGTON, KENTUCKY

COMMONWEALTH OF KENTUCKY
DEPARTMENT OF MINES AND MINERALS
OIL AND GAS DIVISION
P. O. Box 680
Lexington, Ky.

Rec'd 10-6-64

Permit No. 12468 Oil or Gas Well Oil (Kind)

Company John Tuttle
Address Owensboro, Kentucky
Farm Marquess Acres 40
Location (waters)
Well No. #1 Elev. 509'
District County Hopkins
Drilling Commenced Aug 22, 1964
Drilling Completed Aug 29, 1964
Name of Contractor Miro Drlg. Co.
Address of Contractor Owensboro, Ky.
Date Shot From To
With
Open flow /10ths Water in Inch
/10ths Merc. in Inch

Bernice Marquess

Casing and Used in Left in Tubing / Drilling Well

Size
16
13
10
8¼
6¾
5 3/16
3
2
Liners Used

Kind of Packer
Size of
Depth Set
Perf. top
Perf. bottom
Perf. top
Perf. bottom

Casing Cemented Size No. Ft. Date
1563' of 4½"

Formation	Color	Hard or Soft	Top	Bottom	Oil, Gas & Coal or Water	Depth Found	Remarks
sd & gravel			0	19			
shale			19	115			
sand			115	150			
shale			150	160			
shly sd & sd			160	320			
sand			320	344			
Lime			344	350			
sand & sh			350	605			
sd & sd lime			605	730			
Sand			730	740			
lime & sh			740	770			
sd & sh			770	971			
sd lime			971	976			
sh sd			976	994			
sh lime			994	1008			
lime			1008	1044			
L & sh			1044	1125			
sand			1125	1135			
lime			1135	1155			
lime			1155	1201			
L & sh			1201	1459			
shale			1459	1506			
lime			1506	1527			
sh & sd			1527	1588			
sd TS			1588	1600			

Record No: 53748 Permit No: 12468
Farm Name: MARQUESS, BERNICE
Well No: 1
Operator: TUTTLE, JOHN W
Location: 2820 FSL x 1600 FWL 25- J-24
County: HOPKINS Elevation: 509
THE KENTUCKY GEOLOGICAL SURVEY DOES NOT WARRANT
THE ACCURACY OF INFORMATION ON THIS DOCUMENT

P. 12620

NAME OF WELL: ROSS GENTRY #2
OPERATOR: CARTER DRILLING CO., DALE, INDIANA
CONTRACTOR: GRANT MULLENAX, OWENSBORO, KY.
DATE COMMENCED: 9/23/64
DATE COMPLETED: 10/1/64

FORMATION RECORD OF ROSS GENTRY #2, HOPKINS COUNTY, KY.

FROM	TO	FORMATION
0	8	Soil
8	45	Surface Shale
45	55	Sand & Shale
55	170	Sandy Shale
170	350	Sand & Shale
350	360	Hard Lime
360	505	Sand & Shale
505	725	Sandy Lime
725	1030	Sand & Shale
1030	1065	Lime
1065	1100	Sandy Lime
1100	1166	Shale
1166	1219	Sandy Lime
1219	1338	Sand & Shale
1338	1344	Lime
1344	1361	Shale
1361	1373	Lime & Shale
1373	1460	Sandy Lime
1460	1530	Shale
1530	1549	Lime
1549	1675	Lime & Shale
1675	1815	Sand & Shale
1815	1823	Lime
1823	1875	Lime & Shale
1875	1877	Lime
1877	1891	Sand

RECEIVED
FEB 10 1965
DEPT. OF MINES AND MINERALS
LEXINGTON, KENTUCKY

I, the undersigned, do hereby certify that the above is a true and complete copy of the Drillers Log of the Ross Gentry #2, Hopkins County, Ky., as taken from the Daily Drilling Reports.

CARTER DRILLING CO.

Charles Winkler

Record No: 53418 Permit No: 12620
Farm Name: GENTRY, ROSS C
Well No: 2
Operator: MULLENAX, GRANT
Location: 2220 FNL x 1200 FWL 25- J-24
County: HOPKINS Elevation: 508
THE KENTUCKY GEOLOGICAL SURVEY DOES NOT WARRANT
THE ACCURACY OF INFORMATION ON THIS DOCUMENT

P. 12697

Stanhope #2 Elev. 503 2

2650'FSL 900'FWL

Mary Belle Stanhope

RECEIVED
OCT 5 1964
DEPT. OF MINES AND MINERALS
LEXINGTON, KENTUCKY

Well Record

LOCATION: Stanhope #2, Section 25-J-24, Hopkins County, Kentucky
OPERATOR: R. L. Mitchell Oil Co.
CONTRACTOR: Kendall-Davis Drilling Company, Inc.
CASING: Set 63' of 8 5/8" @ 68' w/90 sacks ; Run 1859' of 5 1/2" w/125 sks
STARTED: September 24, 1964
COMPLETED: September 30, 1964

FROM	TO	FORMATION
0	64	Surface
64	155	shale
155	595	shale & sand
595	890	sand
890	990	shly sand & shale
990	1015	lime (U. Kincaid)
1015	1155	lime (Kincaid)
1155	1160	lime & shale
1160	1255	sandy shale & lime
1255	1329	shale & sandy shale
1329	1382	lime & shale (Menard)
1382	1427	lime (Massive Menard)
1427	1440	shale
1440	1448	lime (Little Menard)
1448	1490	shale
1490	1491	lime (Vienna)
1491	1497	shale
1497	1513	lime & shale
1513	1553	shale
1553	1583	shly sand
1583	1600	lime & shale
1600	1642	Shale
1642	1649	lime (Glen Dean)
1649	1746	shale & sand
1746	1790	shly sand & sandy lime
1790	1795	lime
1795	1850	shale & sand
1850		T. D.

I, the undersigned do hereby certify that the foregoing well record of the Stanhope #2, Section 25-J-24, Hopkins County, Kentucky, is a ture and correct well log of the formations encountered, as reflected by the Daily Drilling Report.

BY: Beverly Ann Elder
BEVERLY ANN ELDER

Record No: 53745 Permit No: 12697
Farm Name: STANHOPE, MARY BELLE
Well No: 2
Operator: MITCHELL, R L
Location: 2650 FSL x 900 FWL 25- J-24
County: HOPKINS Elevation: 503
THE KENTUCKY GEOLOGICAL SURVEY DOES NOT WARRANT
THE ACCURACY OF INFORMATION ON THIS DOCUMENT

P-12783

NAME OF WELL: ROSS GENTRY #3
OPERATOR: ~~CARTER DRILLING~~ CO., DALE, INDIANA
CONTRACTOR: GRANT MULLENAX, OWENSBORO, KY.
DATE COMMENCED: 10/9/64
DATE COMPLETED: 10/17/64

Application of Well Building

FORMATION RECORD OF ROSS GENTRY #3, HOPKINS COUNTY, KY. 25-J-24

Elev: 493' 2170' FNL 720' FWL

FROM	TO	FORMATION
0	6	Soil
6	25	Surface Shale
25	150	Sandy Shale
150	340	Sand & Shale
340	375	Water Sand
375	445	Sandy Shale
445	665	Sand
665	750	Sandy Lime
750	900	Sand
900	912	Sandy Shale
912	1011	Sand & Shale
1011	1029	Sandy Lime & Lime
1029	1046	Lime
1046	1100	Lime & Shale
1100	1139	Shale
1139	1186	Lime
1186	1324	Broken Sand & Shale
1324	1404	Lime & Shale
1404	1439	Sandy Lime
1439	1450	Shale
1450	1458	Sand
1458	1506	Shale
1506	1609	Lime
1609	1616	Hard Sand
1616	1657	Shale
1657	1665	Lime (Glendine)
1665	1673	Shale
1673	1743	Sand
1743	1797	Sand
1797	1806	Lime (Golconda)
1806	1855	Shale
1855	1868	Sand

RECEIVED
FEB 10 1965
DEPT. OF MINES AND MINERALS
LEXINGTON, KENTUCKY

I, the undersigned, do hereby certify that the above is a true and complete copy of the Drillers Log of the Ross Gentry #3, Hopkins County, Ky., as taken from the Daily Drilling Report.

CARTER DRILLING CO.

Charles Winkler

Record No: 53417 Permit No: 12783
Farm Name: GENTRY, ROSS C
Well No: 3
Operator: MULLENAX, GRANT
Location: 2170 FNL x 720 FWL 25- J-24
County: HOPKINS Elevation: 493

Record No: 53457 Permit No: 12985
Farm Name: BOWLES, PETER
Well No: 2
Operator: TUTTLE, JOHN W
Location: 1800 FNL x 75 FWL 25- J-24
County: HOPKINS Elevation: 475

THE KENTUCKY GEOLOGICAL SURVEY DOES NOT WARRANT THE ACCURACY OF INFORMATION ON THIS DOCUMENT

COMPANY: John W. Tuttle
ADDRESS: Box 252, Owensboro, Kentucky
COMMENCED DRILLING: November 5, 1964
COMPLETED DRILLING: Dec 15, 1964
CONTRACTOR: Warren Drilling Company
ADDRESS: 1520 Sweeney St., O'boro, Ky.
TOOLS CABLE from 0 to 1350.5
ROTARY from to

SERIAL NO.
PERMIT NO. 12985
Pete Bowles
NO. 2
ACRES: 100
FIELD NAME: Sugar Creek
QUADRANGLE OR TOWNSHIP:
Sec. 25 Twp 3 Rge 2W
COUNTY: Hopkins
STATE: Kentucky
SHOT from to
QUART
1800 FNL 75 FWL

FROM DEPTH	TO	FORMATION
0	14	Sand Rock
14-3	35	Sandy Shale
35	90	Shale
90	128	Sand (Making some Water)
128	218	Sand-Shale and Shale
218	300	Sand HFW
300	303	Sandy Shale
303	310	Lime
310	325	Sand
325	332	Sand and Shale
332	335	Sand
335	340	Sand (Limey)
340	360	Shale
360	375	Sand
375	380	Shale
380	417	Sandy Shale
417	450	Sand (D-S.O.)
450	500	Sand 3-Bailers per hr.
500	605	Sand HFW
605	640	Sand and Shale
640	660	Sand
660	675	Sandy-Shale
675	725	Sand
725	760	Sand and Shale
760	775	Shale
775	810	Sandy-Shale
810	835	Sand
835	885	Sandy Shale
885	895	Shale
895	9 20	Shale and Sandy Shale
920	940	Shale
940	960	Shale and Sandy Shale
960	962	Shale
962	975	Sand
975	984	Shale
984	907	Lime
907	992	Shale
992	1029	Lime
1029	1040	Shale and Lime Shells
1040	1045	Shale
1045	1048	Lime
1048	1065	Shale
1065	1090	Shale and Lime Shells
1090	1132	Shale and Sandy Shale
1132	1162	Lime
1162	1247	Shale and Lime Shells
1247	1274	Lime
1274	1295	Shale and Shells
1295	1308	Lime
1308	1326	Shale and Shells
1326	1360	Lime
1360	1377	Shale and Lime Shells
1377	1417	Lime
1417	1421	Shale
1421	1425	Lime
1425	1436	Shale
1446	1497	Shale
1497	1515	Lime (SLT 1506-1503)
1515	1573	Sandy Shale
1573	1595	Sand
1595	1601	Lime
1601	1640	Lime
1640	1646	Shale and Sandy Shale
1646	1650	Shale
1650	1668	Lime
1668	1705	Shale
1705	1729	Sand (S. Gas)
1729	1740	Sand 1-Bailer per hr.
1740	1750	Sandy Shale
1750	1825	Shale and Lime Shells
1825	1830	Shale
1830	1940	Sand (Hard) SLT
1940	1950	Sand - Oil - Cored
1950	1950.5	Shale
1950.5		TOTAL DEPTH

CASING RECORD

Size	Run	Pulled
13 3/8"	15'	
10"	341'	
8"	1657'	
7"	1925'	
5"	None	
4½"	1950.5	

I hereby certify the within Well Log is a true and correct statement as taken from the Daily Drillers Reports.

BY: John W. Tuttle

RECEIVED
DEC 29 1964
DEPT. OF MINES AND MINERALS
LEXINGTON, KENTUCKY

Form G

WELL RECORD

COMMONWEALTH OF KENTUCKY
DEPARTMENT OF MINES AND MINERALS
OIL AND GAS DIVISION
P. O. Box 688
Lexington, Ky.

RECEIVED
JUL [illegible]
DEPT. OF MINES AND MINERALS
LEXINGTON, KENTUCKY

Permit No. 12986

Oil or Gas Well Oil (Kind)

Company John Tuttle
Address P. O. Box 252-Owensboro, Ky.
Farm Bernice Marquess Acres
Location (waters) 2300'FSLx1350'FWL
Well No. 2 Elev. 481'
District County Hopkins
Drilling Commenced May 22, 1965
Drilling Completed May 27, 1965
Name of Contractor Miro Drilling Co., Inc.
Address of Contractor Owensboro, Kentucky
Date Shot From To
With
Open flow /10ths Water In Inch
/10ths Merc. In Inch

Casing and Used in Left in Tubing Drilling Well

Size
16
13
10
8¼
6¾
5 5/16
3

Kind of Packer
Size of
Depth Set
Perf. top
Perf. bottom
Liners Used
Perf. top
Perf. bottom

Casing Cemented Size 8-5/8" No. Ft. 37' Date
w/10 sx cement

Formation	Color	Hard or Soft	Top	Bottom	Oil, Gas & Coal or Water	Depth Found	Remarks
Surface			0	37			
Shale & Sand			37	155			
Shale & Sand			155	955			
Sand & Lime			955	1000			
Sand & Shale			1000	1087			
Lime & Shale			1087	1127			
Sand & Shale			1127	1266			
Lime & Shale			1266	1440			
Shale			1440	1453			
Lime			1453	1496			
Sand & Shale			1496	1604			
Lime			1604	1609			
Lime & Shale			1609	1625			
Sand & Shale			1625	1692			
Sand & Shale			1692	1761			
Lime & Shale			1761	1829			
Cored			1829	1838			
Total Depth			1838				

Since this well was cored, no electric log was made.

ection
5-J-24

Record No: 53747 Permit No: 12986
Farm Name: MARQUESS, BERNICE
Well No: 2
Operator: TUTTLE, JOHN W
Location: 2300 FSL x 1350 FWL 25- J-24
County: HOPKINS Elevation: 481
THE KENTUCKY GEOLOGICAL SURVEY DOES NOT WARRANT
THE ACCURACY OF INFORMATION ON THIS DOCUMENT

RECEIVED
JUL 13 1965
Kentucky Geological Survey

Record No: 53749 Permit No: 12987
Farm Name: RICKARD, J C
Well No: 2
Operator: TUTTLE, JOHN W
Location: 2850 FNL x 1300 FWL 25- J-24
County: HOPKINS Elevation: 507

THE KENTUCKY GEOLOGICAL SURVEY DOES NOT WARRANT
THE ACCURACY OF INFORMATION ON THIS DOCUMENT LS

285
1300' FWL

RECEIVED
DEC 18 1964
DEPT. OF MINES AND MINERALS
LEXINGTON, KENTUCKY

OIL AND GAS DIVISION
P. O. Box 660
Lexington, Ky.

Permit No. 12987

Oil or Gas Well Oil (Kind)

Company John Tuttle - Box 252
Address Owensboro, Kentucky
Farm J. C. Rickard Acres
Location (waters) 2,350'FNLx1,300'FWL
Well No. 2 Elev. 507'
District County Hopkins
Drilling Commenced November 25, 1964
Drilling Completed December 2, 1964
Name of Contractor Miro Drilling Co., Inc.
Address of Contractor Owensboro, Kentucky
Date Shot From To
With
Open flow /10ths Water in Inch
/10ths Merc. in Inch

Section 25-J-24

Casing and Used in Left in Tubing Drilling Well

Size
16
13
10
8¼
6⅝
5 3/16
3
2
Papers Used

Kind of Packer
Size of
Depth Set
Perf. top
Perf. bottom
Perf. top
Perf. bottom

Casing Cemented Size No. Ft. Date
23 ft-0-5/8" w/6 sks cement

Formation	Color	Hard or Soft	Top	Bottom	Oil, Gas & Coal or Water	Depth Found	Remarks
Surface			0	23			
			23	30			
Sand & shale			30	315			
Sand & shale			315	525			
Sand & shale			525	720			
Sand & shale			720	1010			
Lime			1010	1020			
Lime			1020	1054			
Shale			1054	1136			
Lime			1136	1165			
Lime & shale			1165	1312			
Sand & shale			1312	1380			
Lime			1380	1440			
Shale			1440	1508			
Lime			1508	1525			
Shale & lime			1525	1585			
Sand			1585	1590			
Sand & lime			1590	1635			
Lime & shale			1635	1687			
Lime			1687	1695			
			1695	1746			
Sand & shale			1746	1785			
Sand			1785	1857			
Coring - T.D.			1857	1866			

This well was cored and no electric log was made.

John W. Tuttle

25-J-24

2650 FSL
2220' FWL Elev. 478'

FARM: E.O Laffoon #2 (13693)
OPERATOR: Zogg Oil Company
COMMENCED: May 30, 1965

COUNTY: Hopkins County, Kentucky
CONTRACTOR: Crescent Drilling Company
COMPLETED: June 9, 1965

0	27	Surface Hole
27	120	Sand and Shale
120	315	Shale, Sand & Lime
315	565	Sand and Shale
565	780	Shaly Sand and Lime
780	986	Shale and Sand
986	1012	Upper Kincaid Lime
1012	1024	Shale and Lime
1024	1085	Lime and Shale
1085	1113	Shaly Lime and Shale
1113	1150	Lime Lower Kincaid
1150	1371	Lime and Shale
1371	1387	Shale and Lime
1387	1444	Menard Lime
1444	1485	Shale
1485	1509	Lime Vienna
1509	1548	Shale
1548	1581	Sand
1581	1631	Shale
1631	1639	Lime Glenn
1639	1655	Shale and Sand
1655	1677	Lime and Shale
1677	1715	Sand Hardinsburg
1715	1721	Shale and Sand
1721	1728	Shale and Lime
1728	1770	Golconda Lime
1770	1832	Lime, Shale and Sand
1832	1846	Core #1
1846	1860	Shale
1860	1865	Lime Barlow
1865	1898	Shale
1898	1964	Lime Paint Creek
1964	1985	Paint Creek Sand
1985	2008	Lower Paint Creek Lime
2008	2055	Lime and Shale
2055	2065	Shale and Sand
2065	2115	Renault Lime
2115	2265	Lime
2265'		TOTAL DEPTH

SURFACE CASING RECORD:

Ran 20.97' of 8-5/8" surface casing set at 27', cemented with 30 sacks cement and 1 sack calcium chloride.

PRODUCTION STRING:

Ran 1908' of 4½" casing, cemented with 150 sacks cement.

CERTIFICATION:

The above well log and other data are correct.
Original Signed By
H. W. Hartsough

H. W. Hartsough

Record No: 54164 Permit No: 13693
Farm Name: LAFFOON, E O
Well No: 2
Operator: ZOGG OIL CO, INC
Location: 2650 FSL x 2200 FWL 25- J-24
County: HOPKINS Elevation: 478
THE KENTUCKY GEOLOGICAL SURVEY DOES NOT WARRANT
THE ACCURACY OF INFORMATION ON THIS DOCUMENT

25-8-24
Elev: 506'

1520' FNL
680' FWL

RECEIVED
OCT 8 1965
DEPT. OF MINES AND MINERALS
LEXINGTON, KENTUCKY

13864

NAME OF WELL: Ross C. Gentry #4, Hopkins County, Kentucky
OPERATORS: Grant Mullenax, R.R. #1, Sandoval, Ky.
Neal Drilling Co.,Inc., P. O. Box 14, Carmi, Illinois
CONTRACTOR: Neal Drilling Co.,Inc., P. O. Box 14, Carmi, Illinois
DATE COMMENCED: 5/13/65
DATE COMPLETED: 5/18/65

Formation Record of Ross C. Gentry #4, Hopkins County, Ky.

From	To	Formation
0	120	Surface shale
120	330	Sand & shale
330	510	Shale, sand & lime
510	600	Shale
600	830	Sand, shaley sand & lime
830	1000	Sand & shale
1000	1040	Shale w/ lime streaks
1040	1175	Shale & lime
1175	1320	Lime streaks & shaly shale
1320	1442	Shale & lime
1442	1488	Lime
1488	1545	Lime & shale
1545	1550	Lime & shaley lime
1550	1595	Sand & sandy shale
1595	1605	Shale
1605	1620	Sand
1620	1670	Shale
1670	1675	Lime
1675	1746	Shale & lime
1746	1756	Sandy shale
1756	1833	Lime & shale
1833	1864	Shale
1864	1892TD	Sand

Record No: 53416 Permit No: 13864
Farm Name: GENTRY, ROSS C
Well No: 4
Operator: MULLENAX, GRANT
Location: 1520 FNL x 680 FWL 25- J-24
County: HOPKINS Elevation: 506
THE KENTUCKY GEOLOGICAL SURVEY DOES NOT WARRANT
THE ACCURACY OF INFORMATION ON THIS DOCUMENT

I, the undersigned, do hereby certify that the above is a true and complete copy of the Driller's Log of the Ross C. Gentry #4, Hopkins County, Kentucky, as taken from the daily drilling reports.

RECEIVED
OCT 11 1965
KENTUCKY GEOLOGICAL SURVEY

NEAL DRILLING CO., INC.

John F Walling

P. 14041

From	To	
0	40	Surface shale
40	180	Shale, sand & shells
180	200	Coal
200	385	Shale & sandy shale
385	450	Shale
450	675	Shale & sand
675	680	Lime & sand
680	930	Sand
930	1030	Shale
1030	1065	Lime
1065	1160	Shale & Lime
1160	1198	Lime
1198	1260	SHALE Lime w/sand
1260	1336	SHALE Lime
1336	1340	Lime
1340	1427	SHALE
1427	1450	LIME
1450	1522	Shale
1522	1620	Sand
1620	1635	Shale & sand
1635	1720	Shale & shaley sand
1720	1880TD	Sand

Record No: 53415 Permit No: 14041
Farm Name: GENTRY, ROSS C
Well No: 5
Operator: MULLENAX, GRANT
Location: 1350 FNL x 1300 FWL 25- J-24
County: HOPKINS Elevation: 493

I, the undersigned, ... and complete ... Hopkins County, ...

John T Wallace

Elev 482' 25-J-24 450'FNL 1975'FWL

P. 14342 Jack

FARM: Pressley #1
OPERATOR: Zogg Oil Company
COMMENCED: July 2, 1965

COUNTY: Hopkins County, Kentucky
CONTRACTOR: Crescent Drilling Company
COMPLETED: July 12, 1965

0	67	Surface Hole
67	180	Sand and Shale
180	1021	Shale and Sand
1021	1054	Upper Kaskaskia Lime
1054	1144	Shale and Lime
1144	1222	Lime and Chert
1222	1319	Shaly Sand
1319	1337	Lime and Shale
1337	1354	Shale
1354	1366	Lime Menard
1366	1392	Lime with Chert
1392	1405	Black
1405	1413	Lime
1413	1444	Lime and Shale
1444	1453	Lime Sanded
1453	1463	Shale
1463	1471	Lime Lower Menard
1471	1519	Shale
1519	1539	Lime Frankfort
1539	1561	Shale and Lime
1561	1598	Sand and Shale
1598	1631	Shale and Lime
1631	1673	Shale
1673	1679	Lime Ste. Genevieve
1679	1779	Sand and Shale
1779	1835	Lime and Shale
1835	1845	Sand
1845	1850	Shale
1850	1868	Shale and Lime
1868	1876	Sand
1876	1894	CORE #1
1894		TOTAL DEPTH

SURFACE CASING RECORD:

Ran 41.95' of 10-3/4" surface casing set at 40.95', cemented with 60 sacks cement.

PRODUCTION STRING:

Ran 1779' of 4½" prod. set at 1777½', cemented with 150 sacks Pozmix cement.

Ref. 298141

RECEIVED
NOV 12 1965
DEPT. OF MINES AND MINERALS
LEXINGTON, KENTUCKY

RECEIVED

CERTIFICATE:

The above is the true and correct data and record.

Signed By
H. W. Hartsough

H. W. Hartsough

Form G

WELL RECORD

COMMONWEALTH OF KENTUCKY
DEPARTMENT OF MINES AND MINERALS
OIL AND GAS DIVISION
P. O. Box 660
Lexington, Ky.

RECEIVED
AUG 30 1965
DEPT. OF MINES AND MINERALS
LEXINGTON, KENTUCKY

Permit No. 14513

Oil or Gas Well Oil (Kind)

ection
25-J-24

Company John Tuttle
Address Owensboro, Kentucky
Farm Peter Bowles Heirs Acres
Location (waters) 1320'FNL x 150'FWL
Well No. 3 Elev. 477'
District County Hopkins
Drilling Commenced August 16, 1965
Drilling Completed August 23, 1965
Name of Contractor Miro Drilling Co., Inc.
Address of Contractor Owensboro, Kentucky
Date Shot From To
With
Open flow /10ths Water in Inch
/10ths Merc. in Inch

Casing and Used in Left In Tubing Drilling Well

Size
16
13
10
8¼
6⅝
5 3/16
3
Casing Used
1870' of 4½" pipe cemented
Casing Cemented Size 21 No. Ft. 8-5/8" Feet
w/10/sx cement

Kind of Packer
Size of
Depth Set
Perf. top
Perf. bottom
Perf. top
Perf. bottom

Formation	Color	Hard or Soft	Top	Bottom	Oil, Gas & Coal or Water	Depth Found	Remarks
Surface			0	28			
Sand & Shale			28	1000			
Shale & Lime			1000	1006			
Lime (Upper Kincaid)			1006	1044			
Shale & Lime			1044	1344			
Lime			1344	1360			
Shale & Lime			1360	1507			
Lime & Shale (Vienna?)			1507	1534			
Shale & Lime			1534	1565			
Sand & Shale			1565	1590			
Lime & Shale			1590	1624			
Sand & Shale			1624	1666			
Lime & Shale			1666	1685			
Sand & Shale			1685	1711			
Sand (Hardinsburg)			1711	1756			
Sand			1756	1765			
Lime & Shale			1765	1812			
Lime			1812	1819			
Lime & Shale			1819	1868			
Core #1			1868	1879			
Total Depth			1879				

Record No: 53456 Permit No: 14513
Farm Name: BOWLES, PETER HEIRS
Well No: 3
Operator: TUTTLE, JOHN W
Location: 1320 FNL x 150 FWL 25- J-24
County: HOPKINS Elevation: 477
THE KENTUCKY GEOLOGICAL SURVEY DOES NOT WARRANT
THE ACCURACY OF INFORMATION ON THIS DOCUMENT

August 26, 1965
Miro Drilling Co., Inc.
by James Lowry
Sec-Treas

This well was cored so no electric log was run.

RECEIVED
SEP 7 1965
KENTUCKY GEOLOGICAL SURVEY

Form G

WELL RECORD

cert. 298137

RECEIVED
SEP 11 1965
DEPT. OF MINES AND MINERALS
LEXINGTON, KENTUCKY

920' FNL
2380' FWL

Send to Frankfort

COMMONWEALTH OF KENTUCKY
DEPAETMENT OF MINES AND MINERALS
OIL AND GAS DIVISION
P. O. Box 680
Lexington, Ky.

Permit No. 14514 — Oil or Gas Well Oil (Kind)

Company Zogg Oil Company
Address 1520 Sweeney, Owensboro, Ky.
Farm Wilbur Todd Acres
Location (waters)
Well No. 4 Elev. 502
District 25-J-24 County Hopkins
Drilling Commenced Aug. 2, 1965
Drilling Completed Aug. 10, 1965
Name of Contractor L & H Drilling Co.
Address of Contractor Box 348, O'boro, Ky.
Date Shot From To
With
Open flow /10ths Water in Inch
/10ths Merc. in Inch

Casing and Used in Left In Tubing Drilling Well

Size
16
13
10
8¼
6⅝
5 3/16
3
2
Liners Used

Kind of Packer
Size of
Depth Set
Perf. top
Perf. bottom
Perf. top
Perf. bottom

Casing Cemented Size No. Ft. Date

Formation	Color	Hard or Soft	Top	Bottom	Oil, Gas & Coal or Water	Depth Found	Remarks
Surface Soil			0	15			
Hard Sand			15	75			
Shale & Sand			75	360			
Hard Sand & Shale			360	500			
Sand & Shale			500	800			
Shale & Sand			800	955			
Sand & Shale			955	1042			
Lime, Shale & Sand			1042	1062			
Lime			1062	1085			
Shale, Sand & Lime			1085	1140			
Shale			1140	1180			
Lime			1180	1219			
Shale & Lime			1219	1238			
Lime & Shale			1238	1319			
Lime			1319	1331			
Shale & Lime			1331	1381			
Lime			1381	1479			
Shale			1479	1491			
Lime			1491	1501			
Shale			1501	1546			
Lime			1546	1567			
Shale & sandy shale			1567	1579			
Shale & Sand			1579	1626			
Hard Sand			1626	1631			
Sand & Shale			1631	1669			
Shale			1669	1696			
Lime			1696	1703			
Shale			1703	1710			

Record No: 54163 Permit No: 14514
Farm Name: TODD, WILBUR
Well No: 4
Operator: ZOGG OIL CO, INC
Location: 920 FNL x 2380 FWL 25- J-24
County: HOPKINS Elevation: 502

_____, Inc.

780' FNL
1550' FWL

August 26, 1965

Permit - 14578
25 - J - 24
Elev. 488'
Farm: Jack Pressley #1
County - Hopkins
Dan F Hart

OPERATOR: ~~Walter Sargent~~
CONTRACTOR: Hogue Drilling Co., Inc.
COMMENCED: August 14, 1965
COMPLETED: August 21, 1965
SURFACE: 21' 8 5/8" @ 26'
LONG STRING: Ran 1895' 5 1/2" casing

DRILLER'S LOG

0 -	260	Sand and shale
	480	Sand and shale
	865	Shale and sand
	895	Sand
	1010	Shale and sand
	1060	Lime
	1161	Lime, shale and sand
	1200	Lime
	1417	Shale and lime
	1610	Lime and shale
	1635	Shale and sand
	1695	Sand lime and shale
	1764	Sand and shale
	1886	Shale and sand

Record No: 53776 Permit No: 14578
Farm Name: PRESSLEY, JACK
Well No: 1
Operator: HART, DAN F
Location: 780 FNL x 1550 FWL 25- J-24
County: HOPKINS Elevation: 488
THE KENTUCKY GEOLOGICAL SURVEY DOES NOT WARRANT
THE ACCURACY OF INFORMATION ON THIS DOCUMENT

TO THE BEST OF MY KNOWLEDGE THIS IS A TRUE COPY OF THE DRILLER'S LOG OF YOUR JACK PRESSLEY NO. 1, HOPKINS COUNTY, KENTUCKY.

Permit # 14578
Dan F Hart

HOGUE DRILLING CO., INC.
BY: Stephanie C. Lewellen

sct

Form G

WELL RECORD

RECEIVED
MAY 2 9 1969
DEPT. OF MINES AND MINERALS
LEXINGTON, KENTUCKY

COMMONWEALTH OF KENTUCKY
DEPARTMENT OF MINES AND MINERALS
OIL AND GAS DIVISION
P. O. Box 650
Lexington, Ky.

Permit No. 20186 — Oil or Gas Well Oil

Company Zogg Oil Company
Address 1520 Sweeney-Owensboro, Ky.
Farm Wilbur Todd — Acres
Location (waters) 2835'FNLx1700'FEL
Well No. 6 — Elev. 464'
District — County Hopkins
Drilling Commenced December 5, 1967
Drilling Completed December 14, 1967
Name of Contractor Hire Drilling Co., Inc.
Address of Contractor Owensboro, Ky.
Date Shot — From — To
With
Open flow — /10ths Water in — Inch
/10ths Merc. in — Inch

Casing and Used in Drilling | Left in Well | Tubing

Size
16
13
10
8¼
6⅝
5 3/16
3

Kind of Packer
Size of
Depth Set
Perf. top
Perf. bottom
Liners Used
Perf. top
Perf. bottom

Casing Cemented Size 8-5/8" No. Ft. 225 Date

Formation	Color	Hard or Soft	Top	Bottom	Oil, Gas & Coal or Water	Depth Found	Remarks
Surface			0	27			
Sand & Shale			27	95			
Shale, Sand & Lime			95	335			
Sand & Shale			335	780			
Sand, Shale & Lime			780	1112			
Lime			1112	1220			
Lime, Shale & Sand			1220	1387			
Shale & Lime			1387	1645			
Shale & Sand			1645	1915			
Lime			1915	1940			
Lime, Sand & Shale			1940	2079			
Lime & Shale			2079	2148			
Lime			2148	2170			
TD			2170				

Record No: 54105 Permit No: 20186
Farm Name: TODD, WILBUR
Well No: 6
Operator: ZOGG OIL CO, INC
Location: 2835 FNL x 1700 FEL 25- J-24
County: HOPKINS Elevation: 464
THE KENTUCKY GEOLOGICAL SURVEY DOES NOT WARRANT
THE ACCURACY OF INFORMATION ON THIS DOCUMENT

Form G

WELL RECORD

RECEIVED
MAY 2 9 1969
DEPT. OF MINES AND MINERALS
LEXINGTON, KENTUCKY

25-J-24

COMMONWEALTH OF KENTUCKY
DEPARTMENT OF MINES AND MINERALS
OIL AND GAS DIVISION
P. O. Box 680
Lexington, Ky.

Permit No. 20270

Oil or Gas Well Oil (Kind)

Company Zogg Oil Company
Address 1520 Sweeney, Owensboro, Ky.
Farm Wilbur Todd Acres
Location (waters) 1740'NL - 1380'EL
Well No. 7 Elev. 474
District County Hopkins
Drilling Commenced 12-21-67
Drilling Completed 1-3-68
Name of Contractor Miro Drilling Co.
Address of Contractor Owensboro, Ky.
Date Shot From To
With
Open flow /10ths Water in Inch
/10ths Merc. in Inch

Casing and Used in Left In Tubing
Drilling Well

Size
16
13
10
8¼
6⅝
5 3/16
3
2
Liners Used.

Kind of Packer
Size of
Depth Set.
Perf. top
Perf. bottom
Perf. top
Perf. bottom

Casing Cemented 8 5/8" Size No. Ft. 26' Date

Formation	Color	Hard or Soft	Top	Bottom	Oil, Gas & Coal or Water	Depth Found	Remarks
Surface			0	28			
Sand & Shale			28	105			
Shale, Sand & Lime			105	327			
Sand & Shale			327	766			
Sand, Shale & Lime			766	1119			
Lime			1119	1231			
Lime, Shale & Sand			1231	1398			
Shale & Lime			1398	1661			
Shale & Sand			1661	192			
Lime			1929	1953			
Lime, Sand & Shale			1953	2091			
Lime & Shale			2091	2161			
Lime			2161	2183			
Lime &			2183	2209			
T.D.			2209				

FORMATION RECORD

From	To	Rock Type (describe rock types and other materials penetrated and record occurrences of oil, gas and water from surface to total depth)	From	To	Rock Type (describe rock types and other materials penetrated and record occurrences of oil, gas and water from surface to total depth)
0	240	soil			
240	253	Pennsylvania sandstone-sso			
253	1014	Base, Pennsylvanian System			
1014	1048	Upper Kinkaid limestone			
1144	1178	Lower Kinkaid limestone			
1200	1250	Degonia limestone			
1262	1294	Clore limestone			
1320	1328	Upper Menard limestone			
1344	1444	Middle, Massive Menard limestone			
1454	1464	Lower Menard limestone			
1510	1527	Vienna limestone			
1574	1604	Middle Tar Springs sandstone-sso-vssg			
1676	1682	Glen Dean limestone			
1722	1734	Hardinsburg sandstone-shly			
1798	1805	Golconda limestone			
1852	1876	Jackson sandstone-vsso/wtr			
1891	1900	Barlow limestone			
1914	1936	Cypress sandstone-tight			
1936	1982	Upper Paint Creek limestone			
1992	2004	Paint Creek sandstone-wtr			
2028	2042	Lower Paint Creek limestone			
2068	2085	Bethel sandstone-so			
2094	2130	Upper Renault limestone			
2145	2174	Lower Renault limestone			
2174	2202	Aux Vases limestone			
2202		Top, Ste. Genevieve limestone			
2226	2238	O'Hara Interval			
2240	2252	McClosky "D"			
2360		Birdwell total depth			
2360		Logger total depth			
		Bethel sandstone: 2078'-2085'-oil saturated sandstone with 80% brigh yellow fluorescence with show of live oil and gas when samples broken, very fine to fine grain size, subrounded grain shape, with 20% interbedded shale.			

Record No: 38587 Permit No: 57326
Farm Name: PRESSLEY, JACK
Well No: 2
Operator: ZOGG OIL CO, INC
Location: 420 FSL x 2140 FWL 16- J-24
County: HOPKINS Elevation: 449
THE KENTUCKY GEOLOGICAL SURVEY DOES NOT WARRANT
THE ACCURACY OF INFORMATION ON THIS DOCUMENT

FORMATION RECORD

FROM	TO	ROCK TYPE (DESCRIBE ROCK TYPES AND OTHER MATERIALS PENETRATED AND RECORD OCCURENCES OF OIL, GAS AND WATER FROM SURFACE TO TOTAL DEPTH.)	FROM	TO	ROCK TYPE (DESCRIBE ROCK TYPES AND OTHER MATERIALS PENETRATED AND RECORD OCCURENCES OF OIL, GAS AND WATER FROM SURFACE TO TOTAL DEPTH.)
0	280	Soil, Shale, occ LS	1838	1886	Shale
280	370	Sand, water	1886	1906	Jackson Sandstone SO
370	630	Shale	1906	1942	Shale ; Limestone
630	910	Sand, brackish water, ishale		1942	T.D.
910	1051	Shale; Sandy Shale			
1051	1076	Upper Kinkaid Limestone			
1076	1182	Shale			
1182	1210	Lower Kinkaid Limestone			
1210	1380	Shale: LS			
1380	1496	Menard LS (Menard, Cmmn) w/ occ Shale			
1496	1542	Shale			
1542	1562	Vienna Limestone			
1562	1631	Shale; Sandstone			
1631	1641	Upper Glen Dean Limestone			
1641	1692	Shale			
1692	1701	Lower Glen Dean Limestone			
1701	1720	Shale			
1720	1757	Hardinsburg Sandstone Bkn. VSSO on top			
1757	1830	Shale			
1830	1838	Golconda Limestone			

AFFIDAVIT

Gallagher Drilling, Inc, OPERATOR OF THE WELL CAPTIONED AS PERMIT NUMBER 95402 DOES HEREBY SWEAR THAT THE DEPTH OF THE WELL IS ACCURATE AND CORRECT AND DOES NOT EXCEED THE PERMITTED DEPTH OF 2250.

SIGNATURE OF OPERATOR Shawn Gallagher Vice President 12/10/03
TITLE DATE

SWORN TO AND SUBSCRIBED BEFORE ME THIS 10TH DAY OF December, 2003.

Pamela S. Schultheis
NOTARY PUBLIC

MY COMMISSION EXPIRES: 01/30/08

RECEIVED
DEPARTMENT OF MINES & MINERALS
OIL & GAS

PAMELA S. SCHULTHEIS

FORMATION RECORD

FROM	TO	ROCK TYPE (DESCRIBE ROCK TYPES AND OTHER MATERIALS PENETRATED AND RECORD OCCURENCES OF OIL, GAS AND WATER FROM SURFACE TO TOTAL DEPTH.)	FROM	TO	ROCK TYPE (DESCRIBE ROCK TYPES AND OTHER MATERIALS PENETRATED AND RECORD OCCURENCES OF OIL, GAS AND WATER FROM SURFACE TO TOTAL DEPTH.)
0	150	Clay; Shale Sli Sdy	1809	1860	Shale w/occ Ls.
150	170	Sandy shale	1860	1876	Jackson Sandstone SO.
170	820	Shale w/occ Sd; Lme	1876	1895	Shale
820	890	Sand	1894		Top of Barlow Limestone
890	1015	Shale	1894		T.D. Driller
1015	1050	Upper Kinkaid Limestone			
1050	1153	Shale			
1153	1180	Lower Kinkaid Limestone			
1180	1324	Shale occ Ls stringers			
1324	1448	Menard Limestone			
1448	1458	Shale			
1458	1468	Little Menard Limestone			
1468	1514	Shale			
1514	1534	Vienna Limestone			
1534	1585	Shale			
1585	1620	Upper Glen Dean Limestone			
1620	1662	Shale			
1662	1668	Lower Glen Dean Limestone			
1668	1689	Shale			
1689	1704	Hardinsburg Sandstone VSSO			
1704	1801	Shale			
1801	1809	Golconda Limestone			

0131562002

RECEIVED
DEPARTMENT FOR NATURAL RESOURCES
DIVISION OF OIL & GAS

AFFIDAVIT

Gallagher Drilling, Inc. , OPERATOR OF THE WELL CAPTIONED AS PERMIT NUMBER 99998 DOES HEREBY SWEAR THAT THE DEPTH OF THE WELL IS ACCURATE AND CORRECT AND DOES NOT EXCEED THE PERMITTED DEPTH OF 2250.

SIGNATURE OF OPERATOR Shawn Gallagher V.P (TITLE) 8/21/07 (DATE)

SWORN TO AND SUBSCRIBED BEFORE ME THIS 21 ST DAY OF AUGUST, 2007.

Pamela S. Schultheis
NOTARY PUBLIC

MY COMMISSION EXPIRES: 01/20/2008 Pamela S. Schultheis

Appendix 3 Information on monitoring wells.

	clay	0.0 – 4.5
	soft-hard brown sandstone	4.5 – 12.5
	interbedded shale and ss	12.5 – 21.0
	shaly sandstone	21.0 – 33.0
	shale	33.0 – 49.3
	silty shale to sandy shale	49.3 – 60.8
	shaly sandstone	60.8 – 78.0
	shale	78.0 – 102.8
	coal	102.8 – 104.1
	fine clay to sandy shale	104.1 – 111.0
	sandstone	111.0 – 117.0
	sandy shale to shaly sandstone	117.0 – 130.0
	sandstone	130.0 – 153.0
	coarse-grained hard sandstone	153.0 – 164.3
	coal	164.3 – 164.6
	gray sandstone	164.6 – 175.0
	shale	175.0 – 187.3
	gray to dark sandstone	187.3 – 211.0
	shale	211.0 – 244.3

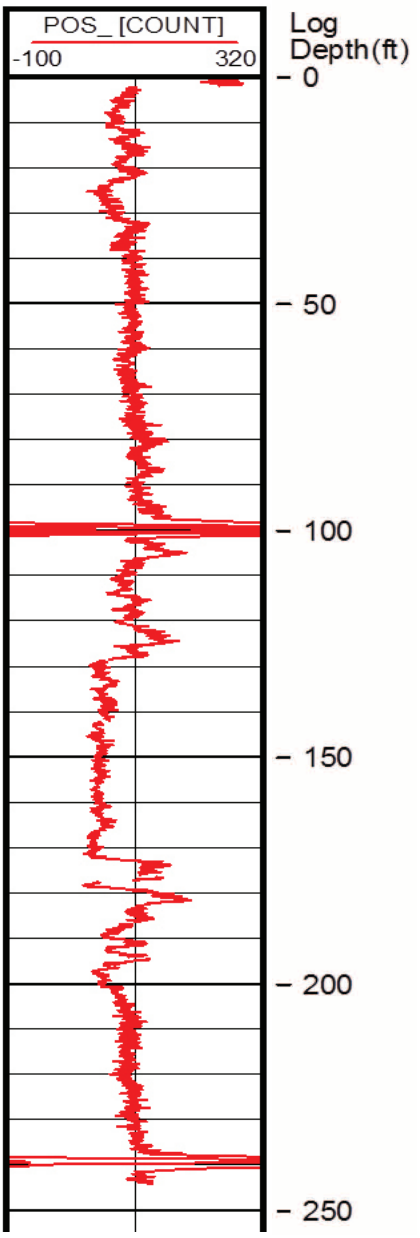

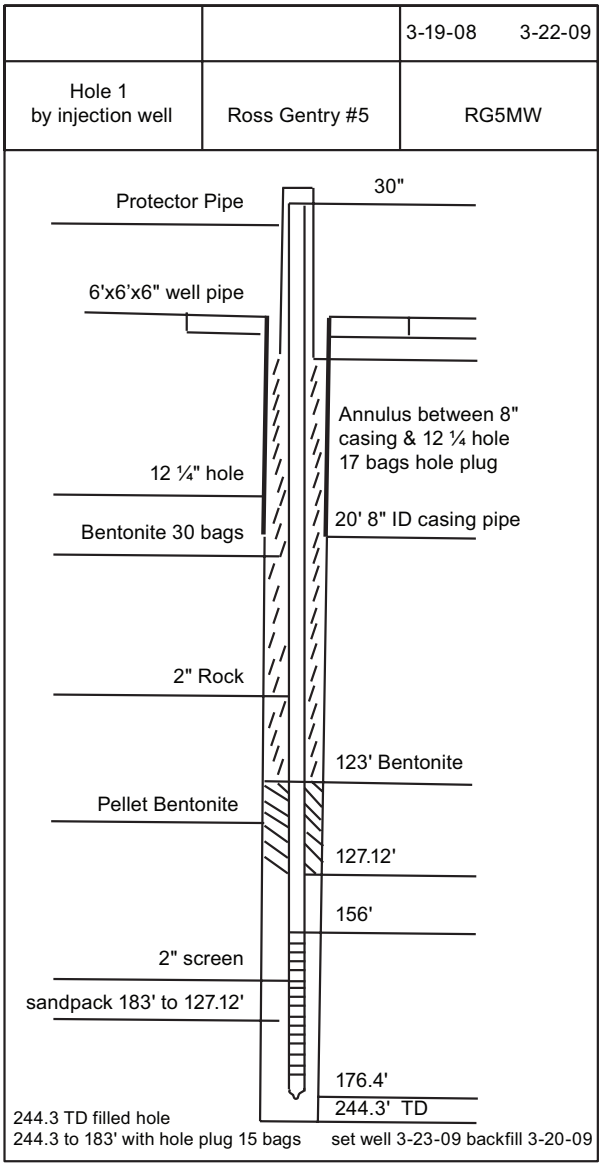

Details of monitoring well construction for RG-5MW, including a stratigraphic column constructed from well driller's log, gamma-ray log, and construction diagram. RG-4MW and PH-1MW were very similar to RG5-MW, so details for those wells are not given here.

Mineralogic composition in weight percent of the Jackson sandstone reservoir and Golconda seal rocks determined from x-ray diffraction analysis.[1]

Well	KGS Permit	Depth (ft)	Qtz	K-SPAR	Na-Plag	Cal	Ank	Dol	Chl	Pyr	Gyp	ML I/S	Illite and mica	Kaol
Jackson Reservoir														
Osburn #1A	12417	1840–1845	83.5	0.2	2.4	3.5	2.6	1.2	3.2	0	0	0	2.2	1.2
Osburn #1A	12417	1845–1850	70.6	0.3	2.3	14.6	1.9	2.6	3.1	0	0	0	3.6	1
Osburn #1A	12417	1850–1855	84.2	0.3	4.1	3.4	1.1	0.5	2.1	0	0	0	2.7	1.6
Harris #3	11987	1795–1800	85.4	0.5	3.1	1.7	0	1.2	4.8	0	0	0	1.7	1.6
Harris #3	11987	1800–1805	79.5	0.4	3.9	3.5	0.8	0	5.4	0	0	0	3.9	2.6
Harris #3	11987	1810–1815	79.7	0.3	3.7	5.1	1.5	0.3	4.1	0	0	0	2.9	2.4
Thomason & Boyd #1	10647	1815–1820	79.3	0.3	1.5	0.6	14.3	0	0	0	0	0	2.2	1.8
Thomason & Boyd #1	10647	1820–1825	80.4	0.3	1.9	0.4	12.8	0	0	0.2	0	0	2	2
Todd #2 (WT-2)	11080	1785–1790	74.1	0.3	2.6	0.9	17.6	0	0	0.2	0	0	2.1	2.2
Todd #2 (WT-2)	11080	1790–1795	75.1	0.2	2.3	0.7	12.9	0	1.9	0.3	0	0	3.4	3.2
Todd #2 (WT-2)	11080	1795–1800	87.6	0.2	3	1.2	1.3	0	1.7	0.1	0	0	2.2	2.7
Laffoon #1 (EL-1)	10574	1735–1740	78	0.3	1.4	0.4	15.8	0	0	0.2	0	0	2.1	1.8
Laffoon #1 (EL-1)	10574	1740–1745	78.4	0.2	4.2	0.7	1.7	0	4.6	0	0	0	3.7	6.5
Laffoon #1 (EL-1)	10574	1745–1750	89.5	0.2	2.9	0.3	2.1	0	0.3	0	0	0	2.1	2.6
Golconda Seal														
Thomason & Boyd #1	10647	1810–1815	25.7	2.4	3.3	5.9	1.9	0	3.5	0.6	0	35.2	18.8	2.7
Todd #2 (WT-2)	11080	1780–1785	25.7	2.4	1.8	8.8	1.7	0	3.5	0.5	0.4	34.5	16.2	4.4
Laffoon #1 (EL-1)	10574	1730–1735	28.6	2.6	2.9	19.4	1.9	0	2.9	0.4	0	19.8	17.9	3.6

[1]Abbreviations: KGS, Kentucky Geological Survey; Qtz, quartz; Cal, calcite; Ank, ankerite; Dol, dolomite; Pyr, pyrite; Gyp, gypsum; ML I/S, mixed layer illite/smectite; Kaol, kaolinite; and Chl, chlorite.

Appendix 5 Jackson brine properties.

Summary of Jackson brine water properties and infrared gas analysis (IRGA) measurements before (Pre-inj.) and after (Post-inj.) CO_2 injection and before and after CO_2 breakthough.[1]

Well and BT date[2]	Period	pH	Alkalinity (mg/L $CaCO_3$)	DIC[3] (mg/L)	TDS (mg/L)	Diss. CO_2 (mg/L)	IRGA CO_2 (%)
RG-1 (09/15/09)	Pre-inj.	7.2, 7.31	557, 764	115, 149	11,124–31,472 (n = 2)	519, 639	1.7–1.9
	Inj. Pre-BT	nd[4]	nd	nd	nd	nd	1.2–3.4
	Inj. Post-BT	5.62–5.9	990–1,201 (i)[4]	423–552 (i)	26,690–29,680 (n = 5)	1,380–2,110 (i)	47.9–90.7
	Post-inj.	5.71–6.29 (i)	1,160–1,754 (i, d)[4]	472–654 (i, d)	26,000–31,010 (n = 13)	1,550–3,130 (d)	41.7–88.4 (d)
RG-2 (05/20/09)	Pre-inj.	6.41–6.93	810–866	170–186	25,668–26,112 (n = 3)	674–774	3.2–6.9
	Inj. Pre-BT	nd	nd	nd	nd	nd	5.8
	Inj. Post-BT	6.22	1,997	657	27,284	3,300	72.4–98.2
	Post-inj.	6.12–6.19	2,116–2,216	664–746	24,580–26,650 (n = 3)	2,870–3,320 (d)	76.8–79.1 (d)
RG-3 (06/10/09)	Pre-inj.	6.56–6.81	832–894	184, 192	23,536–24,734 (n = 3)	736–878	1.6–5.9
	Inj. Pre-BT	6.76	897	177	23,996	843	4.1–6.3
	Inj. Post-BT	5.78–6.31	928–2,412 (i)	337–834 (i)	24,432–28,600 (n = 11)	1,380–3,330 (i)	25.1–90.6 (i)
	Post-inj.	5.92–6.73 (i)	2,210–2,734 (i, d)	735–972 (i, d)	25,480–29,070 (n = 13)	3,070–4,320 (i, d)	78.4–91.4
RG-4 (09/15/09)	Pre-inj.	6.53–7.13	817–854	160–171	18,438–22,316 (n = 3)	653–738	0.5–3.5
	Inj. Pre-BT	6.01–6.92 (d)	804–876	162–207	19,476–22,756 (n = 4)	695–827	2.6–9.7
	Inj. Post-BT	5.68–6.02	1,101–1,651 (i)	468–653 (i)	17,228–23,660 (n = 7)	1,400–3,625 (i, d)	9.9–94.9 (i)

	Post-inj.	5.65–6.17	1,865–2,680 (i)	548–897 (i)	23,720–29,750 (n = 8)	2,350–3,650 (i)	72.2–94.3 (d)
RG-5 (injector)	Pre-inj.	7.2	689	144	20,072	677	nd
PH-1 (10/07/09)	Pre-inj.	6.65–7.51	20–352	19–101	58,056–59,000 (n = 3)	93–410	0, 0.1
	Inj. Pre-BT	6.37–7.79 (d)	290–360	39–73 (d)	58,848–66,640 (n = 3)	208–412 (d)	0–1
	Inj. Post-BT	5.78	1,483	559	62,168	2,390	26–82.7 (i)
	Post-inj.	6.16–6.21	1,969–2,812 (d)	891–963	24,560–26,640 (n = 3)	3,120–4,500 (d)	86–90.7
WT-4 (no BT)	Pre-inj.	6.63–6.84	310–332	66	50,420–58,622 (n = 3)	249–305	0.2–0.8
	Inj. Pre-BT	6.15–7.15	300–361	57–110	55,127–63,410 (n = 11)	230–466	0.7–1.9
	Inj. Post-BT	na	na	na	na	na	na
	Post-Inj.	6.31–6.95	296–588	56–320	51,580–63,470 (n = 12)	305–650	1.0–2.0
WT-9	Pre-inj.	6.67–7.2	858–920 (d)	209	23,720–24,789 (n = 3)	765–787	nd
	Inj. Pre-BT	6.01–7.24 (d, i)	873–1,031 (i)	173–232 (i)	23,872–25,800 (n = 8)	712–1,365	0.3–2.0 (i)
	Inj. Post-BT	na	na	na	23,327–26,020 (n = 5)	na	na
	Post-inj.	6.55–7.21	983–1,068 (i)	226–264 (i)	22,840–25,170 (n = 11)	858–1,375	1.20–3.90 (i, d)

[1] WT-8 is not shown because brine measurements were not conducted; however, IRGA CO_2 measurements in the Inj. Pre-BT and Post-Inj. periods ranged from 0 to 2.9%.
[2] Breakthrough dates given here are based on gas composition (CO_2 concentration); see Table 8-1 for further information.
[3] Abbreviations: DIC, dissolved inorganic carbon; TDS, total dissolved solids; Diss. CO_2, the amount of CO_2 dissolved in solution; IRGA, infrared gas analyzer; nd, no data; na, not applicable.
[4] Parenthetical (i) and (d) refer to increasing and decreasing values for the given period.

Appendix 6 Gas composition from production wells.

Gas composition of gas samples from production wells prior to injected CO_2 breakthrough with minimum air contamination.

Sample	Sample Date	CO_2	O_2 + Ar	N_2	CH_4	C_2H_6	C_3H_8	iC_4H_{10}	nC_4H_{10}	iC_5H_{12}	nC_5H_{12}	C_6H_{14} +
RG1-02	4/8/09	1.88	0.31	<0.01	37.49	15.50	26.32	3.68	11.54	1.53	1.57	0.19
RG1-03	4/28/09	1.70	0.33	1.79	34.39	14.90	26.53	3.80	12.15	1.89	2.13	0.39
RG2-03	4/28/09	7.80	0.26	2.43	39.64	13.93	22.57	2.75	8.09	1.12	1.21	0.20
RG2-04	5/12/09	7.21	0.21	0.67	34.07	13.13	25.20	3.79	11.64	1.71	2.11	0.23
RG3-03	4/28/09	6.51	0.30	3.24	43.49	13.00	20.77	2.69	7.68	1.01	1.12	0.19
RG3-04	5/12/09	7.56	0.52	4.11	34.50	11.78	22.60	3.57	11.26	1.80	1.97	0.35
RG3-04 Dup	5/12/09	7.54	0.54	4.17	34.48	11.77	22.59	3.57	11.25	1.80	1.96	0.35
RG3-08	6/1/09	6.29	0.30	7.71	32.37	11.21	22.59	3.57	11.66	1.86	2.02	0.41
RG4-08	6/1/2009	4.66	1.07	6.90	39.88	10.48	19.18	3.13	10.18	1.81	2.14	0.56
RG4-08 Dup	6/1/2009	4.70	1.09	7.00	39.81	10.46	19.14	3.13	10.16	1.81	2.14	0.56
WT4-1	3/17/09	0.39	0.36	1.04	71.71	5.48	7.79	1.79	7.11	1.87	2.07	0.39
WT4-1 Dup	3/17/09	0.39	0.38	1.12	71.79	5.44	7.73	1.78	7.06	1.86	2.05	0.39
WT4-02	4/8/09	0.49	0.39	0.90	72.93	6.01	8.39	1.48	5.55	1.42	1.94	0.49
WT4-03	4/28/09	0.99	0.03	<0.01	57.79	11.03	17.30	2.47	7.95	1.08	1.18	0.19
WT4-04	5/12/09	1.10	0.45	1.25	55.24	10.70	16.66	2.65	8.51	1.44	1.68	0.32
WT8-1	3/17/09	0.34	0.37	<0.01	38.24	14.99	25.50	3.82	12.22	1.93	2.20	0.38
WT8-02	4/8/09	0.38	0.39	<0.01	41.84	16.08	23.74	3.25	10.34	1.66	1.92	0.42
WT8-02 Dup	4/8/09	0.40	0.31	<0.01	40.87	16.26	24.15	3.31	10.60	1.70	1.98	0.42
WT8-04	5/12/09	0.38	0.42	0.31	38.84	15.78	25.78	3.64	11.06	1.66	1.82	0.30
PH1-03	4/28/09	0.38	0.14	0.57	56.91	9.46	16.75	2.78	9.58	1.52	1.64	0.27

Appendix 7 Pennsylvanian groundwater properties.

Summary of Pennsylvanian groundwater properties before (Pre-inj.), during (Inj.), and after (Post-inj.) CO_2 injection, given as ranges; the number of measurements is in parentheses.

Well	Period	pH	Alkalinity (mg/L $CaCO_3$)	DIC[1] (mg/L)	TDS (mg/L)	Diss. CO_2 (mg/L)
DC-1	Pre-inj.	7.73–7.81 (2)	273–300 (2)	62–66 (2)	396–414 (2)	229–251 (2)
	Inj.	7.37–7.91 (3)	264–280 (3)	63–70 (3)	304–528 (3)	224–284 (3)
	Post-inj.	7.36–8.00 (4)	240–268 (3)	58–67 (4)	304–524 (4)	217–346 (4)
KB-1	Pre-inj.	8.58–8.79 (3)	548–558 (3)	109–120 (3)	732–784 (3)	428–465 (3)
	Inj.	8.34–8.67 (3)	526–555 (3)	114–123 (3)	728–776 (3)	359–664 (3)
	Post-inj.	8.21–9.10 (5)	473–545 (5)	112–117 (5)	688–828 (5)	426–466 (5)
PH-1MW	Pre-inj.	7.01–7.13 (2)	380–416 (2)	106 (1)	828–905 (2)	360–361 (2)
	Inj.	6.69–7.29 (3)	380–404 (3)	94–108 (3)	856–996 (3)	364–464 (3)
	Post-inj.	7.04–7.35 (5)	368–400 (5)	97–103 (5)	772–900 (5)	268–408 (5)
RG-4MW	Pre-inj.	6.75–6.79 (2)	424–466 (2)	119 (1)	800–869 (2)	409–414 (2)
	Inj.	6.72–7.01 (3)	452–452 (3)	113–125 (3)	792–908 (3)	410–468 (3)
	Post-inj.	6.91–7.19 (5)	412–438 (5)	109–118 (5)	776–976 (5)	342–466 (5)
RG-5MW	Pre-inj.	7.10–7.21 (2)	382–434 (2)	109 (1)	724–740 (2)	365–398 (2)
	Inj.	6.78–7.08 (3)	404–438 (3)	106–115 (3)	720–792 (3)	396–524 (3)
	Post-inj.	7.02–7.28 (5)	392–421 (5)	103–110 (5)	712–836 (5)	404–682 (5)
WT-3	Pre-inj.	8.54–8.84 (2)	633–652 (2)	129 (1)	842–1,077 (2)	480–526 (2)
	Inj.	7.92–8.90 (3)	574–680 (3)	129–158 (3)	664–936 (3)	469–530 (3)
	Post-inj.	8.68–9.18 (5)	559–663 (5)	134–147 (5)	804–1,004 (5)	466–665 (5)

[1]Abbreviations: DIC, dissolved inorganic carbon; TDS, total dissolved solids; Diss. CO_2, amount of CO_2 dissolved in solution.

Appendix 8 Jackson brine cation and anion concentrations.

Summary of Jackson brine cation and anion concentrations (mg/L) during the pre-CO_2 injection (Pre-inj.) and post-CO_2 injection (Post-inj.) periods and before and after CO_2 breakthrough (BT). [1]

Well and BT date	Period	Ba	Ca	Fe	K	Mg	Mn	Na	Si	Sr	Al	Br	Cl	HCO_3^-	SO_4
RG-1 (09/15/09)	Pre-inj	1–3.21	248–729	0.007 –0.03	9.3–28.4	96.1–249	0.08– 0.46	3,543– 9,080	4.92– 6.77	161–472	<MDL	25.2– 68.4	6,400– 18,100	679.15– 931.55	31.4– 35.5
	Inj. Pre-BT	nd	nd	nd	nd	nd	nd	nd	nd	nd	nd				
	Inj. Post-BT	2.98– 3.21	649–718 (i)[2]	2.23– 4.433	26.2– 33.3	227–255 (i)	0.21– 0.37	8,810– 9,340	6.11– 7.23	431–493 (i)	<MDL	60.4– 69.4	15,500– 16,400	1,207.11– 1,464.38	43.8– 50.9
	Post-inj.	1.89– 3.38 (d, i)	692–898 (i, d)	<MDL– 2.63 (d)	26.5– 35.1	235–268	0.23– 1.17 (i, d)	8,610– 10,300	6.1–9.15 (i, d)	461–540 (i)	<MDL	57.7–135	14,000– 17,000	1,414.39– 2,138.66	29.9– 85.5
RG-2 (05/20/09)	Pre-inj.	4.39–5.2	558–583	<MDL– 0.007	22.4– 39.8	208–224	0.7–0.09	7,520– 8,413	4.93– 7.49	469–504	<MDL– 0.6	53.7– 61.15	14,300– 15,328.06	987.64– 1,055.92	16.9– 44.9
	Inj. Pre-BT	nd	nd	nd	nd	nd	nd	nd	nd	nd	nd				
	Inj. Post-BT	4.5	863	6.23	23.7	240	1.71	7,460	7.24	596	<MDL	56.6	14,200	2,434.95	44.2
	Post-inj.	1.01– 1.18	887–960 (i)	4.43–14 (i)	24.1– 26.5 (d)	255–275	2.74– 2.81 (d)	8,010– 8,480	8.74– 9.58 (i)	514–590 (i)	<MDL– 0.8 (d)	52.8– 53.2	13,400– 14,600	2,580.05– 2,701.98	95.8– 96.4
RG-3 (06/10/09)	Pre-inj.	4.28– 6.14 (d)	463–523	<MDL– 0.0256	19.2– 33.35	185–199	0.11– 0.16	6,910– 8,079	5.5–7.90	482–537	<MDL	50.2– 53.68	13,200– 13,726.69	1,014.46– 1,090.06	11.2– 42.7
	Inj. Pre-BT	4.8	516	<MDL	22.5	212	0.08	7,140	6.31	554	<MDL	51	12,800	1,093.72	34
	Inj. Post-BT	1.68– 4.55 (d)	523–890 (i)	<MDL– 11.1 (i)	16.4– 31.4 (i)	208–267 (i)	0.12– 2.56 (i)	7,080– 8,740 (i)	3.74– 9.99 (i)	547–769 (i)	<MDL	52.5– 67.1	13,300– 16,100	1,131.51– 2,940.96	20.8– 53.2
	Post-inj.	1.58–2.4 (d)	883– 1,040 (i)	3.26– 19.9 (i)	22.9– 29.3 (d)	252–283 (i)	2.16– 4.16 (i, d)	8,250– 9,140 (i)	8.46– 11.7 (i)	622–886 (d)	<MDL– 0.18 (d)	51.8–105	13,800– 15,000	2,694.66– 3,333.58	52.4– 68.9
RG-4 (09/15/09)	Pre-inj.	2.19– 2.27	371–399	<MDL– 0.04	16.3– 21.5	156–164	0.11– 0.22	5,675– 6,020	5.04– 6.79	459–493	<MDL	38.9– 39.7	10,000– 10,400	996.17– 1,041.29	33.2– 40.7
	Inj. Pre-BT	2.34– 2.48	410–443 (i)	<MDL	13.8– 21.9	175–178	0.04– 0.07	5,850– 6,290	4.74– 6.03	508–518	<MDL	40.8– 44.6	10,300– 11,200	980.32– 1,068.11	38–184
	Inj. Post-BT	1.93– 2.47 (d)	553–696 (i)	3.61– 14.1 (i)	18.8– 22.5 (i)	199–241 (i)	0.68– 1.97 (i)	6,460– 7,260 (i)	4.46– 6.69 (i)	531–592 (i)	<MDL– 0.08	44.9– 53.6	11,300– 12,300	1,342.45– 1,924.06	39.2– 44.3
	Post-inj.	1.07– 1.94 (d)	772– 1,150 (i)	2.83– 7.75 (d)	21.9– 26.2 (i)	239–324 (i)	1.54– 2.32 (i)	7,450– 8,740 (i)	6.95– 9.39 (i)	566–659 (i)	<MDL– 0.09 (d)	50.3– 86.6	13,000– 15,000	2,274– 2,347.16	<MDL– 100
PH-1 (10/07/09)	Pre-inj.	2.02– 5.10	1,480– 1,630	38.3–283	49.4–104	586–613	1.09– 7.76	15,900– 18,857	2.36– 11.16	308–334	0.09	127– 139.55	33,100– 36,506.68	24.39– 429.20	<MDL– 8.3
	Inj. Pre-BT	2.09– 2.54	1,580– 1,670	8.7–35.3	43.4– 45.7	610–643	0.68– 2.18	15,400– 17,560	6.65– 8.82	324–342	0.12	132–139	32,700– 34,400	353.60– 438.95	<MDL– <MDL
	Inj. Post-BT	3.2	1,820	43	50.7	608	1.69	17,370	8.45	365	0.17	51.6–170	13,600– 31,000	1,808.23– 3,428.68	14.8–113
	Post-inj.	1.09– 1.26 (d)	1,095– 1,230	0.02– 11.9	23.5– 28.3	266–289	1.46– 5.09 (d)	7,610– 8,150	9.85– 9.88	339–359	0.10, 0.11	52–61.8	12,800– 14,300	2,400.81– 3,350.65	116–118
WT-4 (no BT)	Pre-inj.	5.12– 5.61	270– 1,581	<MDL– 0.439	50–99.3	570–604	0.232– 0.39	17,340– 17,956	4.27– 7.05	262–275	<MDL– 0.1	125– 130.5	32,100– 34,707.63	377.98– 404.81	54.5– 91.61
	Inj. Pre-BT	4.56– 5.27	1,515– 1,650	<MDL	37.2– 84.4	578–610	0.17– 0.29	15,100– 18,300	4.32– 4.91	266–291	<MDL– 0.1	72.7–179	30,400– 34,900	365.79– 440.17	65.6–144
	Inj. Post-BT	na	na	na	na	na	na	na	na	na	na				
	Post-inj.	4.75– 5.51	1,500– 1,660	<MDL	44.1– 61.7	556–634	0.18– 0.226	17,020– 20,430	3.89– 4.98	285–317	<MDL	106–195	30,300– 35,900	360.91– 716.95	46.4–140
WT-9 (ambiguous; see text))	Pre-inj.	1.81– 2.97	453–473	<MDL– 21	25.2– 42.21	180–183	0.056– 1.63	7,860– 8,023	4.2–8.09	528–576	<MDL– 0.066	51.9– 55.17	13,600– 14,234.74	1,046.16– 1,121.76	23.1– 61.98
	Inj. Pre-BT	2.34– 2.85 (i)	442–497 (i)	<MDL	18.4– 35.9 (i)	182–207 (i)	0.04– 1.96	7,400– 8,820	5.43– 6.67 (d, i)	536–606 (i)	<MDL	51.5– 65.2	8,170– 13,900	1,064.45– 1,171.75	39.5–152
	Inj. Post-BT	na	na	<MDL	na	na	na	na	na	na	na	49.5– 56.3	12,700– 13,500	1,169.31– 1,241.25	77.4–162
	Post-inj.	2.1–3.82 (i)	451–511	<MDL	24.9– 29.8	186–207	0.03– 0.14	7,745– 8,330 (i)	5.89– 6.79	535–648	<MDL	48.3– 81.8	12,900– 14,500	1,198.58– 1,303.22	72.3–156

[1]Concentrations (mg/L) were measured per the previously discussed IC and ICP methods; HCO_3 was calculated from measured alkalinity. Breakthrough dates given here are based on gas composition (CO_2 concentration); see Table 8-1 for further information.

[2]Parenthetical (i) and (d) refer to increasing and decreasing values for the given period. Abbreviations: <MDL, below mean detection limit; nd, not detected.

Appendix 9 Pennsylvanian groundwater cation and anion concentrations.

Summary of Pennsylvanian groundwater cation and anion concentrations (mg/L) before (Pre-inj.), during (Inj.), and after (Post-inj.) CO_2 injection. Concentrations are given as ranges; the number of measurements is shown in parentheses. Concentrations below mean detection limit are shown as <MDL.

Well	Period	Ba	Ca	Fe	K	Mg	Mn	Na	Si	Sr	Br	Cl	HCO_3^-	SO_4
DC-1	Pre-inj.	0.09–0.13 (2)	30.40–31.40 (2)	0.11–0.22 (2)	2.20–2.27 (2)	14.50–15.00 (2)	0.005–0.005 (2)	81–106 (2)	8.81–9.29 (2)	0.44–0.45 (2)	<MDL1–0.1 (2)	5.7–30.2 (2)	333–366 (2)	69–79 (2)
	Inj.	0.13–0.14 (3)	15.20–33.30 (3)	0.08–0.11 (3)	1.83–2.71 (3)	7.70–16.20 (3)	0.003–0.005 (3)	93–120 (3)	8.25–8.80 (3)	0.25–0.50 (3)	<MDL–0.2 (3)	2.7–59.5 (3)	322–341 (3)	42–81 (3)
	Post-inj.	0.08–0.14 (4)	14.50–39.10 (4)	0.02–0.36 (4)	1.78–2.60 (4)	7.50–19.40 (4)	0.003–0.006 (4)	76–123 (4)	7.73–9.46 (4)	0.24–0.55 (4)	<MDL–0.2 (4)	2.9–43.0 (4)	293–327 (4)	41–90 (4)
KB-1	Pre-inj.	0.02–0.03 (3)	2.53–3.03 (3)	<MDL–0.02 (3)	1.47–2.47 (3)	1.22–1.29 (3)	0.002–0.003 (3)	260–295 (3)	4.41–4.65 (3)	0.07–0.09 (3)	0.1–0.1 (3)	12.6–14.6 (3)	668–680 (3)	107–122 (3)
	Inj.	0.05–0.06 (3)	3.06–3.31 (3)	<MDL (3)	2.44–2.65 (3)	1.31–1.38 (3)	0.002–0.002 (3)	259–302 (3)	4.37–4.49 (3)	0.09–0.09 (3)	0.1–0.2 (3)	14.6–33.2 (3)	641–677 (3)	112–156 (3)
	Post-inj.	0.03–0.10 (5)	2.99–3.65 (5)	<MDL (5)	2.14–2.56 (5)	1.33–1.53 (5)	0.002–0.003 (5)	276–393 (5)	4.33–4.61 (5)	0.09–0.10 (5)	<MDL–0.1 (5)	13.5–14.9 (5)	577–665 (5)	104–117 (5)
PH-1MW	Pre-inj.	0.03–0.04 (2)	90.57–92.80 (2)	0.01–0.02 (2)	4.34–4.46 (2)	40.14–41.60 (2)	0.050–0.050 (2)	138–144 (2)	12.60–13.65 (2)	0.79–0.81 (2)	<MDL–1.4 (2)	7.6–9.4 (2)	689–754 (2)	321–373 (2)
	Inj.	0.01–0.02 (3)	89.40–90.80 (3)	0.01–0.31 (3)	4.24–4.35 (3)	38.70–39.90 (3)	0.030–0.040 (3)	135–159 (3)	12.70–13.20 (3)	0.77–0.79 (3)	<MDL–0.1 (3)	6.6–7.3 (3)	689–732 (3)	314–332 (3)
	Post-inj.	0.01–0.02 (5)	90.40–98.10 (5)	0.35–0.41 (5)	4.17–4.39 (5)	39.50–44.20 (5)	0.020–0.020 (5)	138–160 (5)	12.80–13.80 (5)	0.77–0.82 (5)	<MDL–0.1 (5)	6.4–11.2 (5)	667–725 (5)	326–352 (5)
RG-4MW	Pre-inj.	0.04–0.04 (2)	114.00–115.42 (2)	<MDL–0.03 (2)	4.22–4.33 (2)	44.00–45.86 (2)	0.067–0.090 (2)	102–111 (2)	12.90–14.46 (2)	0.50–0.53 (2)	0.1–1.4 (2)	11.4–11.9 (2)	517–568 (2)	278–328 (2)
	Inj.	0.02–0.03 (3)	103.00–109.00 (3)	0.11–0.29 (3)	4.01–4.22 (3)	38.30–40.70 (3)	0.080–0.100 (3)	118–145 (3)	13.40–13.70 (3)	0.47–0.48 (3)	0.1–0.2 (3)	10.6–11.9 (3)	551–551 (3)	284–288 (3)
	Post-inj.	0.02–0.02 (5)	103.00–114.00 (5)	0.18–0.32 (5)	3.85–4.21 (5)	38.70–44.00 (5)	0.070–0.080 (5)	122–149 (5)	13.40–14.60 (5)	0.46–0.50 (5)	<MDL–0.2 (5)	10.1–14.3 (5)	502–534 (5)	288–311 (5)
RG-5MW	Pre-inj.	0.05–0.05 (2)	66.61–81.10 (2)	<MDL (2)	3.89–4.70 (2)	26.42–32.10 (2)	0.038–0.070 (2)	139–158 (2)	11.60–11.92 (2)	0.60–0.75 (2)	<MDL–1.4 (2)	8.2–9.8 (2)	466–529 (2)	244–283 (2)
	Inj.	0.03–0.04 (3)	82.90–83.90 (3)	<MDL (3)	4.51–4.91 (3)	32.60–32.90 (3)	0.050–0.060 (3)	137–161 (3)	12.60–13.00 (3)	0.75–0.78 (3)	0.1–0.2 (3)	9.2–10.2 (3)	2.4–534 (2)	246–254 (3)
	Post-inj.	0.02–0.03 (5)	78.00–88.30 (5)	<MDL (5)	4.73–4.80 (5)	31.70–34.70 (5)	0.035–0.046 (5)	140–161 (5)	12.80–13.40 (5)	0.76–0.78 (5)	<MDL–0.1 (5)	9.0–13.5 (5)	478–513 (5)	250–264 (5)
WT-3	Pre-inj.	0.04–0.07 (2)	1.08–1.82 (2)	0.05–0.20 (2)	0.89–1.46 (2)	0.41–0.62 (2)	0.002–0.004 (2)	313–419 (2)	4.38–4.42 (2)	0.04–0.09 (2)	0.4–2.0 (2)	137.0–227.9 (2)	772–795 (2)	<MDL (2)
	Inj.	0.04–0.06 (3)	1.00–1.60 (3)	0.15–0.20 (3)	1.19–1.44 (3)	0.30–0.53 (3)	0.003–0.003 (3)	287–341 (3)	4.19–4.34 (3)	0.04–0.08 (3)	0.3–0.8 (3)	87.4–196.0 (3)	700–829 (3)	<MDL (3)
	Post-inj.	0.05–0.07 (5)	1.26–1.74 (5)	0.15–0.21 (5)	1.14–1.54 (5)	0.41–0.59 (5)	0.002–0.003 (5)	337–423 (5)	4.20–4.58 (5)	0.05–0.09 (5)	0.4–0.8 (5)	127.0–230.0 (5)	682–808 (5)	<MDL–42 (5)

Appendix 10 Interpretation of Reservoir Saturation Tool logging data.

SUMMARY

Reservoir Saturation Tool (RST) logs were run at Sugar Creek Field to determine whether the injected CO_2 was migrating into zones above the injection zone. The RST is a wireline pulsed neutron logging tool that has as its main measurements the macroscopic capture cross section as well as the neutron porosity of the formation. Other measurements useful to the monitoring of CO_2 in the borehole as well as the formation were also made and will be described later in this appendix. This report is related primarily to the analysis of the RST data collected on one CO_2 injector well and eight oil-producing monitor wells. Conclusions are most accurate within feet from the wellbore and diminish in relevance laterally from the well site in any direction.

The wireline logging program to evaluate the containment of the CO_2 consisted of running two passes of the RST and then overlaying the pertinent data to detect any changes in the fluids in the wellbore or in the formation. The first logging runs (base pass) of the RST were made in late March 2009, prior to injection. In early October 2011, after injection of CO_2 was complete, the monitoring run of the RST log was made in each well.

After making the logging passes, all data were reviewed and reprocessed as necessary to ensure the correct parameters were being used. Next, displays were made to overlay key data from the two logging runs; we looked for indications that the fluids in the borehole or formation had changed. Changes in the fluids are indicated by separations in the overlaid curves. A general interpretation of the data is that the CO_2 remained in the primary zone of injection.

DETAILED DESCRIPTION

Reservoir Saturation Tool Pulsed Neutron Capture (PNC)

The capture mode of the RST can also be referred to as “Sigma mode.” In capture mode, the RST is measuring the rate at which thermal neutrons are captured by the formation. This Sigma measurement (SIGM) is the macroscopic capture cross section. Because chlorine has the greatest ability to capture thermal neutrons and hydrogen has the greatest ability to slow the high energy neutrons to the thermal level, the Sigma measurement is very responsive to saltwater in the pores. If the amount of saltwater decreases and is replaced by hydrocarbons or CO_2, then the capture cross section of the formation will decrease, since hydrocarbons and CO_2 have low Sigma values compared with that of saltwater. The tool also measures thermal neutron porosity in a manner very similar to the open-hole neutron porosity tools. The RST porosity is called TPHI and this porosity will respond to CO_2 very much like gas since both have a very low hydrogen index. Gas and CO_2 both cause neutron porosity to be too low compared to 100% liquid saturation because the neutron porosity measurement is primarily responding to the hydrogen index.

Because of these differences, the Sigma measurement and the porosity measurement from the RST tool can be combined in an analysis to determine the saturation of saltwater and gas/CO_2 in the formation porosity. Gas and CO_2 cannot be differentiated because they have the same neutron porosity response and very similar Sigma values. Both the SIGM and TPHI measurements are intended to be related to the formation properties. Although much has been done to characterize these measurements for changing borehole conditions, it remains difficult to consistently and accurately make borehole corrections when the borehole contains either gas or CO_2. For this reason, additional Sigma and porosity calculations are also made. The log presentation also includes SIGM_TDTL, the computation of Sigma using the same algorithm that was used by the TDT-P tool. This computation is not as robust as the RST Sigma computation under normal conditions, but under some unusual borehole conditions it has been found to be a bit more consistent. Therefore, both are presented for analysis; the thought is that if there is a difference between the two runs and the changes in SIGM and SIGM_TDTL are consistent with each other, the change is in the formation. If there is a difference between the two runs and the changes in SIGM and SIGM_TDTL are not consistent with each other, the change is in the borehole fluids.

The additional porosity presented on the logs is PHIC, a porosity developed for the pulsed neutron tools that is able to provide a porosity computation even in a gas-filled borehole. In a gas-filled borehole, the TPHI porosity will be considerably lower than it should be, even going to zero in larger borehole sizes. As mentioned before, CO_2 and methane cause similar responses to the SIGM and porosity from the RST; therefore, in a CO_2-filled borehole the TPHI porosity will be much too low. The PHIC porosity allows for measurement of a neutron porosity that is responsive to changes in the formation fluids rather than being dominated by changes in the borehole fluids in gas- or CO_2-filled boreholes.

Other Measurements Used from RST

The RST provides other data that can be valuable for monitoring changes in the borehole and primarily borehole fluids. The capture cross section of the borehole (SBNA_FIL) and the inelastic counts from the far detector (INFD_TDTL) are two of these measurements. Just as SIGM is a measurement of the capture cross section of the formation, SBNA_FIL is a measurement of the capture cross section of the borehole. To pulsed neutron tools, the borehole is everything that is not formation. Therefore, the SBNA_FIL measurement includes the capture cross section of all of the cement, all of the different strings of casing and tubing, all of the other hardware such as packers, and all of the fluids in the different casing and tubing strings. In a monitoring case such as this, if the wellbore configuration is not changed, and there are changes in either the SBNA_FIL or INFD_TDTL between runs, then the fluids have likely been changed. If CO_2 or gas has entered the borehole where water once was, both of these measurements would respond to the CO_2. As discussed, with CO_2 in the formation, the capture cross section of CO_2 is low, so with CO_2 anywhere in the borehole, SBNA_FIL would be lower than if saline water was in the wellbore. This may also be true with fluids that have a lower capture cross section; however, the magnitude of the change would be less. INFD_TDTL responds to the hydrogen index and density of the materials in place. It will not respond to changes in water salinity, and any change in liquid-type, such as oil to water, will be too small to be detected. However, CO_2 is unlike both water and oil in that it has a lower density and no hydrogen; if CO_2 is anywhere in the borehole, INFD_TDTL will increase. This response is very similar to that of methane, so again, gas and CO_2 cannot be differentiated.

General Interpretation

The interpretation of pulsed neutron data is normally done by calculating the saturation of the different fluids that may be in the reservoir. For monitoring analysis, a change in saturation can be computed using the change in SIGM measured by the tool. For the wells in the Sugar Creek Field, a cursory look at the data reveals that both SIGM and SIGM_TDTL repeat very well from the base pass to the monitor run, indicating that there is no change in the formation fluids and that CO_2 is not migrating upward into other zones. Because SIGM is the primary measurement from the RST, SIGM forms the basis for the analysis. The TPHI and PHIC can be used as well, but SIGM has less uncertainty and better statistical precision than does the porosity measurement. Also, TPHI will be affected by CO_2 in the wellbore, which may cause slight changes in PHIC as well.

The SBNA_FIL and INFD_TDTL data are the main source of information for identifying fluid changes in the borehole. In several wells, the top of the liquid in the borehole can be identified where the INFD_TDTL curve increases dramatically. SBNA_FIL also decreases, as discussed in the preceding section; but the magnitude of the decrease is much less. Discussion of the data on each well follows.

Detailed Interpretation of Results

Bowles #3 (Appendix 10, figure 1) All data from the monitor run in October 2011 matches the same data from the base pass in March 2009, which indicates no change in formation fluid saturations.

Pressley Hart #1 (Appendix 10, figure 2) Most of the data from the monitor run in October 2011 matches the same data from the base pass in March 2009 up to 89.9 m (295 ft). Above 89.9 m (295 ft), the monitor pass of the RST shows air/gas in the wellbore causing the INFD_TDTL curve to increase and the SBNA_FIL to decrease. From this point up on the monitor pass, TPHI is zero. There are some differences in the base and monitor data for PHIC also. Note that SIGM and SIGM_TDTL are both different in

the base and monitor passes, but not in the same way. SIGM is a little higher on the base pass than on the monitor pass, whereas SIGM_TDTL is a little lower on the base pass than on the monitor pass. Based on the knowledge of the measurement responses described, this result indicates no change in formation fluid saturations. In addition, the fluid in the borehole appears to be different, at least in some intervals. From 366 m to 180 m (1,200 to 590 ft), SBNA_FIL was lower in the monitor run than it was in the base run. With INFD_TDTL repeating very well, this result would indicate a fluid salinity change, not CO_2 or gas/air, which seems to have had some effect on the PHIC computation as well.

Ross Gentry #1 (Appendix 10, figure 3) All data from the monitor run in October 2011 match the same data from the base pass in March 2009, which indicates no change in formation fluid saturations.

Ross Gentry #2 (Appendix 10, figure 4) Most of the data from the monitor run in October 2011 match the same data from the base pass in March 2009. This match is particularly true of the SIGM, SIGM_TDTL and PHIC, indicating no change in formation fluid saturations. However, INFD_TDTL from the monitor pass decreases above 541 m (1,775 ft) relative to the INFD_TDTL from the base pass. The change is abrupt, and one interpretation would be that tubing was run into the well to this point for the monitor pass. This also seems to have had some effect on the TPHI computation.

Ross Gentry #4 (Appendix 10, figure 5) With two exceptions, all data from the monitor run in October 2011 match the same data from the base pass in March 2009 up to 99 m (325 ft). Above 99 m (325 ft) the monitor pass of the RST has air/gas in the wellbore causing the INFD_TDTL curve to increase and the SBNA_FIL to decrease. From this point up on the monitor pass the TPHI is zero. Note that SIGM and SIGM_TDTL are different in the base and monitor passes, but not in the same way. SIGM is a little higher on the base pass than on the monitor pass, whereas SIGM_TDTL is a little lower on the base pass than on the monitor pass. Based on the knowledge of the measurement responses described, no change in formation fluid saturations is indicated. The exceptions mentioned are from 175 m to 166 m (575 to 545 ft) and at 337 m (1,107 ft). In those intervals, INFD_TDTL increases just as if there were a pocket of gas/air or CO_2 in the wellbore. One other helpful measurement is the tension (TENS). Note that for both these occurrences the TENS shifts a bit, indicating that either the tool is "pulling," or the fluid density has changed. Based on this information, it is thought that the open perforations in the well released bubbles or pockets of CO_2 that are migrating to the surface and passed the tool at those points.

Ross Gentry #5 (Appendix 10, figure 6) Most of the data from the monitor run in October 2011 match the same data from the base pass in March 2009, particularly the SIGM, SIGM_TDTL and PHIC, indicating no change in formation fluid saturations. However, INFD_TDTL from the monitor pass increased relative to the INFD_TDTL from the base pass. This well is the CO_2 injector and has 2⅜″ tubing in the well. The increase in INFD_TDTL is likely due to CO_2 being in the tubing casing annulus and seems also to have had some effect on the TPHI computation, causing it to be too low in some places.

Wilbur Todd #4 (Appendix 10, figure 7) All data from the monitor run in October 2011 match the same data from the base pass in March 2009 up to 177 m (580 ft). Above 177 m (580 ft), the base pass of the RST has air/gas in the wellbore, causing the INFD_TDTL curve to increase and the SBNA_FIL to decrease. From this point up on the base pass, the TPHI is zero, and there are some small differences in the base and monitor data for PHIC and SIGM. SIGM_TDTL, however, repeats very well. Based on the knowledge of the measurement responses described, those responses indicate no change in formation fluid saturations.

Wilbur Todd #8 (Appendix 10, figure 8) All data from the monitor run in October 2011 match the same data from the base pass in March 2009 up to 152 m (500 ft). Above 152 m (500 ft), the monitor pass of the RST has air/gas in the wellbore causing the INFD_TDTL curve to increase and the SBNA_FIL to decrease. From this depth up on the monitor pass the TPHI is zero, and there are also some differences in the base and monitor data for PHIC. Note that SIGM and SIGM_TDTL are both different in the base and monitor passes, but not in the same way. SIGM is a little higher on the base pass than on the monitor pass, whereas SIGM_TDTL is a little lower on the base pass than on the monitor pass. Based on the knowledge of measurement responses described, no change in formation fluid saturations is indicated.

Wilbur Todd #9 (Appendix 10, figure 9) All data from the monitor run in October 2011 match the same data from the base pass in March 2009, which indicates no change in formation fluid saturations.

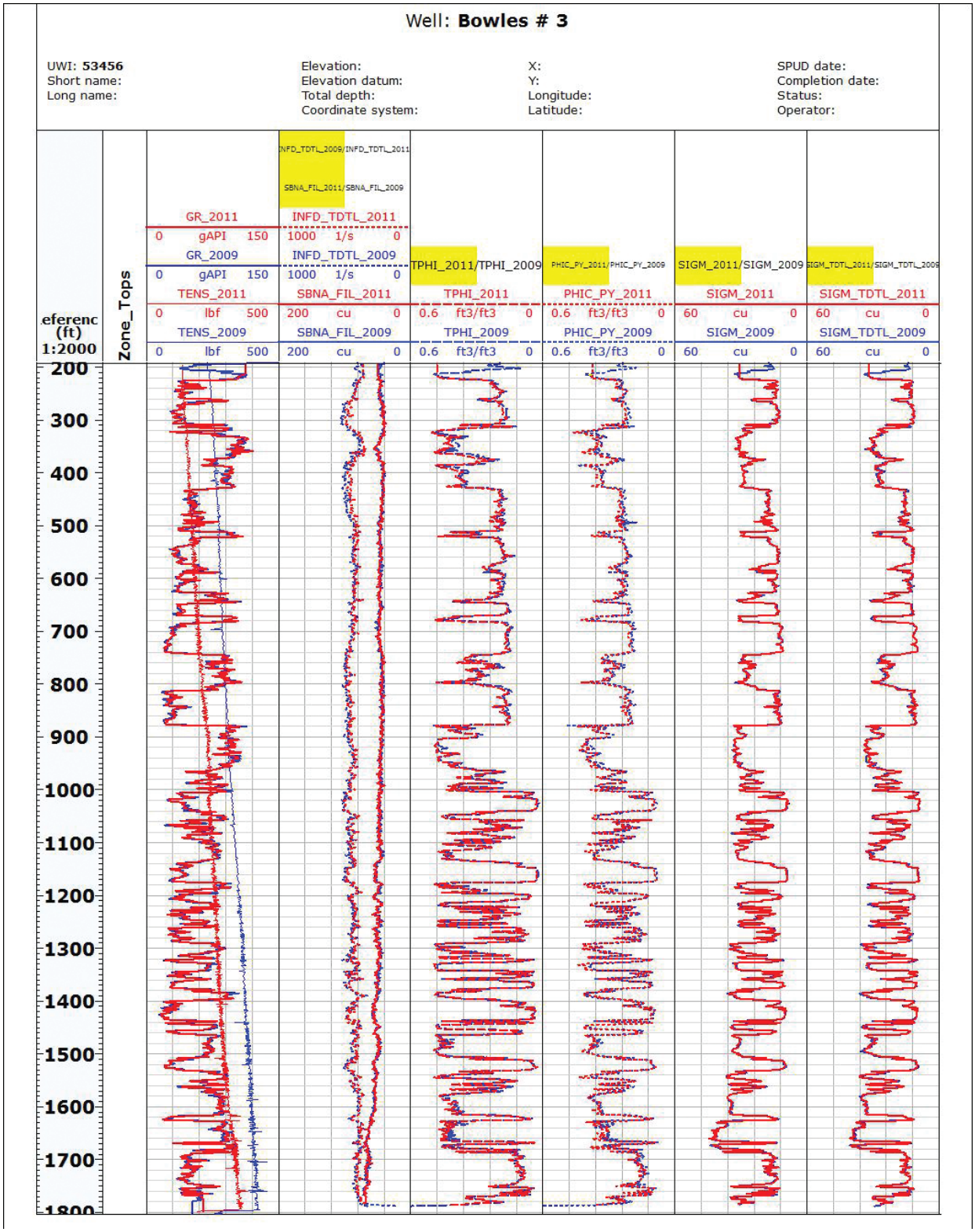

Appendix 10, figure 1 Log analysis for well Bowles #3 (PB-3).

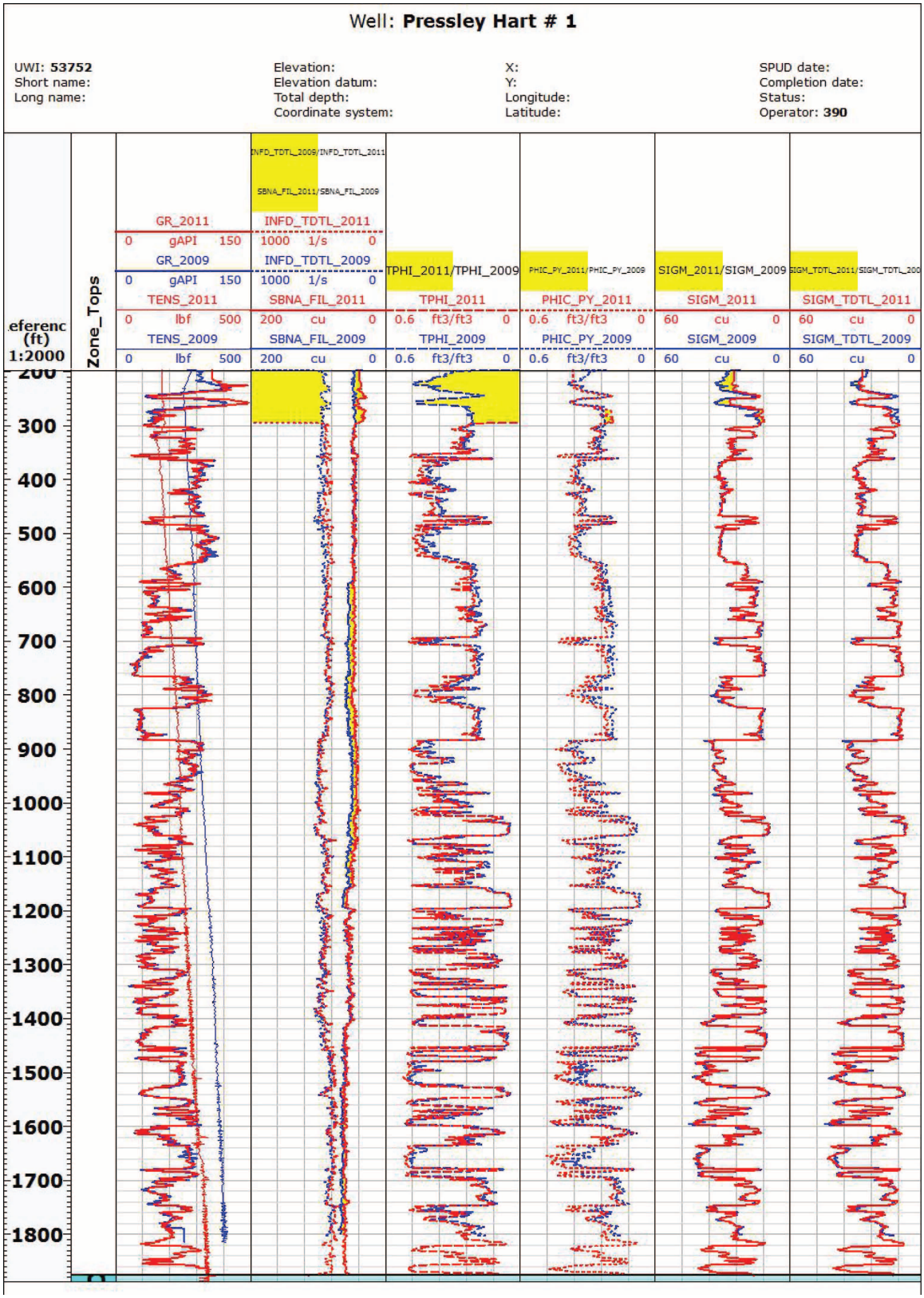

Appendix 10, figure 2 Log analysis for well Pressley Hart #1 (PH-1).

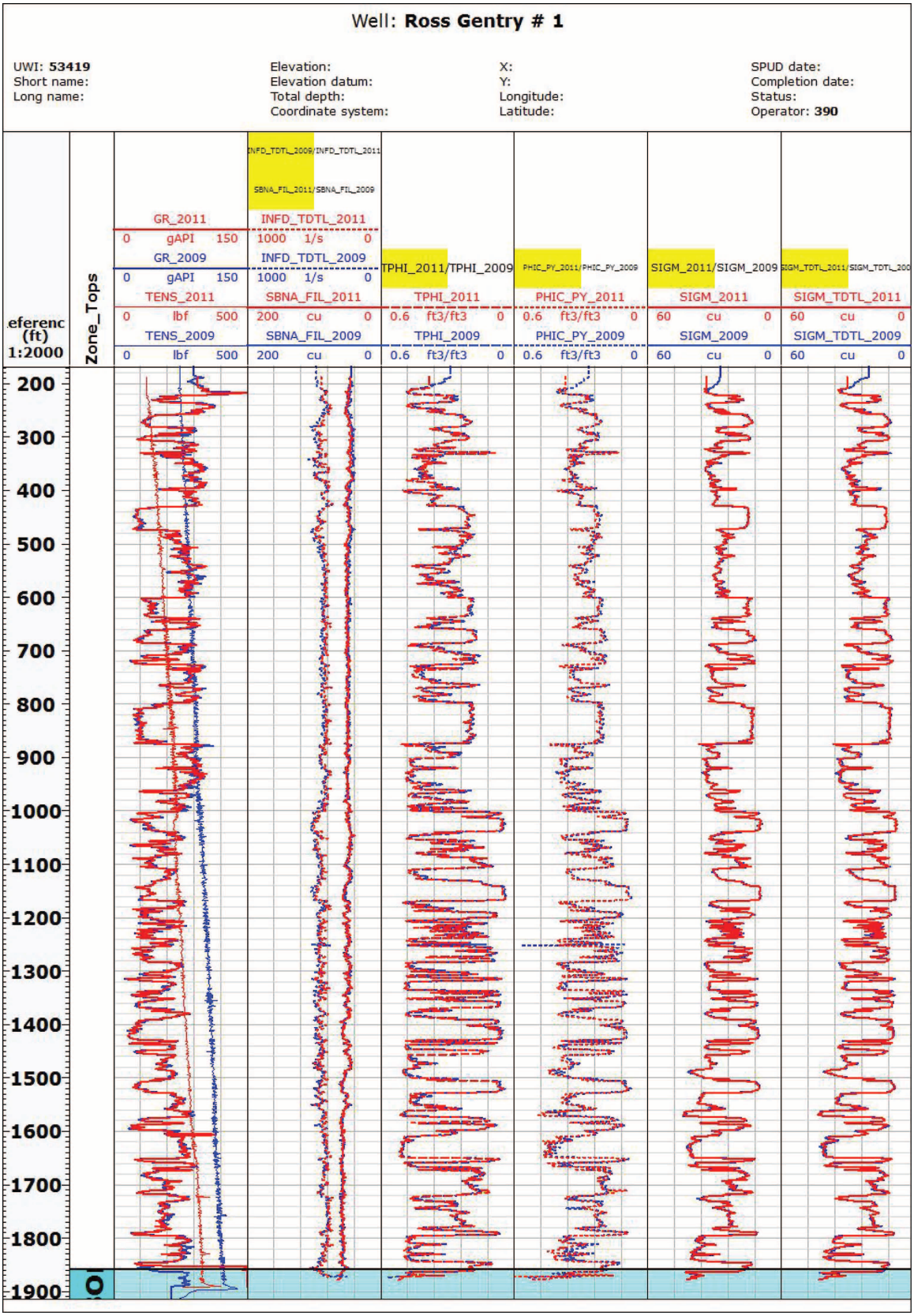

Appendix 10, figure 3 Log analysis for well Ross-Gentry #1 (RG-1).

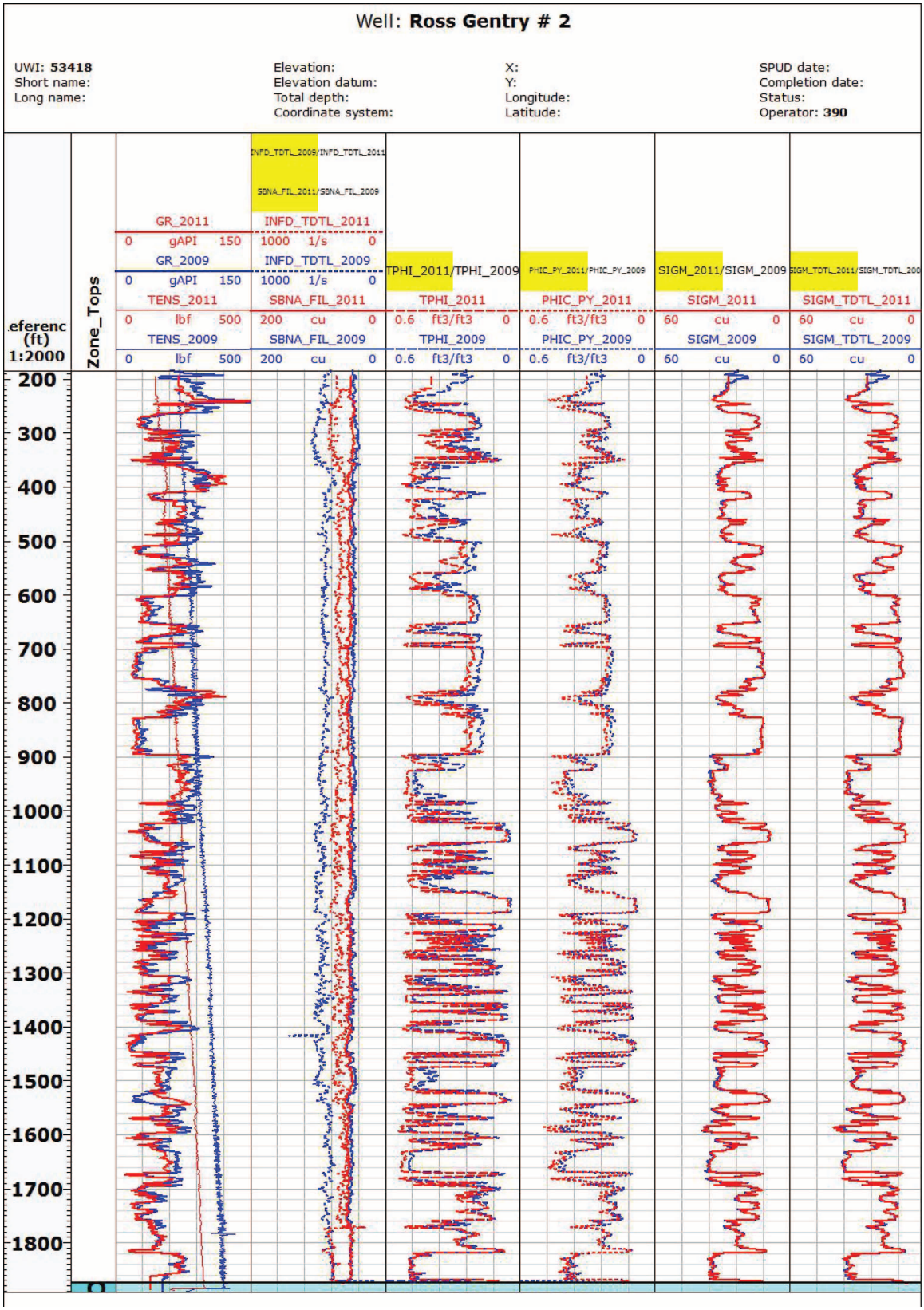

Appendix 10, figure 4 Log analysis for well Ross-Gentry #2 (RG-2).

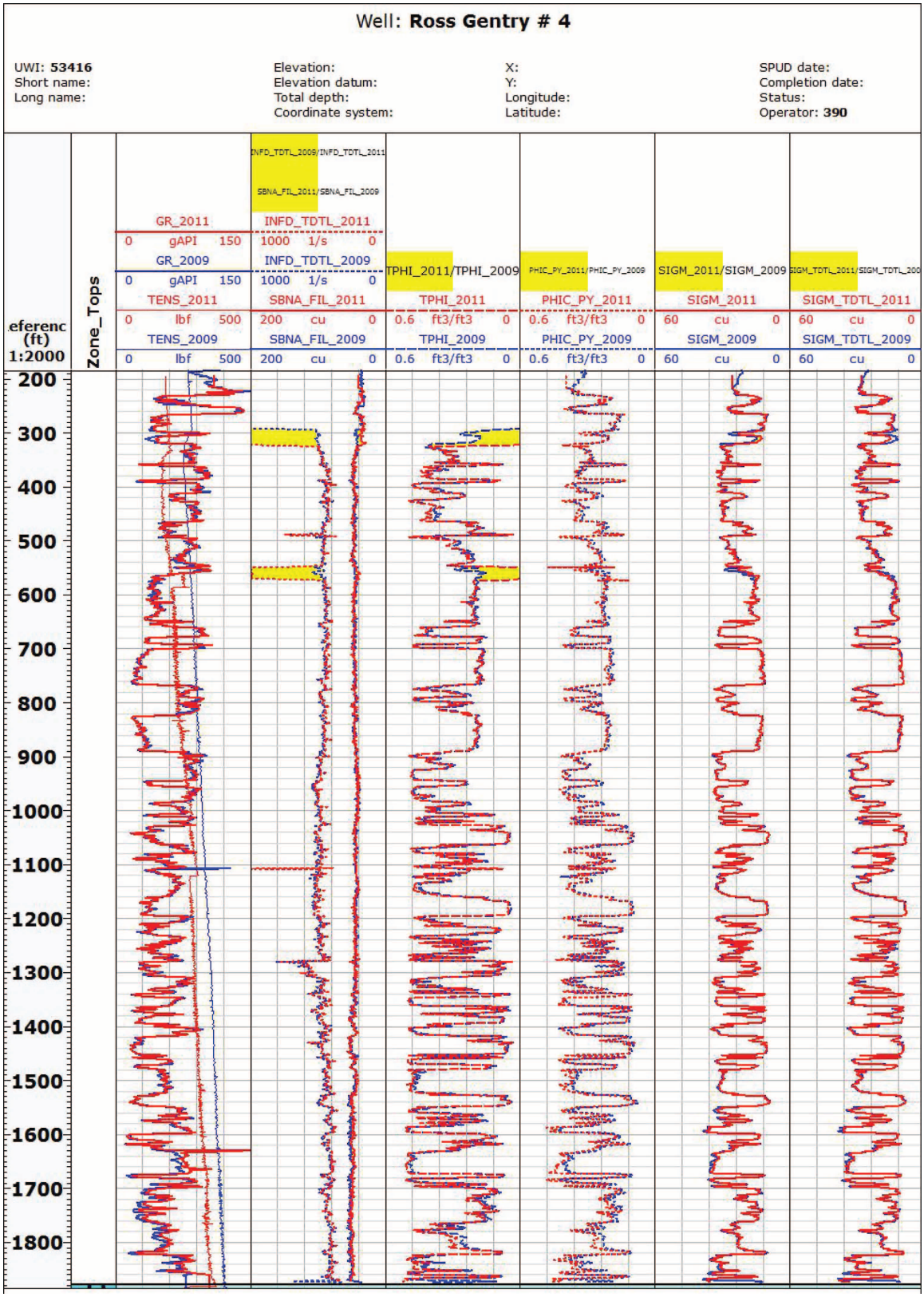

Appendix 10, figure 5 Log analysis for well Ross-Gentry #4 (RG-4).

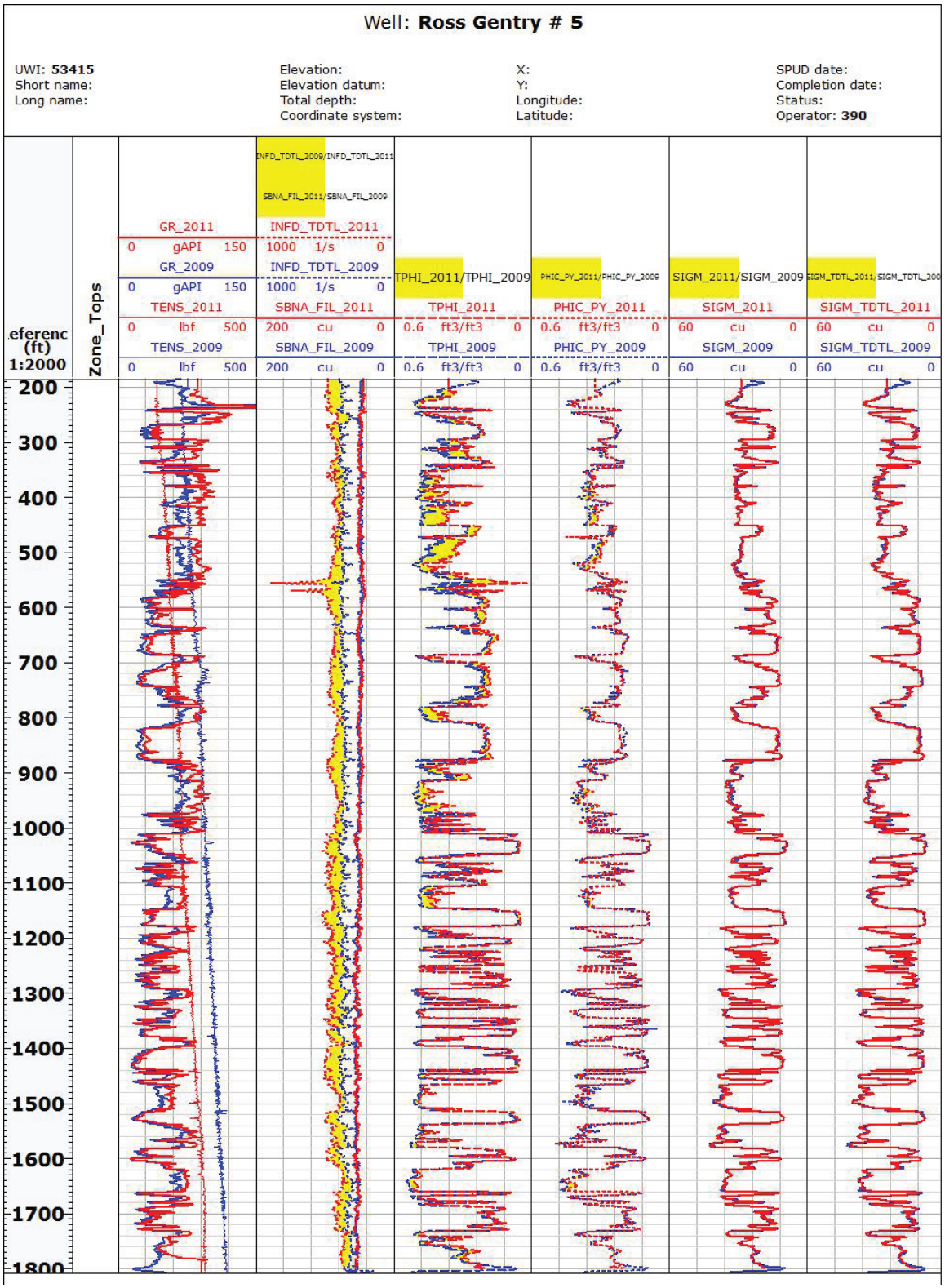

Appendix 10, figure 6 Log analysis for well Ross-Gentry #5 (RG-5).

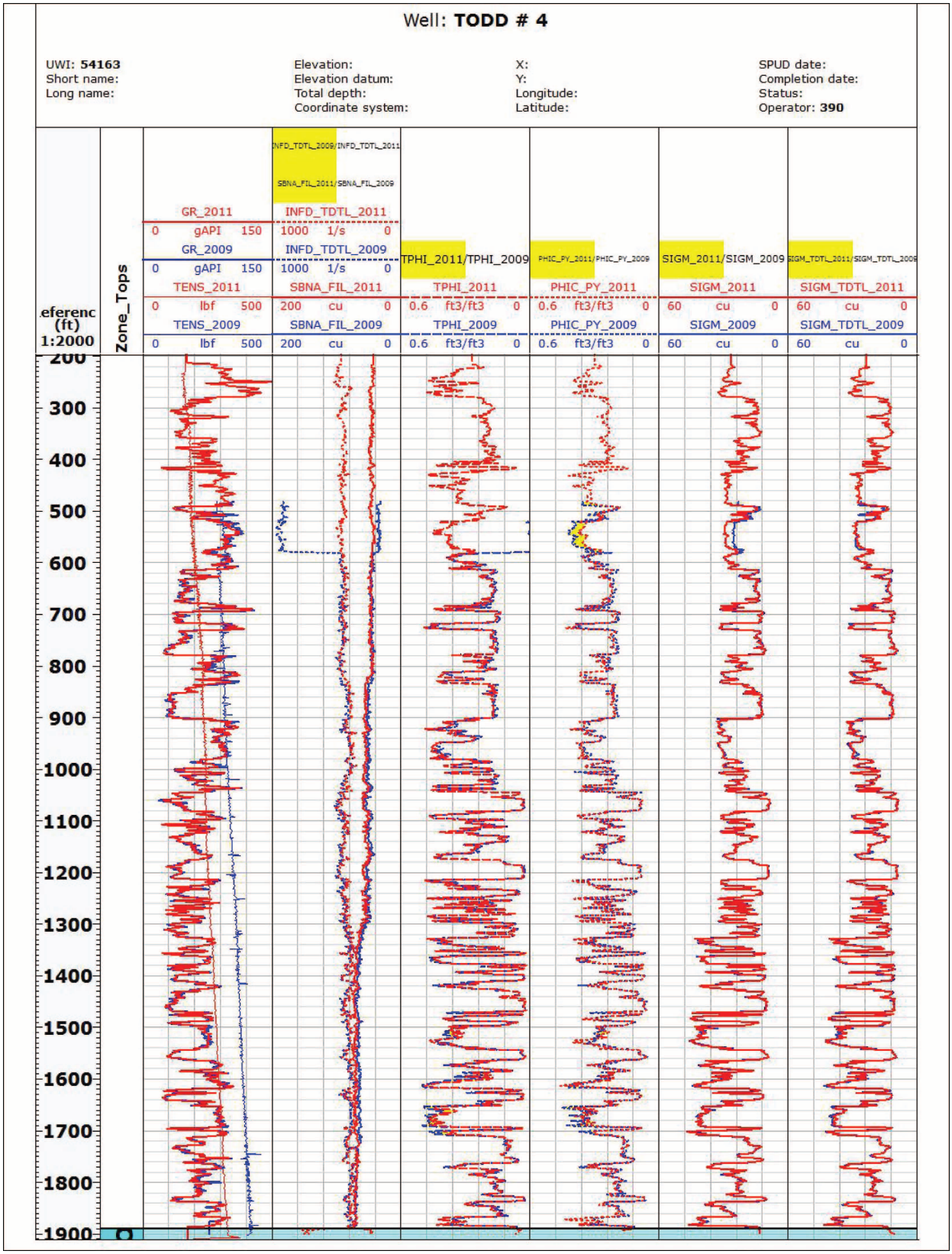

Appendix 10, figure 7 Log analysis for well Todd #4 (WT-4).

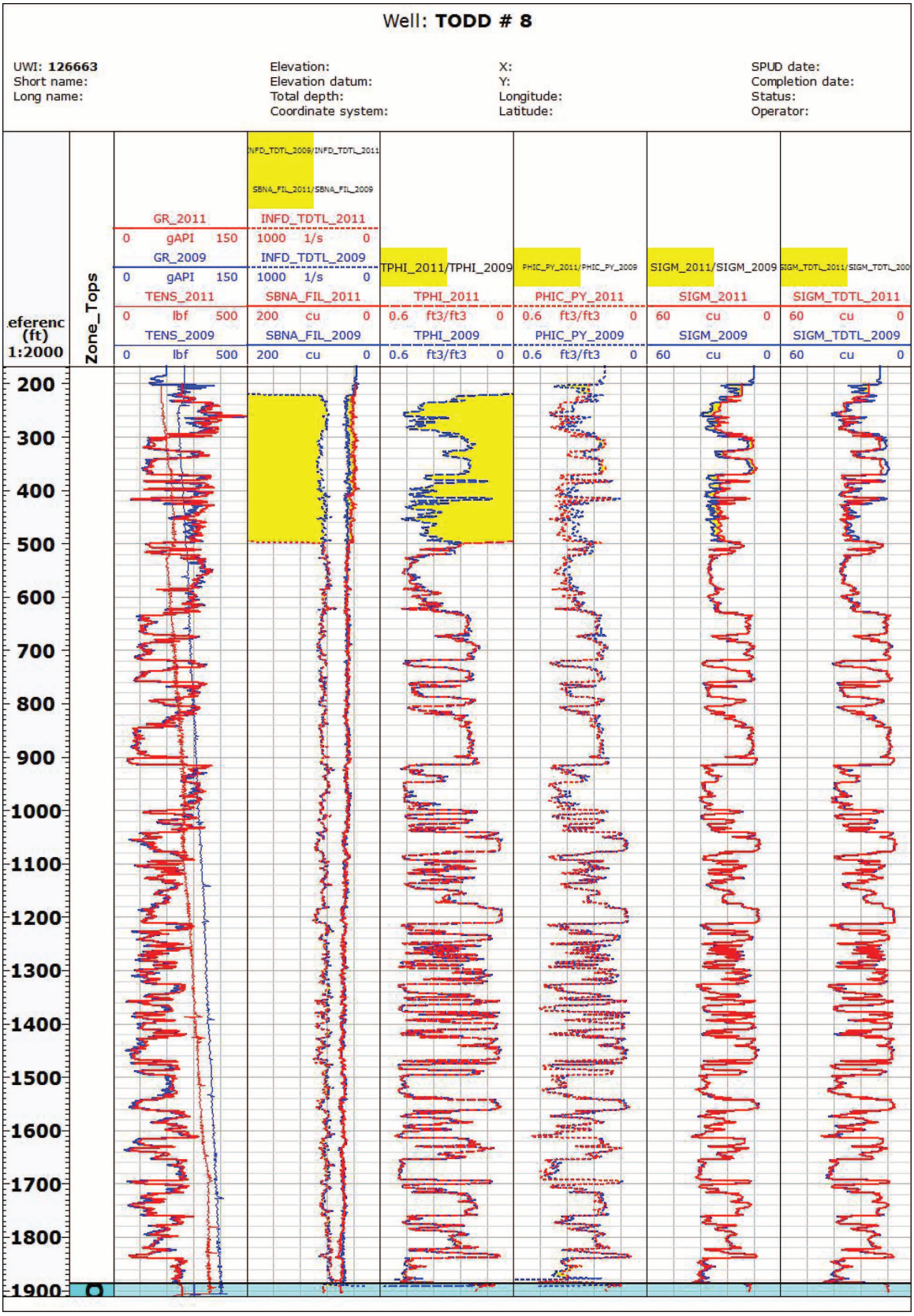

Appendix 10, figure 8 Log analysis for well Todd #8 (WT-8).

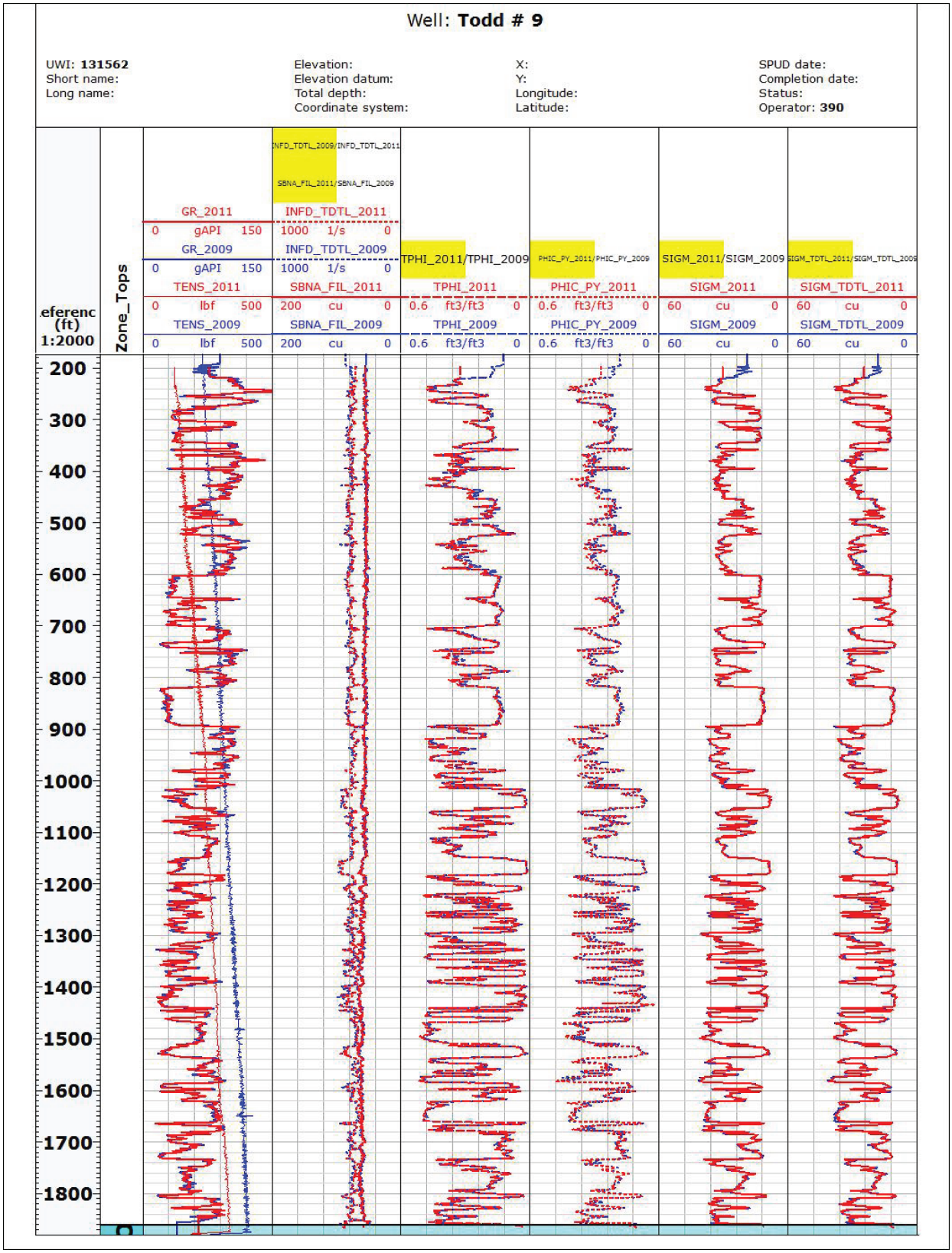

Appendix 10, figure 9 Log analysis for well Todd #9 (WT-9).

Equipment.

Description	Well	Position	Pressure range	Temperature range
Geokon 4500HH Vibrating Wire Pressure Transducer	PH-1, RG-1, RG-2, RG-3, RG-4, WT-4, WT-8	Surface	0–7.5 MPa	–20°C to +80°C
Geokon 4500HH Vibrating Wire Pressure Transducer	RG-5	Surface	0–10 MPa	–20°C to +80°C
Geokon 4500S Vibrating Wire Pressure Transducer	WT-9	Surface	0–700 kPa	–20°C to +80°C
Geokon 4500SH Vibrating Wire Pressure Transducer (Replaced 4500HH on 7/6/09)	RG-5	Surface	0–10 MPa	–20°C to +80°C
Geokon 4500SHI Vibrating Wire Pressure Transducer	PB-3, PZ-1	Downhole	0–10 MPa	–20°C to +80°C
Geokon 4500SHI Vibrating Wire Pressure Transducer	RG-2, RG-5	Downhole	0–20 MPa	–20°C to +80°C
Geokon 4580-1 (Barometer) Vibrating Wire Pressure Transducer	WT-8	Surface	0–17 kPa	–20°C to +80°C
Siemens Sitrans P Pressure Transmitter	RG-3	Surface	0–100 psi	Not recorded
Siemens Sitrans P Pressure Transmitter	JR-1	Surface	0–2300 psi	Not recorded
Campbell Scientific CD295 Display for Enclosure Lid	PH-1, PS, RG-1, RG-2, RG-3, RG-4, RG-5, WT-4, WT-8, WT-9			
Campbell Scientific CR1000 Datalogger	JR-1, PH-1, PS, RG-1, RG-2, RG-3, RG-4, RG-5, WT-4, WT-8, WT-9			
Campbell Scientific AVW200 2-Channel Vibrating Wire Spectrum Analyzer Module	PH-1, RG-1, RG-2, RG-3, RG-4, RG-5, WT-4, WT-8, WT-9			
Campbell Scientific AVW206 2-Channel Vibrating Wire Spectrum Analyzer Module	PB-3, PZ-1			
Campbell Scientific CFM100 CompactFlash Module	JR-1, PH-1, PS, RG-1, RG-2, RG-3, RG-4, RG-5, WT-4, WT-8, WT-9			
Air Link Communications Raven C3211-V Cellular Modem	WT-9			
Campbell Scientific RF401 900-MHz Spread Spectrum Radio Data Transceiver	JR-1, PH-1, PS, RG-1, RG-2, RG-3, RG-4, RG-5, WT-4, WT-8, WT-9			
Sierra Innova-Mass 240 Vortex Meter		Downstream from pumps	0.9–22 gpm	
Cameron NuFlo Liquid Turbine Flowmeter		Downstream from pumps	0.75–7.5 gpm	
Siemens Sitrans P Pressure Transmitter		Upstream from pumps	0–910 psi	
Siemens Sitrans TK-H Temperature Transmitter		Upstream from pumps; downstream from line heater		–30°C to +50°C

PS = pump skid.

Appendix 12 Gas production calculations.

Casing gas flow rates were measured using orifice well testers manufactured by Teledyne Merla. Data required for gas rate calculations included upstream gas temperature, pressure, and specific gravity. The size of orifice plate installed was also required. For most wells, Geokon vibrating wire transducers were installed in pipes venting casing gas to measure both temperature and pressure. One well used a thermistor and Siemens pressure gauge for temperature and pressure measurements. The composition of casing gas was monitored using an infrared gas analyzer in the field, and gas bag samples were collected and analyzed using gas chromatography in the laboratory. The specific gravity of the gas was computed from gas composition and interpolated between measured values based on time.

Teledyne Merla provided tables to correlate gauge pressure and orifice plate size with gas rates at a standard temperature and specific gravity. In addition, equations were required to correct for temperature and specific gravity of gas that deviated from the standards.

The equation for calculating gas rate (GR) was

$$GR = [\text{RateTable (P, orifice plate size)}] \times [520/(460 + T)]^{0.5} \times (0.60/SGG)^{0.5}$$

where

GR is in thousand standard cubic feet per day (Mscfd);

P = gauge pressure in psig;

T = gauge temperature in Fahrenheit degrees;

RateTable(P, orifice plate size) = flow rate for the measured pressure and orifice plate size at standard conditions of 14.65 psia and 60°F and 0.60 specific gravity, as indicated on Teledyne Merla rate table; and

SGG = specific gravity of gas.

Factors taken into consideration in this calculation included temperature, pressure difference, gas gravity of gas, and the need to subtract background CO_2 from measured CO_2 when calculating CO_2 concentrations. Methods for dealing with these factors and other problems included the following:

- Temperature: Temperatures were monitored for anomalies that would make pressure readings inaccurate.
- Gauge pressure: During calibration, each transducer was set to 0 kPag (0 psig) at atmospheric pressure. Many gauges were reading negative values at the beginning of the project and were adjusted to read 0 by adding a pressure offset.
- Gas gravity: Gas gravity was calculated using molecular weight and component concentrations from gas chromatograph (GC) data and interpolated using time to each timestamp in the 1 minute data set. Interpolation was carried out in one of two ways. If CO_2 concentrations exhibited little variation over time based on GC and field infrared readings, the GC data were interpolated using time to each timestamp in the 1 minute data set. Alternatively, a correlation between GC CO_2 concentrations and field IR CO_2 concentrations was created and applied to calculate GC-like readings, and these data were interpolated using time to each timestamp in the 1 minute dataset.
- CO_2 background: CO_2 levels measured prior to injection were averaged to estimate background CO_2 levels.
- Quality control GC data: The GC data was examined for high N_2 or O_2 concentrations (which would suggest atmospheric contamination) and for high deviation and inconsistencies. Data that had high N_2 or O_2 values were removed from the data set.

Appendix 13 Schematics of data acquisition equipment.

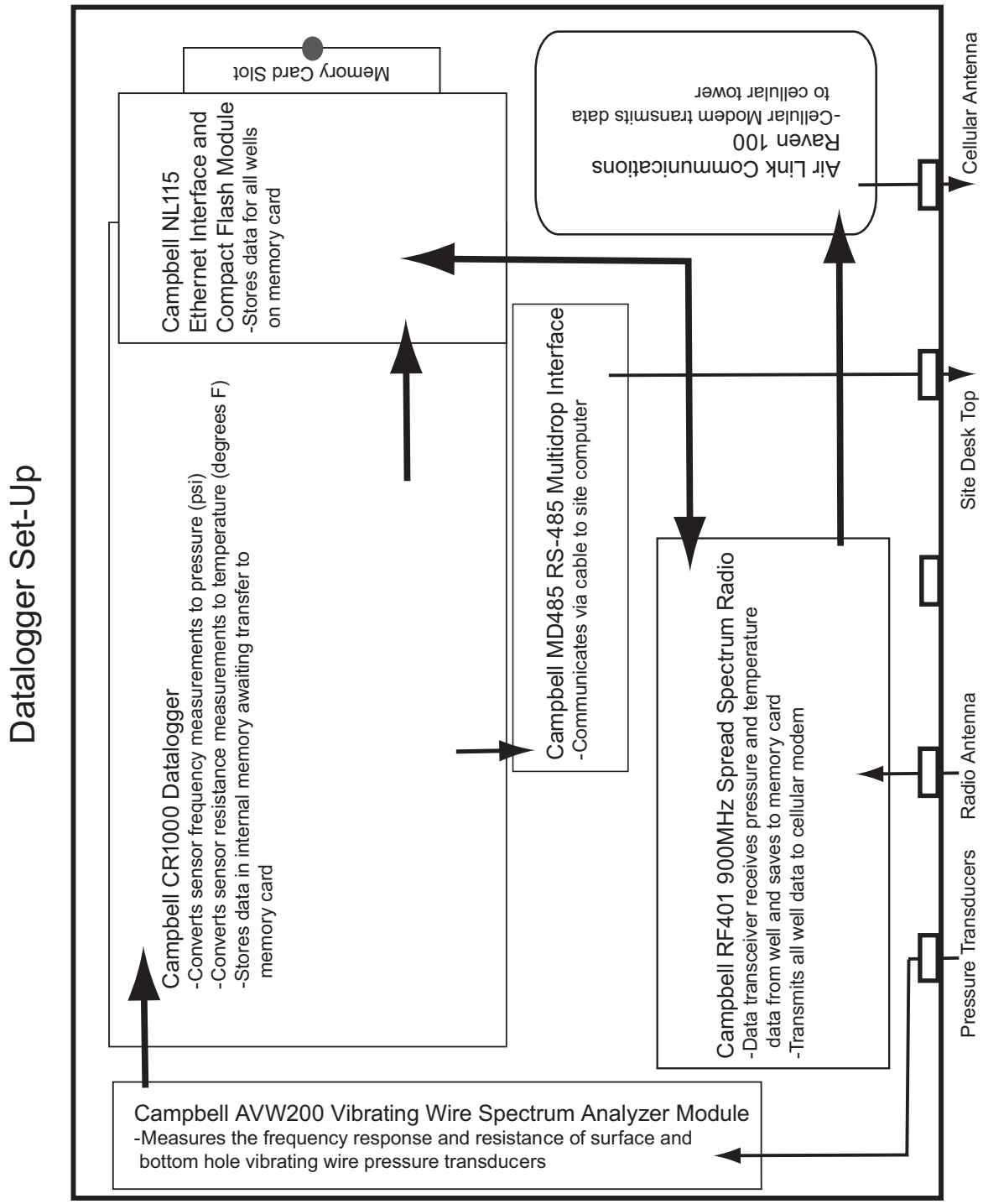

Appendix 14 Timeline of events.

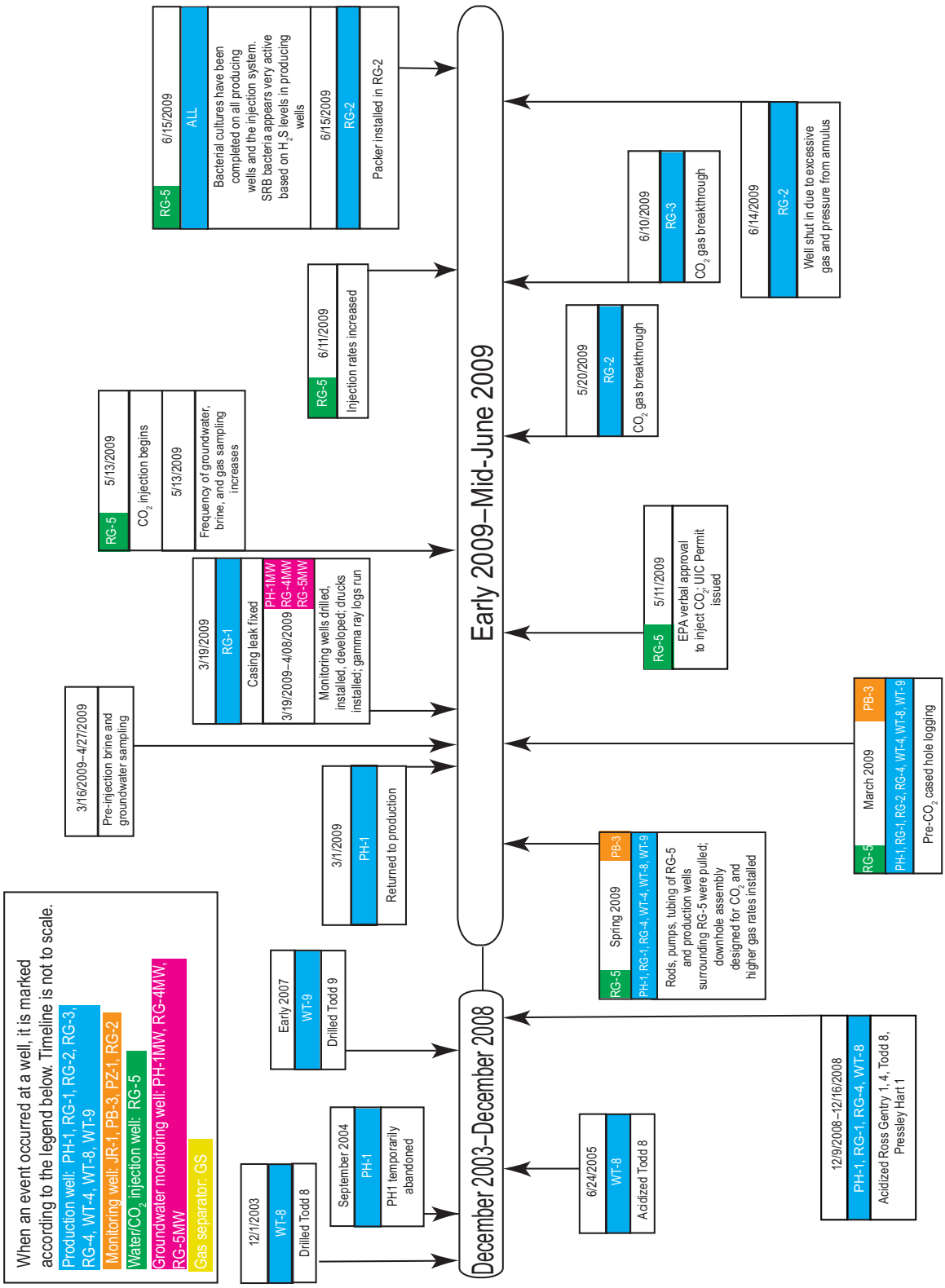

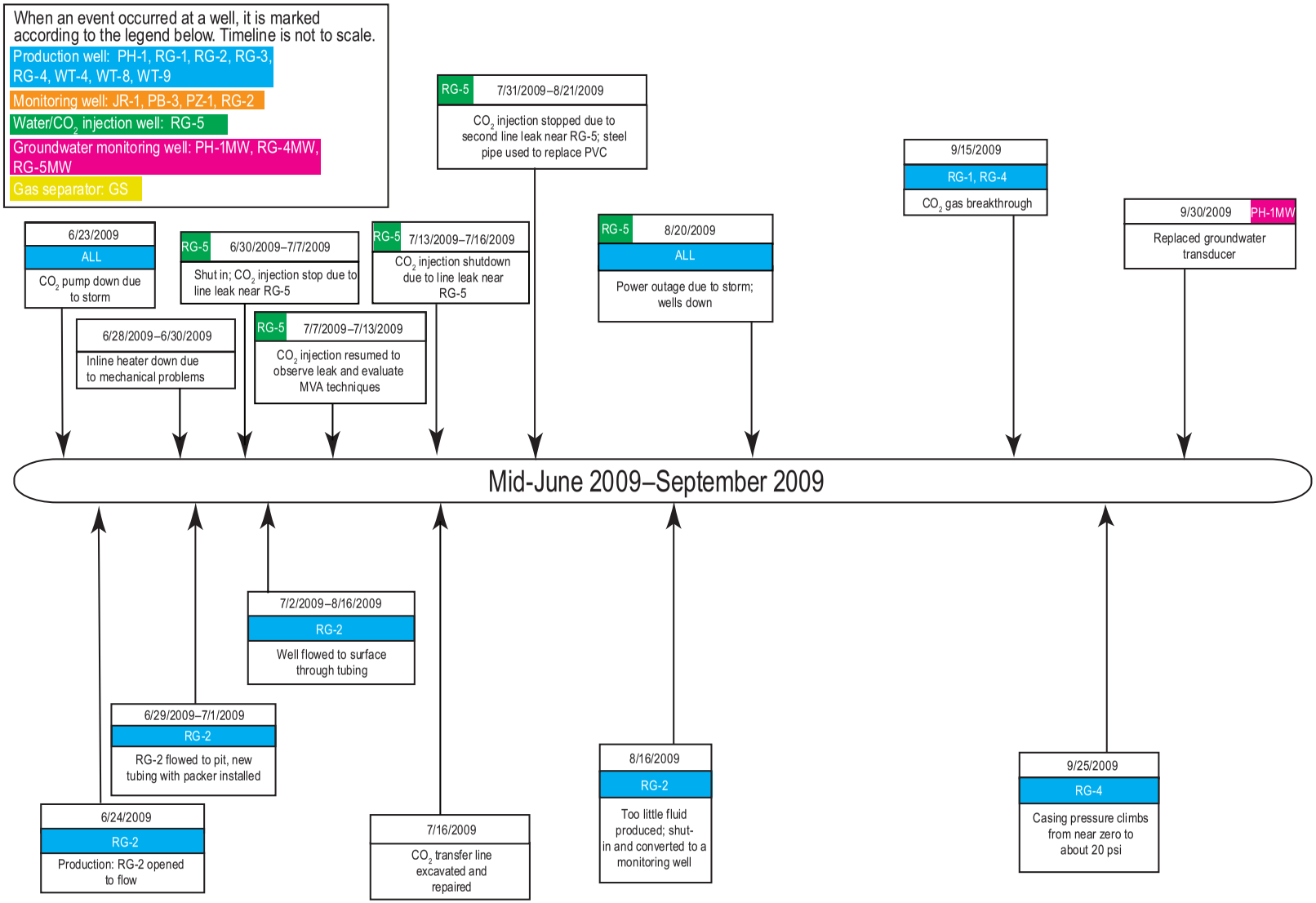
When an event occurred at a well, it is marked according to the legend below. Timeline is not to scale.
Production well: PH-1, RG-1, RG-2, RG-3, RG-4, WT-4, WT-8, WT-9
Monitoring well: JR-1, PB-3, PZ-1, RG-2
Water/CO2 injection well: RG-5
Groundwater monitoring well: PH-1MW, RG-4MW, RG-5MW
Gas separator: GS
6/23/2009
ALL
CO2 pump down due to storm
RG-5 6/30/2009–7/7/2009
Shut in; CO2 injection stop due to line leak near RG-5
RG-5 7/13/2009–7/16/2009
CO2 injection shutdown due to line leak near RG-5
RG-5 7/31/2009–8/21/2009
CO2 injection stopped due to second line leak near RG-5; steel pipe used to replace PVC
RG-5 8/20/2009
ALL
Power outage due to storm; wells down
9/15/2009
RG-1, RG-4
CO2 gas breakthrough
9/30/2009 PH-1MW
Replaced groundwater transducer
6/28/2009–6/30/2009
Inline heater down due to mechanical problems
RG-5 7/7/2009–7/13/2009
CO2 injection resumed to observe leak and evaluate MVA techniques
Mid-June 2009–September 2009
7/2/2009–8/16/2009
RG-2
Well flowed to surface through tubing
6/29/2009–7/1/2009
RG-2
RG-2 flowed to pit, new tubing with packer installed
6/24/2009
RG-2
Production: RG-2 opened to flow
7/16/2009
CO2 transfer line excavated and repaired
8/16/2009
RG-2
Too little fluid produced; shut-in and converted to a monitoring well
9/25/2009
RG-4
Casing pressure climbs from near zero to about 20 psi

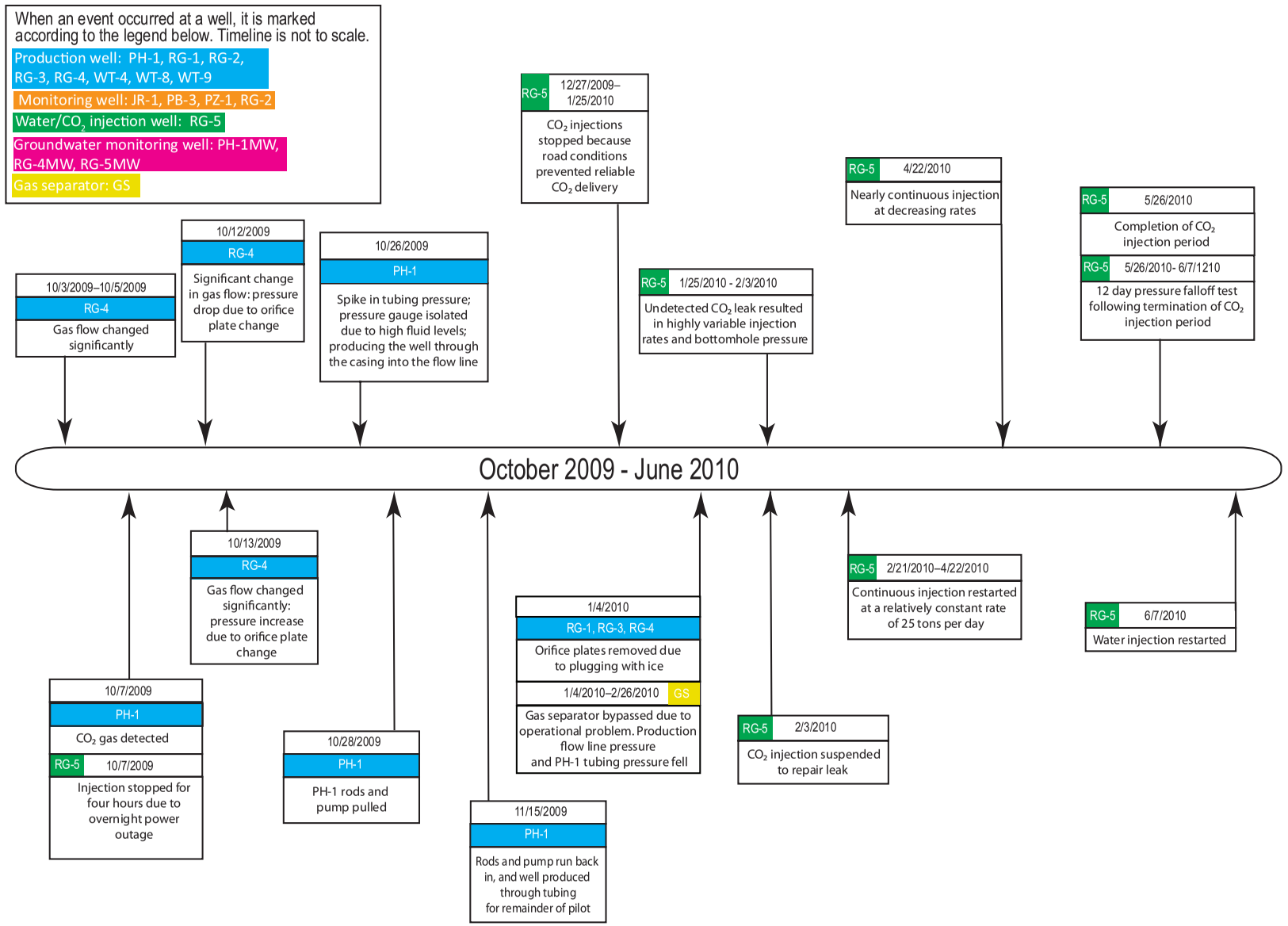
When an event occurred at a well, it is marked according to the legend below. Timeline is not to scale.
Production well: PH-1, RG-1, RG-2, RG-3, RG-4, WT-4, WT-8, WT-9
Monitoring well: JR-1, PB-3, PZ-1, RG-2
Water/CO2 injection well: RG-5
Groundwater monitoring well: PH-1MW, RG-4MW, RG-5MW
Gas separator: GS
October 2009 - June 2010
10/3/2009–10/5/2009
RG-4
Gas flow changed significantly
10/12/2009
RG-4
Significant change in gas flow: pressure drop due to orifice plate change
10/26/2009
PH-1
Spike in tubing pressure; pressure gauge isolated due to high fluid levels; producing the well through the casing into the flow line
RG-5 12/27/2009–1/25/2010
CO2 injections stopped because road conditions prevented reliable CO2 delivery
RG-5 1/25/2010 - 2/3/2010
Undetected CO2 leak resulted in highly variable injection rates and bottomhole pressure
RG-5 4/22/2010
Nearly continuous injection at decreasing rates
RG-5 5/26/2010
Completion of CO2 injection period
RG-5 5/26/2010- 6/7/1210
12 day pressure falloff test following termination of CO2 injection period
10/7/2009
PH-1
CO2 gas detected
RG-5 10/7/2009
Injection stopped for four hours due to overnight power outage
10/13/2009
RG-4
Gas flow changed significantly: pressure increase due to orifice plate change
10/28/2009
PH-1
PH-1 rods and pump pulled
11/15/2009
PH-1
Rods and pump run back in, and well produced through tubing for remainder of pilot
1/4/2010
RG-1, RG-3, RG-4
Orifice plates removed due to plugging with ice
1/4/2010–2/26/2010 GS
Gas separator bypassed due to operational problem. Production flow line pressure and PH-1 tubing pressure fell
RG-5 2/3/2010
CO2 injection suspended to repair leak
RG-5 2/21/2010–4/22/2010
Continuous injection restarted at a relatively constant rate of 25 tons per day
RG-5 6/7/2010
Water injection restarted

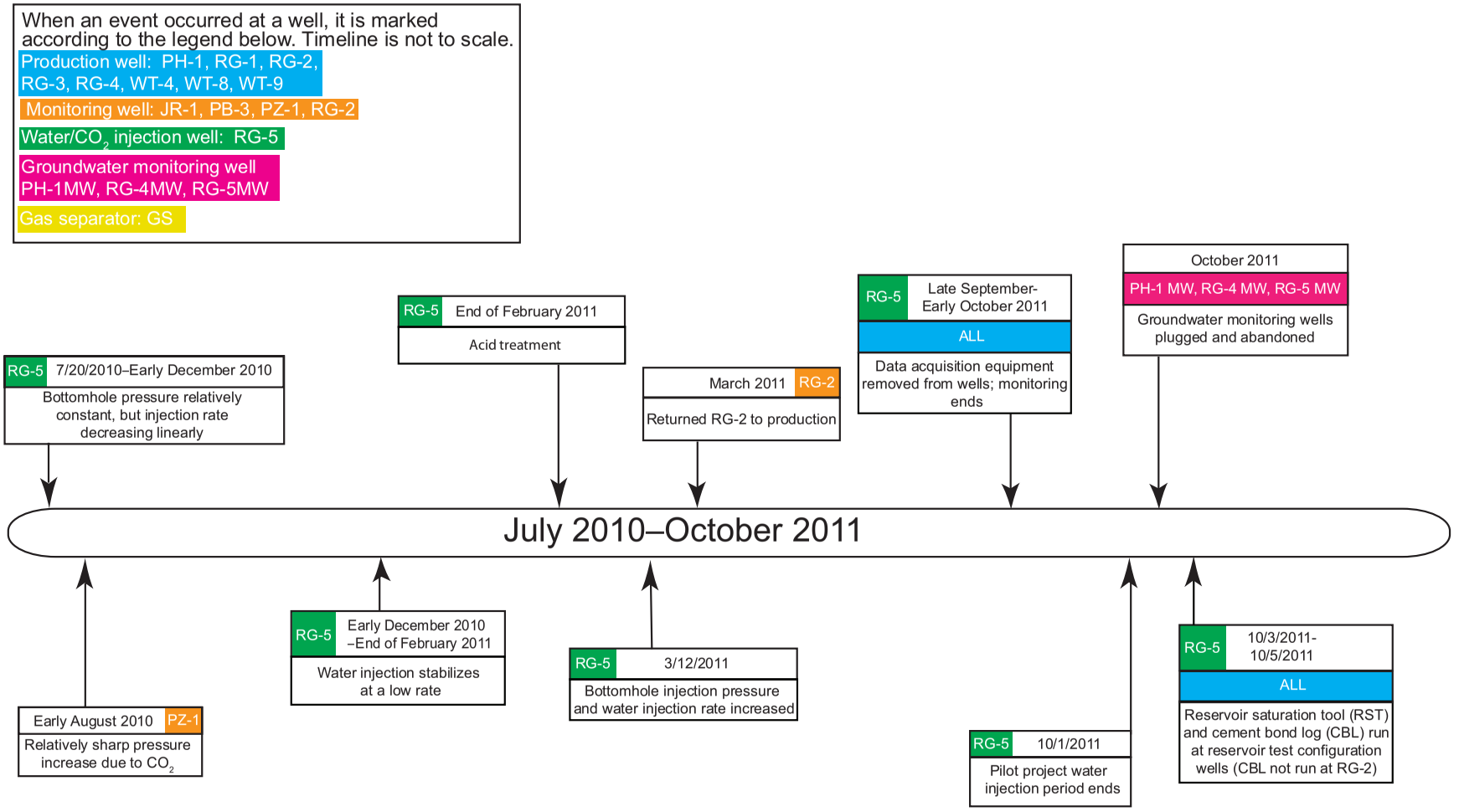
When an event occurred at a well, it is marked according to the legend below. Timeline is not to scale.
Production well: PH-1, RG-1, RG-2, RG-3, RG-4, WT-4, WT-8, WT-9
Monitoring well: JR-1, PB-3, PZ-1, RG-2
Water/CO2 injection well: RG-5
Groundwater monitoring well PH-1MW, RG-4MW, RG-5MW
Gas separator: GS
RG-5 7/20/2010–Early December 2010
Bottomhole pressure relatively constant, but injection rate decreasing linearly
RG-5 End of February 2011
Acid treatment
March 2011 RG-2
Returned RG-2 to production
RG-5 Late September-Early October 2011
ALL
Data acquisition equipment removed from wells; monitoring ends
October 2011
PH-1 MW, RG-4 MW, RG-5 MW
Groundwater monitoring wells plugged and abandoned
July 2010–October 2011
Early August 2010 PZ-1
Relatively sharp pressure increase due to CO2
RG-5 Early December 2010 –End of February 2011
Water injection stabilizes at a low rate
RG-5 3/12/2011
Bottomhole injection pressure and water injection rate increased
RG-5 10/1/2011
Pilot project water injection period ends
RG-5 10/3/2011-10/5/2011
ALL
Reservoir saturation tool (RST) and cement bond log (CBL) run at reservoir test configuration wells (CBL not run at RG-2)

Appendix 15 Water injection rates.

Field water injection rates, January 2008 through December 2010.

Month	Water injected in field (bbl)	Water injection rate for field (bwpd)
January 2008	8,316	268.26
February 2008	8,521	293.83
March 2008	8,959	289.00
April 2008	8,063	268.77
May 2008	7,768	250.58
June 2008	7,702	256.73
July 2008	8,093	261.06
August 2008	7,900	254.84
September 2008	9,348	311.60
October 2008	11,217	361.84
November 2008	9,962	332.07
December 2008	10,281	331.65
January 2009	5,853	188.81
February 2009	1,384	49.43
March 2009	7,380	238.06
April 2009	8,957	298.57
May 2009	6,757	217.97
June 2009	5,589	186.30
July 2009	5,757	185.71
August 2009	5,376	173.42
September 2009	4,650	155.00
October 2009	4,859	156.74
November 2009	4,737	157.90
December 2009	4,855	156.61
January 2010	9,079	292.87
February 2010	8,174	291.93
March 2010	6,794	219.16
April 2010	7,311	243.70
May 2010	7,364	237.55
June 2010	9,561	318.70
July 2010	11,058	356.71
August 2010	10,535	339.84
September 2010	9,677	322.57
October 2010	8,786	283.42
November 2010	9,629	320.97
December 2010	9,148	295.10

Appendix 16 Casing gas production data.

Summary of casing gas production data for the Ross-Gentry and PH-1 wells and the gas separator.

Well name	Total gas production (scm)	Total gas production (Mscf)	CO_2 production (scm)	CO_2 production (Mscf)[1]	CO_2 production (tonnes)[1]	CO_2 production (tons)[1]	Back-ground CO_2 (%)	Corr. CO_2 production (tonnes)[2]	Corr. CO_2 production (tons)[2]	% of injected CO_2 produced at well[3]	Comment
RG-1	56.2989	1,988.18	41,549.167	1,467.295	77.66	85.61	2.00	82.00	83.89	1.16	significant data estimation
RG-2	20.239	714.73	19,475.76	687.78	36.40	40.13	3.20	37.97	38.84	0.54	significant loss during workover
RG-3	142.293	5,025.02	116,514.48	4,114.67	217.78	240.06	8.00	215.894	220.86	3.06	
RG-4	332.866	11,755.1	284,989.24	10,064.3	532.69	587.18	3.50	553.89	566.63	7.84	
PH-1	10.2532	362.09	3,315.34	117.08	6.20	6.83	0.35	6.66	6.81	0.09	assumed plate size of 0.125
GS-1	142.972	5,049.02	117,739.98	4,157.948	220.07	242.59		237.14	242.59	3.36	significant data estimation

[1] Raw data.

[2] After correction (Corr.) for background CO_2 levels.

[3] Percentages were based on a figure of 7,227 tons total CO_2 injected at RG-5. (All measurements were taken in short tons, and tonne equivalents were calculated after the fact.) Elsewhere in this report, the total injected CO_2 is rounded to 7,230 tons, since a level of precision of three significant figures is more in keeping with the amount of uncertainty in the data.

Appendix 17 Isotopic composition of gas phase hydrocarbons from production wells.

Isotopic composition of gas phase hydrocarbons from production wells at Sugar Creek.

Sample ID	$\delta^{13}C\text{-}C_1$	$\delta^{13}C\text{-}C_2$	$\delta^{13}C\text{-}C_3$	$\delta^{13}C\text{-}iC_4$	$\delta^{13}C\text{-}nC_4$	$\delta^{13}C\text{-}iC_5$	$\delta^{13}C\text{-}nC_5$	$\delta D\text{-}C_1$	$\delta D\text{-}C_2$	$\delta D\text{-}C_3$
SC-RG1-90 10/19/11 15:50	–51.0	–35.6	–32.3	–33.2	–32.0	–30.9	–32.3	–185	–172	–124
SC-RG3-90 10/19/11 15:35	–51.8	–35.8	–31.9	–33.3	–32.6	–30.9	–32.5	–184	–162	–130
SC-RG4-90 10/19/11 15:27	–52.2	–35.1	–32.1	–33.3	–32.5	–30.8	–32.4	–185	–171	–128
SC-WT8-90 10/19/11 14:49	–51.0	–35.3	–32.2	–33.3	–32.3	–30.7	–32.3	–185	–170	–125
SC-RG1-91A 11/1/11 13:28	–51.4	–35.5	–32.3	–33.3	–32.4	–30.9	–32.3	–185	–168	–124
SC-RG1-91B 11/1/11 13:31	–51.4	–35.5	–32.2	–33.5	–32.5	–30.9	–32.3	–184	–170	–124
SC-RG2-91A 11/1/11 15:21	– 51.5	–35.3	–32.3	–33.5	–32.7	–31.0	–32.5	–184	–161	–134
SC-RG2-91B 11/1/11 15:22	–50.8	–34.9	–32.3	–33.3	–32.4	–30.9	–32.5	–181	–161	–133
SC-PH1-91A 11/2/11 10:20	–51.6	–35.8	–32.2	–33.4	–32.4	–30.7	–32.4	–181	–166	–129
SC-PH1-91B 11/2/11 10:20	–51.5	–35.7	–32.1	–33.0	–32.4	–30.8	–32.4	–181	–165	–130
SC-WT4-91 11/2/11 11:36	–51.4	–35.4	–32.0	–33.2	–32.3	–30.8	–32.4	–184	–169	–124